

IL  
NUOVO CIMENTO  
ORGANO DELLA SOCIETÀ ITALIANA DI FISICA  
SOTTO GLI AUSPICI DEL CONSIGLIO NAZIONALE DELLE RICERCHE

VOL. III, N. 6

*Serie decima*

1° Giugno 1956

**Introduction of « True Observables »  
into the Quantum Field Equations (\*)**

P. G. BERGMANN

*Department of Physics, Syracuse University, N. Y.*

(ricevuto il 25 Luglio 1955)

**Summary** (+). — In connection with our work on the quantization of general relativity, we have investigated the equations of quantum electrodynamics, with the unrestricted gauge group, that is without specializing to Lorentz or Coulomb gauge. Even before quantization, we formulate the theory in terms of « true observables » only. We define these as dynamical variables generating canonical transformations leading from one permissible state to another; a permissible state, in turn, is a set of values of all canonical variables that obeys the gauge constraints. Similarly an observable in the quantized theory must be a Hermitian operator within the Hilbert space of permissible states; the latter are those obeying the gauge constraints. Transition to the true observables not only eliminates the longitudinal parts, of the vector potential and the scalar potential from the theory, but also the longitudinal components of the electric field strength. Likewise, the operators that create and annihilate charged particles are not themselves observables, but one can construct product combinations that are. Such (gauge-invariant) products involve the product of a creator by an annihilator at different space points, multiplied by a functional that depends on a line integral of the vector potential, the path of integration being any curve connecting the two space points. It turns out that the Hamiltonian can in fact be written in terms of these observables only, and that the infinite self-energy caused by non-transverse photons is eliminated automatically.

(+) *Editor's care.*

(\*) This work was supported by the Office of Naval Research and by the National Science Foundation, and was presented at the International Conference on Elementary Particles held at Pisa, June 1955.

In a previous paper <sup>(1)</sup> it was shown that in the presence of constraints in the Hamiltonian version of a theory the usual group of canonical transformations in phase space may be replaced advantageously by a different group, whose infinitesimal commutators are closely related to the so-called Dirac brackets <sup>(2)</sup>. The new group resembles the group of canonical transformations insofar as it also reproduces the form of the canonical equations of motion, but differs in that it leaves the form of the constraints unchanged. In this transformation group one can also define generators, but in the presence of first-class constraints the relationship between infinitesimal transformations and generating dynamical variables is not one-to-one. Certain dynamical variables cannot serve as generators; on the other hand, there are different transformations belonging to the same generator. In fact, there exists a normal subgroup of infinitesimal transformations belonging to the generator zero. This subgroup represents a group of transformations with respect to which the theory is invariant, e.g. curvilinear coordinate transformations, gauge transformations and the like. It is characteristic for these groups that they depend on arbitrary functions of the time coordinate, unlike, for instance, the Lorentz group. If we form the factor group with respect to the normal subgroup, then we obtain a new (abstract) group that possesses a one-to-one relationship to the admissible generators. The admissible generators are those dynamical variables that are invariant under the normal subgroup. The transition to the factor group eliminates all those generators that are trivially zero, i.e. the constraints of the theory. We shall call these admissible, non-trivial variables «true observables».

The true observables are the physically meaningful variables of a theory. Their values (at a given time) are independent of the choice of the frame of reference (including the gauge frame). Their values can be predicted from one time to another by integration of the canonical equations of motion (or canonical field equations, as the case may be). Any physical situation can be characterized uniquely in terms of the true observables.

The Lie algebra of the true observables affords an improved access to the task of quantizing theories with constraints. It would appear that particularly in theories possessing general covariance the determination of the true observables is a necessary preliminary to their quantization. Unfortunately this determination remains so far an unsolved problem. It was, however, considered a useful «practice» to test out the concept on a theory providing a less formidable challenge, i.e. electrodynamics. That is the topic of this paper.

---

(1) P. G. BERGMANN and I. GOLDBERG: *Phys. Rev.*, **98**, 531, 544 (1955).

(2) P. A. M. DIRAC: *Can. Journ. of Math.*, **2**, 129 (1950); **3**, 1 (1951).



## 1. – The True Observables of Electrodynamics.

We begin by identifying the true observables of classical (relativistic) electrodynamics in which the sources of the field are point charges. Ordinarily such a field is described in the canonical formalism by the four electromagnetic potentials  $\varphi$  and  $A_i$  ( $i = 1, 2, 3$ ), by the four momentum densities  $\pi^4$ ,  $\pi^s$ , and further by the coordinates and momentum components of the point charges  $x_{(n)i}$ ,  $p_{(n)i}$ , where the subscript  $n$  identifies the  $n$ -th particle. These canonical coordinates are subject to two constraints at each space point,

$$(1) \quad \pi^4 = 0, \quad \pi^s_s + \frac{1}{c} \sum_n e_n \delta(\mathbf{x}_n, \mathbf{x}) = 0.$$

The symbol  $\delta$  denotes here the three-dimensional  $\delta$ -function. According to the rules derived earlier <sup>(1)</sup>, and because all the constraints (1) are first-class constraints, the true observables are those dynamical variables that are left over after we have eliminated not only the constraints themselves, but also their canonical conjugates. More precisely, the true observables must be combinations of dynamical variables whose Poisson brackets with all constraints vanish. This requirement is equivalent to the one that the observables must be gauge invariant, because the constraints are actually the generators of infinitesimal gauge transformations. Under an infinitesimal gauge transformation the dynamical variables transform as follows:

$$(2) \quad \delta A_i = \xi_{,i}, \quad \delta \varphi = -\frac{1}{c} \dot{\xi}, \quad \delta x_{(n)i} = 0, \quad \delta p_{(n)i} = \frac{e_n}{c} \xi(\mathbf{x}_n)_{,i},$$

where  $\xi$  is a completely arbitrary function of the space and time coordinates and may even depend on the dynamical variables themselves. This transformation (2) is generated by the functional

$$(3) \quad \mathcal{G} = - \int \left\{ \frac{1}{c} \pi^4 \dot{\xi} + \left[ \pi^s_s + \frac{1}{c} \sum_n e_n \delta(\mathbf{x}_n, \mathbf{x}) \right] \xi \right\} d^3x.$$

It follows, then, that  $\pi^4$ ,  $\varphi$ , and the longitudinal components of  $A_s$  and  $\pi^s$  must be eliminated from the formulation of the theory. Moreover, the canonical momentum components  $p_{(n)i}$  must be replaced by the so-called kinetic momenta  $p'_{(n)i}$ ,

$$(4) \quad p'_{(n)} = p_{(n)} - \frac{e}{c} A(\mathbf{x}_n) = \left( 1 - \frac{\dot{\mathbf{x}}_{(n)}^2}{c^2} \right)^{-\frac{1}{2}} m_n \dot{\mathbf{x}}_{(n)},$$

which are gauge invariant.

We define the longitudinal and transverse components of a vector field as follows:

$$(5) \quad \begin{cases} \mathbf{A} = \mathbf{A}_{(l)} + \mathbf{A}_{(t)}, & \text{curl } \mathbf{A}_{(l)} = 0, & \text{div } \mathbf{A}_{(t)} = 0, \\ \mathbf{A}_{(l)} = -\frac{1}{4\pi} \int \frac{1}{r} \text{grad}' (\text{div}' \mathbf{A}') d^3x', \\ \mathbf{A}_{(t)} = \frac{1}{4\pi} \int \frac{1}{r} \text{curl}' \text{curl}' \mathbf{A}' d^3x', \end{cases} \quad r \equiv |\mathbf{x} - \mathbf{x}'|.$$

If we introduce these quantities into the customary Hamiltonian of the theory, we obtain the following expression:

$$(6) \quad H = \frac{1}{2} \int \left[ \frac{1}{4\pi} (\text{curl } \mathbf{A}_{(t)})^2 + 4\pi e^2 \pi_{(t)}^2 \right] d^3x + \sum_n \left( 1 + \frac{\mathbf{P}_{(n)}'^2}{m_n^2 c^2} \right)^{\frac{1}{2}} m_n c^2 + \sum_{n < n'} \sum \frac{e_n e_{n'}}{|\mathbf{x}_{(n)} - \mathbf{x}_{(n')}|}.$$

Because of the introduction of the gauge-invariant quantities, the Hamiltonian appears as the sum of terms that refer either exclusively to the particle variables or to the (transverse) electromagnetic field. There is no «interaction» term. The actual interaction between field and particles is brought about by the circumstance that the Dirac brackets (identical in this case with ordinary Poisson brackets) between these two kinds of observables do not all vanish. We have, in fact:

$$(7) \quad \{\pi_{(t)i}(\mathbf{x}), p'_{(n)j}\} = \frac{e_n}{c} \left[ \delta_{ij} \delta(\mathbf{x}, \mathbf{x}_{(n)}) + \frac{1}{4\pi} \left( \frac{1}{r_n} \right)_{,ij} \right], \quad r_n = |\mathbf{x}_n - \mathbf{x}|.$$

In the expression (6) we have also eliminated the self-energy terms (Coulomb energy of a particle with itself), which are infinite but  $c$ -numbers and, hence, without effect on the equations of motion of the system. It remains to be seen whether the expression (6) is Lorentz-invariant.

## 2. - Lorentz Invariance of the Formulation.

In a consistently Hamiltonian formulation a four-dimensional notation is feasible only with the introduction of «parameters»<sup>(3)</sup>, i.e. a super-many time formalism. Actually, Lorentz invariance does not depend on a four-

(3) P. G. BERGMANN and J. H. M. BRUNINGS: *Rev. Mod. Phys.*, **21**, 480 (1949).



dimensional notation, and particularly not in the present formulation, in which the quantities employed are not the components of four-vectors or four-tensors. In a Hamiltonian or quasi-Hamiltonian formulation of a theory it is much more appropriate to construct the generator of an infinitesimal Lorentz transformation (which is here a canonical or quasi-canonical transformation) and to show that the theory is invariant with respect to this transformation group. That means that the generator, or rather generators, must be constants of the motion. In view of the circumstance that these generators are physically interesting in themselves, representing the components of the total linear and angular momentum, the energy, and the motion of the center of mass of the whole system, this procedure of proof of Lorentz covariance is doubly advantageous.

We formulate the infinitesimal Lorentz transformation in terms of the coordinates of an arbitrary world point with the help of two constant vectors  $\theta$  and  $v$ ,

$$(8) \quad \delta x = \theta x - vt, \quad \delta t = -\frac{1}{c^2} v \cdot x.$$

The commutator of two such transformations (8), with different sets of values for the two vectors  $\theta$  and  $v$ , is a law of the same form. For the group character of the Lorentz transformations, it is necessary to retain both of these vectors, even though the vector  $\theta$  describes a purely spatial rotation of the coordinate system. On the other hand, the inhomogeneous terms are not necessary to obtain a Lie group. In what follows, we shall omit reference to  $\theta$ , as we need not make explicit use of the group character of the Lorentz transformation.

Without spatial rotation the infinitesimal transformation law for the coordinates of a particle, and for a fixed value of the time coordinate (not « at the same time »!) is

$$(9) \quad \delta x_n = -vt - \dot{x}_n \delta t = -vt + \frac{(v \cdot x_n)}{c^2} \dot{x}_n = \frac{(v \cdot x_n)}{m_n c^2} \frac{P'_n}{\sqrt{1 + (P_n'^2/m_n^2 c^2)}} - vt.$$

It follows immediately, that the generator of an infinitesimal Lorentz transformation,  $\mathcal{L}$ , must contain terms of the form

$$(10) \quad \mathcal{L} = \dots \frac{v \cdot x_n}{c} \sqrt{m_n^2 c^2 + P_n'^2} - (v \cdot p)t.$$

In addition, we must consider the transformation law for the electromagnetic variables. We have for the electromagnetic potentials the transformation laws:

$$(11) \quad \delta A = -\frac{v}{c} \varphi, \quad \delta \varphi = -\left(\frac{v \cdot A}{c}\right).$$

For a point with fixed space and time coordinates (not the same world point), we obtain

$$(12) \quad \left\{ \begin{aligned} \bar{\mathbf{B}} &= -\left(\frac{\mathbf{v}}{c} \cdot \mathbf{E}\right) + t(\mathbf{v} \cdot \nabla) \mathbf{B} - \left(\frac{\mathbf{v}}{c} \cdot \mathbf{x}\right) \text{curl } \mathbf{E}, \\ \bar{\boldsymbol{\pi}} &= -\frac{1}{4\pi c} \left(\frac{\mathbf{v}}{c} \cdot \mathbf{B}\right) + t(\mathbf{v} \cdot \nabla) \boldsymbol{\pi} - \frac{1}{4\pi c} \left(\frac{\mathbf{v}}{c} \cdot \mathbf{x}\right) \left(\text{curl } \mathbf{B} - \frac{4\pi}{c} \mathbf{j}\right), \\ \mathbf{j} &= \sum_n e_n \dot{\mathbf{x}}_n = \sum_n e_n \frac{\mathbf{P}'_n}{m_n \sqrt{1 + (\mathbf{P}'_n/m_n^2 c^2)}}. \end{aligned} \right.$$

From these individual transformation laws for the mechanical and the field quantities one can derive the complete form of the generator of an infinitesimal Lorentz transformation. It is:

$$(13) \quad \mathcal{L} = \mathbf{v} \cdot \left\{ \int \left[ \frac{\mathbf{x}}{c^2} \left( \frac{1}{8\pi} \mathbf{B}^2 + 2\pi c^2 \boldsymbol{\pi}^2 \right) - t(\mathbf{B} \boldsymbol{\pi}) \right] d^3x + \right. \\ \left. + \sum_n \left( \frac{\mathbf{x}_n}{c} \sqrt{m_n^2 c^2 + \mathbf{P}'_n{}^2} - t \mathbf{p}'_n \right) \right\}.$$

This generator is gauge-invariant. It furnishes correctly the transformation laws of any gauge-invariant quantity, but not that of other variables, such as electromagnetic potentials. Actually, the law (11), for instance, is not unique. It is based on a convention as to what is meant by « the same gauge frame » in two different Lorentz frames. If we wish to produce a generator that yields also Eqs. (11), then we must add to the expression (13) terms which contain the constraints (1) as factors and which, therefore, vanish.

The generator (13) is gauge-invariant, but it does not as yet contain only true observables. In order to accomplish this purpose we must separate the vector field  $\boldsymbol{\pi}$  into its longitudinal and its transverse parts. If we do so, we obtain the new expression:

$$(14) \quad \mathcal{L} = \mathbf{v} \cdot \left\{ \int \left[ \frac{\mathbf{x}}{c^2} \left( \frac{1}{8\pi} \mathbf{B}^2 + 2\pi c^2 \boldsymbol{\pi}_t^2 \right) + t(\boldsymbol{\pi}, \mathbf{B}) \right] d^3x + \right. \\ \left. + \sum_n \left( \frac{\mathbf{x}_n}{c} \sqrt{m_n^2 c^2 + \mathbf{P}'_n{}^2} - t \mathbf{p}'_n \right) + \int U \left( \frac{2\pi}{c} \mathbf{x} \sigma - 4\pi \boldsymbol{\pi}_t - t \text{curl } \mathbf{B} \right) d^3x, \right. \\ \left. U = \frac{1}{4\pi c} \sum_n \frac{e_n}{r_n}, \quad \sigma = \sum_n e_n \delta(\mathbf{x}, \mathbf{x}_n) \right\}.$$

In this expression there is one obviously indefinite term:  $\int U(2\pi/c) \mathbf{x} \sigma d^3x$ . Unlike in the expression for the Hamiltonian, Eq. (6), the « self-energy » term here



is multiplied by the coordinate of the charge and will, therefore, make an (infinite) contribution to the Lorentz transformation. The reason is the following: If a charge is at rest, then its electric field strength has precisely the Coulomb type of infinity, which may be subtracted off simply by separating the transverse from the longitudinal electric field (the magnetic field is purely transverse to begin with). But when the point charge is in motion, then even the transverse electric field, as well as the magnetic field, possess singularities, which depend on the velocity of the point charge. Hence a Lorentz transformation changes the transverse fields by an amount which is infinite at the location of each point charge. Accordingly the generator must have a similarly infinite term of its own. It is conceivable that this singularity may be avoided if the total field is not simply separated into longitudinal and transverse part but in such a manner that the quasi-longitudinal part (which will now also have a magnetic component) subtracts off exactly the singularity of each point charge. The quasi-transverse part would still have a vanishing divergence, and the quasi-longitudinal part would be determined completely by the particle coordinates and kinetic momenta. This possibility has not yet been decided.

As for the Lorentz invariance of the Hamiltonian (6), it is sufficient to show that the functional (13) is a constant of the motion under the laws of motion determined by the Hamiltonian (6). This calculation is somewhat lengthy and will not be reproduced here; the result is, however, satisfactory.

### 3. - Dirac Electron Theory.

A more realistic version of quantum electrodynamics starts out not with point charges, but with expressions for current and charge densities that are furnished by the Dirac theory for a single electron. Field quantization of the particle wave functions as well as the electromagnetic field quantities then leads to the situation involving many electrons and the creation and annihilation of pairs.

From the point of view of a « true observables » formalism, the wave functions of charged particles are not gauge-invariant. Hence it becomes necessary to search for combinations that are. A complete theory has not yet been carried out. But instead of the creation and annihilation operators, we must introduce gauge-invariant « transition operators », which may be defined as follows:

$$(15) \quad \varrho(\mathbf{x}_2, \mathbf{x}_1) = \psi^*(\mathbf{x}_2) \exp \left[ \frac{ie}{\hbar c} \int_{\mathbf{x}_1}^{\mathbf{x}_2} (\mathbf{A} \cdot d\mathbf{l}) \right] \psi(\mathbf{x}_1).$$

They depend not only on the two end points but also on the path of integration that connects the two points  $x_1$  and  $x_2$ . However, the ratio between two transition operators with the same end points but different connecting points is a purely electromagnetic and gauge-invariant quantity; it is an exponential function of the magnetic flux through the surface bounded by the two paths of integration. Naturally, the transition operator has two spinor indices, of which one transforms contragrediently to the other. If we interchange the two end points of a transition operator as well as its two spinor indices with the same path of integration, then we obtain the hermitian conjugate of the original operator.

Regardless of whether the transition operator field  $\varrho(x_1, x_2)$  is to describe a Boson or a Fermion field, it always satisfies the same commutation (never anticommutation) relations. These are:

$$(16) \quad [\varrho(x_2, x_1), \varrho(x_4, x_3)] = \delta(x_1, x_4) \varrho(x_2, x_3) - \delta(x_2, x_3) \varrho(x_4, x_1).$$

When we have to deal with a Fermion field, we have, however, the following additional relationship:

$$(17) \quad \varrho(x_2, x_1) \varrho(x_2, x_3) = \delta(x_1, x_2) \varrho(x_2, x_3),$$

as well as its Hermitian conjugate,

$$(18) \quad \varrho(x_2, x_1) \varrho(x_1, x_1) = \delta(x_1, x_1) \varrho(x_2, x_1).$$

It is not clear at present whether the relationships (17), (18) are sufficient to characterize a Fermion field completely. It is possible to set up an algebraic relationship that differentiates between Fermion and Boson fields, of which the relationships (17), (18) are special cases. Provided we normalize the path of integration so that it leads from one end point uniquely to some fixed reference point (say the origin of the coordinate system) and thence to the other end point, these relationships are:

$$\begin{aligned} (19) \quad \varrho(x_1, x_2) \varrho(x_3, x_4) - \delta(x_2, x_3) \varrho(x_1, x_4) &= \\ &= \pm [\varrho(x_3, x_2) \varrho(x_1, x_4) - \delta(x_1, x_2) \varrho(x_3, x_4)] = \\ &= \pm [\varrho(x_1, x_4) \varrho(x_3, x_2) - \delta(x_3, x_4) \varrho(x_1, x_2)]. \end{aligned}$$

The plus sign applies to Bosons, the minus sign to Fermions.

With the help of the electromagnetic field variables and the transition operators, the Hamiltonian of the electron-photon system can be formulated. This system of observables is closed insofar as the time derivative of each (in Heisenberg representation) is a function of these variables only.



## RIASSUNTO (\*)

In connessione col lavoro che stiamo svolgendo sulla quantizzazione della relatività generale, abbiamo investigato le equazioni della elettrodinamica quantistica col gruppo di gauge non ristretto, vale a dire senza specializzarsi al gauge di Lorentz e di Coulomb. Noi formuliamo la teoria, anche prima della quantizzazione, in termini solo di « vere osservabili ». Queste ultime sono definite come variabili dinamiche che generano trasformazioni canoniche che trasformano uno « stato permesso » in un altro, intendendosi per « stato permesso » un insieme di valori di tutte le variabili canoniche che rispettano i vincoli di gauge. Similmente, nella teoria quantizzata, un'osservabile dev'essere un operatore hermitiano nello spazio hilbertiano degli stati permessi. La transizione alle vere osservabili non solo elimina dalla teoria il potenziale scalare e le parti longitudinali del potenziale vettore, ma anche le componenti longitudinali del campo elettrico. Ovviamente, gli operatori che creano e distruggono particelle cariche non sono di per sè osservabili, ma se ne possono costruire combinazioni (in forma di prodotti) che lo sono. Tali prodotti (gauge-invarianti) involgono il prodotto di un creatore per un distruttore in punti differenti dello spazio, moltiplicati per un funzionale che dipende da un integrale di linea del potenziale vettore e calcolato su una qualsiasi curva che connette i due punti suddetti. Ne segue che l'hamiltoniana può essere espressa in termini soltanto di dette variabili e che la selfenergia infinita causata dai fotoni non trasversali è automaticamente eliminata.

---

(\*) *A cura della Redazione.*

## Vanishing of the Renormalized Charge in Electrodynamics and in Meson Theory.

I. POMERANČUK

*Academy of Sciences of the URSS - Moscow*

(ricevuto il 24 Novembre 1955)

**Summary.** (\*). — The author discusses the solutions of the quantum electrodynamics equations for the particles with spin  $\frac{1}{2}$  obtained by various authors firstly with one «smearing out» parameter and subsequently with two parameters. He proves in Sect. 1 that the solutions obtained are correct for all values of the non-renormalized electric charge  $e_1$  ( $e_1 \ll 1$  as well as  $e_1 \gg 1$ ), and that both theories lead to the conclusion that the renormalized charge  $e$  turns out to be zero. In Sect. 2 the author investigates if the same property holds also for the meson charge  $g$  in the pseudo-scalar theory. Using the two-limits technique developed by ABRIKOSOV and HALATNIKOV, he comes to the conclusion that also  $g$  turns out to be zero. In Sect. 3 the author considers in detail the problem of the vanishing of the renormalized meson charge examining the properties of the functions  $G$ ,  $D$  and  $\Gamma$  at arbitrary  $g_1^2$ . The result of this analysis corresponds to the preceding conclusions, and confirms the vanishing of  $g$ .

(\*) *Editor's care.*

### 1. — Vanishing of the Renormalized Charge in Quantum Electrodynamics.

In the paper recently published by LANDAU, ABRIKOSOV and HALATNIKOV <sup>(1)</sup> the solution was found of the quantum electrodynamics equations which determine the Green's functions of the electron  $G$ , of the photon  $D_{\mu\nu}$ , and the vertex part  $\Gamma_\mu$ , corresponding to their electromagnetic interaction. These equations contain the non-renormalized charge  $e_1$  which is a function of the (fictitious) smearing radius  $1/\Lambda$  of the particles. This smearing out, at  $\Lambda \rightarrow \infty$ ,

<sup>(1)</sup> L. D. LANDAU, A. A. ABRIKOSOV and I. M. HALATNIKOV: *Dokl. Akad. Nauk SSSR*, 95, 497, 773, 1177 (1954).



corresponds to the point interaction as a limit of the smeared out one, in the case when the radius of this interaction becomes zero.  $e_1$  grows <sup>(2)</sup> as  $\Lambda$  increases, owing to the vacuum polarization ability to decrease any external charge placed in the vacuum (the dependence of  $e_1$  on  $1/\Lambda$  reflects, roughly speaking, that of the effective electron charge on the distance from its centre). The solutions of the equations of quantum electrodynamics found in <sup>(1)</sup> may be used, according to the evaluations performed in <sup>(1)</sup>, only when  $e_1^2 \ll 1$ . This limitation prevents the study of the properties of quantum electrodynamics at  $\Lambda \rightarrow \infty$  because, at  $\Lambda \rightarrow \infty$ ,  $e_1$  seems likely to become infinite. The above mentioned authors used a very simple «spreading» with one parameter  $1/\Lambda$  in the coordinate space (or  $\Lambda$  in a momentum space). A more general case of smearing out was studied by ABRIKOSOV and HALATNIKOV <sup>(3)</sup> who have introduced the point interaction  $e_1 \bar{\psi}(x) \gamma_\mu \psi(x) A_\mu(x)$  as the limit for the smeared out one:

$$(1.1) \quad e_1 \int F\left(\frac{x-y}{\Lambda_p^{-1}}, \frac{x-z}{\Lambda_k^{-1}}, \frac{y-z}{\Lambda_k^{-1}}\right) \bar{\psi}(x) \gamma_\mu \psi(y) A_\mu(z) dy dz,$$

where the «breadth» of the distribution differs in the cases of  $y$  and  $z$ . They have proved, that the radius of smearing out for  $\Lambda$  (over  $z$ ) always exceeds  $1/\Lambda_p$  (that over  $y$ ), along which  $\psi(y)$  is shifted with respect to  $\psi(x)$ :

$$(1.2) \quad \frac{1}{\Lambda_k} \geq \frac{1}{\Lambda_p}.$$

Using the two-limits smearing out, ABRIKOSOV and HALATNIKOV have obtained the solution of the equations quantum electrodynamics. After renormalization their results coincided with <sup>(1)</sup>, as the renormalized quantities have no parameters of smearing out. The solutions obtained in <sup>(3)</sup> (when  $d_r = 0$  <sup>(1)</sup>) are

$$(1.3) \quad \begin{cases} D_{\mu\nu}(k^2) = \frac{1}{k^2} \frac{\delta_{\mu\nu} - (k_\mu k_\nu / k^2)}{1 + (\nu e_1^2 / 3\pi) \ln(\Lambda_p^2 / k^2)}, & G(p) = \hat{p} - 1, \\ \Gamma_\mu = \gamma_\mu, & p^2 \gg m^2; \quad \Lambda_k^2 \gg k^2 \gg m^2. \end{cases}$$

If  $k^2 > \Lambda_k^2$ , then  $D_{\mu\nu} = \frac{1}{k^2} \left( \delta_{\mu\nu} - \frac{k_\mu k_\nu}{k^2} \right)$ ,  $\Gamma = 0$ .

The connection between the renormalized charge  $e$  and  $e_1$  obtained in <sup>(3)</sup> may

<sup>(2)</sup> B. KÄLLÉN: *Helv. Phys. Acta*, **25**, 417 (1952); H. LEHMANN: *Nuovo Cimento*, **11**, 342 (1954).

<sup>(3)</sup> A. A. ABRIKOSOV and I. M. HALATNIKOV: *Dokl. Akad. Nauk SSSR*, **103**, 993 (1955).

be formulated as

$$(1.4) \quad e^2 = \frac{e_1^2}{1 + (\nu/3\pi)e_1^2 \ln A_p^2 m^{-2}},$$

with  $k^2 = A_k^2$  the  $D$ -function changes discontinuously from the value  $A_k^{-2}[1 + (\nu/3\pi)e_1^2 \ln A_p^2 A_k^{-2}]^{-1}$  up to  $A_k^{-2}$ . In the case of high values of  $(\nu/3\pi)e_1^2 \ln A_p^2 A_k^{-2}$  the  $D$ -function may undergo a large jump. We shall prove below that the « abruptness » of switching off the interaction and the resulting discontinuities of the  $D$ -function are not essential at all. The « cutting off » factor may assume any possible form meeting the demand of the gauge invariance (the transverse polarization current). Such a factor is introduced by substituting  $\gamma_\mu \Phi[p^2 A_p^{-2}, (p-k)^2 A_p^{-2}, k^2 A_k^{-2}]$  instead of  $\gamma_\mu$ . The  $\Phi$ -function, without restricting the necessary generality, may be considered equal to the product of the two functions:

$$(1.5) \quad \left\{ \begin{array}{l} \Phi = f\left(\frac{k^2}{A_p^2}\right) g\left(\frac{p^2}{A_p^2}, \frac{(p-k)^2}{A_p^2}\right) \\ f \rightarrow 0, \quad k^2 > A_k^2; \quad f \rightarrow 1, \quad k^2 < A_k^2, \\ g(x, y) \rightarrow 0, \quad x > 1, \quad y > 1; \quad g(x, y) \rightarrow 1, \quad x < 1, \quad y < 1. \end{array} \right.$$

The  $\Phi$ -function being taken into account, the  $D$ -function and  $\Gamma_\mu$  assume the following form

$$(1.6) \quad \left\{ \begin{array}{l} D_{\mu\nu}(k^2) = k^{-2} \left( \delta_{\mu\nu} - \frac{k_\mu k_\nu}{k^2} \right) \left\{ 1 + \frac{\nu e_1^2}{3\pi} f^2 \left( \frac{k^2}{A_p^2} \right) \ln A_p^2 k^{-2} \right\}^{-1}, \\ \Gamma_\mu(p, p-k; k) = \gamma_\mu \Phi[p^2 A_p^{-2}, (p-k)^2 A_p^{-2}; k^2 A_k^{-2}]. \end{array} \right.$$

(If  $A_p = A_k = A$ , the formulae (1.3), (1.6) become those obtained in <sup>(1)</sup>). We shall consider now the case when  $A_p$  and  $A_k$  satisfy the inequality (\*)

$$(1.7) \quad \ln A_p^2 A_k^{-2} \gg 1, \quad \begin{array}{l} A_p^2 \rightarrow \infty \\ A_k^2 \rightarrow \infty \end{array}.$$

Using this inequality one may prove that formulae (1.3), (1.6) are correct for all values of  $e_1^2$ , low as well as high.

To prove this assertion, we shall consider those terms of the equations determining  $G$ ,  $D$ ,  $\Gamma$  which were treated as small by LANDAU, ABRIKOSOV and HALATNIKOV.

(\*) L. D. LANDAU pointed out the importance of this inequality.



The Dyson-Schwinger equations used in <sup>(1)</sup>, which determine  $G$  and  $D$  are exact. In contradistinction to this,  $\Gamma$  was determined from the approximated «triangular» equation which (in the symbolic form) is

$$(1.8) \quad \Gamma_\mu = \gamma_\mu + \text{triangle diagram} + \dots$$

Graphs which were not taken into account in <sup>(1)</sup> are separated by the vertical line.

All overlapping diagrams and effects connected with the scattering of light by light are not taken into consideration in <sup>(1)</sup>. Let us consider an arbitrary  $n$ -time-overlapping graph, providing the contribution to  $\Gamma$ :

$$(1.9) \quad \Gamma_n = e_1^{2n} \text{triangle diagram with } n \text{ internal lines}$$

There are  $2n$   $G$ -functions,  $n$   $D$ -functions,  $2n$   $\Gamma$ -functions. This graph contains  $n$  4-time integrals over  $\bar{k}_1 \dots \bar{k}_n$ . As is known, all integrations except one do not yield logarithmic divergencies <sup>(+)</sup>. Therefore, we have only single integration in the logarithmic scale. Let the momenta  $p$ ,  $p-k$ ,  $k$  be of the same order and satisfy the inequality:

$$(1.10) \quad p^2 \ll A_k^2, \quad p^2 \sim (p-k)^2 \sim k^2.$$

(In parallel to <sup>(1)</sup>, we may consider all these momenta as space-like). Substituting  $\Gamma_\mu$ ,  $G$  and  $D$  by their values (1.6) in the integral, we shall obtain:

$$(1.11) \quad \Gamma_n \sim e_1^{2n} \int_{p^2} f^{2n} \left( \frac{q^2}{A_k^2} \right) \frac{dq^2}{q^2} \left\{ 1 + \frac{\nu e_1^2}{3\pi} f^2 \left( \frac{q^2}{A_k^2} \right) \ln \frac{A_p^2}{q^2} \right\}^{-n}.$$

It should be pointed out that the upper limit is determined by  $A_k^2$  but not by  $A_p^2$  ( $A_p^2$  appears only in integration over  $p$ ).

Now let us use the condition:

$$(1.11bis) \quad \frac{e_1^2 \nu}{3\pi} \ln \frac{A_p^2}{q^2} \gg 1,$$

resulting from (1.7) in case we are interested in  $e_1^2 \gg 1$ . (1.11bis) leads to the

(+) We assume (here and further on) that  $d_e = 0$  <sup>(1)</sup>.

dropping of  $f$  from equation (1.11), but the integration over  $q^2$  is limited by the condition  $q^2 < A_k^2$ . As the inequality (1.7) ensures a slow (logarithmic) dependence of all functions on  $q^2$ , the substitution of the upper limit of integration for  $A_k^2$  does not cause serious errors. The  $f$ -function falling out (as well as that of  $g$ ) from the other graphs is analogous to that given in the above mentioned example (\*). The independence of the results on the form of  $f$  provides the possibility of an arbitrary type of cutting off. The results obtained do not depend on the form of this cutting off. For the sake of brevity we shall not write the  $f$ -functions explicitly, but we shall introduce a sharp cutting off in the integrals

$$(1.12) \quad \Gamma_n = C_{n-1} \left[ e_1^2 \left\{ 1 - \frac{\nu e_1^2}{3\pi} \ln \frac{A_p^2}{q^2} \right\}^{-1} \right]_{p^2}^{A_k^2} = \\ = C_{n-1} \left\{ e_1^2 \left[ 1 + \frac{\nu e_1^2}{3\pi} \ln A_p^2 A_k^{-2} \right]^{-1} \right\}^{n-1} C_{n-1} \left\{ e_1^2 \left[ 1 + \frac{\nu e_1^2}{3\pi} \ln A_p^2 p^{-2} \right]^{-1} \right\}^{n-1}.$$

$C_{n-1}$  is a numerical factor.

As  $p^2 \ll A_k^2$ , the second member in (1.12) is smaller than the first one and accordingly the order of magnitude  $\Gamma_n$  is equal to

$$(1.13) \quad \Gamma_n \lesssim C_{n-1} \left\{ e_1^2 \left[ 1 + \frac{\nu e_1^2}{3\pi} \ln A_p^2 A_k^{-2} \right]^{-1} \right\}^{n-1}.$$

In the case of very small values of  $e_1^2$ , (1.13) transforms into:

$$(1.14) \quad \Gamma_n \sim C_{n-1} e_1^{2(n-1)},$$

which may lead to the conclusion that for  $e_1^2 \gtrsim 1$  the contribution of the overlapping diagrams may become large. But, if  $(\nu e_1^2/3\pi) \ln A_p^2 A_k^{-2} \gg 1$  (if  $e_1^2 > 1$  this is attained already at not very high values of  $A_p^2 A_k^{-2}$ ) then equation (1.13) gives the following expression, instead of equation (1.14):

$$(1.15) \quad \Gamma_n \sim \frac{C_{n-1}}{[\ln A_p^2 A_k^{-2}]^{n-1}} \ll 1.$$

If, instead of the condition (1.10), the vectors  $p$ ,  $p-k$ , and  $k$  satisfy the inequality

$$(1.16) \quad k^2 \ll A_k^2 \ll p^2 \approx (p-k)^2 \ll A_p^2,$$

then we shall obtain a value of the overlapping graphs lower than in the

(\*) The remark that the  $f$ -function drops away was made by L. D. LANDAU.

case of (1.15). In fact, here the full lines in (1.9) should be substituted for  $\hat{p}^{-1}$  (all  $k$  are small as compared to  $p$ ). Only « dotted » factors will depend on  $k$ , each of them being equal to

$$k^{-2} \left[ 1 + \frac{ve_1^2}{3\pi} \ln A_p^2 k^{-2} \right]^{-1} \left( \delta_{\mu\nu} - \frac{k_\mu k_\nu}{k^2} \right).$$

Taking into account that there are  $2n$  full lines, we obtain the following value of  $\Gamma_n$ , when (1.16) is satisfied:

$$(1.17) \quad \Gamma_n \sim \frac{e_1^{2n}}{p^{2n}} \int d\bar{k}_1 \dots d\bar{k}_n \prod_{\alpha=1}^n k_\alpha^{-2} \left[ 1 + \frac{ve_1^2}{3\pi} \ln \frac{A_p^2}{k_\alpha^2} \right]^{-1} \sim \\ \sim \frac{A_k^{2n}}{p^{2n}} \left\{ e_1^2 \left[ 1 + \frac{ve_1^2}{3\pi} \ln \frac{A_p^2}{A_k^2} \right]^{-1} \right\}^n \lesssim \frac{A_k^{2n}}{p^{2n}} \left[ \ln \frac{A_p^2}{A_k^2} \right]^{-n} \ll 1.$$

Thus the contribution of all the overlapping graphs in  $\Gamma$  is

$$\sum_1^\infty C_n \left\{ e_1^2 \left[ 1 + \frac{ve_1^2}{3\pi} \ln \frac{A_p^2}{A_k^2} \right]^{-1} \right\}^n.$$

It is always small, irrespective of the value of  $e_1^2$ . Though this series seems to be asymptotic <sup>(4)</sup>, nevertheless the value to which this series corresponds is approximated by the first members of the series when these terms decrease rapidly with increasing  $n$ . As it was shown in <sup>(1)</sup>, if the potentials are gauged according to the condition  $d_\perp = 0$ , the contribution of the non overlapping diagrams into  $\Gamma_\mu$

$$(1.18) \quad \begin{array}{c} \text{---} k \text{---} \\ \diagup \quad \diagdown \\ p \quad \text{---} \quad p-k \end{array}$$

turns out to be small, if  $e_1^2 \ll 1$ .

As this operator does not contain logarithmic divergencies, its value has the following order of magnitude:

$$(1.19) \quad \frac{e_1^2}{1 + (ve_1^2/3\pi) \ln (A_p^2/k^2)} < \frac{1}{\ln (A_p^2/k^2)} < \frac{1}{\ln A_p^2 A_k^{-2}} \ll 1,$$

if  $p^2 \sim k^2 \sim (p-k)^2$ . If the inequality  $p^2 \gg A_k^2$  ( $k^2 \ll A_k^2$ ) holds, instead of

<sup>(4)</sup> F. J. DYSON: *Phys. Rev.*, **85**, 631 (1952); W. THIRRING: *Helv. Phys. Acta*, **26**, 33 (1953); C. A. HURST: *Proc. Camb. Phys. Soc.*, **48**, 625 (1952); A. PETERMAN: *Helv. Phys. Acta*, **26**, 291 (1953); R. URYIYAMA and T. IMAMURA: *Prog. Theor. Phys.*, **9**, 431 (1953).



(1.19) we obtain for the operator (1.18) the value

$$(1.20) \quad \sim \frac{e_1^2 A_k^2}{P^2} \left[ 1 + \frac{\nu e_1^2}{3\pi} \ln \frac{A_p^2}{A_k^2} \right]^{-1} \lesssim \frac{A_k^2}{p^2 \ln A_p^2 A_k^{-2}} \ll 1.$$

Up to now we considered the cases when  $p^2 \sim (p-k)^2 \sim k^2$ , or  $p^2 \gg A_k^2 \gg k^2$ . One may easily see that even for the case of the inequality  $A_k^2 \gg p^2 \gg k^2$  the above given values hold for all overlapping operators entering  $\Gamma$ , as well as for (1.18).

We see that all overlapping operators and (1.18) yield a small contribution to  $\Gamma$  at any value of  $e_1^2$ . Let us consider now the effects in  $\Gamma$ , caused by the scattering of light by light. Here the simplest diagram appears as:

$$(1.21) \quad \begin{array}{c} \text{Diagram: A triangle with vertices labeled } k_1, k_2, \text{ and } k_1+k_2-k. \text{ The top vertex is labeled } k. \text{ The bottom-left vertex is labeled } p. \text{ The bottom-right vertex is labeled } p-k. \end{array}$$

We should remember, when evaluating the value of (1.21), that the elementary graph giving the scattering of light by light converges and equals  $e_1^4$ . That is why, under the condition:  $p^2 \sim (p-k)^2 \sim k^2 \ll A_k^2$ , the integral (1.21) in the logarithmic scale is reduced to a single integration ( $k_1^2 \sim k_2^2 \sim (k_1+k_2)^2 \gg k^2$ ) and has the value

$$(1.22) \quad \sim e_1^6 \int_{k^2}^{A_k^2} \frac{dk_1^2}{k_1^2} \left[ 1 + \frac{\nu e_1^2}{3\pi} \ln \frac{A_p^2}{k_1^2} \right]^{-3} \sim \left( 1 + \frac{\nu e_1^2}{3\pi} \ln \frac{A_p^2}{A_k^2} \right)^{-2} e_1^4 < \left[ \ln \frac{A_p^2}{A_k^2} \right]^{-2} \ll 1.$$

In case of an arbitrary graph containing the scattering of light by light one should compare two graphs (\*)

$$(1.23) \quad \begin{array}{c} \text{Diagram: Two boxes labeled } A \text{ and } B \text{ connected by a dashed line. The top line is labeled } k_1. \end{array}$$

$$(1.24) \quad \begin{array}{c} \text{Diagram: Two boxes labeled } A \text{ and } B \text{ connected by a dashed line. The top line is labeled } k_3. \text{ The bottom line is labeled } k_1+k_2-k_3. \end{array}$$

If  $A$  within the logarithmic precision considered here, does not depend on

(\*)  $A$  and  $B$  may be connected with each other by other lines as well. Essential is the fact that (1.24) differs from (1.23) only by a square.

$k_3$ , then the transition from (1.23) to (1.24) leads to the following factor:

$$(1.25) \quad e_1^4 \int_{A_k^2} \frac{d\bar{k}_3}{k_3^2 (k_1 + k_2 - k_3)^2} \left[ 1 + \frac{ve_1^2}{3\pi} \ln \frac{A_p^2}{k_3^2} \right]^{-1} \left[ 1 + \frac{ve_1^2}{3\pi} \ln \frac{A_p^2}{(k_1 + k_2 - k_3)^2} \right]^{-1} \sim \\ \sim e_1^4 \int_{A_k^2} \frac{d\bar{k}_3}{k_3^4} \left[ 1 + \frac{ve_1^2}{3\pi} \ln \frac{A_p^2}{k_3^2} \right]^{-2} \sim e_1^2 \left[ 1 + \frac{ve_1^2}{3\pi} \ln \frac{A_p^2}{A_k^2} \right]^{-1} \lesssim \ln A_p^2 / A_k^2 \ll 1.$$

The independence of  $A$  of  $k_3$  may be realized, for instance, in the following case:

$$\begin{array}{c} \text{---} k_3 \text{---} \\ \boxed{A} \\ \text{---} k_1 + k_2 - k_3 \text{---} \end{array} = \begin{array}{c} \text{---} q \text{---} \\ \boxed{C} \quad \boxed{\phantom{C}} \\ \text{---} k_1 + k - q \text{---} \quad \text{---} k_3 \text{---} \\ \text{---} k_1 + k_2 - k_3 \text{---} \end{array}$$

(the square does not depend on the momenta of the colliding photons if  $k^2 \gg m^2$ ). If, on the contrary,  $A$  does depend on  $k_3$ , then  $A$  decreases as  $k_3$  increases. We may represent roughly this case as follows

$$(1.26) \quad \begin{array}{c} \text{---} k_3 \text{---} \\ \boxed{A} \\ \text{---} k_1 + k_2 - k_3 \text{---} \end{array} = \begin{array}{c} \text{---} 4 \text{---} k_2 \text{---} \\ \boxed{1} \quad \boxed{2} \quad \boxed{3} \\ \text{---} k_1 + k_2 - k_3 \text{---} \end{array}$$

The dependence of the line (2, 3) on  $k_3$  leads to an extra factor  $(\hat{p} - \hat{k}_1 - \hat{k}_2 + \hat{k}_3)^{-1}$ , which ensures the convergence of the integral over  $k_3$ , contrary to the logarithmic divergency of the equation (1.25). Correspondingly going over from equation (1.23) to equation (1.24), if  $A$  depends on  $k_3$ , we obtain a factor, which is even smaller than that appearing in the equation (1.25). Thus the introduction of any graph expressing the light-by-light scattering leads to the series of the same small parameter  $[\ln A_p^2 / A_k^2]^{-1}$ , as in the case of overlapping graphs.

Thus all deviations of  $\Gamma_\mu$  from  $\gamma_\mu$  are small, irrespective of the value of  $e_1^2$ . Due to the logarithmic situation (that means, all essential quantities are slowly changing logarithmic functions), it results from Ward's theorem that with  $\Gamma_\mu = \gamma_\mu$  the Green's function  $G$  of an electron should equal  $\hat{p}^{-1}$ . This may be directly proved by performing calculations of any graph entering the mass operator determining  $G$ .

With  $\Gamma_\mu = \gamma_\mu$  and  $G = \hat{p}^{-1}$ , the  $D$ -function is uniquely determined from the Schwinger-Dyson equation of the type (1.3). The results obtained above prove the possibility of applying equation (1.3) to any  $A_p$  and  $A_k$  satisfying the condition (1.7). This circumstance leads to the following fundamental conclusion: the renormalized charge  $e$  turns out to be zero, in accordance with (1.1):

$$(1.27) \quad e^2 = e_1^2 \left[ 1 + \frac{ve_1^2}{3\pi} \ln \frac{A_p^2}{m^2} \right]^{-1} \rightarrow \frac{3\pi}{v} \frac{1}{\ln A_p^2 / m^2} \rightarrow 0. \quad A_p^2 \rightarrow \infty$$



The physical arguments leading to the vanishing of the charge were given in the paper by L. D. LANDAU and I. Ja. POMERANČUK <sup>(5)</sup> (\*). They were based upon the fact that already at  $e_1^2 \ll 1$  the influence of the action of the free electromagnetic field, according to the equation (1.3), turns out to be quite small. This circumstance makes very probable that the effects of the free field drop out for  $e_1^2 \gg 1$  as well. Then it became possible to draw the conclusion that  $e^2 = 0$ . It should be noted that the use of the two-limits procedure has considerably simplified the analysis of the quantum electrodynamics equations as compared with the analogous situation in the case when one limit is used. In this respect, it should be noted that the condition (1.7) ensures the logarithmic dependence of all functions even for large  $e_1^2$ . This simplifies to a great extent the evaluation of all integrals. If we turn to the one-limit theory, it is likely that we shall see, as a result of a thoroughful consideration, that here the situation quite resembles that of the two-limits theory when both limits are of the same order. Here the contribution of overlapping graphs (and of the effects of light-by-light scattering) does no longer depend on  $e_1^2$  when  $e_1^2$  exceeds unity. That means that the situation with high  $e_1^2$  is equal to that with  $e_1^2 \sim 1$ . As in the case of  $e_1^2 \sim 1$  equations (1.3) hold in order of magnitude, therefore they hold for all values of  $e_1^2$ . Thus, the one-limit theory gives  $e^2 = 0$  as well, but in the last case the whole analysis becomes quite transparent.

The vanishing of  $e$  results from the fact that the naked charge  $e_1$  is surrounded by a cloud of opposite charges under the influence of intensive vacuum polarization; as a result of this process the total charge of the system ( $e_1 +$  polarized charges), at a distance from the centre of the charge hardly exceeding the size of the naked charge  $1/\lambda$ , turns out to be of the order of unity irrespective of how large the  $e_1$  charge would be. The domain of strong interaction does not exist. On the other hand, in the domain of weak interaction  $e$  turns out to be zero, according to (1), with  $\lambda \rightarrow \infty$ .

## 2. — Renormalisation of the Meson Charge in Pseudoscalar Theory with Pseudoscalar Coupling.

In Sect. 1 the result was obtained that the quantum electrodynamics of the particles with spin  $\frac{1}{2}$  leads to the vanishing of the renormalized electron charge. Whether this effect is the property of any point interaction is an important problem. The case of the meson-nucleon interaction is the most essential question. This paper considers the renormalization of the meson charge in the pseudoscalar theory with the pseudoscalar coupling. The considera-

(5) L. D. LANDAU and I. Ja. POMERANČUK: *Dokl. Akad. Nauk SSSR*, **102**, 489 (1955).

(\*) The idea of the vanishing of the charge was also suggested by E. S. FRADKIN.

ion of the problem, as in electrodynamics, is simplified if we use, in the solution of the non-renormalized Schwinger-Dyson equations, the two-limits technique developed by ABRIKOSOV and HALATNIKOV<sup>(3)</sup>. The results obtained by them were deduced in the assumption that the non-renormalized meson charge is small, as compared with unity. This made applicable for the determination of the vertex part  $\Gamma(p, p-k; k)$  the « triangular » equation which takes into consideration only the non-overlapping diagrams<sup>(1)</sup>:

$$(2.1) \quad \Gamma = \gamma_5 + \begin{array}{c} \text{---} \text{---} \text{---} \\ \text{---} \text{---} \text{---} \\ \text{---} \text{---} \text{---} \end{array}$$

The cutting off limits for the nucleon and meson momenta  $\Lambda_p$  and  $\Lambda_k$  satisfy the condition  $\Lambda_p \geq \Lambda_k$ . The Green's functions  $G$  for the nucleon, and  $D$  for the meson, and the vertex part  $\Gamma$  obtained in (3) have the form

$$(2.2) \quad \left\{ \begin{array}{l} G = \hat{p}^{-1} Q(p)^{-3/10}; \quad D = k^{-2} Q(k)^{-4} \left[ 1 + \frac{g_1^2}{\pi} (L_p - L_k) \right]^{-1}; \\ \Gamma = \gamma_5 Q^{1/2}; \quad Q(x) = 1 + \frac{5}{4\pi} g_1^2 (L_k - \ln x^2 m^{-2}) \left[ 1 + \frac{g_1^2}{\pi} (L_p - L_k) \right]^{-1}, \\ L_p = \ln \Lambda_p^2 m^{-2}; \quad x = k \text{ in } D; \\ L_k = \ln \Lambda_k^2 m^{-2}; \quad x = p \text{ in } G. \end{array} \right.$$

In  $\Gamma(p, p-k; k)$   $x^2$  coincides with the largest of the quantities  $p^2$ ,  $(p-k)^2$ ,  $x^2$ , within the logarithmic precision;  $m$  is the nucleon mass. Formulae (2.2) are applicable if

$$(2.3) \quad \left\{ \begin{array}{l} \text{for } G: \quad \Lambda_k^2 \gg p^2 \gg m^2; \\ \text{for } D: \quad \Lambda_k^2 \gg k^2 \gg m^2; \\ \text{for } \Gamma: \quad \Lambda_k^2 \gg p^2, (p-k)^2, k^2 \gg m^2. \end{array} \right.$$

If  $p^2$  or  $k^2$  become smaller than  $m^2$ , then zero should be substituted for the  $\ln x^2 m^{-2}$ . When the above mentioned inequalities are changed to

$$(2.4) \quad \Lambda_p^2 \gg p^2 \gg \Lambda_k^2, \quad k^2 \ll \Lambda_k^2,$$

then the following formulae appear instead of (2.2):

$$(2.5) \quad G = \hat{p}^{-1}, \quad \Gamma = \gamma_5.$$

If  $p^2 > \Lambda_p^2$ , or  $k^2 > \Lambda_k^2$ , then  $\Gamma = 0$ ,  $G = \hat{p}^{-1}$ ,  $D = k^{-2}$ . The connection



between  $g_1$  and the renormalized charge  $g$  is

$$(2.6) \quad g^2 = \frac{g_1^2}{1 + (1/\pi)g^2(L_p + \frac{1}{4}L_k)}; \quad g_1^2 = \frac{g^2}{1 - (1/\pi)g^2(L_p + \frac{1}{4}L_k)}.$$

At  $k^2 = A_k^2$  the  $D$  function changes from  $A_k^{-2}$  to  $A_k^{-2}[1 + (1/\pi)g_1^2(L_p - L_k)]^{-1}$ . This discontinuity is connected with a «sharp» vanishing of the interaction when  $k^2$  increases over  $A_k^2$ .

There is no discontinuity in the case when the vanishing is gradual. One may prove that the  $D$ -function discontinuity is of no importance for the forthcoming evidences, as in electrodynamics.  $g_1^2$  increases with the increase of  $A_p$ ,  $A_k$ . If  $A_p = A_k$  then (2.2) reduce to the «one-limit» formulae of A. A. ABRIKOSOV, A. D. GALANIN and I. M. HALATNIKOV<sup>(7)</sup>. If  $g_1^2 \ll 1$ , but

$$\frac{1}{\pi} g_1^2(L_p - L_k) \gg 1, \quad \frac{1}{\pi} g_1^2 \ln A_p^2 A_k^{-2} \gg 1.$$

then the formulae (2.2) turn into the simpler ones:

$$(2.7) \quad \left\{ \begin{array}{l} G(p) = \hat{p}^{-1} Q_0^{-3/10}(p); \quad D(k) = k^{-2} Q_0^{-4/5}(k) \frac{\pi}{g_1^2} (L_p - L_k)^{-1}; \\ I(p, p-k; k) = \gamma_5 Q_0^{1/5}(x); \quad Q_0(x) = 1 + \frac{5}{4} \frac{L_k - \ln x^2 m^{-2}}{L_p - L_k}. \end{array} \right.$$

The formula (2.7) suggests the possibility to ignore the influence of the free meson field in the Lagrangian. In fact,  $\varphi$  enters the equations only together with  $g_1$ , in the combination  $g_1\varphi$ . Therefore, the average over the vacuum of the quantity:  $T\langle\varphi(x)\varphi(y)\rangle$  to which the  $D$ -function is proportional, becomes proportional to  $g_1^{-2}$  (similarly to the case in electrodynamics<sup>(5,8)</sup> (\*)). The  $G$

(\*) This result is clearly seen in the case when the function is used in the form of a functional integral<sup>(10)</sup>:

$$D(xy) = \int T\varphi(x)\varphi(y) \exp \left[ i \int (g_1\varphi) \right] \delta\varphi / \int \exp \left[ i \int (g_1\varphi) \right] \delta\varphi.$$

Here we ignore the part of the action coming from the free field. Substituting the variables  $\varphi \rightarrow g_1\varphi$  we immediately see that  $D \sim g_1^{-2}$ .

(6) I. JA. POMERANČUK: *Dokl. Akad. Nauk SSSR*, **104**, 51 (1955); **105**, 461 (1955).

(7) A. D. GALANIN, A. A. ABRIKOSOV and I. M. HALATNIKOV: *Dokl. Akad. Nauk SSSR*, **97**, 793 (1954).

(8) I. JA. POMERANČUK: *Dokl. Akad. Nauk SSSR*, **103**, 1005 (1955).

(9) J. SCHWINGER: *Proc. Nat. Acad. Sci. USA*, **37**, 455, 459 (1951).

(10) I. M. GELFAND and R. A. MINLOS: *Dokl. Akad. Nauk SSSR*, **97**, 209 (1954); E. S. FRADKIN: *Dokl. Akad. Nauk SSSR*, **98**, 47 (1954); N. N. BOGOLJUBOV: *Dokl.*

function, being the average value over vacuum of  $T\bar{\psi}(x)\psi(y)$ , should not depend on  $g_1^2$  under these conditions. The vertex part being proportional to  $(^9)$

$$\left\{ \frac{\delta}{\delta g_1 \varphi(z)} G^{-1}[x, y, g_1 \varphi(z)] \right\}_{g_1 \varphi=0},$$

would not depend on  $g_1^2$  either. These dependences are fixed in (2.7).

We arrive at the conclusion that even at small values of  $g_1^2$  the free field action plays no important role. It may be assumed that the role of the free field would be even less important with the further increase of  $g_1^2$ . Therefore, the dependence of all quantities on  $g_1^2$  must correspond to (2.7) by  $g_1^2 \gg 1$  as well. Hence, the function  $g_1^2 D$  should not depend on  $g_1^2$  and, consequently, its dependence on  $k^2$  at higher  $g_1^2$  will be the same as at small values of  $g_1^2$ . That means that at any value of  $g_1^2$  (i.e. at any high value of  $A_p$  and  $A_k$  in the formula (2.6))  $\Gamma$ ,  $D$  and  $G$  should coincide with (2.7). Hence, in the formula connecting  $g_1^2$  and  $g^2$ ,

$$g^2 = \frac{g_1^2}{1 + (1/\pi)g_1^2(L_p + \frac{1}{4}L_k)},$$

$L_p$  and  $L_k$  ( $A_p$ ,  $A_k$ ) may tend to the infinity. Therefore,  $g^2$  turns out to be as in electrodynamics  $(^{5,8})$  equal to zero. The importance of this result makes it desirable to prove it by a direct consideration of the equations determining  $G$ ,  $D$  and  $\Gamma$  at  $g_1^2 > 1$ .

### 3. — On the Vanishing of the Renormalized Meson Charge in Pseudoscalar Theory with Pseudoscalar Coupling.

The previous Section contained certain general considerations proving the fact that the renormalized meson charge  $g$  vanishes in the pseudoscalar meson theory with the pseudoscalar interaction.

Let us consider this problem in details examining the properties of  $G$ ,  $D$  and  $\Gamma$  at arbitrary  $g_1^2$  basing our reasoning upon the two-limits technique given by A. A. ABRIKOSOV and I. M. HALATNIKOV  $(^3)$ .

The formulae (2.2), (2.5), (2.7) were deduced considering only the non-overlapping graphs  $(^1)$ . The overlapping graphs, as well as those containing the of the meson by another, were not taken into account. Let us determine the

*Akad. Nauk SSSR*, **99**, 225 (1954); K. YAMAZAKI: *Prog. Theor. Phys.*, **7**, 449 (1952); S. F. EDWARDS and R. E. PEIERLS: *Proc. Roy. Soc., A* **224**, 24 (1954); P. T. MATTHEWS and A. SALAM: *Nuovo Cimento*, **12**, 563 (1954); K. SYMANZIK: *Zeits. f. Naturfor.*, **9a**, 809 (1954); U. A. GELFAND: *Zu. Èksper. Teor. Fiz.*, **28**, 140 (1955).



scattering contribution of all the terms which were neglected. We shall consider the  $n$ -multiple-overlapping graph entering  $\Gamma$ . We assume the following inequalities to be fulfilled:

$$(3.1) \quad p^2 \sim (p-k)^2 \sim k^2 \ll A_k^2 \ll A_p^2.$$

Taking into account the fact that this diagram contains only one logarithmic integration, we obtain (with a procedure analogous to that used in electrodynamics <sup>(8)</sup>):

$$\begin{aligned} (3.2) \quad \Gamma_n &\sim g_1^{n^2} \int_{p^2}^{A_k^2} \frac{dq^2}{q^2} Q(q)^{-(3/10)2n - (4/5)n + (1/5)(2n+1)} \left[ 1 + \frac{1}{\pi} g_1^2 (L_p - L_k) \right]^{-n} = \\ &= \frac{4\pi}{5} \frac{1}{n - \frac{6}{5}} \left\{ g_1^2 \left[ 1 + \frac{1}{\pi} g_1^2 (L_p - L_k) \right]^{-1} \right\}^{n-1} Q(q)^{(6/5)-n} \Big|_{p^2}^{A_k^2} = \\ &= \frac{4\pi}{5n-6} \left\{ g_1^2 \left[ 1 + \frac{1}{\pi} g_1^2 (L_p - L_k) \right]^{-1} \right\}^{n-1} \cdot \\ &\quad \cdot \left\{ 1 - \left[ 1 + \frac{5}{4\pi} g_1^2 \left( (L_k - \ln \frac{p^2}{m^2}) \right) \left[ 1 + \frac{1}{\pi} g_1^2 (L_p - L_k) \right]^{-1} \right]^{(6/5)-n} \right\}. \end{aligned}$$

The second term in brackets is  $\leq 1$  and at  $p^2 \ll A_k^2$  is quite small. If this term is not taken into account,  $\Gamma_n$  increases. Accordingly, we obtain:

$$(3.3) \quad \Gamma_n \lesssim C_n \left\{ g_1^2 \left[ 1 + \frac{1}{\pi} g_1^2 (L_p - L_k) \right]^{-1} \right\}^{n-1},$$

$C_n$  being a numerical factor.

At very small  $g_1^2$ ,  $\Gamma_n = C_n g_1^{2(n-1)}$ . This relation may lead to the conclusion that  $\Gamma_n$  increases infinitely at high values of  $g_1^2$ . But it would not be correct. Even in case of  $L_p \sim L_k \sim 1$  (i.e. at  $A_p^2 \sim A_k^2$ ) and  $g_1^2$  being increased,  $\Gamma_n$  does not exceed a limit equal to

$$(3.4) \quad \Gamma_n \lesssim C_n \left( \frac{\pi}{L_p - L_k} \right)^{n-1}.$$

If we assume now that the transition to the point nucleon is going as:  $A_p^2 \rightarrow \infty$ ,  $A_k^2 \rightarrow \infty$ ,  $A_p^2 A_k^{-2} \gg 1$  then, according to (3.4),  $\Gamma_n$  turns out to be small at any value of  $g_1^2$ . The series of all overlapping diagrams runs as follows:

$$(3.5) \quad \sum C_n \left\{ g_1^2 \left[ 1 + \frac{1}{\pi} g_1^2 (L_p - L_k) \right]^{-1} \right\}^n.$$

This series seems to be asymptotic <sup>(4)</sup>. At small  $g_1^2$  its sum is small, because of  $g_1^2$  being small. At higher  $g_1^2$  the same result follows from the high value

of  $L_p - L_k$ . However, if  $L_p - L_k \sim 1$  the function expressed by (3.5), for  $g_1^2 \gtrsim 1$ , does not depend on  $g_1^2$ , though it cannot be accurately presented as in (3.5). But the independence of this function on  $g_1^2$  makes it possible to neglect it because at  $g_1^2 \sim 1$  the sum (3.5) is also of the order of unity; while determined by (2.7) will be about  $(L_k - \ln p^2 m^{-2})^{\frac{1}{2}} \gg 1$ , under these conditions, if  $p^2 \ll A_k^2$ .

Until now we supposed that the condition (3.1) is fulfilled. If the nucleon momentum exceeds  $A_k$ :

$$(3.6) \quad k^2 \ll A_k^2 \ll p^2 \ll A_p^2,$$

the evaluation of the function  $\Gamma_n$  is performed in the following way. All nucleon lines may be changed to  $\hat{p}^{-1}$  (as in <sup>(8)</sup>). The integrals over the meson momenta are determined mainly by the domain  $k^2 \sim A_k^2$ : here  $D \sim k^{-2} [1 + (1/\pi)g_1^2 \cdot (L_p - L_k)]^{-1}$ . As a result of that we obtain:

$$(3.7) \quad \Gamma_n \sim \gamma_5 \left( \frac{A_k^2}{p^2} \right)^n \left\{ g_1^2 \left[ 1 + \frac{1}{\pi} g_1^2 (L_p - L_k) \right]^{-1} \right\}^n.$$

In this case  $\Gamma_n$  turns out to be small not only in consequence of the factor  $L_p - L_k$  in the denominator, but also in consequence of the additional factor  $(A_k^2 p^{-2})^n$ . Thus, in the case given by (3.6) the overlapping diagrams play no role as well.

Let us pass now to the diagrams containing the meson-meson scattering. The simplest graph of this type entering  $\Gamma_n$  has the form:

$$(3.8) \quad \begin{array}{c} \text{Diagram showing a meson-meson scattering process. A horizontal line represents the meson line with momentum } p. \text{ It splits into two branches, each with momentum } p - k_1 \text{ and } p - k_1 - k_2. \text{ These branches meet at a vertex where a meson line with momentum } k \text{ is emitted. The internal meson lines have momenta } k_1 \text{ and } k_2. \text{ The final meson line has momentum } p - k. \end{array}$$

Suppose that  $p^2 \sim (p - k)^2 \sim k^2$ .

The matrix element for the meson-meson scattering, according to (2.2), is:

$$(3.9) \quad \begin{array}{c} \text{Diagram showing a meson-meson scattering process. A horizontal line represents the meson line with momentum } p. \text{ It splits into two branches, each with momentum } p - k_1 \text{ and } p - k_1 - k_2. \text{ These branches meet at a vertex where a meson line with momentum } k \text{ is emitted. The internal meson lines have momenta } k_1 \text{ and } k_2. \text{ The final meson line has momentum } p - k. \end{array}$$

$$= b \left[ g_1^4 \int_{k^2}^{A_k^2} Q^{-(4 \cdot 3/10) + (4/5)} \frac{dk^2}{k^2} + g_1^4 (L_p - L_k) \right] =$$

$$= b g_1^4 \left[ 1 + \frac{1}{\pi} g_1^2 (L_p - L_k) \right] \left\{ Q^{(3/5)}(k) - 1 \right\} \frac{4\pi}{3} + b g_1^4 (L_p - L_k).$$

$b$  is a numerical factor (of the order 1), and  $k$  is the largest of all vectors:  $k_1, k_2, k_3, k_1 + k_2 - k_3$ .

The first term in (3.9) originates from the nucleon momenta which are within the limits  $A_k^2 \gg p^2 \gg k^2$ , the second from the momenta within the limits  $A_p^2 \gg p^2 \gg A_k^2$ . In (3.9) the term  $-1$  is small as compared with  $Q^3$  and we can omit it. In this way we can only overestimate the meson-meson scattering. Introducing (3.9) into (3.8) and taking into account that (3.8) contains only one logarithmic integration, we obtain for the expression (3.8) the value:

$$\begin{aligned} & \sim b g_1^4 \left[ 1 + \frac{1}{\pi} g_1^2 (L_p - L_k) \right]^{-3} \int_{p^2}^{A_k^2} Q^{-(12/5)}(k) \frac{dk^2}{k^2} \left\{ \frac{4\pi}{3} Q^{(3/5)}(k) \cdot \right. \\ & \quad \cdot \left[ 1 + \frac{1}{\pi} g_1^2 (L_p - L_k) \right] + g_1^2 (L_p - L_k) \left. \right\} = b g_1^2 \left[ 1 + \frac{1}{\pi} g_1^2 (L_p - L_k) \right]^{-1} \cdot \\ & \quad \cdot \frac{4\pi^2}{3} Q^{-(4/5)}(k) \Big|_{p^2}^{A_k^2} + \frac{4\pi}{7} b g_1^4 (L_p - L_k) \left[ 1 + \frac{1}{\pi} g_1^2 (L_p - L_k) \right]^{-2} Q^{-(6/5)}(k) \Big|_{p^2}^{A_k^2} = \\ & = \frac{4\pi^2}{3} b g_1^2 \left[ 1 + \frac{1}{\pi} g_1^2 (L_p - L_k) \right]^{-1} \left\{ 1 - \left[ 1 + \frac{5g^2}{4\pi} \frac{L_k - \ln p^2 m^{-2}}{(L_p - L_k)(g_1^2/\pi) + 1} \right]^{-\frac{4}{5}} \right\} + \\ & + \frac{4\pi}{7} b g_1^4 \left[ 1 + \frac{g_1^2}{\pi} (L_p - L_k) \right]^{-2} (L_p - L_k) \cdot \left\{ 1 - \left[ 1 + \frac{5g_1^2}{4\pi} \frac{L_k - \ln p^2 m^{-2}}{1 + (1/\pi)g_1^2(L_p - L_k)} \right]^{-\frac{7}{5}} \right\}. \end{aligned}$$

The second term is small in both big brackets if  $p^2 \ll A_k^2$  and can be omitted (this increases the value of (3.8)). We obtain for the expression (3.8) the value:

$$(3.10) \quad \sim \frac{4\pi^2}{3} b g_1^2 \left[ 1 + \frac{1}{\pi} g_1^2 (L_p - L_k) \right]^{-1} + \\ + \frac{4\pi}{7} b g_1^4 (L_p - L_k) \left[ 1 + \frac{1}{\pi} g_1^2 (L_p - L_k) \right]^{-2}.$$

At high values of  $g_1^2$  we obtain for the expression (3.8) the value:

$$(3.11) \quad \sim \frac{1}{L_p - L_k}.$$

Thus, (3.8) ceases to depend on  $g_1^2$  when  $g_1^2$  becomes large. The limiting value of (3.8) turns out to be small at  $L_p - L_k \gg 1$ .

Though the effect of single meson-meson scattering turns out to be small, it should be pointed out that the series of successive acts of the meson-meson scattering does not yield a convergent series even in the case when the two-limits technique is used. Let us compare the two diagrams:

$$(3.12) \quad \begin{array}{cc} \begin{array}{c} \text{---} k_1 \text{---} \\ \square \\ \text{---} k_2 \text{---} \quad \text{---} k_3 \text{---} \end{array} & \begin{array}{c} \text{---} k_1 \text{---} \quad k_1 + k_2 - f \text{---} \\ \square \quad \square \\ \text{---} k_3 \text{---} \quad f \text{---} \quad k_3 \text{---} \end{array} \end{array}$$



(A) is the first member of (3.9). (B) contains only the logarithmic integral over  $f^2$  and, according to (3.9), turns out to be equal to:

$$(3.13) \quad B \sim b^2 \int_{k^2}^{A_k^2} \frac{df^2}{f^2} \left\{ \frac{4\pi^2}{3} g_1^2 \left[ 1 + \frac{1}{\pi} g_1^2 (L_p - L_k) \right] Q^{(3/5)}(f) + \right. \\ \left. + \frac{4\pi}{7} g_1^4 (L_p - L_k) \right\}^2 Q^{-(8/5)}(f) \left[ 1 + \frac{1}{\pi} g_1^2 (L_p - L_k) \right]^{-2}.$$

$k$  is the largest of the vectors:  $k_1, k_2, k_3, k_1 + k_2 - k_3$ . While calculating (3.13) the term containing  $g_1^2 (L_p - L_k)$  can be omitted if  $k^2 \ll A_k^2$  ( $Q(k) \gg 1$ ), and we obtain

$$(3.14) \quad B \approx g_1^2 \left[ 1 + \frac{1}{\pi} g_1^2 (L_p - L_k) \right] Q^{(3/5)}(k).$$

(3.14) coincides in the order of magnitude with (3.9), if  $Q \gg 1$ , ( $k^2 \ll A_k^2$ ). Thus, (B) and (A) are of the same order. This fact makes it quite desirable to consider in details the totality of all diagrams of the meson-meson scattering. However, taking into account the general considerations based on the falling out of the part of the action integral coming from the free field at already low values of  $g_1^2$ , and the fact that:

1) the totality of all overlapping diagrams turns out to be small;

2) each diagram entering  $\Gamma$  and corresponding to meson-meson scattering contains the small factor (3.11)  $(L_p - L_k)^{-1}$ , we may assert, that with high degree of probability, the expressions for  $G, D$  and  $\Gamma$  given in (2.2), are correct at any value of  $g_1^2$  (i.e. at any high value of  $A_p$  and  $A_k$ ). This circumstance leads to the fact that the renormalized meson charge, according to (2.6), turns out to be zero<sup>(6)</sup>. This result corresponds to the conclusion from the quantum electrodynamics of particles with spin  $\frac{1}{2}$ <sup>(5,8)</sup>. Recently L. P. GOR'KOV and I. M. HALATNIKOV found that the quantum electrodynamics of particles with spin 0 leads to the conclusion that also in this theory the renormalized charge of particles is equal to zero<sup>(11)</sup>.

The above mentioned facts of the vanishing of renormalized charges makes it plausible that all point interactions should lead to the same result. From this point of view, it would be most important to clear up the fact whether the vector coupling leads to an analogous result or not.

The vanishing of the charges of point particles would demand radical changes in the fundamentals of the existing physical theories. First of all

<sup>(11)</sup> L. P. GOR'KOV and I. M. HALATNIKOV: *Dokl. Akad. Nauk SSSR*, **104**, 197 (1955).

such a change would introduce a new length into the theory, and this fact would make, roughly speaking, impossible the increasing of  $\Lambda$  to infinity.

One should remember that the new length  $r_0$  cannot be too small. In this case, according to (2.6),  $g^2$  will also be small. It follows from the formula

$$g^2 = \frac{g_1^2}{1 + (1/\pi)g_1^2(L_p + \frac{1}{4}L_k)}$$

that, at a given value of  $\Lambda_p$  and  $\Lambda_k$ ,  $g^2$  attains its maximum if  $g_1^2 = \infty$ :

$$g^2 \leq \frac{\pi}{L_p + \frac{1}{4}L_k}.$$

Assuming that  $L_p = L_k = L$  and substituting  $\ln(1/m^2 r_0^2)$  for  $L$  ( $\Lambda = 1/r_0$ ), we obtain:

$$g^2 \leq \frac{4\pi}{5} \left[ \ln \frac{1}{r_0^2 m^2} \right]^{-1}.$$

If  $r_0 \ll 1/m$ ,  $g^2 \ll 1$ . This value of  $g^2$  contradicts the data obtained from the interactions of  $\pi$ -mesons and nucleons (particular attention should be drawn to the Kroll-Ruderman theorem <sup>(12)</sup>). Thus,  $r_0$  should be of the order or above the Compton length of the nucleon,  $2 \cdot 10^{-14}$  cm. Most probably,  $r_0$  would be within the limits  $10^{-14} < r_0 < 10^{-13}$ . But, as it was noted by L. D. LANDAU, the evaluation of this value may involve some difficulties, if we remember the existence of the showers composed of a large number of  $\pi$ -mesons and nucleons, that is, the so-called explosive showers. If one treats these showers on the basis of the Fermi <sup>(13)</sup> - Landau <sup>(14)</sup> theory, then one inevitably arrives to the conclusion of the great probability of large momentum transfer, up to the magnitude of about  $100 m$ . (This corresponds to an energy of the fast nucleon, if the collision is of the type nucleon-nucleon, of about  $10^{13}$  eV in the laboratory system). On the other side, if  $r_0 \sim 1/m$ , then in case of a somewhat « naive » understanding of  $r_0$  one should consider the transfer of the momentum much over  $m$  to be very improbable. The difficulty with the explosive showers (if they really are explosive) once more points out the necessity of a thorough consideration of such problems as the meson-meson scattering in the pseudoscalar coupling (\*), the pseudovector coupling and more

<sup>(12)</sup> N. KROLL and M. RUDERMAN: *Phys. Rev.*, **93**, 233 (1954).

<sup>(13)</sup> E. FERMI: *Prog. Theor. Phys.*, **5**, 570 (1950).

<sup>(14)</sup> L. D. LANDAU: *Izv. Akad. Nauk SSSR, Ser. Fiz.*, **17**, 51 (1953).

(\*) Recently K. A. TER-MARTIROSIAN and V. V. SUDAKOV made a very fine calculation of the meson-meson scattering and demonstrated, that it does not violate the conclusion about  $g^2=0$ . The same result was obtained by the author by assuming  $\ln A_p^2 m^{-2} \gg \ln A_k^2 m^{-2}$  ( $A_p \rightarrow \infty$ ,  $A_k \rightarrow \infty$ ).

general types of point interactions. However, it may happen that the now existing theories of  $\pi$ -meson showers must be reconsidered, and that in fact there are no great momentum transfers. Experiments revealing the existence of the new fundamental length might be of vital importance for the progress of the theory of the elementary particles.

Experiments with  $\pi$ -mesons, nucleons and other elementary particles with *strong* interaction *cannot* directly serve this purpose. The unambiguous interpretation of these experiments will hardly be possible until a new theory is created, because of the fact that in case of strong interaction all processes are very complicated (we may think that, from the theoretical point of view,  $\pi$ -particles, nucleons and their likes are too complicated. As far as the atomic physics is concerned, they would correspond rather to complex atoms than to hydrogen-like atoms). The basic experiments must be performed with particles with weak interaction (electron-electron, electron- $\gamma$  quantum,  $\gamma$  quantum- $\mu$  particle).

\* \* \*

In conclusion I would like to express my gratitude to L. D. LANDAU for his valuable remarks, as well as to A. A. ABRIKOSOV, B. L. IOFFE, E. S. FRADKIN and I. M. HALATNIKOV for their active participation in the discussion of this work.

#### RIASSUNTO (\*)

L'autore discute le soluzioni delle equazioni dell'elettrodinamica quantistica per le particelle con spin  $\frac{1}{2}$ , soluzioni ottenute da vari autori dapprima con un solo parametro di « smearing out » e in seguito con due parametri. Egli dimostra nella Sez. 1 che le soluzioni ottenute sono valide per tutti i valori della carica elettrica non rinormalizzata  $e_2$  (tanto per  $e_1 \ll 1$  quanto per  $e_2 \gg 1$ ), e che entrambe le teorie portano alla conclusione che la carica rinormalizzata  $e$  risulta essere zero. Nella Sez. 2 l'autore ricerca se la stessa proprietà valga anche per la carica mesonica  $g$  nella teoria pseudoscalare. Usando la teoria dei due limiti sviluppata da ABRIKOSOV e HALATNIKOV, egli giunge alla conclusione che anche  $g$  risulta essere zero. Nella Sez. 3 l'autore esamina minutamente il problema dello svanire della carica mesonica rinormalizzata esaminando le proprietà delle funzioni  $G$ ,  $D$  e  $F$  per valori arbitrari di  $g_1^2$ . Il risultato di questa analisi corrisponde alle conclusioni precedenti, e conferma lo svanire di  $g$ .

(\*) A cura della Redazione.



## Radiation with a Finite Rest-mass and the Heat Balance of the Earth.

L. BASS

*Dublin Institute for Advanced Studies*

(ricevuto il 25 Gennaio 1956)

**Summary.** — The theory of the photon with a finite rest-mass is applied to the problem of the distribution of radioactive elements in the body of the earth. The small amount of the conduction loss of heat observed on the surface of the earth could hitherto be only explained by assuming *ad hoc* that the radioactive sources of heat are effectively confined to a thin surface layer of some 20 km depth. It is shown that even a *uniform* distribution of radioactivity throughout the earth (with the density given by the measured surface value) is compatible with the heat balance if an otherwise allowable small rest-mass of the photon is assumed. In that case the surplus energy is carried away by longitudinal photons straight from the hot core of the earth. The upper limit for the admissible rest-mass ( $10^{-47}$  g, as imposed by independent considerations) is used for the present estimate. The very small magnitude of this rest-mass is the cause of the very weak interaction between longitudinal photons and matter and thus makes possible the cooling mechanism described in the paper; it also accounts for the fact that longitudinal photons had not been detected by direct measurements.

---

### 1. — Introduction.

In a recent paper BASS and SCHRÖDINGER <sup>(1)</sup> had pointed out that a finite rest-mass of the photon is compatible with the present experimental knowledge of radiation. Observations (of rotating binary stars and of the earth's magnetic field) set an *upper limit* to the admissible rest-mass,  $m \lesssim 10^{-47}$  g. The existence of such a small rest-mass would lead to a new, experimentally undetected cooling mechanism effective in very massive hot bodies. Following

<sup>(1)</sup> L. BASS and E. SCHRÖDINGER: *Proc. Roy. Soc., A* **232**, 1 (1955).

a suggestion of P. FELLGETT <sup>(2)</sup> we shall apply this theory to the problem of the distribution of radioactive elements in the body of the earth. It will be shown that, as a consequence of the cooling, the sources of radioactive heat within the earth may be considerably more abundant than had hitherto been thought permissible on account of the observed heat outflow through the surface of the earth.

## 2. — The Radiation with a Finite Rest-Mass.

When the rest-mass  $m$  is finite there exist both transverse and longitudinal waves (in vacuo),  $T$ -waves and  $L$ -waves for short. The former are nearly identical with the ordinary Maxwellian ones, the latter are distinguished by an exceedingly weak interaction with matter. In terms of the quantum theory  $L$ -photons, compared with  $T$ -photons of the same frequency, are very rarely emitted, absorbed or scattered by individual atoms; nevertheless, as pointed out in <sup>(1)</sup>, sufficiently massive celestial bodies may emit  $L$ -waves abundantly. The interaction of  $L$ -waves with matter is, roughly speaking, proportional to  $m^2$ . Maxwell's theory is obtained by going to the limit  $m = 0$ . It is shown in Appendix I that the respective cross-sections  $\sum (L)$ ,  $\sum (T)$  for all first-order radiation processes (e.g. absorption or emission) and some of the second-order processes are connected by the approximate relation

$$(1) \quad \sum (L) \approx \left( \frac{mc^2}{h\nu} \right)^2 \sum (T),$$

which enables us to estimate cross-sections for  $L$ -interactions from the known cross-sections for ordinary light. It can also be shown that  $L$ -photons probably cannot be detected directly by our instruments, *not* because they are necessarily rare, but because by (1) they interact too weakly to be registered and moreover because an  $L$ -perturbation, even when effective, leaves the affected atom in a state which is the same as that which a  $T$ -photon of the same frequency would cause with an enormously greater probability.

According to the law of equipartition there would be, in temperature equilibrium, on the average one  $L$ -photon for every two  $T$ -photons. A massive body of density  $\varrho$  and thickness  $x$  at constant temperature  $T$  throughout, black for  $T$ -waves but semi-transparent for  $L$ -waves will emit, by an appropriate generalization of the Stefan-Boltzmann law (see Appendix II)

$$(2) \quad \approx \sigma T^4 \left[ 1 + \frac{1}{2} \left( 1 - \exp \left| - \frac{x}{l_L} \right| \right) \right] \text{erg} \cdot \text{s}^{-1} \cdot \text{cm}^{-2},$$

<sup>(2)</sup> P. FELLGETT: Private communication.

where  $l_L = (\bar{k}q)^{-1}$  is the mean free path of an  $L$ -photon in the body,  $\bar{k}$  the mean  $L$ -absorption coefficient and  $\sigma$  the Stefan-Boltzmann constant. For a completely black body,  $l_L \ll x$ , (2) reduces to approximately three halves of the Maxwellian value (this factor is due to the additional longitudinal direction of polarization). For  $l_T \ll x \ll l_L$  we obtain the emissivity

$$(3) \quad \approx \sigma T^4 \left( 1 + \frac{1}{2} \frac{x}{l_L} \right),$$

where the first term gives the  $T$ -emission and the second the  $L$ -emission (per unit time and surface area).

### 3. — The Problem of the Distribution of Radioactivity.

The value of the mean thermal conductivity and temperature gradient on the surface of the earth is established by measurements, from which the loss of heat by conduction is deduced. While this loss corresponds to only about  $3 \cdot 10^{-5}$  of the solar constant it represents, according to current theories, the net heat loss of the earth. If the radioactive elements were distributed approximately uniformly throughout the body of the earth with the density known empirically on the surface, then the heat balance would, according to current views <sup>(3)</sup>, be considerably upset by the production of  $7 \cdot 10^{-6}$  erg  $\cdot$  g $^{-1}$   $\cdot$  s $^{-1}$  of radioactive heat, corresponding to about 200 times the amount of the observed conduction loss. Thus the geophysicists are forced to assume that radioactivity is effectively confined to a surface layer so thin that the factor of 200 is accounted for, i.e. corresponding to a layer of constant density and some 20 km depth. It is not possible to account for the factor of 200 by assuming only that the earth is not in a stationary state. For even if the earth had been originally cold, a roughly uniform radioactive distribution (with the measured surface density throughout) would, up to the present time, cause a mean temperature of the order of  $10^5$  degrees, even disregarding the heat from gravitational contraction.

We propose to show that even if the distribution of radioactive elements were near to uniform, all excess energy could be carried away by  $L$ -waves straight from the hot core of the earth. The observed conduction loss would then be only a fraction of the total energy loss of the earth, but the latter loss (per unit time and surface area) would still be very small as compared with the solar constant.

<sup>(3)</sup> H. JEFFREYS: *The Earth* (Cambridge, 1952), 3rd edition.



#### 4. — The Estimate of the $L$ -Emission.

We shall use for our computations the *upper limit*  $m \approx 10^{-47}$  g. We are therefore allowed to *underestimate* in the calculation the  $L$ -emission in other respects, as long as the resulting estimate suffices to account for the excess heat. For if the *exact* amount of  $L$ -energy loss which results from our chosen value of  $m$  and which is really larger than our underestimate, happened to be too large to agree with the knowledge of the radioactive distribution, we should regard it only as an indication that the true value of  $m$  is appropriately lower than the upper limit imposed by independent considerations. We shall use a rough model of the earth (the estimate being rather insensitive to details of the model) taking the *core* (radius  $r_{\text{core}} \approx 4 \cdot 10^8$  cm) to be at  $\approx 5000$  °K throughout, on account of the high thermal conductivity of liquid Fe. All  $T$ -radiation and some of the  $L$ -radiation from the core is absorbed by the colder *crust* which we shall consider as an absorber only, with some plausible temperature gradient. We further assume a uniform density of radioactivity throughout the earth. Thus we assume all the excess energy to come away from the core as  $L$ -waves although much of the heat is generated in the crust. However, this circumstance will merely modify the theoretical temperature gradient in the crust (below the depth accessible to measurements) while we are concerned only with the total heat balance of the earth as a whole.

Now the  $L$ -term in (3) for the core-surface must be at least of the order of the total heat production in the earth, i.e.  $\approx 4 \cdot 10^{22}$  erg·s<sup>-1</sup>, if  $L$ -waves are to suffice for the maintenance of the balance. This leads to the condition for the mean free path  $l_L$ :

$$l_L \lesssim 10^6 r_{\text{core}} \approx 4 \cdot 10^{14} \text{ cm.}$$

For the estimate of the mean free path we shall use Kramers' law of absorption in the continuous region <sup>(4)</sup> in the approximate form

$$(4) \quad \bar{k} \approx 4 \cdot 10^{25} \varrho T^{-7/2},$$

multiplied by the factor  $(mc^2/h\nu)^2$  according to (1). The application of Kramers' law is in keeping with the nature of our estimate since by disregarding resonance interactions this law leads to an underestimate of the  $L$ -emission (due to the overestimate of the mean free path  $l_L$ ). Since in (4) the mean absorption coefficient  $k$  is an average over the frequencies  $\nu$  we shall use in (1) the frequency corresponding to the maximum intensity at the temperature of the

<sup>(4)</sup> A. S. EDDINGTON: *The Internal Constitution of the Stars* (Cambridge, 1930).

emitter by Wien's law:  $\nu \approx 5 \cdot 10^{14} \text{ s}^{-1}$ ,  $(mc^2/h\nu)^2 \approx 10^{-29}$ . Taking the density  $\rho \approx 15 \text{ g} \cdot \text{cm}^{-3}$  in the core we obtain indeed  $l_L \approx 10^{14} \text{ cm}$  as required above.

Finally, the opacity of  $3 \cdot 10^8 \text{ cm}$  of the *crust* with respect to the outgoing  $L$ -radiation from the core is, according to (1), approximately equivalent to the opacity of  $\approx 3 \cdot 10^8 \cdot 10^{-29} = 3 \cdot 10^{-21} \text{ cm}$  of the crust material with respect to ordinary  $T$ -radiation. Hence the  $L$ -radiation from the core passes through the crust without appreciable absorption, and through our measuring devices without being noticed. The choice of another set of permissible data for the interior of the earth is not likely to reduce the amount of  $L$ -emission. Thus the choice of a core-temperature  $\approx 3000 \text{ }^\circ\text{K}$  and density  $\approx 12 \text{ g} \cdot \text{cm}^{-3}$  would more than double the outgoing  $L$ -energy while further reducing the accuracy of Kramers' law.

## 5. — Discussion.

We are thus faced, in principle, with the following two points of view:

(i)  $m = 0$ . Radioactivity is confined to the very surface of the earth.

(ii)  $0 < m \lesssim 10^{-47} \text{ g}$ . Corresponding to the true value of  $m$ , the true distribution of the radioactive elements is somewhere between that in (i) and a uniform one.

With regard to the hypothesis (i) it is not easy to see *a priori* why, in a heavy gravitating body which is partly liquid, the very heaviest (i.e. radioactive) elements should be concentrated on the surface (this remark may be helpful when conclusions are drawn from the composition of comparatively light solid meteorites). The author is not aware that any plausible mechanism of such concentration has ever been suggested, and the empirical evidence supporting an upward concentration of radioactivity is confined to the depth of merely a few kilometers of solid crust. Moreover, the theory of geomagnetism might require energy sources inside the earth more abundant than those compatible with (i).

For these reasons (ii) may be considered preferable to (i) and this situation may be regarded as an indication that the photon rest-mass is actually finite.

As a result of (1) and (4) it is very likely that the  $L$ -energy loss of the very hot and highly ionized sun and stars will not be excessively strong. In particular it is clear that  $L$ -radiation emitted by the sun and absorbed by the earth is of no significance for the present estimate. Supposing that the solar  $L$ -emission is comparable in intensity with the known  $T$ -emission, then the  $L$ -energy loss of the earth calculated above corresponds to  $\approx 6 \cdot 10^{-3}$  of the solar constant for  $L$ -radiation. On the other hand the mean free path of the solar  $L$ -photons

in the earth is at least of the order of  $10^6 \cdot r_{\text{core}}$  (in fact considerably longer since the mean frequency in (1) corresponds to the temperature of the sun) so that the earth loses by  $L$ -emission about  $10^4$  times the  $L$ -energy absorbed from the sun rays.

\* \* \*

The author is grateful to professors E. SCHRÖDINGER and H. BONDI and to Dr. P. FELLGETT for valuable discussions.

# APPENDIX I

## The Cross-Sections for Processes Involving $L$ -Photons.

The radiation with a finite rest-mass  $m$  is described by the set of four Klein-Gordon equations governing the four-potential  $(\mathbf{A}, V)$

$$(I.1) \quad \left\{ \begin{array}{l} \left( \Delta - \frac{1}{c^2} \frac{\partial^2}{\partial t^2} - k_0^2 \right) \mathbf{A} = 0, \\ \left( \Delta - \frac{1}{c^2} \frac{\partial^2}{\partial t^2} - k_0^2 \right) V = 0, \\ k_0 = \frac{mc}{\hbar}, \quad \hbar = \frac{h}{2\pi}, \end{array} \right.$$

with the Lorentz condition

$$\text{div } \mathbf{A} + \frac{1}{c} \dot{V} = 0,$$

which is fulfilled by the coefficients of the Fourier expansion:

$$(I.2) \quad \left\{ \begin{array}{l} \mathbf{A} = \frac{1}{L^3} \sum_{\mathbf{k}} \mathbf{q}_{\mathbf{k}} \exp[i\mathbf{k}\mathbf{r}], \\ V = \frac{1}{L^3} \sum_{\mathbf{k}} \frac{(\mathbf{q}_{\mathbf{k}} \mathbf{k})}{\omega} \exp[i\mathbf{k}\mathbf{r}], \end{array} \right.$$

where  $\omega = 2\pi\nu/c$ ,  $|\mathbf{k}| = 2\pi/\lambda$  and  $L^3$  is the volume of the periodicity cube. The dispersion is indicated by

$$(I.3) \quad \omega^2 - k^2 = k_0^2.$$



We further introduce three polarization vectors  $\mathbf{e}_\lambda$ ,

$$\begin{aligned} \mathbf{q}_k &= \sum \mathbf{e}_\lambda \mathbf{q}_\lambda^k, & (\mathbf{e}_\lambda \mathbf{e}_{\lambda'}) &= \delta_{\lambda\lambda'}, & \lambda &= 1, 2, 3, \\ (\mathbf{e}_1 \mathbf{k}) &= |\mathbf{k}|, & (\mathbf{e}_2 \mathbf{k}) &= (\mathbf{e}_3 \mathbf{k}) = 0; & [\mathbf{e}_1 \mathbf{k}] &= 0 \text{ etc.}, \end{aligned}$$

and new Fourier amplitudes (chosen so that the eigenvalues of the product matrices  $a \cdot a^*$  are integers)

$$\left\{ \begin{aligned} q_1^k &= \frac{1}{k_0} \sqrt{\hbar c \omega} (a_1^k + a_1^{-k*}), \\ q_\lambda^k &= \sqrt{\frac{\hbar c}{\omega}} (a_\lambda^k + a_\lambda^{-k*}), \end{aligned} \right. \quad \lambda = 2, 3.$$

( $q_\lambda^k = q_\lambda^{-k*}$ , since the field is real) and the commutation relations <sup>(5)</sup>

$$[a_\lambda^k, a_{\lambda'}^{k*}] = \delta_{\mathbf{k}\mathbf{k}'} \delta_{\lambda\lambda'}.$$

Using also the explicit time-dependence of the Fourier amplitudes we then obtain from (I.2) ( $a_\lambda^k \equiv a_\lambda$ ),

$$(I.4) \quad \left\{ \begin{aligned} \mathbf{A} &= \frac{1}{L^{\frac{3}{2}}} \sqrt{\hbar c} \sum_{\mathbf{k}} \left[ \frac{1}{\sqrt{\omega}} \sum_{\lambda=2,3} \mathbf{e}_\lambda (a_\lambda \exp[i(\mathbf{k}\mathbf{r} - \omega t)] + a_\lambda^* \exp[-i(\mathbf{k}\mathbf{r} - \omega t)]) \right. \\ &\quad \left. + \mathbf{e}_1 \frac{\sqrt{\omega}}{k_0} (a_1 \exp[i(\mathbf{k}\mathbf{r} - \omega t)] + a_1^* \exp[-i(\mathbf{k}\mathbf{r} - \omega t)]) \right] \\ V &= \frac{1}{L^{\frac{3}{2}}} \sqrt{\hbar c} \sum_{\mathbf{k}} \frac{1}{\sqrt{\omega}} \frac{|\mathbf{k}|}{k_0} (a_1 \exp[i(\mathbf{k}\mathbf{r} - \omega t)] + a_1^* \exp[-i(\mathbf{k}\mathbf{r} - \omega t)]) \end{aligned} \right.$$

where  $a, a^*$  denote the well known operators for creation and annihilation of photons, respectively. We observe that the  $\mathbf{e}_1$ -term in the expansion of  $\mathbf{A}$  in (I.4) is a three-gradient of a scalar potential  $\varphi$ ,

$$\varphi = \frac{1}{L^{\frac{3}{2}}} \sqrt{\hbar c} \sum_{\mathbf{k}} \left[ -i \frac{\sqrt{\omega}}{k_0} \frac{1}{|\mathbf{k}|} (a_1 \exp[i(\mathbf{k}\mathbf{r} - \omega t)] - a_1^* \exp[-i(\mathbf{k}\mathbf{r} - \omega t)]) \right],$$

from which we can construct the corresponding four-gradient  $[\text{grad } \varphi, -(1/c)\dot{\varphi}]$ . Now according to Dirac's theory such a four-gradient can only affect the phase of the wave-function of the system with which the radiation field (I.4) interacts, and this phase does not enter into the expressions for transition probabilities arising from the interaction. We therefore subtract this four-gradient from the four-potential (I.4), making use also of (I.3). We then construct

<sup>(5)</sup> G. WENTZEL: *Quantum Theory of Fields* (New York, 1949).

the appropriate perturbation Hamiltonian of the system:

$$(I.5) \quad H' = e[(\boldsymbol{\alpha}\mathbf{A}) - V] = U + U^*,$$

$$U = \frac{e}{L^{\frac{3}{2}}} \sqrt{ch} \sum_{\mathbf{k}} \frac{1}{\sqrt{\omega}} \left[ \sum_{\lambda=2,3} (\boldsymbol{\alpha} \mathbf{e}_{\lambda}) a_{\lambda} + \frac{k_0}{\omega} a_1 \right] \exp[i(\mathbf{k}\mathbf{r} - \omega ct)].$$

We note that the subtraction of the irrelevant four-gradient has made the longitudinal part of the perturbation (i.e. the part involving  $a_1$  and  $a_1^*$ ) considerably smaller than the transversal part, since  $k_0$  is very small. This is the reason for the relatively weak interaction of  $L$ -photons with matter. The remaining, effective  $L$ -perturbation is proportional to  $k_0$  and goes smoothly to zero when  $m$  goes to zero. The other term is the ordinary  $T$ -perturbation. The  $L$ -term is, for each monochromatic perturbation, of the order  $mc^2/h\nu$  as compared with a corresponding  $T$ -term. Since the transition probabilities and hence the cross-sections for first-order processes are proportional to the square of the respective elements of the perturbation matrix, the formula (1) is indeed obtained.

For the discussion of second-order processes we note that the above argument is independent of whether the states of the system are virtual or real. It is then easily found that, depending on the character (longitudinal or transverse) of the perturbations which bring about the intermediate and final states, either (1) is valid (e.g. for  $L$ -bremsstrahlung or  $T \rightarrow L$  scattering) or the fourth power of the fraction  $mc^2/h\nu$  must be substituted into (1) for the square (e.g. for  $L \rightarrow L$  scattering).

## APPENDIX II

### The Generalization of the Stefan-Boltzmann Law.

Consider a body of thickness  $x$  at constant temperature  $T$  throughout, emitting radiation which has a mean free path  $l$  within this body. If the radiation emitted from a given point has to traverse a distance  $x'$  on its way to the surface of the body, its intensity is reduced by the factor  $\exp[-x'/l]$ . Since  $T$  is constant, integration over all the sources contributing to an outgoing ray, together with the stipulation of black-body emission in the limiting case  $l \ll x$  leads to an emissivity equal to

$$\sigma T^4 \left( 1 - \exp\left[-\frac{x}{l}\right] \right).$$

For the present purpose  $l \ll x$  is always true for  $T$ -radiation but not for  $L$ -radiation. Thus the emissivity with respect to the combined  $L$ - and  $T$ -emis-

sion is approximately equal to

$$\sigma T^4 \left[ 1 + \frac{1}{2} \left( 1 - \exp \left[ -\frac{x}{l_L} \right] \right) \right],$$

in agreement with (2).

We may disregard the factors of the order of unity which would arise from taking into account the directions of the rays and from exact averaging of the mean free path since in previous calculations other approximations of similar inaccuracy have been made.

---

#### RIASSUNTO

La teoria del fotone di massa a riposo finita viene applicata al problema della distribuzione degli elementi radioattivi nel globo terrestre. La piccola perdita di calore per conduzione attraverso la superficie della Terra poteva sino ad ora essere spiegata solo assumendo *ad hoc* che le sorgenti radioattive di calore fossero confinate ad uno sottile strato superficiale di 20 km di profondità all'incirca. Nel presente lavoro si mostra che anche una distribuzione *uniforme* di radioattività nell'interno della Terra (con una densità alla superficie data dal valore noto) è compatibile con l'equilibrio termico se si assume un'appropriata, piccola massa a riposo del fotone. In tal caso l'energia sovrabbondante è trasportata via da fotoni *longitudinali* direttamente dal nucleo ad alta temperatura della Terra. Per tale stima viene usato il limite superiore ammissibile per la massa a riposo ( $10^{-47}$  g, imposto da altre considerazioni); ciò è sufficiente per causare una debolissima interazione tra fotoni longitudinali e materia, che rende così possibile il meccanismo di raffreddamento descritto nel lavoro; tale valore dà pure ragione del fatto che i fotoni longitudinali non sono stati rivelati da misurazioni dirette.



## Transition Amplitudes as Sums over Histories.

W. TOBOCMAN

*Institute for Advanced Study - Princeton, New Jersey*

(ricevuto il 16 Febbraio 1956)

**Summary.** — Explicit sum over histories expressions for the transition amplitude are constructed on the basis of the canonical formalism of quantum mechanics. The sum over histories can be shown to coincide with the Feynman principle when the Hamiltonian is classical in form and quantization is carried out in terms of the commutators of operators. In general, the sum over histories differs somewhat from Feynman's functional integral but still involves the exponential of the action,  $S = \int (p\dot{x} - H) dt$ . However, for the Dirac field, where dynamical independence implies the anti-commutativity of operators, the sum over histories we construct has a form completely different from the Feynman principle.

### 1. — Introduction.

The laws of classical mechanics have two equivalent formulations. One formulation is based on the Lagrangian and the other is based on the Hamiltonian. The quantum generalization of the laws of classical mechanics was first carried out in terms of the Hamiltonian. The Hamiltonian formulation of quantum mechanics has come to be accepted as the standard or canonical formulation. Nevertheless a Lagrangian formulation for the laws of quantum mechanics has always seemed to be desirable because such a derivation would be manifestly covariant.

It was early recognized that the Lagrangian is intimately involved in quantum dynamics. SCHRÖDINGER <sup>(1)</sup> noted that in some cases the solution

---

<sup>(1)</sup> E. SCHRÖDINGER: *Ann. der Phys.*, **79**, 489 (1926); H. GOLDSTEIN: *Classical Mechanics*, Sect. 9-8 (Cambridge, Mass. 1950).

to the Schrödinger equation can be written formally  $\psi = \exp[iS/\hbar]$  where  $S = \int L dt$  is the action (or, to be precise, Hamilton's principle function). This relationship between the Schrödinger wave function and the action was further illuminated by DIRAC <sup>(2)</sup>. DIRAC showed that  $\hbar/i$  times the logarithm of the wave function for a system which is known to have had the coordinates  $q_0$  at time  $t_0$ , that is,

$$\frac{\hbar}{i} \ln \psi(q't) = \frac{\hbar}{i} \ln \langle q't | q'_0 t_0 \rangle = S_0,$$

behaves just like the generator of the canonical transformation which carries  $q_0$  into  $q$  if the momenta conjugate to  $q_0$  and  $q$  can be written as well-ordered functions of  $q$  and  $q_0$ . This, of course, is one of the important properties of Hamilton's principle function in classical mechanics. DIRAC also demonstrated that when the system is macroscopic so that  $S_0$  is large compared to  $\hbar$ , then the dynamical development follows a trajectory along which  $S_0$  is stationary.

A true Lagrangian formulation of quantum mechanics first appeared in the work of R. P. FEYNMAN <sup>(3)</sup> and J. SCHWINGER <sup>(4)</sup>. The equivalence of the two formulations was pointed out by F. J. DYSON <sup>(5)</sup>. FEYNMAN showed that the «sum over histories» representation for the transition amplitude is, namely,

$$(1) \quad \langle q'_0 t_0 | q'_1 t_1 \rangle = K_{01} \int_{q'_1}^{q'_0} \delta q' \exp \left[ \frac{i}{\hbar} S_{01}(q', \dot{q}') \right]$$

where

$$S_{01}(q', \dot{q}') = \int_{t_1}^{t_0} dt L(q'(t), \dot{q}'(t))$$

and

$$K_{01} = \text{a normalization constant,}$$

satisfies the Schrödinger equation when  $L$  has the form appropriate to a point mass moving in a potential field and the functional integration is suitably defined. We will refer to Eq. (1) as the Feynman dynamical principle.

<sup>(2)</sup> P. A. M. DIRAC: *Phys. Zeit. Sowjetunion*, **3**, 64 (1933); *Quantum Mechanics*, Sect. 32, third ed. (Oxford, 1947).

<sup>(3)</sup> R. P. FEYNMAN: *Rev. Mod. Phys.*, **20**, 367 (1948). See also: B. DAVISON *Proc. Roy. Soc., A* **225**, 252 (1954); P. T. MATTHEWS and A. SALAM: *Nuovo Cimento* **2**, 120 (1955).

<sup>(4)</sup> J. SCHWINGER: *Phys. Rev.*, **82**, 914 (1951); **91**, 713 (1953).

<sup>(5)</sup> F. J. DYSON: *Advanced Quantum Mechanics*, lecture notes, 1951.

SCHWINGER <sup>(4)</sup> derived the equations of the canonical formalism for quantum dynamics from his Lagrangian formulation. A similar derivation based on Feynman's Lagrangian formulation was carried out by J. C. POLKINGHORNE <sup>(5)</sup>. The most satisfactory justification of Feynman's Lagrangian formulation is that due to K. SYMANZIK <sup>(7)</sup>. SYMANZIK derived the Feynman principle by means of a functional Fourier analysis applied to the functional equations for the generator of the Green's functions.

In this paper we explore the connection between the Feynman functional integral and the quantum mechanical sum over histories. This is done by constructing the sum over histories expansion for the transition amplitude. In this way the functional integral expression for the transition amplitude is constructed from the usual canonical formalism by means of a straightforward limiting process. We find that the resulting expression has the form of the Feynman functional integral only when the Hamiltonian is classical in form and quantization is carried out in terms of commutators rather than anti-commutators.

In Sect. 2 the sum over histories expansion is constructed for a system which is quantized in terms of commutators. In Sects. 3 and 5 are found alternative constructions of the sum over histories expansion for a free Dirac field. In Sect. 4 we observe that there are representations for the state vectors and operators of the free Dirac field for which the Lagrangian formulation is invalid.

## 2. — Bose Quantization.

Let  $x(t)$  be the operator for the observable characterizing our system, and let  $p(t)$  be its canonical momentum. For the sake of simplicity we restrict ourselves to a system with one degree of freedom. The generalization to a system with  $n$  such degrees of freedom will be obvious. Let  $H(x, p)$  be the Hamiltonian for the system. Then the canonical formalism according to Bose quantization is based on the following fundamental equations:

$$(2) \quad \left\{ \begin{array}{ll} [H, p] = -i\dot{p} \\ [p, p] = 0 & [H, x] = -i\dot{x} \\ [x, x] = 0 & [p, x] = -i \\ h = c = 1. \end{array} \right.$$

All the operators appearing above have the same time argument. Let  $|q't\rangle$

<sup>(6)</sup> J. C. POLKINGHORNE: *Proc. Roy. Soc. (London)*, A **230**, 272 (1955).

<sup>(7)</sup> K. SYMANZIK: *Zeits. f. Naturf.*, **9a**, 809 (1954).

be the eigenstate of  $q(t)$  having the eigenvalue  $q'$ . Then from the canonical equations we can derive the following simple result,

$$(3) \quad \left\{ \begin{aligned} \langle p't + \Delta t | x't \rangle &= \langle p't | \exp [-iH(x, p)\Delta t] | x't \rangle \\ &= \exp [-iH(x', p')\Delta t] \langle p't | x't \rangle \\ &= \frac{1}{\sqrt{2\pi}} \exp [-i\{H(x', p')\Delta t + p'x'\}], \end{aligned} \right.$$

which holds to first order in  $\Delta t$ .

Our goal is to express the transition amplitude  $\langle x'_0 t_0 | x't \rangle$  as a sum over histories. We start by breaking the interval separating  $t_0$  and  $t$  into a large number of parts

$$t_0 > t_1 > t_2 > \dots > t_{N-1} > t_N = t$$

so that  $\Delta t = t_n - t_{n+1}$  is small. Then we expand the transition amplitude into a complete set of states at each interval

$$(4) \quad \langle x'_0 t_0 | x'_N t_N \rangle = \int dx'_1 dx'_2 \dots dx'_{N-1} \langle x'_0 t_0 | x'_1 t_1 \rangle \langle x'_1 t_1 | x'_2 t_2 \rangle \langle x'_2 t_2 | \dots \\ \dots | x'_{N-1} t_{N-1} \rangle \langle x'_{N-1} t_{N-1} | x'_N t_N \rangle.$$

Now take each factor of the integrand and expand it in terms of a complete set of momentum eigenstates

$$(5) \quad \langle x'_{n-1} t_{n-1} | x'_n t_n \rangle = \int dp'_n \left\langle x'_{n-1} t_n + \Delta t | p'_n t_n + \frac{\Delta t}{2} \right\rangle \left\langle p'_n t_n + \frac{\Delta t}{2} | x'_n t_n \right\rangle.$$

Then apply Eq. (3)

$$(6) \quad \langle x'_{n-1} t_{n-1} | x'_n t_n \rangle = \frac{1}{2\pi} \int dp'_n \exp \left[ i \left\{ p'_n \frac{(x'_{n-1} - x'_n)}{\Delta t} - \right. \right. \\ \left. \left. - \frac{H(x'_{n-1}, p'_n) + H(x'_n, p'_n)}{2} \right\} \Delta t \right]$$

Substituting this back into Eq. (4) and allowing  $N \rightarrow \infty$  in a manner that causes  $t_n - t_{n+1} = \Delta t \rightarrow 0$  gives

$$(7) \quad \langle x'_0 t_0 | x't \rangle = \lim_{N \rightarrow \infty} \int \frac{dp'_1}{2\pi} dx'_1 \frac{dp'_2}{2\pi} dx'_2 \dots dx'_{N-1} \frac{dp'_N}{2\pi} \\ \cdot \exp \left[ i \sum_{n=1}^N \Delta t \left\{ p'_n \frac{(x'_{n-1} - x'_n)}{\Delta t} - \frac{H(x'_{n-1}, p'_n) + H(x'_n, p'_n)}{2} \right\} \right] = \\ = \int_{x'}^{x'_0} \delta x'(t) \int \delta \left( \frac{p'(t)}{2\pi} \right) \exp \left[ i \int_{t'}^{t_0} dt \{ p' \dot{x}' - H(x', p') \} \right].$$



Thus we have succeeded in writing the transition amplitude in the form of a sum over histories. These histories correspond to classical trajectories in that the coordinate and momentum are specified at each instant. However these are not true classical trajectories since there is no relationship between velocity and momentum. Eq. (7) was derived by FEYNMAN<sup>(8)</sup> by means of a functional Fourier analysis. Our functional integral is the result of a limiting process in which each trajectory is specified with ever increasing detail.

If  $H(x', p')$  has the form

$$(8) \quad H(x', p') = \frac{p'^2}{2M} + p'B(x') + C(x'),$$

the integration over  $p$  can be performed with the result

$$(9) \quad \left\{ \begin{aligned} \langle x'_0 t_0 | x' t \rangle &= \lim_{N \rightarrow \infty} \left( \sqrt{\frac{M}{2\pi i \Delta t}} \right)^N \int dx'_1 dx'_2 \dots dx'_{N-1} \exp \left[ i \sum_{n=1}^N \Delta t L_n \right] \\ &= K \int \delta x' \exp \left[ i \int dt L(x', \dot{x}') \right], \end{aligned} \right.$$

where

$$(10) \quad L_n = \frac{M}{2} \frac{(x'_{n-1} - x'_n)^2}{(\Delta t)^2} + \frac{M}{2} \left[ \frac{B(x'_{n-1}) + B(x'_n)}{2} \right]^2 - \\ - M \frac{(x'_{n-1} - x'_n)}{\Delta t} \left[ \frac{B(x'_{n-1}) + B(x'_n)}{2} \right] - \frac{C(x'_{n-1})}{2} - \frac{C(x'_n)}{2}.$$

Eq. (9) is a sum over truly classical trajectories. Thus for the particular type of Hamiltonian shown in Eq. (8), the canonical formalism does lead to the Feynman principle. However this must be regarded as a special case of Eq. (7).

### 3. - Dirac Quantization.

Consider next the Dirac field  $\psi_\alpha(x)$ . Let  $\psi_\alpha^+(x)$  be the Hermitian conjugate field. The Hamiltonian density (in the charge symmetric theory) is

$$(11) \quad \mathcal{H}(x) = -\frac{1}{2} \psi^\dagger (i\boldsymbol{\alpha} \cdot \nabla - \beta m) \psi - \frac{1}{2} \psi (i\boldsymbol{\alpha}^T \cdot \nabla + \beta^T m) \psi^\dagger,$$

where

$$\{\alpha_j, \alpha_k\} = 2\delta_{jk}, \quad \{\alpha_j, \beta\} = 0, \quad \beta^2 = 1.$$

<sup>(8)</sup> R. P. FEYNMAN: *Phys. Rev.*, **84**, 108 (1951).

The canonical equations according to Dirac quantization are

$$(12) \quad \begin{cases} \{\psi_\alpha(x), \psi_\beta(y)\} = 0 \\ \{\psi_\alpha(x), \psi_\beta^\dagger(y)\} = \delta_{\alpha\beta} \delta(\mathbf{x} - \mathbf{y}) \\ [H, \psi_\beta(x)] = -i\dot{\psi}_\beta(x), \end{cases}$$

where

$$H = \int d^3x \mathcal{H}(x)$$

and all the operators have the same time argument. For our discussion it will be convenient to use the momentum space representation. In momentum space we have

$$(13) \quad \psi_\sigma(x) = \sum_{\mathbf{k}, r} a_r(\mathbf{k}, t) u_\sigma^{(r)}(\mathbf{k}) \frac{\exp[i\mathbf{k} \cdot \mathbf{x}]}{\sqrt{V}},$$

where

$$(\boldsymbol{\alpha} \cdot \mathbf{k} + \beta m) u^{(r)}(\mathbf{k}) = \omega_r(\mathbf{k}) u^{(r)}(\mathbf{k}) = \pm \sqrt{k^2 + m^2} u^{(r)}(\mathbf{k})$$

and

$$(14) \quad H = \int d^3x \mathcal{H}(x) = \sum_{\mathbf{k}, r} \frac{\omega_r(\mathbf{k})}{2} [a_r^+(\mathbf{k}) a_r(\mathbf{k}) - a_r(\mathbf{k}) a_r^+(\mathbf{k})].$$

The canonical equations in momentum space are

$$(15) \quad \begin{cases} \{a_r(\mathbf{k}, t), a_s^+(\mathbf{q}, t)\} = \delta_{rs} \delta(\mathbf{k} - \mathbf{q}) \\ \{a_r, a_s\} = 0 \\ [H, a_r] = -i\dot{a}_r. \end{cases}$$

To carry out our program of expressing the transition amplitude as a sum over histories we will need a representation in which the field operators are simultaneously diagonalized. Since  $a$  and  $a^+$  are not Hermitian operators, it is not convenient to work with them. Therefore we make the substitution(\*)

$$(16) \quad \begin{cases} \zeta_s = a_s^+ + a_s \\ \xi_s = i(a_s^+ - a_s). \end{cases}$$

---

(\*) From this point on we will lump the momentum coordinates with the spin coordinates in the subscript.

In terms of  $\zeta$  and  $\xi$  the Hamiltonian is

$$(17) \quad H = \sum_s \frac{\omega_s}{2} i \zeta_s \xi_s.$$

The commutation relations for  $\zeta$  and  $\xi$  are

$$(18) \quad \begin{cases} \{\zeta_r, \zeta_s\} = \{\xi_r, \xi_s\} = 2\delta_{rs}, \\ \{\zeta, \xi\} = 0. \end{cases}$$

Since the operators in this theory anti-commute with each other, they can be simultaneously diagonal only if their eigenvalues also anti-commute. Thus we must use for the base field of our Hilbert space a field which has a non-commutative algebra rather than the field of complex numbers. To be concrete, we will suppose that the matrix elements of our Hilbert space operators and the components of our Hilbert space vectors are not complex numbers but infinite dimensional matrices. In the usual occupation number representation the operators  $\zeta_s$  and  $\xi_s$  are represented by infinite dimensional matrices whose elements are restricted to the numbers 0, 1, and  $i = \sqrt{-1}$ : Let us represent these matrices by the symbols  $\hat{\zeta}_s$  and  $\hat{\xi}_s$ . We construct our operators  $\zeta_s$  and  $\xi_s$  from the matrices  $\hat{\zeta}_s$  and  $\hat{\xi}_s$  by replacing the numbers 0, 1, and  $i$  by the matrices

$$\mathbf{0} = \begin{pmatrix} 0 & 0 & 0 & . & . \\ 0 & 0 & 0 & . & . \\ 0 & 0 & 0 & . & . \\ . & . & . & . & . \end{pmatrix}, \quad \mathbf{1} = \begin{pmatrix} 1 & 0 & 0 & . & . \\ 0 & 1 & 0 & . & . \\ 0 & 0 & 1 & . & . \\ . & . & . & . & . \end{pmatrix} \text{ and } i\mathbf{1}.$$

The two eigenvalues of the operator  $\zeta$  will be represented by  $\zeta' = \pm \hat{\zeta}$  and the two eigenvalues of  $\xi$  will be  $\xi' = \pm \hat{\xi}$ . We will call the matrices like  $\zeta$  and  $\xi$ , whose elements are matrices, hypermatrices. The name hypervector will be used for vectors whose elements are matrices rather than complex numbers.

To provide a simple example of the construction described above let us assume that we are dealing with a Dirac field that has only 2 degrees of freedom instead of four spin degrees of freedom and  $\infty^3$  momentum degrees of freedom. It will be easy to generalize the results of this special example. In the case of 2 degrees of freedom we can represent  $\hat{\zeta}_1$ ,  $\hat{\xi}_1$ ,  $\hat{\zeta}_2$ , and  $\hat{\xi}_2$  by

$$\hat{\zeta}_2 = \begin{pmatrix} 0 & 0 & 1 & 0 \\ 0 & 0 & 0 & 1 \\ 1 & 0 & 0 & 0 \\ 0 & 1 & 0 & 0 \end{pmatrix}, \quad \hat{\xi}_2 = i \begin{pmatrix} 0 & 0 & -1 & 0 \\ 0 & 0 & 0 & -1 \\ 1 & 0 & 0 & 0 \\ 0 & 1 & 0 & 0 \end{pmatrix},$$

$$\hat{\zeta}_1 = \begin{pmatrix} 0 & 1 & 0 & 0 \\ 1 & 0 & 0 & 0 \\ 0 & 0 & 0 & -1 \\ 0 & 0 & -1 & 0 \end{pmatrix}, \quad \hat{\xi}_1 = i \begin{pmatrix} 0 & -1 & 0 & 0 \\ 1 & 0 & 0 & 0 \\ 0 & 0 & 0 & 1 \\ 0 & 0 & -1 & 0 \end{pmatrix}.$$

These matrices anticommute with each other and are square roots of the identity matrix. The hypermatrices  $\hat{\zeta}_1$ ,  $\hat{\xi}_1$ ,  $\hat{\zeta}_2$ , and  $\hat{\xi}_2$  are constructed from  $\hat{\zeta}_1$ ,  $\hat{\xi}_1$ ,  $\hat{\zeta}_2$ , and  $\hat{\xi}_2$  by replacing the elements by the appropriate  $4 \times 4$  matrix. Thus, for example, the hypermatrix for  $\hat{\xi}_1$  is

$$\xi_1 = i \begin{pmatrix} 0 & -\mathbf{1} & 0 & 0 \\ \mathbf{1} & 0 & 0 & 0 \\ 0 & 0 & 0 & \mathbf{1} \\ 0 & 0 & -\mathbf{1} & 0 \end{pmatrix}$$

where

$$\mathbf{1} = \begin{pmatrix} 1 & 0 & 0 & 0 \\ 0 & 1 & 0 & 0 \\ 0 & 0 & 1 & 0 \\ 0 & 0 & 0 & 1 \end{pmatrix} \quad \text{and} \quad \mathbf{0} = \begin{pmatrix} 0 & 0 & 0 & 0 \\ 0 & 0 & 0 & 0 \\ 0 & 0 & 0 & 0 \\ 0 & 0 & 0 & 0 \end{pmatrix}.$$

The hypermatrices  $\hat{\zeta}_1$  and  $\hat{\zeta}_2$  have the four orthogonal simultaneous eigenvectors

$$(20) \quad |\zeta'_1 \zeta'_2\rangle = \frac{1}{\sqrt{2^2}} \begin{pmatrix} \mathbf{1} \\ \zeta'_1 \\ \zeta'_2 \\ \zeta'_2 \zeta'_1 \end{pmatrix}.$$

Similarly, the hypermatrices  $\hat{\xi}_1$  and  $\hat{\xi}_2$  have the four orthogonal simultaneous eigenvectors

$$(21) \quad |\xi'_1 \xi'_2\rangle = \frac{1}{\sqrt{2^2}} \begin{pmatrix} \mathbf{1} \\ i\xi'_1 \\ i\xi'_2 \\ -\xi'_2 \xi'_1 \end{pmatrix}.$$

Each of these two sets of four hypervectors constitute a complete basis of the



Hilbert hyperspace. The transition amplitude from one representation to the other is just

$$\langle \zeta'_1 \zeta'_2 | \xi'_1 \xi'_2 \rangle = \frac{1}{2^2} (\mathbf{1} + i \zeta'_1 \xi'_1) (\mathbf{1} + i \zeta'_2 \xi'_2).$$

To construct the corresponding quantities for the case of  $n+1$  degrees of freedom from the  $n$  degrees of freedom case we use the following simple algorithms

$$(22) \quad \left\{ \begin{array}{l} \hat{\zeta}_j^{(n+1)} = \begin{pmatrix} \hat{\zeta}_j^{(n)} & \mathbf{0}^{(n)} \\ \mathbf{0}^{(n)} & -\hat{\zeta}_j^{(n)} \end{pmatrix} \quad \hat{\xi}_j^{(n+1)} = \begin{pmatrix} \hat{\xi}_j^{(n)} & \mathbf{0}^{(n)} \\ \mathbf{0}^{(n)} & -\hat{\xi}_j^{(n)} \end{pmatrix} \\ \hat{\zeta}_{n+1}^{(n+1)} = \begin{pmatrix} \mathbf{0}^{(n)} & \mathbf{1}^{(n)} \\ \mathbf{1}^{(n)} & \mathbf{0}^{(n)} \end{pmatrix} \quad \hat{\xi}_{n+1}^{(n+1)} = i \begin{pmatrix} \mathbf{0}^{(n)} & -\mathbf{1}^{(n)} \\ \mathbf{1}^{(n)} & \mathbf{0}^{(n)} \end{pmatrix} \end{array} \right. \quad j \leq n,$$

$$(23) \quad |\zeta'_1 \dots \zeta'_{n+1}\rangle = \frac{1}{\sqrt{2}} \begin{pmatrix} |\zeta'_1 \dots \zeta'_n\rangle \\ \zeta'_{n+1} |\zeta'_1 \dots \zeta'_n\rangle \end{pmatrix} \quad |\xi'_1 \dots \xi'_{n+1}\rangle = \frac{1}{\sqrt{2}} \begin{pmatrix} |\xi'_1 \dots \xi'_n\rangle \\ i \xi'_{n+1} |\xi'_1 \dots \xi'_n\rangle \end{pmatrix}$$

$$(24) \quad \langle \zeta'_1 \dots \zeta'_{n+1} | \xi'_1 \dots \xi'_{n+1} \rangle = \frac{1}{2} (\mathbf{1} + i \zeta'_{n+1} \xi'_{n+1}) \langle \zeta'_1 \dots \zeta'_n | \xi'_1 \dots \xi'_n \rangle = \prod_{s=1}^{n+1} \frac{1}{2} (\mathbf{1} + i \zeta'_s \xi'_s),$$

where the quantities bearing the superscript  $(m)$  are  $2^m$ -dimensional matrices (\*). For the construction of the sum over histories we will need the infinite dimensional analogue of Eq. (24), namely,

$$(25) \quad \langle \zeta' | \xi' \rangle = \langle \zeta'_1 \zeta'_2 \dots | \xi'_1 \xi'_2 \dots \rangle = \prod_{s=1}^{\infty} \frac{1}{2} (\mathbf{1} + i \zeta'_s \xi'_s) = \langle \xi' | \zeta' \rangle,$$

where  $s$  ranges over all possible combinations of spin and momentum variables. We will also need the matrix element of the Hamiltonian.

$$(26) \quad \left\{ \begin{array}{l} \langle \zeta' | H | \xi' \rangle = \sum_s \frac{\omega_s}{2} \langle \zeta' | i \zeta'_s \xi'_s | \xi' \rangle \\ \quad = - \sum_s \frac{\omega_s}{2} \frac{(\mathbf{1} - i \zeta'_s \xi'_s)}{2} \prod_{r \neq s} \frac{1}{2} (\mathbf{1} + i \zeta'_r \xi'_r) \\ \quad = \langle \xi' | H | \zeta' \rangle. \end{array} \right.$$

(\*) For some applications it is of interest to have matrices which anti-commute with all the matrices  $\hat{\zeta}_j^{(n)}$  and  $\hat{\xi}_j^{(n)}$ . For a given value of  $n$  this can be done by introducing  $\hat{\zeta}_{n+1}^{(n+1)}$ ,  $\hat{\zeta}_{n+1}^{(n+1)}$ ,  $\hat{\xi}_{n+2}^{(n+2)}$  etc., by increasing the size of the matrices representing the  $\hat{\zeta}_j$  and  $\hat{\xi}_j$ . If we need only one quantity which anti-commutes with all the  $\hat{\zeta}_j$  and  $\hat{\xi}_j$ , it is not necessary to enlarge the algebra since  $\prod_j \hat{\zeta}_j \hat{\xi}_j$  will serve the purpose.

We proceed in the construction of the sum over histories as we did in the Bose case

$$(27) \quad \langle \zeta'(0)t_0 | \zeta'(N)t_N \rangle = \sum_{\zeta'(1), \zeta'(2), \dots, \zeta'(N-1)} \langle \zeta'(0)t_0 | \zeta'(1)t_1 \rangle \langle \zeta'(1)t_1 | \dots \\ \dots | \zeta'(N-1)t_{N-1} \rangle \langle \zeta'(N-1)t_{N-1} | \zeta'(N)t_N \rangle,$$

where  $N$  is a very large integer and  $\Delta t = t_n - t_{n+1}$  is very small. Next expand each factor on the left side of Eq. (27) as follows:

$$(28) \quad \left\{ \begin{aligned} \langle \zeta'(r-1)t + \Delta t | \zeta'(r)t \rangle &= \\ &= \sum_{\xi'(r)} \langle \zeta'(r-1)t + \Delta t | \xi'(r)t + \frac{\Delta t}{2} \rangle \langle \xi'(r)t + \frac{\Delta t}{2} | \zeta'(r)t \rangle \\ &= \sum_{\xi'(r)} \langle \zeta'(r-1) | \mathbf{1} - i \frac{\Delta t}{2} H | \xi'(r) \rangle \langle \xi'(r) | \mathbf{1} - i \frac{\Delta t}{2} H | \zeta'(r) \rangle. \end{aligned} \right.$$

By using Eqs. (25) and (26) to get explicit representations for the matrix elements we find:

$$(29) \quad \langle \zeta'(r-1)t + \Delta t | \zeta'(r)t \rangle = \sum_{\xi'(r)} \prod_s \frac{1}{4} \left\{ (\mathbf{1} + \zeta'_s(r-1)\zeta'_s(r)) + \right. \\ \left. + i(\zeta'_s(r-1) + \zeta'_s(r))\xi'_s(r) + i\Delta t \frac{\omega_s}{2} (\mathbf{1} - \zeta'_s(r-1)\zeta'_s(r)) \right\}.$$

Since each  $\xi'_s(r)$  assumes the values  $\pm \xi_s$  in the summation, the sum is easily performed by changing the order of  $\Pi$  and  $\Sigma$ . The result is merely to eliminate the second term and introduce a factor 2.

$$(30) \quad \langle \zeta'(r-1)t + \Delta t | \zeta'(r)t \rangle = \\ = \prod_s \frac{1}{2} \left\{ (\mathbf{1} + \zeta'_s(r-1)\zeta'_s(r)) + i\Delta t \frac{\omega_s}{2} (\mathbf{1} - \zeta'_s(r-1)\zeta'_s(r)) \right\}.$$

Eqs. (27) and (30) define (in the limit  $\Delta t \rightarrow 0$ ) the sum over histories representation for the transition amplitude  $\langle \zeta'(0)t_0 | \zeta'(N)t_N \rangle$ . The right side of Eq. (30) does not have the form of an exponential. Thus the procedure which yields the Feynman principle in the case of Bose quantization leads to something quite different in the Dirac case.

The sum over histories has such a simple form in the Dirac case that the sum is easily performed.

Let us make the following simplifications in notation:

$$(31) \quad \begin{cases} \nu^{(s)} = \frac{1}{2} i \Delta t \omega_s \\ A_{\alpha\beta}^{(s)} = \frac{1}{2} (\mathbf{1} + \zeta_s'(\alpha) \zeta_s'(\beta)) \\ B_{\alpha\beta}^{(s)} = \frac{1}{2} (\mathbf{1} - \zeta_s'(\alpha) \zeta_s'(\beta)) \end{cases}$$

Since  $\zeta_s' = \pm \hat{\zeta}_s$  and  $\hat{\zeta}_s^2 = \mathbf{1}$ ,  $A$  and  $B$  can be only  $\mathbf{1}$  or  $\mathbf{0}$ . Also let us define the operation

$$(32) \quad A_{\alpha\beta}^{(s)} \circ B_{\alpha\beta}^{(s)} = \sum_{\zeta_s'(\beta) = \pm \hat{\zeta}_s} A_{\alpha\beta}^{(s)} B_{\alpha\beta}^{(s)}.$$

Then Eq. (30) becomes

$$(30A) \quad \langle \zeta'(r-1)t + \Delta t | \zeta'(r)t \rangle = \prod_s \{ A_{r-1r}^{(s)} + \nu^{(s)} B_{r-1r}^{(s)} \},$$

and combining this with Eq. (27) we have

$$(30) \quad \langle \zeta'(0)t_0 | \zeta'(N)t_N \rangle = \prod_s \{ A_{01}^{(s)} + \nu^{(s)} B_{01}^{(s)} \} \circ \{ A_{12}^{(s)} + \nu^{(s)} B_{12}^{(s)} \} \circ \dots \circ \{ A_{N-1N}^{(s)} + \nu^{(s)} B_{N-1N}^{(s)} \}.$$

The product in Eq. (33) can be evaluated with the help of the following multiplication table for the operation defined by Eq. (32).

$U_{\alpha\beta} \circ W_{\beta\gamma}$	$A_{\beta\gamma}$	$B_{\beta\gamma}$
$A_{\alpha\beta}$	$A_{\alpha\gamma}$	$B_{\alpha\gamma}$
$B_{\alpha\beta}$	$B_{\alpha\gamma}$	$A_{\alpha\gamma}$

The result is

$$(34) \quad \langle \zeta'(0)t_0 | \zeta'(N)t_N \rangle = \prod_s (A_{0N}^{(s)} V_N^{(s)} + B_{0N}^{(s)} W_N^{(s)})$$

where

$$(35) \quad V_n = \sum_{m=0} S_1^{2m-1}(n+1-2m) \nu^{2m}, \quad W_n = \sum_{m=0} S_1^{2m}(n-2m) \nu^{2m+1}$$

and

$$(36) \quad S_r^m(n) = \sum_{\alpha_m=1}^n \sum_{\alpha_{m-1}=1}^{\alpha_m} \dots \sum_{\alpha_1=1}^{\alpha_2} (\alpha_1)^r.$$

The function  $S_r^m(n)$  defined above can be shown <sup>(9)</sup> to satisfy the following

<sup>(9)</sup> G. CHRYSTAL: *Algebra*, chap. XX (London, 1904).

recursion relation

$$(37) \quad (r+1)S_r^m(n) = S_{r+1}^{m-1}(n+1) - S_1^{m-2}(n+1) - \sum_{\lambda=0}^{r-1} \frac{(r+1)!}{\lambda! (r+1-\lambda)!} S_\lambda^m(n),$$

when we set  $S_r^{-1}(n) = 1$  and  $S_r^0(n) = n^r$ . From eq. (37) we can easily show that

$$(38) \quad S_r^m(n) \xrightarrow{n \rightarrow \infty} \frac{r!}{(r+m)!} n^{r+m}.$$

Thus in the limit as  $n \rightarrow \infty$ , Eq. (35) becomes

$$(39) \quad \left\{ \begin{array}{ll} V_n \rightarrow \sum_{m=0} \frac{(n\nu)^{2m}}{(2m)!}, & W_n \rightarrow \sum_{m=0} \frac{(n\nu)^{2m+1}}{(2m+1)!}, \\ \rightarrow \cos \frac{\omega}{2} (t_0 - t_N), & \rightarrow i \sin \frac{\omega}{2} (t_0 - t_N). \end{array} \right.$$

Combining Eqs. (31), (34), and (39) gives us our final result

$$\langle \zeta' t_0 | \zeta'' t_1 \rangle = \prod_s \frac{1}{2} \left\{ \mathbf{1} \exp \left[ i \frac{\omega_s}{2} (t_0 - t_1) \right] + \zeta_s' \zeta_s'' \exp \left[ -i \frac{\omega_s}{2} (t_0 - t_1) \right] \right\}.$$

Of course, the physical results of the theory are usually expressed in terms of matrix elements involving the eigenstates of the number operator. However, they can also be expressed in terms of the eigenstates of  $\zeta$  since these are related in a simple way to the eigenstates of the number operator. In fact the one column matrix representation for the eigenhypervectors of  $\zeta$  and  $\xi$  given by Eqs. (20), (21) and (23) is a representation in occupation number space. Thus in the 2 degrees of freedom case we have,

$$\text{the vacuum state} = |0\rangle = \begin{pmatrix} \mathbf{1} \\ \mathbf{0} \\ \mathbf{0} \\ \mathbf{0} \end{pmatrix}$$

$$\text{the state when there is a particle in cell 1} = \frac{1}{2}(\zeta_1 - i\xi_1)|0\rangle = \begin{pmatrix} \mathbf{0} \\ \mathbf{1} \\ \mathbf{0} \\ \mathbf{0} \end{pmatrix}$$

etc.

In the  $N$ -dimensional case let us represent the state in which there are  $n_i$



particles in the  $i$ 'th cell ( $n_i = 0, 1$ ) by the hypervector

$$n_1 n_2 \dots \rangle = (a_1^+)^{n_1} (a_2^+)^{n_2} \dots |0\rangle = \frac{(\zeta_1 - i\xi_1)^{n_1}}{2} \frac{(\zeta_2 - i\xi_2)^{n_2}}{2} \dots |0\rangle.$$

Then the transition amplitudes connecting the several representations are

$$\langle n_1 n_2 \dots | \zeta' \rangle = \frac{1}{\sqrt{2^N}} (\zeta'_1)^{n_1} (\zeta'_2)^{n_2} \dots (\zeta'_N)^{n_N},$$

$$\langle n_1 n_2 \dots | \xi' \rangle = \frac{1}{\sqrt{2^N}} (i\xi'_1)^{n_1} (i\xi'_2)^{n_2} \dots (i\xi'_N)^{n_N},$$

$$\langle \zeta' | \xi' \rangle = \frac{1}{2^N} (\mathbf{1} + i\zeta'_1 \xi'_1) (\mathbf{1} + i\zeta'_2 \xi'_2) \dots (\mathbf{1} + i\zeta'_N \xi'_N).$$

#### 4. - Disagreement with the Lagrangian Formulation.

We have seen that the sum over histories expression for the transition amplitude between eigenstates of  $\zeta_s = a_s^+ + a_s$  and  $\xi_s = i(a_s^+ - a_s)$  does not involve the exponential of the action  $S = \int L dt$ . Thus the sum over histories does not provide a Lagrangian formulation of the dynamics of the Dirac field. In this connection it is of interest to note that our description of the Dirac field, based on the canonical formalism, does not obey the fundamental assumption of Schwinger's Lagrangian formulation.

Schwinger's Lagrangian formulation postulates that the generators of infinitesimal transformations are the momenta conjugate to the operators involved. Thus it is assumed that, say, for a point mass in one dimension

$$(41) \quad (1 - ip\delta x') |x'\rangle = |x' + \delta x'\rangle.$$

For the Dirac field the operator conjugate to  $\zeta$  is  $i\zeta/2$  so that according to the Lagrangian formulation

$$(42) \quad (1 + \frac{1}{2} \sum_s \zeta_s \delta \zeta'_s) |\zeta'\rangle = |\zeta' + \delta \zeta'\rangle.$$

In the above expression  $\delta \zeta'_s$  is a quantity which anti-commutes with all the eigenvalues  $\zeta'_s$  and  $\xi'_s$ . However a direct calculation yields the following result

$$(43) \quad (1 + \frac{1}{2} \sum_s \zeta_s \delta \zeta'_s) |\zeta'\rangle = |\zeta' + \delta \zeta'\rangle (1 - \frac{1}{2} \sum_s \xi'_s \delta \xi'_s).$$

Suppose we had constructed a representation of the Bose commutation relations:

$$(44) \quad [px] = -i, \quad [pp] = [xx] = 0.$$

Then a calculation like the one referred to above would yield in general

$$(45) \quad (1 - ip \delta x') |x'\rangle = |x' + \delta x'\rangle (1 + if(x') \delta x'),$$

which can be written

$$(46) \quad (1 - i[p + f(x')] \delta x') |x'\rangle = |x' + \delta x'\rangle.$$

Now the quantity  $p + f(x')$  satisfies the same commutation relations as  $p$  and so can replace  $p$  as a representation for the conjugate of  $x$ . Thus for all practical purposes Eq. (44), the canonical equations, are equivalent to Eq. (41), the Lagrangian equation.

Returning to Eq. (43) we see that there is no way of making a change of representation that will convert it to Eq. (42). The reason is that the operator  $\zeta_s$  on the left side of Eqs. (42) and (43) can be replaced by  $\zeta'_s$  since it operates on an eigenvector. Thus these equations do not really involve operators and are therefore quite independent of how the operators are represented.

Let us say the same thing in slightly different words. We could, if we like, construct an operator  $\bar{\zeta}_s$  which has the same commutation properties as  $\zeta_s$  and which in addition generates displacements of the eigenvector  $|\zeta'\rangle$ . However  $|\zeta'\rangle$  will not be the eigenvector of such an operator so that we still do not arrive at the Lagrangian formalism postulate, Eq. (42).

## 5. - Alternate Formulation for the Dirac Field.

In this section we will construct a sum over histories for the Dirac field in terms of eigenstates of the annihilation and creation operators  $a_s$  and  $a_s^\dagger$ . This representation is similar to that used by SCHWINGER<sup>(10)</sup>. We will find that in spite of the fact that the Lagrangian postulate that momenta generate displacements is true in this representation, we still do not get the Feynman type of sum over histories.

For the sake of simplicity we will assume our system has only one degree of freedom. Then there will only be two eigenstates of the number operator  $a^\dagger a$ : the vacuum state and the one particle state. The restriction to one degree of

<sup>(10)</sup> J. SCHWINGER: *Phys. Rev.*, **92**, 1283 (1953).

freedom entails no real loss of generality since a representation for  $N$  degrees of freedom is provided by the outer product of  $N$  one degree of freedom representations.

The base field for our Hilbert space will be  $4 \times 4$  matrices of complex numbers. We define the following symbols:

$$(47) \quad \left\{ \begin{array}{l} \hat{a} = \begin{pmatrix} 0 & 1 & 0 & 0 \\ 0 & 0 & 0 & 0 \\ 0 & 0 & 0 & -1 \\ 0 & 0 & 0 & 0 \end{pmatrix} \quad \hat{a}^\dagger = \begin{pmatrix} 0 & 0 & 0 & 0 \\ 1 & 0 & 0 & 0 \\ 0 & 0 & 0 & 0 \\ 0 & 0 & -1 & 0 \end{pmatrix} \quad \mathbf{0} = \begin{pmatrix} 0 & 0 & 0 & 0 \\ 0 & 0 & 0 & 0 \\ 0 & 0 & 0 & 0 \\ 0 & 0 & 0 & 0 \end{pmatrix} \\ \hat{b} = \begin{pmatrix} 0 & 0 & 1 & 0 \\ 0 & 0 & 0 & 1 \\ 1 & 0 & 0 & 0 \\ 0 & 1 & 0 & 0 \end{pmatrix} \quad \hat{c} = i \begin{pmatrix} 0 & 0 & -1 & 0 \\ 0 & 0 & 0 & -1 \\ 1 & 0 & 0 & 0 \\ 0 & 1 & 0 & 0 \end{pmatrix} \quad \mathbf{1} = \begin{pmatrix} 1 & 0 & 0 & 0 \\ 0 & 1 & 0 & 0 \\ 0 & 0 & 1 & 0 \\ 0 & 0 & 0 & 1 \end{pmatrix} \end{array} \right.$$

We represent the Dirac field operators by

$$(48) \quad a = \begin{pmatrix} \mathbf{0} & \hat{b} \\ \mathbf{0} & \mathbf{0} \end{pmatrix} \quad a^\dagger = \begin{pmatrix} \mathbf{0} & \mathbf{0} \\ \hat{b} & \mathbf{0} \end{pmatrix}.$$

The factor  $\hat{b}$  has been introduced so that the operators will anti-commute with their eigenvalues. These operators have the eigenstates

$$(49) \quad \left\{ \begin{array}{l} |\hat{\hat{b}}\hat{\hat{a}}\rangle = \begin{pmatrix} \hat{\hat{a}}^\dagger \\ \hat{\hat{a}}^\dagger \hat{\hat{a}} \end{pmatrix} \quad |\hat{\hat{b}}\hat{\hat{a}}\rangle^+ = \begin{pmatrix} \hat{\hat{a}}^\dagger \hat{\hat{a}} \\ \hat{\hat{a}}^\dagger \end{pmatrix} \\ |\hat{\hat{b}}\hat{\hat{a}}^+\rangle = \begin{pmatrix} \hat{\hat{a}} \\ \hat{\hat{a}} \hat{\hat{a}}^\dagger \end{pmatrix} \quad |\hat{\hat{b}}\hat{\hat{a}}^+\rangle^\dagger = \begin{pmatrix} \hat{\hat{a}} \hat{\hat{a}}^\dagger \\ \hat{\hat{a}} \end{pmatrix}, \end{array} \right.$$

where the eigenvalue equation now has the form

$$(50) \quad a |\hat{\hat{b}}\hat{\hat{a}}\rangle = \hat{\hat{b}} |\hat{\hat{b}}\hat{\hat{a}}\rangle \hat{\hat{a}}, \quad a^\dagger |\hat{\hat{b}}\hat{\hat{a}}\rangle^+ = \hat{\hat{b}} |\hat{\hat{b}}\hat{\hat{a}}\rangle^+ \hat{\hat{a}}, \quad \hat{\hat{a}} = \hat{\hat{a}}, \hat{\hat{a}}^\dagger.$$

Each pair of eigenstates forms a complete orthonormal set. The Hamiltonian is

$$(51) \quad H = \frac{\omega}{2} (a^\dagger a - a a^\dagger) = H(a).$$

The sum over histories is particularly easy to get in this representation because the matrix element of  $H(a)$  between two eigenstates of  $a$  is quite simple.

$$(52) \quad \langle \hat{b}\hat{g}_1 | H(a) | \hat{b}\hat{g}_2 \rangle = \delta_{12} H(\hat{g}_1).$$

Thus

$$(53) \quad \langle \hat{b}\hat{g}_1 t + \Delta t | \hat{b}\hat{g}_2 t \rangle = \langle \hat{b}\hat{g}_1 | 1 - H(a) \Delta t | \hat{b}\hat{g}_2 \rangle \\ = \delta_{12} (1 - iH(\hat{g}_1) \Delta t).$$

Finally,

$$(54) \quad \langle \hat{b}\hat{g}_0 t_0 | \hat{b}\hat{g}_N t_N \rangle = \sum_{\substack{\hat{a}_1, \hat{a}_2, \dots, \hat{a}_N \\ \hat{g}_1, \hat{g}_2, \dots, \hat{g}_N}} \langle \hat{b}\hat{g}_0 t_0 | \hat{b}\hat{g}_1 t_1 \rangle \langle \hat{b}\hat{g}_1 t_1 | \dots | \hat{b}\hat{g}_N t_N \rangle \\ = \delta_{0,N} \exp[-iH(\hat{g}_0)(t_0 - t_N)].$$

We see that since the Hamiltonian is diagonal in this representation, the sum over histories reduces to one history.

We end by showing that  $-ia^+$ , the canonical conjugate to  $a$ , does generate displacements in the eigenstates of  $a$ .

$$(55) \quad (1 - a^+ \delta \hat{a}) | \hat{b}\hat{a} \rangle = \begin{pmatrix} \hat{a}^+ \\ \hat{b} \delta \hat{a} \hat{a}^+ + \hat{a}^+ \hat{a} \end{pmatrix}.$$

Now in order that  $\delta \hat{a}$  anti-commute with eigenvalues as well as with operators we write

$$\delta \hat{a} = \hat{b} \hat{c} \delta \varepsilon,$$

where  $\delta \varepsilon$  is a small complex number. Then Eq. (55) becomes

$$(56) \quad (1 - a^+ \hat{b} \hat{c} \delta \varepsilon) | \hat{b}\hat{a} \rangle = \begin{pmatrix} \hat{a}^+ \\ a^+ (\hat{a} + \hat{c} \delta \varepsilon) \end{pmatrix} \\ = | \hat{b}(\hat{a} + \hat{c} \delta \varepsilon) \rangle \\ = | \hat{b}\hat{a} + \hat{b}\hat{c} \delta \varepsilon \rangle.$$

\* \* \*

The author is indebted to many people, particularly Drs. G. FELDMAN, R. L. ARNOWITT, R. UTIYAMA, and C. N. YANG, for helpful discussions on the subject matter of this paper. I also wish to thank Professor J. R. OPPENHEIMER and the Institute for Advanced Study for the hospitality which has been extended to me.



## RIASSUNTO (\*)

Sulla base del formalismo canonico della meccanica quantistica si costruiscono per l'ampiezza di trasmissione espressioni composte da somme esplicite sulle storie. Si può dimostrare che la somma sulle storie coincide col principio di Feynman quando l'hamiltoniana ha la forma classica e la quantizzazione si esegue in termini dei commutatori degli operatori. In generale la somma sulle storie differisce alquanto dall'integrale funzionale di Feynman ma comprende ancora l'esponentiale dell'azione  $S = \int (p\dot{x} - H) dt$ . Tuttavia, per il campo di Dirac, in cui l'indipendenza dinamica implica l'anticommutatività degli operatori, la somma sulle storie che costruiamo ha forma completamente differente dal principio di Feynman.

(\*) *Traduzione a cura della Redazione.*

## Kopplung nichtrelativistischer Teilchen mit einem quantisierten Feld.

### 1. Das Exziton im schwingenden, polaren Kristall.

H. HAKEN

*Institut für Theoretische Physik der Universität - Erlangen*

(ricevuto il 20 Febbraio 1956)

**Zusammenfassung.** — Es werden die stationären Zustände eines Exzitons (Elektron-Defektelektron-Paares) im schwingenden Gitter mit einem für eine beliebige Stärke der Kopplung zwischen Einzelteilchen und Gitterschwingungen brauchbaren, angenäherten Variationsverfahren bestimmt, wobei die Einteilchenlösungen im schwingenden Gitter als bekannt vorausgesetzt werden. Die Gültigkeit des Verfahrens für genügend große Exzitonenradien wird ausführlich nachgewiesen. Auf die Anwendbarkeit der Methode zur nichtrelativistischen Behandlung der Kopplung von Nukleonen über ein Mesonenfeld (im divergenzfreien Fall) wird hingewiesen.

### 1. — Einleitung.

Die Wechselwirkung von Teilchen mit einem quantisierten Feld tritt in verschiedenen Gebieten der Physik entgegen. Einmal nennen wir hier die Quantenfeldtheorie, wo neben der Quantenelektrodynamik in letzter Zeit besonders die Mesonentheorie mit ihrer Behandlung der Wechselwirkung zwischen Nukleonen und Mesonen <sup>(1)</sup> in den Vordergrund des Interesses getreten ist. Zum anderen möchten wir die Wechselwirkung zwischen Elektronen und Gitterschwingungen im festen Körper hervorheben. Als ein wesentlicher Zug b

---

<sup>(1)</sup> Eine zusammenfassende Darstellung findet sich etwa bei H. A. BETHE u. F. DE HOFFMANN: *Mesons and Fields* (New York, 1955), vol. II.

der Behandlung der Wechselwirkung zwischen Teilchen und Feld erscheint die Tatsache, daß die Kopplung in vielen Fällen so stark ist, daß die geläufige störungstheoretische Methode versagt und daher neue mathematische Methoden zu entwickeln sind, wie sie beispielsweise in der Tamm-Dancoff-Methode <sup>(2)</sup> oder in Tomonagas Methode <sup>(3)</sup> der mittelstarken Kopplung vorliegen. Das Schwergewicht derartiger Untersuchungen lag bisher bei der Entwicklung und Erprobung neuer Verfahren für den Fall *eines* Teilchens in Wechselwirkung mit einem quantisierten Feld. In dem wohl einfachsten Falle — nicht-relativistisches Teilchen in skalarer Wechselwirkung mit einem skalaren Feld — sind diese Lösungsmethoden, speziell auch im Hinblick auf das Polaronenproblem der Festkörperphysik, besonders weit vorangetrieben worden <sup>(4)</sup>. Nachdem hier die Bereiche schwacher bis mittlerer sowie starker Kopplung bereits seit einiger Zeit brauchbar behandelt worden sind <sup>(5)</sup>, lassen es die Lösungsansätze von HÖHLER <sup>(6)</sup> und von FEYNMAN <sup>(7)</sup> erhoffen, daß auch der Bereich mittlerer bis starker Kopplung bald befriedigend behandelt werden kann.

In der vorliegenden Arbeit soll unter der Annahme, daß das Problem der Wechselwirkung eines nichtrelativistischen Teilchens mit dem quantisierten Feld bereits gelöst ist, die Wechselwirkung mehrerer solcher Teilchen mit dem quantisierten Feld untersucht werden. Der wichtigste Gesichtspunkt bei einem derartigen Problem ist, wie bekannt, dadurch gegeben, daß durch die Wechselwirkung der Teilchen mit dem Feld eine direkte Wechselwirkung zwischen den Teilchen selbst geschaffen wird. Wir werden uns deshalb besonders der Untersuchung dieser direkten Wechselwirkung widmen, wobei wir sogleich mit dem konkreten Beispiel des Exzitons im schwingenden Gitter, also mit einem Zweiteilchenproblem beginnen. Dieses Beispiel hat vor allem den Vorteil, daß wir die Einteilchenlösungen, wenigstens in der Kontinuumsnäherung, bereits (wie schon hervorgehoben) ziemlich genau kennen. Das im folgenden zu beschreibende Verfahren läßt sich ohne weiteres auch auf *mehrere* Teilchen ausdehnen.

<sup>(2)</sup> I. TAMM: *Journ. Phys. USSR*, **9**, 449 (1950); S. M. DANCOFF: *Phys. Rev.*, **78**, 382 (1950).

<sup>(3)</sup> S. TOMONAGA: *Prog. Theor. Phys.*, **2**, 6 (1947).

<sup>(4)</sup> Zusammenfassende Darstellungen bei H. FRÖHLICH: *Advances in Physics*, **3**, 325 (1954); H. HAKEN: Bericht in *Halbleiterprobleme*, II, herausgegeben von W. SCHOTTKY (Braunschweig, 1955).

<sup>(5)</sup> Wir nennen hier vor allem: H. FRÖHLICH, H. PELZER und S. ZIENAU: *Phil. Mag.*, **41**, 221 (1951); T. LEE, F. LOW und D. PINES: *Phys. Rev.*, **90**, 197 (1953); M. GURARI: *Phil. Mag.*, **44**, 329 (1953); S. V. TJABLIKOV: *Žu. Eksper. Teor. Fiz.*, **25**, 688 (1953); S. J. PEKAR: *Untersuchungen über die Elektronentheorie der Kristalle* (Berlin, 1953) (Deutsche Übersetzung).

<sup>(6)</sup> G. HÖHLER: *Zeits. f. Naturf.*, **9a**, 801 (1954); *Zeits. f. Phys.*, **140**, 192 (1955); *Nuovo Cimento*, **2**, 691 (1955).

<sup>(7)</sup> R. P. FEYNMAN: *Phys. Rev.*, **97**, 660 (1955).

## 2. — Das Exziton im schwingenden Gitter.

Der von FRENKEL<sup>(8)</sup> eingeführte Begriff des Exzitons, der einen Energie-transport ohne gleichzeitigen Ladungstransport wie auch feinere Züge der Eigenabsorption der Kristalle verständlich macht, ist für den Fall des ruhenden Gitters bereits vor langem von WANNIER<sup>(9)</sup> in die Begriffsbildungen des Bändermodells eingebaut worden. Nach dieser Wannierschen Vorstellung besteht das Exziton aus einem Elektron und einem Defektelektron, die einander auf einer wasserstoffähnlichen Bahn umkreisen. Die Wechselwirkung des Exzitons mit den Gitterschwingungen, die in den polaren Kristallen besonders stark ausgeprägt ist, wurde, von einigen ersten Ansätzen<sup>(10)</sup> abgesehen, erst vor kurzem von H. J. G. MEYER<sup>(11)</sup> behandelt. MEYER läßt die Gitterdeformation (bzw. die Polarisierung des Kristalls) der Bewegung des Exzitons pauschal folgen, wobei er die über das Polarisationsfeld geschaffene Wechselwirkung zwischen Elektron und Defektelektron wenigstens teilweise erfaßt.

Die folgende Untersuchung bringt eine Verbesserung dieses Ansatzes mit sich und hat, wie uns scheint, außerdem den Vorzug, daß sie die anschaulichen « Teilchen-Aspekte » besonders deutlich hervortreten läßt. Als diese « anschaulichen Aspekte » sehen wir insbesondere die beiden folgenden an:

Der erste betrifft die direkte Wechselwirkung zwischen Elektron und Defektelektron, die über die Wechselwirkung der Teilchen mit den Gitterschwingungen zustandekommt. Einen Hinweis, wie diese Wechselwirkung etwa aussieht, liefert uns die klassische Elektrodynamik. Fassen wir dazu den polaren Kristall als ein homogenes Dielektrikum auf, so wird nach Aussagen der klassischen Elektrodynamik das Anziehungspotential zwischen zwei ruhenden Punktladungen  $e$  und  $-e$ , das im Vakuum  $-e^2/r_{12}$  lautet, zu  $-e^2/\epsilon r_{12}$  abgeschwächt. Wesentlich für unsere folgende Untersuchung ist es, daß diese Abschwächung — wie bekannt — zum einen auf der Polarisierung der Elektronenhüllen bei festgehaltenen Atomkernen beruht, was für sich auf das Gesetz  $-e^2/\epsilon_\infty r_{12}$  führen würde, zum anderen aber auch auf der zusätzlichen Verschiebung der Ionen basiert:

$$-\frac{e^2}{\epsilon r_{12}} = -\frac{e^2}{\epsilon_\infty r_{12}} + \frac{e^2}{r_{12}} \left( \frac{1}{\epsilon_\infty} - \frac{1}{\epsilon} \right).$$

<sup>(8)</sup> J. FRENKEL: *Phys. Rev.*, **37**, 17, 1276 (1931).

<sup>(9)</sup> G. H. WANNIER: *Phys. Rev.*, **52**, 191 (1937). Weitere neue Gesichtspunkte bei der Behandlung des Exzitons im ruhenden Gitter bringt die Arbeit von W. R. HELLMER und A. MARKUS: *Phys. Rev.*, **84**, 809 (1951).

<sup>(10)</sup> J. FRENKEL: l. c. <sup>(8)</sup>; sowie *Phys. Zeits. Sowjetunion*, **9**, 158 (1936); R. PEIERLS *Ann. der Phys.*, **13**, 905 (1932).

<sup>(11)</sup> H. J. G. MEYER: *Physica*, **22**, 109 (1956). Herrn Dr. MEYER bin ich für die Überlassung eines Vorabdruckes sehr zu Dank verpflichtet.



Bewegen sich die Punktladungen, so werden sich die Elektronenhüllen praktisch trägheitslos dem jeweiligen Ort von Überschuß- und Defektelektron anpassen, während die Ionen nicht momentan folgen können. Daher kann sich, wie bereits von FRÖHLICH<sup>(12)</sup> ausführlich für den Einelektronenfall dargelegt wurde, der Teil der Polarisierung, der auf der Ionenverschiebung allein beruht, nicht voll ausbilden, sodaß wir eine Abänderung des Gesetzes  $(e^2/r_{12})((1/\varepsilon_\infty) - (1/\varepsilon))$  zu erwarten haben, das jedoch in geeigneten Grenzfällen wieder in  $e^2/r_{12} \cdot ((1/\varepsilon_\infty) - (1/\varepsilon))$  übergehen wird. Während es der Theorie des Exzitons im ruhenden Gitter überlassen bleiben muß, das Gesetz  $-e^2/\varepsilon_\infty r_{12}$  zu begründen bzw. zu verfeinern, wird es im folgenden unsere Aufgabe sein, die von den Ionenverschiebungen hervorgerufene Wechselwirkung zwischen den Teilchen zu bestimmen und besonders auf den Grenzfall  $(e^2/r_{12})((1/\varepsilon_\infty) - (1/\varepsilon))$  zu untersuchen.

Als zweiten anschaulichen Aspekt sehen wir die Tatsache an, daß in Translationsgittern, deren Ionen auch noch Schwingungen ausführen dürfen, sich Elektron bzw. Defektelektron wie freie Teilchen mit einer bestimmten scheinbaren Masse<sup>(13)</sup> verhalten. Wir werden erwarten, daß diese scheinbaren Massen, wenigstens in geeigneter Näherung, auch in der resultierenden Gleichung für die gemeinsame Bewegung von Elektron und Defektelektron auftreten werden. Bei der nun folgenden Behandlung des Problems werden wir also besonders auf diese beiden Gesichtspunkte: Form der direkten Wechselwirkung zwischen den beiden Teilchen und Erfassung ihrer scheinbaren Massen achten.

### 3. — Die Schrödingergleichung.

Der Hamiltonoperator des Systems besteht aus den drei Teilen

$$(3.1) \quad H = H_{\text{Exziton}} + H_{\text{Oszillatoren}} + H_{\text{Wechselw.}}$$

Der erste beschreibt die Bewegung des Exzitons im ruhenden Gitter, wobei wir im Anschluss an WANNIER annehmen, daß sich das Exziton aus einem Elektron und einem Defektelektron zusammensetzt, deren jedes sich in einem ruhenden, periodischen Potentialfeld bewegt und die untereinander noch durch eine direkte, abstandsabhängige Wechselwirkung gekoppelt sind:

$$(3.2) \quad H_{\text{Exziton}} = H_{\text{Elektron}} + H_{\text{Defektelektron}} + H_{\text{w}}^{(1)},$$

$$H_j = -\frac{\hbar^2}{2m} \Delta_j + V_j(\mathbf{r}_j), \quad j = \begin{cases} \text{Elektron} \\ \text{Defektelektron,} \end{cases} \quad H_{\text{w}}^{(1)} = H_{\text{w}}^{(1)}(r_{12}).$$

<sup>(12)</sup> H. FRÖHLICH: l. c. <sup>(4)</sup>.

<sup>(13)</sup> Wenigstens solange keine freien Quanten vorhanden sind.

Die Energie der Gitterschwingungen geben wir durch

$$(3.3) \quad H_{\text{Oszillatoren}} = \sum_{\mathbf{w}} \hbar \omega_{\mathbf{w}} b_{\mathbf{w}}^+ b_{\mathbf{w}},$$

( $\omega_{\mathbf{w}}$ : Frequenz der Gitterwelle mit dem Ausbreitungsvektor  $\mathbf{w}$ ) wieder, während wir die Wechselwirkung dieser Schwingungen mit Elektron und Defektelektron in ziemlich allgemeiner Weise durch

$$(3.4) \quad H_{\text{WW}_e} = \sum_{\mathbf{w}} \{ b_{\mathbf{w}} (W_{\mathbf{w}}^{(1)}(\mathbf{r}_1) + W_{\mathbf{w}}^{(2)}(\mathbf{r}_2)) + \text{konj. kompl.} \}$$

mit  $W_{\mathbf{w}}^{(i)}(\mathbf{r}_i) = \tilde{W}_{\mathbf{w}}^{(i)}(\mathbf{r}_i) \exp[i\mathbf{w} \cdot \mathbf{r}_i]$ ,  $\tilde{W}$ : gitterperiodisch, darstellen. Die  $b_{\mathbf{w}}^-$  und  $b_{\mathbf{w}}$  sind die bekannten Erzeugungs- und Vernichtungsoperatoren für Schallquanten (bzw. Polarisationsquanten), die den Bose-Vertauschungsrelationen genügen. Gemäß unserem Ansatz für die Schrödingergleichung können wir es uns vorläufig vorbehalten, ob wir die Wechselwirkung von Elektron und Defektelektron mit den Gitterschwingungen in mikroskopischer Weise beschreiben wollen, oder ob wir zu einer schon halb makroskopischen Behandlung übergehen, bei der Elektron und Defektelektron mit den *Polarisationsschwingungen* eines homogenen, kontinuierlichen Dielektrikums in Wechselwirkung stehen. Diese letztere Beschreibung wurde bisher bei der Untersuchung des Polaronenproblems (Überschußelektron im polaren Kristall) fast ausschließlich zugrundegelegt.

#### 4. — Der Lösungsansatz.

Bei der geläufigen störungstheoretischen Methode würde man nun die Schrödingergleichung in der Weise lösen, daß man zuerst die Eigenzustände von  $H_{\text{Exziton}}$  und  $H_{\text{Oszillatoren}}$  bestimmt und dann das Wechselwirkungsglied (3.4) als kleine Störung ansieht. Da diese Wechselwirkung in polaren Kristallen aber durchaus nicht klein ist, schlagen wir einen grundsätzlich anderen Weg ein. Wir nehmen nämlich an, daß wir die Bewegung der Einzelteilchen im *schwingenden* Gitter bereits kennen, also daß wir die Lösung der Schrödingergleichung

$$(4.1) \quad \left\{ H_0 + \sum_{\mathbf{w}} \hbar \omega_{\mathbf{w}} b_{\mathbf{w}}^+ b_{\mathbf{w}} + \sum_{\mathbf{w}} (b_{\mathbf{w}} W_{\mathbf{w}}^{(j)}(\mathbf{r}_j) + \text{konj. kompl.}) \right\} \varphi^{(j)} = E^{(j)} \varphi^{(j)}$$

bereits besitzen. Für unsere weitere Untersuchung ist es wesentlich, daß die Lösungen die Form <sup>(14)</sup>

$$(4.2) \quad \varphi^{(j)} = \exp[i\mathbf{k} \cdot \mathbf{r}] u_{\mathbf{k}}^{(j)}(\mathbf{r}_j, b^+) \Phi_0 = \chi_{\mathbf{k}}^{(j)}(\mathbf{r}_j, b^+) \Phi_0$$

<sup>(14)</sup> H. HAKEN: *Zeits. f. Naturf.*, **9a**, 228 (1954).

haben. Dabei ist  $\Phi_0$  der tiefste ungestörte Schwingungszustand des Kristalls. Die Lösungen (4.2) stellen in bestimmter Weise modulierte ebene Wellen dar, die die Bewegung von Elektron bzw. Defektelektron zusammen mit der sie jeweils begleitenden Gitterdeformation (bzw. « Polarisationswolke ») beschreiben. Jedes der beiden Teilchen erzeugt so, besonders in seiner Umgebung, eine bestimmte Zahl von Schallquanten, die die Gitterdeformation bewirken. Wenn die Teilchen sich nicht in einem zu kleinen Abstand bewegen, so werden sich die mitlaufenden Gitterdeformationen bzw. die Erzeugungsprozesse für die Schallquanten fast ungestört überlagern. Diese Überlagerung wird durch den Ansatz

$$(4.3) \quad \varphi_{f_1 f_2}(\mathbf{r}_1, \mathbf{r}_2, b^+) \Phi_0 = \exp [i f_1 \mathbf{r}_1] u_{f_1}^{(1)}(\mathbf{r}_1, b^+) \exp [i f_2 \mathbf{r}_2] u_{f_2}^{(2)}(\mathbf{r}_2, b^+) \Phi_0$$

beschrieben. Elektron und Defektelektron bewegen sich nun natürlich nicht nur in dem von ihnen jeweils allein geschaffenen Polarisationsfelde, sondern in einem Felde, das gleichzeitig auch von dem anderen Teilchen herrührt. Auf diese Weise entsteht über das Feld der Gitterschwingungen eine direkte Wechselwirkung zwischen den Teilchen, die zu der schon im ruhenden Gitter vorhandenen Wechselwirkung  $H_w^{(1)}$  hinzutritt. Zur vorläufigen Berechnung dieser neuen Wechselwirkung gehen wir mit dem Ansatz (4.3) in die Schrödingergleichung mit dem Hamiltonoperator (3.1) ein. Beachten wir dabei die aus den Vertauschungsrelationen sofort hervorgehenden Beziehungen

$$(4.4) \quad \begin{cases} b^+ \chi^{(1)} \chi^{(2)} \Phi_0 = \chi^{(1)} b^+ \chi^{(2)} \Phi_0 = \chi^{(2)} b^+ \chi^{(1)} \Phi_0 \\ b \chi^{(1)} \chi^{(2)} \Phi_0 = \chi^{(1)} b \chi^{(2)} \Phi_0 + \chi^{(2)} b \chi^{(1)} \Phi_0 \\ b^+ b \chi^{(1)} \chi^{(2)} \Phi_0 = \chi^{(1)} b^+ b \chi^{(2)} \Phi_0 + \chi^{(2)} b^+ b \chi^{(1)} \Phi_0 \end{cases}$$

so erhalten wir unter Berücksichtigung der Tatsache, daß die  $\chi^{(i)} \Phi_0$  den Gleichungen (4.1) genügen:

$$(4.5) \quad H \varphi_{f_1 f_2} = (E^{(1)}(f_1) + E^{(2)}(f_2) + H_w^{(1)}) \varphi_{f_1 f_2} \Phi_0 + \\ + \sum_w (W_w^{(1)} \chi_{f_1}^{(1)} b_w \chi_{f_2}^{(2)} \Phi_0 + W_w^{(2)} \chi_{f_2}^{(2)} b_w \chi_{f_1}^{(1)} \Phi_0).$$

Das neben  $H_w^{(1)}$  auftretende Summenglied stellt, wenigstens näherungsweise, bereits die zusätzliche Wechselwirkung infolge der Gitterschwingungen dar.

Infolge der beiden Wechselwirkungsglieder  $H_w^{(1)}$  und  $H_w^{(2)} = \sum_w (\dots)$  werden

Übergänge zwischen den verschiedenen  $f_1, f_2$ -Zuständen geschaffen, sodaß die stationären Lösungen erst wieder durch Linearkombinationen der Form

$$(4.6) \quad \Psi(\mathbf{r}_1, \mathbf{r}_2, b^+) = \iint c_{f_1 f_2} \varphi_{f_1 f_2}(\mathbf{r}_1, \mathbf{r}_2, b^+) \Phi_0 d f_1 d f_2$$

gegeben sind. (4.6) ist bereits der unserer jetzigen Untersuchung zugrundegelegte Lösungsansatz. Die in ihm noch frei wählbaren Koeffizienten  $c_{f_1 f_2}$  sind mit Hilfe des Variationsprinzips

$$(4.7) \quad \left\langle \int \Psi^* H \Psi d\tau \right\rangle = \text{Min!}, \quad \left\langle \int \Psi^* \Psi d\tau \right\rangle = 1,$$

zu bestimmen.

### 5. — Näherungsweise Lösung von (4.7).

Zur Berechnung des Variationsintegrals (4.7) multiplizieren wir als erstes (4.5) mit  $c_{f_1 f_2}$  und integrieren über  $f_1, f_2$ . Damit haben wir zunächst  $H\Psi$  bestimmt. Nun multiplizieren wir mit  $\Psi^*$  (s. (4.6)), integrieren über die Koordinaten von Elektron und Defektelektron und bilden bezüglich der Schallquanten den Erwartungswert. Berücksichtigen wir noch (4.3), so erhalten wir:

$$(5.1) \quad \begin{aligned} & \iiint \iiint \int c_{f_1' f_2'}^* c_{f_1 f_2} [E^{(1)}(f_1) + E^{(2)}(f_2) + H_w^{(1)}] \exp [i r_1(f_1 - f_1') + i r_2(f_2 - f_2')] \cdot \\ & \cdot \langle \Phi_0 u_{f_1}^{(1)*} u_{f_2}^{(2)*} u_{f_1}^{(1)} u_{f_2}^{(2)} \Phi_0 \rangle d r_1 d r_2 d f_1' d f_2' d f_1 d f_2 + \\ & + \iiint \iiint \int c_{f_1' f_2'}^* c_{f_1 f_2} \exp [i r_1(f_1 - f_1') + i r_2(f_2 - f_2')] \cdot \\ & \cdot \Phi_0 u_{f_1}^{(1)*} u_{f_2}^{(2)*} \sum_w (W_w^{(1)} u_{f_1}^{(1)} b_w u_{f_2}^{(2)} + W_w^{(2)} u_{f_2}^{(2)} b_w u_{f_1}^{(1)}) \Phi_0 \rangle d r_1 d r_2 d f_1' d f_2' d f_1 d f_2, \end{aligned}$$

und ganz entsprechend für das Normierungsintegral

$$(5.2) \quad \begin{aligned} & \iiint \iiint \int c_{f_1' f_2'}^* c_{f_1 f_2} \exp [i r_1(f_1 - f_1') + i r_2(f_2 - f_2')] \cdot \\ & \cdot \langle \Phi_0 u_{f_1}^{(1)*} u_{f_2}^{(2)*} u_{f_1}^{(1)} u_{f_2}^{(2)} \Phi_0 \rangle d r_1 d r_2 d f_1' d f_2' d f_1 d f_2. \end{aligned}$$

Hier und im folgenden bezeichnen wir den Ausdruck

$$(5.3) \quad \langle \Phi_0 u_{f_1}^{(1)*} u_{f_2}^{(2)*} u_{f_1}^{(1)} u_{f_2}^{(2)} \Phi_0 \rangle \quad \text{mit} \quad G_{f_1, f_2, f_1', f_2'}.$$

Wir beginnen mit der Untersuchung des Normierungsintegrals (5.2), das wir wie auch die Integrale (5.1), wesentlich vereinfachen können. Beschränken wir uns nämlich auf den Fall, daß das Elektron mit einem großem Bahnradius das Defektelektron umkreist, und daß sich außerdem das gesamte Exziton nur langsam bewegt, so liefern zum Integral nur solche Funktionen  $c_{f_1 f_2}$  einen wesentlichen Beitrag, für welche die  $f_i$  klein sind. Denkt man sich daher



$G_{\mathbf{f}'_1, \mathbf{f}'_2, \mathbf{f}_1, \mathbf{f}_2}$  in eine Potenzreihe nach  $\mathbf{f}_i, \mathbf{f}'_i$  entwickelt, so sind die Glieder mit Potenzen von  $\mathbf{f}_i, \mathbf{f}'_i$  gegenüber dem Glied  $G_{0,0,0,0}$  zu vernachlässigen. Die bisher bekannt gewordenen Einelektronen-Lösungen, die bei der Berechnung von (5.3) eingehen, geben uns die Möglichkeit, diese qualitative Aussage zu einer quantitativen zu verschärfen, worauf wir im Anhang genauer eingehen.

Neben dieser Vereinfachung, die in ähnlicher Weise auch schon bei der Theorie der scheinbaren Masse eines Elektron im ruhenden Gitter verwendet wird <sup>(15)</sup>, können wir noch eine zweite Vereinfachung vornehmen. Nehmen wir nämlich wie schon eben an, daß nur kleine  $\mathbf{f}_i$  wesentlich sind, und zwar jetzt genauer so, daß  $|\mathbf{f}_\alpha| < 1$  ( $\alpha$ : Basisvektor einer Gitterzelle), so ist die Exponentialfunktion in (5.1) und (5.2) in einer Gitterzelle nur langsam veränderlich. Bei der Integration über  $\mathbf{r}_1, \mathbf{r}_2$  liefert also praktisch nur die über eine Gitterzelle (im Konfigurationsraum!) gemittelte Funktion

(5.4) 
$$\bar{G}_{0,0,0,0}(\mathbf{r}_1, \mathbf{r}_2) = \frac{1}{V_{0,i}^2} \int \int_{\text{Gitterzelle } \mathbf{r}_1, \mathbf{r}_2} G_{0,0,0,0}(\mathbf{r}'_1, \mathbf{r}'_2) d\mathbf{r}'_1 d\mathbf{r}'_2$$

einen Beitrag, sodaß wir im folgenden der Einfachheit halber gleich diese geglättete Funktion  $\bar{G}_{0,0,0,0}$  verwenden werden.

Die weitere Behandlung des Problems ist dadurch festgelegt, daß es uns auf die anschaulichen Aspekte, also auf die Beschreibung der Bewegung der Teilchen im Ortsraum ankommt. Den Übergang in den Ortsraum erreichen wir durch die Substitution

(5.5) 
$$U(\mathbf{r}_1, \mathbf{r}_2) = \sqrt{\bar{G}_{0,0,0,0}(\mathbf{r}_1, \mathbf{r}_2)} \int \int e_{\mathbf{f}_1, \mathbf{f}_2} \exp [i\mathbf{f}_1 \mathbf{r}_1 + i\mathbf{f}_2 \mathbf{r}_2] d\mathbf{f}_1 d\mathbf{f}_2 .$$

Das Normierungsintegral läßt sich dann zu der Form

(5.6) 
$$\int \int U^*(\mathbf{r}_1, \mathbf{r}_2) U(\mathbf{r}_1, \mathbf{r}_2) d\mathbf{r}_1 d\mathbf{r}_2 ,$$

vereinfachen. Läßt man die Integration über die Teilchenkoordinaten weg, so ersieht man fast unmittelbar, daß  $|U(\mathbf{r}_1, \mathbf{r}_2)|^2$  — wenigstens näherungsweise — die Wahrscheinlichkeit wiedergibt, das Elektron am Orte  $\mathbf{r}_1$ , das Defektelektron am Orte  $\mathbf{r}_2$  zu finden.

Unsere folgende Aufgabe wird es sein, auch die übrigen Integralausdrücke (5.1) in Integrale über  $U(\mathbf{r}_1, \mathbf{r}_2), U^*(\mathbf{r}_1, \mathbf{r}_2)$  umzuformen und daraus dann die Schrödingergleichung für  $U$  zu gewinnen. Bei der Berechnung dieser Integrale ist es zweckmässig, dafür zu sorgen, daß diese Integrale automatisch reell sind. Wir erreichen dies dadurch, daß wir im Variationsintegral den Hamilton-

(15) Siehe hierzu besonders S. J. PEKAR: l. c. <sup>(b)</sup>.

operator  $H$  zur Hälfte nach rechts auf  $\Psi$ , zur Hälfte nach links auf  $\Psi^*$  wirken lassen. Damit können wir dann für das erste Integral in (5.1) (für den Elektronenteil) schreiben:

$$(5.7) \quad \frac{1}{2} \iiint \iiint \iiint c_{\mathbf{f}_1 \mathbf{f}_2}^* c_{\mathbf{f}_1' \mathbf{f}_2'} [E^{(1)}(\mathbf{f}_1) + E^{(1)}(\mathbf{f}_1')] \cdot \\ \cdot \exp [i \mathbf{r}_1 (\mathbf{f}_1 - \mathbf{f}_1') + i \mathbf{r}_2 (\mathbf{f}_2 - \mathbf{f}_2')] \bar{G}_{0,0,0,0} d\mathbf{f}_1' d\mathbf{f}_2' d\mathbf{f}_1 d\mathbf{f}_2 d\mathbf{r}_1 d\mathbf{r}_2.$$

Dabei haben wir bezüglich  $G_{\mathbf{f}_1', \mathbf{f}_2', \mathbf{f}_1, \mathbf{f}_2}$  die gleichen Vereinfachungen wie im Normierungsintegral, nämlich Ersatz von  $G_{\mathbf{f}_1', \mathbf{f}_2', \mathbf{f}_1, \mathbf{f}_2}$  durch  $G_{0,0,0,0}$  und Mittelung von  $G_{0,0,0,0}$  über eine Gitterzelle vorgenommen. Wir denken uns nun  $E^{(1)}$  in der Form  $E_0^{(1)} + \hbar^2 k^2 / 2m_1$  dargestellt, wodurch bekanntlich  $E^{(1)}$  in der Umgebung des Minimums gut angenähert wird<sup>(16)</sup>. (Stillschweigen wird dabei wieder vorausgesetzt, daß die Funktion  $\varphi_{\mathbf{f}_1 \mathbf{f}_2}$  (in (4.6)) der Umgebung dieses Minimums entstammt, was wiederum bedeutet, daß der Bahnradius nicht zu klein sein darf.) Im Gegensatz zu unserer Behandlung von  $G_{\mathbf{f}_1', \mathbf{f}_2', \mathbf{f}_1, \mathbf{f}_2}$ , bei der wir die Potenzreihenentwicklung nach dem ersten Gliede abbrechen, müssen wir bei  $E^{(1)}$  das Glied mit  $k^2$  beibehalten, da konstante Zusätze zu  $H$  für die Lösungsfunktion ohne Bedeutung sind und der erste, die gesuchte Wellenfunktion  $U$  beeinflussende und nicht verschwindende Beitrag von  $E^{(1)}$  von  $\hbar^2 k^2 / 2m_1$  herrührt<sup>(17)</sup>. Beachten wir nun, daß wir statt  $\mathbf{f}_1^2 \exp [i \mathbf{r}_1 (\mathbf{f}_1 - \mathbf{f}_1')] \exp [-i \mathbf{r}_1 \mathbf{f}_1'] (-\Delta_1) \exp [i \mathbf{r}_1 \mathbf{f}_1]$  schreiben, dürfen, so können wir sofort in (5.7) die Transformation (5.5) vornehmen und erhalten dann:

$$(5.8) \quad \frac{1}{2} \int \int \sqrt{\bar{G}_{0,0,0,0}} \left\{ U^* \left( E_0^{(1)} - \frac{\hbar^2}{2m_1} \Delta_1 \right) \frac{U}{\sqrt{\bar{G}_{0,0,0,0}}} + \right. \\ \left. + U \left( E_0^{(1)} - \frac{\hbar^2}{2m_1} \Delta_1 \right) \frac{U^*}{\sqrt{\bar{G}_{0,0,0,0}}} \right\} d\mathbf{r}_1 d\mathbf{r}_2.$$

Das entsprechende Ergebnis erhalten wir für den von  $E^{(2)}$  herrührenden Teil von (5.1).

Die Umformung des zweiten Integrals in (5.1) bereitet keinerlei Schwierigkeiten und gibt unter der Annahme, daß  $H_w^{(1)}$  räumlich langsam veränderlich ist, sofort:

$$(5.9) \quad \iint U^*(\mathbf{r}_1, \mathbf{r}_2) H_w^{(1)} U(\mathbf{r}_1, \mathbf{r}_2) d\mathbf{r}_1 d\mathbf{r}_2.$$

<sup>(16)</sup> Auf Ausnahmefälle, wie sie z.B. schon im ruhenden Gitter beim Germanium vorliegen, wo mehrere Minima und zwar bei  $k \neq 0$  auftreten, gehen wir hier nicht ein.

<sup>(17)</sup> Das gesamte von  $E$  herrührende Glied in (5.1) können wir deshalb nicht völlig vernachlässigen, weil es den Operator für die kinetische Energie des «angezogenen» Teilchens liefert und die kinetische und die potentielle Energie infolge eines (angenähert gültigen) Virialsatzes die gleiche Größenordnung haben.

Schließlich müssen wir noch das letzte Glied in (5.1) umformen. Wir setzen darin zur Abkürzung

(5.10) 
$$F_{\mathfrak{f}_1', \mathfrak{f}_2', \mathfrak{f}_1, \mathfrak{f}_2} = \frac{1}{2} \{ \langle \Phi_0 u_{\mathfrak{f}_1}^{(1)*} u_{\mathfrak{f}_2}^{(2)*} (\sum_w W_w^{(1)} u_{\mathfrak{f}_1}^{(1)} b_w u_{\mathfrak{f}_2}^{(2)} + W_w^{(2)} u_{\mathfrak{f}_2}^{(2)} b_w u_{\mathfrak{f}_1}^{(1)} ) \Phi_0 \rangle + \\ + \Phi_0 (\sum_w u_{\mathfrak{f}_2}^{(2)*} b_w^+ u_{\mathfrak{f}_1}^{(1)*} W_w^{(1)*} + u_{\mathfrak{f}_1}^{(1)*} b_w^+ u_{\mathfrak{f}_2}^{(2)*} W_w^{(2)*} ) u_{\mathfrak{f}_1}^{(1)} u_{\mathfrak{f}_2}^{(2)} \Phi_0 \rangle \} ,$$

behalten dann von der Potenzreihenentwicklung von  $F_{\mathfrak{f}_1', \mathfrak{f}_2', \mathfrak{f}_1, \mathfrak{f}_2}$  nach  $\mathfrak{f}_1', \mathfrak{f}_2', \mathfrak{f}_1, \mathfrak{f}_2$  nur das erste Glied bei und denken uns außerdem gleich  $F$  über eine Gitterzelle gemittelt:

(5.11) 
$$\iiint \iiint \iiint c_{\mathfrak{f}_1 \mathfrak{f}_2}^* c_{\mathfrak{f}_1 \mathfrak{f}_2} \exp [ i r_1 (\mathfrak{f}_1 - \mathfrak{f}_1') + i r_2 (\mathfrak{f}_2 - \mathfrak{f}_2') F_{0,0,0,0} d\mathfrak{f}_1' d\mathfrak{f}_2' d\mathfrak{f}_1 d\mathfrak{f}_2 d\mathbf{r}_1 d\mathbf{r}_2 .$$

Um nun schließlich  $U(\mathbf{r}_1, \mathbf{r}_2)$  als neue Funktion einzuführen, erweitern wir den Integranden in (5.11) mit  $\bar{G}_{0,0,0,0}$  und können dann mit Hilfe von (5.5) schreiben:

(5.12) 
$$\iint U^*(\mathbf{r}_1, \mathbf{r}_2) U(\mathbf{r}_1, \mathbf{r}_2) \frac{\bar{F}_{0,0,0,0}}{\bar{G}_{0,0,0,0}} d\mathbf{r}_1 d\mathbf{r}_2 .$$

Das Normierungsintegral wie auch das gesamte zu variierende Integral haben wir damit unter der Voraussetzung, daß der Bahnradius Elektron-Defektelektron nicht zu klein und die Bewegung des Exzitons nicht zu schnell ist, auf die folgende Summe der Ausdrücke (5.6), (5.8), (5.9), (5.12)

(5.13) 
$$N = \iint U^*(\mathbf{r}_1, \mathbf{r}_2) U(\mathbf{r}_1, \mathbf{r}_2) d\mathbf{r}_1 d\mathbf{r}_2 = 1 ,$$

(5.14) 
$$H = \frac{1}{2} \iint \sqrt{\bar{G}_{0,0,0,0}} \cdot \\ \cdot \left\{ U^* \left( E_0^{(1)} - \frac{\hbar^2}{2m_1} \Delta_1 \right) \frac{U}{\sqrt{\bar{G}_{0,0,0,0}}} + U \left( E_0^{(2)} - \frac{\hbar^2}{2m_1} \Delta_1 \right) \frac{U^*}{\sqrt{\bar{G}_{0,0,0,0}}} \right\} d\mathbf{r}_1 d\mathbf{r}_2 + \\ + \frac{1}{2} \iint \sqrt{G_{0,0,0,0}} \left\{ U^* \left( E_0^{(2)} - \frac{\hbar^2}{2m_2} \Delta_2 \right) \frac{U}{\sqrt{G_{0,0,0,0}}} + U \left( E_0^{(2)} - \frac{\hbar^2}{2m_2} \Delta_2 \right) \frac{U^*}{\sqrt{G_{0,0,0,0}}} \right\} d\mathbf{r}_1 d\mathbf{r}_2 + \\ + \iint U^*(\mathbf{r}_1, \mathbf{r}_2) \left\{ H_w^{(1)} + \frac{F_{0,0,0,0}}{\bar{G}_{0,0,0,0}} \right\} U(\mathbf{r}_1, \mathbf{r}_2) d\mathbf{r}_1 d\mathbf{r}_2$$

reduziert. Die Schrödingergleichung für  $U$  erhalten wir in bekannter Weise durch Variation von  $H$  und  $U^*$  unter Berücksichtigung der Normierungs-

bedingung  $N=1$  nach kurzer Rechnung zu

$$(5.15) \quad \left( E_0^{(1)} + E_0^{(2)} - \frac{\hbar^2}{2m_1} A_1 - \frac{\hbar^2}{2m_2} A_2 + H_w^{(1)}(r_{12}) + \frac{F_{0,0,0,0}(r_1, r_2)}{G_{0,0,0,0}(r_1, r_2)} \right) \cdot U(r_1, r_2) = EU(r_1, r_2),$$

wobei wir

$$\frac{\hbar^2}{2m_1} \frac{\bar{G}_{x_1}^2 + \bar{G}_{y_1}^2 + \bar{G}_{z_1}^2}{\bar{G}^2} \quad \text{und} \quad \frac{\hbar^2}{2m_2} \frac{\bar{G}_{x_2}^2 + \bar{G}_{y_2}^2 + \bar{G}_{z_2}^2}{\bar{G}^2},$$

vernachlässigt haben <sup>(18)</sup>. Die Lösung der Gleichung (5.15) kann, wenn  $H_w^{(1)}$  und  $\bar{F}_{0,0,0,0}/\bar{G}_{0,0,0,0}$  bekannt sind, mit den bekannten Standardmethoden erfolgen, worauf wir hier nicht weiter einzugehen brauchen. Von wesentlichem Interesse ist hier lediglich die Berechnung und Diskussion von  $\bar{F}_{0,0,0,0}/\bar{G}_{0,0,0,0}$ , der wir uns nun zuwenden.

## 6. – Diskussion der Schrödingergleichung.

Die ersten beiden konstanten Glieder  $E_0^{(1)}$  und  $E_0^{(2)}$  sind schon von der Behandlung der Bewegung von Elektron bzw. Defektelektron im schwingenden Gitter her bekannt. Diese Einzelenergien setzen sich zum einen aus der Energie von Elektron bzw. Defektelektron im ruhenden Gitter, zum anderen aber aus der zusätzlichen Selbstenergie der Teilchen infolge ihrer Wechselwirkung mit den Gitterschwingungen zusammen. In den beiden nächsten Ausdrücken für die kinetische Energie stellen  $m_1$  und  $m_2$  die scheinbaren Massen von Elektron und Defektelektron im schwingenden Gitter dar. Der Wert dieser Massen rührt zum einen von der Wirkung des ruhenden, streng periodischen Gitterpotentials, zum anderen wiederum von der Wechselwirkung des Elektrons bzw. Defektelektrons mit den Gitterschwingungen her. Da uns das folgende Wechselwirkungsglied  $H_w^{(1)}$  bereits, und zwar schon von der Theorie des Exzitons im ruhenden Gitter her, vorgegeben ist, haben wir nur noch den vorläufig unbekannten Ausdruck  $H_w^{(2)} = \bar{F}_{0,0,0,0}(r_1, r_2)/\bar{G}_{0,0,0,0}(r_1, r_2)$  zu untersuchen.

Wir zeigen zuerst, daß dieser Ausdruck im wesentlichen eine nur von der Relativkoordinate abhängige Funktion ist. Dazu untersuchen wir zuerst

$$(6.1) \quad \bar{G}_{0,0,0,0}(r_1, r_2) = \frac{1}{V^2} \iint \langle \Phi_0 | U_0^{(1)}(r'_1, b^+) U_0^{(2)}(r'_2, b^+) |^2 \Phi_0 \rangle dr'_1 dr'_2,$$

wobei die Integration über eine Gitterzelle mit dem Mittelpunkt  $(r_1, r_2)$  (im Konfigurationsraum) gehen sollte.

<sup>(18)</sup> Die Rechtfertigung dieser Vernachlässigungen findet sich im Anhang II.



Wir betrachten die simultane Koordinatenverschiebung

(6.2) 
$$\mathbf{r}_1 \rightarrow \mathbf{r}_1 + \mathbf{m}, \quad \mathbf{r}_2 \rightarrow \mathbf{r}_2 + \mathbf{m},$$

wobei  $\mathbf{m}$  noch ein Gittervektor ist. Auf der rechten Seite in (6.1) verwandeln wir diese Ersetzung sofort in eine der Integrationsvariablen

(6.3) 
$$\mathbf{r}'_1 \rightarrow \mathbf{r}'_1 + \mathbf{m}, \quad \mathbf{r}'_2 \rightarrow \mathbf{r}'_2 + \mathbf{m}.$$

Zu dieser letzteren Substitution fügen wir unter dem Erwartungswert «  $\langle \dots \rangle$  » noch die Substitution

(6.4) 
$$b_{\mathbf{w}} \rightarrow b_{\mathbf{w}} \exp[-i\mathbf{w}\mathbf{m}], \quad b_{\mathbf{w}}^+ \rightarrow b_{\mathbf{w}}^+ \exp[i\mathbf{w}\mathbf{m}]$$

hinzu, wodurch natürlich der Erwartungswert nicht verändert wird. Wir können aber die Tatsache benutzen, daß die  $u^{(i)}(\mathbf{r}_i, b^+)$  gegenüber der gemeinsamen Substitution

(6.5) 
$$\mathbf{r}_i \rightarrow \mathbf{r}_i + \mathbf{m}, \quad b_{\mathbf{w}}^+ \rightarrow b_{\mathbf{w}}^+ \exp[i\mathbf{w}\mathbf{m}]$$

invariant sind. Daher bleibt schließlich bei der Substitution (6.2) die gesamte Funktion  $\bar{G}_{0,0,0,0}(\mathbf{r}_1, \mathbf{r}_2)$  unverändert. Nehmen wir nun an, daß  $\bar{G}_{0,0,0,0}(\mathbf{r}_1, \mathbf{r}_2)$  innerhalb einer Gitterzelle nur langsam veränderlich ist, eine Annahme, die in praktisch allen interessierenden Fällen gerechtfertigt ist, so kann bei der Substitution (6.2) statt des Gittervektors  $\mathbf{m}$  auch ein beliebiger Vektor benutzt werden, wobei also  $\bar{G}_{0,0,0,0}(\mathbf{r}_1, \mathbf{r}_2)$  wiederum (näherungsweise) invariant ist. Daraus folgt aber sofort, daß  $\bar{G}_{0,0,0,0}(\mathbf{r}_1, \mathbf{r}_2)$  nur vom Relativabstand  $\mathbf{r}_1 - \mathbf{r}_2$  abhängt.

Der Nachweis, daß auch  $\bar{F}_{0,0,0,0}(\mathbf{r}_1, \mathbf{r}_2)$  nur vom Relativabstand abhängt, ergibt sich ganz genauso. Wir haben dabei lediglich außerdem noch zu beachten, daß die Operatoren  $W_{\mathbf{w}}^{(i)}(\mathbf{r}_i)b_{\mathbf{w}}$ , die gemäß (5.10) in  $\bar{F}$  auftreten, ebenso wie die  $u^{(i)}(\mathbf{r}_i, b^+)$  gegenüber der Substitution (6.5) invariant sind.

7. – Explizite Berechnung des Wechselwirkungsgliedes  $H_w^{(2)}$ .

Zur weiteren Diskussion von Gleichung (5.15) berechnen wir das Wechselwirkungsglied  $H_w^{(2)}$  explizit. Da sich  $H_w^{(2)}$  aus  $\bar{G}_{0,0,0,0}$  und  $\bar{F}_{0,0,0,0}$  zusammensetzt, die wiederum nach ihrer Definition (5.3) bzw. (5.10) von den Einteilchenlösungen  $u^{(i)}(\mathbf{r}_i, b^+)$  und den Wechselwirkungsgliedern  $W_{\mathbf{w}}^{(i)}(\mathbf{r}_i)$  (s. S. 5) abhängen, sind wir auf die bisher explizit untersuchten Einteilchenprobleme angewiesen. Wir beschränken uns dazu von vornherein auf den Fall polarer

Medien, da hier gerade eine starke Wechselwirkung vorliegt <sup>(19)</sup> und wählen das Wechselwirkungsglied im Anschluß an die bisherigen Arbeiten in der Form <sup>(20)</sup>

$$(7.1) \quad W_{\mathbf{w}}^{(i)}(\mathbf{r}_i) = \pm \gamma_{\mathbf{w}} \exp[i\mathbf{w} \cdot \mathbf{r}_i] \quad \text{mit} \quad \gamma_{\mathbf{w}} = -i\hbar\omega \left( \frac{4\pi\alpha}{uV} \right)^{\frac{1}{2}} \frac{1}{W}.$$

Die verschiedenen Vorzeichen rühren von dem verschiedenen Ladungsvorzeichen von Elektron und Defektelektron her. Im einzelnen bedeuten:

$\omega$ : longitudinal Reststrahlfrequenz,

$\alpha = \frac{1}{2} \left( \frac{1}{\epsilon_{\infty}} - \frac{1}{\epsilon} \right) \frac{e^2 u}{\hbar\omega}$ : dimensionslose Kopplungskonstante,

$\sqrt{\epsilon_{\infty}}$ : Berechnungsindex im optischen Gebiet vor dem Einsetzen der Ultraviolettabsorption,

$\epsilon$ : statische Dielektrizitätskonstante,

$u^{-1} = (2m^*\omega/\hbar)^{-\frac{1}{2}}$ : Konstante von der Dimension einer Länge ( $10^{-7}$  cm),

$m^*$ : scheinbare Masse. Da  $m^*$  im Kopplungsglied herausfällt, kann die Wahl von  $m^*$  zunächst noch offen bleiben.

Die Lösungsfunktionen  $u^{(i)}(\mathbf{r}_i, b^+)$  werden in fast allen bisherigen Arbeiten unter den folgenden Vereinfachungen der Einteilchengleichung (4.1) gewonnen:

- 1) Das periodische Gitterpotential  $V^{(i)}(\mathbf{r}_i)$  (s. (3.2)) wird mit Hilfe der Methode der scheinbaren Masse eliminiert.
- 2) Alle Oszillatoren besitzen die gleiche Frequenz  $\omega$ .

Bei unserer jetzigen Wahl der  $u^{(i)}$  haben wir im Hinblick auf die bisherige Behandlungsweise des Einteilchenproblems zwischen dem Grenzfall schwacher bis mittlerer und dem starker Kopplung zu unterscheiden.

a) *Grenzfall schwacher bis mittlerer Kopplung.* – Wir beginnen mit dem ersten Grenzfall und wählen hierbei die von LEE, LOW und PINES <sup>(21)</sup> angegebenen Funktionen, die in diesem Grenzfall gute Resultate geben und die außerdem sehr handlich sind. Nach diesen Autoren besitzen die  $u^{(i)}(\mathbf{r}_i, b^+)$  die Form

$$(7.2) \quad N_i \cdot \exp \left\{ \sum_{\mathbf{w}} b_{\mathbf{w}}^+ (\pm) \gamma_{\mathbf{w}}^* \frac{\exp[-i\mathbf{w} \cdot \mathbf{r}_i]}{\hbar^2 w^2 / 2m_i^* + \hbar\omega} \right\}, \quad N_i: \text{ Normierungsfaktor.}$$

<sup>(19)</sup> Genauer gesagt: eine mittelstarke Kopplung.

<sup>(20)</sup> H. FRÖHLICH: l. c. (4).

<sup>(21)</sup> T. LEE, F. LOW und D. PINES: l. c. (5).

Wir erhalten mit diesen Funktionen für  $G_{0,0,0,0}$ :

(7.3) 
$$|N_1|^2 |N_2|^2 \left\langle \Phi_0 \exp \left\{ \sum_{\text{w}} b_{\text{w}} \gamma_{\text{w}} \left( \frac{\exp[i\text{w} r_1]}{\hbar^2 w^2 / 2m_1^* + \hbar \omega} - \frac{\exp[i\text{w} r_2]}{\hbar^2 w^2 / 2m_2^* + \hbar \omega} \right) \right\} \cdot \right. \\ \left. \cdot \exp \left\{ \sum_{\text{w}} b_{\text{w}}^+ \gamma_{\text{w}}^* \left( \frac{\exp[-i\text{w} r_1]}{\hbar^2 w^2 / 2m_1^* + \hbar \omega} - \frac{\exp[-i\text{w} r_2]}{\hbar^2 w^2 / 2m_2^* + \hbar \omega} \right) \right\} \Phi_0 \right\rangle .$$

Zur Auswertung des Erwartungswertes entwickeln wir im Anschluß an HÖHLER <sup>(22)</sup> (Einteilchenfall) die Exponentialfunktion in eine Potenzreihe in  $b_{\text{w}}$ ,  $b_{\text{w}}^+$  und beachten

(7.4) 
$$\langle \Phi_0 b^n (b^+)^m \Phi_0 \rangle = \delta_{n,n} \cdot m! .$$

Wir erhalten dann nach Aufsummation:

(7.5) 
$$G_{0,0,0,0} = |N_1|^2 |N_2|^2 \exp \left\{ \sum_{\text{w}} |\gamma_{\text{w}}|^2 \left| \frac{\exp[i\text{w} r_1]}{\hbar^2 w^2 / 2m_1^* + \hbar \omega} - \frac{\exp[i\text{w} r_2]}{\hbar^2 w^2 / 2m_2^* + \hbar \omega} \right|^2 \right\} .$$

Die Berechnung von  $F_{0,0,0,0}$  verläuft entsprechend und ergibt

(7.6) 
$$F_{0,0,0,0} = G_{0,0,0,0} \cdot \frac{1}{2} \sum_{\text{w}} |\gamma_{\text{w}}|^2 \cdot \left\{ \frac{\exp[i\text{w}(r_1 - r_2)]}{\hbar^2 w^2 / 2m_1^* + \hbar \omega} + \frac{\exp[i\text{w}(r_1 - r_2)]}{\hbar^2 w^2 / 2m_2^* + \hbar \omega} + \text{konj. kompl.} \right\} .$$

Die Summe führen wir in ein Integral über, das sich geschlossen auswerten läßt. Insgesamt erhalten wir dann

(7.7) 
$$H_w^{(2)} = \frac{F_{0,0,0,0}}{G_{0,0,0,0}} = \left( \frac{1}{\varepsilon_\infty} - \frac{1}{\varepsilon} \right) \frac{e^2}{r_{12}} \left( 1 - \frac{\exp[-u_1 r_{12}] + \exp[-u_2 r_{12}]}{2} \right) ,$$

mit  $u_i = \sqrt{2m_i^* \omega / \hbar}$  (s. Def. S. 13).

Für  $r_{12} > 1/u_i$  erhalten wir das klassisch zu erwartende Gesetz, das wir auf S. 4 bereits diskutierten:

(7.8) 
$$H_w^{(2)} \approx \left( \frac{1}{\varepsilon_\infty} - \frac{1}{\varepsilon} \right) \frac{e^2}{r_{12}} .$$

b) *Grenzfall starker Kopplung.* - Von HÖHLER <sup>(23)</sup> und TJABLIKOV <sup>(24)</sup>

<sup>(22)</sup> G. HÖHLER: l. c. <sup>(6)</sup>.  
<sup>(23)</sup> G. HÖHLER: l. c. <sup>(6)</sup>.  
<sup>(24)</sup> S. V. TJABLIKOV: l. c. <sup>(5)</sup>.

wurde für den Grenzfall starker Kopplung die folgende Verbesserung des bekannten Pekarschen <sup>(25)</sup> Produktansatzes angegeben:

$$(7.9) \quad u_0^{(i)}(r_i, b^+) = N_i \int \Psi_i(r_i - r'_i) \exp \{ d_{w0}^{(i)} b^+ \exp [-i w r'_i] \} dr'_i,$$

$N_i$ : Normierungsfaktor

Darin ist  $\Psi_i(r)$  eine wasserstoffartige Funktion

$$(7.10) \quad \Psi_i(r) = M_i \exp [-\beta_i r],$$

während die « Oszillatorverschiebungen »  $d_{w0}^{(i)}$  durch

$$(7.11) \quad d_{w0} = \mp \frac{\gamma_{w0}^* \varrho_{w0}^{(i)*}}{\hbar \omega}, \quad \varrho_{w0}^{(i)} = \int |\Psi_i(r)|^2 \exp [-i w r] dr = \frac{1}{[1 + (w/2\beta)^2]^2},$$

gegeben sind.

Mit den Funktionen (7.9) lautet  $G_{0,0,0,0}$ :

$$(7.12) \quad |N_1|^2 |N_2|^2 \iiint \Psi_1^*(r_1 - r'_1) \Psi_1(r_1 - r''_1) \Psi_2^*(r_2 - r'_2) \Psi_2(r_2 - r''_2) \cdot \\ \cdot \exp \left( \sum_w |d_{w0}^{(1)}|^2 \exp [i w (r'_1 - r''_1)] + |d_{w0}^{(2)}|^2 \exp [i w (r'_2 - r''_2)] + \right. \\ \left. + d_{w0}^{(1)} d_{w0}^{(2)*} \exp [i w (r'_1 - r''_2)] + d_{w0}^{(2)} d_{w0}^{(1)*} \exp [i w (r'_2 - r''_1)] \right) dr'_1 dr''_1 dr'_2 dr''_2,$$

wobei wir den Erwartungswert bezüglich der Oszillatoren genau wie bei dem eben behandelten Fall mittlerer Kopplung ausgewertet haben. Nehmen wir nun an, daß der Abstand  $r_{12}$  groß gegenüber der Ausdehnung  $1/\beta_i$  der Ladungswolken  $|\Psi_i|^2$  ist, so dürfen wir in guter Näherung in der Exponentialfunktion in den Gliedern, die zugleich  $r'_1$  und  $r''_2$  bzw.  $r'_2$  und  $r''_1$  enthalten,

$$r'_1 = r''_1 = r_1, \quad r'_2 = r''_2 = r_2$$

setzen.

Wir erhalten dann

$$(7.13) \quad G_{0,0,0,0} \sim A_1 A_2 \exp \left\{ \sum_w d_{w0}^{(1)} d_{w0}^{(2)} \exp [i w (r_2 - r_1)] + \text{konj. kompl.} \right\}$$

mit

$$A_i = \iint \Psi_i^*(r_i - r'_i) \Psi_i(r_i - r''_i) \exp \left( \sum_w |d_{w0}^{(i)}|^2 \exp [i w (r'_i - r''_i)] \right) dr'_i dr''_i.$$

<sup>(25)</sup> S. J. PEKAR: l. c. <sup>(5)</sup>.



Unter den entsprechenden Vereinfachungen erhalten wir für  $F_{0,0,0,0}$ :

(7.14) 
$$F_{0,0,0,0} = G_{0,0,0,0} \frac{1}{2} \left\{ \sum_w \gamma_w d_w^{(2)} \exp[iw(r_1 - r_2)] - \gamma_w d_w^{(1)} \exp[iw(r_2 - r_1)] + \right. \\ \left. + \text{konj. kompl.} \right\}.$$

Zur Auswertung der Summe setzen wir die Ausdrücke (7.1) und (7.11) ein und verwandeln die Summe in ein Integral. Dieses Integral ließe sich in geschlossener Form auswerten. Da wir aber ohnehin bei der Berechnung von  $G_{0,0,0,0}$  wie auch von  $F_{0,0,0,0}$  unter der Voraussetzung  $r_{12} > 1/\beta_i$  Vereinfachungen durchführten, ist es sinnvoll, hier ebenfalls die entsprechenden Vereinfachungen <sup>(26)</sup> vorzunehmen. Wir erhalten dann sofort:

(7.15) 
$$H_w^{(2)} = \frac{F_{0,0,0,0}}{G_{0,0,0,0}} = \left( \frac{1}{\varepsilon_\infty} - \frac{1}{\varepsilon} \right) \frac{e^2}{r_{12}}.$$

8. – Eine Modifikation des Variationsansatzes (4.6).

Sowohl in den Grenzfällen schwacher bis mittlerer als auch starker Kopplung liefert, wie wir eben zeigten, die Überlagerung der die Einzelteilchen begleitenden Polarisationswolken für große Teilchenabstände das klassisch zu erwartende Wechselwirkungsgesetz (7.8) (bzw. (7.15)). Wesentlich bei dieser Untersuchung ist, daß nichts über die Größe des Kopplungsparameters zwischen Teilchen und Feld vorausgesetzt werden muß, sondern daß die zur Herleitung der Schrödingergleichung (5.15) gemachten Annahmen lediglich einen nicht zu kleinen Bahnradius voraussetzen. Die physikalische Bedeutung dieser Bedingung liegt, wie wir im Anhang ausführlich zeigen, darin, daß die effektive Wechselwirkung zwischen den Teilchen, die durch den Austausch von Schallquanten hervorgerufen wird und die in unserem hier betrachteten Falle durch (7.8) gegeben ist, kleiner als die Energie eines Schallquants ist.

Bei kleineren Bahnradien erscheinen die Vereinfachungen in Abschnitt 5, insbesondere die Vernachlässigung der f-Abhängigkeit von  $G'_{f_1, f_2', f_1, f_2}$  und  $F'_{f_1, f_2', f_1, f_2}$  nicht mehr als gerechtfertigt. Dies ist an sich zunächst kein Einwand gegen die Brauchbarkeit des Variationsansatzes (4.6) bei kleineren Radien, da man die Variationsaufgabe (4.7) — wenigstens im Prinzip — mit dem Ansatz (4.6) auch ohne die eben erwähnten Vernachlässigungen hätte lösen können (wobei natürlich die anschaulichen Züge verloren gehen würden, was hier aber im Moment nicht zur Diskussion steht). Indessen ist auch der Ansatz (4.6)

<sup>(26)</sup> Die hierbei eingehende Vereinfachung besteht darin, daß im Nenner von  $d_w$  das Glied  $(w/2\beta)^2$  gegenüber 1 vernachlässigt wird. Die Rechtfertigung hierfür liefert die Sattelpunktmethode, nach der in dem Integral  $\int f(w) \exp[i(wr)] dw$  für  $r \rightarrow 1/\beta$  nur Glieder mit  $w < \beta$  einen wesentlichen Beitrag liefern.

nicht vollständig, da er nur «angezogene» Teilchen ohne zusätzliche freie Quanten benutzt. Gerade die oben ausgesprochene Bedingung, daß die durch das Feld der Gitterschwingungen hervorgerufene Wechselwirkung zwischen den Teilchen kleiner als die Energie eines Quants ist, zeigt, daß bei kleineren Radien der Ansatz (4.6) durch Produkte aus solchen Einteilchenfunktionen (4.2)<sup>27</sup> zu erweitern ist, bei denen zusätzlich noch freie Quanten (27) angeregt sind. Während eine Erweiterung dieser Art zur Untersuchung thermischer Effekte (27) zweifellos sehr sinnvoll ist, so möchten wir doch im folgenden noch auf eine andere Modifikation des Variationsansatzes (4.6) hinweisen, die folgendermaßen nahegelegt wird:

Beim Ansatz (4.6) wird die gesuchte Funktion in bestimmter Weise als Überlagerung von Einteilchenfunktionen (4.2) aufgebaut, deren jede die Bewegung eines Teilchens zusammen mit der begleitenden Gitterdeformation beschreibt. Die Gestalt dieser Gitterdeformation (bzw. Polarisationswolke) ist für die verschiedenen Bewegungszustände der Teilchen (verschiedene  $\mathbf{k}$ -Zustände) verschieden, was durch die  $\mathbf{k}$ -Abhängigkeit des Modulationsfaktors  $u_{\mathbf{k}}(\mathbf{r}, b^+)$  in (4.2) erfaßt wird. Wesentlich für unsere jetzige Überlegung ist nun, daß bei dieser  $\mathbf{k}$ -Abhängigkeit eine geradlinige Bewegung von Teilchen + Gitterdeformation vorausgesetzt ist. Wenn jedoch die beiden im Exziton gebundenen Teilchen dauernd ihre Richtung ändern, so wird sich die « $\mathbf{k}$ -Deformation» der Polarisationswolke nicht voll ausbilden. Diese «Behinderung der  $\mathbf{k}$ -Abhängigkeit» kann man ohne weiteres im Ansatz (4.6) durch eine einfache Modifikation der Eielektronenlösungen (4.2) erfassen (28). Auf den besonders einfachen Fall, in dem die  $\mathbf{k}$ -Abhängigkeit völlig aufgegeben wird, wurden wir schon auf Grund anderer Überlegungen geführt (29). In diesem Fall hängt also  $u$  nicht mehr von  $\mathbf{k}$  ab und die exakte Berechnung des Variationsintegrals (4.7), die wir unter Verwendung der Funktionen von Lee, Low und Pines durchführten, bereitet keinerlei Schwierigkeiten. Die Variation nach  $\Psi^*$  liefert dann ohne jede Vernachlässigung eine Gleichung von genau der gleichen Form wie (5.15) mit dem Wechselwirkungsglied (7.7), wobei jedoch im wesentlichen Unterschied zu (5.15) für die Massen  $m_i$  die im ruhenden Gitter zu setzen sind.

Daß dieses sich hier wiederum ergebende Wechselwirkungsglied (7.7) für große Abstände richtig ist, wissen wir bereits. Es zeigt aber auch bei kleinen Abständen, zumindest qualitativ, das richtige Verhalten. Im Grenzfall sehr kleiner Bahnradien kompensiert sich nämlich, wie wir an anderer Stelle aus-

(27) Ein derart erweiterter Ansatz ist auch bei großen Bahnradien dann nötig, wenn freie Quanten angeregt sind, was man zu berücksichtigen hat, wenn man etwa die thermische Dissoziation des Exzitons oder seine Streuung an angeregten Gitterwellen untersuchen will.

(28) Bei den Einteilchenlösungen bei schwacher bis mittlerer Kopplung erreicht man dies einfach dadurch, daß man in (I.1. Anhang)  $\eta_i$  noch als frei wählbar ansieht.

(29) Eine ausführliche Darstellung erscheint in *Zeits. f. Phys.*

fürlich zeigen, die Wechselwirkungsenergie (7.7) gegen die Selbstenergie der beiden Teilchen. Dies bedeutet nichts anderes, als daß bei sehr kleinen Radien das Exziton für die Polarisationswellen als elektrisch neutral erscheint <sup>(30)</sup>, sodaß keine Wechselwirkung mit diesen Wellen und damit auch keine direkte Wechselwirkung zwischen den Teilchen zustandekommt. Da es dann auch kein Mitlaufen der Polarisationswolken mit den *einzelnen* Teilchen mehr gibt, besitzen diese Teilchen nicht mehr die scheinbare Masse im schwingenden, sondern die im ruhenden Gitter <sup>(31)</sup>. Wenn wir nun zwischen dem bei großen Radien realisierten Grenzfall der vollen  $f$ -Abhängigkeit und dem bei kleinen Radien einen eine (vermutlich!) brauchbare Näherung darstellenden Grenzfall verschwindender  $f$ -Abhängigkeit interpolieren, so wird das Wechselwirkungsglied (7.8) (bei der hier betrachteten schwachen bis mittleren Kopplung: Teilchen-Feld) seine Form behalten, während wir eine Änderung der scheinbaren Massen zu erwarten haben.

Unsere Aussage, daß wir hier im wesentlichen schon das richtige Wechselwirkungsglied vor uns haben, während die Untersuchung des Verhaltens der scheinbaren Massen bei kleinen Abständen noch weiterhin sorgfältig untersucht werden muß, wird auch noch von einem allgemeinen Gesichtspunkt her gestützt: Bekanntlich liefern Variationsverfahren auch bei nicht sehr guten Funktionen brauchbare Energiewerte. Da nun — wenn wir an das Wasserstoffproblem denken — die Energie von der Kernladung  $Z$  quadratisch, von der Elektronenmasse hingegen nur linear abhängt, so können wir schließen, daß das Variationsverfahren das Wechselwirkungsglied genauer als die scheinbare Masse liefert. Eine entsprechende Erfahrung liegt, *mutato mutandis*, bereits aus der Polaronentheorie vor, da hier bekanntlich die Energieabsenkung (= Selbst-Wechselwirkungs-Energie!) nur wenig von dem Näherungsansatz, die scheinbare Masse des Teilchens hingegen sehr empfindlich davon abhängt.

Unsere Ausführungen in den Abschnitten 4 und 5 hatten keinerlei Gebrauch von der genauen Form der Einteilchenlösungen (außer von der Gestalt (4.2)) gemacht, wie auch von dem Wechselwirkungsglied (3.4) (implizit) lediglich vorausgesetzt wurde, daß es keine Ableitungen nach der Ortskoordinate der Teilchen enthält. Es darf aber sehr wohl noch die Operatoren des

---

<sup>(30)</sup> Zu der Aussage, daß die « effektive » Kopplung des Exzitons an die Polarisations-schwingungen kleiner ist als beim Einteilchenproblem, gelangte bereits MEYER <sup>(11)</sup>. Allerdings gibt unsere Rechnung nur im Limes  $r_{12} \rightarrow 0$  eine verschwindende Kopplung, während bei dem Ansatz von MEYER diese Wechselwirkung überdies auch im Falle, daß die scheinbaren Massen (im ruhenden Gitter) der beiden Teilchen einander gleich sind, für beliebige Bahnradien identisch verschwindet. Wie sich zeigt <sup>(29)</sup>, liegt der Energie-Erwartungswert unseres oben diskutierten Ansatzes ( $f \rightarrow 0$ ) durchwegs tiefer als der entsprechende von MEYER.

<sup>(31)</sup> Bei dieser gesamten Diskussion denken wir an die Kontinuumsnäherung für das Gitter. Die Berücksichtigung der atomistischen Struktur erfordert neue Gesichtspunkte, auf die wir hier nicht näher eingehen.

Spins oder des Isotopenspins enthalten. Deshalb sind die Ergebnisse der Abschnitte 4 bis 6 sofort auch für die Behandlung der Kopplung von Nukleonen über ein Mesonenfeld heranzuziehen. Die Bedingung für die Brauchbarkeit des in diesen Abschnitten beschriebenen Verfahrens, daß die effektive Wechselwirkungsenergie Nukleon-Nukleon kleiner als die Energie eines Feldquants ist, ist wegen der großen Ruhe-Energie der Mesonen, wie man leicht überschlägt, zumindest bei den leichteren Atomkernen erfüllt. Vorausgesetzt ist dabei natürlich (gemäß Abschnitt 5) eine nichtrelativistische Behandlung der Nukleonenbewegung und die Divergenzfreiheit des Problems. Zwar wäre eine Renormierung von Gl. (5.15) sofort möglich, doch soll hier nicht weiter darauf eingegangen werden, da die dann sofort auftretende Frage nach dem Zusammenhang mit den üblichen Renormierungskonstanten den Rahmen dieser Arbeit übersteigen würde.

\* \* \*

Den Herren Professoren F. HUND und H. VOLZ sowie den Mitarbeitern von Prof. Hund danke ich für interessante Diskussionen.

## ANHANG I

**Die Bedingung für die Vernachlässigbarkeit der  $f$ -Abhängigkeit von  $G_{t_1, t_2, t_3, t_4}$  (zu S. 8).**

a) *Schwache bis mittlere Kopplung.* — Wir benutzen wieder die Einteilchenlösungen von LEE, LOW und PINES <sup>(32)</sup>:

$$u_{f_i}^{(i)}(r_i, b^+) = \exp \left[ -\frac{1}{2} \sum_w |f_{w,i}^{(f_i)}|^2 \right] \exp \left[ \sum_w b_w^+ f_{w,i}^{(f_i)} \exp [-i w r_i] \right],$$

mit

$$(I.1) \quad f_{w,i}^{(f_i)} = \mp \frac{\gamma_w^*}{[\hbar \omega - (w f_i \hbar^2 / m_i^*) (1 - \eta_i) + (\hbar^2 w^2 / 2 m_i^*)]}.$$

Das darin auftretende  $\gamma_w$  ist in (7.1) definiert, während  $\eta$  näherungsweise (für  $\hbar^2 k^2 / 2 m_i^* \lesssim \hbar \omega$ ) durch  $\eta_i = (\alpha_i / 6) / (1 + \alpha_i / 6)$  gegeben ist. Für den Gültigkeitsbereich der Lösung von Lee, Low und Pines, der etwa durch die Kopplungskonstante  $\alpha_i < 6$  gegeben ist, ist  $0 \leq \eta_i < 1$ . Die Lösungen (I.1) sind außerdem

<sup>(32)</sup> T. LEE, F. LOW und D. PINES: I. c. <sup>(5)</sup>.



auf den Bereich

(I.2) 
$$k_i < \sqrt{2m_i^* \omega / \hbar} \, ,$$

beschränkt.

Die Berechnung von  $G_{\mathbf{f}_1, \mathbf{f}_2, \mathbf{f}_1, \mathbf{f}_2}^{\mathbf{f}_1', \mathbf{f}_2'}$  mit (I.1), die genau wie die von  $G_{0,0,0,0}$  auf S. 14 verläuft, liefert

(I.3) 
$$\begin{aligned} \exp \Big[ - \frac{1}{2} \sum_{j=1,2} \sum_{\mathbf{w}} ( |f_{\mathbf{w},j}^{(\mathbf{f}_j')}|^2 + |f_{\mathbf{w},j}^{(\mathbf{f}_j)}|^2 ) + \sum_{j=1,2} \sum_{\mathbf{w}} f_{\mathbf{w},j}^{(\mathbf{f}_j')*} f_{\mathbf{w},j}^{(\mathbf{f}_j)} + \\ + \sum_{\mathbf{w}} ( f_{\mathbf{w},1}^{(\mathbf{f}_1')*} f_{\mathbf{w},2}^{(\mathbf{f}_2)} \exp [i\mathbf{w}(\mathbf{r}_1 - \mathbf{r}_2)] + f_{\mathbf{w},2}^{(\mathbf{f}_2')*} f_{\mathbf{w},1}^{(\mathbf{f}_1)} \exp [i\mathbf{w}(\mathbf{r}_2 - \mathbf{r}_1)] \Big] . \end{aligned}$$

Um die weiteren Ausführungen nicht zu verwickelt zu gestalten, greifen wir eine der obigen Exponentialfunktionen heraus und behandeln als Beispiel etwas ausführlicher:

(I.4) 
$$\exp \Big[ \sum_{\mathbf{w}} f_{\mathbf{w},1}^{(\mathbf{f}_1')*} f_{\mathbf{w},2}^{(\mathbf{f}_2)} \exp [i\mathbf{w}(\mathbf{r}_1 - \mathbf{r}_2)] \Big] .$$

Wir spezialisieren unser Beispiel — ohne dabei wesentliche Gesichtspunkte zu vernachlässigen — noch weiter, indem wir  $\mathbf{f}_2 = 0$ ,  $m_1^* = m_2^* = m$  und  $\eta_1 = \eta_2 = \eta$  setzen. Wir betrachten zunächst den Exponenten, der nach Einsetzen der  $f_{\mathbf{w}}$  und der Umformung der Summe in ein Integral die folgende Form hat:

(I.5) 
$$\frac{\hbar^2 \omega^2 4 \pi \alpha}{u(2\pi)^3} \iiint \frac{\exp [i\mathbf{w}(\mathbf{r}_1 - \mathbf{r}_2)]}{\left( \hbar \omega - \frac{\mathbf{w} \mathbf{f} \hbar^2}{m} (1 - \eta) + \frac{\hbar^2 \omega^2}{2m} \right) \left( \hbar \omega + \frac{\hbar^2 \omega^2}{2m} \right)} \frac{d\mathbf{w}}{w^2} .$$

Da ferner  $0 \leq \eta < 1$  ist, bleiben wir in der richtigen Größenordnung, wenn wir  $1 - \eta$  einfach durch 1 ersetzen. Die Reihenentwicklung von (I.5) nach Potenzen von  $k$  liefert

(I.6) 
$$\frac{\hbar^2 \omega^2 4 \pi \alpha}{u(2\pi)^3} \sum_v \iiint \frac{\exp [i\mathbf{w}(\mathbf{r}_1 - \mathbf{r}_2)] \left( \frac{\hbar^2}{m} \mathbf{w} \mathbf{f} \right)^v}{\left( \hbar \omega + \frac{\hbar^2 \omega^2}{2m} \right)^{v+2}} \frac{d\mathbf{w}}{w^2} .$$

Da wir ohnehin schon wissen, daß die  $\mathbf{f}_i$ , die in (I.6) auftreten, klein sein müssen, daß also speziell der Exzitonenradius  $r_{12}$  hinreichend groß sein muß, beschränken wir uns von vornherein auf große  $r_{12}$  und zwar im Hinblick auf (I.2):  $r_{12} > \sqrt{\hbar/2m\omega}$ .

Die Behandlung des Integrals nach der Sattelpunktmethode lehrt dann sofort, daß die wesentlichen Beiträge zum Integral nur von  $w$ -Werten mit  $wr \approx 1$ , also  $w \approx \sqrt{2m\omega/\hbar}$  herrühren. Wir erhalten dann, wenn wir  $\mathbf{w} \mathbf{f}$  durch

$wk$  abschätzen:

$$(I.7) \quad \left\{ \begin{aligned} &\approx \frac{\hbar^2 \omega^2 4\pi\alpha}{u(2\pi)^3} \sum_{\nu} \frac{1}{\hbar^2 \omega^2} \left( \frac{\hbar}{m\omega} \right)^{\nu} \left( \frac{2m\omega}{\hbar} \right)^{\nu/2} k^{\nu} \iint \frac{\exp[iw(r_1 - r_2)]}{w^2} dw \\ &\approx \frac{\alpha}{ur_{12}} \sum_{\nu} \frac{1}{(2m\omega/\hbar)^{\nu/2}} (2)^{\nu/2} k^{\nu} . \end{aligned} \right.$$

Mit  $u = \sqrt{2m\omega/\hbar}$  erhalten wir (unter der Voraussetzung  $k < u/\sqrt{2}$ ) für die betrachtete Exponentialfunktion (I.4)

$$(I.8) \quad \approx \exp \left\{ \frac{\alpha}{ur_{12}} \frac{1}{1 - \sqrt{2}k/u} \right\} \approx \exp \left\{ \frac{\alpha}{ur_{12}} \right\} \left\{ 1 + \frac{\sqrt{2}\alpha}{ur_{12}} \frac{k}{u} + \dots \right\} .$$

Diese Endformel liefert uns sofort die gewünschte Abschätzung, da sich die Potenzreihenentwicklung von  $G'_{f_1, f_2, f_1, f_2}$  nach  $f_i, f'_i$  einfach aus Produkten der Form (I.8) zusammensetzt. Die Bedingung, daß wir die Potenzen von  $f$  gegenüber  $f_0$  vernachlässigen dürfen, lautet unter der Annahme  $r_{12} > 1/u$ :  $\alpha k/u < 1$  oder wegen  $r_{12} \sim 1/k$  <sup>(33)</sup>

$$(I.9) \quad r_{12} > \frac{\alpha}{u} .$$

Der Bahnradius des Exzitons muß also dieser Bedingung genügen, damit die auf S. 8 gemachten Vernachlässigungen der  $f$ -Abhängigkeit von  $G'_{f_1, f_2, f_1, f_2}$  gerechtfertigt sind. Die anschauliche Bedeutung dieser Bedingung erhellt sofort, wenn wir  $\alpha$  und  $u$  gemäß S. 13 durch die experimentell gegebenen Größen ausdrücken:

$$\left( \frac{1}{\varepsilon_{\infty}} - \frac{1}{\varepsilon} \right) \frac{e^2}{r_{12}} < \hbar\omega .$$

Die in Rede stehende Vernachlässigung ist also dann gerechtfertigt, wenn die Wechselwirkungsenergie zwischen den Teilchen, die über das Feld der Gitterschwingungen zustandekommt, etwa kleiner als die Anregungsenergie für ein Quant der Gitterschwingung ist.

b) *Starke Kopplung.* – Wir benutzen bei der Diskussion die von HÖHLER <sup>(34)</sup> bzw. TJABLIKOV <sup>(35)</sup> für diesen Grenzfall angegebene Lösungsfunktion von

<sup>(33)</sup> Bei dieser hier und im folgenden benutzten Relation wird in gewissen Sinne  $U(r_1, r_2)$  mit  $\iint c_{f_1 f_2} \exp[i f_1 r_1 + i f_2 r_2] dr_1 dr_2$  identifiziert. Wie sich unter Benutzung der gleichen Schlüsse, wie sie hier in Anhang I und II benutzt werden, zeigen läßt, ist dieses Vorgehen für  $r_{12} > 1/U$  tatsächlich erlaubt, worauf wir hier aber aus Raumgründen nicht näher eingehen.

<sup>(34)</sup> G. HÖHLER: l. c. <sup>(6)</sup>.

<sup>(35)</sup> S. V. TJABLIKOV: l. c. <sup>(5)</sup>.

der Form:

$$\exp [i \mathfrak{f} r] u_{\mathfrak{f}}(r, b^+) =$$
$$= \exp [i \mathfrak{f} r] \int \exp [i \mathfrak{f}(r' - r)] \Psi(r - r') \exp \left[ \sum_{\mathfrak{w}} d_{\mathfrak{w}} b_{\mathfrak{w}}^+ \exp [-i \mathfrak{w} r'] \right] dr',$$

mit den auf S. 15 definierten  $\Psi$  und  $d_{\mathfrak{w}}$ .

Nach diesem Ansatz sind die  $d_{\mathfrak{w}}$  nicht von  $\mathfrak{f}$  abhängig, was, wie TAJBLIKOV hervorhebt, eine ziemlich einschneidende Vereinfachung darstellt, sodaß insbesondere sich die scheinbare Masse nur halb so groß wie nach der Pekarschen Rechnung ergibt. Insofern kann unsere nachfolgende Abschätzung nur zu einer vorläufigen Orientierung dienen.

Genau wie auf S. 15 können wir  $G_{\mathfrak{f}_1, \mathfrak{f}_2, \mathfrak{f}_1, \mathfrak{f}_2}$  bei Abständen  $r_{12}$ , die größer als die Ausdehnung der Ladungswolken  $|\Psi|^2$  sind, näherungsweise in der Form schreiben

$$G_{\mathfrak{f}_1, \mathfrak{f}_2, \mathfrak{f}_1, \mathfrak{f}_2} \approx A_{1, \mathfrak{f}_1, \mathfrak{f}_1} \cdot A_{2, \mathfrak{f}_2, \mathfrak{f}_2} \exp \left[ \sum_{\mathfrak{w}} d_{\mathfrak{w}}^{(1)} d_{\mathfrak{w}}^{(2)} \exp [i \mathfrak{w}(r_2 - r_1)] + \text{konj. kompl.} \right],$$

mit

$$A_{i, \mathfrak{f}_i, \mathfrak{f}_i} = \iint \exp [-i \mathfrak{f}_i(r'_i - r_i)] \Psi_i^*(r_i - r'_i) \cdot$$
$$\cdot \exp [i \mathfrak{f}_i(r''_i - r_i)] \Psi_i(r_i - r''_i) \exp \left[ \sum_{\mathfrak{w}} |d_{\mathfrak{w}}^{(i)}|^2 \exp [i \mathfrak{w}(r'_i - r''_i)] dr'_i dr''_i \right].$$

Ohne den Beweisgang wesentlich zu beeinträchtigen, betrachten wir nur  $A_1$  und setzen darin  $\mathfrak{f}'_2 = 0$  (und  $\mathfrak{f}_1 = \mathfrak{f}$ ,  $r_1 = r$ ). Die Reihenentwicklung von  $A_1$  nach Potenzen von  $\mathfrak{f}$  liefert:

$$\sum_{\nu=0}^{\infty} \frac{i^{\nu}}{\nu!} \iint [\mathfrak{f}(r - r'')]^{\nu} \Psi(r - r') \Psi(r - r'') \exp \left[ \sum_{\mathfrak{w}} |d_{\mathfrak{w}}|^2 \exp [i \mathfrak{w}(r' - r'')] \right] dr' dr''.$$

Einen Einblick in die Größenordnung der einzelnen Glieder erhalten wir, wenn wir überall zu den Beträgen übergehen und  $\mathfrak{f}(r - r')$  durch  $k |r - r'|$  ersetzen:

$$\approx \exp \left[ \sum |d_{\mathfrak{w}}|^2 \right] \int \Psi(r - r'') dr'' \cdot \sum_{\nu=0}^{\infty} \frac{1}{\nu!} k^{\nu} \int |r - r'|^{\nu} \Psi(r - r') dr'.$$

Da wir Glieder mit  $k^{\nu}$ ,  $\nu \neq 0$  gegenüber dem mit  $k^0$  abschätzen wollen, können wir von dem vor der Summe stehenden gemeinsamen Faktor absehen. Mit

$$\Psi = \left( \frac{\beta^3}{\pi} \right)^{\frac{1}{2}} \exp [-\beta r],$$

ergibt sich das Integral

$$\int r^{\nu} \Psi(r) dr \quad \text{zu} \quad (\nu + 2)! \frac{1}{\beta^{\nu+3}} 4\pi \left( \frac{\beta^3}{\pi} \right)^{\frac{1}{2}}.$$

Der schon alles Wesentliche zeigende Vergleich der ersten beiden Glieder  $k^{\nu}$

und  $k^+$  führt auf die Beziehung

$$2! \frac{1}{\beta^3} 4\pi \left( \frac{\beta^3}{\pi} \right)^{\frac{1}{2}} > 3! \frac{1}{\beta^4} 4\pi \left( \frac{\beta^3}{\pi} \right)^{\frac{1}{2}} \cdot k,$$

also

$$k < \frac{2}{3} \beta,$$

und da nach PEKAR<sup>(36)</sup>  $\beta \approx 0.6u \cdot \alpha$ , lautet die Bedingung:  $k < \frac{1}{3}\alpha u$ , die bei einer großen Kopplungskonstanten  $\alpha$  natürlich leicht erfüllt ist.

Die Abschätzung der höheren Glieder der Reihenentwicklung von  $F'_{f'_1, f'_2, f_1, f_2}$  verläuft ganz entsprechend und führt wiederum auf Gl. (I.9).

## ANHANG II

**Die Berechtigung der Vernachlässigung von  $|U|^2(G_x^2/G^2)$  gegenüber  $U^* \Delta U$**   
(zu S. 11).

a) *Schwache bis mittlere Kopplung.* — Wir gehen von dem Ausdruck (7.5) für  $G_{0,0,0,0}$  aus, quadrieren im Exponenten aus und untersuchen die beiden noch von  $r_1 - r_2$  abhängigen Glieder

$$(II.1) \quad \sum_w |\gamma_w|^2 \left\{ \frac{\exp[iw(r_1 - r_2)]}{(\hbar^2 w^2 / 2m + \hbar\omega)^2} + \text{konj. kompl.} \right\},$$

wobei wir der Einfachheit zuliebe  $m_1 = m_2 = m$  gesetzt haben. Es genügt die erste Summe zu betrachten. Einsetzen von  $\gamma_w$  (s. S. 13) und Umformung der Summe in ein Integral liefert den gleichen Ausdruck (I.5), Anhang I, mit  $f = 0$ . Für  $r_{12} > 1/u$  liefert die Abschätzung dieses Integrals

$$(II.2) \quad \int \dots dw \lesssim \frac{1}{\hbar^2 \omega^2} \int \frac{\exp[iw(r_1 - r_2)]}{w^2} dw \approx \frac{4\pi}{\hbar^2 \omega^2} \frac{1}{r_{12}}.$$

Wir erhalten also (II.1)  $\lesssim (\alpha/u)(1/r_{12})$ .

Insgesamt ergibt sich damit:

$$(II.3) \quad |U|^2 \frac{G_x^2}{G^2} \lesssim \left( \frac{\alpha}{u} \right)^2 \frac{1}{r_{12}^4} |U|^2.$$

Nehmen wir andererseits  $U$  als wasserstoffartige Funktion

$$U(r_1 - r_2) \sim \exp[-r_{12}/r_0],$$

<sup>(36)</sup> S. J. PEKAR: l. c. <sup>(5)</sup>.



an, so ergibt sich größenordnungsmäßig:

$$(II.4) \quad U^* A U \approx \frac{1}{r_0^2} |U|^2.$$

Da wir in (II.3) für  $r_{12}$  ebenfalls größenordnungsmäßig  $r_0$  zu setzen haben, erhalten wir unmittelbar durch Vergleich von (II.3) und (II.4) die Abschätzung

$$\frac{\alpha}{u} \frac{1}{r_0} < 1,$$

also genau die gleiche Bedingung wie oben [Formel (I.9), Anhang I].

b) *Starke Kopplung.* — Wir benutzen für  $G_{0,0,0}$  die vereinfachte Form (7.12) (s. auch Anhang I), bei der vorausgesetzt ist, daß  $r_{12}$  groß gegenüber der Ausdehnung der einzelnen Ladungswolken ist. Substituieren wir in  $A_i$ :  $r_i$  durch  $\tilde{r}_i'$  und  $r_i - r_i''$  durch  $\tilde{r}_i''$ , so sehen wir sofort, daß die gesamte Abhängigkeit der Funktion  $G_{0,0,0}$  von  $r_1$  und  $r_2$  im Exponentialfaktor enthalten ist. Wir schätzen den Exponenten der Exponentialfunktion ab. Unter Benutzung der Ausdrücke (7.11) für die  $d_{10}^{(i)}$  erhalten wir unter nochmaliger Verwendung der Voraussetzung, daß  $r_{12}$  groß gegenüber der Ausdehnung der beiden Ladungswolken ist:

$$\text{Exponent} \approx \frac{\alpha}{u} \frac{1}{r_{12}}.$$

Damit erhalten wir wegen  $G \sim \exp [(\alpha/u)(1/r_{12})]$  unmittelbar

$$\frac{G_x^2}{G^2} \approx \left(\frac{\alpha}{u}\right)^2 \frac{1}{r_{12}^4}.$$

Insgesamt ergibt sich somit genau das gleiche Ergebnis wie im Falle (II.a):

$$r_{12} > \frac{\alpha}{u}.$$

#### RIASSUNTO (\*)

Si determinano gli stati stazionari di un eccitone (coppa elettrone-elettrone difettivo) nel reticolo vibrante, per mezzo di un procedimento variazionale approssimato utilizzabile per una qualsiasi intensità dell'accoppiamento tra particelle singole e vibrazioni del reticolo, presumendo note le soluzioni monoparticellari nel reticolo vibrante. Si sviluppa la dimostrazione della validità del procedimento per raggi dell'eccitone sufficientemente grandi. Si accenna alla validità del metodo per il trattamento non relativistico dell'accoppiamento di nucleoni ad un campo mesonico (nel caso non divergente).

(\*) Traduzione a cura della Redazione.

## On Thermoelastic Waves in Liquids.

A. CARRELLI and E. GROSSETTI

*Istituto di Fisica dell'Università - Napoli*

(ricevuto il 5 Marzo 1956)

**Summary.** (\*) — This paper investigates the thermomechanical properties of some liquids and solutions (water, glycerine, saturated solution of NaCl, saturated solution of  $\text{Na}_2\text{SO}_4$ ) already pointed out by R. LUCAS <sup>(1)</sup>. The existence of the force predicted by LUCAS has been confirmed by us with different methods which have yielded practically coincident results (account taken of the difficulties inherent to the measures). It should be underlined that the various methods employed are differently quick; an optical method which detects the thermal behaviour has shown that the latter proceeds practically in accord with the force measured by us.

(\*) *Editor's Translation.*

In a paper by LUCAS <sup>(1)</sup> we find the following reasoning: A volume  $\Delta V$  of a liquid, the thermal capacity and the density of which are respectively  $c$  and  $\rho$ , under an increase  $\Delta T$  of temperature will acquire a quantity  $Q$  of heat:

$$Q = \rho c \Delta V \Delta T.$$

This thermal energy expands from a point of the fluid to another in a certain way; connected with this flow of energy there will be the flow of a momentum  $G$ ; the variation  $\Delta G$  will be connected to  $Q$  by the equation:

$$\frac{Q}{\Phi} = \Delta G,$$

where  $\Phi$  is a velocity. If this variation of momentum occurs in the time  $\Delta t$

(<sup>1</sup>) R. LUCAS: *Journ de Phys.*, série VII, n. 10, p. 441 (1937).

on the volume unity of the fluid will act a force  $f$  given by

$$f = \frac{1}{\Phi} \frac{1}{\Delta V} \frac{dQ}{dt} = \frac{\rho c}{\Phi} \frac{dT}{dt}.$$

Referring to the heat transfer equation, we can express the derivative of  $T$  with respect to  $t$  in the following way:

$$\frac{\partial T}{\partial t} = \frac{K}{\rho c} \Delta^2 T,$$

where  $K$  is the thermal conductivity of the fluid.

If the heat flow takes place along the direction  $x$  one can write more particularly:

$$\frac{\partial T}{\partial t} = \frac{K}{\rho c} \frac{\partial^2 T}{\partial x^2}.$$

If in a liquid we consider two planes  $x_1$  and  $x_2$  at the temperatures  $T_1$  and  $T_2$ , between these two planes there will be a difference of hydrostatic pressure given by  $\int_{x_1}^{x_2} \rho g dx$  and a difference of pressure due to the presence of this heat flow, given by:

$$\Delta p = \frac{K}{\Phi} \left[ \left( \frac{\partial T}{\partial x} \right)_{x_1} - \left( \frac{\partial T}{\partial x} \right)_{x_2} \right];$$

if the plane  $x_2$  is very far from  $x_1$ , where the thermal action may still be felt, one can write:

$$\Delta p = \frac{K}{\Phi} \frac{\partial T}{\partial x_1},$$

and therefore the total force acting on a floating body will be given by:

$$F = S \cdot \Delta p = \frac{SK}{\Phi} \frac{\partial T}{\partial x} + S \int_{x_1}^{x_2} \rho g dx.$$

From the study of the thermal conductivity one may calculate  $\Delta T$  as a function of  $t$  at a distance  $x$ :

$$\Delta T = \Delta T_0 [1 - 2\varepsilon],$$

where

$$\varepsilon = \frac{1}{\sqrt{\pi}} \int_0^{\xi} e^{-\xi} d\xi$$

with

$$\xi = \frac{x}{2} \sqrt{\frac{\rho c}{K}} \frac{1}{\sqrt{t}},$$

from which one deduces:

$$\frac{\partial T}{\partial x} = -\frac{\Delta T_0}{\sqrt{\pi}} \sqrt{\frac{\rho c}{Kt}} \cdot \exp \left[ -\frac{\rho c}{Kt} x^2 \right];$$

therefore after a time  $t_m$  one obtains a maximum given by

$$t_m = \frac{x^2 \rho c}{2K}.$$

The maximum for  $\partial T / \partial x$  gives also a maximum of the force  $F = fS$ :

$$F = fS \left| \frac{\partial}{\partial x} \right| \frac{\Delta T_0}{\pi e} \sqrt{\frac{\rho c}{Kt}} \frac{KS}{\Phi}.$$

Knowing  $F$  we are thus able to calculate  $\Phi$ . One must also take account of the term  $\int_{x_1}^{x_2} \rho g dx$  which may be calculated at any moment if we know the thermic distribution of the liquid.

As the density of the liquid increases with time because of the temperature decrease one can say that a floating body originally in equilibrium in the liquid is pushed upward when the liquid becomes colder. On the contrary, through the thermoelastic action it is pushed downwards.

For our measurements we used—as did Prof. LUCAS—a very sensitive balance (2.2 divisions for 1 mg and for a total weight of 200 g), having an oscillation period of about 20 s (Fig. 1). On the axis of the knife of the yoke we placed a little mirror  $S$  so that the displacement taking place

as a consequence of the thermal waves could be photographically registered on a photographic recorder.

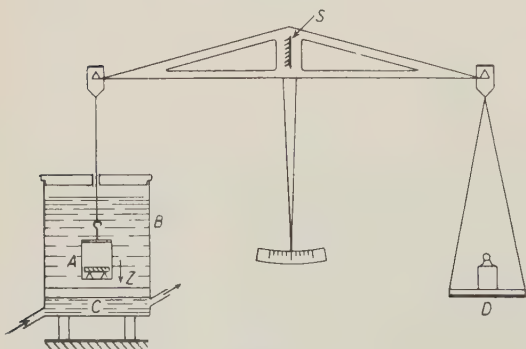


Fig. 1.



The floating body *A* consists of a glass cylinder on the basis of which are fixed two brass discs about 0.5 mm thick. This body is hanged on one arm of the balance and plunged in a container *B* filled up with the liquid; the balance is then put again in equilibrium with some weights placed on plate *D*. The bottom *F* of the container is made of copper sheet 2 mm thick and is kept at room temperature by means of water circulation. A second pump allows, by the turning of a two-way tap, to substitute cold water of 2 °C in the space *C* thus causing a sudden lowering of the temperature of the bottom of container *B*.

The substitution of the water at room temperature with cold water requires about 10 s which is a short time in comparison with the 260 s required for reaching the maximum force against the bottom. After having measured the sensibility of the balance one is able to obtain from the registered deflection the value of the acting force. From Lucas' equation, as we know the maximum value  $F_m$  of the force, we can obtain the value of  $\Phi$  and compare this value with the speed of the longitudinal waves in the liquid under examination, value given by  $V = 4c/3$ , where  $c$  is the velocity of sound in the liquid.

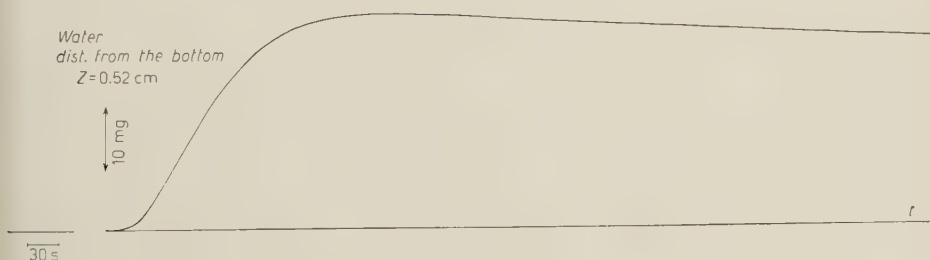


Fig. 2.

In Fig. 2 and 3 are given plots of the force acting on the body immersed respectively in water or in glycerin against time when the variation  $\Delta T$  of temperature is about 14 °C (cooling from 15 °C to 1 °C). In every in-

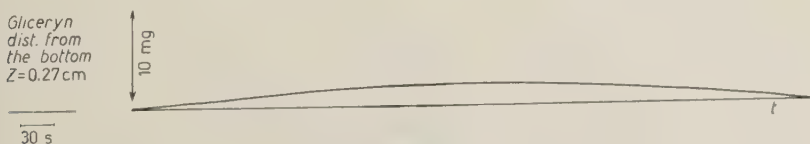


Fig. 3.

stance, as already put in evidence by LUCAS, one observes with all liquids first a movement of the floating body towards the bottom and then an opposite motion during the variation of the liquid's density, due to cooling.

In Table I we show the values we obtained for water, glycerin and two watery solutions.

TABLE I. —  $c = \text{velocity of sound}$ .

	$V = \frac{4}{3}c$	$\Phi$
Water . . . . .	$1.44 \cdot 10^5 \text{ cm/s}$	$4.0 \cdot 10^5 \text{ cm/s}$
Glycerin . . . . .	$1.92 \cdot 10^5 \text{ »}$	$1.46 \cdot 10^5 \text{ »}$
NaCl in water (saturated) . . . .	$2.34 \cdot 10^5 \text{ »}$	$7.66 \cdot 10^5 \text{ »}$
$\text{Na}_2\text{SO}_4$ in water (saturated) . . .	$2.08 \cdot 10^5 \text{ »}$	$5.18 \cdot 10^5 \text{ »}$

We experimented with 2 liquids having not very different values of  $V$  namely water and glycerin and we found for  $\Phi$  two very different values which are quite in accord with the values found by LUCAS. We then determined  $V$  in watery solutions in order to see if variations obtained in this way for  $V$  do correspond to the variations obtained for  $\Phi$ . The ratios do not result very different; one has indeed to bear in mind that the measurements of  $\Phi$  are not very exact, the probable error being of the order of 30%.

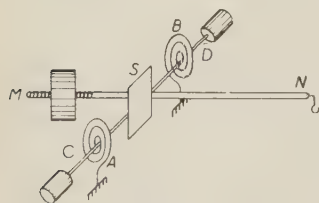


Fig. 4.

With these first measurements we verified the results found by LUCAS; we then tried to make the same measurements with a different method. We employed a much prompter arrangement (Fig. 4); it consists of two counteracting spirals A and B. We suspended the floating body on  $MM'$  which is free to turn around the axis  $CD$ ; a little mirror  $S$  allowed to measure by means of optical amplification the force  $A$  against time. The sensibility of this device was about  $\frac{1}{3}$  of the sensibility of the balance we previously used.

With such a system we obtained for water values of  $\Phi$  a little higher than those obtained with the balance.

As it is essential that the measurements be independent of the time employed by the experimental device to achieve the measure of the acting force, we considered also the determination of  $\Phi$  employing

another system even quicker than the last one and able to measure very little variations of pressure  $\Delta p$  (Fig. 5).

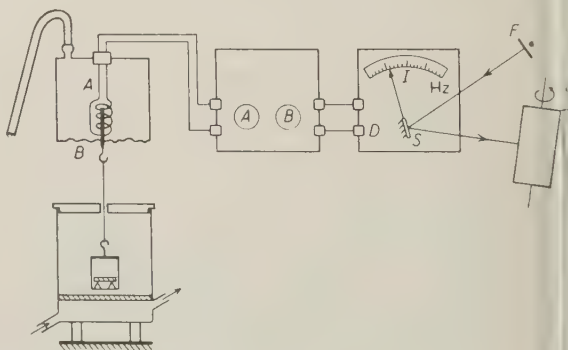


Fig. 5.

The sensitive head to which the pressures under measurement are applied, consists of a membrane  $A$  made of undulated brass sheet and fitted with a central hook on which the floating body is suspended. The sensitivity of this arrangement is about half the sensitivity of the balance.

The elastic membrane  $A$  with its displacements modifies an inductance which is part of an oscillating circuit  $A$  working at about 100 kHz. The frequency changes thus obtained are compared with a fixed frequency generated by an oscillator.

The resulting beating frequency is a function of  $\Delta p$  and is measured in Hertz by means of a frequencymeter  $D$ .

The frequency generated by the second circuit  $A$  is regulated by turning a knob in order to obtain a beating frequency lower than 30 kHz (this is the field width of the frequencymeter), while it is also necessary to have the lowest possible frequency in order to obtain the maximum sensibility of the measurements. We obtain that employing a series of capacities which can be included or excluded for the big variations, while the settings are made with a variable capacitor inserted in parallel with the fixed inductance of the second oscillator  $B$ .

The two oscillators are identical so that the external causes affect equally both frequencies. It is for this reason that the inductance of oscillator  $B$  has been included in the same sensitive head. To ensure the constance of zero against the atmospheric variations, the inside of the head has been put in connection with the external room by means of a rubber pipe. On the vertical rotation axis of the index  $I$  of the frequencymeter we placed a little mirror  $S$  so that the displacements of  $I$  are amplified by an optical lever and registered on recorder  $T$ .

The measurements of the beating frequency after adjustment allow the determination of the  $\Delta p$  acting on the membrane, and therefore to deduce the force. The system is, as we said, very quick.

In Fig. 6 we report a measurement made with this arrangement for water, from which we can see that the general pattern is like the one obtained

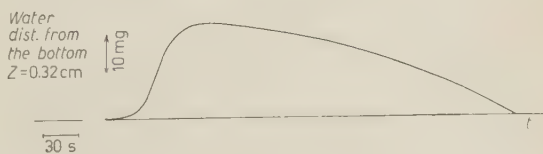


Fig. 6.

with the balance, but we have observed that the time after which the maximum force  $F_m$  is registered is shorter.

The values obtained for  $\Phi$  with this method are about twice the ones found with the precision balance.

We wanted also to find the optical behaviour of the liquid placed between the floater and the bottom of the container, the variation of the refracted index being dependent on the temperature required to establish

whether the density variation in time was identical to the variation of the force. When the liquid cools we obtain a variation of its density and therefore a variation of the refracting index, thus from the variation of the index we may deduce the fluctuation of the density.

The method we adopted is the well known one of Töpler (Fig. 7). An achromatic objective  $L_1$  gives, of an horizontal illuminated slit  $F$ , an image  $F_1$  at a distance of about 5 m from  $F$  in the horizontal plane passing through the optical axis of the system. A cylindrical lens  $L_2$  is so placed as to focus the image of  $F_1$  on the recorder.

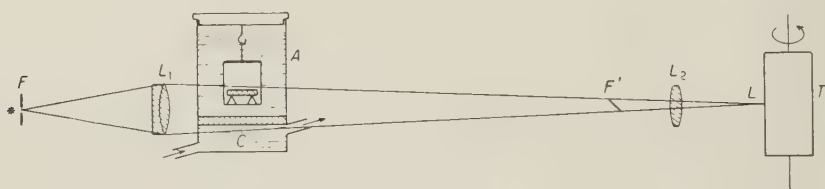


Fig. 7.

The trough  $A$  made of optical glass with plane parallel sides is situated just behind the objective  $L_1$  at such a height that the liquid between the bottom and the body  $B$  may be crossed by a slightly converging light beam which comes from  $L_1$ . As the distance of  $F$  from  $F_1$  is great, the system constitutes an optical lever which can be used to put in evidence little perturbations which interest the crossed layer of the liquid.

Water at room temperature is circulated through container  $C$  and in these conditions it is possible to register on recorder  $T$  the zero positions characterized by a rectilinear pattern. When a sudden refrigeration of the bottom of the container is produced, the light beam passing through the liquid zone which has changed its temperature undergoes a variation of the refracting index and the image is variously displaced in the different layers, which signifies that the observed image becomes larger. One can see that the pattern of the enlargement against time (using the same recorder of Fig. 1) follows exactly the pattern of the force against time.

We have thus confirmed the existence of the force found by LUCAS, for which we measured with different methods obtaining practically the same results (considering the difficulty of the measurements).

Finally it is to be remarked that the different methods are differently quiet and that their results are yet in good agreement.

## RIASSUNTO

In questo lavoro sono state studiate le proprietà termomeccaniche di alcuni liquidi e soluzioni (acqua, glicerina, soluzione satura di NaCl, soluzione satura di  $\text{Na}_2\text{SO}_4$ ) già messe in evidenza da R. LUCAS <sup>(1)</sup>. L'esistenza della forza prevista dal LUCAS è stata da noi confermata con metodi diversi che hanno portato a risultati praticamente coincidenti (tenuto conto delle difficoltà presentate da queste misure). È da sottolineare che i vari metodi usati sono diversamente pronti; un metodo ottico che dà l'andamento termico ha mostrato come questo proceda praticamente in accordo con la forza da noi misurata.



## A High Accuracy Approximation for Solving Multiple Scattering Problems in Infinite Homogeneous Media.

C. C. GROSJEAN (\*)

*Interuniversitair Instituut voor Kernwetenschappen  
Centrum van de Rijksuniversiteit Gent, Belgium*

(ricevuto il 5 Marzo 1956)

**Summary.** — Making use of a result published by the author two years ago, an approximate formula describing the steady-state density of isotropically scattered particles emitted by a point source in an infinite homogeneous medium is obtained and compared with the exact distribution. The agreement is remarkably good for all values of the parameters. Without being more complicated, the present approximation turns out to be much better than all the formulae previously derived from other approximate theories. In an infinite homogeneous medium, it can be applied in the calculation of the particle density in the presence of a given source distribution. The method by which the formula has been deduced, permits a direct generalization to the case of non-isotropic scattering. Attention is drawn upon the fact that the obtained results could be of basic importance in the development of a more complete formalism, which would also permit the solution of multiple scattering problems in finite media with the same high accuracy.

---

In a recent article, RICHARDS <sup>(1)</sup> has developed a new approximate formalism for solving problems of multiple isotropic scattering which possesses important advantages compared to diffusion theory and may therefore, in our opinion, be considered as an interesting contribution. However, we believe that at least in the case of homogeneous media, it must be possible to build an approximate theory yielding results which have the apparently paradoxical

---

(\*) Address: Natuurk. Laboratorium, Universiteit Gent, Rozier, 6, Gent, Belgium.  
(<sup>1</sup>) P. I. RICHARDS: *Phys. Rev.*, **100**, 517 (1955).

properties of being simpler and nevertheless more accurate than those derived from Richards's formalism. In the present paper, we have no intention to work out a complete theory of multiple isotropic scattering of particles in all kinds of media, but we want to draw the attention upon some formulae on which such a theory could possibly be based. Therefore, we shall limit ourselves to the case of an infinite homogeneous medium, but we hope to generalize this first attempt to finite media in a later, more complete article.

Our statement is based on the following facts. In one of our papers on multiple scattering <sup>(2)</sup>, we have presented the exact solution for a non-isotropic random flight problem in the case of a non-isotropic point source which radiates particles in an infinite homogeneous medium. The path probabilities were left arbitrary. Applying the results to the case of thermal neutrons, we obtained the exact expressions for density and current components [G (85), (86), (87)] and due to the fact that they contained integrals which cannot be worked out in a closed form, we discussed various ways to obtain useful approximations. Finally, we concluded that the simplest formula which can represent the steady-state density sufficiently well, can be written as

$$(G\ 117) \quad \varrho(r, \alpha) \cong \frac{S_0}{4\pi v} \frac{\exp[-r/\lambda]}{r^2} + \frac{S_0 \lambda_c \lambda}{4\pi v \lambda_s L'^2} \frac{\exp[-r/L']}{r} + \frac{S_1 \cos \alpha}{4\pi v L} \frac{\exp[-r/L]}{r} \left(1 + \frac{L}{r}\right),$$

in which:  $S_0$  and  $S_1$  resp. represent the isotropic and non-isotropic source strengths;

$v$  is the particle velocity;

$\lambda_s$ ,  $\lambda_c$ ,  $\lambda$  resp. represent the scattering, capture and total mean free paths;

$L'$  and  $L$  are the positive square roots of

$$L'^2 = \frac{\lambda \lambda_c}{3[1 - (\lambda/\lambda_s) \overline{\cos \gamma}]} \left(1 + \frac{\lambda}{\lambda_c} + \frac{\lambda^2}{\lambda_c^2} \overline{\cos \gamma}\right), \quad L^2 = \frac{\lambda \lambda_c}{3[1 - (\lambda/\lambda_s) \overline{\cos \gamma}]},$$

$\overline{\cos \gamma}$  being the average cosine of the scattering angle.

In the case of an isotropic point source ( $S_1 = 0$ ) and isotropic scattering ( $\overline{\cos \gamma} = 0$ ), (G 117) becomes

$$(1) \quad \varrho(r) \cong \frac{S_0}{4\pi v} \frac{\exp[-r/\lambda]}{r^2} + \frac{S_0 \lambda_c \lambda}{4\pi v \lambda_s L'^2} \frac{\exp[-r/L']}{r},$$

<sup>(2)</sup> C. C. GROSJEAN: *Nuovo Cimento*, **11**, 11 (1954). References to formulae of this paper will be preceded by the symbol G.

in which

$$L'^2 = \frac{\lambda\lambda_c}{3} \left(1 + \frac{\lambda}{\lambda_c}\right).$$

Introducing the notation  $\omega = \lambda/\lambda_c$ , we finally get

$$(2) \quad \frac{4\pi r^2 v \varrho(r)}{S_0} \cong \exp[-r/\lambda] + \frac{3\omega}{(2-\omega)} \frac{r}{\lambda} \exp\left[-\frac{r}{\lambda} \left(3 \frac{1-\omega}{2-\omega}\right)^{\frac{1}{2}}\right].$$

More generally,  $\omega$  represents the average number of secondaries emitted after a collision. In (2), it can only vary in the interval  $0 \leq \omega \leq 1$ , because for  $\omega > 1$  a finite steady-state solution is no longer possible.

As the exact solution of the point source problem has been tabulated<sup>(3)</sup> some time ago for various values of  $r$  and  $\omega$ , we have been able to examine the validity of (2) in full detail. In our discussion, we shall need the exact expression for the quantity on the left hand side of (2). This can easily be deduced from the rigorous particle density which has been established independently by several authors using different methods. One finds:

$$(3) \quad \frac{4\pi r^2 v \varrho(r)}{S_0} = \exp[-r/\lambda] + \frac{2\omega}{\pi} \cdot \frac{r}{\lambda} \int_0^\infty \frac{(\operatorname{arctg} u)^2}{u - \omega \operatorname{arctg} u} \sin \frac{r}{\lambda} u \, du.$$

In Appendix C of reference<sup>(3)</sup>, it has been shown that (3) can be brought in a second mathematical form. In our notations, this can be written as

$$(4) \quad \frac{4\pi r^2 v \varrho(r)}{S_0} = -\frac{dK^2}{d\omega} \cdot \frac{r}{\lambda} \exp\left[-K \frac{r}{\lambda}\right] + \frac{r}{\lambda} \int_0^1 g(\omega, \mu) \exp\left[-\frac{r}{\mu\lambda}\right] \frac{d\mu}{\mu^2},$$

in which

$$g(\omega, \mu) \equiv \frac{1}{(1 - \omega\mu \operatorname{argth} \mu)^2 + [(\pi/2)\omega\mu]^2}$$

and  $K$  is the positive root of the transcendental equation:

$$(4') \quad \omega = \frac{K}{\operatorname{argth} K}.$$

Our approximation (2) has the following properties:

---

<sup>(3)</sup> K. M. CASE, F. DE HOFFMANN and G. PLACZEK: *Introduction to the Theory of Neutron Diffusion* (Washington, D.C., 1953), Vol. 1, Chapter IV.

1) The way in which (G 117) was obtained implies that both the zeroth and the second order moments of (2) are rigorous, namely:

$$(5) \quad \frac{4\pi v}{S_0} \int_0^\infty r^2 \varrho(r) dr = \frac{\lambda}{(1-\omega)}; \quad \frac{4\pi v}{S_0} \int_0^\infty r^4 \varrho(r) dr = \frac{2\lambda^3}{(1-\omega)^2}.$$

2) When  $\omega$  vanishes, (2) becomes identical to the rigorous solution.

3) When  $\omega = 1$ , our formula gives

$$(6) \quad \frac{4\pi r^2 v \varrho(r)}{S_0} \cong \exp[-r/\lambda] + 3 \frac{r}{\lambda}.$$

This can be nicely compared with (4) which can now be written as

$$(7) \quad \frac{4\pi r^2 v \varrho(r)}{S_0} = 3 \frac{r}{\lambda} + \exp[-r/\lambda] - \frac{r}{\lambda} \int_0^1 [1 - g(1, \mu)] \exp\left[-\frac{r}{\mu\lambda}\right] \frac{d\mu}{\mu^2},$$

in which the integral contributes very little to the right hand side for all values of  $r \geq 0$ , so that (2) is a very good approximation in this case.

4) In the region around the origin and for all possible values of  $\omega$ , the rigorous formula (3) and our approximation (2) respectively behave as

$$(8) \quad 1 - \frac{r}{\lambda} \left(1 - \frac{\pi^2 \omega}{4}\right) \quad \text{and} \quad 1 - \frac{r}{\lambda} \left(1 - \frac{3\omega}{2-\omega}\right),$$

showing that (2) always starts at the exact value, namely unity for  $r = 0$ . It can also be seen that the slope of (2) at  $r = 0$  will be respectively smaller, equal or larger than the exact slope for  $0 < \omega < 2 - 12/\pi^2$ ,  $\omega = 2 - 12/\pi^2 = 0.78415$ , and  $2 - 12/\pi^2 < \omega \leq 1$ .

However, the most convincing way to examine the validity of (2) has been a numerical comparison with the exact distribution. This has been carried out for ten values of  $\omega$ , namely  $\omega = 0.1, 0.2, \dots$  up to 1.0. Reference (3) contains tables of  $4\pi r^2 v \varrho(r)/S_0$  for  $\omega = 0.3$  and  $\omega = 0.9$ . When  $\omega$  is put equal to one of the other values, similar tables for this quantity can easily be computed from the tabulated  $\varepsilon$ -function (pp. 91-92) and the ratio  $\varrho_{as}/\varrho$  (pp. 102-103). Examples of the obtained results are given in Tables I and II, in which our formula (2) is not only compared with the rigorous distribution, but also with

TABLE I. — *Values of  $4\pi r^2 v_Q(r)/S_0$  from different theories when  $\omega = 0.9$ .*

$r/\lambda$	Rigorous	our approxim. (2)	Richards's approxim. (19)	simple diffusion theory	Diffusion theory with rigorous diff. length
0.0	1.0000	1.0000	2.5000	0	0
0.1	1.1211	1.1378	2.3065	0.2840	0.2846
0.2	1.2343	1.2610	2.1764	0.5377	0.5401
0.3	1.3384	1.3704	2.0836	0.7636	0.7687
0.4	1.4326	1.4670	2.0159	0.9639	0.9725
0.5	1.5168	1.5518	1.9657	1.1407	1.1534
0.6	1.5914	1.6254	1.9279	1.2958	1.3133
0.7	1.6567	1.6887	1.8990	1.4312	1.4537
0.8	1.7130	1.7424	1.8762	1.5485	1.5764
0.9	1.7607	1.7873	1.8576	1.6492	1.6826
1.0	1.8006	1.8239	1.8417	1.7348	1.7739
1.5	1.8974	1.9052	1.7727	1.9788	2.0461
2.0	1.8660	1.8627	1.6843	2.0063	2.0978
2.5	1.7547	1.7451	1.5680	1.9071	2.0164
3.0	1.5992	1.5868	1.4301	1.7403	1.8607
3.5	1.4239	1.4113	1.2815	1.5439	1.6692
4.0	1.2454	1.2340	1.1312	1.3418	1.4670
4.5	1.0742	1.0644	0.9862	1.1479	1.2690
5.0	0.9158	0.9082	0.8506	0.9699	1.0843
6	0.6483	0.6441	0.6170	0.6730	0.7694
7	0.4467	0.4450	0.4361	0.4541	0.5307
8	0.3018	0.3014	0.3020	0.3001	0.3587
9	0.2007	0.2010	0.2060	0.1952	0.2386
10	0.1318	0.1325	0.1388	0.1254	0.1568

Richards's formula (19) for the isotropic point source (\*) and with the distributions deduced from the simple and the « corrected » diffusion theory. The values contained in these tables give rise to the curves shown in Fig. 1 and 2. It can be seen that our approximation is by far the most accurate for  $\omega = 0.9$  over the entire range of values for the distance. When  $\omega = 0.3$ , Richards's approximation fits the exact curve better than in the previous case for  $r > 0.3\lambda$ , but our formula is still considerably more accurate. In this strong

(\*) In Table II, the values of the fourth column derived from Richards's point source solution do not agree with those computed for  $\omega = 0.3$  by the mentioned author and presented in his article [ref. (1)]. We find a closer agreement between his formula and the exact distribution in this case. That Richards's values could certainly not all be correct, can be seen even before any recalculation. Indeed, all his values are larger than the corresponding exact ones. This is impossible considering that the integral of  $4\pi r^2 v_Q(r)/S_0$  from zero to infinity is rigorous in Richards's approximation.



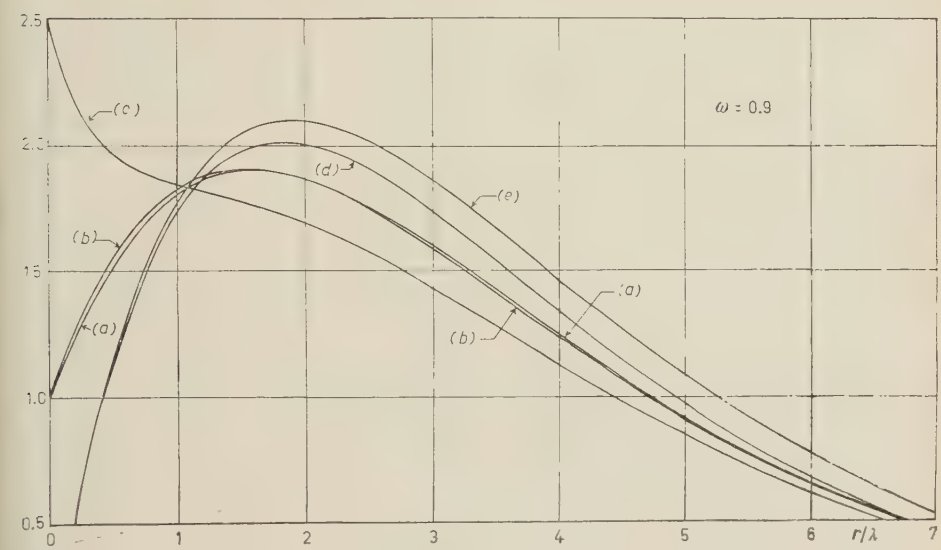


Fig. 1. — Curves for  $4\pi r^2 v_Q(r)/S_0$  given by different theories in the case of  $\omega = 0.9$ : (a) rigorous; (b) our approximation (2); (c) Richards's approximation (19); (d) simple diffusion theory; (e) diffusion theory with rigorous diffusion length.

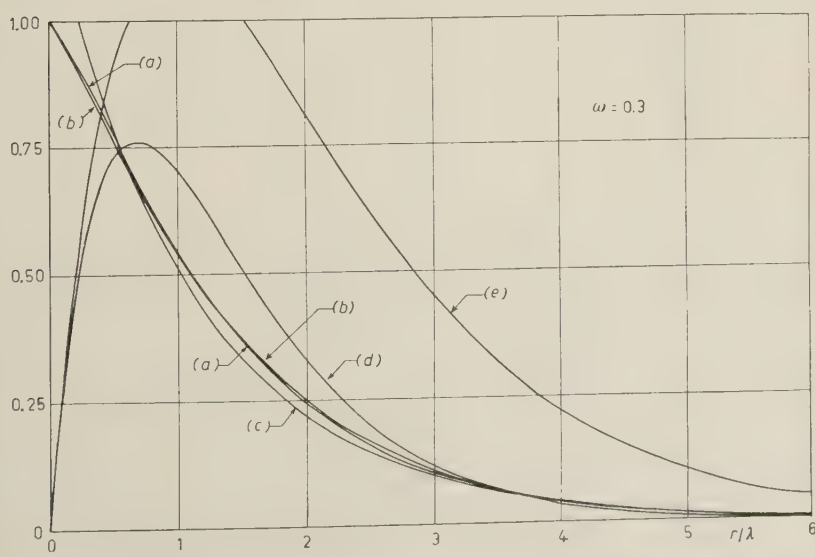


Fig. 2. — Curves for  $4\pi r^2 v_Q(r)/S_0$  given by different theories in the case of  $\omega = 0.3$ : (a) rigorous; (b) our approximation (2); (c) Richards's approximation (19); (d) simple diffusion theory; (e) diffusion theory with rigorous diffusion length.

TABLE II. — *Values of  $4\pi r^2 v_0(r)/S_0$  from different theories when  $\omega = 0.3$ .*

$r/\lambda$	Rigorous	our approxim. (2)	Richards's approxim. (19)	simple diffusion theory	Diffusion theory with rigorous diff. length
0.0	1.0000	1.0000	1.2500	0	0
0.1	0.9644	0.9522	1.1340	0.2595	0.2715
0.2	0.9196	0.9035	1.0319	0.4490	0.4915
0.3	0.8710	0.8546	0.9418	0.5827	0.6673
0.4	0.8209	0.8061	0.8601	0.6721	0.8052
0.5	0.7708	0.7584	0.7868	0.7268	0.9110
0.6	0.7215	0.7119	0.7204	0.7545	0.9894
0.7	0.6737	0.6668	0.6600	0.7615	1.0447
0.8	0.6277	0.6234	0.6052	0.7529	1.0806
0.9	0.5838	0.5818	0.5552	0.7327	1.1003
1.0	0.5421	0.5421	0.5096	0.7043	1.1065
1.5	0.3675	0.3730	0.3341	0.5119	1.0078
2.0	0.2441	0.2500	0.2204	0.3307	0.8162
2.5	0.1599	0.1643	0.1459	0.2003	0.6196
3.0	0.1037	0.1064	0.0967	0.1165	0.4516
3.5	0.0668	0.0681	0.0641	0.0658	0.3200
4.0	0.0427	0.0432	0.0425	0.0365	0.2221
4.5	0.0272	0.0271	0.0281	0.0199	0.1517
5.0	0.0173	0.0170	0.0186	0.0107	0.1024
6	0.0069	0.0065	0.0081	0.0030	0.0453
7	0.0028	0.0025	0.0035	0.00083	0.0195
8	0.0011	0.0009	0.0015	0.00022	0.0082
9	0.0004	0.0003	0.0006	0.00006	0.0034
10	0.0002	0.0001	0.0003	0.00002	0.0014

absorption case, the simple and the « corrected » diffusion theory both lead to rather poor approximations. For the remaining values of  $\omega$ , we have always found the same kind of remarkable agreement between (2) and (3), at least in the interval  $0 \leq r \leq 10\lambda$ .

In general, our approximation shows a very tiny oscillation around the exact curve, cutting the latter in a first point in the vicinity of  $r = \lambda$  and in a second point around  $r = 6\lambda$ . The deviation generally varies between 0 and 2 or 3 percent as it can be seen for  $\omega = 0.3$  and  $\omega = 0.9$  and one should consider that both examples are by no means the most favorable cases. Indeed, the deviations are the smallest for  $\omega$  in the vicinity of zero and  $2 - 12/\pi^2$ . For  $\omega = 0.7$ , e.g., the deviation does not exceed 1 percent in the interval  $0 \leq r \leq 7\lambda$ .

In our opinion, it is quite remarkable that a simple approximation as (2) can fit the rigorous distribution so well for all possible values of  $\omega$  and for

all distances at once. This is still more true when one considers the amount of mathematics involved to find several approximations for (3), each valid in a certain region of  $r$  and  $\omega$  (see e.g. ref. (3)). It should also be noted that (2) is much simpler and much easier to use than Richards's formula (19). In fact, (2) consists of a superposition of two functions: an exponential term due to the « direct beam » of particles and a distribution of scattered particles having the same mathematical form as the one given by diffusion theory.

Therefore, in each case in which (2) will be applied, the amount of computation required will be practically the same as if diffusion theory itself were used, but the accuracy of the result will be considerably increased.

Another remarkable fact concerns the coefficient of  $r/\lambda$  appearing in the exponential of the second term in (2). This factor can be denoted as  $K(\omega)$  since it appears to be an approximation for the rigorous  $K(\omega)$  defined by (1'). In our approximation, it is given by

$$(9) \quad K(\omega) = \left[ \frac{3(1-\omega)}{(2-\omega)} \right]^{\frac{1}{2}}.$$

From a numerical comparison with the exact  $K(\omega)$  tabulated in ref. (3) (p. 60), it follows that for all values of  $\omega$ , (9) is more accurate than the expression  $[3(1-\omega)]^{\frac{1}{2}}$  for  $K$  used in simple diffusion theory. However, our formula seems to be only sufficiently precise when  $\omega > 0.5$ . Under this condition, it gives more accurate values than Richards's approximation for  $K(\omega)$ . This can also be seen analytically by comparing the expansions of the various expressions for  $K(\omega)$  with each other in the vicinity of  $\omega = 1$  :

$$(\text{rigorous}) \quad \frac{K(\omega)}{\sqrt{3(1-\omega)}} = 1 - \frac{2}{5}(1-\omega) - \frac{12}{175}(1-\omega)^2 - \dots,$$

$$(\text{approx. (9)}) \quad \frac{K(\omega)}{\sqrt{3(1-\omega)}} = 1 - \frac{1}{2}(1-\omega) + \frac{3}{8}(1-\omega)^2 - \dots,$$

$$(\text{Rich. approx.}) \quad \frac{K(\omega)}{\sqrt{3(1-\omega)}} = 1 - (1-\omega) + \frac{3}{2}(1-\omega)^2 - \dots,$$

$$(\text{diff. theory}) \quad \frac{K(\omega)}{\sqrt{3(1-\omega)}} = 1.$$

Our formula is clearly the closest approximation when  $(1-\omega)$  is small. As  $\omega$  approaches zero, (9) converges towards  $(3/2)^{\frac{1}{2}} = 1.22474$  instead of towards unity. However, this deviation for small  $\omega$  is really unimportant as we know already from our previous successful comparison between the distri-

butions (2) and (3) for all  $\omega$ . This must be attributed to the fact that in cases of strong capture, the contributions of the second terms in (2) and (3) to the density become less and less important, so that the deviation of  $K(\omega)$  does not matter very much. On the other hand, when  $(1 - \omega)$  is small, the contribution of the scattered particles largely predominates and in these cases, a highly accurate  $K(\omega)$  is needed. These conditions are quite well fulfilled in our approximation (2). Finally, the fact that the latter fits the exact distribution equally well for small  $\omega$  as for  $\omega$  in the region of unity shows once more, that it is not always the approximation containing the most precise  $K(\omega)$  which will be the most successful. A similar conclusion was reached by Richards's after comparison of the ordinary diffusion theory with the one containing the rigorous  $K(\omega)$ .

Considering the previous analysis, it is sufficiently clear that it would be very interesting to develop an approximate one-velocity theory of multiple scattering based on the approximation (2). As we stated in the beginning, we regard a detailed development of such a theory outside the scope of the present note. However, as a starting point, we want to discuss a few formulae applicable to sources in an infinite homogeneous medium.

Let  $S(\mathbf{r}')d\mathbf{r}'$  describe an arbitrary distribution of isotropic sources present in such a medium. Then the approximate particle density will be given by

$$(10) \quad \varrho(\mathbf{r}) \cong \frac{1}{4\pi v} \iiint_{-\infty}^{\infty} S(\mathbf{r}') \frac{\exp[-|\mathbf{r} - \mathbf{r}'|/\lambda]}{|\mathbf{r} - \mathbf{r}'|^2} d\mathbf{r}' + \\ + \frac{1}{4\pi v \lambda} \cdot \frac{3\omega}{(2 - \omega)} \iiint_{-\infty}^{\infty} S(\mathbf{r}') \frac{\exp\left[-\frac{|\mathbf{r} - \mathbf{r}'|}{\lambda} \left(3 \frac{1 - \omega}{2 - \omega}\right)^{\frac{1}{2}}\right]}{|\mathbf{r} - \mathbf{r}'|} d\mathbf{r}'.$$

The first term in this formula represents the exact density due to the unscattered particles and may therefore be denoted as  $\varrho_d(\mathbf{r})$  (referring to the « direct beam »). The second term represents the contribution of the scattered particles which we may call  $\varrho_s(\mathbf{r})$ , so that

$$(11) \quad \varrho(\mathbf{r}) \cong \varrho_d(\mathbf{r}) + \varrho_s(\mathbf{r}).$$

By a straightforward calculation, one can show that  $\varrho_s(\mathbf{r})$  satisfies the second order partial differential equation

$$(12) \quad \nabla^2 \varrho_s(\mathbf{r}) - \frac{3}{\lambda^2} \left( \frac{1 - \omega}{2 - \omega} \right) \varrho_s(\mathbf{r}) + \frac{3\omega S(\mathbf{r})}{(2 - \omega)v\lambda} = 0.$$

This equation differs from the stationary diffusion equation by the following

particularities:

- the diffusion length  $\lambda/\sqrt{3(1-\omega)}$  is replaced by  $\lambda\sqrt{(2-\omega)/3(1-\omega)}$ ;
- the source term appears to be multiplied by the factor  $\omega/(2-\omega)$ ;
- the total density  $\varrho(\mathbf{r})$  is replaced by  $\varrho_s(\mathbf{r})$ .

Apart from this third particularity, it can be seen that the difference between (12) and the ordinary diffusion equation is not very important in the case of weak capture ( $\omega \cong 1$ ). On the contrary, the difference is really important when capture predominates. Equation (12) will probably play a basic role in the more general approximate theory mentioned above.

The density  $\varrho_s(\mathbf{r})$  as it is given by the second term of (10) represents the physically acceptable solution of (12), which vanishes at infinity. It is also interesting to note that  $\varrho_s(\mathbf{r})$  can be written as a useful Fourier integral. Indeed, applying the threedimensional complex Fourier transform to the second term in (10) or to the equation (12), one easily finds after taking the Fourier inverse:

$$(13) \quad \varrho_s(\mathbf{r}) = \frac{3\omega}{8\pi^3(2-\omega)r\lambda} \iint\limits_{-\infty}^{\infty} \frac{F(\mathbf{k}) \exp[-i\mathbf{k} \cdot \mathbf{r}]}{|\mathbf{k}|^2 + \frac{3}{\lambda^2} \left( \frac{1-\omega}{2-\omega} \right)} d\mathbf{k},$$

in which

$$(13') \quad F(\mathbf{k}) \equiv \iiint\limits_{-\infty}^{\infty} S(\mathbf{r}) \exp[i\mathbf{k} \cdot \mathbf{r}] d\mathbf{r}.$$

Finally, we wish to point out that the present approximate formulae can most easily be generalized to include the first degree of non-isotropic scattering. This follows directly from (G 117) and the way in which this formula has been obtained. Indeed, suppose that the angular distribution of the secondaries after a collision is described by the probability distribution

$$(14) \quad p(\gamma) \frac{\sin \gamma d\gamma}{2} = (1 + 3 \overline{\cos \gamma} \cos \gamma) \frac{\sin \gamma d\gamma}{2},$$

in which  $\gamma$  represents the scattering angle and  $\overline{\cos \gamma}$  the average of its cosine.

Applying (G 117), one finds directly:

$$(15) \quad \frac{4\pi r^2 v \varrho(r)}{S_0} \cong \exp\left[-\frac{r}{\lambda}\right] + \frac{3\omega(1 - \overline{\cos \gamma})}{[2 - \omega + (1 - \omega)^2 \overline{\cos \gamma}]} \cdot \frac{r}{\lambda} \exp\left\{-\frac{r}{\lambda} \left( \frac{3(1 - \omega)(1 - \omega \overline{\cos \gamma})}{[2 - \omega + (1 - \omega)^2 \overline{\cos \gamma}]} \right)^{\frac{1}{2}} \right\}.$$



This formula possesses essentially all the properties which we have mentioned for (2): it is a high accuracy approximation with rigorous zeroth and second order moments, starting at the exact value, namely unity, at  $r = 0$  and becoming the rigorous solution when  $\omega$  vanishes. As it has the same mathematical form as (2), the formulae (10), (12) and (13) can readily be generalized to include first order non-isotropy. In (10) and (13), one should simply replace

$$\text{the factor } \frac{3\omega}{(2-\omega)} \quad \text{by} \quad \frac{3\omega(1-\omega \overline{\cos \gamma})}{[2-\omega + (1-\omega)^2 \overline{\cos \gamma}]}$$

$$\text{and } \left(3 \frac{(1-\omega)}{(2-\omega)}\right)^{\frac{1}{2}} \quad (\text{under the integral signs}) \quad \text{by} \quad \left(\frac{3(1-\omega)(1-\omega \overline{\cos \gamma})}{[2-\omega + (1-\omega)^2 \overline{\cos \gamma}]}\right)^{\frac{1}{2}}.$$

Equations (12) changes into

$$(16) \quad \nabla^2 \varrho_s(\mathbf{r}) - \frac{3}{\lambda^2} \cdot \frac{(1-\omega)(1-\omega \overline{\cos \gamma})}{[2-\omega + (1-\omega)^2 \overline{\cos \gamma}]} \varrho_s(\mathbf{r}) + \frac{3\omega(1-\omega \overline{\cos \gamma})S(\mathbf{r})}{[2-\omega + (1-\omega)^2 \overline{\cos \gamma}]} = 0$$

A further generalization of our formulae which would correct them for higher orders of non-isotropy appears to be impossible without altering the approximation method which led to (G 117). This would finally cause the substitution of (2) and the other approximate formulae by more complicated distributions. The reason for this can be derived from the following considerations. The method by which the second term in (2) was found, provided at once its form as a function of  $r$  and the right expressions for the coefficients in this function. Afterwards, it could be shown directly that the zeroth and the second order moments of (2) were rigorous. However, suppose that by some way or another, we had concluded that a formula like

$$(17) \quad \exp\left(-\frac{r}{\lambda}\right) + ar \exp[-br]$$

could be a good approximation for the exact distribution (3). Then the factors  $a$  and  $b$  could have been calculated from the requirement that the zeroth and the second order moments of (17) should be rigorous.

The exact values of the latter can be deduced from an appropriate Fourier transformation of both sides of (3). By this procedure we would have found exactly the same coefficients as in (2). The equivalence of both methods lead to the conclusion that an easy way to generalize our formula (2) to all cases of non-isotropic scattering in which there is circular symmetry around the incoming direction, consists in putting the zeroth and the second order moments of (17) equal to those of the exact distribution. This is possible because

the general problem, in which the angular distribution of the secondaries after a collision is left arbitrary, has been rigorously solved <sup>(4)</sup>. By means of this solution, it can be shown that if the angular distribution is given by the arbitrary Legendre expansion

$$(18) \quad p(\gamma) \frac{\sin \gamma \, d\gamma}{2} = \left[ \sum_{l=0}^{\infty} A_l P_l(\cos \gamma) \right] \frac{\sin \gamma \, d\gamma}{2},$$

in which  $A_0 = 1$ ,  $A_1 = 3 \overline{\cos \gamma}$  and generally  $A_l = (2l+1) \overline{P_l(\cos \gamma)}$ , the zeroth and the second order moments of  $4\pi r^2 v \varrho(r)/S_0$  are given by

$$(19) \quad \frac{4\pi v}{S_0} \int_0^{\infty} r^2 \varrho(r) \, dr = \frac{\lambda}{(1-\omega)}; \quad \frac{4\pi v}{S_0} \int_0^{\infty} r^4 \varrho(r) \, dr = \frac{2\lambda^3}{(1-\omega)^2(1-\omega \cos \gamma)}.$$

Both moments are *entirely independent* of the coefficients  $A_l$  ( $l \geq 2$ ) appearing in (18). Putting them equal to those of (17) yields our approximation (15) and determines it completely. Hence, a generalization of (15) which would make it dependent on the higher order coefficients  $A_2, A_3, \dots$  is impossible, unless some suitable correction terms are added. Nevertheless, (15) will certainly be a useful approximation in all cases in which the coefficients  $A_2, A_3, \dots$  appearing in the expansion of the non-isotropic scattering law are small with respect to unity.

### Note Added in Print.

In each one of our Tables I and II, the last two columns have been calculated using the approximate formula

$$(a) \quad \frac{4\pi r^2 v \varrho(r)}{S_0} = 3 \frac{r}{\lambda} \exp \left[ -K \frac{r}{\lambda} \right],$$

in which we have replaced  $K$  respectively by the approximation  $[3(1-\omega)]^{\frac{1}{2}}$  (simple diffusion theory) and by its rigorous value namely the positive root of eq. (4') (corrected diffusion theory) (\*). In this respect, we followed RICHARDS who makes the remark that (a) only gives the correct total number of particles if the first mentioned expression for  $K$  is used. As a matter of fact, eq. (a) even has a rigorous second order moment in this case and therefore leads to the exact mean square distance traveled

(4) C. C. GROSJEAN: *Verhand. Kon. Vl. Acad. Wet. (België)*, **13**, n. 36 (1951); *Physica*, **19**, 29 (1953).

(\*) Throughout the present discussion, it is only necessary to consider isotropic scattering.

by the particles

$$\overline{r^2} = 2\lambda^2/(1 - \omega).$$

Putting the rigorous value of  $K$  in eq. (a) constitutes one possible way to try to correct diffusion theory, but then none of the moments of (a) is any longer exact and it was shown that the procedure does not at all improve the accuracy. Compared with the rigorous solution of the point source problem, the formula (a) with rigorous  $K$  generally yields much too high values (see e.g.: curves (e) in Fig. 1 and 2).

However, we wish to point out that there is another and in fact more logical way of trying to correct simple diffusion theory, namely introducing the rigorous value of  $K$  not only in the exponential term of (a) but also in the proportionality factor preceding this term. This can easily be done considering the point source solution as it is primarily obtained by elementary diffusion theory:

$$(b) \quad \varrho(r) = \frac{S_0}{4\pi D} \cdot \frac{\exp[-r/L]}{r},$$

in which  $D$  represents the diffusion constant and  $L$  the diffusion length. Using the notations of our article, we can write:

$$L = \frac{\lambda}{K} \quad \text{and} \quad D = \frac{v\lambda(1 - \omega)}{K^2},$$

so that (b) becomes

$$(c) \quad \frac{4\pi r^2 \varrho(r)}{S_0} = \frac{K^2}{(1 - \omega)} \cdot \frac{r}{\lambda} \exp\left[-K \frac{r}{\lambda}\right].$$

Whatever the value of  $K$  introduced in this formula, the zeroth order moment will always be correct.

Replacing  $K^2$  by  $3(1 - \omega)$  in (c) yields the previously mentioned simple diffusion approximation and constitutes the *only* way to adjust the second order moment. In the special cases  $\omega=0.9$  and  $\omega=0.3$ , this evidently leads to the columns and curves denoted with «simple diffusion theory».

However, replacing  $K^2$  by its rigorous value in (c) yields a formula differing from the corresponding one resulting from (a) by a constant proportionality factor and will have now

$$\text{approx. (c)} = \frac{K_{\text{exact}}^2}{3(1 - \omega)} \cdot \text{approx. (a)}.$$

In practice, as  $K_{\text{exact}}^2$  is generally smaller than  $3(1 - \omega)$  (see Table I, reference (1)), this means that correcting simple diffusion theory on the basis of approx. (c) instead of using approx. (a) will lead to smaller values. In the cases  $\omega=0.9$  and  $\omega=0.3$  the curves (c) on Fig. 1 and 2 will be lowered by a factor 0.9203 and 0.4737 respectively bringing them closer to the exact curves for  $r \gtrsim \lambda$ . However, multiplying the sixth column of our Tables I and II with the appropriate factor and comparing the results with the values in the other columns, we can conclude that none of our previous statements undergoes any modification. Although it yields better results than the old attempt to correct simple diffusion theory, the new attempt still fails to give rise

a much more accurate formula than the one given by diffusion theory itself. Therefore, no further comparison is needed: our formulae (2), (10), etc., still remain by far the most accurate among the simple approximations which can be proposed.

\* \* \*

We are indebted to the Institut Interuniversitaire des Sciences Nucléaires and to Prof. Dr. J. L. VERHAEGHE for his valuable interest in this work.

---

### RIASSUNTO (\*)

Utilizzando un risultato pubblicato dall'autore due anni or sono, si ricava una formula approssimata che descrive la densità dello stato stazionario di particelle disperse isotropicamente, emesse da una sorgente puntiforme in un mezzo infinito omogeneo e la si confronta con la distribuzione esatta. L'accordo è notevolmente buono per tutti i valori dei parametri. Senza essere più complicata la presente approssimazione risulta essere assai migliore di tutte le formule precedentemente ricavate dalle altre teorie approssimate. In un mezzo omogeneo infinito si può utilizzare per il calcolo della densità di particelle in presenza di una data distribuzione di sorgenti. Il metodo col quale la formula è stata ricavata permette una generalizzazione diretta al caso dello scattering non isotropico. Si accenna al fatto che i risultati ottenuti potrebbero essere d'importanza fondamentale nello sviluppo di un formalismo più completo che permetterebbe anche la soluzione di problemi di scattering multiplo in mezzi finiti con lo stesso elevato grado di esattezza.

---

(\*) *Traduzione a cura della Redazione.*

## Electromagnetic Cross-Section of a Small Circular Disc with Unidirectional Conductivity (\*).

G. TORALDO DI FRANCIA

*Istituto Nazionale di Ottica - Arcetri, Firenze*

(ricevuto il 6 Marzo 1956)

**Summary.** — The scattering of an electromagnetic field by a small circular disc is investigated with the assumption that the disc can conduct current in only one direction. The analysis follows closely that given by Bethe in a similar case. Although Bethe's theory is open to criticism and leads to some wrong results, the present discussion appears to the author to be perfectly correct. Both the scattering cross-section and the angular momentum cross-section are evaluated. This is sufficient for explaining why the experimental measurement of the torque exerted upon the screen is in poor quantitative agreement with the theory based on the geometric cross-section.

### 1. — Introduction.

We shall consider a plane screen of vanishing thickness, having infinite conductivity in one direction and being perfectly insulating in the orthogonal direction. Physically, such a screen can be realized with great approximation by means of a parallel-wire grating with very close spacing. It is interesting to investigate the scattering of an electromagnetic wave by a screen of this kind.

A similar device can find application in some electromagnetic technique. For example, an elegant experiment has been described by CARRARA <sup>(1)</sup>, which allows a direct measurement of the angular momentum carried by an electric

---

(\*) The present research was made in partial fulfillment of Contract AF 61 (514)-4-4 between the European Office of the Air Research and Development Command, United States Air Force, and the Centro Microonde del C.N.R.

<sup>(1)</sup> N. CARRARA: *Nuovo Cimento*, **6**, 50 (1949); *Nature*, **164**, 882 (1949).



magnetic wave circularly polarized. In the simplest version of the experiment, the wave is incident on a parallel-wire grating, which reflects the component with the electric force parallel to the wires, while leaving the other component undisturbed. Both reflected and transmitted waves are linearly polarized and do not carry angular momentum. The whole angular momentum of the incident wave is therefore absorbed by the grating, which is consequently subjected to a torque. By measuring this torque, one can derive the angular momentum of the incident wave (or, what amounts to the same, the spin of the photons). Apart from its theoretical interest, a device of this kind can be very useful for power measurements in a wave guide.

An approximate evaluation of the torque on the grating can be carried out on the basis of the geometrical cross-section. However, this procedure can hardly be justified when the dimensions of the screen are not very large compared with the wavelength. A proper evaluation of the torque can only be carried out by taking into account diffraction.

In the present paper we shall discuss the diffraction of an electromagnetic wave in the case where the unidirectional screen is a circular disc of very small diameter. The analysis will be closely analogous to that given by BETHE <sup>(2)</sup> in his discussion of diffraction through a small hole. It is known that Bethe's theory is open to criticism <sup>(3)</sup> and that some of its results are incorrect. The same criticism does not seem to apply in the present case. The following analysis seems to be perfectly correct, within the limits of the required approximation.

## 2. — Evaluation of Currents and Charges on the Screen.

Let the screen  $\Sigma$  be a circular disc in the  $xy$  plane with the center at the origin of coordinates. The radius  $a$  will be assumed to be very small compared with the wavelength. Conductivity on the screen will be infinite in the  $x$  direction and zero in the  $y$  direction.

Let the incident field be represented by the electric force

$$(1) \quad \mathbf{E}^i \exp [-i\omega t].$$

In the following treatment the time factor  $\exp [-i\omega t]$  will be omitted throughout.

The field (1) will induce in the screen a current parallel to the  $x$  axis.

<sup>(2)</sup> H. A. BETHE: *Phys. Rev.*, **66**, 163 (1944).

<sup>(3)</sup> C. J. BOUWKAMP: *Philips Res. Rep.*, **5**, 321 (1950); *Rep. Progr. Phys.*, **17**, 35 (1954).

The surface density of this current will be denoted by  $\mathbf{I}(x, y)$ . By virtue of the equation of continuity, we shall also have a surface charge  $\sigma$  given by

$$(2) \quad ikc\sigma = \frac{\partial I}{\partial x}.$$

The resulting vector and scalar potentials will be given by <sup>(4)</sup>

$$(3) \quad A(P) = \mu \iint_{\Sigma} I(P') G(P, P') d\Sigma_{P'},$$

$$(4) \quad \varphi(P) = \frac{1}{\varepsilon} \iint_{\Sigma} \sigma(P') G(P, P') d\Sigma_{P'},$$

where

$$(5) \quad G(P, P') = \frac{\exp[ik|P - P'|]}{4\pi|P - P'|}.$$

The vector potential is parallel to the  $x$  axis. The field vectors can be derived in the usual way from the potentials. If  $P$  does not lie in the plane  $xy$ , some easy transformations give

$$(6) \quad \mathbf{E}(P) = \iint_{\Sigma} \left[ ikZ \mathbf{I}(P') G - \frac{1}{\varepsilon} \sigma(P') \text{grad}_P G \right] d\Sigma_{P'},$$

$$(7) \quad \mathbf{H}(P) = \iint_{\Sigma} \text{grad}_P G \wedge \mathbf{I}(P') d\Sigma_{P'},$$

where  $Z$  represents the intrinsic impedance of free space.

Now, by taking into account (2), we note that in the vicinity of the screen the first term in the integral (6) is of the order of  $(ka)^2$  times the second. As a consequence, if  $a$  is small in comparison with the wavelength, the first term can be neglected and the electric force can be determined by the scalar potential alone

$$(8) \quad \mathbf{E} = -\text{grad } \varphi.$$

<sup>(4)</sup> The notations are those adopted in: G. TORALDO DI FRANCA: *Electromagnetic Waves* (New York, 1955). It is only to be noted that here the time factor  $\exp[-i\omega t]$  instead of  $\exp[i\omega t]$ . This amounts to the same as changing the sign of in all the formulas.

Further, the retardation can be neglected in and near the screen, so that (4) becomes

$$(9) \quad \varphi(P) = \frac{1}{4\pi\epsilon} \iint_{\Sigma} \frac{\sigma(P')}{|P - P'|} d\Sigma_{P'}.$$

The only boundary condition to be fulfilled is that the  $x$  component of the total electric field should vanish on both sides of the screen. Consequently, the scattered field (8) on the screen must be equal and opposite to the  $x$  component of the incident field (1). Thus, by combining (8) and (9), we obtain

$$(10) \quad \frac{1}{4\pi\epsilon} \frac{\partial}{\partial x} \iint_{\Sigma} \frac{\sigma(P')}{|P - P'|} d\Sigma_{P'} = E_x^i(P),$$

where  $P$  is a point of the screen. This is an integro-differential equation for  $\sigma$ , which must be solved without introducing inadmissible singularities at the edge of  $\Sigma$ . The charge density must be integrable over any finite region of  $\Sigma$ . Further, the current must vanish at the rim of  $\Sigma$ .

Now we note with Bethe that, if  $a$  is very small,  $E_x^i$  can be considered to be constant over the screen and that the charge distribution  $\sigma$  which gives a constant field inside the screen is readily found by considering the screen to be the limiting case of a rotational ellipsoid with a uniform spatial distribution of dipoles parallel to  $x$ . This easily leads to the solution of equation (10)

$$(11) \quad \sigma = \frac{8\epsilon x E_x^i}{\pi \sqrt{a^2 - x^2 - y^2}}.$$

The charge density becomes infinite at the rim of the screen, however it is readily verified that the charge itself is finite over any portion of the screen.

From (2) and (11) the current  $I$  is found to be

$$(12) \quad I = -\frac{8ikE_x^i}{\pi Z} \sqrt{a^2 - x^2 - y^2},$$

with no ambiguity, since in our case it is evident that  $I$  must vanish at the rim of the screen, for physical reasons.

### 3. - The Scattered Field.

The scattered field at infinity is most readily found by observing that the screen, when seen from a large distance, is equivalent to an electric dipole

of moment

$$L = \iint_{\Sigma} x \sigma \, d\Sigma,$$

parallel to the  $x$  direction. By substituting expression (11) for  $\sigma$ , we find, after integration

$$(13) \quad L = \frac{16}{3} E_x^i \varepsilon a^3.$$

The scattered field at a large distance is given then by

$$(14) \quad \mathbf{E} = \frac{16}{3} E_x^i k^2 a^3 G(\mathbf{s} \wedge \mathbf{i}) \wedge \mathbf{s}, \quad Z\mathbf{H} = \mathbf{s} \wedge \mathbf{E},$$

where  $G$  is the function defined by (5) and  $\mathbf{s}$ ,  $\mathbf{i}$  are unit vectors in the direction of the ray and of  $x$  respectively.

The evaluation of the scattered field in or near the screen is more complicated. Fortunately we can utilize a result due to BOUWKAMP<sup>(3)</sup>, who has given explicit expressions, valid near the origin for the complementary field generated by magnetic (instead of electric) charges and currents of the type<sup>(11)</sup>,<sup>(12)</sup>. The field components are expressed in terms of oblate-spheroidal coordinates  $u$ ,  $v$ ,  $\varphi$  defined by

$$(15) \quad z = auv, \quad x = a\sqrt{(1-u^2)(1+v^2)} \cos \varphi, \quad y = a\sqrt{(1-u^2)(1+v^2)} \sin \varphi$$

where  $0 \leq u \leq 1$ ,  $-\infty < v < \infty$ ,  $0 \leq \varphi \leq 2\pi$ . From BOUWKAMP's results<sup>(3)</sup> we find, by making the necessary transpositions, the field components for  $z \geq 0$ :

$$(16) \quad E_x/E_x^i = -1 + \frac{2}{\pi} \left( \operatorname{arctg} v + \frac{v}{u^2 + v^2} \right) + \frac{2(x^2 - y^2)v}{\pi a^2(u^2 + v^2)(1 + v^2)^2},$$

$$(17) \quad E_y/E_x^i = \frac{4xyv}{\pi a^2(u^2 + v^2)(1 + v^2)^2}, \quad E_z/E_x^i = \frac{4xu}{\pi a(u^2 + v^2)(1 + v^2)^2},$$

$$(18) \quad ZH_x = 0, \quad ZH_y/E_x^i = -2ikz + \frac{4}{\pi} ikau(1 + v \operatorname{arctg} v),$$

$$(19) \quad ZH_z/E_x^i = -iky + \frac{2}{\pi} iky \left( \operatorname{arctg} v + \frac{v}{1 + v^2} \right).$$

---

<sup>(5)</sup> BOUWKAMP's paper contains an obvious misprint:  $E_x$  and  $E_z$  should be interchanged.

On the screen we have  $v = 0$  and the field reduces to

$$(20) \quad E_x = -E_x^i, \quad E_y = 0, \quad E_z = \frac{4E_x^i x}{\pi\sqrt{a^2 - x^2 - y^2}},$$

$$(21) \quad ZH_x = 0, \quad ZH_y = \frac{4}{\pi} E_x^i k \sqrt{a^2 - x^2 - y^2}, \quad ZH_z = -E_x^i k y.$$

On the plane  $xy$  outside the screen we have  $u = 0$  and the field components are found by substituting  $v = \sqrt{x^2 + y^2 - a^2}/a$  in the general expressions (16)-(19). From the resulting expressions and from (20), (21) it is apparent that some components of the field become infinite at the rim of the screen. However, the infinities are of an admissible type, which is common in diffraction problems <sup>(6)</sup>.

#### 4. - Scattering Cross-Section and Angular Momentum Cross-Section.

Knowing the dipole moment of the screen, it is easy to calculate the total scattering cross-section. The power radiated by an electric dipole of moment  $L$  is given by

$$W = \frac{k^4}{12\pi} c^2 Z L L^*,$$

where an asterisk denotes the complex conjugate. By substituting expression (13), we find

$$(22) \quad W = \frac{64}{27\pi Z} E_x^i E_x^{i*} k^4 a^6.$$

Let the incident wave be a plane wave at any angle of incidence. If the electric vector has unit amplitude and makes an angle  $\alpha$  with the  $x$  axis, we shall have  $E_x^i = \cos \alpha$ .

Now, the power carried by the incident wave per unit surface is  $1/2Z$  so that the scattering cross-section turns out to be

$$(23) \quad A = \frac{128}{27\pi} k^4 a^6 \cos^2 \alpha.$$

As was to be expected, this cross-section is much smaller than the geometrical cross-section when  $a$  is small compared with the wavelength. It is interesting

<sup>(6)</sup> C. J. BOUWKAMP: *Physica*, **12**, 467 (1946).



to note that when  $\alpha = 0$ , i.e. when the electric vector is parallel to  $x$ , the cross-section (23) is equal to the cross-section of a disc perfectly conducting in all directions for a plane wave travelling in the  $z$  direction (7). This is not at all obvious, since in the latter case the current has also an  $y$  component. We want also to point out the independence of the cross-section from the angle of incidence, when the electric vector is perpendicular to a fixed plane of incidence.

Let us now consider a plane wave circularly polarized, travelling in the  $z$  direction. This wave will be split into two components, the first represented by

$$(24) \quad E_x^i = \exp [ikz]$$

and the second represented by

$$(25) \quad E_y^i = -i \exp [ikz].$$

The total wave carries an angular momentum about the  $z$  axis. The amount of the angular momentum carried across a unit surface of the  $xy$  plane per unit time (8) is equal to  $S/kc$ ,  $S$  being the time average of the Poynting vector.

To evaluate the angular momentum cross-section of the screen, we note that, by virtue of equation (2), the dipole moment can be expressed by

$$L = \iint_{\Sigma} x \sigma \, d\Sigma = \frac{1}{ikc} \iint_{\Sigma} x \frac{\partial I}{\partial x} \, d\Sigma.$$

Carrying out an integration by parts, and taking into account that  $I$  vanishes at the rim of the screen, we obtain

$$L = -\frac{1}{ikc} \iint_{\Sigma} I \, d\Sigma.$$

The electric field (25) acts upon the dipole with an average mechanical moment about the  $z$  axis given by

$$M = \frac{1}{2kc} \operatorname{Re} \iint_{\Sigma} I \, d\Sigma,$$

where  $\operatorname{Re}$  denotes the real part. Dividing by the angular momentum per unit

(7) C. J. BOUWKAMP: *Philips Res. Rep.*, **5**, 401 (1950).

(8) N. CARRARA, T. FAZZINI, L. RONCHI and G. TORALDO DI FRANCA: *Alta Frequenza*, **24**, 100 (1955).

surface carried by the incident wave, we get the angular momentum cross-section

$$(26) \quad A_{am} = \frac{1}{2S} \operatorname{Re} \iint_{\Sigma} I \, d\Sigma.$$

Next we evaluate the power carried by the scattered field, by integrating the outward  $z$  component of Poynting's vector over both faces of the screen. Taking into account that  $H_x = 0$ , and that by (24)  $E_x = -E_x^i = -1$ , we obtain the power

$$W = - \operatorname{Re} \iint_{\Sigma} H_y \, d\Sigma$$

and the scattering cross-section

$$(27) \quad A = - \frac{1}{S} \operatorname{Re} \iint_{\Sigma} H_y \, d\Sigma.$$

On the other hand, since the field  $H_y$  is created by the current  $I$ , it is readily seen that  $I = -2H_y$ , so that, upon comparison of (26) and (27), we get

$$(28) \quad A_{am} = A.$$

It is worth noting that the above proof of (28) is rigorous and valid for a screen of any shape and size.

In our approximation, the scattering cross-section for the circularly polarized wave is obtained by averaging  $\cos^2 \alpha$  over both directions  $\alpha = 0$  and  $\alpha = \pi/2$  of the component waves (24) and (25). We thus obtain for the angular momentum cross-section of the disc

$$(29) \quad A_{am} = \frac{64}{27\pi} k^4 a^6.$$

When the screen is small compared to the wavelength, this cross-section is of a much smaller order of magnitude than the geometrical cross-section. No wonder then that the torque evaluated on the basis of the geometrical cross-section is in poor quantitative agreement with the one measured experimentally <sup>(1)</sup>.

An interesting remark can be made about equation (28). Let us assume that the screen is very large in comparison with the wavelength. In this case, if the screen were conducting in all directions, the scattering cross-section

would be twice the geometrical cross-section<sup>(9)</sup>. Now, our unidirectional screen scatters only the component (24) of the circularly polarized wave, so that its scattering cross-section becomes equal to the geometrical cross-section. Then (28) states that the angular momentum cross-section of a large screen is equal to the geometric cross-section, as it should be, for physical reasons.

---

(<sup>9</sup>) G. TORALDO DI FRANCA: *Rend. Acc. Naz. Linc.*, **8**, 369 (1950).

---

### RIASSUNTO

Viene studiata la diffrazione di un'onda elettromagnetica da parte di un disco sottile, di piccolo diametro, perfettamente conduttore in una direzione e isolante nella direzione ad essa ortogonale. Si applica un metodo già seguito da BETHE nel caso di un foro circolare in uno schermo perfettamente conduttore. Viene calcolata la sezione efficace di assorbimento di momento angolare. Viene dimostrato un teorema generale che mette in relazione questa sezione efficace con la sezione di scattering.

## Observations on Electromagnetic Cascades in Nuclear Emulsions.

K. PINKAU

*H. H. Wills Physical Laboratory - University of Bristol*

(ricevuto il 9 Marzo 1956)

**Summary.** — Four cascades, each initiated by a single photon, have been studied in detail. Target diagrams are made at different depths and the energy of every particle plotted has been determined by multiple scattering measurements. The results are compared with shower theory for lateral and longitudinal development under approximation A of Rossi and Greisen <sup>(5)</sup>. The theory is found to give a consistent picture within the fluctuation possibilities up to a primary energy of  $10^6$  MeV. The distribution of particles very near the core is consistent with a law like  $r^{s-2}$ . Comparison is done with the calculations of the root mean square lateral displacement by Chartres and Messel <sup>(21)</sup>.

### 1. — Introduction.

With the introduction of stripped emulsion techniques it has become possible to investigate the development of an electromagnetic shower for considerable distances. Attempts to study these phenomena with glass backed emulsions <sup>(1)</sup> have not been successful because of the limited length of observation available.

The increasing interest in high energy phenomena, the interpretation of unusual electromagnetic events such as first reported by SCHEIN <sup>(2)</sup> and the doubts in the validity of cross-sections of elementary processes like trident

(1) J. E. HOOPER, D. T. KING and A. H. MORRISH: *Can. Journ. Phys.*, **29**, 545 (1951).

(2) M. SCHEIN, D. M. HASKIN and R. G. GLASSER: *Phys. Rev.*, **95**, 855 (1954); A. DEBENEDETTI, C. M. GARELLI, L. TALLONE, M. VIGONE and G. WATAGHIN: *Nuovo Cimento*, **12**, 954 (1954); A. JURAK, M. MIESOWICZ, O. STANISZ and W. WOLTER: *Bull. Pol. Acad. Sc. Cl. III*, **3**, no. 7 (1955).

production at very high energies, expressed recently by KAPLON and KOSHIBA <sup>(3)</sup>, justify a renewed attack on the problem of cascade development.

The advantages of using nuclear emulsions for an investigation of these phenomena come from the high cross-sections of all elementary processes (they are essentially proportional to  $Z^2$  which is very high in nuclear emulsion), and the possibility of observation of individual processes such as pair creation, trident production etc.

The principle problem arising in cascade theory is to obtain the probability, as a function of the space coordinates, of finding a particle (negatron, positron or photon) with an energy lying between  $E$  and  $E+dE$  striking volume element  $dv$ . The boundary conditions are given by the initiating process (incident photon, electron or several particles, and their direction).

The problem in its most general form has been discussed theoretically by a number of authors <sup>(4)</sup>, but no complete numerical results are yet available.

The theoretical discussion is easier, if we consider the three distinct parts of the question separately.

- a) The average longitudinal spread;
- b) The average lateral spread;
- c) The fluctuations from this average.

All three parts have been investigated with the help of cloud chambers, ionization chambers, counter tubes and only very recently with emulsions <sup>(6)</sup>.

Quantitative agreement has been achieved so far only with question a), especially with the Monte Carlo calculations of R. R. WILSON <sup>(7)</sup>, up to a primary energy of about 500 MeV. These experiments were done by NASSAR and HAZEN <sup>(8)</sup> and later, using incident particles with known energies from synchrotrons, by BLOCKER, KENNEY and PANOFSKY <sup>(9)</sup>, by CROWE and HAYWARD <sup>(10)</sup> and by SHAPIRO <sup>(11)</sup>.

<sup>(3)</sup> M. KOSHIBA and M. F. KAPLON: *Phys. Rev.*, **100**, 327 (1955).

<sup>(4)</sup> a) L. JÁNOSSY: *Proc. Phys. Soc.*, A **63**, 241 (1950); b) H. MESSEL: *Proc. Phys. Soc.*, A **64**, 807 (1951); c) B. A. CHARTRES and H. MESSEL: *Phys. Rev.*, **96**, 1651 (1954).

<sup>(5)</sup> B. ROSSI: *High Energy Particles* (New York, 1952); B. ROSSI and K. GREISEN: *Rev. Mod. Phys.*, **13**, 240 (1941).

<sup>(6)</sup> Summary in ROSSI's book. Some examples not mentioned there are: ref. <sup>(3)</sup> and W. E. HAZEN, R. W. WILLIAMS and C. A. RADNALL: *Phys. Rev.*, **93**, 578 (1954); H. L. KRAYBILL: *Phys. Rev.*, **93**, 1362 (1954); G. M. BRANCH: *Phys. Rev.*, **84**, 147 (1951); W. E. HAZEN: *Phys. Rev.*, **85**, 455 (1952); K. E. RELF: *Phys. Rev.*, **97**, 172 (1955).

<sup>(7)</sup> R. R. WILSON: *Phys. Rev.*, **86**, 261, 590 (1952).

<sup>(8)</sup> S. NASSAR and W. E. HAZEN: *Phys. Rev.*, **69**, 298 (1946).

<sup>(9)</sup> W. BLOCKER, R. W. KENNEY and W. K. PANOFSKY: *Phys. Rev.*, **79**, 419 (1950).

<sup>(10)</sup> K. M. CROWE and E. HAYWARD: *Phys. Rev.*, **80**, 40 (1950).

<sup>(11)</sup> A. M. SHAPIRO: *Phys. Rev.*, **82**, 307 (1951).



The present experiment is concerned with questions *a*) and *b*) for incident photons with energies between  $10^5$  and  $10^6$  MeV. The statistics available on problem *c*) are not sufficient to enable any conclusion to be drawn.

The experimental data are compared with the theoretical results for the longitudinal development derived under approximation A of ROSSI and GREISEN <sup>(5)</sup>, by LANDAU and RUMER <sup>(12)</sup>, and with the numerical tables for lateral spread given by EYGES and FERNBACH <sup>(13)</sup>. In addition the radial distribution of the particles for small radii is compared with the  $r^{s-2}$  law given by MIGDAL and others <sup>(14)</sup>.

There are two main difficulties of high energy cascade work in general and in nuclear emulsion in particular:

1) The initial energy  $E_0$  must be determined.

2) Accurate measurements are possible only within a certain disc around the core of the cascade. At large radii there may be confusion with background, and high angular divergence makes the definition of tracks as belonging to the same shower very difficult.

We therefore shall adopt the following line of argument: From the number of particles within a given radius  $R$  of the core, at depth  $t'$  and with energy exceeding  $E'$  the primary energy  $E_0$  is deduced, after correcting for the loss of particles outside the disc, by using the tables of EYGES and FERNBACH <sup>(13)</sup>. From cascade theory, the distribution of particles with energy for various values of  $t$  is then calculated and compared with experimental results.

It is of interest to note, that in one case an independent estimate could be obtained for the primary energy  $E_0$ , and that this agreed rather closely with the estimate based on cascade theory.

## 2. — Theoretical Summary.

### 2.1. Definitions.

i) Shower axis. The shower axis is given by the direction of the primary particle. The point where it intersects the target diagram (perpendicular to the direction of the shower) will be taken as given by the centroid of the electrons in this target diagram, weighted according to their energy.

<sup>(12)</sup> L. LANDAU and G. RUMER: *Proc. Roy. Soc.*, **166**, 213 (1938).

<sup>(13)</sup> L. L. EYGES and S. FERNBACH: *Phys. Rev.*, **82**, 23, 287, 288 (1951).

<sup>(14)</sup> *a*) A. MIGDAL: *Journ. Phys. USSR*, **9**, 183 (1945); *b*) I. POMERANČUK: *Journ. Phys. USSR*, **8**, 17 (1944); *c*) J. NISHIMURA and K. KAMATA: *Prog. Theor. Phys.*, **5**, 899 (1950); *d*) **6**, 262, 628 (1951); *e*) **7**, 185 (1952).

ii) The distances  $t$  from the origin of the cascade are measured in cascade units, where

$$\begin{aligned} 1 \text{ cascade unit} &= 1 \text{ radiation length (r. l.)} \\ &= 2.9 \text{ cm for emulsion.} \end{aligned}$$

iii) The following notations will be used for the experimentally obtained particle distributions:

$n_r dr dE$  denotes the number of particles within a given energy interval and lying between radii  $r$  and  $r+dr$  from the shower axis;

$N_r(E) dr$  gives the number of particles in this annulus with energy exceeding  $E$ , thus

$$N_r(E) = \int_E^{\infty} n_r dE,$$

$n_R dE$  denotes the number within a radius  $R$ , i.e.

$$n_R = \int_0^R n_r dr,$$

and the total number  $n$  is given by the limit of  $n_R$  as  $R \rightarrow \infty$ .

Similarly

$$N_R(E) = \int_0^R N_r(E) dr,$$

and  $N$  is again the total number in the limit  $R \rightarrow \infty$ .

**2.2. Longitudinal Spread.** — We restrict ourselves to the case where the energy of the electrons under consideration is sufficiently high compared with the critical energy, (see ref. (5)) (100 MeV was chosen as lower energy limit) for us to neglect processes such as the Compton effect, multiple scattering, knock-on etc. This is known as approximation A of ROSSI and GREISEN (5). Only the knowledge of the cross-sections for Bremsstrahlung and pair production (asymptotic formulae) are required, higher order processes (trident production etc.) are not taken into account. Under these assumptions LANDAU and RUMER (12) have solved the diffusion equations of this problem by means of the Mellin transformation.

We shall measure the depth in our single photon initiated cascades from the point of creation of the first pair. We therefore consider the shower to be a superposition of two electron-initiated cascades with equipartition (\*) of the primary photon energy  $E_0$  amongst the two electrons. When the uncertainties in the conversion distance of the primary photon are excluded in such a manner the fluctuations are decreased. The solution of LANDAU and RUMER will have, under these assumptions, the form

$$(1) \quad \Pi(E_0, E, t) = \frac{2H''_{II}(s)}{\sqrt{2\pi}[\lambda''(s)t + (1/s^2)]^{\frac{1}{2}}} \frac{1}{s} \frac{1}{2^s} \left(\frac{E_0}{E}\right)^s \exp[\lambda(s)t],$$

where  $\Pi$  is the average number of electrons at a distance  $t$  from the point of creation of the first pair. The functions  $H''_{II}(s)$ ,  $\lambda(s)$ ,  $\lambda'(s)$ ,  $\lambda''(s)$  are tabulated by ROSSI and GREISEN<sup>(5)</sup> and by JÁNOSSY and MESSEL<sup>(15)</sup>, who also give tables for the calculation of  $\Pi$ . The parameter  $s$  is given by the equation

$$(2) \quad \ln \frac{E_0}{2E} - \frac{1}{s} + \lambda'(s)t = 0.$$

This  $s$ , which is the exponent of the fraction  $E_0/E$ , is often called « shower age » with the meaning that parts of the shower with  $s < 1$  are « young »,  $s = 1$  « at maximum » and  $s > 1$  « old ». Under approximation A, therefore, a cascade, at every distance from its origin, is « young », « at maximum » and « old » with respect to the ratio  $E_0/E$  under consideration. For too large distances  $t$  this is of course no longer valid, since  $E$  cannot be diminished infinitely without leaving the region of validity for approximation A.

The total track length travelled by all electrons in the cascade with energy above  $E$  is (ref. (5))

$$(3) \quad \int_0^\infty \Pi(E_0, E, t) dt = 0.437 E_0/E.$$

Note the power 1 for  $E_0/E$  which means  $s = 1$  for the track length spectrum.

In the experimental part, we will compare total numbers  $N$  with (1), hence

$$(4) \quad N(E, t) = \Pi(E_0, E, t).$$

(\*) As Dr. DALITZ remarked to me, the development of the cascade will not depend critically on the assumption that  $E_0$  is divided *equally* between the first two electrons. We use the theoretical function (1) mainly in the region for  $s$  from 0.7 to 1.0. Even if the whole primary energy  $E_0$  goes to one electron alone, the difference between  $2(E_0/2E)^s$  and  $(E_+/E)^s + (E_-/E)^s$  is only about 20% for  $s = 0.7$ .

(15) L. JÁNOSSY and H. MESSEL: *Proc. Roy. Ir. Acad.*, A 54, 15 (1951).

2'3. *Lateral Spread.* — Landau's <sup>(16)</sup> equations for lateral spread have, for a long time, been the basis of calculations by various authors <sup>(13,14,16,17,19)</sup>. Recently GREEN and MESSEL <sup>(20)</sup> criticized the use of Landau's <sup>(18)</sup> equations even in media with constant density, because 4th and higher angular moments for Coulomb scattering have been neglected. Only calculations of the second moment of their new distribution function have been published so far <sup>(21)</sup>. For the actual distribution of particles we are left with the calculations on the basis of Landau's equations.

i) The distribution function for not too small radii. — Numerical tables for the lateral distribution function under approximation have been calculated by EYGES and FERNBACH <sup>(13)</sup>. They give no information about the behaviour very near the core of the shower, or assume Molière's <sup>(14)</sup> calculations to be correct for small radii. In their notation we denote the proportion of electrons with energy between  $E$  and  $E+dE$  with a lateral displacement between  $r$  and  $r+dr$  from the shower axis by  $P(x)(r/r_1)(dr/r_1)dE$  where  $x = Er/Kr_1$ . Here  $K$  is a characteristic energy which is about 21 Mev and  $r_1$  is the cascade unit.

$P(x)$  depends on the shower age  $s$  which contains the dependence of  $P(x)$  on  $E_0$  and  $t$ . For this case, the appropriate shower age  $s$  is given by the expression

$$(5) \quad \ln \frac{E_0}{2E} + \lambda'(s)t = 0,$$

(which coincides with the definition (2.55) of ROSSI and GREISEN <sup>(5)</sup> for the differential energy spectrum). Note, that  $P(x)$  depends weakly on  $E_0$  if the primary energy is sufficiently high in comparison with the energy  $E$  of the electrons. Tables of  $P(x)$  are given by EYGES and FERNBACH <sup>(13)</sup> for  $s = 0.1, 1.0$ ; and  $1.5$ .  $P(x)$  is normalized such that

$$\int_0^{\infty} P(x)x dx = 1.$$

In terms of  $P(x)$ , the following expressions will be used for comparison with

<sup>(16)</sup> L. LANDAU: *Journ. Phys. USSR*, **3**, 237 (1940).

<sup>(17)</sup> G. MOLIÈRE: *Cosmic Radiation*, ed. W. HEISENBERG (New York, 1940).  
G. MOLIÈRE: *Phys. Rev.*, **77**, 715 (1949).

<sup>(18)</sup> J. M. BLATT: *Phys. Rev.*, **75**, 1584 (1949).

<sup>(19)</sup> J. ROBERG and J. W. NORDHEIM: *Phys. Rev.*, **75**, 444 (1949).

<sup>(20)</sup> H. S. GREEN and H. MESSEL: *Phys. Rev.*, **88**, 331 (1952).

<sup>(21)</sup> B. A. CHARTRES and H. MESSEL: *Proc. Phys. Soc.*, A **67**, 158 (1954).

our experimental quantities:

$$(6) \quad n_r \, d \frac{r}{r_1} \, dE = A P(x) \frac{r}{r_1} \, d \frac{r}{r_1} \, dE,$$

$$(7) \quad n_R \, dE = A \, dE \int_0^R P(x) \frac{r}{r_1} \, d \frac{r}{r_1},$$

$$(8) \quad N_r \, d \frac{r}{r_1} = A \frac{r}{r_1} \, d \frac{r}{r_1} \int_E^\infty P(x) \, dE,$$

$$(9) \quad N_R = A \int_E^\infty dE \int_0^R P(x) \frac{r}{r_1} \, d \frac{r}{r_1},$$

where  $A$  normalizes the total number of particles to equal the observed number. The values of  $s$  for which the functions are calculated are given in the graphs.

In equations (8) and (9) we will approximate the integral spectrum by a constant power law, since we keep  $s$  constant during the integration over  $E$ . Actually formula (8) will be used only in connection with the track length spectrum for which  $s = 1$  for *all* energies (eq. (3)). For the case of  $A 7$  and function (9) we also approximate the integral spectrum in Fig. 1 by two straight lines for energies above 500 MeV. The line from 500 MeV to 2000 MeV has slope  $-1$  ( $s = 1$ ) and the other above 2000 MeV has slope  $-1.5$  ( $s = 1.5$ ). The normalization was chosen to give best agreement with the theoretical spectrum in Fig. 1. In terms of  $P(x)$  this approximation is then

$$(10) \quad N_R(500 \text{ MeV}) = A_1 \int_{500}^{2000} dE \int_0^R P(x) \Big|_{s=1} \frac{r}{r_1} \, d \frac{r}{r_1} + A_2 \int_{2000}^\infty dE \int_0^R P(x) \Big|_{s=1.5} \frac{r}{r_1} \, d \frac{r}{r_1},$$

with the normalization factors  $A_1$  and  $A_2$  calculated from the total numbers  $n$  and  $N$  given in the graph.

ii) The behaviour very near the core of the shower. — POMERANČUK, MIGDAL, and NISHIMURA and KAMATA <sup>(14)</sup> derived a law

$$(11) \quad N_r(E) \frac{1}{r} \sim r^{s-2},$$

for very small radii.

Here the parameter  $s$  has to satisfy the equation [ref. <sup>(14a)</sup> eq. (5); ref. <sup>(14c)</sup>



eq. (13)]

$$(12) \quad \ln \frac{E_0 r}{2Kr_1} + \lambda'(s)t = 0.$$

Following MIGDAL, we may say that this definition is essentially the same as eq. (5), the main contribution to the integral

$$N_r(E) = \int_E^{\infty} n_r dE,$$

coming from electrons with energy at about  $E = Kr_1/r$ .

iii) The root mean square lateral spread. — CHARTRES and MESSEL consider the root mean square lateral spread, i.e. the quantity

$$(13) \quad \sqrt{\overline{r^2}} = \sqrt{\frac{\int_0^{\infty} r^2 N_r dr}{\int_0^{\infty} N_r dr}},$$

for comparison with the computations of other authors.

In Sect. 5.4 our experimental results are compared with the calculations by CHARTRES and MESSEL<sup>(21)</sup> of the second moment of Messel's<sup>(20)</sup> distribution function, and with ROBERG and NORDHEIM's<sup>(19)</sup> results for integrated energy spectrum on the basis of equations equivalent to LANDAU's<sup>(16)</sup>.

2.4. *The Fluctuation Problem.* — JÁNOSSY and MESSEL<sup>(22)</sup> have derived various moments of the fluctuations in the longitudinal distribution function. The function itself is only approximately known (4<sup>b</sup>), but the second moment gives us the standard deviation from the average number and we shall use this quantity as a measure of our statistical uncertainties. It can be seen from Fig. 4 of ref. (22) that our range in  $t$  and  $E$  is such that Jánosy's deviation only differs appreciably from the Poissonian standard deviation in relative few cases.

The fluctuation in lateral spread is believed to be Poissonian (BLATT)<sup>(12)</sup>

(22) L. JÁNOSSY and H. MESSEL: *Proc. Phys. Soc.*, A **63**, 1101 (1950).

### 3. — Experimental Procedure.

3'1. *Detection of Cascades.* — The showers of the present experiment were detected in three large ( $25\text{ cm} \times 36\text{ cm} \times 10\text{ cm}$ ;  $26\text{ cm} \times 36\text{ cm} \times 16\text{ cm}$ ;  $15\text{ cm} \times 20\text{ cm} \times 5\text{ cm}$ ) blocks of stripped emulsions. The scanning procedure was designed to detect high energy nuclear interactions. The details of the events thus found are given by BRISBOUT *et al.* <sup>(23)</sup>. The minimum number of tracks forming a cascade or part of it found in this manner was 6.

We therefore believe that we have obtained an unbiased sample of cascades, irrespective of inherent fluctuations. It must be emphasized that, in view of the recently reported anomalous events (SCHEIN <sup>(2)</sup>), the size of the stack as well as the detection criteria are very important. For instance by random scanning in small stacks one will always be biased in favour of cascades exhibiting fluctuations towards larger numbers.

3'2. *The Origin.* — Every cascade was followed back to its origin. In the case of showers apparently induced by single photons, we cannot a priori exclude the possibility that several photons are actually responsible for the creation of the cascade. However, several arguments may be given to show, that in our case the probability for such an occurrence is very small.

i) Assuming that each of our showers was due to a single photon originating outside the stack, we can apply a maximum likelihood method to calculate the conversion length from the measured distances of the origin from the emulsion edge, measured parallel to the shower axis (\*). The value obtained for the photon conversion length is  $4.3^{+1.1}_{-0.8}\text{ cm}$  to be compared with the theoretical value of 3.75 cm. If a large fraction of our cascades were of multiple photon origin, we would have expected a smaller value than 3.75 cm.

ii) Two  $\gamma$ -rays from the same  $\pi^0$  in one cascade can be detected due to their relative lateral displacement. (The angle of divergence between 2  $\gamma$ -rays from the same  $\pi^0$  is by about a factor 200 larger than the opening angle of the first pair of cascades). Moreover, in such a case there is a certain probability of finding associated shower tracks.

Hence we shall always assume that the cascades we investigated have been produced by a single photon.

<sup>(23)</sup> F. A. BRISBOUT, C. DAHANAYAKE, A. ENGLER, Y. FUJIMOTO and D. H. PERKINS: to be published in *Phil. Mag.*

(\*) For details see our « Letter to the Editor » in *Nuovo Cimento* 3, 1156 (1956).

From our 19 photon-initiated cascades, 4 examples have been chosen with a length greater than 1 cm per plate for detailed examination. This was the only criterion in our selection, as scattering measurements are very sensitive to the dip of the tracks.

**3.3. Target Diagram.** — Each shower was examined at three different distances,  $t$ , from the origin. These points were mainly determined by the primary energy of the cascade and the quality of the actual plate. For very high energy cascades,  $t$  must be large enough to permit significant scattering measurements and also to allow resolution of individual tracks. Upper limits for  $t$  are the size of the stack and the fact, that for too large values of  $t$  the fraction of low energy tracks diverging into neighbouring plates can lead to serious errors.

At each point of examination (which we shall hereafter call a « cut ») a target diagram was made of the tracks belonging to the cascade. The point of exit of a black track through the glass side of emulsion was chosen as a point of reference, with respect to which the dip (coordinate  $z$ ) and the lateral displacement (coordinate  $y$ ) were measured. The  $z$ -coordinates were later corrected for shrinkage of the emulsion.

The tracks included had to satisfy the following criteria:

- i) Blob density = plateau value.
- ii) They should have approximately the same length per plate as the easily visible core of the cascade.
- iii) They should be roughly parallel to the core (such that the angle between the track and the core of the cascade did not exceed  $25^\circ$ ).

We believe that no tracks within  $25^\circ$  were missed, since every target diagram was checked a second time during scattering measurements. The error in the number of particles at a depth  $t$  will have two sources:

- i) Missing of tracks with angles greater than  $25^\circ$ .
- ii) Tracks outside our plate, i.e. beyond a distance  $R$  from the shower axis.

The first error can be neglected, since we use 100 MeV as a lower energy limit, which we think is high enough to ensure that tracks within the distance  $R$  (in general of the order of  $200\ \mu\text{m}$ ) should be parallel to the shower axis within  $25^\circ$ .

The loss of tracks outside  $R$  is an important error for which we will correct by calculation on the basis of a lateral distribution function (Sect. 5.2 (iv)).

3.4. *Energy Estimation.* At each cut the energy of every track was determined by multiple scattering measurements. Whenever possible, relative scattering measurements have also been used.

The scattering measurements for electrons in the dense core of cascades suffers from three difficulties:

i) Due to the high track density, the motion of the screw of the scattering stage cannot be made smoothly because of the danger of confusion of tracks, thus the noise is appreciably increased. *The upper limit of reliability of the energy determinations in a particular region of the emulsions was obtained from a comparison of single with relative scattering results.*

ii) The occurrence of pseudo tridents in the dense core is very high. Scattering measurements must be stopped because of confusion of tracks and so the length of some tracks available for measurements is shortened.

iii) We neglected the influence of energy loss due to radiation on our results. The point where the track intersects the plane of the target diagram was chosen to be about the centre of the length of track upon which measurements were made. However, the probability of emission of a high energy photon on this length is small.

As may be seen from our data, the energy values used for experimental evidence are between 100 and 2000 MeV. In this region, spurious scattering is negligible in these stacks (see BRISBOUT *et al.* <sup>(24)</sup>).

The over-all statistical accuracy in the determination of the energy of a track (in the region of reliable scattering results) was of the order of 30%.

In the region of unreliable scattering results, we always obtain lower limits of energy.

The error in  $N_x(E)$  from the uncertainty in energy estimation has been neglected in comparison with the Jánossy standard deviation.

#### 4. — Experimental Results.

The following abbreviations are used, the numbers behind the letters denoting the individual cascade give the distance of the « cut » from the origin in cascade units.

In Table I we collect our measurement results. The numbers express the energy of the particles in MeV. All particles between the same distance limits can be found in the same row. All particles from the same « cut » are in the

<sup>(24)</sup> F. A. BRISBOUT, C. DAHANAYAKE, A. ENGLER, P. H. FOWLER and P. B. JONES: to be published in *Nuovo Cimento*.

cascade	length/plate	1 <sup>st</sup>	2 <sup>nd</sup>	3 <sup>rd</sup> « cut »
<i>A</i>	1.3 cm	<i>A</i> 4	<i>A</i> 5.5	<i>A</i> 7
<i>B</i>	2.0 cm	<i>B</i> 2	<i>B</i> 3	<i>B</i> 4
<i>C</i>	8.0 cm (out of stack)	<i>C</i> 1	<i>C</i> 2	<i>C</i> 2.4
<i>D</i>	1.7 cm	<i>D</i> 2.7	<i>D</i> 4	<i>D</i> 5.5

same column. Since we do not believe that we have determined the shower centre as the centroid of energy to better than  $10 \div 20 \mu\text{m}$  we give in the first row all particles between 0 and  $20 \mu\text{m}$ , later we proceed in steps from 10 to  $10 \mu\text{m}$ . The upper limits of reliability of the energy determinations can be seen from the second row. In *A7* the measurements were extended up to a radius of  $400 \mu\text{m}$ , and the numbers in brackets give the approximate loss of particles in the air gap between the emulsion sheets. The energy of some particles in *A4* could not be determined properly since the core was very dense but rough measurements showed that they had an energy above 1000 MeV they are marked as? Stars \* denote electrons with energy below 100 MeV.

## 5. — Shower Development.

5.1. *The Longitudinal Spread.* — In Fig. 1-4 we show the results from Table I in the form of integral energy spectra. The black dots mark experimental values of  $N_R(R)$  in the zone of reliable scattering measurements. In the energy region where the influence of noise and spurious scattering is serious we denote  $N_R(E)$  by crosses (see Sect. 3'4 i)).

The spectrum is cut-off at 1000 MeV in the case of *A4* for the reasons mentioned in Sect. 4.

Cascade *B* shows a fluctuation which appears at about 800 MeV for (*B2*) at about 400 MeV for (*B3*), and at about 200 MeV for (*B4*). This fluctuation is of interest, because it does not disappear as we proceed down the cascade and because the energy decreases at about  $e^{-1}$  from cut to cut, which is the average energy loss of an electron per radiation length.

i) Estimation of  $E_0$ . — The primary energy will be estimated from one of our measurement points, which we will call  $N'_R(E', t')$ . The theoretical function (1) relates the primary energy  $E_0$  to the given energy  $E'$ , the distance  $t'$ , and to the number  $N'(E', t')$  (eq. (4)). Thus we have to calculate  $N'(E', t')$  from  $N'_R(E', t')$ .

This forces us to introduce the lateral distribution function in the considerations of longitudinal spread. But we want to rely as little as possible on the correctness of this function. The smallest corrections for losses of particles outside  $R$  will be for high  $E'$  since the higher the energy of the electron



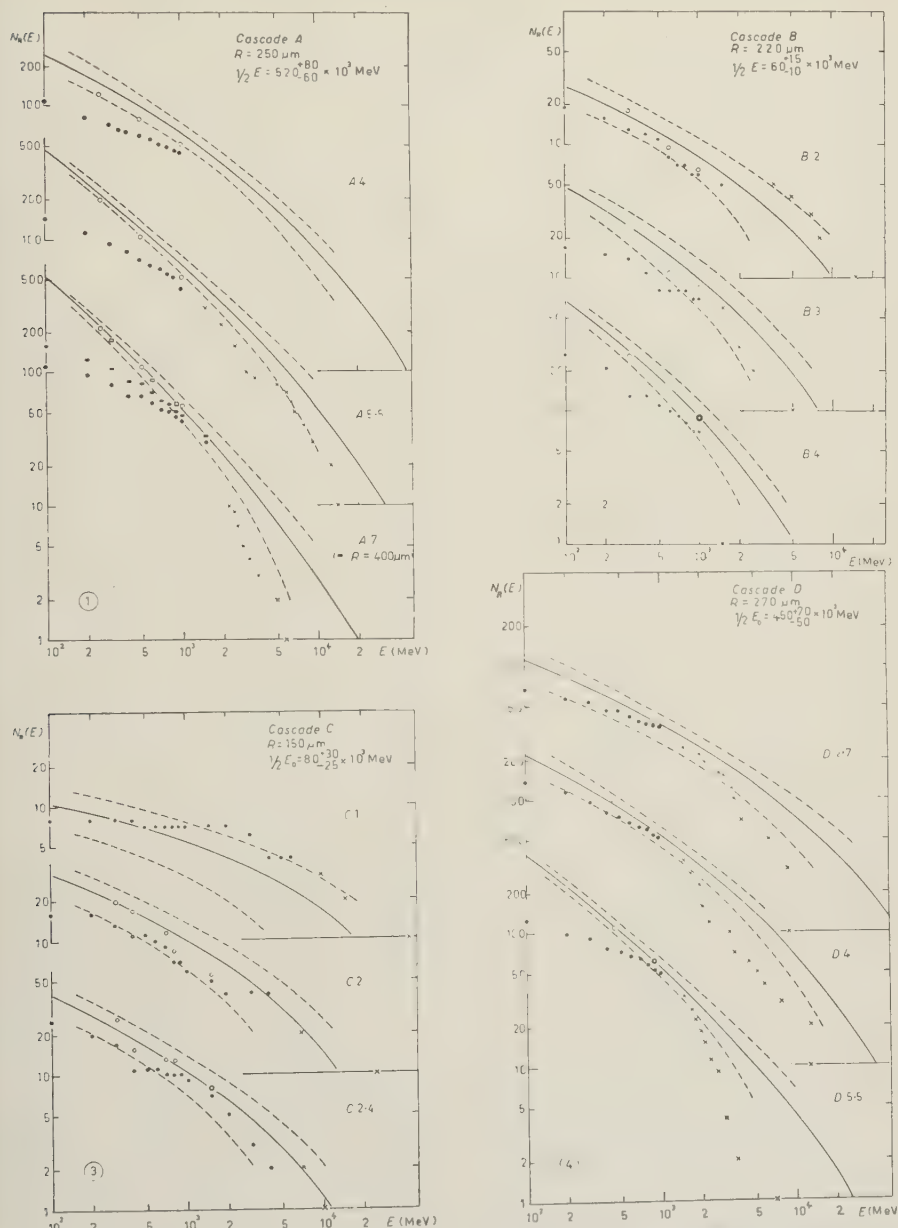


Fig. 1. - 1-4: The integral energy spectra of four cascades at different depths (given in cascade units behind the notation of the shower). The dashed lines represent the Jánossy deviation (in C 1 Poissonian deviation), enlarged by a factor  $\sqrt{2}$  to include the uncertainties in the estimation of  $E_0$ . The full lines represent function (1) fitted for the  $E_0$  given. - •, number of electrons above energy  $E$  within distance  $R$  from the shower axis. - x, the same as above, when the determination of energy was probably not very reliable. - o, these circles are obtained from the dots • after correction is made for losses of particles at distances  $> R$ .

TABLE I. — (Energies are given in MeV).

« cut »:	A 4	A 5.5	A 7	D 2.7	D 4	D 5.5
measurement .. reliable for E smaller than:	1 000	1 000	1 500	1 000	1 000	1 000
<i>r</i> (μm)	3 600	1 120	—	1 150	3 500	7 000
	4 800	130	—	9 000	8 000	1 000
	2 400	290	—	2 000	13 000	1 500
0 ÷ 20	2 300	—	—	6 500	2 300	1 800
	5 000	—	—	3 800	4 500	—
	3 400	—	—	3 200	440	—
	2 300	—	—	1 150	380	—
	?	—	—	2 000	620	—
	?	—	—	9 000	—	—
	?	—	—	1 400	—	—
	270	—	—	3 900	—	—
	470	—	—	4 100	—	—
	330	—	—	920	—	—
	830	—	—	960	—	—
	380	—	—	120	—	—
	*	—	—	640	—	—
	*	—	—	630	—	—
	—	—	—	630	—	—
	—	—	—	380	—	—
	—	—	—	110	—	—
	—	—	—	120	—	—
20 ÷ 30	2 200	—	3 100	3 100	2 000	1 000
	2 500	—	1 200	6 500	2 000	1 700
	2 400	—	1 300	*	1 700	2 100
	120	—	—	1 100	180	3 000
	940	—	—	3 000	2 100	2 000
	800	—	—	2 000	13 000	2 600
	?	—	—	9 000	1 100	1 000
	?	—	—	3 500	1 200	1 700
	700	—	—	4 000	540	—
	780	—	—	*	*	—
	530	—	—	2 800	*	—
	*	—	—	—	380	—
	*	—	—	—	440	—
	*	—	—	—	5 400	—
	*	—	—	—	580	—
	—	—	—	—	3 600	—
30 ÷ 40	5 400	940	290	3 700	360	2 300
	140	250	1 800	1 400	1 700	2 700
	6 000	1 330	2 000	*	*	*

TABLE I (continued)

$r$ ( $\mu\text{m}$ )	$A$ 4	$A$ 5.5	$A$ 7	$D$ 2.7	$D$ 4	$D$ 5.5
30 $\div$ 40	960	550	120	100	*	*
	420	960	270	3 500	3 400	130
	140	240	—	—	800	2 000
	230	*	—	—	1 200	1 700
	5 000	340	—	—	670	330
	3 800	2 100	—	—	850	*
	—	—	—	—	—	130
40 $\div$ 50	300	160	270	*	1 000	*
	*	1 000	*	300	1 800	*
	1 300	220	1 300	200	*	170
	290	2 700	1 400	780	700	330
	*	420	1 600	520	320	—
	3 500	660	1 900	1 300	310	—
	6 400	5 200	—	—	1 000	—
	2 600	2 300	—	—	1 600	—
	—	820	—	—	*	—
	—	3 000	—	—	2 000	—
	—	730	—	—	550	—
50 $\div$ 60	1 400	1 000	250	*	6 000	3 000
	380	2 400	200	2 400	650	500
	*	620	110	—	1 700	130
	120	6 000	*	—	270	300
	130	260	300	—	210	890
	1 700	540	1 150	—	—	2 100
	2 000	*	—	—	—	160
	2 700	300	—	—	—	*
	*	9 500	—	—	—	290
	—	*	—	—	—	330
	—	240	—	—	—	—
	—	1 400	—	—	—	—
	—	*	—	—	—	—
	—	290	—	—	—	—
	—	6 800	—	—	—	—
60 $\div$ 70	480	170	*	1 500	*	800
	1 400	3 000	250	120	1 800	1 300
	190	15 000	1 000	—	1 600	*
	*	3 100	1 700	—	120	740
	3 600	270	1 700	—	300	—
	?	1 900	1 100	—	370	—
	—	13 000	270	—	150	—
	—	230	—	—	300	—
	—	—	—	—	380	—
	—	—	—	—	500	—
	—	—	—	—	1 800	—
	—	—	—	—	—	—

TABLE I (continued)

$r$ ( $\mu\text{m}$ )	A 4	A 5.5	A 7	D 2.7	D 4	D 5.5
70 ÷ 80	2 000	1 000	650	1 800	190	130
	?	*	110	370	680	1 200
	300	*	2 500	—	900	770
	380	*	190	—	1 400	700
	*	1 200	3 600	—	1 800	1 200
	*	1 100	1 900	—	840	*
	150	*	—	—	1 200	1 300
	300	280	—	—	1 800	—
80 ÷ 90	680	1 190	500	170	1 400	1 000
	150	140	*	*	2 000	2 800
	2 600	1 400	2 400	190	150	1 600
	120	220	1 250	380	1 400	1 500
	190	1 700	1 500	2 400	280	3 600
	2 100	510	250	—	1 700	110
	—	2 200	—	—	520	220
	—	380	—	—	—	540
	—	3 500	—	—	—	*
	—	340	—	—	—	240
	—	160	—	—	—	—
	—	220	—	—	—	—
	—	730	—	—	—	—
	—	—	—	—	—	—
90 ÷ 100	180	820	*	2 300	2 200	2 400
	180	980	*	650	170	120
	570	*	*	—	*	960
	170	1 000	*	—	210	290
	110	190	*	—	230	820
	—	570	2 200	—	1 500	110
	—	750	460	—	2 300	390
	—	910	—	—	3 300	2 200
	—	190	—	—	—	110
	—	*	—	—	—	—
	—	6 500	—	—	—	—
	—	*	—	—	—	—
100 ÷ 110	*	460	1 000	170	290	2 800
	1 700	1 000	540	120	150	*
	*	1 100	*	—	*	330
	1 700	120	1 700	—	1 200	2 000
	?	230	—	—	—	*
	190	—	—	—	—	170
	780	—	—	—	—	200
	—	—	—	—	—	920
	—	—	—	—	—	1 700
	—	—	—	—	—	1 700
	—	—	—	—	—	*

TABLE I (continued)

$r$ ( $\mu\text{m}$ )	$A$ 4	$A$ 5.5	$A$ 7	$D$ 2.7	$D$ 4	$D$ 5.5
$110 \div 120$	*	330	780	540	110	*
	350	490	*	*	820	*
	430	310	250	—	1 100	420
	—	1 900	700	—	—	—
	—	110	5 000	—	—	—
	—	310	250	—	—	—
	—	1 600	370	—	—	—
	—	460	320	—	—	—
	—	490	1 700	—	—	—
	—	2 200	*	—	—	—
	—	8 000	370	—	—	—
$120 \div 130$	130	2 700	580	300	*	*
	—	310	2 000	160	1 700	*
	—	1 800	840	*	120	*
	—	190	1 200	*	1 100	1 600
	—	500	—	—	1 400	—
	—	740	—	—	930	—
	—	500	—	—	150	—
	—	350	—	—	—	—
$130 \div 140$	1 300	870	670	1 000	240	*
	380	1 800	*	1 200	600	120
	*	380	2 800	—	1 900	*
	150	160	170	—	*	380
	*	*	280	—	110	*
	*	180	*	—	—	*
	*	2 200	*	—	—	1 600
	100	*	—	—	—	1 800
$140 \div 150$	*	*	570	*	*	*
	8 600	200	*	1 300	370	300
	270	1 100	*	550	280	880
	*	1 800	*	—	200	580
	—	110	1 700	—	220	1 800
	—	190	650	—	360	*
	—	420	—	—	—	—
	—	1 800	—	—	—	—
	—	1 000	—	—	—	—
$150 \div 160$	4 500	240	2 500	270	1 200	*
	120	480	*	—	*	*
	310	1 250	850	—	140	*
	*	—	360	—	390	740
	—	—	*	—	510	—
	—	—	310	—	470	—
	—	—	*	—	180	—



TABLE I (continued)

$r$ ( $\mu\text{m}$ )	$A$ 4	$A$ 5.5	$A$ 7	$D$ 2.7	$D$ 4	$D$ 5.5
150 $\div$ 160	—	—	*	—	—	—
	—	—	600	—	—	—
	—	—	2 000	—	—	—
	—	—	670	—	—	—
	—	—	1 600	—	—	—
160 $\div$ 170	170	2 800	1 100	1 200	*	1 300
	340	100	110	*	2 100	*
	2 500	*	860	*	800	350
	150	170	*	—	2 100	1 200
	1 100	*	160	—	110	*
	1 200	—	—	—	1 300	480
	710	—	—	—	470	150
	140	—	—	—	490	—
	800	—	—	—	—	—
170 $\div$ 180	*	200	910	290	1 100	*
	2 200	*	1 700	—	*	*
	*	*	170	—	120	*
	*	*	130	—	240	400
	*	390	200	—	*	2 700
	*	1 000	320	—	—	—
	*	700	*	—	—	—
	*	170	—	—	—	—
180 $\div$ 190	*	2 600	*	500	1 800	*
	*	610	*	—	260	2 100
	*	*	200	—	410	1 200
	170	190	190	—	800	110
	—	1 300	670	—	—	*
	—	—	310	—	—	600
	—	—	*	—	—	1 000
	—	—	—	—	—	*
	—	—	—	—	—	850
	—	—	—	—	—	1 400
	—	—	—	—	—	—
190 $\div$ 200	390	420	250	—	250	*
	1 800	160	2 000	—	*	*
	500	180	1 500	—	320	730
	140	2 400	1 700	—	400	—
	*	*	6 000	—	1 200	—
	—	210	1 000	—	240	—
	—	120	100	—	—	—
	—	*	310	—	—	—
	—	110	—	—	—	—
	—	180	—	—	—	—
	—	*	—	—	—	—
	—	110	—	—	—	—
	—	—	—	—	—	—

TABLE I (continued)

$r$ ( $\vartheta$ m)	$A$ 4	$A$ 5.5	$A$ 7	$D$ 2.7	$D$ 4	$D$ 5.5
$200 \div 210$	—	140	1 500	550	100	*
	—	130	*	—	*	*
	—	*	*	—	*	520
	—	*	540	—	330	280
	—	—	*	—	—	*
	—	—	*	—	—	320
	—	—	240	—	—	1 800
	—	—	*	—	—	250
	—	—	*	—	—	*
$210 \div 220$	*	470	*	1 300	730	140
	*	400	2 400	—	220	170
	*	*	230	—	220	0
	*	—	1 600	—	160	130
	960	—	—	—	*	150
	—	—	—	—	180	*
	—	—	—	—	—	*
	—	—	—	—	—	*
$220 \div 230$	120	300	1 800	—	190	1 700
	*	—	*	—	*	230
	—	—	*	—	*	*
	—	—	280	—	—	*
$230 \div 240$	250	200	130	390	*	110
	150	*	*	—	350	150
	100	530	330	—	—	*
	*	280	690	—	—	1 500
	—	280	2 000	—	—	980
	—	330	340	—	—	1 200
	—	120	1 700	—	—	300
	—	—	*	—	—	140
$240 \div 250$	*	280	830	—	*	*
	*	240	580	—	—	710
	150	870	*	—	—	130
	130	600	340	—	—	*
	240	200	390	—	—	490
	—	*	640	—	—	1 100
	—	—	400	—	—	—
	—	—	*	—	—	—
	—	—	*	—	—	—
$250 \div 270$	not measured			380	310	600
				—	*	190
				—	*	390
				—	*	100
				—	260	610
				—	480	*
				—	120	390
				—	920	160
				—	—	100
				—	—	400
				—	—	330
				—	—	530

TABLE I (continued)

250 ÷ 400	A 7					
	250-300 $\mu\text{m}$	300-350 $\mu\text{m}$	350-400 $\mu\text{m}$			
	*	150	100			
100	*	*	100			
*	*	*	*			
170	*	*	*			
640	190	*	*			
340	350	*	360			
140	1 600	*	*			
450	*	*	*			
100	*	*	*			
220	*	630	*			
330	*	*	*			
340	*	770	*			
*	450	(11)	*			
1 200	1 900	—	—			
340	120	—	—			
—	(14)	—	—			
270	—	—	—			
700	—	—	—			
950	—	—	—			
*	—	—	—			
*	—	—	—			
(6)	—	—	—			

« cut »:	B 2	B 3	B 4	C 1	C 2	C 2.4
limit reliability:	1 500	1 000	1 000	6 000	4 000	4 000
$r$ ( $\mu\text{m}$ )	8 000	2 100	—	44 000	25 000	10 000
	7 000	5 000	—	15 000	4 000	2 400
0 ÷ 20	14 000	120	—	10 000	720	*
	180	*	—	3 000	—	—
	510	*	—	500	—	—
	—	—	—	300	—	—
20 ÷ 30	5 000	1 700	*	—	1 600	370
	580	2 500	—	—	*	—
	400	—	—	—	—	—
30 ÷ 40	—	*	200	6 000	300	1 800
			*			

TABLE I (continued)

$r$ ( $\mu\text{m}$ )	$B\ 2$	$B\ 3$	$B\ 4$	$C\ 1$	$C\ 2$	$C\ 2.4$
$40 \div 50$	3700 — — —	1900 * 240 1400 *	1300 230 810 —	— — — —	— — — —	110 — — —
$50 \div 60$	210 180 240	370 1600 890	1300 220 —	2800 — —	700 300 —	370 — —
$60 \div 70$	290 — — — —	— — — — —	110 270 480 — —	— — — — —	500 4000 7000 * —	7000 210 100 2500 130
$70 \div 80$	640 * — — —	— — — — —	* * — — —	— — — — —	230 — — — —	1000 * 280 * 300
$80 \div 90$	* —	150 —	250 —	— —	200 950	— —
$90 \div 100$	— — —	370 — —	780 630 1300	— — —	1300 290 —	1700 970 —
$100 \div 110$	— — —	— — —	1400 — —	— — —	* 620 —	1100 110 3300
$110 \div 120$	380 — —	— — —	120 140 220	— — —	— — —	390 630 200
$120 \div 130$	— —	— —	* 1300	— —	— —	370 —
$130 \div 140$	* —	400 —	570 —	— —	— —	130 —
$140 \div 150$	200 —	— —	— —	— —	— —	310 —

TABLE I (continued)

$r$ ( $\mu\text{m}$ )	$B\ 2$	$B\ 3$	$B\ 4$	$C\ 1$	$C\ 2$	$C\ 2.4$
$150 \div 160$	— —	470 —	470 1 000	not measured		
$160 \div 170$	—	—	—			
$170 \div 180$	1 150	—	1 200			
$180 \div 190$	530 —	440 —	170 240			
$190 \div 200$	—	390	270			
$200 \div 210$	810	—	190			
$210 \div 220$	—	—	—			

the more they are concentrated around the shower axis. An upper limit for useful  $E'$  is given by the limitations of scattering measurements. (Region of the dots).

The actual process of correction is described in Sect. 5'2 iv. It will appear there that it is essential to know the value of  $s'$  from eq. (5) for the energy  $E'$ . This involves a previous knowledge of  $E_0$ . We apply, therefore, a process of successive approximations in order to determine  $E_0$ .

Inserting  $N'_R(E', t')$  in eq. (4) we obtain a first approximation  $E'_0$  to  $E_0$ . This  $E'_0$  gives  $s'$  as a function of  $E'$  from eq. (5). With the help of  $s'$  we find  $N'(E', t')$  from  $N'_R(E', r')$  (see Sect. 5'2 iv)). Now inserting this  $N'(E', t')$  in eq. (4) we find that the next approximation to  $E_0$  does not differ seriously from  $E'_0$ , because  $E'$  was high and therefore the correction small.

On the other hand, since  $E_0$  appears in eq. (5) under a logarithm, the change from  $E'_0$  to  $E_0$  does not alter  $s'$  appreciably and the correction to  $N'_R(E', t')$  remains essentially the same. Thus we may finish the process of successive approximation after one step.

The limits of error for  $E_0$  are taken from the fluctuation uncertainties of  $N'(E')$  using eq. (4).

These uncertainties are relatively smallest when the number of particles is large. Hence, we have chosen the cut  $t'$  with the largest number of particles at  $E'$  in order to determine  $E_0$ .

The numbers  $N'(E', t')$  used are the points  $E' = 1000$  MeV in  $A\ 7$ ,  $B\ 5$ , and  $D\ 5.5$ , and the point  $E' = 1500$  MeV in  $C\ 2.4$ .



With this  $E_0$  we can predict from eq. (4) the numbers  $N(E, t)$  for all other depths and energies in the same cascade. Function (1) is represented in Fig. 1-4 by the full lines. We calculated Jánossy's standard deviation from  $N(E, t)$  multiplying it by a factor of  $\sqrt{2}$  to include the uncertainties in the estimation of  $E_0$ . These limits are given by the dashed lines in the diagrams. For  $t = 1$  Jánossy has not given the deviation and therefore the Poissonian standard deviation times a factor  $\sqrt{2}$  is drawn in *C1*.

It will be realized that the measurement points  $N'_r(E', t')$  are generally within the Jánossy deviation from  $N'(E', t')$ . Therefore, even if our correction to  $N'_r(E', t')$  was in error by 100%, the result for  $E_0$  would still lie within the given limits of error for  $E_0$ . We therefore shall always assume  $E_0$  to be practically independent of the detailed correctness of the lateral spread function. Not here, that the energy balance from *C1* (Table I) is about 80 000 MeV, which after correction for invisible photon energy (about a factor of 2) agrees rather closely with the value of  $E_0$  determined by this method (Fig. 3).

ii) Having now obtained  $E_0$  and a scale of  $s$  from eq. (5) for all depths and energies, we are able to correct several other measurement points for losses outside the disc of measurement. The results of our corrections are represented by the circles in Fig. 1-4. In case *A7* corrections from full squares are marked as open squares. The actual values of  $E$  for which corrections are made can be seen from Table II.

TABLE II.

$x_0$	$E$ in MeV					Proportion excluded: $\chi$		
	400 $\mu\text{m}$	270 $\mu\text{m}$	250 $\mu\text{m}$	220 $\mu\text{m}$	150 $\mu\text{m}$	$s = 1$	$s = 0.6$	$s = 1.5$
0.05	75	111	125	145	200	0.78	—	—
0.1	150	222	250	290	400	0.62	0.37	0.87
0.2	300	445	500	580	800	0.42	0.18	0.67
0.4	600	890	1000	1200	1600	0.21	0.06	0.46
0.6	900	1300	1500	1750	2400	0.12	—	—
0.8	1200	1800	2000	2400	3200	—	—	0.24
1.6	2400	3600	4000	4600	6400	—	—	0.08

In cascade *C* two more corrected points in each cut are obtained by multiplying  $N_r$  (300 MeV) and  $N_r$  (700 MeV) with the correction factors  $1/(1 - \chi)$  (Sect. 5'2 iv)) for 400 and 800 MeV respectively. Note the fluctuation to lower numbers at *A4* and *A5.5* which in *A4* lies outside the Poissonian standard deviation.

5'2. *The Lateral Spread.* — For comparison of  $P(x)$  with experiment we have to select certain energy intervals in which we can assume  $s$  to be constant because the tables (ref. (13)) are calculated under the assumption of constant  $s$  for values  $s = 0.6; 1.0; 1.5$ . No energy interval with  $s = 1.5$  can be found

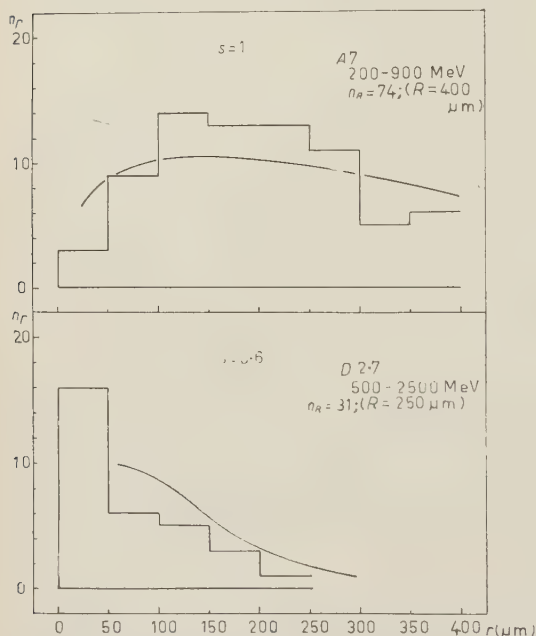


Fig. 5. — The differential lateral distribution of electrons with energy between the given limits. The line represents the function (6), normalized so that the total number of particles inside the disc of radius  $R$  equals the observed number.

with the experiment. One will see from Fig. 9 by comparison with the theory of MIDGAL and others (14) that  $D2.7$  seems to be a fluctuation to a very peaked core, so that eq. (6) for  $s = 0.6$  may not be such a poor approximation as suggested by Fig. 5.

ii) *The track length distribution.* — As said before, we obtain  $s = 1$  for the whole energy range in the track length spectrum (eq. (3)).

We tried an admittedly poor approximation of the integral  $\int_0^\infty \Pi(E_0, E, t) dt$  by the sum

$$(14) \quad 2 \cdot (D 2.7) + (D 4) + 2 \cdot (D 5.5),$$

which approximates to the integral  $\int_{1.5}^{6.5} \Pi(E_0, E, t) dt$ . 1000 MeV is taken as  $t$

in our cuts. For  $s = 1$  we choose the interval from 200–900 MeV in  $A7$  for comparison, because it is measured up to  $R = 400 \mu m$  and provides us with the best statistics. The range from 500–2500 MeV in  $D2.7$  is the most suitable for comparison with  $P(x)$  for  $s = 0.6$ . All other choices suffer from poor statistics, and also from the fact that, since  $P(x)$  is tabulated only for  $x = Er/Kr_1 > 0.2$ , a high value of  $r$  must be chosen for small  $r$  in order to have values of  $x$  in the appropriate region.

The result is given in Fig. 5, where the normalization has been chosen so that observed and theoretical numbers of particles equal each other in the disc with radii 400  $\mu m$  and 250  $\mu m$  respectively.

The theoretical curve (6) does not appear to be in disagreement

lower energy limit in  $N_r(E)$  in order that the influence from the missing part  $\int_0^\infty \Pi(E_0, E, t) dt$  be very small. Very near the core we expect differences, because the integral  $\int_0^\infty \Pi(E_0, E, t) dt$  is not included and for small  $t$  one can expect the particles to be near the shower axis.

Fig. 6 shows the comparison of our approximation eq. (14) with eq. (8) calculated for  $s = 1$ . The error due to the uncertainty in the position of the shower axis may influence the experimental results very near the core, so that the error there may be greater than Poissonian.

iii) Corrections for the integral spectrum. — Assume  $N_r(E)$  to be the experimentally obtained number which we want to correct for losses of particles outside the disc of radius  $R$ . We know that particles of higher energy are closer to the core than particles of lower energy. It will be clear therefore that mainly electrons with energy just above  $E$  are lost outside the disc of measurement. Thus the distribution function (9) will be determined in the region from  $R$  to  $\infty$  by the value  $s$  for  $E$  from eq. (5).

For example, in A7 we have  $E = 500$  MeV for  $s = 1$ . We calculated the function (9) for  $s = 1$ , i.e. we approximated the integral spectrum by a power law with  $s = 1$  over the entire energy range. The result is shown as a dashed line in Fig. 7. The full line represents the better approximation (10) with two values of  $s$  for the energy range above  $E$ . It can be seen from Fig. 7 that there is a big difference only near the core, while beyond  $R = 150 \mu\text{m}$  both

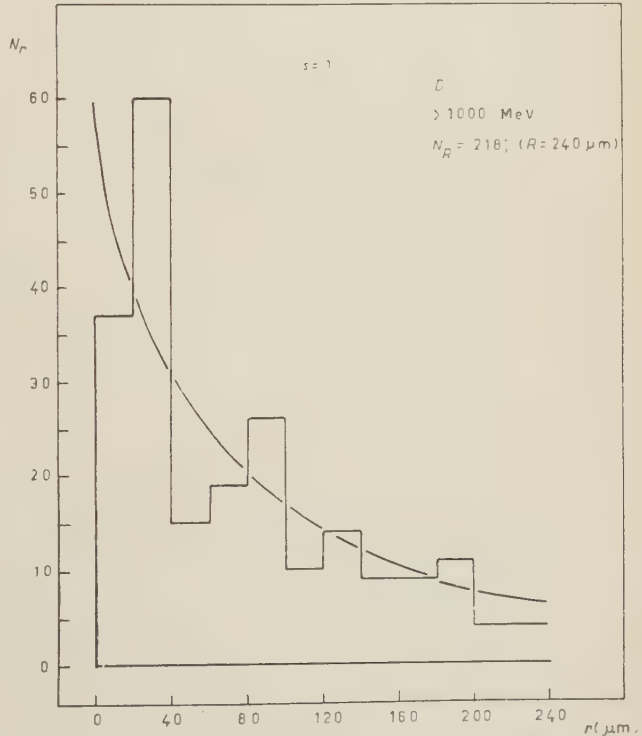


Fig. 6. — The track length distribution. The experimental values are taken from approximation (14), the theoretical line represents function (8), the normalization is such that the theoretical number of particles inside  $R$  is equal to that observed.

functions approach each other and are then in good agreement with the experimental data. Hence we shall always assume that approximation (9) is good enough for the calculation of the proportional loss outside the radius  $R$ , because we use it only for radii larger than the values of  $R$  given in Fig. 1.

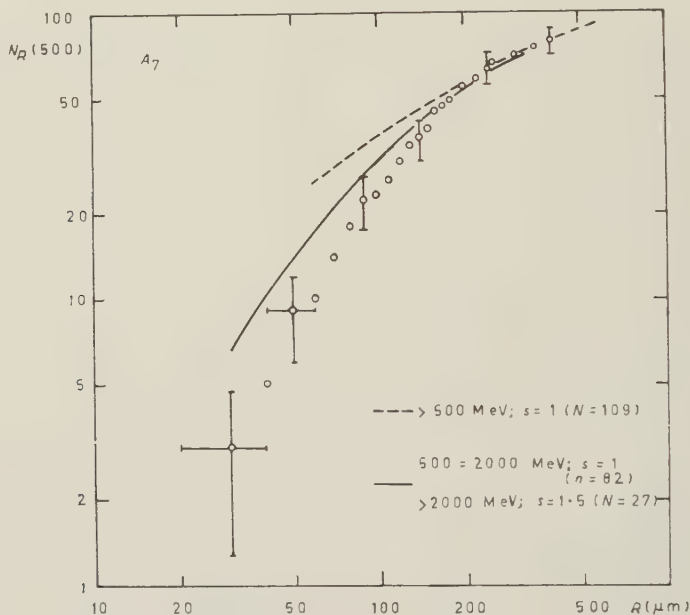


Fig. 7. — Integral lateral distribution for electrons with energy above 500 MeV. The dashed line is function (9) for  $s = 1$ , the full line function (10). In both cases the normalization was chosen to give a total number of particles  $N = 109$  as taken from  $A_7$  in fig. 1.

iv) The method of correction. — We calculated the proportional loss of particles with energy above  $E$  (in MeV) outside the disc with radius  $R$  from the shower axis from the integral

$$(15) \quad \chi = \int_{x_0}^{\infty} x \left( 1 - \left( \frac{x_0}{x} \right)^s \right) P(x) dx.$$

The total number  $N(E)$  is then obtained from  $N_R(E)$  by

$$(16) \quad N(E) = N_R(E) \frac{1}{1 - \chi},$$

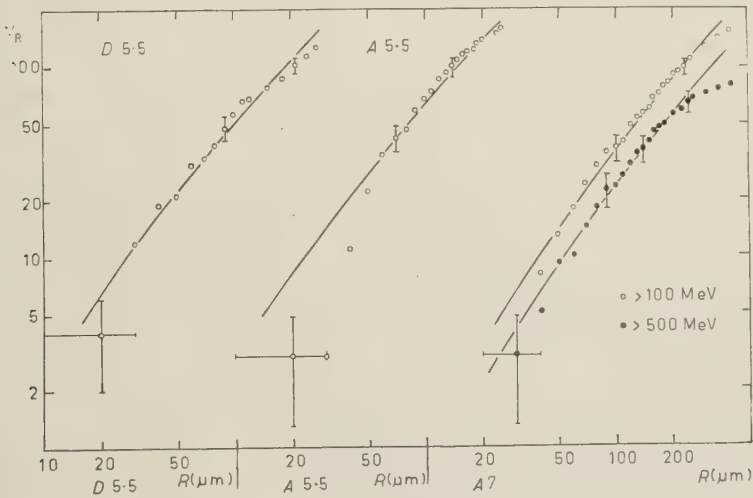
where  $x_0 = ER/Kr_1$ . The function  $\chi$  is given in Table II for  $s = 0.6, 1.0, 1.5$ .

In practice, for a given energy  $E$ ,  $s$  is calculated from eq. (5) and the value  $\chi$  obtained from Table II by interpolation for the same  $x_0 = ER/Kr_1$ . The results for  $N(E)$  from eq. (16) are marked as circles in Fig. 1-4.

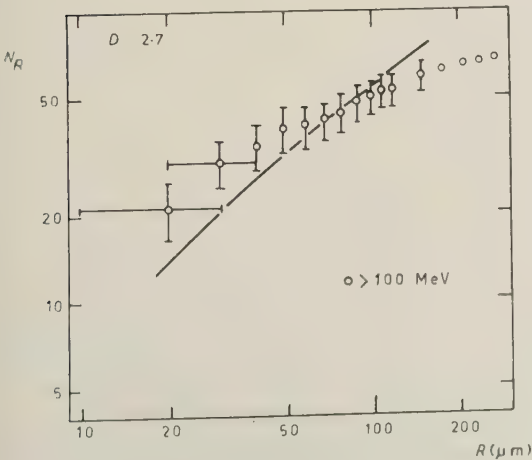
5.3. *The Behaviour Very Near the Core.* – We compare the experimental results  $N_R(E)$  as a function of  $R$  with eq. (11) integrated over  $r$ , i.e. with the function

(17) 
$$N_R(E) = CR^s,$$

where  $s$  is given by eq. (12) and  $C$  is a constant factor chosen to give the best fit with the experimental values. Eq. (17) should be valid for small radii, but exact upper limits are not known from the theory.



← Fig. 8.



← Fig. 9

Figs. 8 and 9. – Integral lateral distribution of electrons above 100 MeV (○) and 500 MeV (●). Theoretical curves correspond to the function (11).



Since  $s$  in eq. (12) is not dependent on the energy  $E$  of the particles, we expect the same slope for other values of  $E$ . Experimental points with  $E = 100$  MeV are drawn for  $D$  5.5 and  $A$  5.5 in Fig. 8 and for  $D$  2.7 in Fig. 9. For  $A$  7 (Fig. 8) we give the  $E = 100$  and 500 MeV measurement points. It seems that  $E$  has an influence only on the upper limit of validity of eq. (17).

There is only one example (Fig. 9) where it is difficult to see agreement between the theoretical curve and the experimental points. But the difference is in the same direction as that in Fig. 5 when compared with the theory of Eyges and Fernbach. So we assume that  $D$  2.7 is a fluctuation, however it must be remembered that extreme deviations are possible in lateral spread.

5.4. *The Root Mean Square Lateral Spread.* - The root mean square lateral spread  $\sqrt{r^2}$  defined from eq. (13) will be compared with the experimental quantity

$$(18) \quad \sqrt{r^2} = \sqrt{\frac{\sum_i r_i^2}{N_R(E)}},$$

where the sum is over all particles of energy exceeding  $E$  within radius  $R$ .

The comparison is shown in Fig. 10. The curves are taken from ref. (21). Fig. 2, the line for 7 r.l. is obtained by interpolation. The dashed line gives the value calculated by ROBERG and NORDHEIM (19) for the root mean square lateral spread of particles above energy  $E$  at the maximum of the cascade.

Since we only record tracks within distance  $R$  from the shower axis, we have selected a very high value of  $E$  to ensure that essentially all electron tracks which have undergone multiple scattering only will be included in this region. However, it is still possible that occasional electrons which have suffered large angle scattering earlier in the cascade may lie outside the region considered. On the other hand the increasing uncertainty in energy determination gives an upper limit for the value of  $E$  selected, we used the number given in the second column of Table III.

No track with energy exceeding  $E$  has been found at a larger distance than  $R_{\max}$  from the shower axis (Table III), while measurements have been made up to the distance  $R$ .

One standard deviation is drawn in Fig. 10 as a measure of the statistical uncertainties.

Assuming that all electrons, recorded to be above 2000 MeV were above 3000 MeV, we calculated the new position of the points  $\times$  and  $\circ$  in Fig. 10 and marked the shift by arrows. For the calculation of the influence of unreliable energy estimation this is certainly a pessimistic assumption, because some of the particles, particularly those with large values of  $r$  will not in fact

have energies higher than 3000 MeV, so  $\sqrt{r^2}$  should be correspondingly reduced.

Our results (Fig. 10) lie consistently lower than those predicted by Messel's calculation. This may in part be due to the limited size  $R$  of our disc. Therefore we may miss one or two cases of large single scattering. Table III gives in the last two columns the distances from the shower axis (in  $\mu\text{m}$ ) at which 1 or 2 particles respectively would have had to be found in order to give agreement with Messel's theory.

TABLE III.

« cut »	$E$ (MeV)	$R_{\text{max}}$ ( $\mu\text{m}$ )	$R$ ( $\mu\text{m}$ )	1 part. at $r$ ( $\mu\text{m}$ )	2 part. at $r$ ( $\mu\text{m}$ )
$C$ 1	1000	60	150	—	—
$C$ 1	2000	60	150	—	—
$D$ 2.7	1500	100	270	460	330
$D$ 4	1500	190	270	1000	700
$D$ 5.5	1500	240	270	1300	900
$A$ 5.5	2000	200	250	750	550
$A$ 7	1500	300	400 (?)	1500	1100
$A$ 7	2000	240	400 (?)	700	500

A small part of the disc with the radius 400  $\mu\text{m}$  in  $A$  7 has not been checked because of the air gap between the emulsion sheets.

In the case of  $C$  1 our distribution is completely reliable. The development of this cascade was followed from the origin up to one cascade unit, and 3 particles with energies below 500 MeV have been found to leave the disc of observation. So we are certain that no particle with energy exceeding 1000 MeV has been missed (\*).

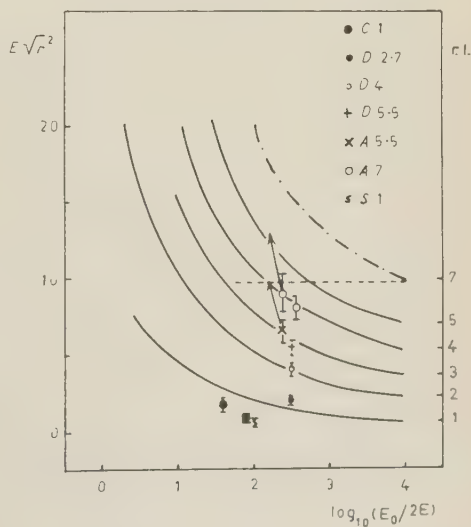


Fig. 10. — The root mean square lateral spread. The curves are copied from ref. <sup>(21)</sup> Fig. 2. The dot-dashed line is obtained by interpolation. The errors shown are standard deviations, the arrows are explained in the text.

(\*) After writing the paper, another flat cascade ( $S$ ) has been found and followed for one cascade unit in the same manner as cascade  $C$ . It is believed that no particle lies outside the measured area. The experimental point is drawn in Fig. 10 as a small  $s$ .

However, even if no particles lying at large  $r$  have been missed in the showers discussed above, it is still not necessarily inconsistent with the theory of Messel and Chartres <sup>(21)</sup> that we find values of  $\sqrt{r^2}$  lying consistently below their calculated values. In contrast with LANDAU <sup>(16)</sup>, these authors have included the effects of single scattering of electrons through large angles (see MOLIÈRE <sup>(25)</sup>). Although these large angle scatters are rare, they will contribute strongly to the average value calculated for  $\sqrt{r^2}$ , and may cause the frequency distribution for  $\sqrt{r^2}$  to be skew.

For the case  $A\ 7$ , which is near shower maximum, the values of  $\sqrt{r^2}$  agree with the calculations of ROBERG and NORDHEIM <sup>(19)</sup> for the shower maximum on the basis of equations equivalent to Landau's.

## 6. — Discussion.

Even if the criticism expressed by MESSEL and GREEN <sup>(20)</sup> of the older lateral spread theory was justified, we think that the influence on our calculations for losses outside the disc of measurement would be small. This is because the difference in the theories affects only the very small number of particles which may suffer single scattering, while we are interested only in the main contribution from particles being deflected by multiple scattering.

It is to be hoped that detailed calculations of the lateral distribution function for differential and integral energy spectrum and different shower ages  $s$  are soon made available for all radii.

From a consideration of the longitudinal spread, no sign of a very important trident influence could be seen. This does not mean that the theoretical trident cross-section must be correct, but that the trident cross-section is negligible in comparison with bremsstrahlung and pair production. As mentioned by KOSHIBA and KAPLON <sup>(3)</sup>, the result of a very much larger cross-section for higher order processes would be a shorter cascade unit, i.e. the shower would become older more rapidly than is predicted by theory. No sign of such behaviour can be seen in our 4 cascades.

## 7. — Conclusions.

The photographic emulsions technique offers a very powerful approach to the problem of quantitative investigation of longitudinal and lateral development of electronic showers at very high energies. We believe that our

---

<sup>(25)</sup> G. MOLIÈRE: *Phys. Rev.*, **93**, 636 (1954).

investigations give a strong argument for the validity of present shower theory under approximation A within the expected fluctuations, although higher order processes may not have been detected. But we believe that they are negligible in comparison with bremsstrahlung and pair production, even at energies above  $10^5$  MeV.

Our measurements are not in disagreement with the computations of EYGES and FERNBACH <sup>(13)</sup>.

The behaviour very near the core is consistent with the law

$$N_r(E) \frac{1}{r} \sim r^{s-2},$$

suggested by MIGDAL and others <sup>(14)</sup>.

All values obtained for the root mean square lateral spread are lower by a factor of about 2 than the predictions by CHARTRES and MESSEL <sup>(21)</sup>.

\* \* \*

The author wishes to acknowledge his indebtedness to Professor C. F. POWELL for affording him the facilities of this laboratory, and to Professor E. BAGGE, the Rotary Club Hamburg and the Studienstiftung des deutschen Volkes for a scholarship to the University of Bristol.

He is very grateful to Dr. Y. FUJIMOTO for many ideas in the initial stage of this experiment and he wishes to thank Dr. A. ENGLER and Dr. R. H. DALITZ for many discussions and help with the manuscript. Finally, he is very much obliged to Miss S. BULT for the great amount of work done in the course of the tiring scattering measurements and in the target diagrams.

---

#### RIASSUNTO (\*)

Si sono studiate in dettaglio quattro cascate iniziate da un fotone singolo. Si danno diagrammi del bersaglio a differenti profondità e l'energia di ogni particella rappresentata è stata determinata per mezzo di misure di scattering multiplo. I risultati si confrontano colla teoria degli sciami per lo sviluppo laterale e longitudinale nell'approssimazione A di ROSSI e GREISEN <sup>(5)</sup>. Si trova che la teoria fornisce un quadro compatibile, nell'ambito delle possibilità di fluttuazione fino ad un'energia primaria di  $10^6$  MeV. La distribuzione delle particelle molto prossime al core si accorda con una legge del tipo  $r^{s-2}$ . Si fa un confronto coi calcoli dello spostamento quadratico medio laterale di CHARTRES e MESSEL <sup>(21)</sup>.

---

(\*) Traduzione a cura della Redazione.

## On the Ionization Loss of Fast $\mu$ -Mesons.

G. N. FOWLER

*Department of Theoretical Physics - University of Manchester*

(ricevuto il 15 Marzo 1956)

**Summary.** — The fluctuation in the ionisation loss of fast  $\mu$ -mesons due to resonance effects is discussed in detail using a modification of Landau's method. Numerical results for oxygen neon and other inert gases are compared with experiment and it is concluded that most of the observed large fluctuation can be accounted for when atomic resonance effects are included and the effect of primary excitation loss on the phenomenon is taken into account.

### 1. — Introduction.

When a fast particle traverses matter the energy lost in producing ions in the medium is subject to fluctuations as a result of the fluctuation both in the number of collisions in a given length of track and in the energy lost in each collision. The resulting distribution is approximately gaussian with a pronounced tail in the region of high energy losses. It has been shown by BOHR <sup>(1,2)</sup> and WILLIAMS <sup>(3)</sup> that the basic features of the distribution may be most easily explained in terms of an energy  $\xi$  given by

$$\xi = \frac{2\pi N e^4 \rho x}{m v^2} \frac{\sum Z}{\sum A},$$

where  $e$  and  $m$  are the charge and mass of the electron,  $x$  the thickness of

<sup>(1)</sup> N. BOHR: *Phil. Mag.*, **30**, 581 (1915).

<sup>(2)</sup> N. BOHR: *Dan. Mat.-Fys. Medd.*, **18**, 8 (1948).

<sup>(3)</sup> E. J. WILLIAMS: *Proc. Roy. Soc.*, **125**, 420 (1929).



absorber traversed,  $\rho$ ,  $Z$ ,  $A$ , the density, atomic and mass numbers of the absorbers  $v$  the velocity of the incident particle and  $N$  is Avogadro's number.

Broadly speaking, there will be many collisions in which the energy loss  $\varepsilon < \xi$  and these produce a gaussian fluctuation. The few collisions in which the loss  $\varepsilon > \xi$  are responsible for the tail.

In order to include the effects due to atomic binding the collisions are divided into two classes, the resonant collisions in which the atomic binding is important and the free collisions in which it is not. It may be shown that the effect of the former group on the fluctuation is unimportant when  $\xi$  is large compared with the atomic ionization potentials. In this case we speak of a thick absorber and it is with such absorbers that most of the theoretical work has been concerned (cf. the authors quoted above, and, more recently, LANDAU <sup>(4)</sup> and SYMON <sup>(5)</sup>).

The experimental work on this question falls into two classes: direct measurements of energy loss in thin foils (GOLDWASSER, MILLS and HANSON) <sup>(6)</sup> and measurements of distributions of ion pairs. When proportional counters are used, the latter are converted into measurements of energy loss by assuming that the ion pair and energy loss distributions are the same and calibrating by means of X-rays of known frequency. Both types of measurement have been carried out in recent times on thin absorbers and fluctuations have been found considerably in excess of those predicted by WILLIAMS and LANDAU. The details of much of this work are summarized in a review article by CRANSHAW <sup>(7)</sup>. More recent investigations have been carried out by WEST <sup>(8,9)</sup> and EYEIONS *et al.* <sup>(10)</sup>.

So far as the direct measurements of energy loss are concerned BLUNCK and LEISEGANG <sup>(11)</sup> have modified Landau's calculation to include the effects of atomic resonance on the fluctuation and have in fact found a larger theoretical fluctuation which, however, in the case of some thin absorbers, is even greater than that found experimentally. On the other hand, MOYAL <sup>(12)</sup> has found no significant increase in fluctuation when resonant collisions are included. In the following we have attempted to clarify the situation with reference to measurements of ion pairs and we show that resonance effects do lead to a

<sup>(4)</sup> L. LANDAU: *Journ. Phys. USSR*, **8**, no. 4, 201 (1944).

<sup>(5)</sup> S. K. SYMON: *Harvard University Thesis* (1948).

<sup>(6)</sup> E. L. GOLDWASSER, F. E. MILLS and A. O. HANSON: *Phys. Rev.*, **88**, 1137 (1952).

<sup>(7)</sup> T. E. CRANSHAW: *Progress in Nuclear Physics*, **2**, 271 (1952).

<sup>(8)</sup> D. WEST: *Proc. Phys. Soc.*, A **66**, 306 (1953).

<sup>(9)</sup> D. WEST: *Progress in Nuclear Physics*, **3**, 18 (1953).

<sup>(10)</sup> D. EYEIONS, B. G. OWEN, B. T. PRICE and J. G. WILSON: *Proc. Phys. Soc.*, A **68**, 793 (1955).

<sup>(11)</sup> O. BLUNCK and S. LEISEGANG: *Zeits. f. Phys.*, **128**, 500 (1950).

<sup>(12)</sup> J. E. MOYAL: *Phil. Mag.*, **46**, 263 (1955).

significant increase in fluctuation in the case of thin absorbers. The method of calculation is derived from that used by LANDAU and, though approximate, it does permit the various types of collision to be taken into account in a consistent way. It also allows of a simple and concise discussion of much of the previous theoretical work on the subject.

The comparison between the theoretical energy loss distribution and the experimental distribution of ion pairs may be made provided the ion pair distribution for a given energy loss and the energy loss per ion pair is known. In connection with the latter quantity it is necessary to examine more closely the part played in the phenomena by the primary optical excitation loss, which is the energy lost by the primary particle in exciting atoms of the medium, the energy transfers being too small to admit of the formation of ion pairs after the excitation. Thus if we denote the primary optical excitation loss by  $E_x$  and the ionisation loss by itself by  $E_I = N\bar{e}$ , where  $\bar{e}$  is some mean energy expended in producing an ion pair and  $N$  is the total number of ion pairs produced the energy loss per ion pair is

$$\eta = \bar{e} + E_x/N.$$

Now the number of primary collisions in which an atom is excited is very large and so we may assume that  $E_x$  remains sensibly constant for all traversals of the absorbing medium. Thus we have that, if, in two traversals, the total number of ion pairs produced are  $N_1$  and  $N_2$ , then

$$\eta_1 = \bar{e} + E_x/N_1 \neq \eta_2.$$

Now it is reasonable to assume that  $\bar{e}$  is a constant over most of the distribution (with the possible exception of the high energy tail) so that, if  $\eta$  is to have the same property we must exclude primary optical excitation from the calculation. For this reason we have omitted the contribution of primary optical excitation from the calculation of the energy loss distribution. (An estimate of the magnitude of this contribution will be given at a later stage).

As has already been mentioned some of the experimental results are given in terms of a total loss found from calibration by means of X-rays. Underlying this procedure is the assumption that the total loss is proportional to the number of ion pairs over the whole distribution, which we have seen is not the case when primary optical excitation is included, as it is when X-rays are used. Thus these experimental results are to be regarded as being measurements of relative numbers of ion pairs and the comparison with the theoretical distribution is to be made after the experimental results have been scaled down so that the two values of the most probable loss agree. The result then shows a much better agreement between theory and experiment than has been found previously.

## 2. - General Formula for the Energy Loss Distribution.

The method is a combination of the work of WILLIAMS <sup>(3)</sup> and LANDAU <sup>(4)</sup>. We first denote by  $f(x, \Delta)$  the probability that the meson of given initial energy will lose an energy lying between  $\Delta$  and  $\Delta + d\Delta$  in traversing a thickness  $x$  of the medium. If now  $\omega(\varepsilon)d\varepsilon$  is the probability per unit length of path of a collision in which the energy loss lies between  $\varepsilon$  and  $\varepsilon + d\varepsilon$  then the function  $f(x, \Delta)$  satisfies the following equation

$$(1) \quad \frac{\partial f}{\partial x} = \int_{\varepsilon_0}^{\varepsilon_{\max}} \omega(\varepsilon) [f(x, \Delta - \varepsilon) - f(x, \Delta)] d\varepsilon,$$

where  $\varepsilon_0$  is the smallest atomic ionization potential and  $\varepsilon_{\max}$  is the maximum transferable energy. It is assumed that the initial energy  $E$  is so large that we can neglect the effect on  $\omega(\varepsilon)$  of the decrease in particle energy.

Following LANDAU we solve this equation by means of the Laplace transformation

$$(2) \quad \varphi(p, x) = \int_0^\infty f(x, \Delta) \exp[-p\Delta] d\Delta.$$

The solution is then

$$(3) \quad f(x, \Delta) = \frac{1}{2\pi i} \int_{-i\infty + \sigma}^{+i\infty + \sigma} \exp \left[ p\Delta - x \int_{\varepsilon_0}^{\varepsilon_{\max}} \omega(\varepsilon) (1 - \exp[-p\varepsilon]) d\varepsilon \right] dp.$$

To evaluate the integral over  $p$  we take (cf. BUTLER <sup>(13)</sup>)

$$\begin{aligned} \omega(\varepsilon) &= \omega_1(\varepsilon) & \varepsilon \leq \varepsilon' \\ &= \omega_2(\varepsilon) & \varepsilon > \varepsilon' \end{aligned}$$

and write

$$(4) \quad \int_{\varepsilon_0}^{\varepsilon_{\max}} \omega(\varepsilon) (1 - \exp[-p\varepsilon]) d\varepsilon = \int_{\varepsilon_0}^{\varepsilon'} \omega_1(\varepsilon) (1 - \exp[-p\varepsilon]) d\varepsilon + \int_{\varepsilon'}^{\varepsilon_{\max}} \omega_2(\varepsilon) (1 - \exp[-p\varepsilon]) d\varepsilon.$$

<sup>(13)</sup> S. T. BUTLER: *Proc. Phys. Soc.*, A **63**, 599 (1950).

We expand the first term of the second member of (4) by means of the series

$$(5) \quad \int_{\varepsilon_0}^{\varepsilon'} \omega_1(\varepsilon)(1 - \exp[-p\varepsilon]) d\varepsilon = p \int_{\varepsilon_0}^{\varepsilon'} \varepsilon \omega_1(\varepsilon) d\varepsilon - \frac{p^2}{2} \int_{\varepsilon_0}^{\varepsilon'} \varepsilon^2 \omega_1(\varepsilon) d\varepsilon + \\ + \frac{p^3}{6} \int_{\varepsilon_0}^{\varepsilon'} \varepsilon^3 \omega_1(\varepsilon) d\varepsilon \dots \equiv p\bar{\varepsilon} - \frac{p^2}{2} \bar{\varepsilon}^2 + \frac{p^3 \bar{\varepsilon}^3}{6} - \dots$$

retaining only the first three terms.

The energy  $\varepsilon'$  is to be determined in such a way that the following approximation is valid:

$$(6) \quad \int_{-\infty + i\sigma}^{+\infty + i\sigma} \exp \left[ p\Delta - x \int_{\varepsilon_0}^{\varepsilon_{\max}} \omega(\varepsilon)(1 - \exp[-p\varepsilon]) d\varepsilon \right] \approx \exp \left[ -x \int_{\varepsilon'}^{\varepsilon_{\max}} \omega_2(\varepsilon) d\varepsilon \right] \cdot \\ \cdot \left[ \int_{-\infty + i\sigma}^{+\infty + i\sigma} \exp \left[ p\Delta - p\bar{\varepsilon}x - \frac{1}{2} p^2 \bar{\varepsilon}^2 x \right] \left\{ 1 - p^3 \bar{\varepsilon}^3 x / 6 + x \int_{\varepsilon'}^{\varepsilon_{\max}} \omega_2(\varepsilon) \exp[-p\varepsilon] d\varepsilon \right\} dp \right].$$

On carrying out the integration over  $p$ , using (6), we find for  $f(x, \Delta)$  the result

$$(7) \quad f(x, \Delta) = e^{-Q} [e^{-t^2} (1 - A) + B] / (2\pi)^{\frac{1}{2}} a.$$

Here

$$A = \frac{2\bar{\varepsilon}^3}{a^3} \left( t - \frac{2t^3}{3} \right), \quad B = x \int_{\varepsilon'}^{\varepsilon_{\max}} \omega_2(\varepsilon) \exp[-(\Delta - \Delta_0 - \varepsilon)^2 / a^2] d\varepsilon, \\ C = x \int_{\varepsilon'}^{\varepsilon_{\max}} \omega_2(\varepsilon) d\varepsilon, \quad t = (\Delta - \Delta_0) / a, \\ \Delta_0 = x\bar{\varepsilon}, \quad a = (2x\bar{\varepsilon}^2)^{\frac{1}{2}}.$$

The first term in the bracket of (7) represents the contribution of the many collisions in all of which the energy loss  $\varepsilon < \varepsilon'$  and the second term allows for the contribution from one collision only, on traversing the thickness  $x$ , in which the energy loss  $\varepsilon > \varepsilon'$ .

The expression for the most probable energy loss

$$A_0 = x \int_{\varepsilon_0}^{\varepsilon'} \varepsilon \omega_1(\varepsilon) d\varepsilon ,$$

is very similar to that given by LANDAU:

$$A_{0L} = x \int_{\varepsilon_0}^{\varepsilon} \varepsilon \omega_1(\varepsilon) d\varepsilon .$$

In order that (7) be valid it is sufficient that  $A, B \ll 1$ . It will be seen that  $A$  is an increasing and  $B$  a decreasing function of  $\varepsilon'$ . We therefore choose  $\varepsilon'$  so as to satisfy  $A = B$ , with  $t$  fixed so that  $A$  is maximised.

One important remark should be made concerning the dependence of the result on  $\varepsilon'$ . The terms in (7) relating to the many collisions in which the energy loss  $\varepsilon < \varepsilon'$  obviously cannot include ionizing collisions involving electrons whose ionization potential  $I > \varepsilon'$ . Such collisions should be included in the term in (7) which gives the contribution due to a single collisions in which the energy loss  $\varepsilon > \varepsilon'$ . This point will be referred to again below.

### 3. - Ion Pair Distribution.

The theoretical ion pair distribution for a given energy loss is discussed by WEST<sup>(9)</sup>. The result is a gaussian distribution with variance, in the case of ion pairs produced in a proportional counter, given by

$$V = n_0/k + n_0 ,$$

where  $n_0$  is the most probable number of ions pairs and  $2 \leq k \leq 3$ .

If no account is taken of the fluctuation due to the counter multiplication process, we have the cloud chamber case when

$$V = n_0/k .$$

The experimental ion pair distribution of HANNA, KIRKWOOD and PONTECORVO<sup>(14)</sup> using proportional counters, is to a very good approximation a gaussian with variance approximately  $n_0$ . This result disagrees with the theory

<sup>(14)</sup> G. C. HANNA, D. N. KIRKWOOD and B. PONTECORVO: *Phys. Rev.*, **75**, 985 (1949).



in predicting an additional fluctuation due to counter multiplication which is smaller than that to be expected. In the following we have taken  $k = 3$  as being the best theoretical value and one which should lead to an upper limit on the theoretical fluctuation.

If, now, we exclude contributions from primary optical excitation we may define a quantity  $\chi$ , constant over the distribution as discussed above by

$$\chi = n_{\Delta}/\Delta,$$

where  $\Delta$  is the energy lost in ionization in a given traversal and  $n_{\Delta}$  is the most probable number of ion pairs produced when this energy is transferred.

The distribution of numbers of ion pairs for a given energy loss may thus be written

$$g(x, n) = \frac{r^{\frac{1}{2}} \exp [-(n - n_{\Delta})^2 r / n_{\Delta}]}{(\pi n_{\Delta})^{\frac{1}{2}}} = \frac{r^{\frac{1}{2}} \exp [-(n - \chi \Delta)^2 r / \chi \Delta]}{(\pi \chi \Delta)^{\frac{1}{2}}}.$$

From this we find for  $F$ , the ion pair distribution function

$$F(x, n) = \int_0^{\infty} f(x, \Delta) g(x, n, \Delta) d\Delta,$$

where  $r = \frac{3}{4}$  or 3 for counters and cloud chambers respectively (we have assumed  $k = 3$ ).

The integrals required are of the form  $\partial^k I / \partial n_{\Delta_0}^k$  with  $k = 0, 1, 2$ , and

$$I = \int_0^{\infty} \exp [-(\Delta - n_{\Delta_0} / \chi)^2 / a^2] \frac{\exp [-(n - \chi \Delta)^2 r / \chi \Delta]}{(\chi \Delta)^{\frac{1}{2}}} d\Delta.$$

To evaluate  $I$  we expand the first factor in a Taylor series about the point  $\Delta = n/\chi$  and use the result

$$\int_0^{\infty} \exp [-n^2/t - pt] t^{p-1} dt = 2p^{p/2} n^{-p} K_p(2p^{\frac{1}{2}}n)$$

where  $K_p$  is the Bessel function defined by WATSON<sup>(15)</sup>. The result is then

$$(7') \quad F(x, s) \approx f(x, s) + \frac{1}{2r\chi a} \frac{df}{ds} + \frac{n}{2r(\chi a)^2} \frac{d^2f}{ds^2},$$

where  $s = (n - n_{\Delta_0})/\chi a$  and the correction terms  $A$  and  $B$  have been neglected.

(15) G. N. WATSON: *A treatise on theory of Bessel functions*, C.U.P., 77 (1944).

In the present application  $\chi a$  is large enough for the second and third terms to be  $< 5\%$  of the leading term. We may therefore directly compare the experimental ion pair distribution with the theoretical energy loss distribution given by (7) and then make a small correction.

#### 4. — Comparison with the Results of Other Authors.

It is of interest to see how the result (7) is related to that of the other authors referred to above.

If we determine  $\varepsilon'$  by the condition  $U = 1$ , omit the term in  $\bar{\varepsilon}^3$  in the approximation (6) we recover the result given by WILLIAMS when only one collision of energy transfer  $\varepsilon > \varepsilon'$  is taken into account.

If we take  $\varepsilon'$  so small that only the first term in (5) need be included and then evaluate the result numerically without making the further approximation (6) we recover Landau's result.

It is worth discussing the approximation implied in this case in more detail because a similar method has been used by BLUNCK and LEISEGANG <sup>(11)</sup> to take into account resonant collisions.

The assumptions that are of interest here are, firstly, referring to (5) and considering only the the contribution of the resonant collisions,

$$p\bar{\varepsilon}_{\text{res}} \gg p^2\varepsilon_{\text{res}}^2$$

and so the resonance contribution is to be included in the evaluation of the most probable energy loss only. The second assumption is that the successive terms in (5) corresponding to the free collisions similarly decrease rapidly in magnitude. This implies that we can find an  $\varepsilon'$  such that

$$(11) \quad \log \varepsilon'/\varepsilon_0 \gg \varepsilon'p/2.$$

Now the main contribution to the resulting integral over  $p$  comes from the values of  $p \sim \xi^{-1}$ , and so we can satisfy (11), if we can find an  $\varepsilon'$  such that

$$\varepsilon_0 \ll \varepsilon' \ll \xi,$$

where  $\varepsilon_0$  is the smallest atomic ionization potential.

The first assumption is invalid in the case of thin absorbers particularly at high incident energies when the resonance contributions become more important as a result of the logarithmic increase in resonance loss. The second assumption is also invalid for thin absorbers for which  $\varepsilon_0 \sim 10$  eV and  $\xi \sim 1000$  eV, since it is then not possible to satisfy (11) accurately.

Turning now to the work of BLUNCK and LEISEGANG we may recover their result from that given by LANDAU by adding a term  $p^2 \varepsilon_{\text{res}}^2/2$  to the first term in the expression (5). Here  $\varepsilon_{\text{res}}^2$  is given, according to these authors, by

$$(12) \quad \varepsilon_{\text{res}}^2 = 1.5\xi \sum_s I_s n_s \log \left\{ \frac{2E}{I_s(1 - v^2/c^2)} \right\} / Z,$$

where the summation is over the atomic electrons. This formula is then an approximate expression for the mean square energy loss in resonant collisions. This avoids the first assumption referred to in the discussion of Landau's treatment but not the second. There is, in addition, a further possible objection to this procedure arising from the fact that the inner shell electrons are to be included in the summation over  $s$  in (12). This is only legitimate when  $\xi$  is so large that  $\varepsilon'$  may be taken larger than all the  $I_s$ . For thin gaseous absorbers this is not satisfied for the innermost electrons so that they should be omitted from the sum (12). Their inclusion leads to fluctuations considerably in excess of those observed experimentally.

It is appropriate to discuss at this point the method used and the results obtained by MOYAL, referred to above. This author evaluates the integral (3) by the method of steepest descent. The result is

$$(7'') \quad f(x, \Delta) = \frac{1}{d} [2\pi Q R''(p)] \exp [Q(R(p) - R'(p))],$$

where

$$\begin{aligned} R(p) &= \int_0^\infty (\exp[-p\varepsilon] - 1)\varphi(\varepsilon) d\varepsilon \\ Q &= x \int_{\varepsilon_0}^{\varepsilon_{\text{max}}} \omega(\varepsilon) d\varepsilon, \\ \varphi &= x\omega(\varepsilon)/Q, \end{aligned}$$

$d$  is a normalization constant, and  $\Delta$  is connected with  $p$  by the relation

$$(13) \quad \Delta = -QR'(p);$$

primes here denote derivatives. The method of steepest descent gives the first term of an asymptotic expansion in  $Q^{\frac{1}{2}}$  of (3) (JEFFREYS<sup>(16)</sup>) so that we may expect (7'') to be valid only for large  $Q$ .

(16) H. JEFFREYS and B. S. JEFFREYS: *Mathematical Physics*, C.U.P. (1946).

The author then finds the following approximate expression for  $R(p)$  by neglecting powers of  $p$  compared with  $\log p$ , which is legitimate when  $Q > 20$ ,

$$(14) \quad k(p) = I_0 p(f - 1 + \log(I_0 p)),$$

where  $f$  is Euler's constant and the Rutherford cross-section is used for  $\omega(\varepsilon)$ . An attempt is made to include resonant collisions by taking for  $\omega(\varepsilon)$  the expression

$$(15) \quad \omega(\varepsilon) d\varepsilon = \frac{(\xi/x) d\varepsilon}{(\varepsilon - I_0)^2 + I^2},$$

whence

$$Q = \pi \xi / 2I.$$

The expression (14) now becomes, with the same approximation as before,

$$(16) \quad R(p) = 2Ip(f - 1 + \log Ip)/\pi$$

and now

$$(17) \quad QR(p) = \xi p(f - 1 + \log Ip).$$

In order to elucidate the physical restrictions involved in the approximate expression (17) we will derive the corresponding expression according to Landau's method, using (15) for the cross-section. If  $I', I_0 \ll \varepsilon' \ll \xi$  and  $p\varepsilon' \ll 1$ , necessary requirements in Landau's method, then

$$(18) \quad (QR(p))_L = -\xi p \log(\varepsilon'/I') + \xi p(f - 1 + \log p\varepsilon'),$$

which agrees exactly with (17). In this approximation it may readily be shown that  $p^2\varepsilon_{\text{res}}^2$  may be neglected and so the conclusion is that the approximations made in deriving the two equations (17) and (18) are entirely equivalent and that both neglect the effect of resonance collisions on the fluctuation. In fact (17) requires  $Q \gg 1$  which implies  $\xi/I' \gg 1$ , the condition of validity of (18). The difference in the results of these authors arises from the fact that MOYAL evaluates (3) by the method of steepest descent and then uses (17) whereas LANDAU evaluates (3) numerically using (18) in the integrand. ((The remark made in a postscript to MOYAL's paper, that resonance effects on the fluctuation are included, seems to rest on an error in his equation (6.6) involving the omission of a factor  $2/\pi$ .) In fact neglecting powers of  $p$  compared with  $\log p$  involves neglecting the resonance contribution to the fluctuation which, as has been shown, depends on  $p^2\varepsilon_{\text{res}}^2$ .

## 5. — Results and Discussion.

The details of the auxiliary formulae used in evaluating the results are as follows:

$\varepsilon < \varepsilon'$ . The quantities  $\bar{\varepsilon}$ ,  $\varepsilon^2$ , and  $\varepsilon^3$  have contributions from both free and resonant collisions. The former have been calculated excluding the  $K$  electrons (denoted in the formulae by the notation  $\xi'$  in place of  $\xi$ ) using  $\omega_1(\varepsilon) = \xi'/\varepsilon^2$ , the latter with the help of a formula of FOWLER and JONES (17) modified to fit experimental results in a way which will be described in detail later. This formula is the following

$$(19) \quad \bar{\varepsilon}^n = \frac{2e^2c}{\hbar v^2\pi} \sum_{i=s,p} n_i \int_{\omega_{1i}}^{\omega_{2i}} \frac{\varepsilon^{n-1}}{|\eta(\omega)|^2} \left\{ \frac{1}{2} \log \frac{4v^2}{(3.17)^2 b_0^2 \omega^2 |1 - \beta^2 \eta(\omega)|^2} - \theta \cot \theta + |1 - \beta^2 \eta(\omega)| \theta \operatorname{cosec} \theta \right\} \sigma_i(\omega) d\omega$$

where

$$(20) \quad \eta(\omega) = 1 + K \sum_{i=s,p} \frac{\omega_{2i} - \omega}{\omega \omega_{2i}} \log \frac{\omega_{2i} - \omega}{\omega - \omega_{1i}} - \frac{\omega_{2i} + \omega}{\omega \omega_{2i}} \log \frac{\omega_{2i} + \omega}{\omega_{1i} + \omega} + i \frac{\gamma \pi K (\omega_{2i} - \omega) \delta_i}{\omega \omega_{2i}} + \frac{8\pi \alpha N e^2}{m(\omega^2 - \omega_0^2)},$$

and  $\beta = v/c$

$$\theta = \arg (1 - \beta^2 \eta(\omega)),$$

$$b_0 = 10^{-8} \text{ cm},$$

$$\delta_{s,p} = 1 \text{ for } \omega_{1s} \leq \omega \leq \omega_{2s}, \omega_{1p} \leq \omega \leq \omega_{2p},$$

$$= 0 \text{ otherwise,}$$

$\sigma_i$  is the photo effect cross-section,

$$K = \hbar c \, 2.2 \cdot 10^{-17} / \pi,$$

$\omega_0/2\pi$  is the frequency of the principal excitation line,

and  $N$  is the number of atoms per  $\text{cm}^3$ .

The quantities  $\omega_{1s}$ ,  $\omega_{2s}$  and  $\omega_{1p}$ ,  $\omega_{2p}$ , are the lower and approximate upper

(17) G. N. FOWLER and the late G. M. D. B. JONES: *Proc. Phys. Soc.*, A **66**, 579 (1953).



limits of the  $s$  and  $p$  ionization continua respectively, and  $\gamma$  and  $\alpha$  are parameters to be determined from experiment.

$\varepsilon > \varepsilon'$ . The function  $\omega_2(\varepsilon)$  which occurs in the term  $B$  in equation (7) is given by the expression

$$(21) \quad \omega_2(\varepsilon) = \frac{\xi}{\varepsilon^2} + \frac{2Ne^2}{\pi\hbar c} \left\{ \log \frac{2E\lambda_\mu}{I_K a_K} - 1 \right\} \frac{1820(Z-0.3)^6(\hbar c)^4}{\varepsilon^5},$$

where  $\lambda_\mu = \hbar/m_\mu c$ ,  $E$  is the energy of the particle and  $a_K$  is the radius of  $K$  orbit. The second term on the right hand side of (21) corresponds to the possibility of ionisation from the  $K$  shell. It has been obtained by using the WILLIAMS<sup>(18)</sup> result for the energy loss due to resonance effects and inserting a theoretical photoeffect cross-section appropriate to X-rays taken from COMPTON and ALLISON<sup>(19)</sup>.

The formula (7) has been evaluated numerically in the cases of oxygen and neon, the results of which, together with the experimental observations are shown in Figs. 1-4.

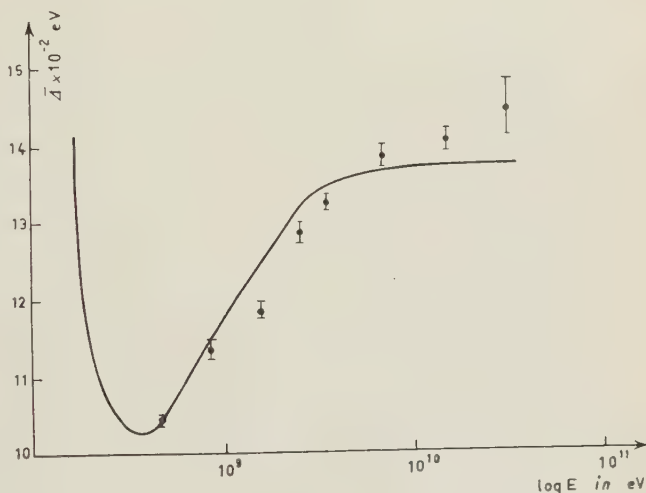


Fig. 1. — Mean energy loss of fast  $\mu$ -mesons in oxygen. The solid curve is the theoretical result for  $\alpha = 2$ ,  $\gamma = 4$ .

(i) *Oxygen*. The experimental results are due to GOSH, JONES and WILSON<sup>(20)</sup>, and we have taken into account here two sets of measurements, the variation in the mean number of ion pairs per cm with the energy of the incident particle and the fluctuation in ion pairs per cm for particles of energy corresponding to the minimum mean number of ion pairs per cm. The first set of measurements has been compared with the mean energy loss calculated using (19), account being taken of the contribution from the free collisions and from the  $K$  electrons with the help of (21). For the photoeffect cross-

<sup>(18)</sup> E. J. WILLIAMS: *Dan. Mat.-Fys. Medd.*, **13**, 4 (1935).

<sup>(19)</sup> A. H. COMPTON and S. K. ALLISON: *X-rays in theory and experiment* (New York, 1935), p. 560.

<sup>(20)</sup> S. K. GHOSH, the late G. M. D. B. JONES and J. G. WILSON: *Proc. Phys. Soc.*, **A 67**, 331 (1954).

section in (19) we have used the theoretical results of Bates *et al.* <sup>(21)</sup> for the  $2p$  electrons, and a cross-section of similar shape has been assumed for the  $2s$  electrons. This permits the two parameters  $\gamma$  and  $\alpha$  to be determined; the values found are 4 and 2 respectively. These two quantities correspond to an additional damping not taken into account in the derivation of the dielectric constant (20) and to the oscillator strength for the transition to the group of states corresponding to the principal lines in the oxygen atomic spectrum which have been taken from the M.I.T. wave length tables (1939). The fit between theory and experiment is shown in Fig. 1 and this gives 27 eV as the mean loss in ionization per ion pair.

With regard to the ionization loss distribution for a particle of an energy corresponding to the minimum in the mean loss curve, we find that  $\epsilon' = 333$  eV,  $\xi' = 96$  eV, and the variance of the gaussian term,  $a$  is 280 eV. The quantity  $\xi'/I_0 = 7$  so that the condition of validity of Landau's approximation (and so that of MOYAL) is not satisfied. The most probable energy loss in ionization alone is 971 eV, a loss per ion pair of 24.2 eV, calculated from the most probable number of ion pairs per cm. The difference between this and the mean loss in ionization per ion pair is rather large and difficult to understand. In fact the mean exceeds the most probable loss by a resonant contribution from the  $K$  electrons and a contribution from free collisions in which the energy transfer lies between  $\epsilon'$  and  $\epsilon_{\max}$  where  $\epsilon_{\max}$  is here an upper limit to the energy transfers imposed by the experimental conditions. (In this case  $\epsilon_{\max}$  was 1000 eV). These two contributions are approximately equal and their sum is  $\sim 200$  eV. The mean and most probable numbers of ion pairs, however, differ by only 4 ion pairs. In order to remove this discrepancy it has been suggested that the bulk of the energy loss when a  $K$  electron is ejected is carried off by an X-ray which does not produce further ion pairs sufficiently close to the track to be included in the count. In fact on re-examining the oxygen data EYEIONS <sup>(22)</sup> did not find as many large clusters of ion pairs corresponding to energy transfers of the order of the  $K$  shell ionization potential as would be expected if Auger or fast knock-on electrons were always produced close to the track after the ejection of a  $K$  shell electron. It would therefore seem that in the cloud chamber at least the  $K$  shell electrons make a negligible contribution to the phenomena. If this is accepted a value of 245 eV is found as the mean loss in ionization per ion pair in good agreement with that found from the most probable loss.

The value of  $\Delta_{0L}$  found from Landau's formula is 1020 eV which is reduced to 900 eV when the  $K$  shell electrons are excluded. This value which is super-

<sup>(21)</sup> D. R. BATES, R. A. BUCKINGHAM, H. S. W. MASSEY and J. J. UNWIN: *Proc. Roy. Soc.*, A **170**, 322 (1939).

<sup>(22)</sup> D. EYEIONS: private communication.

posed to include a contribution from primary optical excitation should be larger than the 971 eV found above. That it is not so is due to the approximate character of Landau's expression for the most probable loss, especially for small  $\xi$ . This point will be discussed further below.

In comparing the theoretical and experimental fluctuations in loss we have used 24.2 eV as the energy loss/ion pair and the two curves are shown in Fig. 2. The comparison between the two distributions may be made in terms of  $\delta A/\Delta_0$ ,

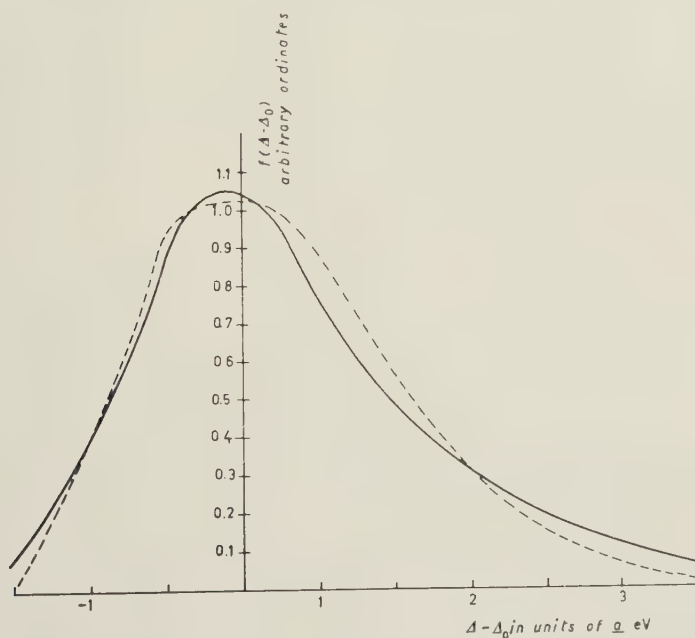


Fig. 2. — Fluctuation in ionization loss of fast  $\mu$ -mesons in oxygen. — Theoretical.  
----- Experimental.

the ratio of the width at half maximum to the most probable loss. The result, together with the predictions of LANDAU, corrected to exclude excitation loss using results of the present calculations, is given in the Table I.

TABLE I. —  $(\delta A/\Delta_0) \cdot 100$  for oxygen and neon.

Gas	Exp.	Theoretical	
		present calc.	LANDAU
Oxygen	81	74	48
Neon	67	53	39

Small corrections to the theoretical result arise from the effect of two or more collisions with loss  $\varepsilon > \varepsilon'$  and the correction terms of (7') with  $r = 3$ . These give an increase of the theoretical value of  $\delta A/A_0$  of  $\sim 5\%$ .

The conclusion is that the theory and experiment are in good agreement and that the enhanced fluctuation in the energy loss compared with the pre-

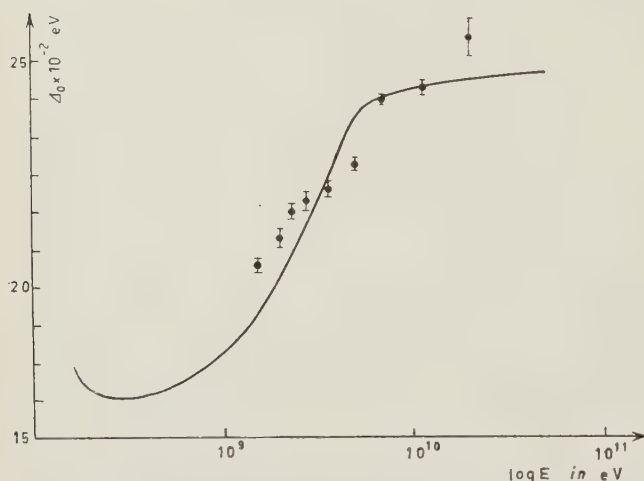


Fig. 3. — Most probable ionization loss of fast  $\mu$ -mesons in neon. The solid curve is the theoretical result for  $\alpha = \frac{1}{2}$ ,  $\gamma = 1$ .

tivity is obtained from calibration with standard 5 keV X-rays.

The two sets of measurements we have used in this case are the variations of the most probable number of ion pairs with particle energy and the fluctuation in the number of ion pairs produced by particles of energy 7 GeV for which the number of observations is greatest. The comparison between theory and experiment is a little more complicated in this case because the most probable loss depends on  $\gamma$  and  $\alpha$  through (20) and also through  $\varepsilon'$ . However, the most probable loss is not sensitive to  $\varepsilon'$  in this case so that it suffices to determine  $\gamma$  and  $\alpha$  from the first set of data and then to determine  $\varepsilon'$  as described in the appendix, using the values of  $\gamma$  and  $\alpha$  already found. The photoelectric cross-section used in (20) is that found experimentally by PO LEE and WEISSLER<sup>(23)</sup>. It is found that  $\gamma = 1$ ,  $\alpha = \frac{1}{2}$ , and that  $\varepsilon'$  and the most probable loss are 615 and 2370 eV respectively, with  $\xi' = 205$  eV and  $a = 650$  eV. The parameter  $\xi'/I_0 \sim 10$  and again Landau's condition is now well satisfied. Landau's value for  $A_0$  is 4.7 keV which reduces to 4.3 keV on excluding the  $K$  shell electrons. It will be seen by comparing this with the

predictions of LANDAU, is due partly to the effect of resonance collisions and partly to the exclusion of primary excitation from the most probable value of the loss.

(ii) *Neon*. In this case the experiments have been carried out by EYEIONS, OWENS, PRICE and WILSON<sup>(10)</sup>. The results are given in terms of the total energy lost by the particle in traversing the counter and this quantity

<sup>(23)</sup> P. LEE and G. L. WEISSLER: *Proc. Roy. Soc., A* **220**, 71 (1953).

2370 eV previously obtained that in this case the contribution from optical excitation is much larger.

The distributions are compared by scaling down the experimental results, given in terms of energy loss, so that the two values of most probable loss agree. In this way the contribution of the primary optical excitation loss to the fluctuation is removed.

We can estimate the energy loss per ion pair in ionization and excitation by assuming that the appropriate cross-sections are the same as for oxygen and using the oxygen data corrected for the particle energy. The result is 26 and 18.8 eV ion pair respectively. This compares with a mean total loss of 36.8 eV/ion pair found by JESSE and SADAUSKIS<sup>(24)</sup> using  $\alpha$  particles.

The value of  $\delta A/A_0$  is given in the table. The two distributions are given in Fig. 4.

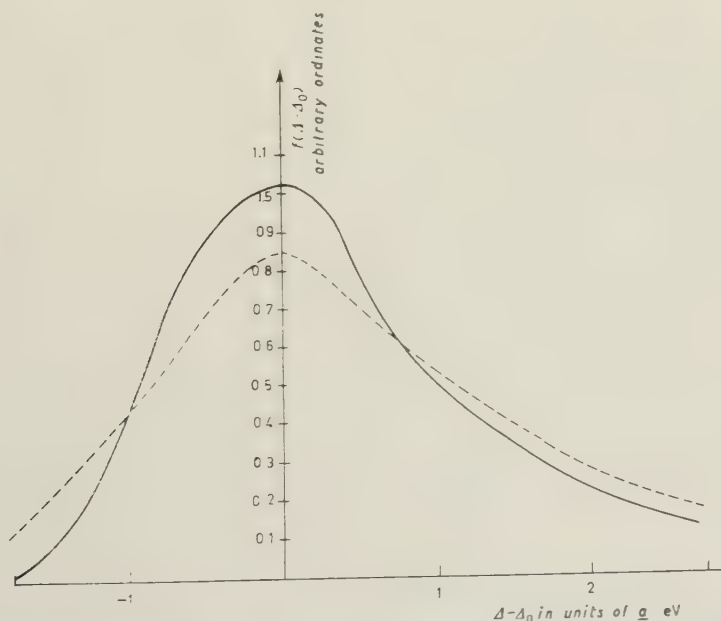


Fig. 4. - Fluctuation in ionization loss of fast  $\mu$ -mesons in neon. — Theoretical; ----- Experimental.

The corrections to the theoretical result are again  $\sim 5\%$  when we take  $r = 1$  in (7'). The agreement between theory and experiment is not so good as that found for oxygen.

(iii) *Measurements on other Gases.* Similar measurements, using a proportional counter, have been made by WEST<sup>(25)</sup> on other inert gases, with small

(24) W. P. JESSE and J. SADAUSKIS: *Phys. Rev.*, **90**, 1120 (1953).



admixtures of hydrocarbons, when the incident particles were electrons of energies 1-2 MeV. The results are expressed in terms of  $\delta\Delta/\Delta_0$  and it is found that the values of this quantity for the various gases lie on a smooth curve when plotted against  $\xi/I_0Z$ , where  $I_0$  is 13.5 eV and  $\overline{I_0Z}$  is an average taken over the constituents of the fillings gas. This curve is reproduced in Fig. 5 together with a point representing the results on oxygen discussed above, for which the  $\mu$ -mesons concerned had corresponding energies.

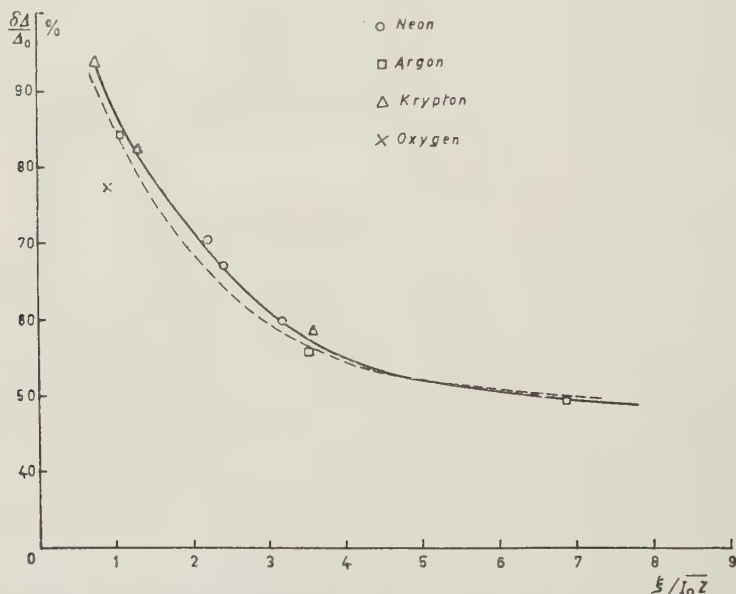


Fig. 5. Fractional width of observed energy loss distributions in various gases [see Sect. 5 (iii)]. The dashed curve is the best fit for  $\delta\Delta/\Delta_0$  satisfying  $\delta\Delta/\Delta_0 = p[1 + g(I_0Z/\xi)]^{\frac{1}{2}}$ .

An interpretation of West's results may be attempted on the basis of the calculations given above. In the first place, with the method presented here the bulk of the fluctuation, for not too large energy losses, is given by the gaussian contribution and for a rough estimate of  $\delta\Delta/\Delta_0$  we may neglect the contribution from the tail. Thus we have, at least for thin absorbers,

$$\Delta_0 = l\xi \quad \text{and} \quad \delta\Delta = (m\xi^2 + n\xi)^{\frac{1}{2}},$$

where  $m$  and  $n$  refer to contributions from the free and resonant collisions respectively.

For thin absorbers  $l$  is approximately independent of  $Z$  since the resonant collisions give the main contribution to  $\Delta_0$  and so the atomic structure only

enters into  $l$  through a logarithmic term (cf. equation (20)). On the other hand, taking (12) as an approximation to  $n\xi$  one finds, at least for the inert gases, that

$$\sum n_s I_s \sim qZ^2,$$

when the outer shells only are considered. It should be remembered that only those electrons for which  $I_s < \varepsilon'$  should be included in this summation. In the present case this means that for the heavier gases it is necessary to omit some of the  $L$  shell electrons.

Thus we are led to an expression of the following form for  $\delta\Delta/\Delta_0$

$$(22) \quad \delta\Delta/\Delta_0 \sim p(1 + gI_0\bar{Z}/\xi)^{\frac{1}{2}}.$$

The dashed curve in Fig. 5 is found with  $p = 41.4$  and  $g = 3.22$ .

Taken literally this result implies that the resonance contribution required by experiment is larger than that found by calculation by a factor of three. Bearing in mind, however, the contribution of the high energy tail of the distribution to  $\delta\Delta/\Delta_0$  and the fact that in (22) we should have  $\xi'$  rather than  $\xi$ , this is certainly an overestimate. We may, however, interpret the fact that the resonance contribution gives a curve of the required shape as further confirmation that resonance effects give rise to a considerable increase in the fluctuation in energy loss in thin absorbers.

## 6. — The Limiting Value of $\delta\Delta/\Delta_0$ for Large $\xi/I_0Z$ .

One remark which is appropriate in discussing West's results concerns the limiting value of  $\delta\Delta/\Delta_0$  when  $\xi/I_0Z$  is large. It would appear that this quantity tends to a limit which is larger than predicted by LANDAU. This conclusion is confirmed in a recent paper by EYEIONS<sup>(25)</sup> and we suggest that part of this increase in the limiting value may be explained in the following way.

It has already been noted that primary optical excitation loss should be excluded from  $\Delta_0$  and we will show that when this is done the ratio  $\delta\Delta/\Delta_0$  is then in somewhat better agreement with experiment. An estimate of the excitation loss may be found by starting from the Williams formula

$$(23) \quad \bar{\varepsilon}_{\text{res}} = \frac{2Ne^2}{\pi\hbar c} \int \log \frac{E\lambda_\mu}{\hbar\nu a} \cdot \sigma_{\hbar\nu} d(\hbar\nu).$$

If  $I$  is some mean atomic excitation potential,  $I_0$  the smallest ionization

<sup>(25)</sup> D. EYEIONS: to be published.

potential and  $f_{on}$  the oscillator strength for the transition to the  $n$ -th state we have

$$(24) \quad \bar{\varepsilon}_{\text{res}} \approx \frac{\xi'}{Z'} \log \frac{2mc^2 I_0}{(1 - v^2/c^2) I^2} \left( \sum_n + \int d\varepsilon \right) f_{on}.$$

The prime indicates that  $K$  electrons are excluded.

Evidently the contribution of optical excitation and ionization to (24) will depend on the extent to which the appropriate transitions contribute to  $(\sum_n + \int d\varepsilon) f_{on}$ . In the case of oxygen and neon considered above, we can estimate the contributions of the ionization continua as approximately  $\frac{1}{2}$  and  $\frac{3}{8}$  of the total. For oxygen this would give as upper limits to the most probable loss 1550 eV and for neon 5.2 keV. In the case of oxygen the mean loss is 1410 eV, using 32 eV as the mean loss per ion pair, and the mean and most probable should differ by approximately  $\xi' \log 1000/333$ , excluding the  $K$  electrons (see above), since a cut-off in energy transfer at 1000 eV is imposed by the experimental technique employed. This gives 1300 eV for the most probable loss or 32.5 eV/ion pair.

In the limiting case of large  $\xi$  the inner shell electrons would contribute to  $\Delta_0$  but, for not too large  $Z$ , optical excitation would still account for an appreciable part of the most probable loss. In fact for large  $\xi$  the mean and the most probable losses are the same and resonant and free collisions contribute approximately equally. If the greater part of the resonant loss is optical excitation, which should be excluded, it will be seen that the theoretical value of  $\delta\Delta/\Delta_0$  is in better agreement with experiment.

It is worth remarking that the reason for the rather large contribution from primary excitation loss is that, although in each collision the energy transfer is small, the number of such transfers varies as  $1/h\nu$ . Also we may remark that the photons produced by de-excitation will be absorbed very close to the path of the particle so one would not expect to observe any measurable effect from optical excitation. This has been confirmed by BARCLAY and GELLEY<sup>(26)</sup>.

Before we leave this question there are certain additional remarks which should be made.

In the first place the value of the total most probable energy loss which has been found for oxygen is larger than that predicted by LANDAU and it is necessary to enquire into the reason for this. Landau's result may be written (with the  $K$  electrons included)

$$\Delta_{0L} = \xi' \log \xi'/I_0 + \xi' \log \frac{2mc^2 I_0}{(1 - v^2/c^2) I^2} \left( \sum_n + \int d\varepsilon \right) f_{on}/Z'.$$

(26) F. R. BARCLAY and J. V. GELLEY: *Nuovo Cimento*, **2**, 27 (1955).

Here  $I = 13.5 Z \text{ eV}$ . As the  $K$  electrons do not contribute to  $\Delta_{0L}$  in the present examples the value of  $I$  should certainly be considerably less than  $13.5 Z \text{ eV}$ . In fact a more reasonable value would be  $\bar{I} \sim I_0$ . With this value for  $\bar{I}$  we find agreement with the results calculated here. For larger  $Z$  and thicker absorbers we would expect Landau's value of  $I$  to be more accurate.

In the second place we would expect the most probable loss per ion pair to be rather larger than the mean loss per ion pair since the contribution from primary excitation to the most probable loss is relatively larger. In this connection it is noteworthy that CRANSHAW (?) found experimental values for  $\Delta_0$ , in terms of ion pairs, which were considerably smaller than those deduced from  $\Delta_{0L}$ . However these were found by assuming that the mean and most probable energy loss per ion pair were the same. With a larger most probable loss per ion pair the agreement is much improved.

Finally one further point is that, except for small  $Z$ , the agreement between Landau's theory and the experimental observations on energy loss in thin foils is not disturbed by the present proposal.

## 7. — Polarization Effects.

The polarization of the medium affects the results at high incident energies, as one would expect, by introducing a plateau into the resonant contribution to the most probable loss and the fluctuation in loss. Thus the absolute value of the fluctuation increases until the plateau is reached. It is found, however, that the quantity  $\delta\Delta/\Delta_0$  falls as the energy of the incident particle is increased. This is borne out by the experimental results on neon.

## 8. — Conclusions.

In conclusion we may say that in all cases the resonant collisions play an important part in increasing the energy loss fluctuation above that predicted by LANDAU, and that theory and experiment are in fair agreement when the effect of primary optical excitation loss is duly discounted.

\* \* \*

Thanks are due to Dr. B. G. OWEN and Mr. D. EYEIONS for many helpful discussion, and to the staff of the Manchester Electronic Computing Machine for their guidance and advice in the use of the machine.

## RIASSUNTO (\*)

Si discute dettagliatamente la fluttuazione della perdita di ionizzazione dei mesoni  $\mu$  veloci per effetto di risonanza usando una modificazione del metodo di Landau. Confrontano con l'esperienza i risultati numerici per l'ossigeno, il neon ed altri gas inerti e si conclude che ci si può render conto della maggior parte della fluttuazione se si tien calcolo degli effetti di risonanza atomica e dell'effetto della perdita di eccitazione primaria dovuta a tale fenomeno.

---

(\*) Traduzione a cura della Redazione.



**Remarks on the Operation of the Diffusion Cloud Chamber - II (\*).**

P. E. ARGAN and A. GIGLI

*Istituto di Fisica dell'Università - Genova**Istituto Nazionale di Fisica Nucleare - Sezione Aggregata di Genova*

N. D'ANGELO

*Istituto Superiore di Sanità, Laboratorio di Fisica - Roma*

(ricevuto il 16 Marzo 1956)

**Summary.** — The first results of our theory on the operation of the diffusion cloud chamber have already been published in a previous paper. The particular problem then resolved will now be faced from a more general point of view, with regard to the nature and the pressure of the filling gas and ion load, while retaining the geometrical characteristics of the chamber, the temperatures imposed at the bottom and at the top, and the nature of the organic vapour used (methyl alcohol). We will establish a relation which has to be satisfied by the parameters characterising a chamber (nature and pressure of the gas and ion load) if the height of the sensitive layer has to remain unchanged, and a second relation which directly furnishes the height of the sensitive layer as a function of these parameters once it is known for a particular set of them. This relation will be discussed in detail and calculated for  $H_2$ ,  $D_2$ , He,  $CO_2$ , A and Air, for pressures between 0.5 and 20 atm and assuming an ion load,  $n$  (number of ions that are formed per  $cm^3/s$  in the interior of the chamber) between 2 and 100. We will show further how it is possible to calculate in a simple and direct way the temperature gradient, in the zone of the chamber sensitive to the ionizing particles, as a function of its height. The results of the calculation will be compared with the experimental results. The particular problem considered in our previous paper, in which the various parameters were considered to be functions of a horizontal co-ordinate as well as functions of the height measured from the bottom of the chamber (two-dimensional case) will now be studied in a more general way, keeping still the same geometry of the instrument, the temperatures imposed on the bottom and top, and the organic vapour used. We will assume various temperature and vapour pressure distributions

(\*) This work was supported in part by a grant from the I.N.F.N. - Sezione Acceleratore.

on the side walls of the chamber (or on plates of any material placed vertically in it) and will show how the geometry of the sensitive layer will thereby be changed. Similarly to what was done in the one-dimensional case, one can consider gases of various natures and pressures with different ion loads. We shall discuss the various cases considered and establish the criteria to follow (when imposing the temperature and vapour pressure distributions) so that the distance from the walls or plates, to which tracks of ionizing particles are still observable, may be the smallest possible. The stability conditions of the chamber in varying the ion load are also discussed. The above criteria are applied to the particular case of a chamber operating with methyl alcohol in air at normal pressure.

## 1. — Introduction.

In a previous work <sup>(1)</sup> a theoretical study was carried out on the characteristics of a cloud chamber of permanent sensitivity functioning by diffusion of vapours of methyl alcohol in air at normal pressure and under a strong temperature gradient. The theory of the instrument was treated both one-dimensionally and two-dimensionally; the picture of the physical problem assumed was found to be particularly advantageous 1) in evaluating the distribution of the supersaturation taking into account the condensation of vapour on electrically charged centres, and 2) in the two-dimensional treatment of the problem. In the latter case it has been shown that it is possible to obtain information on the perturbation introduced on the shape of the sensitive layer by the side walls of the chamber (or by plates of material introduced vertically in it) when given temperature and vapour pressure distributions are imposed on such structures. The problem was considered in the most general way possible, compatible with the approximations we have introduced. The successive utilisation of simple physical considerations have afforded us adequate results consistent with the experimental observations either with regard to the height of the sensitive layer and the temperature gradient as a function of the ion load, or with regard to the form of the sensitive zone, with some restrictions as to particular temperature and vapour pressure conditions imposed on the side walls of the chamber.

Based on the considerations of I, and in the case of a one-dimensional treatment, it is shown in this work, that it is easily possible to establish

<sup>(1)</sup> P. E. ARGAN, N. D'ANGELO and A. GIGLI: *Nuovo Cimento*, **1**, 761 (1955). Regarding the notations we have used see this paper which, in the following, will be indicated with I, while, on the other hand, with (I, 4) will be indicated, for example, the formula (4) and with Fig. I, 4 the Fig. 4 of that paper.

relation between the parameters which characterise a chamber (pressure and nature of the gas, temperature distribution, number of ions that are formed per  $\text{cm}^3/\text{s}$ , etc.) so that the height of the sensitive layer remains unchanged (Sect. 2'1); furthermore it is possible to arrive at a relation which directly gives the height of the sensitive layer once it is known for a particular set of values of the above parameters (Sect. 2'2).

Finally the two-dimensional treatment of the theory was extended to the case of more general boundary conditions (Sect. 3). First, the case in which the side walls (or plates of material introduced vertically in the chamber) are in part or totally impenetrable to the vapour, i.e. the cases when on such structures the vapour does not condense, was considered. On the other hand we considered the case when the temperature distributions are different from those considered in I.

## 2. — One-Dimensional Treatment of the Problem.

2'1. — We shall take the formula (I, (21a)) and re-write it in a more convenient form:

$$(1) \quad \Delta\Phi = (1 - \varepsilon_f)\Phi = \frac{4}{3}\pi\bar{n}\bar{r}^3 \frac{\delta}{M} \xi_f.$$

Formula (1) gives the relation we have assumed between the quantity of organic liquid which is deposited in the form of drops per  $\text{cm}^2/\text{s}$  on the bottom of the chamber, the average number,  $\bar{n}$ , of ions created per  $\text{cm}^3/\text{s}$ , the height of the sensitive layer  $\xi_f$  and the average value of the cube of the radius of the drops of methyl alcohol at the bottom of the chamber. Let us assume, further, that the number  $\bar{n}$  of ions that are formed per  $\text{cm}^3/\text{s}$  is expressed by (2)

$$(2) \quad \bar{n} = n_0 P \left[ \frac{273}{T^*(y)} \right] \left( \frac{\tau Z}{2Z_a} \right),$$

when one wants to examine the case of a chamber filled with gas at pressure  $P$  and atomic number  $Z$  and with the number  $\tau$  of atoms per molecule; in (2)  $n_0$  is the number of ions that are formed per  $\text{cm}^3/\text{s}$  in air at N.T.P.,  $Z_a$  the average atomic number of air. The averages which appear in (1) and (2) are calculated for  $0 \leq y \leq \xi_f$ .

Starting with these two expressions we propose to establish a criterion of comparison between diffusion cloud chambers functioning with the same organic

---

(2) R. P. SHUTT: *Rev. Sci. Instr.*, **22**, 730 (1951).

vapour but with different gases, the total pressure and ion loads being possibly different. We shall limit our comparison to the case of two chambers of the same height  $h$  and with the same conditions for the vapour pressure and the temperature both for  $y = 0$  and for  $y = h$ . In the following, with the expression « behaving similarly » we shall indicate two chambers of equal height functioning with the same organic vapour, in which the heights of sensitive layer are equal.

Substituting (2) in (1) one obtains:

$$(3) \quad (1 - \varepsilon_f) \Phi = \frac{4}{3} \pi \bar{r}^3 n_0 P \left[ \frac{273}{T^*(y)} \right] \frac{\tau Z}{2 Z_a} \xi_f \frac{\delta}{M}.$$

The term  $\bar{r}^3$  which appears in this relation can be written (see Appendix) in the form:

$$(4) \quad \bar{r}^3 = K \left( \frac{D_1}{P} \right)^\alpha,$$

where  $K$  is, in general, a function of  $\xi_f$  and of the nature of the gas (through its viscosity coefficient),  $D_1$  the diffusion coefficient of the organic vapour in the gas at atmospheric pressure and at temperature  $T_1$ ,  $P$  the total pressure and  $\alpha$  a constant.

Suppose we write eq. (3) for the two chambers whose behaviour we wish to compare, labeling with 1 and 2 the magnitudes of the first and the second respectively; dividing the two equations term by term results in

$$(5) \quad \frac{T_2^*(y)}{T_1^*(y)} \frac{K_1}{K_2} \frac{D_{11}^\alpha}{D_{12}^\alpha} \frac{P_2^\alpha}{P_1^\alpha} \frac{n_{01}}{n_{02}} \frac{\tau_1 Z_1}{\tau_2 Z_2} \frac{P_1}{P_2} \frac{\xi_{f1}}{\xi_{f2}} = \frac{1 - \varepsilon_{f1}}{1 - \varepsilon_{f2}} \frac{\Phi_1}{\Phi_2},$$

where  $T_1^*(y)$  and  $T_2^*(y)$  represent the temperature distributions in the first and second case.

If one considers chambers « behaving similarly » eq. (5) is reduced to

$$(6) \quad \frac{P_2^\alpha}{P_1^\alpha} \frac{K_1}{K_2} \frac{D_{11}^\alpha}{D_{12}^\alpha} \frac{n_{01}}{n_{02}} \frac{\tau_1 Z_1}{\tau_2 Z_2} \frac{P_1}{P_2} = \frac{D_{11}}{D_{12}} \frac{P_2}{P_1}.$$

In fact, with equal  $\xi_f$ , the vapour pressure distribution remains unchanged together with  $\varepsilon_f$  and the temperature distribution (\*). From this last co

(\*) It's not difficult to verify these statements, by keeping in mind the content of Sect. 2.3 of I. From (I, 16) it follows that  $p_1^* \approx \beta B P \varepsilon_0 = \text{const.}$  (according to the meaning of  $\beta$ ,  $B$  and  $\varepsilon_0$ , once  $\xi_f$  is fixed) and independent of  $D$ . Furthermore the distribution  $T^*(y)$  of the temperature remains unchanged since  $\eta'$  [formulae (I, 12) and (I, 13)] is a function only of  $\xi_f$  [see formula (I, 16), which is the same in any situation of application of the method of successive approximations discussed in I and, therefore, in particular, for  $\eta'_{ff}$ ,  $\varepsilon'_{ff}$ ,  $\xi_f$ ].

dition it follows that we can write the second member of (5) in the form (6) (formula (I.10)).

Eq. (6) is equivalent to:

$$(7) \quad K_1 D_{11}^{\alpha-1} P_1^{2-\alpha} n_{01} \tau_1 Z_1 = K_2 D_{12}^{\alpha-1} P_2^{2-\alpha} n_{02} \tau_2 Z_2.$$

The meaning of  $K$  and  $\alpha$  for this case (cloud chambers « behaving similarly ») is given in the Appendix. With the values shown there, (7) obviously reduces to:

$$(8) \quad \mu_1 D_{11}^{-\frac{1}{3}} P_1^{\frac{5}{3}} n_{01}^{\frac{2}{3}} (\tau_1 Z_1)^{\frac{4}{3}} = \mu_2 D_{12}^{-\frac{1}{3}} P_2^{\frac{5}{3}} n_{02}^{\frac{2}{3}} (\tau_2 Z_2)^{\frac{4}{3}},$$

where  $\mu_i$  ( $i = 1, 2$ ) is the viscosity coefficient of the gas-vapour mixture in the two cases under consideration.

Eq. (8) gives a condition sufficient for the two chambers to behave similarly. It was previously obtained by R. P. SHUTT<sup>(2)</sup> in his one-dimensional theory, with a procedure extremely complicated as compared to that described here. Such a formula was discussed in detail by SHUTT and later by A. R. BEVAN<sup>(3)</sup>; according to these authors it gives with good approximation the relation which the parameters must satisfy in order for the temperature distribution to provide the condensation of organic vapour on the charged centres, at temperatures below 260 °K. Shutt's numerical calculations indicate further that for a given set of such parameters there is a minimum temperature gradient for a satisfactory operation of the chamber. The limits of validity of the formula have been discussed and experimentally established by BEVAN, using a diffusion cloud chamber of 9 inches in diameter, filled with gases of different nature and various pressures and with an ion load widely varied and realised with a 7  $\mu$ C <sup>60</sup>Co,  $\gamma$ -source.

This author considers further, in some detail, the process of condensation of vapour in order to estimate in the most correct way possible, the parameter which gives the number of centres of condensation; in particular Shutt's results are also extended to the case in which, not only the ions, that are formed in the interior of the chamber, are responsible for the condensation of vapour, but also the uncharged centres which, according to Farkas' calculations<sup>(4)</sup>, are formed in the gas in strong correlation with positive variations of temperature.

We shall not insist on discussing (8); we consider that equation (8) has been satisfactorily established and verified. We refer the reader to the two exhaustive works quoted, and limit ourselves to report in Table I the numerical values, calculated by Shutt, of the pressures of various gases in relation

<sup>(3)</sup> A. R. BEVAN: *Jour. Scient. Instr.*, **31**, 45 (1954).

<sup>(4)</sup> L. FARKAS: *Zeits. Phys. Chem.*, **125**, 236 (1927).



to that of the air, for which the temperature distributions should be the same if one wants to obtain the same height of the sensitive layer.

TABLE I.

		H <sub>2</sub>	D <sub>2</sub>	He	A
$P/P_{\text{air}}$	$T < 260^\circ\text{K}$	9.7	7.7	5.6	0.70
	$T > 260^\circ\text{K}$	6.1	4.5	3.7	0.75

2'2. — Extending the considerations of the previous paragraph, we now show how it is possible to write a relation which represents the dependence of the height  $\xi_f$  of the sensitive layer on the various parameters which characterise a chamber, once such a height is known for a particular set of their values.

Also in this case we shall limit our remarks to the behaviour of a chamber of height  $h$  with given temperatures both for  $y = 0$  and  $y = h$  and, therefore, with linear temperature distribution and independent of the particular nature or pressure of the gas (at least in a first approximation), when the condensation of organic vapour on charged centres is neglected.

For this purpose we shall discuss the relation (A.6) of the Appendix:

$$(9) \quad \bar{r}_3 = \frac{1}{\xi_f} \left( G \mu \frac{D_1}{P} \right)^{\frac{2}{n}} \cdot \int_0^{\xi_f} \psi^{\frac{1}{n}} dy,$$

where

$$(10) \quad \psi(\xi_f, y) = \int_0^y \left( \frac{T^*}{T_1} \right)^n (\varrho_v^* - \varrho_0) dy,$$

is, in general, a function of  $\xi_f$  and  $y$  and  $G = 18/\sigma^2 g = \text{const.}$  For  $n = 2$  (1) and under the hypothesis that the organic vapour can be considered as perfect gas, the integral (10) can be written (in a first approximation) in the form

$$(11) \quad \psi(\xi_f, y) \cong \frac{M}{T_1^2 R} \int_0^y T^* (p^* - p_0) dy.$$

We are dealing now with the calculation of the integral in eq. (11).

---

(\*) It must be observed that the exponent  $n$  which appears in (10) is, generally equal to 1.75 or 2, depending on the nature of the gas. In particular as in the case of Hydrogen, Deuterium and Helium,  $n$  is equal to 1.75. Having taken  $n = 2$  for all gases, however, does not affect sensibly the final results.

Eq. (9) can be transformed, with good approximation, into

$$(12) \quad \bar{r}^3 \cong \left[ G\mu \frac{D_1}{R} \frac{M}{P} \frac{P}{4} \beta (1 - \varepsilon'_f \xi_f) \right]^{\frac{3}{2}} C \xi_f^{\frac{3}{2}},$$

with  $C = \text{const}$  as specified by (A.14) of the Appendix.

On comparison of (12) with (4) it follows that

$$(13) \quad K = \left[ G\mu \frac{M}{R} \frac{\beta P}{4} (1 - \varepsilon'_f \xi_f) \right]^{\frac{3}{2}} C \xi_f^{\frac{3}{2}}.$$

If we take up again eqs. (5) and (13) and keep in mind that, with good approximation,  $\bar{T}_1^*(y) \cong \bar{T}_2^*(y)$  for  $0 \leq y \leq \xi_f$  we obtain

$$(14) \quad \frac{D_{11}^{-\frac{1}{2}} \mu_1^{\frac{3}{2}} P_1^{\frac{5}{2}} n_{01} \tau_1 Z_1}{D_{12}^{-\frac{1}{2}} \mu_2^{\frac{3}{2}} P_2^{\frac{5}{2}} n_{02} \tau_2 Z_2} = \frac{(1 - \varepsilon_{f1})(1 - \varepsilon'_{f2} \xi_{f2})^{\frac{3}{2}} \xi_{f2}^{\frac{3}{2}}}{(1 - \varepsilon_{f2})(1 - \varepsilon'_{f1} \xi_{f1})^{\frac{3}{2}} \xi_{f1}^{\frac{3}{2}}},$$

where the indices 1 and 2 refer in this case to two generic values which the various parameters considered can assume for the same chamber.

Now, the term  $(1 - \varepsilon'_{fi} \xi_{fi})$ , (with  $i = 1, 2$ ), which appears in the second member of (14) is nothing else but the parameter  $\varepsilon_{fi}$ , the meaning of which was discussed in I (formula (I.14)); that parameter is related to the fractional reduction of the vapor flux at the bottom of the chamber and depends on the number of ions that are formed per  $\text{cm}^3/\text{s}$  in its interior. This represents, in other words, the final value assumed by the parameter  $\varepsilon_0$  at the end of the successive approximation procedure discussed in I (in the case of a chamber operating by diffusion of methyl alcohol in air at normal pressure) to account for the condensation of vapour on charged centres.

From the discussion in this and the previous paragraph it is clear that  $\varepsilon_0$  and hence  $\varepsilon_{fi}$  now take on a more general significance. They depend, as a consequence of (2), on  $n$  and therefore on the gas pressure  $P$ , on the nature of the gas through the term  $\tau Z$  and, because of (3), (4), (A.1) and (A.2) on the diffusion coefficient  $D$  and on the viscosity coefficient of the gas-vapour mixture. In dealing with chambers which (geometrical conditions, organic vapour and temperature boundary values being the same) have to satisfy different requirements (for different values of ions load and pressure and nature of the filling gas, of course) a suitable choice of  $\varepsilon_0$  would be made, to which a definite value of  $\xi_f$  would correspond. Such a criterion could be applied from time to time following the general lines of procedure outlined in I. Nevertheless eq. (14) allows a direct evaluation of the height of the sensitive layer once this height is known for a particular set of values of the parameters characterising the chamber under consideration. In fact, the graph shown in Fig. 4 of I indi-

cates that for values of  $\varepsilon_0 < 0.8$  the corresponding value of  $\varepsilon_f$  is sensibly constant; it follows, therefore, that (14) can be written, in first approximation in the form:

$$(15) \quad \frac{D^{-1} \mu_1^3 P_1^2 n_{01} \tau_1 Z_1}{D^{-1} \mu_2^3 P_2^2 n_{02} \tau_2 Z_2} \cong \frac{\xi_{f2}^5}{\xi_{f1}^5},$$

from which, if we put  $D^{-1} \mu^3 P^2 n_0 \tau Z = \Delta$  (the « characteristic parameter » of the chamber) we would get:

$$(16) \quad a) \quad \frac{\Delta_1}{\Delta_2} \cong \frac{\xi_{f2}^5}{\xi_{f1}^5},$$

or also

$$b) \quad \xi_f = \sim \Delta \Delta^{-\frac{1}{5}},$$

where  $\Delta$  is a constant of proportionality, whose value is determined once particular set of values of the various parameters and the height of the corresponding sensitive layer are known.

The formulae (16a) and (16b) can be directly utilised for fairly accurate calculations of  $\xi_f$  within the interval in which  $\varepsilon_f$  is sensibly constant i.e. for values of  $\varepsilon_0 < 0.8$ . In general this possibility arises, other conditions being equal, whenever the ion load is not too small. For low values of  $n_0$ , in particular for low values of the gas pressure, (16a) and (16b) are no longer correct. In general, therefore, one has to go back to eq. (14). This has been calculated numerically for  $H_2$ ,  $D_2$ , He,  $CO_2$ , A and Air for pressures between 0.5 and 20 atm and assuming an ion load variable between 2 and 100. The data of reference used to calculate eq. (14) have been taken from measurements performed with a chamber  $\cong 20$  cm high, filled with hydrogen at 20 atm. With methyl alcohol as organic vapour and temperatures at the bottom and the top of  $\cong 213$  °K and  $\cong 293$  °K respectively, the height  $\xi_f$  of the sensitive layer is equal to  $\sim 6$  cm under normal ion load ( $n_0 = 2$ ). These values, together with those shown in Table II for hydrogen, have been introduced into eq. (14) for the terms labeled with index 1. From the graphs of Fig. I, 3 and

TABLE II. — Constants for different gases. Values of  $D$  and  $\mu$  are for 0 °C.

Gas	$D$	$\mu \cdot 10^{-4}$	$Z$	$\tau$
Hydrogen . . . . .	0.506	0.84	1	2
Deuterium . . . . .	0.350	1.20	1	2
Helium . . . . .	0.358	1.87	2	1
Argon . . . . .	0.096	2.09	18	1
Carbon-Dioxide . . . . .	0.088	1.37	14.67	3
Air . . . . .	0.133	1.71	7.2	2

Fig. 1, 4, the correspondence between the terms  $(1 - \epsilon_{fi})$  and  $\xi_{fi}$  has been deduced. The values for  $D_2$ , He,  $\text{CO}_2$ , A and Air given in Table II have been utilized subsequently for the terms of eq. (14) labeled with index 2.

The results of the calculations are shown in Figs. 1, 2, 3, 4, 5 and 6; the

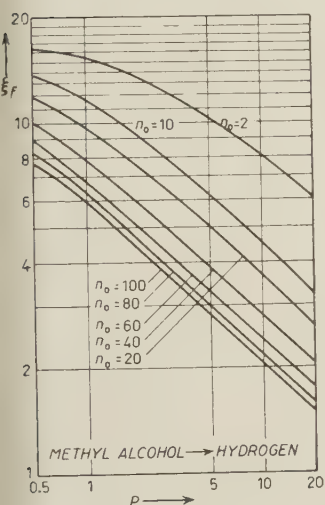


Fig. 1. - Filling gas: Hydrogen.

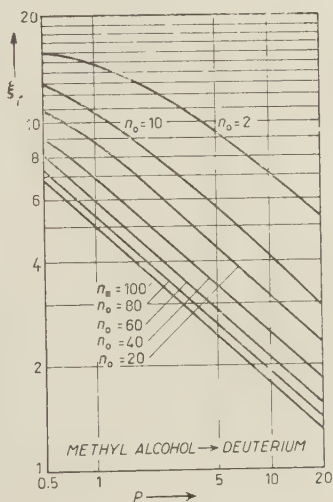


Fig. 2. - Filling gas: Deuterium.

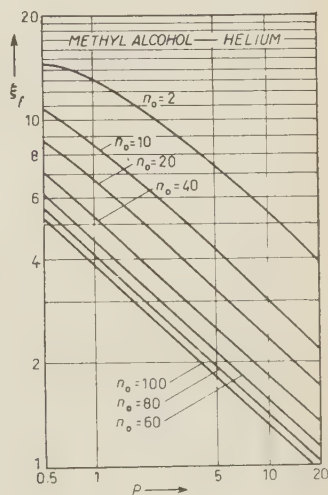


Fig. 3. - Filling gas: Helium.

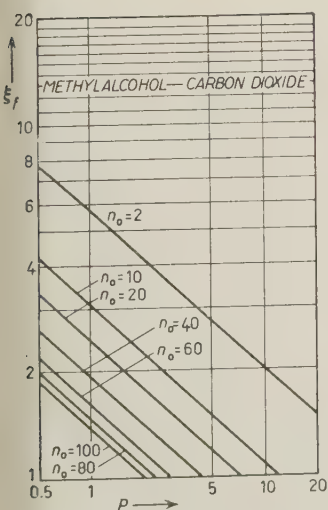


Fig. 4. - Filling gas: Carbon-Dioxide.

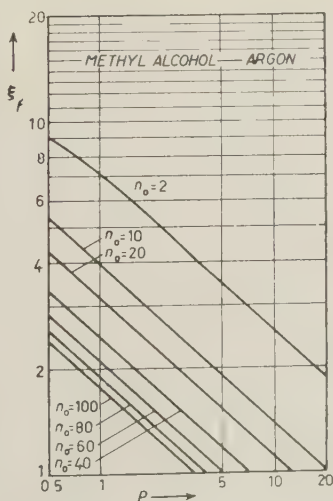


Fig. 5. - Filling gas: Argon.

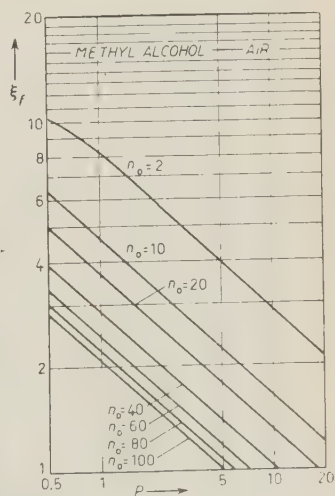


Fig. 6. - Filling gas: Air.

Fig. 1-6. - The height  $\xi_f$  of the sensitive layer (one-dimensional theory) as a function of the filling gas pressure  $P$ .  $\xi_f$  in cm,  $P$  in atm,  $n_0$  number of ions per  $\text{cm}^3/\text{s}$  in Air at N.T.P.

curves have been calculated for  $n_0 = 2, 10, 20, 40, 60, 80$  and  $100$ . The abscissae are the pressures  $P$  of the gas and the ordinates the heights of the sensitive layer. In general, for sufficiently high values of  $P$  and  $n_0$  the approximation afforded by (16a) and (16b) is satisfactory (linear portions of the curves) whilst for low values of  $P$  and  $n_0$  the deviations from linearity mean that the effect due to the term  $(1 - \varepsilon_{fi})$  is no longer negligible. Such an effect is fairly strong for Hydrogen, Deuterium and Helium, also for high ion loads and for pressures lower than  $\sim 10$  atm; for heavier gases such as Argon, Carbon Dioxide and Air it arises only for ion loads less than 10 and, anyhow, for pressures lower than 1 atm. The graphs in Figs. 1, 2, 3, 4, 5 and 6 can be of practical use in so far as they give immediately the height of the sensitive layer, once the type and the pressure of the gas and the ion load are chosen (the distance  $h = 20$  cm, between the bottom and the top of the chamber and the temperatures,  $T_1 = 213^\circ\text{K}$  and  $T_2 = 293^\circ\text{K}$ , are never varied). Such graphs should, however, be used with some caution; in fact, at the basis of our theory lies the hypothesis that the gas is macroscopically at rest. Such a condition is equivalent to  $\mathbf{I}_2 = 0$  or  $\mathbf{v}_2 = 0$ , where  $\mathbf{I}_2 = c_2 \mathbf{v}_2$  is the current vector of the gas ( $c_1$  is the concentration and  $\mathbf{v}_2$  the average velocity of the gas). This hypothesis almost certainly corresponds, at least at first approximation, to the real physical situation when the chamber operates with low values of the temperature of the vapour source and with heavy gases. As it has been observed by other authors<sup>(3)</sup>, operating with light gases (e.g. Hydrogen and Helium) and with a temperature  $T_2$  of the source higher than room temperature, results in permanent conditions of instability due to the convective motion of the gas: the sensitive layer is no longer uniform. Such an effect is particularly evident when the temperature of the source and the nature of the gas are such that the density of the gas-vapour mixture,  $d_s$ , near the source exceeds the density  $d_{ef}$ , at the top of the sensitive layer. The condition  $d_s > d_{ef}$  is more easily realizable with light gases, with vapour source temperatures slightly exceeding room temperature and with low pressures, than with heavy gases, other conditions being equal.

A. R. BEVAN<sup>(3)</sup> discusses and studies experimentally such processes. His results are not, always, directly comparable with the results of our theory due to the fact that the temperatures at the bottom and the top of the chamber and the distances between bottom and source are, sometimes, markedly different in the two cases. When a comparison is possible the agreement is, however, satisfactory. The conclusions of A. R. BEVAN on the stability of operation can, in our view, be assumed as an indication of the limits of validity of our conclusions summarized in the graphs of Figs. 1, 2, 3, 4, 5 and 6: the condition  $d_s < d_{ef}$  holds for light gases (Hydrogen, Deuterium and Helium) with pressures greater than 10 atm and for heavy gases (Carbon Dioxide, Argon, Air) for pressures greater than 1 atm.



The results of the theory are consistent with the results we obtained with an experimental chamber<sup>(5)</sup> filled with air at the pressure of 1 atm ( $h = 20$  cm,  $T_1 \cong 213$  °K,  $T_2 \cong 293$  °K). For an ion load  $n_0$  between 2 and 10,  $\xi_f$  lies between 7 and 15 cm respectively, in good agreement with the data of the curves in Fig. 6.

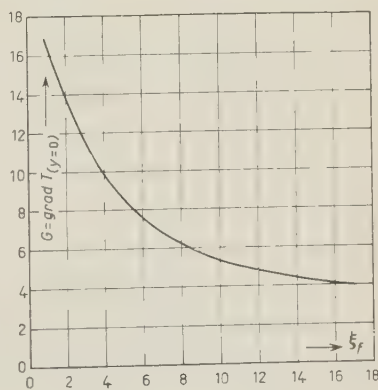
We wish to point out that information on the dependence of the temperature gradient on the height of the sensitive layer can be deduced in a very simple way using (I.16). Since (I.16) is valid in any step of the successive approximation procedure discussed in I, one obtains, substituting for  $\varepsilon'$ ,  $\eta'$  and  $\xi$  respectively  $\varepsilon'_f$ ,  $\eta'_f$  and  $\xi_f$ :

$$(17) \quad \eta'_f = \frac{1 - \varepsilon_f}{\varepsilon_f \xi_f} \left( 1 - \frac{A}{B} \xi_f \right),$$

which expresses  $\eta'_f$  as a function of  $\varepsilon_f$  and  $\xi_f$ . Introducing (17) in (I.12) which represents the temperature distribution for  $0 \leq y < \xi_f$ , when the condensation of the vapour is taken into account, by means of (I.13) one can find, with easy calculations, the temperature gradient  $G$  for  $y = 0$  as a function of  $\xi_f$

$$(18) \quad G = \text{grad } T_{(y=0)} = A + B \frac{1 - \varepsilon_f}{\varepsilon_f \xi_f} \left( 1 - \frac{A}{B} \xi_f \right).$$

Fig. 7. — The temperature gradient  $G$  at the bottom of the chamber as a function of the height  $\xi_f$  of the sensitive layer.  $G$  in °C/cm,  $\xi_f$  in cm.



$\text{Grad } T_{(y=0)}$  as a function of  $\xi_f$  is shown in Fig. 7. For the calculation of the curve shown there, the graphs of Figs. I, 3 and I, 4 have been used.

### 3. — Two-Dimensional Treatment.

3.1. — In I, Sect. 3, the problem was treated for the case in which the various quantities involved are considered to depend both on the height above the bottom of the chamber and a horizontal coordinate. Only the case of a chamber

(5) P. E. ARGAN, N. D'ANGELO and A. GIGLI: *Ric. Sci.*, **24**, 1006 (1954).

operating with methyl alcohol in air at normal pressure was considered, with given temperature and vapour pressure distributions on the side walls (or on plates of any material put vertically inside).

A solution was obtained neglecting, as a first approximation, the condensation of the vapour both on charged and uncharged centers; condensation was subsequently taken into account, by means of a suitable extension of the procedure applied in the one-dimensional case. Let us recall we were dealing with the problem of the integration of the system

$$(19) \quad \begin{cases} T\Delta_2 u - \text{grad } T \times \text{grad } u = 0, \\ \Delta_2 T - \alpha \Delta_2 u = 0, \end{cases} \quad \alpha = \text{const}$$

where  $T(x, y)$  is the temperature and  $u(x, y) = \ln(P - p_1)$ ;  $P$  is the total pressure and  $p_1(x, y)$  the vapour pressure. In eq. (19)  $\alpha = \Delta_1 P \bar{D} / \bar{K} R$  where  $\Delta_1$  is the specific heat at constant pressure of the vapour and  $\bar{D}$  and  $\bar{K}$  the average values of the diffusion coefficient of the vapour and the heat transfer coefficient of the gas-vapour mixture, respectively, in the temperature interval from the bottom to the top of the chamber. Eqs. (19) have been solved with the following boundary conditions:

$$(20) \quad T_{fd} \begin{cases} T(x, 0) = 213^\circ \text{K}, & T(x, b) = 293^\circ \text{K}, \\ T(0, y) = T(a, y) = \begin{cases} 213 + 8y & \text{for } 0 \leq y \leq b/2 \\ 213 & \text{for } b/2 \leq y \leq b \end{cases} \end{cases}$$

For sake of simplicity we assumed that the gas is macroscopically at rest i.e.  $\mathbf{I}_2 = 0 = \mathbf{v}_2$ , where  $\mathbf{I}_2$  and  $\mathbf{v}_2$  represent the current vector and the velocity of the gas, respectively. Let us emphasize again that this assumption is not

in general strictly valid; nevertheless it provides a good picture of the actual situation when the boundary conditions for both temperature and vapour pressure are suitably chosen. In this paragraph we propose to discuss some of the results obtained by integration of eqs. (19) in the parallelogram  $ABCD$ .

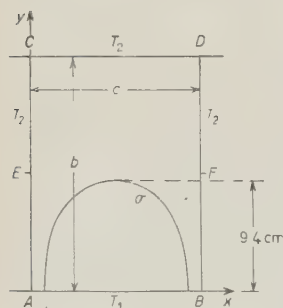


Fig. 8. — The parallelogram  $ABCD$  represents the area taken for the integration of the equations system (19) (two-dimensional theory). The curve  $\sigma$  represents the structure of the top of the sensitive layer as a result of the integration of equation system (19) with the boundary conditions discussed in I (case I of this paper).  $a = 15$  cm,  $b = 20$  cm.

in Fig. 8, with boundary conditions that seem to be reasonably in accordance with the assumption  $I_2 = 0 = v_2$ . We wish to emphasize that they are (as we have discussed already in Appendix III of I) limiting cases; nevertheless some of them seem to be very close to actual physical situations. In the following, number 1 will refer to the particular problem considered in I and numbers 2, 3, 4 and 5 will refer to those to be discussed in this section.

In problems 2 and 3 the temperature distribution on the boundary  $fd$  of  $ABCD$  is the same as that which has already been considered in problem 1(20); in problem 2 we impose the condition  $p_1 = p_{1s}(T)$  (saturated vapour pressure) on  $EC$ ,  $DF$ ,  $AB$  and  $CD$  and  $\partial p_1/\partial x \equiv 0$  on  $AE$  and  $BF$ . In problem 3,

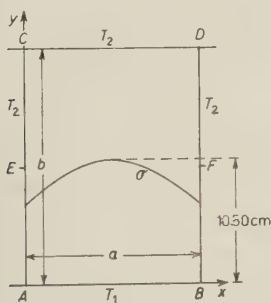


Fig. 9. — The structure of the top of the sensitive layer (curve  $\sigma$ ) in case 2.

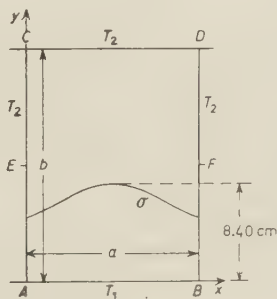


Fig. 10. — The structure of the top of the sensitive layer (curve  $\sigma$ ) in case 3.

$p_1 = p_{1s}(T)$  on  $AB$  and  $CD$ , while  $\partial p_1/\partial x = 0$  on  $AC$  and  $DB$ . The condition  $\partial p_1/\partial x = 0$  means that the horizontal component of the vapour current vector vanishes. In other words on the wall portions where this condition holds, vapour condensation does not occur. The condition  $p_1 = p_{1s}(T)$  is easily realisable in practice (for instance by means of velvet saturated with alcohol), while the condition  $\partial p_1/\partial x = 0$  seems to be more difficult to obtain experimentally.

Curves  $\sigma$  of Figs. 9 and 10 represent the shapes of the sensitive layers we obtain by integrating eqs. (19), <sup>(6)</sup> with the boundary conditions 2 and 3, respectively. On comparison of the solutions of these two problems with the solution of problem 1 (curve  $\sigma$  of Fig. 8) it seems to be possible to draw the following conclusions:

a) condensation of the organic vapour on the side walls of the chamber prevents tracks of ionizing particles from forming in the immediate neigh-

<sup>(6)</sup> Reports of the Istituto Nazionale per le Applicazioni del Calcolo del C.N.R., Roma, 1955 (unpublished).

bourhood. This happens when, for optical reasons, the side walls of the chamber are covered with black velvet that, in steady conditions of operation, becomes wetted by alcohol. The order of magnitude of the insensitive zone near the walls is  $1 \div 2$  cm. If a sensitive layer is desired extending very close to the walls, condensation of the vapour has to be prevented;

b) on comparison of 2 with 3 it is possible to state that, other things being equal, the greater the surface, that is a source of vapour, the thicker is the sensitive layer.

We wish to point out that the zero approximation solutions <sup>(6)</sup> of the problems 1, 2 and 3 provide the same temperature distribution inside the chamber. In case 3 the vapour pressure  $p_1(x, y)$  comes out to be independent of  $x$ . In this case the distribution of the supersaturation depends on  $x$  only because of  $T(x, y)$ , of which  $p_{1s}$  is a function.

In problems 4 and 5 the temperature distribution is linear on  $AC$  and  $BD$ , between the same values on the bottom and the top, as considered in the previous cases, i.e.

$$(21) \quad T_{fd} \begin{cases} T(x, 0) = 213^\circ\text{K}, & T(x, b) = 293^\circ\text{K}, \\ T(0, y) = T(a, y) = 213 + 4y & \text{for } 0 \leq y \leq b. \end{cases}$$

In problem 4,  $p_1 = p_{1s}(T)$  on all  $fd$ ; in problem 5,  $p_1 = p_{1s}(T)$  both on  $AB$  and  $CD$ , while on the remaining part of  $fd$  we have imposed the condition  $\partial p_1 / \partial x \equiv 0$ . Curve  $\sigma$  of Fig. 11 represents the shape of the sensitive layer in case 4 <sup>(6)</sup>. The solution of problem 5 is practically the same as in the one-dimensional case; the sensitive layer is uniform and its height is 17 cm.

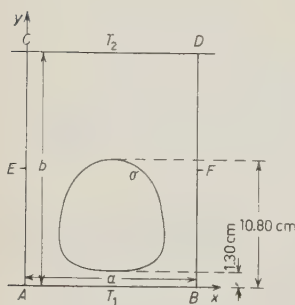


Fig. 11. — The structure of the top of the sensitive layer (curve  $\sigma$ ) in case 4.

The result of problem 4 confirms the necessity of preventing condensation on the side walls. A comparison of 4 and 5 shows that, at least when condensation of vapour on charged and uncharged centers is neglected, a large surface wet with alcohol does not mean necessarily that we get thick sensitive layers. Vector  $I_1$  can be oriented towards the side walls, on a large part of these, so that a certain amount of vapour supplied by the portions of the walls

which are at high temperature condenses on the parts that are at lower temperature and does not contribute to the thickness of the sensitive layer. A similar effect seems to produce the insensitive zone near the bottom of the chamber in problem 4. An analogous effect is to be expected, but to a much lesser extent, in case 1. On the other hand a large surface wet with alcohol and at high temperature can really act as a vapour source, as is shown by comparison of 2 and 3.

In Sect. 3'1 of I we demonstrate that the solution of eqs. (19) with the given boundary conditions is not very dependent on the value of the constant  $\alpha$ . This constant is a function of a number of quantities and they determine completely the behaviour of the gas-vapour mixture, when condensation is neglected. Then in considering the behaviour of the shape of the sensitive layer as function both of the type and the pressure of the gas, same consideration of the constant  $\alpha$  will be needed. It follows from the definition of the diffusion coefficient  $D$  that  $\alpha$  does not depend on the internal pressure. Furthermore, when consideration is limited to a given type of organic vapour, i.e. to a given  $A_1$ , it is easy to see that the values of  $\bar{D}$  and  $\bar{K}$  for  $H_2$ ,  $D_2$ , He,  $CO_2$ , A and Air provide values of  $\alpha$  very close to one another and the differences in temperature distributions corresponding to the various cases never exceed 1-2 °C. The shapes of the sensitive layers of Figs. 8, 9, 10 and 11 turn out to be independent, ceteris paribus, of the particular type of gas and of the internal pressure. So far the condensation of the vapour on charged and uncharged centers of condensation has been neglected. In this approximation the conclusion seems to be valid that the best conditions for operation are obtained when vapour condensation on the side walls is prevented and also the temperature gradient is uniform there, from the bottom to the top of the chamber. We propose now to show how, when condensation is taken into account, this conclusion has to be modified.

3'2. - The successive approximations procedure applied in order to take condensation into account, and discussed in I, is not directly applicable in problems 2, 3, 4, 5, as was also the case in problem 1 (I, Sect. 3'2). Also in these cases our considerations will be valid only for the central part of the chamber, where, for symmetry reasons, it is still possible to evaluate the decrease of the thickness of the sensitive layer when the average value of the vapour flux  $\bar{I}_{x=7.5}^{(y)} = \bar{\Phi}$  is known.

The criteria established in I, Sect. 3'2, will not be applied directly now. We shall show how, by means of simple considerations, it is possible to illustrate the dependence of the height of the sensitive layer on  $\sqrt{r^3}$  for the cases 1, 2, 3, 4, 5 as in Fig. I, 5 for the one-dimensional case.

Our starting point will be eq. (18), giving, in the one-dimensional theory,



the dependence of  $\text{grad } T_{(v=0)}$  on  $\xi_f$ . Suppose we draw, beside the curve in Fig. 7, the corresponding curve for the central part of the chamber in the two-dimensional case (problem 1). It is easy to see that the two curves, as  $\xi_f$  decreases, tend to become parallel. For values of  $\xi_f$  not exceeding  $6 \div 7$  cm they are practically parallel. Then, with an accuracy of a few percent, for any value of  $\xi_f$  between 0 and 7 cm, we can write

$$(22) \quad \left[ \frac{dG}{d\xi} \right]_u = \left[ \frac{dG}{d\xi} \right]_b,$$

where indices  $u$  and  $b$  refer to one-dimensional and two-dimensional cases, respectively. We wish to note that for these values of  $\xi$  the quantity  $\varepsilon_f$  of the one-dimensional theory can be considered to be a constant (the corresponding parameter  $\varepsilon_0$  is certainly  $< 0.8$  (Fig. I, 3 and I, 4)). The same statement does not hold for  $\varepsilon_f$  in the two-dimensional theory, when the same ion loads are considered, for values of  $\xi$  close to  $6 \div 7$  cm.

Eq. (22) can be put in the following form

$$(23) \quad \frac{1 - \varepsilon_{fb}}{\varepsilon_{fb}\xi} + \frac{d\varepsilon_{fb}}{d\xi} \cdot \frac{1}{\varepsilon_{fb}^2} = \frac{1 - \varepsilon_{fu}}{\varepsilon_{fu}\xi},$$

if the term  $(A/B)\xi$ , appearing in eq. (18), is neglected with respect to unity. This approximation seems to be reasonable, especially when we propose, as we now do, to calculate only orders of magnitude, and when the values of  $\xi$  are sufficiently small ( $A = 4$  and  $B = 213$ ). Eq. (23) can be rewritten as

$$(24) \quad \frac{1}{\varepsilon_{fu}} - \frac{1}{\varepsilon_{fb}} = \left[ \frac{1 - \varepsilon_{fu}}{\varepsilon_{fu}\xi_{0b}} \right] \xi_{fb}.$$

Now eq. (I.27), by means of (I.18), can be rewritten as

$$(25) \quad \frac{\tilde{\Phi}_b \xi_{fu} (1 - \varepsilon_{fb})}{\tilde{\Phi}_u \xi_{fb} (1 - \varepsilon_{fu})} = \frac{\xi_{0b}^{\frac{3}{2}}}{\xi_{0u}^{\frac{3}{2}}},$$

where  $\xi_{fu}$  and  $\xi_{fb}$  are the heights of the sensitive layers resulting from the successive approximations procedure discussed in I, for corresponding values of  $\varepsilon_{0u}$  and  $\varepsilon_{0b}$ , shown there; i.e. when the values of  $nr^3$  are the same (chamber operating with air at 1 atm).

From eqs. (24) and (25) it follows that

$$(26) \quad \xi_{fb} \cong \frac{\xi_{fu} \bar{\Phi}_b \xi_{0u}^3 \xi_{0b}}{\xi_{00}^3 \bar{\Phi}_u + \bar{\Phi}_b \xi_{fu} \xi_{0u}^3},$$

where we have assumed  $\varepsilon_{fb} \cong \varepsilon_{fu}$ , as it can be seen to be. Eq. (26) has general validity and provides a useful relation between the heights of the sensitive layer  $\xi_{fb}$  at the center of the two-dimensional, the height  $\xi_{0u}$  and the flux  $\bar{\Phi}_u$  (all of which are known quantities (Fig. I, 1)), the height  $\xi_{fu}$  of the sensitive layer in the one-dimensional theory, whose dependence on  $nr^3$  is also known (Fig. I, 5), and the corresponding quantities  $\xi_{0b}$  and  $\bar{\Phi}_b$  for the various cases considered in the two-dimensional theory, whose numerical values can be easily calculated <sup>(6)</sup>. Then the height of the sensitive layer at the center of the chamber can be evaluated, for different values of  $nr^3$ , in the various cases taken into consideration. Eq. (26) has been evaluated using the data of Table III.

TABLE III.

Problem no.	$\xi_{0b}$	$\bar{\Phi}_b = I_{x=7.5}^{(y)}$
1	9.4	$5.228 \cdot 10^{-8}$
2	10.5	$5.567 \cdot 10^{-8}$
3	8.4	$4.118 \cdot 10^{-8}$
4	10.8	$2.644 \cdot 10^{-8}$
5	17.0	$3.700 \cdot 10^{-8}$
(one-dimensional)		

The results of the calculations are plotted in Fig. 12. This shows, in addition to the curve of Fig. I, 5, the curves for the various cases of the two-dimensional theory. It seems possible to draw the following conclusions. A linear temperature distribution on the side walls hinders stable operation (dotted-curve). With ion loads slightly greater than those corresponding to normal conditions of operation the height of the sensitive layer is considerably reduced;

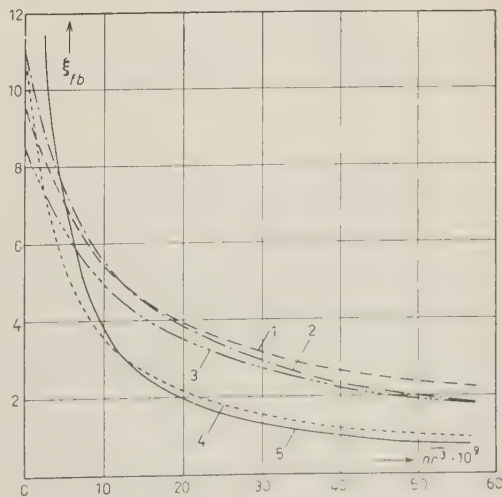


Fig. 12. — The dependence of the height  $\xi_f$  (in cm) of the sensitive layer from  $nr^3 \cdot 10^9$  in cases 1, 2, 3, 4 and 5 discussed in the text.

with higher loads it becomes practically the same as in the one-dimensional case (or case 5). On the other hand it seems to be useful to impose a linear temperature distribution on the lower part of the side walls (in our case for  $0 \leq y \leq b/2$ ), while the upper part is at constant temperature (room temperature). In cases 1, 2, 3,  $\xi_{fb}$  decreases slowly as the ionic load increases. The heights of the sensitive layer, in these three cases, and for high ionic loads, are greater than those obtained in cases 4 and 5, at least by a factor of two. Of these cases 1, 2, 3 the most stable seems to be case 3. In this case, nevertheless, the height of the sensitive layer is smaller than in the first two cases and the stability conditions are about the same. The best conditions seem to be those of cases 1 and 2, as far as the temperature distribution on the side walls is concerned. When the boundary conditions for the vapour pressure are also considered, the conditions of case 2 appear to be the best, because:

- a) the height of the sensitive layer is a maximum for low ionic loads;
- b) for higher loads this condition still applies approximately;
- c) the possibility of ion track formation near the side walls more than offsets the disadvantage of a lower stability of operation.

We wish now to emphasize the fact that when the height of the sensitive layer at the center of the chamber has to be evaluated, for conditions of operation different from those considered above, Fig. 1, 2, 3, 4, 5 and 6 for  $H_2$ ,  $D_2$ , He,  $CO_2$ , A and Air and eq. (26) can be utilized. The quantities  $\xi_{ou}$  and  $\xi_{ob}$  of eq. (26) are in fact fairly independent of the nature and the pressure of the gas; furthermore the dependence of  $\Phi_b$  and  $\Phi_u$  on  $P$  is of the same type. For any value of  $\xi_{fu}$  i.e. for any  $n\bar{r}^3$  given by curves of Fig. 1, 2, 3, 4, 5 and 6, eq. (26) provides the values of  $\xi_{fb}$  corresponding to the same value of  $n\bar{r}^3$ . In this way curves similar to those of Fig. 12 can be obtained, for  $H_2$ ,  $D_2$ , He,  $CO_2$ , A and Air, for pressures between 0.5 and 20 atm. By means of the discussion of Sect. 2.2 the conditions of maximum stability of operation could be deduced.

#### 4. — Conclusions.

Relatively simple calculations provide a fairly good representation of the physical facts determining the behaviour of a diffusion chamber. Our picture of the problem seems to represent the experimental facts adequately despite its generality. Both one-dimensional and two-dimensional treatments are possible, for extremely varied operating conditions (pressure and type of the gas, ionic load etc.). It is necessary to consider only one type of organic vapour (methyl alcohol) and particular geometrical conditions, which are never changed

in developing the theory. However, theory is only able to indicate orders of magnitude; further details we think are not of great importance. The results obtained for a particular organic vapour and given geometrical conditions can be utilized in practice, in order to determine the best conditions of efficiency and stability of any diffusion cloud chamber. The following conclusions can be drawn from I and II:

1) The curves of Fig. 1, 2, 3, 4, 5 and 6 are the results of the one-dimensional theory and provide directly the height of the sensitive layer for given conditions of operation. The starting point in calculating these curves are the measurements by various authors on a chamber operating with methyl alcohol in hydrogen at 20 atm, under normal ionic load. The information that can be obtained from these graphs for different gases, at different filling pressures, and with high ionic loads, seems to be consistent with the experimental results.

2) The curve of Fig. 7 gives directly the value of the temperature gradient at the bottom of the chamber as function of the height of the sensitive layer. This curve can be assumed to have general validity.

3) Integration of eqs. (19) over the parallelogram of Fig. 8, with the boundary conditions already discussed, gives information on the deformation of the sensitive layer due to given temperature and vapour pressure distributions on the side walls of the chamber (or on plates of any material put vertically inside). The results of our theory, given in Figs. 8, 9, 10 and 11, for a chamber filled with  $H_2$ ,  $D_2$ , He,  $CO_2$ , A and Air at various pressures, have been deduced for the cases in which the gas can be considered to be macroscopically at rest. This assumption seems to be compatible with the boundary conditions we have considered. These results are valid only when condensation on charged and uncharged centers can be neglected; nevertheless the statement is valid that the sensitive zone can be allowed to reach the side walls of the chamber provided these are suitably treated, so as to prevent condensation. This conclusion is consistent with experimental observations <sup>(5)</sup>, <sup>(7)</sup>.

4) From curves of Fig. 12 one may deduce immediately the conditions to be satisfied by temperature and vapour pressure distributions on the side walls, in order to get the greatest stability when the ionic load is varied. In particular, for a chamber operating with air at one atmosphere, these conditions are realized with a linear distribution of the temperature on the lower part of the side walls and a constant value in the upper part (in our case for  $b/2 < y < b$ ). As far as the vapour pressure is concerned, the alcohol evaporation

---

(7) C. SUCCI: private communication.

surface, at room temperature, has to be as great as possible and condensation on the lower part of the side walls should be prevented.

The criterion for evaluating the conditions of maximum stability is easily shown to hold also in the cases in which the chamber is operated at pressures between 0.5 and 20 atm, with  $H_2$ ,  $D_2$ , He,  $CO_2$ , A and Air.

\* \* \*

We wish to express thanks to prof. E. PANCINI and to prof. M. AGENO for the interest shown in this work.

We are particularly grateful to prof. M. PICONE, Director of the Istituto Nazionale per le Applicazioni del Calcolo del C.N.R., who has given us permission to carry out the integration of the differential equation system (19) at his Institute.

#### APPENDIX

**A.1** - The following relation gives the law of increase of drop-size with time <sup>(\*)</sup>:

$$(A.1) \quad r^2 = 2D \frac{\varrho_v - \varrho_0}{\sigma} t,$$

where  $\varrho_v$  is the vapour density measured at a great distance from the drop,  $\varrho_0$  the corresponding density of the saturated vapour,  $\sigma$  the density of the drop and  $D$  the diffusion coefficient.

Let us assume further Stokes' law for the speed of fall of the drop

$$(A.2) \quad v = \frac{2}{9} \frac{r^2}{\mu} g \sigma. \quad (\sigma \gg \varrho_v)$$

From these two relations we obtain

$$(A.3) \quad \frac{d(r^4)}{dy} = -18D \frac{\varrho_v - \varrho_0}{\sigma^2} \frac{\mu}{g},$$

which integrated between the heights  $y = 0$  and  $y$  gives

$$(A.4) \quad r^4 = \int_0^y d(r^4) = G\mu \frac{D_1}{P} \int_y^0 \left( \frac{T^*}{T_1} \right)^n (\varrho_v^* - \varrho_0) dy,$$

(\*) J. G. WILSON: *The principle of Cloud-Chamber Technique* (Cambridge, 1951).



for the radius at the bottom of the chamber of a droplet which has started to form at the height  $y$ .

We put  $G = 18/\sigma^2 g$  and recall that  $D = (D_1/P)/(T^*T_1)^n$ . Let us assume that the integral which appears in (A.4) depends only on  $\xi_f$  and on  $y$  (due to the fact that  $T^*(y)$  and  $p_1^*(y)$  do not depend sensibly on the type of gas and on the pressure  $P$ ). Eq. (A.4) gives for the radius  $r$  of the droplet the expression

$$(A.5) \quad r = \sqrt[4]{G\mu \frac{D_1}{P} \psi(\xi_f, y)},$$

where  $\psi(\xi_f, y)$  indicates the integral in eq. (A.4). Consequently, for  $\bar{r}^3$  we get

$$(A.6) \quad \bar{r}^3 = \frac{1}{\xi_f} \left( G\mu \frac{D_1}{P} \right)^{\frac{3}{4}} \int_0^{\xi_f} \psi^3 dy.$$

If, as discussed in the text, only those conditions are considered for which, operating with chambers at different pressures and gases, other things being equal, the heights of sensitive layers  $\xi_f$  (and consequently vapour pressure and temperature distributions) are the same, the integral in (A.6) could be considered as a constant. One can then write (A.6) in the form:

$$(A.7) \quad \bar{r}^3 = \text{const} \left( G\mu \frac{D_1}{P} \right)^{\frac{3}{4}}.$$

Comparing eq. (4) of the text with (A.7) the quantities  $K$  and  $\alpha$  are defined as follows

$$(A.8) \quad K = \text{const} (G\mu)^{\frac{3}{4}} \quad \text{and} \quad \alpha = \frac{3}{4}.$$

**A.2** - Let us consider the integral (11) of the text. Due to the behaviour of  $T^*(y)$  and  $p^*(y)$  we have, with good approximation,

$$(A.9) \quad \frac{M}{T_1^2 R} \int_0^y T^*(p^* - p_0) dy \cong \frac{M}{T_1^2 R} T^* p^*(y/2) \int_0^y \left( 1 - \frac{p_0}{p^*} \right) dy,$$

where  $T^* p^*(y/2)$  is the product of  $T^*$  and  $p^*$ , calculated at  $y/2$ . According to (A.5) we can then write for  $\bar{r}^3$

$$(A.10) \quad \bar{r}^3 = \frac{[ \sqrt[4]{G\mu(D_1/P)} (\overline{M/T_1^2 R}) ]^3}{\xi_f} \int_0^{\xi_f} \left( \sqrt[4]{T^* p^*(y/2) \int_0^y (1 - (p_0/p^*)) dy} \right)^3 dy,$$

which, can be reduced to

$$(A.11) \quad \bar{r}^3 = \frac{[ \sqrt[4]{G\mu(D_1/P)} (\overline{M/T_1^2 R}) T^* p^*(\xi_f/4) ]^3}{\xi_f} I(\xi_f),$$

where

$$(A.12) \quad I(\xi_f) = \int_0^{\xi_f} \left( \sqrt[4]{\int_0^y (1 - (p_0/p^*)) dy} \right)^3 dy.$$

Now, from (12) and (17) we find

$$(A.13) \quad T^*p^*(\xi_f/4) \cong P\beta B(1 - \varepsilon'_f \xi_f) \frac{\xi_f}{4} \left( A \frac{\xi_f}{4} + B \right) \left( 1 + \eta'_f \frac{\xi_f}{4} \right) = \\ = P\beta B(1 - \varepsilon'_f \xi_f) \left[ A \frac{\xi_f^2}{16} + \eta'_f \frac{\xi_f^3 A}{64} + B \frac{\xi_f}{4} + \frac{B \eta'_f \xi_f^2}{16} \right],$$

and it is easy to verify that the fourth root of the term in square bracket in eq. (A.13) is

$$(A.14) \quad \cong \sqrt[4]{\frac{B \xi_f}{4}} \quad \text{and that} \quad I(\xi_f) = C \xi_f^2 \quad (C = \text{const. of prop.})$$

If we take again (A.11) introducing (A.14) into it and consider (A.13) it is not difficult to obtain eqs. (12) and (13) of the text.

## RIASSUNTO

I primi risultati della teoria da noi svolta sul funzionamento della camera a diffusione sono già stati pubblicati in un precedente lavoro. Il particolare problema allora risolto viene ora affrontato da un punto di vista più generale, per quel che riguarda la natura e la pressione del gas di riempimento e il carico ionico, ferme restando le caratteristiche geometriche della camera, le temperature imposte sul fondo e la sommità e la natura del vapore organico impiegato (alcool metilico). Si stabilisce una relazione che rappresenta il legame che deve intercorrere tra i parametri che caratterizzano una camera (natura e pressione del gas e carico ionico) affinché l'altezza dello strato sensibile risulti invariata ed una seconda relazione che fornisce direttamente l'altezza dello strato sensibile in funzione dei detti parametri una volta che essa sia nota per un particolare insieme di essi. Questa relazione viene dettagliatamente discussa e calcolata numericamente per  $H_2$ ,  $D_2$ , He,  $CO_2$ , A ed Aria per pressioni comprese tra 0.5 e 20 atm ed assumendo un carico ionico,  $n$ , (numero di ioni che si formano per  $cm^3/s$  nell'interno della camera) variabile tra 2 e 100. Si mostra inoltre come sia possibile calcolare, in modo semplice e diretto, il gradiente di temperatura limitatamente alla zona della camera sensibile alle particelle ionizzanti, in funzione della sua altezza. I risultati del calcolo vengono messi a confronto con i risultati sperimentali. Anche il problema particolare considerato nel nostro precedente lavoro, in cui i vari parametri erano ritenuti funzione oltre che della quota misurata a partire dal fondo della camera

anche di una coordinata orizzontale (caso bidimensionale), viene ora affrontato in modo più generale, ferma restando la geometria dello strumento, le temperature imposte sulla base e sulla sommità ed il vapore organico impiegato. Si immagina di imporre diverse distribuzioni di temperatura e di tensione di vapore sulle pareti della camera (o su setti di materiale introdotti verticalmente in essa) e si mostra come la geometria dello strato sensibile ne risulti alterata. Analogamente a quanto fatto nel caso unidimensionale si considerano gas di natura e pressione di riempimento diverse con carico ionico pure diverso. I vari casi considerati vengono discussi e si stabiliscono i criteri da seguire nella imposizione della distribuzione di temperatura dall'esterno e della distribuzione della tensione di vapore (trattamento delle pareti o dei setti) affinché la distanza dalle pareti o dai setti, a cui sono ancora osservabili tracce di particelle ionizzanti risulti minima. Si stabiliscono inoltre i criteri da applicare al caso particolare di una camera funzionante con alcool metilico e riempita di aria alla pressione di 1 atmosfera affinché, unitamente all'estensione della zona sensibile fino alle pareti, si realizzi la condizione di massima stabilità di funzionamento della camera al variare del carico ionico.

## Conformal Invariance and Conservation Laws for Relativistic Wave Equations for Zero Rest Mass (\*).

J. A. McLENNAN JR. (+)

*Department of Physics, Lehigh University - Bethlehem, Pennsylvania*

(ricevuto il 16 Marzo 1956)

**Summary.** — It is shown that the relativistic wave equations obtained by GÄRDING for particles of zero rest mass and arbitrary spin are invariant under the conformal transformations of space-time. Conservation laws corresponding to this invariance are obtained. They are formally identical with those found by BESSEL-HAGEN for the electromagnetic field, with the exception of those found for the scalar field. For this case, the conservation laws contain extra terms which arise from the fact that the trace of the energy-momentum tensor is not zero.

### 1. — Introduction.

In 1910, CUNNINGHAM <sup>(1)</sup> and BATEMAN <sup>(2)</sup> discovered that Maxwell's equations are invariant under, not only the inhomogeneous Lorentz group, but the larger group of all conformal, or angle preserving, transformations in four dimensions. This fact was used by BESSEL-HAGEN <sup>(3)</sup>, in conjunction with NOETHER'S theorem <sup>(4)</sup>, to obtain two new conservation laws for the electromagnetic field, in addition to the usual ones for energy-momentum and angular momentum.

(\*) A short account of some of the results of this paper was given in: J. A. McLENNAN JR. and P. HAVAS: *Phys. Rev.*, **87**, 898 (1952).

(+) This research was done while the author was holder of an A.E.C. Pre-Doctoral Fellowship, 1950-1952.

(1) E. CUNNINGHAM: *Proc. Lond. Math. Soc.*, **8**, 77 (1910).

(2) H. BATEMAN: *Proc. Lond. Math. Soc.*, **8**, 223 (1910).

(3) E. BESSEL-HAGEN: *Math. Ann.*, **84**, 258 (1921).

(4) E. NOETHER: *Nachr. Akad. Wiss. Göttingen, Math.-Physik. Kl.*, 235 (1918).  
See also E. L. HILL: *Rev. Mod. Phys.*, **23**, 253 (1951).

gular momentum. The conservation laws he obtained are ( $\times$ )

$$(1.1) \quad \frac{\partial}{\partial x_j} T_{jk} = 0,$$

$$(1.2) \quad \frac{\partial}{\partial x_i} M_{ijk} = 0, \quad M_{ijk} \equiv T_{ij}x_k - T_{ik}x_j,$$

$$(1.3) \quad \frac{\partial}{\partial x_i} (x_j T_{ij}) = 0,$$

$$(1.4) \quad \frac{\partial}{\partial x_i} (2x_k x_j T_{ij} - T_{ik} x_j x_i) = 0,$$

where  $x_j = (x, y, z, ict)$  and  $T_{jk}$  is the energy-momentum tensor for the electromagnetic field. As is well known, (1.2) follows from (1.1), provided that  $T_{jk}$  is symmetric. Similarly, (1.3) and (1.4) follow from (1.1), provided that  $T_{jk}$  is symmetric and has zero trace. Nevertheless, these laws all have independent physical meaning, as was discussed by BESSEL-HAGEN.

The conformal invariance of equations other than Maxwell's has been studied by DIRAC (<sup>5</sup>), SCHOUTEN and HAANTJES (<sup>6</sup>), PAULI (<sup>7</sup>), BHABHA (<sup>8</sup>), and others. From the results obtained by these authors it follows that rest-mass is not a conformal invariant, and that the conformal invariance of Maxwell's equations is closely related to the fact that the photon has zero rest mass. In addition, it is known (<sup>1</sup>) that the scalar equation for zero rest mass

$$(1.5) \quad \square u = 0$$

is conformally invariant. Thus one might expect that other wave equations for fields with zero rest-mass are conformally invariant.

In this paper we investigate the conformal invariance of wave equations for particles with zero rest-mass and arbitrary spin. The equations studied are those given by GÄRDING (<sup>9</sup>), which include the equations obtained by DIRAC (<sup>10</sup>) and FIERZ (<sup>11</sup>) for zero rest-mass. It is shown here that all of Gårding's equations are conformally invariant (but not all of his « minimum sets »; see Sect. 3 below.)

( $\times$ ) The Einstein summation convention is used for both tensor (Latin) and spinor (Greek) indices.

(<sup>5</sup>) P. A. M. DIRAC: *Ann. of Math.*, **37**, 429 (1936).

(<sup>6</sup>) J. SCHOUTEN and J. HAANTJES: *Proc. Kon. Akad. v. Wet.*, **39**, 1059 (1936).

(<sup>7</sup>) W. PAULI: *Helv. Phys. Acta*, **13**, 204 (1940).

(<sup>8</sup>) H. J. BHABHA: *Proc. Camb. Phil. Soc.*, **32**, 622 (1936).

(<sup>9</sup>) L. GÄRDING: *Proc. Camb. Phil. Soc.*, **41**, 49 (1945).

(<sup>10</sup>) P. A. M. DIRAC: *Proc. Roy. Soc. London (A)*, **155**, 447 (1936).

(<sup>11</sup>) M. FIERZ: *Helv. Phys. Acta*, **12**, 3 (1939); **13**, 45 (1940).



In addition, the conservation laws are found for those of Gårding's equations for which a Lagrangian formalism is available; this includes examples of all spin values. For all cases except the scalar field, the conservation laws are formally identical with those found by BESSEL-HAGEN. In the case of the scalar field, they contain extra terms due to the fact that the trace of the energy-momentum tensor is not zero.

## 2. - Notation.

We use the spinor notation as given by VAN DER WAERDEN <sup>(12)</sup> and LAPORTE and UHLENBECK <sup>(13)</sup>. Define the four quantities

$$(2.1) \quad \begin{cases} x_{11} = x_3 + ix_4, & x_{12} = x_1 + ix_2, \\ x_{21} = x_1 - ix_2, & x_{22} = -x_3 + ix_4. \end{cases}$$

Then if the  $x_j$  undergo a Lorentz transformation <sup>(14)</sup>

$$(2.2) \quad x'_j = L_{jk} x_k,$$

it can be shown that the corresponding transformation on the  $x_{\alpha\dot{\beta}}$  ( $\alpha = 1, 2$ ;  $\dot{\beta} = \dot{1}, \dot{2}$ ) factors into

$$(2.3) \quad x'_{\alpha\dot{\beta}} = t_{\alpha}^{\lambda} t_{\dot{\beta}}^{\dot{\lambda}} x_{\lambda\dot{\lambda}}$$

if the Lorentz transformation is proper, and

$$(2.4) \quad x'_{\alpha\dot{\beta}} = t_{\alpha}^{\dot{\lambda}} t_{\dot{\beta}}^{\lambda} x_{\lambda\dot{\lambda}}$$

if the Lorentz transformation is improper. The transformation coefficients  $t_{\alpha}^{\lambda}$ ,  $t_{\dot{\beta}}^{\dot{\lambda}}$ , or  $t_{\alpha}^{\dot{\lambda}}$ ,  $t_{\dot{\beta}}^{\lambda}$ , are determined uniquely, except for sign, by the  $L_{jk}$ .

<sup>(12)</sup> B. L. VAN DER WAERDEN: *Nachr. Akad. Wiss. Göttingen, Math.-physik. Kl.*, 100 (1929).

<sup>(13)</sup> O. LAPORTE and G. E. UHLENBECK: *Phys. Rev.*, **37**, 1380 (1931). See also W. L. BADE and H. JEHL: *Rev. Mod. Phys.*, **25**, 714 (1953).

<sup>(14)</sup> Our meaning of « Lorentz transformation » agrees with that of H. J. BHABHA: *Rev. Mod. Phys.*, **21**, 451 (1949), i.e., the time-reversing or antichronous transformations are included in the term. The proper (improper) transformations are those for which  $\det(L_{jk}) = +1$  ( $-1$ ). (Spinor representations of the antichronous transformations have been given by S. WATANABE: *Phys. Rev.*, **84**, 1008 (1951) and KEN-ITI GOTO: *Prog. Theor. Phys.*, **6**, 990 (1951).

A spinor  $a_{\alpha_1 \dots \alpha_m \dot{\beta}_1 \dots \dot{\beta}_n}$ , symmetric in each kind of index, transforms irreducibly under  $L^+$ , the proper Lorentz group, its transformation law being <sup>(13)</sup>

$$(2.5) \quad a'_{\alpha_1 \dots \alpha_m \dot{\beta}_1 \dots \dot{\beta}_n} = t_{\alpha_1}^{\lambda_1} \dots t_{\alpha_m}^{\lambda_m} t_{\dot{\beta}_1}^{\dot{\rho}_1} \dots t_{\dot{\beta}_n}^{\dot{\rho}_n} a_{\lambda_1 \dots \lambda_m \dot{\rho}_1 \dots \dot{\rho}_n}.$$

If  $m \neq n$ , two symmetric objects  $a_{\alpha_1 \dots \alpha_m \dot{\beta}_1 \dots \dot{\beta}_n}$  and  $b_{\dot{\alpha}_1 \dots \dot{\alpha}_m \beta_1 \dots \beta_n}$  are needed to provide a representation of the full Lorentz group  $L$ . They transform irreducibly under  $L$ , both quantities transforming as in (2.5) for the proper transformations, and like

$$(2.6) \quad \begin{cases} a'_{\alpha_1 \dots \alpha_m \dot{\beta}_1 \dots \dot{\beta}_n} = t_{\alpha_1}^{\dot{\rho}_1} \dots t_{\alpha_m}^{\dot{\rho}_m} t_{\dot{\beta}_1}^{\lambda_1} \dots t_{\dot{\beta}_n}^{\lambda_n} b_{\dot{\rho}_1 \dots \dot{\rho}_m \lambda_1 \dots \lambda_n} \\ b'_{\dot{\alpha}_1 \dots \dot{\alpha}_m \beta_1 \dots \beta_n} = t_{\dot{\alpha}_1}^{\rho_1} \dots t_{\dot{\alpha}_m}^{\rho_m} t_{\beta_1}^{\dot{\lambda}_1} \dots t_{\beta_n}^{\dot{\lambda}_n} a_{\rho_1 \dots \rho_m \dot{\lambda}_1 \dots \dot{\lambda}_n} \end{cases}$$

for the improper transformations. The  $b_{\dot{\alpha}_1 \dots \dot{\alpha}_m \beta_1 \dots \beta_n}$  may be taken as the complex conjugates of the  $a_{\alpha_1 \dots \alpha_m \dot{\beta}_1 \dots \dot{\beta}_n}$ , but this is not necessary and is not done here unless specifically stated. If  $m = n$ ,  $a_{\alpha_1 \dots \alpha_m \dot{\beta}_1 \dots \dot{\beta}_n}$  transforms irreducibly under  $L$ .

Upper spinor indices are defined according to  $a^1 = a_2$ ,  $a^2 = -a_1$ , and similarly for dotted indices. With this convention  $a_2 b^2$  is invariant under  $L^+$ .

### 3. — Gårding's Equations.

GÅRDING obtained the most general possible Lorentz invariant equations which are linear and homogeneous in the first partial derivatives of a symmetric spinor. From these equations he then formed « minimum sets » with the property that all solutions to the equations of a minimum set are also solutions to the second order wave equation

$$(3.1) \quad \square u = 0,$$

while no minimum set possesses a proper subset with this property. Thus Gårding's minimum sets describe particles with zero rest mass and arbitrary spin.

The results obtained depend on whether invariance under the full Lorentz group  $L$  or the proper Lorentz group  $L^+$  is required. For  $L^+$ , let the wave function be a symmetric spinor  $u_{\alpha_2 \dots \alpha_m \dot{\beta}_2 \dots \dot{\beta}_n}$  ( $m = 1$  or  $n = 1$  denotes the absence of undotted or dotted indices). Define the symbol

$$p^{\alpha\dot{\beta}} = \frac{\partial}{\partial x_{\alpha\dot{\beta}}}.$$

Let  $s$  be an operator which makes a spinor symmetric in the undotted indices

where it is not already symmetric, e.g.

$$sp^{\alpha_1\dot{\beta}_1}u^{\alpha_2\cdots\alpha_m\dot{\beta}_2\cdots\dot{\beta}_n} = p^{\alpha_1\dot{\beta}_1}u^{\alpha_2\cdots\alpha_m\dot{\beta}_2\cdots\dot{\beta}_n} + p^{\alpha_2\dot{\beta}_1}u^{\alpha_1\alpha_3\cdots\alpha_m\dot{\beta}_2\cdots\dot{\beta}_n} + \dots + p^{\alpha_m\dot{\beta}_1}u^{\alpha_1\cdots\alpha_{m-1}\dot{\beta}_2\cdots\dot{\beta}_n}$$

and similarly for  $\dot{s}$ . Then Gårding's equations are

$$(3.2) \quad s\dot{s}p^{\alpha_1\dot{\beta}_1}u^{\alpha_2\cdots\alpha_m\dot{\beta}_2\cdots\dot{\beta}_n} = 0,$$

$$(3.3) \quad sp^{\alpha_1}_{\dot{\beta}_2}u^{\alpha_2\cdots\alpha_m\dot{\beta}_2\cdots\dot{\beta}_n} = 0,$$

$$(3.4) \quad \dot{s}p^{\dot{\beta}_1}_{\alpha_2}u^{\alpha_2\cdots\alpha_m\dot{\beta}_2\cdots\dot{\beta}_n} = 0,$$

$$(3.5) \quad p^{\alpha_1}_{\dot{\beta}_2}u^{\alpha_2\cdots\alpha_m\dot{\beta}_2\cdots\dot{\beta}_n} = 0.$$

These equations transform irreducibly, since they are symmetric in all indices. Furthermore, they are the only such equations, since there are  $4mn$  equations in the  $4mn$  expressions  $p^{\alpha_1\dot{\beta}_1}u^{\alpha_2\cdots\alpha_m\dot{\beta}_2\cdots\dot{\beta}_n}$ .

For the full Lorentz group  $L$ , the wave function consists of the two symmetric objects  $u^{\alpha_2\cdots\alpha_m\dot{\beta}_2\cdots\dot{\beta}_n}$  and  $v^{\alpha_2\cdots\alpha_m\dot{\beta}_2\cdots\dot{\beta}_n}$ , provided that  $m \neq n$ . The equations analogous to (3.2)-(3.5) are

$$(3.6) \quad s\dot{s}p^{\alpha_1\dot{\beta}_1}u^{\alpha_2\cdots\alpha_m\dot{\beta}_2\cdots\dot{\beta}_n} = 0, \quad s\dot{s}p^{\alpha_1\dot{\beta}_1}v^{\alpha_2\cdots\alpha_m\dot{\beta}_2\cdots\dot{\beta}_n} = 0,$$

$$(3.7) \quad sp^{\alpha_1}_{\dot{\beta}_2}u^{\alpha_2\cdots\alpha_m\dot{\beta}_2\cdots\dot{\beta}_n} = 0, \quad \dot{s}p^{\alpha_1}_{\dot{\beta}_2}v^{\alpha_2\cdots\alpha_m\dot{\beta}_2\cdots\dot{\beta}_n} = 0,$$

$$(3.8) \quad \dot{s}p^{\dot{\beta}_1}_{\alpha_2}u^{\alpha_2\cdots\alpha_m\dot{\beta}_2\cdots\dot{\beta}_n} = 0, \quad sp^{\dot{\beta}_1}_{\alpha_2}v^{\alpha_2\cdots\alpha_m\dot{\beta}_2\cdots\dot{\beta}_n} = 0,$$

$$(3.9) \quad p^{\alpha_1}_{\dot{\beta}_2}u^{\alpha_2\cdots\alpha_m\dot{\beta}_2\cdots\dot{\beta}_n} = 0, \quad p^{\alpha_1}_{\dot{\beta}_2}v^{\alpha_2\cdots\alpha_m\dot{\beta}_2\cdots\dot{\beta}_n} = 0,$$

provided that  $|m - n| \neq 2$ . If  $n - m = 2$ , the equations (3.7) do not transform irreducibly, but are replaced by

$$(3.7a) \quad sp^{\alpha_3}_{\dot{\beta}_2}u^{\alpha_1\cdots\alpha_m\dot{\beta}_2\cdots\dot{\beta}_m} + \dot{s}p^{\dot{\beta}_3}_{\alpha_2}v^{\dot{\beta}_1\cdots\dot{\beta}_m\alpha_2\cdots\alpha_m} = 0,$$

$$(3.7b) \quad sp^{\alpha_3}_{\dot{\beta}_2}u^{\alpha_1\cdots\alpha_m\dot{\beta}_2\cdots\dot{\beta}_m} - \dot{s}p^{\dot{\beta}_3}_{\alpha_2}v^{\dot{\beta}_1\cdots\dot{\beta}_m\alpha_2\cdots\alpha_m} = 0,$$

each of which transforms irreducibly. (Obviously (3.7) and (3.7a,b) are completely equivalent for all but group theoretical purposes.) If  $m - n = 2$  (3.8) splits up similarly.

If  $m = n$ , the wave function is  $u^{\alpha_2\cdots\alpha_m\dot{\beta}_2\cdots\dot{\beta}_m}$  and Gårding's equations are

$$(3.10) \quad s\dot{s}p^{\alpha_1\dot{\beta}_1}u^{\alpha_2\cdots\alpha_m\dot{\beta}_2\cdots\dot{\beta}_m} = 0,$$

$$(3.11) \quad \dot{s}p_{\dot{\beta}_2}^{\alpha_1} u^{\alpha_2 \dots \alpha_m \dot{\beta}_2 \dots \dot{\beta}_m} = 0, \quad \dot{s}p_{\alpha_2}^{\dot{\beta}_1} u^{\alpha_2 \dots \alpha_m \dot{\beta}_2 \dots \dot{\beta}_m} = 0,$$

$$(3.12) \quad p_{\alpha_2 \dot{\beta}_2} \dot{u}^{\alpha_2 \dots \alpha_m \dot{\beta}_2 \dots \dot{\beta}_m} = 0.$$

Note that equations (3.3), (3.5), (3.7) and (3.9) do not exist if  $n = 1$ , and similarly for (3.4), (3.5), (3.8), (3.9), (3.11) and (3.12) if  $m = 1$ .

Although equations (3.2)-(3.5) were required to be invariant for the proper Lorentz group only, (3.2) and (3.5) with  $m = n$  are also invariant under the improper Lorentz transformations, and are included in (3.10) and (3.12). The remainder of (3.2)-(3.5) are not invariant under the improper Lorentz transformations.

In writing equations (3.2)-(3.12), GÄRDING used a subscript  $\tau$  to indicate the behavior of the wave function under the space- and time-like reflections. However, this distinction is unimportant for our purposes, and so the subscript has been dropped,

If a spinor vanishes, its irreducible parts must also vanish. Thus equations (3.2)-(3.12) are the most general possible equations that are linear and homogeneous in the first partial derivatives of the wave function. However, the solutions to any one of (3.2)-(3.12) will not necessarily satisfy the second order equation (3.1), and so the minimum sets will, possibly, have to include more than one irreducible equation. The structure of the minimum sets was determined by GÄRDING, and may be summed up as follows. If  $m = 1$  or  $n = 1$ , any one of the irreducible equations is sufficient to form a minimum set. In all other cases, any two irreducible equations form a minimum set, with the exception that (3.3) and (3.4) with  $m = n$  do not constitute a minimum set. (Equations (3.7a,b) are to be counted together as a single equation, and similarly for the two equations replacing (3.8) if  $m = n = 2$ .)

As pointed out by GÄRDING, a minimum set made up from (3.3) and (3.5) may be written

$$(3.13) \quad p_{\dot{\beta}_2}^{\alpha_1} u^{\alpha_2 \dots \alpha_m \dot{\beta}_2 \dots \dot{\beta}_n} = 0.$$

The minimum sets made up from (3.4) and (3.5), (3.7) and (3.9), (3.8) and (3.9), and (3.11) and (3.12) may be written in a similar way.

Some of GÄRDING's minimum sets are not useful for the description of wave fields, since they do not possess plane wave solutions. It is easily shown that the equations (3.2), (3.6), and (3.10) do not have plane wave solutions, other than the trivial ones of zero frequency.

Consider now the equations (3.10)-(3.12). Since (3.10) does not have plane wave solutions, the only physically useful minimum sets are those made up from (3.11) and (3.12). Since the wave function is a spinor of even rank, these

equations may be transcribed into tensor notation <sup>(13)</sup>; the result is

$$(3.14) \quad \left\{ \begin{array}{l} \frac{\partial}{\partial \bar{x}_i} u_{jkl...} - \frac{\partial}{\partial x_j} u_{ikl...} = 0, \\ \frac{\partial}{\partial x_j} u_{jkl...} = 0, \end{array} \right.$$

where  $u_{ijkl...}$  is a symmetric tensor with zero trace. But all solutions to this set of equations are of the form

$$(3.15) \quad u_{jkl...} = \frac{\partial}{\partial x_j} \frac{\partial}{\partial x_k} \frac{\partial}{\partial x_l} \dots u, \quad \text{where} \quad \square u = 0.$$

Thus the minimum sets made up from (3.11) and (3.12) are equivalent (in the sense of (3.15)) to the scalar or pseudoscalar wave equation.

Now we collect Garding's minimum sets, excluding those which do not have plane wave solutions, and using (3.13). For  $L^-$  the minimum sets are

$$(3.16) \quad p_{\beta_2}^{\alpha_1} u^{x_2 \dots \alpha_m \dot{\beta}_2 \dots \dot{\beta}_n} = 0,$$

$$(3.17) \quad p_{\alpha_2}^{\dot{\beta}_1} u^{x_2 \dots \alpha_m \dot{\beta}_2 \dots \dot{\beta}_n} = 0,$$

$$(3.18) \quad sp_{\beta_2}^{\alpha_1} u^{x_2 \dots \alpha_m \dot{\beta}_2 \dots \dot{\beta}_n} = 0, \quad \dot{s}p_{\alpha_2}^{\dot{\beta}_1} u^{x_2 \dots \alpha_m \dot{\beta}_2 \dots \dot{\beta}_n} = 0. \quad (m \neq n).$$

For  $L$  with  $m \neq n$  the minimum sets are

$$(3.19) \quad p_{\beta_2}^{\alpha_1} u^{x_2 \dots \alpha_m \dot{\beta}_2 \dots \dot{\beta}_n} = 0, \quad p_{\beta_2}^{\dot{\alpha}_1} v^{\alpha_2 \dots \dot{\alpha}_m \dot{\beta}_2 \dots \beta_n} = 0,$$

$$(3.20) \quad \left\{ \begin{array}{l} sp_{\beta_2}^{\alpha_1} u^{x_2 \dots \alpha_m \dot{\beta}_2 \dots \dot{\beta}_n} = 0, \quad \dot{s}p_{\beta_2}^{\dot{\alpha}_1} v^{\alpha_2 \dots \dot{\alpha}_m \dot{\beta}_2 \dots \beta_n} = 0, \\ \dot{s}p_{\alpha_2}^{\dot{\beta}_1} u^{x_2 \dots \alpha_m \dot{\beta}_2 \dots \dot{\beta}_n} = 0, \quad sp_{\alpha_2}^{\beta_1} v^{\alpha_2 \dots \dot{\alpha}_m \dot{\beta}_2 \dots \beta_n} = 0. \end{array} \right.$$

For  $L$  with  $m = n$ , all minimum sets are equivalent to the scalar or pseudo-scalar wave equation

$$(3.21) \quad \square u = 0.$$

We will not consider the conformal invariance of the minimum sets not included in (3.16)-(3.21).



#### 4. — Conformal Transformations.

The conformal transformations on the four variables  $x_j$  are those transformations which preserve geometry in the small; the interval

$$ds^2 = dx_j dx_j$$

transforms like

$$(4.1) \quad ds'^2 = \varrho ds^2,$$

where  $\varrho$  may be a function of the coordinates. These transformations form a group. LIE <sup>(15)</sup> has shown that all the conformal transformations can be compounded from the inhomogeneous Lorentz transformations plus the inversions

$$(4.2) \quad x'_i = kx_i / (x_j x_j),$$

where  $k$  is a real (positive or negative) constant.

The infinitesimal conformal transformations can be obtained by forming linear combinations of the following fifteen independent infinitesimal transformations

$$(4.3) \quad x'_j = x_j + \beta_j,$$

$$(4.4) \quad x'_j = x_j + \varepsilon_{jk} x_k, \quad (\varepsilon_{jk} = -\varepsilon_{kj})$$

$$(4.5) \quad x'_j = (1 + \nu) x_j,$$

$$(4.6) \quad x'_j = (1 + 2\alpha_k x_k) x_j - \alpha_j x_k x_k$$

where  $\beta_j$ ,  $\varepsilon_{jk}$ ,  $\nu$ , and  $\alpha_k$  are infinitesimal parameters.

The space- and time-like reflections and the inversions cannot be obtained from the infinitesimal transformations. We call  $C^+$  the group generated by the infinitesimal transformations and  $C$  the complete conformal group including the reflections and inversions. The group  $C$  can be obtained by adding either the reflections or the inversions to  $C^+$ ; this is expressed by the following

*Lemma:* The full Lorentz group can be obtained from the inhomogeneous proper orthochronous Lorentz transformations plus the inversions. Furthermore, the inversions can be obtained from the infinitesimal transformations (4.3)-(4.6) plus the reflections.

This lemma, which we shall use in the following, is proved in the appendix.

<sup>(15)</sup> S. LIE and F. ENGEL: *Theorie der Transformationsgruppen* (Leipzig, 1893). vol. III, p. 347 ff.

## 5. — Conformal Invariance of the Irreducible Equations.

We first consider the behavior of equations (3.2)-(3.12) under the inversion. Equations (3.2)-(3.5) with  $m \neq n$  and (3.3), (3.4) with  $m = n$  are not invariant under the inversion. This follows from the fact that they are invariant under the inhomogeneous proper Lorentz transformations, and this, coupled with invariance under the inversions, would require by our lemma that they be invariant under the improper Lorentz transformations, which they are not.

The remainder of the equations (3.6)-(3.12) are invariant under the inversion. To show this, first consider the transformation law for the derivative operator  $p^{\alpha\dot{\beta}}$ . From (4.2) it follows that

$$p'^{\alpha\dot{\beta}} = \frac{\partial x_{\mu\dot{\nu}}}{\partial x'_{\alpha\dot{\beta}}} p^{\mu\dot{\nu}} = \frac{1}{k} (x^2 \delta_{\mu}^{\alpha} \delta_{\dot{\nu}}^{\dot{\beta}} + x_{\mu\dot{\nu}} x^{\alpha\dot{\beta}}) p^{\mu\dot{\nu}},$$

where  $x^2 = x_{\alpha\dot{\beta}} x^{\alpha\dot{\beta}} = -2x_j x_j$  and  $\delta_{\mu}^{\alpha} = \delta_{\dot{\mu}}^{\dot{\alpha}}$  is the Kronecker delta. Using the spinor identities given by LAPORTE and UHLENBECK<sup>(13)</sup> one may reduce this to

$$(5.1) \quad p'^{\alpha\dot{\beta}} = \frac{1}{k} x_{\nu}^{\alpha} x_{\mu}^{\dot{\beta}} p^{\mu\nu}.$$

Thus, when written in spinor notation, the inversion factors in the same way as the Lorentz transformations, providing for the possibility of transformations on spinors of arbitrary rank, with the transformation coefficients  $x_{\nu}^{\alpha}$ . Since the Jacobian determinant of the transformation (4.2) is not constant, but is proportional to  $(x^2)^{-1}$ , it is also possible to have « spinor densities » whose transformation law contains as a factor some power of  $x^2$ . Thus we try the transformation law

$$(5.2) \quad \begin{cases} u'^{\alpha_1 \dots \alpha_m \dot{\beta}_1 \dots \dot{\beta}_n} = A x^{2t} x_{\dot{\alpha}_2}^{\alpha_1} \dots x_{\dot{\alpha}_m}^{\alpha_m} x_{\dot{\lambda}_2}^{\dot{\beta}_1} \dots x_{\dot{\lambda}_n}^{\dot{\beta}_n} v^{\dot{\alpha}_2 \dots \dot{\alpha}_m \dot{\lambda}_2 \dots \dot{\lambda}_n} \\ v'^{\dot{\alpha}_1 \dots \dot{\alpha}_m \beta_1 \dots \beta_n} = A x^{2t} x_{\dot{\alpha}_2}^{\dot{\alpha}_1} \dots x_{\dot{\alpha}_m}^{\dot{\alpha}_m} x_{\dot{\lambda}_2}^{\beta_1} \dots x_{\dot{\lambda}_n}^{\beta_n} v^{\dot{\alpha}_2 \dots \dot{\alpha}_m \dot{\lambda}_2 \dots \dot{\lambda}_n} \end{cases}$$

where  $t$  is a constant to be determined. The constant  $A$  is arbitrary, but may be chosen so as to make the transformation (5.2) self-inverse, in accordance with that property of the coordinate transformation (4.2). If this is done, it is found<sup>(16)</sup> that  $A$  has the value

$$(5.3) \quad A = \pm 2^{-t} k^{-\frac{1}{2}(2t+m+n-2)}.$$

<sup>(16)</sup> For details of this and later calculations, see J. A. MCLENNAN Jr.: *On the Invariance Properties and Conservation Laws for Relativistic Wave Equations. Particularly for Zero Rest Mass* (Lehigh University, Thesis, 1952).

If the transformations (5.1) and (5.2) are substituted into equations (3.6)-(3.12), it is found that those equations are in fact invariant, provided that  $t$  has the values given in Table I. The calculations are straightforward but

TABLE I. — *Values of  $t$  necessary for conformal invariance of equations (3.2)-(3.12).*

Equation	$t$
3.2, 3.6	$-m-n+2$
3.3, 3.7	$-m+2$
3.4, 3.8	$-n+2$
3.5, 3.9	2
3.10	$-2m+2$
3.11	$-m+2$
3.12	2

quite lengthy, and so we will indicate them here for one case only. Consider equation (3.6), which we assume to hold in the primed system of coordinates:

$$(5.4) \quad s\dot{s}p'^{\alpha_1\dot{\beta}_1}u'^{\alpha_2\cdots\alpha_m\dot{\beta}_2\cdots\dot{\beta}_n}=0, \quad s\dot{s}p'^{\dot{\alpha}_1\beta_1}v'^{\dot{\alpha}_2\cdots\dot{\alpha}_m\beta_2\cdots\beta_n}=0.$$

Substituting into this equation the transformations (5.1) and (5.2), one finds

$$(5.5) \quad s\dot{s}p'^{\alpha_1\dot{\beta}_1}u'^{\alpha_2\cdots\alpha_m\dot{\beta}_2\cdots\dot{\beta}_n}=\frac{A}{k}x^{2t}s\dot{s}x_{\mu_1}^{\alpha_1}\cdots x_{\mu_m}^{\alpha_m}x_{\nu_1}^{\dot{\beta}_1}\cdots x_{\nu_n}^{\dot{\beta}_n}p^{\dot{\mu}_1\nu_1}v^{\dot{\mu}_2\cdots\dot{\mu}_m\nu_2\cdots\nu_n}+ \\ +\frac{A}{k}s\dot{s}x_{\mu_1}^{\alpha_1}x_{\nu_1}^{\dot{\beta}_1}v^{\dot{\mu}_2\cdots\dot{\mu}_m\nu_2\cdots\nu_n}p^{\dot{\mu}_1\nu_1}[x^{2t}x_{\mu_2}^{\alpha_2}\cdots x_{\mu_m}^{\alpha_m}x_{\nu_2}^{\dot{\beta}_2}\cdots x_{\nu_n}^{\dot{\beta}_n}].$$

The operators  $s$  and  $\dot{s}$  in the first term above produce a sum over permutations of  $\alpha_1\cdots\alpha_m$  and  $\dot{\beta}_1\cdots\dot{\beta}_n$ ; in this sum, we may permute the dummy indices to obtain

$$(5.6) \quad s\dot{s}x_{\mu_1}^{\alpha_1}\cdots x_{\mu_m}^{\alpha_m}x_{\nu_1}^{\dot{\beta}_1}\cdots x_{\nu_n}^{\dot{\beta}_n}p^{\dot{\mu}_1\nu_1}v^{\dot{\mu}_2\cdots\dot{\mu}_m\nu_2\cdots\nu_n}= \\ =x_{\mu_1}^{\alpha_1}x_{\mu_m}^{\alpha_m}x_{\nu_1}^{\dot{\beta}_1}\cdots x_{\nu_n}^{\dot{\beta}_n}s\dot{s}p^{\dot{\mu}_1\nu_1}v^{\dot{\mu}_2\cdots\dot{\mu}_m\nu_2\cdots\nu_n}.$$

Furthermore, on taking the derivative indicated in the second term of (5.5), one obtains a sum of terms which differ by permutations of the indices  $\alpha_1\cdots\alpha_m$ ,  $\dot{\beta}_1\cdots\dot{\beta}_n$ ; the operators  $s$  and  $\dot{s}$  then have the effect of collapsing this sum to a single term

$$(5.7) \quad s\dot{s}x_{\mu_2}^{\alpha_2}x_{\nu_1}^{\dot{\beta}_1}v^{\dot{\mu}_2\cdots\dot{\mu}_m\nu_2\cdots\nu_n}p^{\dot{\mu}_1\nu_1}[x^{2t}x_{\mu_2}^{\alpha_2}\cdots x_{\mu_m}^{\alpha_m}x_{\nu_2}^{\dot{\beta}_2}\cdots x_{\nu_n}^{\dot{\beta}_n}]= \\ = (t+m+n-2)x^{2t}x_{\nu_2}^{\alpha_2\dot{\beta}_1}x_{\mu_2}^{\alpha_2}\cdots x_{\mu_m}^{\alpha_m}x_{\nu_2}^{\dot{\beta}_2}\cdots x_{\nu_n}^{\dot{\beta}_n}p^{\dot{\mu}_1\nu_1}v^{\dot{\mu}_2\cdots\dot{\mu}_m\nu_2\cdots\nu_n}.$$

Thus equation (5.5) reduces to

$$(5.8) \quad \begin{aligned} \dot{s}\dot{s}p'^{\alpha_1\dot{\beta}_1}u'^{\alpha_2\cdots\alpha_m\dot{\beta}_2\cdots\beta_n} &= \frac{A}{k} x^{2t} x_{\mu_1}^{\alpha_1} \cdots x_{\mu_m}^{\alpha_m} x_{\nu_1}^{\dot{\beta}_1} \cdots x_{\nu_n}^{\dot{\beta}_n} \dot{s}\dot{s}p^{\mu_1\nu_1} \cdots \mu_m\nu_m \cdots \nu_n \\ &+ \frac{A}{k} (t+m+n-2) x^{2t} x_{\mu_1}^{\alpha_1\dot{\beta}_1} x_{\mu_2}^{\alpha_2} \cdots x_{\mu_m}^{\alpha_m} x_{\nu_2}^{\dot{\beta}_2} \cdots x_{\nu_n}^{\dot{\beta}_n} \nu^{\mu_2\cdots\mu_m\nu_2\cdots\nu_n}. \end{aligned}$$

It is now apparent that equation (5.4) is invariant under the inversion if  $t+m+n-2=0$ . We have considered the transformation of only half of equation (3.6), but the other half may be treated in the same way, the only difference being an interchange of dotted and undotted indices. The invariance of the remaining equations (3.7)-(3.12), with the values of  $t$  given in Table I, follows from a similar treatment.

The transformation (4.6) can be obtained from an inversion, followed by an infinitesimal translation, followed by the original inversion. Thus it follows from their invariance under inversions that equations (3.6)-(3.12) are also invariant under (4.6). (In addition they are invariant under the change of scale (4.5), as is obvious from their homogeneity.) The explicit transformation law for the wave function, for the transformation (4.6), can be obtained by transforming the wave function in three steps corresponding to the three coordinate transformations which result in (4.6). Before giving the results of this calculation, we consider the transformation law for the derivative operator, which, from (4.6), is

$$p'^{\alpha\dot{\beta}} = [(1 + \alpha_{\lambda\dot{\rho}} x^{\lambda\dot{\rho}}) \delta_{\mu}^{\alpha} \delta_{\nu}^{\dot{\beta}} + \alpha^{\alpha\dot{\beta}} x_{\mu\nu} - \alpha_{\mu\nu} x^{\alpha\dot{\beta}}] p^{\mu\nu},$$

where  $\alpha_{\lambda\dot{\beta}}$  is obtained from  $\alpha_j$  in the manner of (2.1). Using the identities of spinor analysis and ignoring second order terms in  $\alpha_{\lambda\dot{\beta}}$ , one can reduce this to

$$(5.9) \quad p'^{\alpha\dot{\beta}} = a_{\mu}^{\alpha} a_{\nu}^{\dot{\beta}} p^{\mu\nu},$$

where

$$(5.10) \quad a_{\mu}^{\alpha} = \delta_{\mu}^{\alpha} - \alpha_{\lambda}^{\alpha} x_{\mu}^{\dot{\lambda}} = (a_{\mu}^{\dot{\lambda}})^*.$$

The transformation law for the wave function in terms of the  $a_{\mu}^{\alpha}$ , as obtained by the above mentioned process, is

$$(5.11) \quad \begin{cases} u'^{\alpha_2\cdots\alpha_m\dot{\beta}_2\cdots\dot{\beta}_n} = (1 + t\alpha_{\lambda_2}^{\alpha_2} x^{\lambda_2\dot{\rho}}) a_{\lambda_2}^{\alpha_2} \cdots a_{\lambda_m}^{\alpha_m} a_{\rho_2}^{\dot{\beta}_2} \cdots a_{\rho_n}^{\dot{\beta}_n} u^{\lambda_2\cdots\lambda_m\rho_2\cdots\rho_n} \\ v'^{\dot{\alpha}_2\cdots\dot{\alpha}_m\beta_2\cdots\beta_n} = (1 + t\alpha_{\lambda_2}^{\dot{\alpha}_2} x^{\lambda_2\dot{\rho}}) a_{\lambda_2}^{\dot{\alpha}_2} \cdots a_{\lambda_m}^{\dot{\alpha}_m} a_{\rho_2}^{\beta_2} \cdots a_{\rho_n}^{\beta_n} v^{\lambda_2\cdots\lambda_m\rho_2\cdots\rho_n} \end{cases}$$

where  $t$  has the values given in Table I. The transformation (5.11) makes equations (3.6)-(3.12) invariant under (4.6), but from the complete reduc-

bility of (5.11) it is apparent that equations (3.2)-(3.5) are also invariant under (4.6), with  $u^{\alpha_2 \dots \alpha_m \dot{\beta}_2 \dots \dot{\beta}_n}$  transforming as in (5.11).

Thus all of the equations (3.2)-(3.12) are invariant under the group  $C^+$ , while equations (3.6)-(3.12) are in addition invariant under  $C$ .

## 6. — Conformal Invariance of the Minimum Sets.

Now we examine the conformal invariance of Gårding's minimum sets. Note first that all minimum sets are invariant under the change of scale (4.5). However, it does not follow without further discussion that those minimum sets containing two irreducible equations are invariant under either the inversion or the transformation (4.6), since the transformation laws are different for the different irreducible equations.

Consider the minimum set (3.21), which is just the scalar or pseudoscalar wave equation. This equation is known to be conformally invariant (<sup>1</sup>). Under the inversion, the wave function transforms like

$$(6.1) \quad u' = \frac{1}{k} x_j x_j u,$$

and for (4.6) the transforming law is

$$(6.2) \quad u' = (1 - 2\alpha_j x_j) u.$$

The minimum set (3.19) is also invariant under the inversion and under (4.6). For the inversion, the wave function transforms like

$$(6.3) \quad \begin{cases} u^{\alpha_2 \dots \alpha_m \dot{\beta}_2 \dots \dot{\beta}_n} = x^2 C_{\mu_2 \dots \mu_m}^{\alpha_2 \dots \alpha_m} x_{\nu_2}^{\dot{\beta}_2} \dots x_{\nu_n}^{\dot{\beta}_n} v^{\mu_2 \dots \mu_m \nu_2 \dots \nu_n} \\ v^{\dot{\alpha}_2 \dots \dot{\alpha}_m \beta_2 \dots \beta_n} = x^2 C_{\mu_2 \dots \mu_m}^{\dot{\alpha}_2 \dots \dot{\alpha}_m} x_{\nu_2}^{\beta_2} \dots x_{\nu_n}^{\beta_n} u^{\mu_2 \dots \mu_m \nu_2 \dots \nu_n} \end{cases}$$

where  $C_{\mu_2 \dots \mu_m}^{\alpha_2 \dots \alpha_m}$  and  $C_{\mu_2 \dots \mu_m}^{\dot{\alpha}_2 \dots \dot{\alpha}_m}$  are arbitrary constant spinors. The correctness of this transformation law can be demonstrated by explicit calculation (<sup>16</sup>). For the transformation (4.6), the minimum set (3.19) is invariant if the wave function transforms like

$$(6.4) \quad \begin{cases} u^{\alpha_2 \dots \alpha_m \dot{\beta}_2 \dots \dot{\beta}_n} = (1 + \alpha_{\lambda \bar{\rho}} x^{\lambda \bar{\rho}}) a_{\nu_2}^{\dot{\beta}_2} \dots a_{\nu_n}^{\dot{\beta}_n} u^{\alpha_2 \dots \alpha_m \dot{\nu}_2 \dots \dot{\nu}_n}, \\ v^{\dot{\alpha}_2 \dots \dot{\alpha}_m \beta_2 \dots \beta_n} = (1 + \alpha_{\lambda \bar{\rho}} x^{\lambda \bar{\rho}}) a_{\nu_2}^{\beta_2} \dots a_{\nu_n}^{\beta_n} v^{\dot{\alpha}_2 \dots \dot{\alpha}_m \nu_2 \dots \nu_n}. \end{cases}$$

Similar transformations leave the minimum sets (3.16) and (3.17) invariant under (4.6), while they are not invariant under the inversions, since they are not invariant under the improper Lorentz transformations.



The remaining minimum sets (3.18) and (3.20) are not invariant under either the inversions or the transformations (4.6). This may be seen as follows. First, to show that (3.20) is not invariant under the inversions, try a transformation law of the form

$$(6.5) \quad \begin{cases} u^{\alpha_2 \dots \alpha_m \dot{\beta}_2 \dots \dot{\beta}_n} = S_{\mu_2 \dots \mu_m \nu_2 \dots \nu_n}^{\alpha_2 \dots \alpha_m \dot{\beta}_2 \dots \dot{\beta}_n} v^{\mu_2 \dots \mu_m \dot{\nu}_2 \dots \dot{\nu}_n}, \\ v^{\alpha_2 \dots \alpha_m \beta_2 \dots \beta_n} = S_{\mu_2 \dots \mu_m \nu_2 \dots \nu_n}^{\alpha_2 \dots \alpha_m \beta_2 \dots \beta_n} u^{\mu_2 \dots \mu_m \dot{\nu}_2 \dots \dot{\nu}_n}, \end{cases}$$

which, with the help of the lemma of Sect. 4, can be shown to be the most general possible linear transformation law corresponding to an inversion. On substituting this and (5.1) into (3.20) one finds a set of conditions which must be satisfied by  $S_{\mu_2 \dots \mu_m \nu_2 \dots \nu_n}^{\alpha_2 \dots \alpha_m \dot{\beta}_2 \dots \dot{\beta}_n}$  and  $S_{\mu_2 \dots \mu_m \nu_2 \dots \nu_n}^{\alpha_2 \dots \alpha_m \beta_2 \dots \beta_n}$  in order for (3.20) to be invariant. However, these conditions are contradictory unless  $S_{\mu_2 \dots \mu_m \nu_2 \dots \nu_n}^{\alpha_2 \dots \alpha_m \dot{\beta}_2 \dots \dot{\beta}_n} = 0$ , and hence (3.20) cannot be made invariant with a linear transformation law for the wave function.

Now, from the invariance of (3.20) under the improper Lorentz transformations and the lack of invariance under the inversions, it follows by the lemma of Sect. 4 that (3.20) is not invariant under (4.6.) Furthermore, it is apparent on comparing (3.18) and (3.20) that if (3.18) were invariant under (4.6), then (3.20) would be also; thus (3.18) is not invariant under (4.6).

The results of this section are thus that the minimum sets (3.16), (3.17) and (3.19) are invariant under  $C^+$ , while (3.19) is also invariant under  $C$ . The minimum sets (3.18) and (3.20) are invariant under neither the inversions nor the transformations (4.6).

## 7. — The Conservation Laws.

It is well known that the existence of groups of transformations which leave a set of equations invariant is closely related to the existence of first integrals, or conservation laws, for the equations. An explicit statement of this fact is provided by a theorem due to NOETHER<sup>(4)</sup>. If a variational principle based on a Lagrangian is known to be invariant under a group of transformations, then Noether's theorem provides a direct method for obtaining the corresponding conservation laws. Thus, if an invariant Lagrangian can be given for any of Gårding's equations, it follows that corresponding conservation laws exist.

However, as noted in the introduction, all that is necessary for the validity of Bessel-Hagen's conservation laws (1.3) and (1.4) is that the symmetric energy-momentum tensor have zero trace. The only case for which this trace does not vanish and for which we have to make explicit use of Noether's theorem

rem is that of the scalar or pseudoscalar wave equation (3.21). This equation can be derived from the Lagrangian <sup>(17)</sup>

$$(7.1) \quad L = \frac{1}{2} \frac{\partial u}{\partial x_j} \frac{\partial u}{\partial x_j}.$$

The canonical energy-momentum tensor, which is symmetric, is

$$(7.2) \quad T_{jk} = \frac{\hat{\partial} u}{\partial x_j} \frac{\partial u}{\partial x_k} + L \delta_{jk}.$$

The variational principle depending on the Lagrangian (7.1) is conformally invariant, and the corresponding conservation laws follow directly from Noether's theorem. We obtain the expressions

$$(7.3) \quad \frac{\partial}{\partial x_j} \left( T_{jk} x_k - u \frac{\partial u}{\partial x_j} \right) = 0,$$

$$(7.4) \quad \frac{\partial}{\partial x_j} \left[ 2x_i x_k T_{jk} - x_k x_k T_{ij} + \delta_{ij} u^2 - 2x_i u \frac{\partial u}{\partial x_j} \right] = 0,$$

which can be verified by direct calculation. The terms involving  $T_{jk}$  are the same as in Bessel-Hagen's laws.

Next consider the case of non-zero spin. Gårding's equations provide more than one minimum set for each field with spin greater than one, since a field with spin  $f$  is represented by a spinor with  $2f$  indices, and such a spinor may have its indices distributed in  $2f+1$  ways between dotted and undotted indices. For some of the minimum sets corresponding to higher spin values, a simple Lagrangian formulation does not appear to be possible. Because of the intimate connection between conservation laws and the Lagrangian formalism, we will only consider those minimum sets for which a Lagrangian is available. However, in a certain sense the different wave equations for a fixed spin value are equivalent, as discussed by FIERZ <sup>(11)</sup>.

Consider first the fields of half-integral spin. If the wave function has a number of dotted indices differing by one from the number of undotted indices, then, following FIERZ <sup>(11)</sup>, we can form the Lagrangian

$$(7.5) \quad L = u_{\alpha_1 \dots \alpha_m \dot{\beta}_2 \dots \dot{\beta}_m} \dot{p}_{\dot{\beta}_1}^{\alpha_1} u^{\alpha_2 \dots \alpha_m \dot{\beta}_1 \dots \dot{\beta}_m} + \\ + v^{\dot{\alpha}_1 \dots \dot{\alpha}_m \beta_2 \dots \beta_m} p_{\beta_1}^{\dot{\alpha}_1} v^{\dot{\alpha}_2 \dots \dot{\alpha}_m \beta_1 \dots \beta_m} - \text{complex conjugate}.$$

$u^{\alpha_2 \dots \alpha_m \dot{\beta}_1 \dots \dot{\beta}_m}$  and  $v^{\dot{\alpha}_2 \dots \dot{\alpha}_m \beta_1 \dots \beta_m}$  are the complex conjugates of  $u^{\alpha_1 \dots \alpha_m \dot{\beta}_1 \dots \dot{\beta}_m}$  and

<sup>(17)</sup> G. WENTZEL: *Quantum Theory of Fields* (New York, 1949).

$\dot{q}^{\alpha_2 \dots \alpha_m \dot{\beta}_1 \dots \dot{\beta}_m}$  respectively. The Euler equations obtained from this Lagrangian are just the equations (3.7) with  $n = m + 1$ , plus their complex conjugates. These equations do not form a minimum set except when  $m = 1$ , but may be considered as «field equations», with the remaining equations necessary for a minimum set considered as «supplementary conditions».

The canonical energy-momentum tensor obtained from the Lagrangian (7.5) is

$$(7.6) \quad T_{\alpha\dot{\beta},\lambda\dot{q}}^c = u_{\alpha\alpha_2 \dots \alpha_m \dot{\beta}_2 \dots \dot{\beta}_m} \dot{p}_{\lambda\dot{q}}^{\alpha_2 \dots \alpha_m \dot{\beta}_2 \dots \dot{\beta}_m} + \\ + v_{\dot{\beta}_2 \dots \dot{\beta}_m \alpha_2 \dots \alpha_m} \dot{p}_{\lambda\dot{q}}^{\dot{\beta}_2 \dots \dot{\beta}_m \alpha_2 \dots \alpha_m} - \text{complex conjugate}.$$

Suppressing the dummy indices, one may write this more compactly as

$$(7.7) \quad T_{\alpha\dot{\beta},\lambda\dot{q}}^c = u_{\alpha} \dot{p}_{\lambda\dot{q}}^{\alpha} u_{\dot{\beta}} + v_{\dot{\beta}} \dot{p}_{\lambda\dot{q}}^{\dot{\beta}} v_{\alpha} - u_{\dot{\beta}} \dot{p}_{\lambda\dot{q}}^{\alpha} u_{\alpha} - v_{\alpha} \dot{p}_{\lambda\dot{q}}^{\dot{\beta}} v_{\dot{\beta}}.$$

This tensor, which is not symmetric, satisfies the conservation law

$$(7.8) \quad p^{\alpha\dot{\beta}} T_{\alpha\dot{\beta},\lambda\dot{q}}^c = 0.$$

However, if the wave function satisfies  $\square u = 0$ , then

$$p^{\alpha\dot{\beta}} T_{\lambda\dot{q},\alpha\dot{\beta}}^c = 0.$$

Thus the symmetric tensor

$$(7.9) \quad T_{\alpha\dot{\beta},\lambda\dot{q}} = \frac{1}{2}(T_{\alpha\dot{\beta},\lambda\dot{q}}^c + T_{\lambda\dot{q},\alpha\dot{\beta}}^c)$$

also satisfies the conservation law (7.8). Now, the trace of this symmetric tensor is zero by virtue of (3.7), and thus it follows that the conservation laws (1.3) and (1.4) are satisfied. These conservation laws are applicable to both minimum sets (3.19) and (3.20) with  $n = m + 1$ .

For integral spin, FIERZ <sup>(11)</sup> has studied the equations

$$(7.10) \quad \begin{cases} \square A_{jkl\dots} = 0, \\ \frac{\partial}{\partial x_j} A_{jkl\dots} = 0, \end{cases}$$

where  $A_{jkl\dots}$  is a symmetric tensor with zero trace. In analogy to the electromagnetic field, FIERZ treats the  $A_{jkl\dots}$  as «potentials» and defines the «fields» by

$$(7.11) \quad B_{[ij]kl\dots} = \frac{\partial A_{jkl\dots}}{\partial x_i} - \frac{\partial A_{ikl\dots}}{\partial x_j}.$$

Then the fields satisfy the first order equations

$$(7.12) \quad \frac{\partial}{\partial x_i} B_{[ij]kl\dots} = 0.$$

According to FIERZ, the above equations can be written in spinor notation as

$$(7.13) \quad p_{\dot{\beta}_2}^{\alpha_2} u^{\alpha_1\dots\alpha_m \dot{\beta}_2\dots\dot{\beta}_m} = 0, \quad p_{\beta_2}^{\dot{\alpha}_2} v^{\dot{\alpha}_1\dots\dot{\alpha}_m \beta_2\dots\beta_m} = 0.$$

$u^{\alpha_1\dots\alpha_m \dot{\beta}_2\dots\dot{\beta}_m}$  and  $v^{\dot{\alpha}_1\dots\dot{\alpha}_m \beta_2\dots\beta_m}$  are related to the tensor  $B_{[ij]kl\dots}$  in a manner similar to that used by LAPORTE and UHLENBECK (<sup>13</sup>) for the electromagnetic field. If  $B_{[ij]kl\dots}$  is to represent a real field, then  $u^{\alpha_1\dots\alpha_m \dot{\beta}_2\dots\dot{\beta}_m}$  and  $v^{\dot{\alpha}_1\dots\dot{\alpha}_m \beta_2\dots\beta_m}$  must be complex conjugates. Equations (7.13) are Gårding's minimum sets (3.19) with  $n = m - 2$ .  $u^{\alpha_1\dots\alpha_m \dot{\beta}_2\dots\dot{\beta}_m}$  and  $v^{\dot{\alpha}_1\dots\dot{\alpha}_m \beta_2\dots\beta_m}$  may be written in terms of potentials as

$$(7.14) \quad \begin{cases} u^{\alpha_1\dots\alpha_m \dot{\beta}_2\dots\dot{\beta}_m} = \dot{s} p_{\alpha_3}^{\dot{\beta}_2} \varphi^{\alpha_3\dots\alpha_m \dot{\beta}_3\dots\dot{\beta}_m}, \\ v^{\dot{\alpha}_1\dots\dot{\alpha}_m \beta_2\dots\beta_m} = s p_{\alpha_3}^{\beta_2} \varphi^{\dot{\alpha}_3\dots\dot{\alpha}_m \beta_3\dots\beta_m}. \end{cases}$$

The symmetric spinor  $\varphi^{\alpha_3\dots\alpha_m \dot{\beta}_3\dots\dot{\beta}_m}$  corresponds to the tensor  $A_{jkl\dots}$  (FIERZ did not use the operators  $s$  and  $\dot{s}$  in defining the fields in terms of the potentials. However, it follows from the Lorentz condition

$$\frac{\partial}{\partial x_j} A_{jkl\dots} = 0,$$

that our definition is equivalent to his.)

Now consider the Lagrangian

$$(7.15) \quad L = u_{\alpha_1\dots\alpha_m \dot{\beta}_2\dots\dot{\beta}_m} u^{\alpha_1\dots\alpha_m \dot{\beta}_2\dots\dot{\beta}_m} + v_{\dot{\alpha}_1\dots\dot{\alpha}_m \beta_2\dots\beta_m} v^{\dot{\alpha}_1\dots\dot{\alpha}_m \beta_2\dots\beta_m}$$

where  $u$  and  $v$  are to be considered as functions of  $\varphi$  as in (7.14). The equations of motion derived from this Lagrangian are

$$(7.16) \quad s p_{\dot{\beta}_2}^{\alpha_2} u^{\alpha_1\dots\alpha_m \dot{\beta}_2\dots\dot{\beta}_m} + \dot{s} p_{\alpha_2}^{\dot{\beta}_2} v^{\dot{\alpha}_1\dots\dot{\alpha}_m \beta_2\dots\beta_m} = 0.$$

From (7.14) it follows that

$$(7.17) \quad s p_{\dot{\beta}_2}^{\alpha_2} u^{\alpha_1\dots\alpha_m \dot{\beta}_2\dots\dot{\beta}_m} - \dot{s} p_{\alpha_2}^{\dot{\beta}_2} v^{\dot{\alpha}_1\dots\dot{\alpha}_m \beta_2\dots\beta_m} = 0.$$

Equations (7.16) and (7.17) are Gårding's equations (3.7a) and (3.7b). They

do not form a minimum set unless  $m = 3$ , which gives Maxwell's equations. However, they are a part of both minimum sets (3.19) and (3.20). As with the cases of half-integral spin, (7.16) and (7.17) may be considered as field equations, with the remaining equations necessary to form a minimum set as supplementary conditions.

The energy-momentum tensor found by FIERZ for these equations is

$$(7.18) \quad T_{jk} = B_{[ik]mn\dots} B_{[ij]mn\dots} - \frac{1}{4} \delta_{jk} B_{[mn]rs\dots} B_{[mn]rs\dots}.$$

This tensor is obviously symmetric, and has zero trace. Thus it satisfies the conservation laws (1.3) and (1.4). It was given by FIERZ for the field equations (7.12) only. However, it can be shown that it satisfies the conservation law (1.1) even if only the weaker conditions corresponding to (7.16) and (7.17) are satisfied. Thus the tensor (7.18) is applicable to both minimum sets (3.19) and (3.20) with  $m = n - 2$ .

## 8. - Summary.

It has been shown that all of Gårding's irreducible equations (3.2)-(3.12) are invariant under the restricted conformal group  $C^+$ , while (3.6)-(3.12) are in addition invariant under the full conformal group  $C$ . It has also been shown that the minimum sets (3.16) and (3.17) are invariant under  $C^+$ , (3.19) and (3.21) are invariant under  $C$ , while the minimum sets (3.18) and (3.20) are not invariant under either the inversion (4.2) or the transformation (4.6).

In addition, the conservation laws corresponding to the conformal invariance have been given, for those minimum sets for which a Lagrangian is available. These minimum sets include the scalar wave equation and the equations given by FIERZ for zero rest mass. In all cases the conservation laws are formally identical with those found by BESSEL-HAGEN, with the exception of the scalar field, whose conservation laws contain extra terms arising from the fact that the trace of the energy-momentum tensor is not zero. The new conservation laws (1.3) and (1.4) have been shown to hold for certain of the minimum sets (3.20), even though these minimum sets are not conformally invariant. The reason for this is that conformal invariance of the field equations only is sufficient to assure the existence of the conservation laws.

\* \* \*

The author wishes to express his appreciation to Professor PETER HAVAS, who suggested this problem and made numerous valuable suggestions during the course of the work.



## APPENDIX

The lemma of Sect. 4 is apparently known to mathematicians, but we have not been able to find an explicit reference to it. Consequently a proof is presented here. It is most easily proven by treating the conformal transformations of space-time as linear homogeneous transformations of a five-dimensional projective space<sup>(5,8)</sup>. Let  $y_\mu$  ( $\mu = 1, \dots, 6$ ) be homogeneous coordinates in the five dimensional space. Then points on the hyperquadric

$$(A.1) \quad y_\mu y_\mu = 0,$$

correspond to the points of space-time as

$$(A.2) \quad x_j = \frac{y_j}{y_5 + iy_6},$$

$y_4$  and  $y_6$  are pure imaginary, while all others are real. Then the conformal transformations of the  $x_j$  correspond to those linear homogeneous transformations of the  $y_\mu$  which leave equation (A.1) invariant, i.e., the transformations

$$y'_\mu = a_{\mu\nu} y_\nu,$$

where

$$a_{\mu\nu} a_{\mu\lambda} = k \delta_{\nu\lambda}.$$

In particular, the infinitesimal transformations

$$(A.3) \quad y'_\mu = y_\mu + \xi_{\mu\nu} y_\nu, \quad \xi_{\mu\nu} = -\xi_{\nu\mu},$$

induce the infinitesimal transformations (4.3)-(4.6).

Also a reflection in the  $y$ -space, say

$$y'_1 = -y_1,$$

$$y'_\mu = y_\mu, \quad \mu \neq 1,$$

corresponds to

$$x'_1 = -x_1,$$

$$x'_j = x_j, \quad j \neq 1,$$

while the reflection

$$y'_5 = -y_5,$$

$$y'_\mu = y_\mu, \quad \mu \neq 5,$$

corresponds to the inversion

$$x'_j = x_j / (x_k x_k) .$$

To prove the lemma, note that from the infinitesimal transformations (A.3), or (4.3)-(4.6), a finite transformation can be obtained which corresponds to the rotation in  $y$ -space

$$(A.4) \quad \begin{cases} y'_1 = y_5 , \\ y'_5 = -y_1 , \\ y'_\mu = y_\mu , \end{cases} \quad \mu \neq 1, 5 ;$$

If this is followed by the inversion

$$\begin{aligned} y'_5 &= -y_5 , \\ y'_\mu &= y_\mu , \end{aligned} \quad \mu \neq 5 ,$$

and then the inverse of the transformation (A.4), the result is the reflection

$$\begin{aligned} y'_1 &= -y_1 , \\ y'_\mu &= y_\mu , \end{aligned} \quad \mu \neq 1 ,$$

or

$$\begin{aligned} x'_1 &= -x_1 , \\ x'_j &= x_j , \end{aligned} \quad j \neq 1 .$$

From this reflection and the proper orthochronous Lorentz transformations one can obtain all improper orthochronous Lorentz transformations. The antichronous transformations can then be obtained by addition of the transformation  $x'_j = -x_j$ , which in turn results from two inversions with constants  $k, -k$ . This proves the first part of the lemma.

To prove the second part, make the transformation (A.4), then the reflection

$$\begin{aligned} y'_1 &= -y_1 , \\ y'_\mu &= y_\mu , \end{aligned} \quad \mu \neq 1 ,$$

or

$$\begin{aligned} x'_1 &= -x_1 , \\ x'_j &= x_j , \end{aligned} \quad j \neq 1 ,$$

and then the inverse of (A.4). The result is the inversion.

## RIASSUNTO (\*)

Si dimostra che le equazioni d'onda relativistiche ottenute da GÄRDING per particelle di massa a riposo nulla e spin arbitrario sono invarianti nelle trasformazioni conformi dello spazio-tempo. Si ottengono leggi di conservazione corrispondenti a detta invarianza. Sono formalmente identiche a quelle trovate da BESSEL-HAGEN per il campo elettromagnetico, ad eccezione di quelle trovate per il campo scalare. Per questo caso le leggi di conservazione contengono termini aggiuntivi che originano dal fatto che la traccia del tensore energia-impulso non è zero.

---

(\*) *Traduzione a cura della Redazione.*

# The Coupling Constant of $p$ -Wave Pion Nucleon Scattering.

M. CINI

*Istituto di Fisica dell'Università - Catania*  
*Istituto Nazionale di Fisica Nucleare - Sezione di Torino*

S. FUBINI

*Istituto di Fisica dell'Università - Torino*  
*Istituto Nazionale di Fisica Nucleare - Sezione di Torino*

A. STANGHELLINI

*Istituto di Fisica dell'Università - Bologna*  
*Istituto Nazionale di Fisica Nucleare - Gruppo di Bologna*

(ricevuto il 17 Marzo 1956)

**Summary.** — Introducing the experimental data for the phase-shift  $\delta_{33}$  of the pion-nucleon scattering, in the Low equation, we have determined the renormalized  $p$ -wave coupling constant  $f^2$ , and we have obtained:  $f^2 = 0.107 \pm 0.006$ . The reliability of this result is discussed.

## 1. — Introduction.

One of the main problems of meson theory is the determination of the renormalised  $p$ -wave coupling constant  $f^2$  from experiments. A major step in this direction has been performed by G. F. CHEW and F. Low <sup>(1)</sup> by giving an approximate solution of the one-meson approximation of the Low <sup>(2)</sup> equation in the form of an effective range formula for the dominant  $\delta_{33}$  phase-shift. Since the experimental values of the phase-shift lie with good appro-

<sup>(1)</sup> G. F. CHEW and F. E. Low: *Proc. Fifth Rochester Conf.* (1955), p. 21 and ff.; see also: *Theory of  $p$ -wave pion nucleon scattering at low energies*, preprint.

<sup>(2)</sup> F. E. Low: *Phys. Rev.*, **97**, 1392 (1955).

ximation on the straight line,

$$(1) \quad \frac{k^3}{\omega_k} \cotg \delta_{33} = 9.3 \left( 1 - \frac{\omega_k^*}{2.15} \right) \quad \omega_k^* = \omega_k + \frac{k^2}{2M},$$

by extrapolating to zero energy one obtains:

$$(2) \quad f^2 = \frac{3}{4} \frac{1}{9.3} = 0.081.$$

However some criticism has been raised against the above mentioned procedure especially because CASTILLEJO, DALITZ and DYSON<sup>(3)</sup> have shown that an infinite set of solutions are possible for the Low equation in the one-meson approximation and no particular reason seems to exist for choosing the one selected by Chew and Low. Furthermore the zero energy extrapolation does not seem very reliable because no strong theoretical argument exists predicting a linear behaviour in the gap between zero and the meson rest energy.

In addition the slope of the straight line (1) is not clearly determined from experiment.

The purpose of the present work is to determine  $f^2$ , not by attempting an explicit solution of the Low equation, but rather by using this equation as an exact sum rule relating real and imaginary parts of the scattering amplitudes.

## 2. - The Low Equation as a Sum-Rule.

We write the Low equation for the scattering amplitude  $g_3(\omega)$  (i.e. the eigenvalue of the transition matrix  $-\pi T(\omega)$  in the state  $J = \frac{3}{2}$ ,  $T = \frac{3}{2}$ )<sup>(4)</sup>. For purely elastic scattering  $g_3 = \exp[i\delta_{33}] \sin \delta_{33}$

$$(3) \quad \text{Re } g_3(\omega_q) = \frac{4}{3} f^2 \frac{q^3 v^2(q)}{\omega_q} + \frac{q^3 v^2(q)}{\pi} P \int_1^\infty \frac{d\omega_p}{p^3 v^2(p)} \cdot \left\{ \frac{\text{Im } g_3(\omega_p)}{\omega_p - \omega_q} + \frac{1}{9} \frac{\text{Im} [4g_1(\omega_p) + 4g_2(\omega_p) + g_3(\omega_p)]}{\omega_p + \omega_q} \right\},$$

$P$  means principal value.  $r^2(q)$  is the source form factor whose only property

(3) Y. CASTILLEJO, R. H. DALITZ and F. J. DYSON: *Phys. Rev.*, **101**, 453 (1956).

(4) See e.g. M. CINI and S. FUBINI: *Nuovo Cimento*, **3**, 764 (1956), eqs. (3), (7), (15). In the following all energies and momenta will be measured in units of the meson mass.



used in the following is:

$$v^2(q) = 1 \quad \text{for} \quad \omega_q \leq \xi,$$

where  $\xi$  does not need to be precisely specified as long as it is taken greater than  $\sim 4$ .

For the values  $\omega_q$  well below the cut-off in which we are interested  $v^2(q) = 1$  and  $\text{Re } g_3 = \sin \delta_{33} \cos \delta_{33}$ . We remark that, for these same values of  $\omega_q$  the contributions to the integrals arising from energies above the cut-off  $\xi$  can be approximated by neglecting  $\omega_q$  in the denominators compared with  $\omega_p$ . In the low energy region the contributions of the scattering amplitudes  $g_1(\omega_p)$ ,  $g_2(\omega_p)$  are completely negligible both because of their smallness and because they appear with  $\omega_p + \omega_q$  in the denominator.

By defining:

$$(4) \quad X(\omega_q) = \frac{1}{\pi} P \int_1^{\xi} \frac{d\omega_p}{p^3} \text{Im } g_3(\omega_p) \left[ \frac{1}{\omega_p - \omega_q} + \frac{1}{9} \frac{1}{\omega_p + \omega_q} \right],$$

$$(5) \quad Y = \frac{1}{\pi} \int_{\xi}^{\infty} \frac{d\omega_p}{\omega_p p^3 v^2(p)} \text{Im} \left[ \frac{10}{9} g_3(\omega_p) + \frac{4}{9} g_2(\omega_p) + \frac{4}{9} g_1(\omega_p) \right],$$

eq. (3) becomes:

$$(6) \quad \left[ \frac{\sin \delta_{33}(\omega_q) \cos \delta_{33}(\omega_q)}{q^3} - X(\omega_q) \right] \omega_q = \frac{4}{3} f^2 + Y \omega_q.$$

By introducing in eqs. (6) and (4) the experimental data we will deduce:

a) the best value of the renormalized coupling constant  $f^2$  suggested by the experiment;

b) the order of magnitude of the essential positive parameter  $Y$  which summarizes all the unknown high energy effects.

### 3. — Numerical Results and Discussion.

Our analysis will be limited to energies of the incident pion  $\omega_q$  below the resonance, which occurs approximately at 190 MeV ( $\omega_q \sim 1.9$ ). The reasons for this are twofold: first because the experimental situation is not very clear at higher energies, and second because our assumption of the energy independence of the parameter  $Y$  begins to be less justified when  $\omega_q$  approaches the cut-off.

The values of  $\text{Im } g_3(\omega_q)$  to be introduced in the integral of eq. (4) are obtained from the available experimental data <sup>(5)</sup> of  $\delta_{33}$  up to  $\omega_p = 2.4$  (300 MeV in the laboratory system) using the relation:

$$\text{Im } g_3(\omega_p) = \sin^2 \delta_{33}.$$

Since above this energy no reliable phase-shift analysis can be performed because of the importance of inelastic processes we shall use the relation:

$$\text{Im } g_3(\omega_p) = 8\pi p^2 \sigma^+(\omega_p),$$

where  $\sigma^+(\omega_p)$  is the total positive pion cross-section <sup>(6)</sup>. We remark that the error introduced with this assumption is extremely small since the contribution to  $X(\omega_p)$  from the energy range  $3 \lesssim \omega_p \lesssim \xi$  is of the order of a few percent at most. The function  $X(\omega_q)$  has been calculated numerically after having subtracted the singularity, namely

$$P \int \frac{f(\omega_p)}{\omega_p - \omega_q} d\omega_p = f(\omega_q) P \int \frac{d\omega_p}{\omega_p - \omega_q} + \int \frac{f(\omega_p) - f(\omega_q)}{\omega_p - \omega_q} d\omega_p,$$

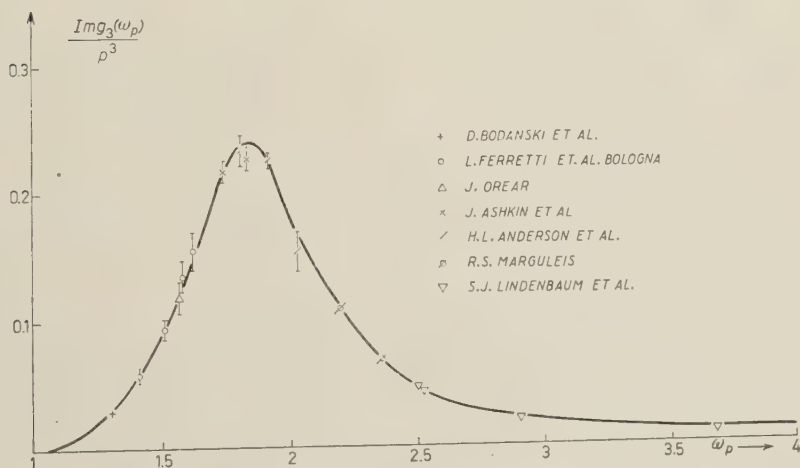


Fig. 1. — Experimental points  $[\text{Im } g_3(\omega_p)]/p^3$  plotted versus pion total energy in c. m. s. For reference see <sup>(5)</sup> and <sup>(6)</sup>.

<sup>(5)</sup> J. OREAR: *Phys. Rev.*, **96**, 176, 1417 (1955); L. FERRETTI, E. MANARESI, G. PUPPI, G. QUARENI and A. RANZI: *Nuovo Cimento*, **1**, 1238 (1955); G. PUPPI: *Proc. of Rochester Conf.* (1956); J. ASHKIN, J. P. BLASER and M. O. STERN: preprint; H. L. ANDERSON and M. GLICKSMAN: *Phys. Rev.*, **100**, 268 (1955); H. L. ANDERSON, W. C. DAVIDON, M. GLICKSMAN and V. E. KRUSE: *Phys. Rev.*, **100**, 279 (1955); H. TAFT: preprint; R. S. MARGULEIS: *Bulletin of the American Society*, **7** (1955).

<sup>(6)</sup> S. J. LINDENBAUM and L. C. L. YUAN: *Phys. Rev.*, **100**, 306 (1955). In this equation  $\sigma^+$  is measured in units  $\mu^2$ . The conversion in millibarns must be done by using  $(\hbar/\mu c)^2 \cong 20 \text{ mb}$ .

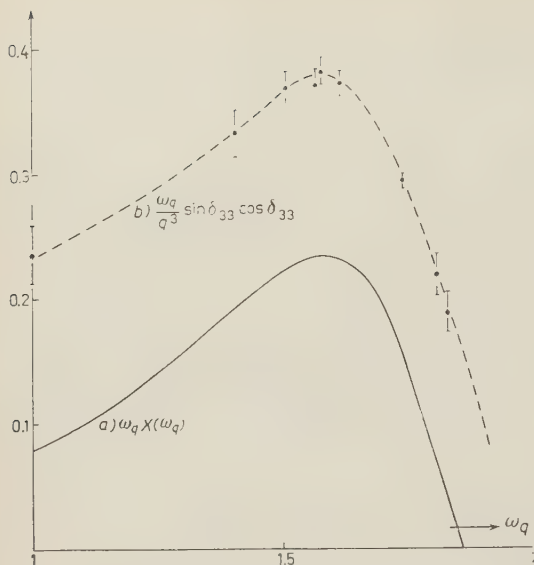


Fig. 2. - Curve *a* represents  $\omega_q X(\omega_q)$  as obtained from numerical calculation. Curve *b* is a line connecting the experimental points

$$\omega_q (\sin \delta_{33} \cos \delta_{33}) / q^3.$$

reference between the ordinates of the two curves suggests, according to eq. (6) that  $Y = 0$ . In Fig. 3 this difference is plotted. The errors on this difference have been evaluated by taking into account, in addition to the experimental errors of curve *b*) (Fig. 2), also a relative error in  $X(\omega_q)$  equal to the relative error of  $\sin^2 \delta_{33}(\omega_q)$ .

The parameters  $f^2$  and  $Y$  have been evaluated with a least squares fit to the points in Fig. 3. The result is

$$f^2 = 0.126 \pm 0.012,$$

$$Y = -0.010 \pm 0.012.$$

Fig. 3. - The differences of curve *a* and *b* Fig. 2 are plotted versus  $\omega_q$ .  $f^2 = 0.07 \pm 0.010$  represents the mean value of the ordinates when  $Y$  is taken equal to zero.

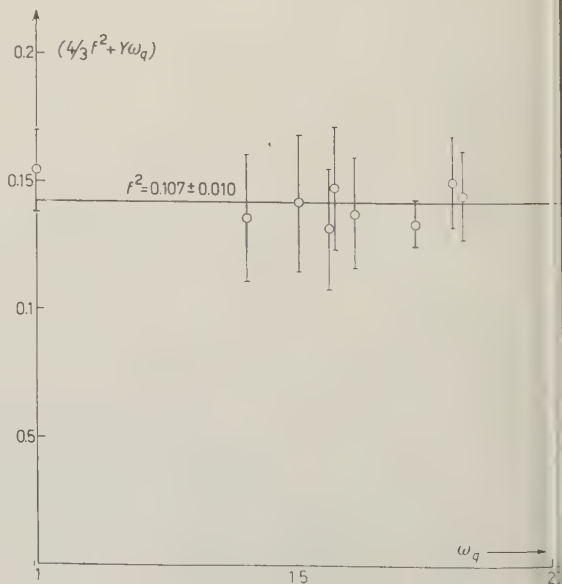
where the function  $f(\omega_p) = \text{Im } g_3(\omega_p) / p^3$  given by experiment is plotted in Fig. 1. Curve *a*) in Fig. 2 represents  $\omega_q X(\omega_q)$  obtained with the procedure outlined above.

The points of curve *b*) in Fig. 2 represent the experimental values of the quantity

$$(\omega_q \sin \delta_{33} \cos \delta_{33}) / q^3 \quad (5).$$

Errors for these points are deduced from the errors in the phase-shifts given by the respective authors when available, and in other cases by attributing to  $\delta_{33}$  the error in the total cross section. The error in the points at zero kinetic energy has been estimated of the order of 10%.

The constance of the difference



We notice that no inconsistency arises from the slightly negative value of  $Y$  (essentially a positive quantity) because the error is larger than its absolute value. The most reliable value for  $Y$  seems therefore  $Y = 0$ . In this case  $f^2$  obtained from the average of the experimental points is

$$(7) \quad f^2 = 0.107 \pm 0.006,$$

the error is the standard error.

Some additional information can be obtained with the aid of other considerations about the zero kinetic energy behaviour of  $\delta_{33}$ . Very general quantum mechanical arguments which hold for all short range interactions suggest that the low energy dependence of  $\delta_{33}$  should be of the type

$$(8) \quad \delta_{33}(\omega_q) = \alpha q^3.$$

Therefore

$$(9) \quad \left[ \frac{d}{d\omega_q} \left( \frac{\sin \delta_{33}(\omega_q) \cos \delta_{33}(\omega_q)}{q^3} \right) \right]_{q=0} = \left[ \frac{d}{d\omega_q} \left( \frac{\delta_{33}(\omega_q)}{q^3} \right) \right]_{q=0} = 0.$$

Relation (9) does not contain the constant  $\alpha$  and therefore has the advantage of giving a determination of  $f^2$  independent of the zero kinetic energy experimental point. Differentiation of eq. (6) yields:

$$(10) \quad \frac{4}{3} f^2 - \left[ \frac{d}{d\omega_q} X(\omega_q) \right]_{q=0} = \frac{1}{\pi} \int_1^\xi \sin^2 \delta_{33} \left[ \frac{1}{p^3} \left[ \frac{1}{(\omega_p - 1)^2} - \frac{1}{9(\omega_p - 1)^2} \right] \right] d\omega_q.$$

The integral in eq. (10) has the advantage that the square power in the denominator ensures a very rapid convergence, thus minimizing the effect of the imperfect knowledge of the phase-shifts at energies above resonance. In fact the contributions above  $\omega_p \sim 2.5$  amount to less than 1%. Eq. (10) gives:

$$(11) \quad f^2 = 0.1.$$

Comparison between (11) (deduced without need of specifying  $Y$ ) and the value (7) confirms our choice of  $Y = 0$ .

Another check is obtained by considering the behaviour in the neighbourhood of  $\delta_{33} = 45^\circ$ . The following argument illustrates the reason of this choice. The quantity  $\sin \delta_{33} \cos \delta_{33}$  vanishes both for  $\delta_{33} = 0$  and  $\delta_{33} = 90^\circ$ . Its expression:

$$(12) \quad \sin \delta_{33} \cos \delta_{33} = q^3 \left[ \frac{4}{3} \frac{f^2}{\omega_q} + X(\omega_q) \right],$$

reaches a maximum value in the interval between  $\omega_q = 1$  and  $\omega_q \cong 1.9$ . The value of this maximum must be exactly 0.5; a larger value is obviously inconsistent, and a smaller value would mean that the phase-shift cannot reach  $45^\circ$ . In this case for reason of continuity the phase-shift would decrease to zero at  $\omega_q \cong 1.9$ , in contrast with the experimental resonance. By imposing the fulfillment of this condition one obtains another determination of  $f^2$  which turns out to be in remarkable agreement with eqs. (11) and (7):

$$(13) \quad f^2 = 0.103 .$$

We therefore conclude that the value (7) can be considered a reliable evaluation of the coupling constant for  $p$ -wave pion nucleon scattering from experiment. It is remarkable that this value is not very different from the one obtained by CHEW and LOW. However the results of a recent investigation (4) show that the one-meson approximation may lead to strong inconsistencies and therefore, in our opinion, should not be trusted too much.

We want to emphasize that the theoretical assumptions, underlying this determination, are only the validity of the Low sum-rule (based essentially only on causality) and the neglect of nucleon recoil in the low energy region.

---

#### RIASSUNTO

Introducendo i dati sperimentali per la fase  $\delta_{33}$  dello scattering pione-nucleone nell'equazione di Low, si è determinato la costante d'accoppiamento per le onde  $p$  e si è ottenuto:  $f^2 = 0.107 \pm 0.006$ . Si discute l'attendibilità di questo risultato.



# On the Production of Heavy Mesons in the Nucleon-Nucleon Collisions at Energies Near the Threshold.

P. BROVETTO and S. FERRONI

*Istituto Nazionale di Fisica Nucleare - Sezione di Torino*

(ricevuto il 26 Marzo 1956)

**Summary.** — Calculations based on the statistical theory are made for the production of pions and heavy mesons in nucleon-nucleon collision energies below 10 GeV in the laboratory system. Multiplicities are derived as functions of energy, and the energy spectra for the various kinds of particles are given. Average multiplicities as a function of the energy spectrum of the protonic component in cosmic radiation are also given.

## 1. — Introduction.

In the statistical treatment of nucleon collisions at high energy (\*), the probabilities for elastic scattering and for scattering with production of one or more pions are related to the corresponding statistical weights obtainable from the fundamental equation:

$$(1) \quad S(n, s) = \frac{\Omega^{n+s}}{(8\pi^3 \hbar^3)^{n+s}} \frac{dQ(W)}{dW}.$$

In equation (1)  $n$  and  $s$  are the numbers of pions and nucleons respectively,  $\Omega$  is the volume of interaction,  $W$  is the total energy in the center of mass system, and  $Q(W)$  is the volume of the momentum space inside the surface of energy  $W$ .

---

(\*) G. WATAGHIN: *Symposium sobre Raios Cosmicos* (Rio de Janeiro, 1941);  
E. FERMI: *Progr. Theor. Phys.*, **5**, 570 (1950).

## 2. - Statistical Formulae.

Equation (1) can be immediately extended to processes of production in which heavy mesons would compete with pions.

In this case, the conservation of energy in the center of mass system, can be written:

$$(2) \quad \sum_1^s \frac{p_i^2}{2M} + \sum_1^r \frac{p_j^2}{2m} + \sum_1^n cp_k = W - sMc^2 - rmc^2.$$

In equation (2),  $s$  and  $M$  are the number and mass of nucleons, respectively,  $r$  and  $m$  the number and mass of heavy mesons,  $W$  the total energy.

We have supposed, following Fermi, that nucleons are classical and pions extremely relativistic particles. Because of the considerable rest mass, we have treated the heavy mesons as classical particles. As a matter of fact the conservation of momentum and angular momentum further limits the volume of phase space available for the system. By evaluating the volume of the phase space included in the surface of equation (2) (\*) and taking into account the conservation of momentum, we obtain immediately the generalized expression for the statistical weights:

$$(3) \quad S(n, r, s) = K(s, w) \frac{1}{(3w)^{(r/2)}} \left( \frac{m}{\mu} \right)^{(3r/2)} \left( \frac{s}{s + r(m/M)} \right)^{\frac{3}{2}} \cdot \frac{\left[ \frac{2}{(3\pi)^{\frac{1}{2}}} \frac{M}{\mu} \frac{1}{w^{\frac{1}{2}}} \left( w - s - r \frac{m}{M} \right) \right]^{3n + 3(s+r)/2 - \frac{5}{2}}}{\Gamma \left( 3n + 3 \frac{s + r - 1}{2} \right)}$$

In equation (3)  $w$  is the energy  $W$  expressed in  $Mc^2$  units,  $\mu$  is the mass of pions, and  $K(s, w)$  for  $s = 2$  is a normalization coefficient irrelevant for the determination of the probabilities of  $n$  and  $r$ .

Using the statistical procedure we have just outlined, we may also deduce the energy spectrum for both pions and classical particles.

For this purpose, it is sufficient to evaluate the part of the surface (2) relative to an infinitesimal interval of the momentum of the particle we con-

(\*) For the procedure see for example: J. WILLARD GIBBS: *Elementary Principles in Statistical Mechanics* (Yale University Press, 1948); J. V. LEPORE and R. M. STUART: *Phys. Rev.*, **94**, 1724 (1954).

sider. As a function of kinetic energy  $\vartheta$  we obtain:

$$(4) \quad P(\vartheta) d\vartheta = \frac{2}{\sqrt{\pi}} \frac{I[\frac{3}{2}(s+r) + 3n]}{I[\frac{3}{2}(s+r-1) + 3n]} \frac{\sqrt{\vartheta}}{(W - sMc^2 - rmc^2)^{\frac{3}{2}}} \cdot \left[ 1 - \frac{\vartheta}{W - sMc^2 - rmc^2} \right]^{\frac{3}{2}(s+r) + 3n - \frac{5}{2}} d\vartheta,$$

for the classical particles, and

$$(4') \quad P(\vartheta) d\vartheta = \frac{1}{2} \frac{I[\frac{3}{2}(s+r) + 3n]}{I[\frac{3}{2}(s+r) + 3(n-1)]} \frac{\vartheta^2}{(W - sMc^2 - rmc^2)^3} \cdot \left[ 1 - \frac{\vartheta}{W - sMc^2 - rmc^2} \right]^{\frac{3}{2}(s+r) + 3n - 4} d\vartheta,$$

for extremely relativistic particles.

From equations (4), (4'), we obtain for the mean values of kinetic energy

$$\bar{\vartheta}_{\text{class.}} = \frac{W - sMc^2 - rmc^2}{s + r + 2n}; \quad \bar{\vartheta}_{\text{rel.}} = 2 \frac{W - sMc^2 - rmc^2}{s + r + 2n}.$$

For the most probable values, we obtain the equations

$$\vartheta_{\text{P class.}} = \frac{W - sMc^2 - rmc^2}{3(s+r-1) + 6n-1}; \quad \vartheta_{\text{P rel.}} = 4 \frac{W - sMc^2 - rmc^2}{3(s+r-1) + 6n-1},$$

i.e., the mean kinetic energy of pions is twice the mean kinetic energy of nucleons and heavy mesons; on the other hand, for the most probable values, we obtain 4 as a factor.

### 3. - Discussion.

By means of equation (4) and putting  $M = 1840 m_e$ ,  $m = 966 m_e$ ,  $\mu = 273 m_e$  we have evaluated (Table I) the relative probabilities of elastic

TABLE I. - Probabilities of events with  $n$  pions and  $r$  heavy mesons for some values of kinetic energy (Lab. system) of the incident nucleon.

	1.5 GeV		3 GeV		5 GeV			7.5 GeV				10 GeV			
	0	1	0	1	0	1	2	0	1	2	3	0	1	2	3
$n \backslash r$															
0	29.4	3.8	4.4	9.9	0.6	3.6	1.4	0.1	0.9	1.2	0.1	—	0.2	0.6	0.3
1	57.3	—	42.1	3.4	17.4	7.3	0.2	5.4	5.2	1	—	1.9	2.8	1.2	0.1
2	9.1	—	32.7	0.2	38.3	2.6	—	25.6	5.5	0.2	—	14.3	5.7	0.6	—
3	0.4	—	6.7	—	22.4	0.3	—	31.9	2	—	—	29.5	4.0	0.1	—
4	—	—	0.6	—	5.3	—	—	16	0.3	—	—	24.5	1.2	—	—
5	—	—	—	—	0.6	—	—	4	—	—	—	10.1	0.2	—	—
6	—	—	—	—	—	—	—	0.6	—	—	—	2.4	—	—	—
7	—	—	—	—	—	—	—	—	—	—	—	0.3	—	—	—

collision and collision with production of  $n$  pions and  $r$  heavy mesons for several values of the kinetic energy in the laboratory system. The multipli-

cities of the pions remain substantially those predicted by FERMI.

Heavy mesons at low energies are found mostly not associated with pions.

When the energy increases, the most probable events are those in which the heavy mesons are found together with one, two or, at most three pions.

The mean multiplicities  $\bar{n}_\pi$ ,  $\bar{n}_K$  of the pions and the heavy mesons are given in Fig. 1 as a function of the kinetic energy in the laboratory system.

The curve for  $\bar{n}_K$  shows near 2.6 GeV a sudden variation which corresponds to the threshold for the production of two heavy mesons.

In the same figure we also give  $\varrho = \bar{n}_K/(\bar{n}_\pi + \bar{n}_K)$ ; for energies just above the threshold,  $\varrho$  passes through a maximum.

From these results, the proportion of heavy mesons appears to be too great in relation to the available experimental data.

The energy spectra for classical and extremely relativistic particles, calculated by means of equations (4) and (4') are given in Fig. 2, for the case in which one pion and one heavy meson are produced at the energy of 5 GeV in the laboratory system.

Further improvements of the theory, such as the introduction of angular momentum conservation and of statistical correlations among the particles, would lower the multiplicities.

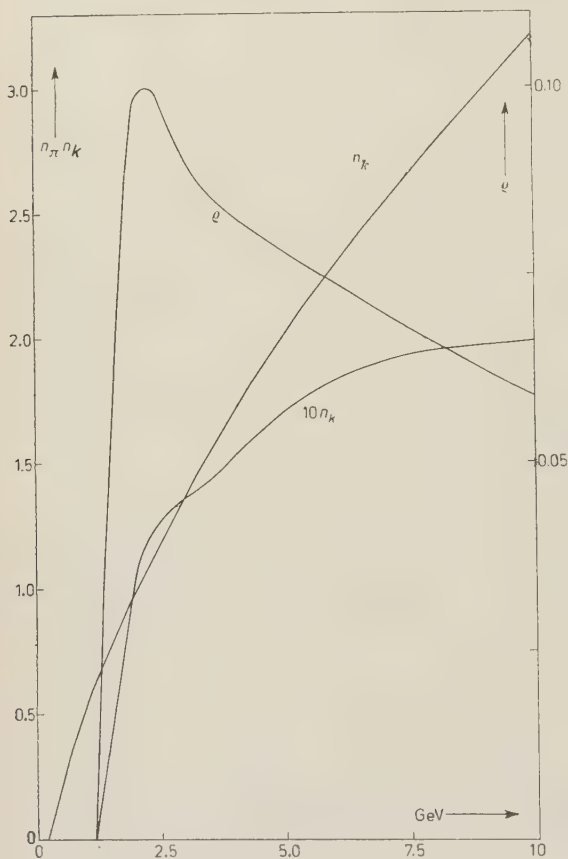


Fig. 1. — Graph showing the average multiplicities  $\bar{n}_\pi$  and  $\bar{n}_K$  of pions and heavy mesons, and the relative multiplicity  $\varrho = \bar{n}_K/(\bar{n}_\pi + \bar{n}_K)$  of heavy mesons as functions of kinetic energy (lab. system) of the incident nucleon.

Also charge effects would alter the multiplicities (\*). The usefulness of these corrections is however somewhat doubtful because the approximation of treating the pion as extremely relativistic and the nucleons and heavy mesons as classical particles introduces errors at least as great as those produced by the omission of the mentioned corrections.

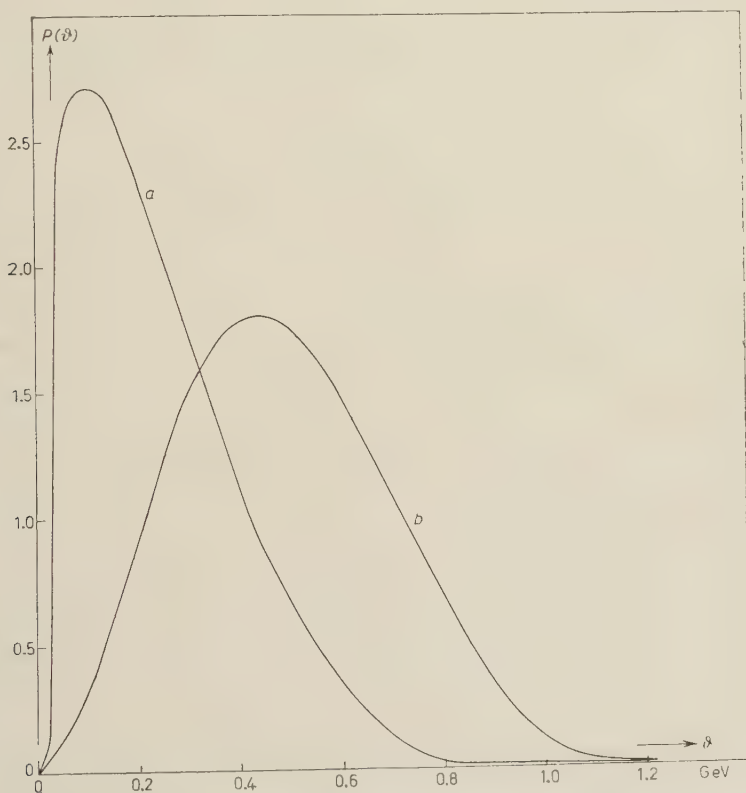


Fig. 2. -- Energy spectra in the center of mass system for classical (curve *a*) and relativistic (curve *b*) particles.

Our results give therefore only qualitative tendencies. For energies greater than 10 GeV, it may be a better approximation to consider heavy mesons as extremely relativistic particles.

In that case their multiplicity differs from the multiplicity of the pions only because of statistical weights associated to spin and isotopic spin.

Consequently when the primary energy goes above 10 GeV, heavy meson

(\*) U. HABER-SCHAIM, Y. YEIVIN and G. YEKUTIEL: *Phys. Rev.*, **94**, 184 (1954).



multiplicities grow rapidly and become for high energies, of the same order of the pion multiplicities.

In other words, as a consequence of the statistical hypothesis the curve of the relative multiplicity shows a maximum near the threshold, a minimum near 10 GeV and gradually grows up to a practically constant value for energies of the order of  $10^3 \div 10^4$  GeV.

Taking into account the energy spectrum of the protons in cosmic radiation (\*), we have calculated for energies between 1 and 10 GeV (Table II) the mean probabilities of the events for various numbers of the two types of particles. The mean values for the number of pions and heavy mesons are respectively  $\bar{n}_\pi = 1.3$ ,  $\bar{n}_K = 0.11$ , corresponding to  $\rho = \bar{n}_K / (\bar{n}_\pi + \bar{n}_K) = 0.078$ .

This value is slightly lower if the considered energy range starts from values greater than 1 GeV.

TABLE II. — Probabilities of events with  $n$  pions and  $r$  heavy mesons for the proton component of cosmic radiation in the energy range from 1 to 10 GeV.

$n \backslash r$	0	1	2
0	11.8	7	0.3
1	43.1	2.5	0.1
2	23.6	0.9	—
3	7.8	0.2	—
4	2.1	—	—
5	0.5	—	—
6	0.1	—	—

From Table II we see that the greatest probability is for the case of heavy mesons produced not associated to pions.

It is evident that if the observed energy range starts from values above 1 GeV, the probability becomes favorable to heavy mesons accompanied by one or more pions.

\* \* \*

The authors wish to thank Prof. G. WATAGHIN for his constant interest and for many stimulating discussions.

(\*) W. HEISENBERG: *Kosmische Strahlung* (Berlin, 1953).

## RIASSUNTO

Si eseguiscano calcoli, mediante la teoria statistica, sulla produzione di pioni e mesoni K nelle collisioni di nucleoni ad energie inferiori a 10 GeV nel sistema del laboratorio. Si deducono le molteplicità in funzione dell'energia e gli spettri di energia per i vari tipi di particelle. Sono pure date le molteplicità medie in funzione dello spettro di energia della componente protonica nella radiazione cosmica.

## Exclusion Principle Inhibition of Bound Hyperon Mesonic Decay.

H. PRIMAKOFF

*Physics Department, Washington University (\*) - St. Louis, Missouri, U.S.A.  
Clarendon Laboratory, Oxford University - Oxford, England*

(ricevuto il 26 Marzo 1956)

**Summary.** — An explanation is given of the variation with  $A$ ,  $Z$ , of 1): the ratio of the probabilities of mesonic to nonmesonic decay of hyperfragments and 2): the mean life of the hyperfragments. The explanation involves an exclusion principle inhibition of the bound hyperon mesonic decay. Some evidence is presented in favor of a  $\Lambda^0$  hyperon spin and parity (relative to a nucleon) of  $\frac{1}{2}^-$  (or less probably, of  $\frac{1}{2}^+$  or  $\frac{3}{2}^+$ ) (+).

In a general theoretical treatment of the non-mesonic decay of a  $\Lambda^0$  hyperon bound to a nuclear fragment (<sup>1</sup>), relations for the various mean lives:

$$\tau^{-1}(A, Z) = \tau_{\text{bound; mesonic}}^{-1} + \tau_{\text{bound; nonmesonic}}^{-1},$$

$$(1) \quad R(A, Z) = \frac{\text{number of hyperfragments (of given } A, Z) \text{ decaying with pion emission}}{\text{number of hyperfragments (of given (same) } A, Z) \text{ decaying without pion emission}} = \\ = \left( \frac{\tau_{\text{bound; mesonic}}^{-1}}{\tau_{\text{bound; nonmesonic}}^{-1}} \right) \mathcal{P},$$

were obtained and discussed. Thus it was shown (<sup>2</sup>) that for not too heavy

(\*) Assisted by the joint program of the U.S.O.N.R. and the U.S.A.E.C.

(+) *Note added in proof:* Conclusions similar to those reached here have been developed more fully by M. RUDERMAN and R. KARPLUS: *Phys. Rev.*, **102**, 247 (1956). See also, K. NISHIJIMA: *Prog. Teor. Phys.*, **14**, 527 (1955); R. GATTO: *Nuovo Cimento*, **3**, 499 (1956); T. K. FOWLER: *Phys. Rev.*, **102**, 844 (1956).

(<sup>1</sup>) W. CHESTON and H. PRIMAKOFF: *Phys. Rev.*, **92**, 1537 (1953).

(<sup>2</sup>) See eqs. (16b)-(18) of ref. (<sup>1</sup>).

hyperfragments,

$$(2) \quad \tau_{\text{bound; nonmesonic}}^{-1} \approx \tau_{\text{free; mesonic}}^{-1} \gamma g^2 \left( \frac{\alpha^2(A, Z) + \beta^2(A, Z)}{2} \right)^{-\frac{3}{2}} A \equiv \\ \tau_{\text{free; mesonic}}^{-1} K(A, Z) A,$$

where  $\gamma$  is a dimensionless constant depending on the spin and parity of the  $\Lambda^0$ ,  $g(\hbar c)^{\frac{1}{2}}$  is an effective pion-nucleon coupling constant and  $\alpha(A, Z)\hbar/M_{\pi}c$ ,  $\beta(A, Z)\hbar/M_{\pi}c$  are effective radii of the 1s nucleon and 1s hyperon orbits within the hyperfragment. Also,  $\alpha(A, Z)$ ,  $\beta(A, Z)$  are, respectively, some  $1.5 \div 2$  times larger in  ${}^3\text{H}_{\Lambda}$  than in any  ${}_Z^AX_{\Lambda}$  (with  $2 < Z \lesssim 10$ ,  $6 < A \lesssim 20$ ), because of the greater binding energy of the hyperon and of the nucleons within the heavier hyperfragments; thus,  $K(A, Z)$  increases by a factor  $\approx 5$  as  $A$  increases from 3 to values  $> 6$ . Further,  $\varphi$ , the probability of a (real) pion emitted by the bound hyperon actually emerging from the fragment, varies between 1 and  $(3/2)\varrho$  as  $\varrho = \{\text{effective mean free path for } (25 \div 50 \text{ MeV}) \text{ pion absorption within nuclear matter} : \text{effective linear dimension (diameter) of hyperfragment}\}$  varies between values  $\gg 1$  and  $\ll 1$ ; hence, in all hyperfragments of interest (i.e., with  $3 \leq A \lesssim 20$ ),  $\varphi \approx 1$  since  $\varrho$  may be estimated as  $\ll 4 \div 2$ . We therefore see that  $R(A, Z)$  decreases with increasing  $A$  as  $[K(A, Z)A]^{-1}$  if  $\tau_{\text{bound; mesonic}}^{-1}$  is assumed independent of  $A$ ; in reference (1) such an assumption was indeed provisionally made and in fact  $\tau_{\text{bound; mesonic}}^{-1}$  was there approximated by  $\tau_{\text{free; mesonic}}^{-1}$ .

On the other hand, the now available experimental data on hyperfragments (3) seem to indicate that, 1)  $R(A, Z)$  decreases with increasing  $Z$ ,  $A$  even faster than  $[K(A, Z)A]^{-1}$ , and that, 2)  $\tau(A, Z)$  is never appreciably shorter than  $\tau_{\text{free; mesonic}}$  and does not decrease monotonically, but may even increase, as  $Z$  increases from 1 to values  $> 2$ . In more detail, 30 mesonic and 1 non-mesonic decays have so far been observed in  ${}^{3,4}_1\text{H}_{\Lambda}$ , 13 mesonic and 7 non-mesonic decays in  ${}^{4,5}_2\text{He}_{\Lambda}$ , 4 mesonic and about  $60 \div 80$  nonmesonic decays in  ${}_Z^AX_{\Lambda}$  (with  $2 < Z \lesssim 10$ ,  $6 < A \lesssim 20$ ); also, of these  $115 \div 135$  hyperfragment decays, only 4, two  ${}^3_1\text{H}_{\Lambda}$ , a  ${}^4_2\text{He}_{\Lambda}$  and a  ${}^4_0\text{F}_{\Lambda}$  occurred in flight. A plausible explanation of this experimentally found dependence of  $R(A, Z)$ ,  $\tau(A, Z)$  on  $Z$ ,  $A$  involves modification of the assumption that  $\tau_{\text{bound; mesonic}}^{-1} \approx \tau_{\text{free; mesonic}}^{-1}$  actually one expects  $\tau_{\text{bound; mesonic}}^{-1}$  to be less than  $\tau_{\text{free; mesonic}}^{-1}$  because of exclusion principle restrictions on the relatively low energy ( $\approx 5 \text{ MeV}$ ) proton produced

(3) For the sake of the numbers quoted, we have, in those cases where several alternative decay modes are given by the authors, adopted that one decay mode which seems to fit best the overall variation of  $B.E._{\Lambda}$  with  $A, Z$ . We have also been rather conservative in including supposed nonmesonic decays in cases where the «hyperfragment» track is very short.

via:

$$(3) \quad \Lambda_{\text{bound}}^0 \rightarrow p + \pi^-.$$

In fact, the proton in eq. (3) has in the rest frame of the  $\Lambda_{\text{bound}}^0$  a momentum  $\mathbf{q}$  of magnitude  $[2(M_p M_\pi / M_p + M_\pi) 37 \text{ MeV}]^{1/2} = 95 \text{ MeV}/c$  so that this proton's momentum in the lab. frame is  $\mathbf{q} + \mu \mathbf{p}_\Lambda$  ( $\mu \equiv M_p / M_\Lambda$ ) where  $\mathbf{p}_\Lambda$  is the  $\Lambda_{\text{bound}}^0$  momentum at the instant of decay; if now the proton momentum state within the hyperfragment with momentum  $\mathbf{q} + \mu \mathbf{p}_\Lambda$  is usually occupied by another proton, the decay of eq. (3) will be strongly inhibited by the exclusion principle. More quantitatively:

$$(4) \quad \tau_{\text{bound; mesonic}}^{-1} = \tau_{\text{free; mesonic}}^{-1} I_\Lambda(A, Z),$$

so that, from eqs. (1), (2), (4),

$$(5) \quad \begin{cases} R(A, Z) \approx \frac{I_\Lambda(A, Z)}{K(A, Z)A}, \\ \tau^{-1}(A, Z) \approx \tau_{\text{free; mesonic}}^{-1} [I_\Lambda(A, Z) + K(A, Z)A], \\ \approx \tau_{\text{free; mesonic}}^{-1} I_\Lambda(A, Z) [1 + R^{-1}(A, Z)]; \end{cases}$$

here  $I_\Lambda(A, Z)$ , the exclusion principle inhibition factor, is approximately:

$$(6) \quad \begin{aligned} I_\Lambda(A, Z) &\approx 1 - \int P_{\text{pr}}(\mathbf{q} + \mu \mathbf{p}_\Lambda) P_\Lambda(\mathbf{p}_\Lambda) d\mathbf{p}_\Lambda = \\ &= 1 - \left\{ \frac{1}{2} \left[ \frac{p_0 - q}{|p_0 - q|} \operatorname{erf} \left( \frac{|p_0 - q|}{\mu \alpha} \right) + \operatorname{erf} \left( \frac{p_0 + q}{\mu \alpha} \right) \right] \right. \\ &\quad \left. - \frac{\mu \alpha}{2\pi^2 q} \left( \exp \left[ -\frac{(p_0 - q)^2}{\mu^2 \alpha^2} \right] - \exp \left[ -\frac{(p_0 + q)^2}{\mu^2 \alpha^2} \right] \right) \right\}, \end{aligned}$$

with  $P(\mathbf{p}_\Lambda) d\mathbf{p}_\Lambda = \pi^{-3/2} \alpha^{-3} \exp[-\mathbf{p}_\Lambda^2 / \alpha^2] d\mathbf{p}_\Lambda$ , the (assumed Gauss type) probability of the momentum of the  $\Lambda_{\text{bound}}^0$  lying between  $\mathbf{p}_\Lambda$  and  $\mathbf{p}_\Lambda + d\mathbf{p}_\Lambda$ , and,  $P_{\text{pr}}(\mathbf{q} + \mu \mathbf{p}_\Lambda) = 1, 0$  as  $|\mathbf{q} + \mu \mathbf{p}_\Lambda| \leq p_0$ , the (assumed Fermi type) probability that the proton ( $\mathbf{q} + \mu \mathbf{p}_\Lambda$ )-momentum state within the hyperfragment is already occupied. An equivalent approximate expression for  $I_\Lambda(A, Z)$  is:

$$(7) \quad I_\Lambda(A, Z) \approx 1 - \sum_\alpha |C_{\alpha\Lambda}|^2 \int \Phi_\alpha^*(\mathbf{x}) \exp[-i\mathbf{Q} \cdot \mathbf{x}] \Phi_\Lambda(\mathbf{x}) d\mathbf{x},$$

where  $\hbar \mathbf{Q}$  is the lab. frame momentum of the emitted pion;  $\Phi_\Lambda(\mathbf{x})$ ,  $\Phi_\alpha(\mathbf{x})$  are (individual particle) bound hyperon, proton wave functions with the  $\sum_\alpha \dots$



running over all already occupied proton states;  $C_{\alpha\Lambda}$  is a factor (normalized so that  $\sum_{\alpha} |C_{\alpha\Lambda}|^2 = 1$ ) whose numerical value is determined by the spin and  $\Lambda^0$ -parity dependence of the hyperon-nucleon-pion coupling and by the spin quantum numbers characterizing the  $\Phi_{\Lambda}$  and  $\Phi_{\alpha}$  states.

Eq. (6) now predicts a rapid decrease of  $I_{\Lambda}(A, Z)$ , and so of  $\tau_{\text{bound; mesonic}}^{-1}$  and of  $R(A, Z)$  as  $Z$  increases from 1 to values  $> 2$ . For  ${}^3_1\text{H}_{\Lambda}$ ,  ${}^4_1\text{H}_{\Lambda}$ , rough estimates of possible forms for  $P_{\Lambda}$ ,  $P_{\text{pr}}$  (based on the corresponding hyperon and proton binding energies) lead to the equivalent parameters:  $\alpha \approx (0.3 \div 0.6)q$ ,  $p_0 \approx (0.5 \div 0.8)q$ , yielding  $I_{\Lambda}(3 \text{ or } 4, 1) \approx 1$ . On the other hand,  $\alpha \approx (2M_{\Lambda}B.E._{\Lambda})^{\frac{1}{2}} \approx (1.2 \div 0.8)q$ ,  $p_0 \approx (2.0 \div 2.4)q$  for  ${}^4_Z\text{X}_{\Lambda}$ , yielding,  $I_{\Lambda}(6 < A \lesssim 20, 2 < Z \lesssim 10) \approx 0.18 \div 0.005$ ; thus from eq. (5):

$$(8) \quad \left\{ \begin{array}{l} R(12, 6) \approx \frac{.05}{K(12, 6) \cdot 12}; \quad R(3, 1) \approx \frac{1}{K(3, 1) \cdot 3}; \quad \frac{R(12, 6)}{R(3, 1)} \approx \frac{1}{400}, \\ \tau^{-1}(12, 6) \approx \tau_{\text{free; mesonic}}^{-1}(.05)[1 + R^{-1}(12, 6)]; \\ \tau^{-1}(3, 1) \approx \tau_{\text{free; mesonic}}^{-1}(1)[1 + R^{-1}(3, 1)], \end{array} \right.$$

where  $I_{\Lambda} = .05$  (corresponding to  $\alpha = 1q$ ,  $p_0 = 2.2q$ ) has been used for the exclusion principle inhibition factor in the heavier hyperfragments. Since experimentally  $R^{-1}(3, 1) \ll 1$  and  $R^{-1}(12, 6) \approx 70/4$ , one also has:

$$(9) \quad \tau^{-1}(12, 6) \approx \tau_{\text{free; mesonic}}^{-1} \cdot 7/8; \quad \tau^{-1}(3, 1) \approx \tau_{\text{free; mesonic}}^{-1}$$

both eqs. (8), (9) being consistent with the above mentioned presently available experimental data (4). Alternatively, from the viewpoint of eq. (7), one can suppose that  $\Phi_{\Lambda}$  is effectively a  $1s$  orbital at least in the heavier fragments where  $B.E._{\Lambda}$  is appreciable. Then, for  $Z > 2$ , the  $\sum_{\alpha} \dots$  runs over the two  $1s$  orbitals  $\Phi_{\pm}$ ,

(4) Using eqs. (2), (5), one has:

$$\gamma = \frac{I_{\Lambda}(A, Z) \{[\alpha^2(A, Z) + \beta^2(A, Z)]/2\}^{\frac{3}{2}}}{R(A, Z)Aq^2},$$

which with  $I_{\Lambda}(12.6) \approx .05$ ,  $\alpha(12.6) \approx \beta(12.6) \approx 1.4$ ,  $R(12.6) \approx 4/70$ ,  $q^2 \approx 10$ , gives an « experimental value » for  $\gamma \approx 1/50$ . On the other hand, crude but purely theoretical estimates for  $\gamma$  yield:  $\gamma \approx 1$  for  $S_{\Lambda} = \frac{1}{2}^{+}$  [the spin, parity (relative to a nucleon) assumed in ref. (1)] and for  $S_{\Lambda} = \frac{3}{2}^{+}$ ;  $\gamma \gg 1$  for  $S_{\Lambda} = \frac{3}{2}^{-}, \frac{5}{2}^{\pm}, \frac{7}{2}^{\pm}, \dots$ ;  $\gamma \approx 1/30$  for  $S_{\Lambda} = \frac{1}{2}^{-}$ . The theoretical estimate of  $\gamma$  in the case  $S_{\Lambda} = \frac{1}{2}^{+}$  has already been given in ref. (1); the theoretical estimates of  $\gamma$  for the other  $S_{\Lambda}$  are also obtained by the method of ref. (1) using correspondingly suitable expressions for the  $\Lambda^0$ -nucleon-pion interactions, e.g.  $\Psi_{\pi}^{*}\beta\Psi_{\Lambda}\Phi_{\pi}$  for the case  $S_{\Lambda} = \frac{1}{2}^{+}$ . It is seen that the experimental and theoretical values of  $\gamma$  agree best when  $S_{\Lambda} = \frac{1}{2}^{+}$ .

occupied by other protons and it is just for these orbitals that the  $\Phi_\Lambda$ ,  $\Phi_\alpha$  overlap is greatest. Thus for  $Z = 2$ , the  $\sum \dots$  is likely to be considerably larger, and the  $I_\Lambda(A, Z)$  correspondingly smaller, than for  $Z = 1$  where the  $\sum \dots$  runs over just one of the two 1s proton orbitals <sup>(5)</sup>, and where besides,  $B.E._\Lambda$  is so low that  $\Phi_\Lambda$  probably overlaps no worse with several higher energy proton orbitals than with the 1s. Quantitative results, however, are even more uncertain if calculated from eq. (7), than from eq. (6).

It is also worth mentioning that a very similar exclusion principle inhibition enters into the phenomenon of negative muon capture by nuclei; here the basic process is  $\mu + p \rightarrow n + \nu$  with the neutron possessing a momentum  $\approx M_\mu c(1 - M_\mu/2M_n) = 100 \text{ MeV}/c = 1.05q$  in a common rest frame of the muon and proton. The exclusion principle inhibition in the muon capture case, at least in the lighter nuclei where the neutron excess is zero or small, is then roughly as severe as in the bound hyperon case, the latter inhibition being actually rather more stringent since the momentum spectrum of the proton which captures the muon in general extends to higher values than the momentum spectrum of the bound hyperon. The exclusion principle inhibition factor in the muon capture,  $I_\mu(A, Z)$ , is essentially given by the equation <sup>(6)</sup>:

$$(10) \quad \tau_{\text{capt}}^{-1}(A, Z) = \tau_{\text{capt}}^{-1}(1, 1) Z^1 I_\mu(A, Z) ;$$

theoretical calculation of  $\tau_{\text{capt}}^{-1}(1, 1)$ , assuming a muon-neutrino-nucleon interaction identical in strength with the electron-neutrino-nucleon beta decay interaction, and comparison with experimental values of  $\tau_{\text{capt}}^{-1}$  for  $A, Z$  from  ${}^{12}_6\text{C}$  to  ${}^{32}_{16}\text{S}$  indicates that  $I_\mu(A, Z)$  is more or less independent of  $A, Z$  in the range mentioned and has a numerical value  $\approx 1/6$ . On the other hand, fairly detailed calculations of  $\tau_{\text{capt}}^{-1}(A, Z)$  for  $\mu + {}^3_2\text{He} \rightarrow {}^3_1\text{H} + \nu$  <sup>(6)</sup> indicate that where the 1s orbit is available to the neutron the exclusion principle inhibition is unimportant and  $I_\mu$  is not far from 1. Supposing that these results apply, at least approximately, to the case of exclusion principle inhibition in bound hyperon decay, we see that one can expect  $I_\Lambda$  to be fairly close to 1 for  $Z < 2$  ( $A \leq 3$  or 4) whereas for  $Z > 2$  ( $A > 6$  or 7)  $I_\Lambda$  should be considerably smaller than 1, say  $\approx 1/10$ . One therefore anticipates again a difference by a factor of some 200 between  $R(3, 1)$  and, say,  $R(12, 6)$ .

<sup>(5)</sup> This argument would indicate that the mesonic decay mode:  ${}^3_1\text{H}_\Lambda \rightarrow {}^3_2\text{He} + \pi$  should compete favorably with the mesonic decay modes:  ${}^3_1\text{H}_\Lambda \rightarrow {}^2_1\text{H} + p + \pi^-$ , etc.: available experimental results appear consistent with such a conclusion. A mode of decay of  ${}^4_2\text{He}_\Lambda$  (as yet unobserved) which might also be fairly frequently expected (at least if:  $\Lambda^0_{\text{free}} \rightarrow n + \pi^0$  is not too rare compared to  $\Lambda^0_{\text{free}} \rightarrow p + \pi^-$ ) is  ${}^4_2\text{He}_\Lambda \rightarrow {}^4_2\text{He} + \pi^0$ .

<sup>(6)</sup> H. PRIMAKOFF: *Proceedings of the Fifth Annual Rochester Conference on High-Energy Physics* (New York, 1955), p. 174.

\* \* \*

I wish to thank the members of the emulsion group at Bristol University for a helpful discussion about hyperfragments.

## RIASSUNTO (\*)

Si dà una spiegazione della variazione con  $A, Z$ : 1) del rapporto delle probabilità dei decadimenti mesonico e non mesonico degli iperframmenti; 2) della vita media degli iperframmenti. La spiegazione richiede l'inibizione del principio d'esclusione riferito al decadimento mesonico dell'iperone legato. Si presentano deboli prove in favore di spin e parità di un iperone  $\Lambda^0$  (rispetto a un nucleone)  $\frac{1}{2}^-$  (o, meno probabilmente,  $\frac{1}{2}^+$  o  $\frac{3}{2}^+$ ).

---

(\*) *Traduzione a cura della Redazione.*

## Spurious Scattering in Nuclear Emulsions.

F. A. BRISBOUT, C. DAHANAYAKE (\*), A. ENGLER, P. H. FOWLER  
and P. B. JONES (+)

*H. H. Wills Physical Laboratory - University of Bristol*

(ricevuto il 27 Marzo 1956)

**Summary.** — Spurious scattering has been investigated in three stacks of stripped emulsions; one of these has been exposed to the 4.5 GeV  $\pi$ -meson beam at Berkeley, the other two to cosmic radiation. Multiple scattering measurements performed on flat tracks of high energy particles show that the spurious scattering in two of these stacks is appreciably smaller than that obtained by BISWAS *et al.*, LOHRMANN and TEUCHER, and FAY and that reliable measurements up to 5 GeV (for singly charged particles) can be made using a basic cell size of one mm. Clearly spurious scattering is a function of the quality of the stack. A procedure for eliminating spurious scattering is suggested which in particular cases permits measurements to be extended to higher energy regions.

### Introduction.

During the past year several investigations (<sup>1-3</sup>), concerning the various limitations of scattering measurements in nuclear emulsions have been published. The first and most important of these is the work of BISWAS, PETERS and RAMA. These authors arrived at the following conclusions:

a) Besides the well-known effects of *C* and *S*-shaped distortion due to differential shear with depth in the emulsion, small dislocations can give rise

(\*) On leave of absence from the University of Ceylon.

(+) On leave of absence from the Cavendish Laboratory, Cambridge.

(<sup>1</sup>) S. BISWAS, B. PETERS and RAMA: *Proc. Ind. Acad.*, A **41**, 154 (1955).

(<sup>2</sup>) H. FAY: *Zeits. f. Naturfor.*, **10a**, 572 (1955).

(<sup>3</sup>) E. LOHRMANN and M. TEUCHER: *Nuovo Cimento*, **3**, 59 (1956).

to « spurious scattering » which seriously impairs measurements at high energies.

b) The intensity of this effect is generally *the same* for all Ilford G5 emulsions.

c) The spurious scattering in individual tracks increases with the cell length ( $t$ ) very nearly as  $t^{\frac{3}{2}}$  and hence

d) Reliable scattering measurements are possible only on tracks of protons with energy below 600 MeV and heavy nuclei with energy below 300 MeV per nucleon.

These results were later substantially confirmed by FAY <sup>(2)</sup> and LOHRMANN and TEUCHER <sup>(3)</sup>, the only difference being in the rate of increase of spurious scattering with cell size. The latter authors claim that it rises linearly with  $t$  and that therefore, using very large cells, measurements can be extended to energies higher than those given by BISWAS *et al.*

These results, if correct, seem to rule out any systematic investigation of high energy phenomena recorded in nuclear emulsions, since these rely essentially on energy determinations by multiple scattering measurements. (Relative scattering, however, is unaffected by spurious scattering). It seemed therefore of importance to investigate this problem in the various stacks of emulsions available.

Previous experiments in this laboratory, although not contradicting the existence of spurious scattering, definitely indicate its influence to be considerably less than that found by BISWAS *et al.* WADDINGTON <sup>(4)</sup> has pointed out that if spurious scattering were present to the extent predicted by BISWAS *et al.* then the integral energy spectrum of primary  $\alpha$ -particles, as determined from scattering measurements, should have an exponent of 3.3. Instead, DAINTON, FOWLER and KENT <sup>(5)</sup> using glass backed emulsions obtained a value of 1.9, while recently in a stripped emulsion stack WADDINGTON <sup>(4)</sup> has obtained a value of 1.8. Thus it would appear that in at least two stacks the influence of spurious scattering is less than that found by BISWAS *et al.*

The present results have been obtained from an investigation of three stacks of stripped emulsions. One was exposed to the 4.5 GeV  $\pi$ -meson beam of the Berkeley Bevatron, the other two to cosmic radiation.

Sect. 1 gives a short description of the experimental procedure generally adopted in this laboratory for multiple scattering measurements. The information obtained from the stack exposed to a beam of particles of unique and known energy is particularly important and will be dealt with in Sect. 2.

<sup>(4)</sup> C. J. WADDINGTON: *Nuovo Cimento* (1956, in press).

<sup>(5)</sup> A. D. DAINTON, P. H. FOWLER and D. W. KENT: *Phil. Mag.*, **43**, 729 (1952).



The last Section deals with the information obtained from tracks of high energy particles found in the stacks exposed to cosmic radiation.

## 1. — Experimental Procedure.

The methods described in this Section for multiple scattering measurements have, on the whole, been employed in this laboratory for several years, and will therefore be dealt with briefly.

CookeM 4000 microscopes were used throughout this investigation. The influence of temperature noise and mechanical vibration was kept at a minimum.

For accurate measurements it is important to know the variation of stage noise with cell size. The stage noise of two of the microscopes used has been determined by interferometric measurements (GOTTSTEIN <sup>(6)</sup>). By adding a constant contribution for «reading» and «grain noise» of 0.1  $\mu\text{m}$ , the resultant total noise was found to vary with cell size as  $t^x$ , with  $x = 0.25$ . An identical result was obtained with the same microscopes from scattering measurements on the track of an extremely energetic singly charged particle. The length of this track exceeds 8 cm per plate and it produces a high energy «jet» of 650 GeV. The values of the mean second differences  $\bar{D}$  obtained for various cell sizes were plotted against  $t$  (in units of 100  $\mu\text{m}$ ) and the total noise found to obey the same power law ( $x = 0.25$ ). This track gave a value of  $\bar{\alpha} = 0.0001^\circ$  per 100  $\mu\text{m}$ , and hence appears to be practically unaffected by any large scale distortion or spurious scattering. The various observers calibrated their microscopes using the same track over a length of 5 cm and the total noise in each case was found to be approximately represented by a power law  $t^x$  with  $x$  between 0.20 and 0.45. The standard deviation of the exponent  $x$  for individual microscopes is about  $\pm 0.05$  but the error introduced thereby in the determination of  $\bar{\alpha}$  is negligible.

Assuming i)  $\bar{D}^2 = \bar{\alpha}^2 t^3 + at^{2x}$  ( $a = \text{constant}$ ) and ii) the absence of large scale distortion or spurious scattering, the parameter  $\bar{\alpha}$  is given, by

$$(1) \quad \bar{\alpha} = A \sqrt{\frac{\bar{D}_2^2 - (t_2/t_1)^{2x} \bar{D}_1^2}{t_2^3 - (t_2/t_1)^{2x} t_1^3}},$$

where  $A$  is a constant depending upon the magnification.

It must be pointed out that this method of noise elimination will also remove a certain fraction of spurious scattering.

<sup>(6)</sup> K. GOTTSTEIN: *Nuovo Cimento*, **12**, 619 (1954).

To decide whether a particular value of  $\bar{x}$  obtained from scattering measurements is significant it is necessary that certain criteria be satisfied. These criteria though arbitrary, ensure to a large extent that the contribution of the total noise to the measured scattering parameter  $\bar{D}$ , is a suitable fraction of the total signal observed. A very convenient criterion is given by

$$(2) \quad \left( \frac{\bar{D}_2}{\bar{D}_1} \right)^2 \geq \left( \frac{t_2}{t_1} \right)^{2x+1}.$$

This convention has proved very useful in scattering measurements of tracks of medium energy up to 1 GeV. Clearly the above relation, though necessary, is by no means sufficient to ensure that the actual scattering parameter determined from relation (1) is due to Coulomb scattering alone.

## 2. - Scattering Measurements on the Tracks of 4.5 GeV $\pi$ -Mesons.

A stack of 80 stripped emulsions  $20 \text{ cm} \times 30 \text{ cm} \times 600 \mu\text{m}$  was exposed to the  $\pi$ -meson beam of the Bevatron at Berkeley. According to the data of exposure the mean momentum of the pions is  $4.49 \pm 0.03 \text{ GeV}/c$ . The  $\mu$ -meson contamination of the pion beam is about 4% and could be neglected. The mean length per plate of the  $\pi$ -meson tracks was about 1.5 cm.

**2.1 Relative Scattering Measurements on Pairs of  $\pi$ -Meson Tracks.** - In order to obtain an accurate value of the energy of the beam, independent of the measurements made at Berkeley, relative scattering measurements were performed on 43 pairs of closely spaced parallel tracks. Since the experimental evidence so far (<sup>1-3</sup>) supports the assumption that such measurements are free from spurious scattering and conventional distortion, the results of these observations may be compared with those obtained by scattering measurements on the individual tracks in order to examine the effects of spurious scattering. Moreover, by using the energy value quoted by Berkeley, we can obtain a value for the scattering constant at this energy.

The selected pairs had to obey the following criteria:

a) Both tracks must remain within a projected distance of  $50 \mu\text{m}$  from each other for at least one cm. This ensures a minimum of twenty 500  $\mu\text{m}$  cells.

b) The difference in depth between the two tracks should not exceed  $20 \mu\text{m}$  (in unprocessed emulsion) along the whole length used. This criterion was imposed in order to eliminate the influence of distortion or spurious scattering which may vary from layer to layer in the emulsion. Also the requirement that both tracks should lie in the same layer of emulsion will reduce the noise due to the movement of the fine focus.

It must be pointed out that condition *a*) introduces a small bias toward tracks which exhibit smaller relative scattering than the average. However we estimate this error to be of the order of 1% only.

The multiple scattering on all the pairs was determined using a basic cell size of 500  $\mu\text{m}$ . The values of  $\bar{\alpha}$  obtained by using overlapping cells are given in Table I. Large angle Coulomb single scattering has been removed by a cut-off with replacement (7) (\*). Assuming the  $\pi$ -mesons to have a unique energy of 4.49 GeV we obtain the values of the scattering constant  $K$  given in column 3 of Table I, in excellent agreement with the calculations of VOJVODIC and PICKUP (8).

TABLE I. — The values of  $\bar{\alpha}$  and  $K$  from relative scattering measurements.

cell size (in units of 100 $\mu\text{m}$ )	$\bar{\alpha}_{(100\mu\text{m})}$	$K$ experimental	$K$ expected
5 $\div$ 10	$0.00888 \pm 0.00030$	$28.2 \pm 1.0$	28.7
5 $\div$ 15	$0.00878 \pm 0.00040$	$27.9 \pm 1.4$	29.2
10 $\div$ 20	$0.00900 \pm 0.00050$	$28.6 \pm 1.7$	29.6

For 19 pairs, the grain and reading noise were eliminated according to the method of BISWAS *et al.* by repeating the measurements at points displaced 50  $\mu\text{m}$  along the track. The values obtained in this manner are

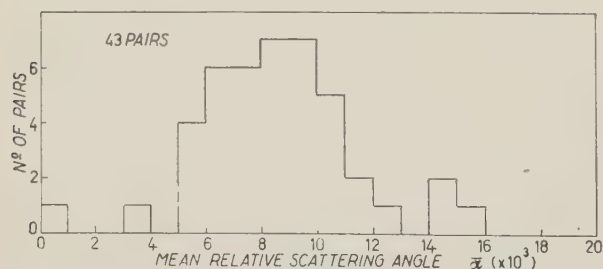


Fig. 1. — The distribution of  $\bar{\alpha}$ -values for pairs of 4.5 GeV  $\pi$ -meson tracks. These were calculated, from the observed second differences for cell sizes  $t = 5$  and  $t = 15$ , by the method of overlapping cells. The mean value observed is  $\bar{\alpha} = 0.00878$  deg. per 100  $\mu\text{m}$ . The standard deviation for individual pairs is  $\sigma$  (observed) = 0.0028 and  $\sigma$  (expected) = .0026.

$\bar{\alpha}$	$t$
$0.0098 \pm 0.0004$	5
$0.0096 \pm 0.0006$	10
$0.0096 \pm 0.0008$	15

in good agreement with the values found by the method of overlapping cells for noise elimination.

Therefore in the case where stage noise and spurious scattering may be neglected both methods yield identical results.

A histogram of the va

(\*) In this procedure, every signal which exceeds four times  $\bar{D}$ , the mean of the second differences, is replaced by  $4\bar{D}$ .

(7) P. H. FOWLER and D. H. PERKINS: private communication.

(8) L. VOJVODIC and E. PICKUP: *Phys. Rev.*, **85**, 91 (1952).

ues of  $\bar{\alpha}$  obtained for overlapping cells of  $t = 5$  and  $t = 15$  is shown in Fig. 1. The spread of this distribution is that to be expected from statistical errors.

**2.2. Scattering Measurements on Individual Tracks.** — The multiple scattering of 292 tracks of 4.5 GeV  $\pi$ -mesons recorded in 40 emulsions has been determined by four observers, using four different microscopes. These tracks belong to two groups: in the first were the 86 tracks which formed the pairs on which relative scattering measurements were performed; the second consists of 206 particles which produced nuclear interactions.

The average length of an individual track along which measurements were made, was 15 mm. The basic cell size chosen was 500  $\mu\text{m}$  and the scattering parameter  $\bar{\alpha}$  on higher cell sizes was determined by the method of overlap. Large angle Coulomb single scattering has been removed as mentioned previously. The distortion vector perpendicular to the tracks was very small ( $\sim 30$  covans); the total distortion vector was  $\sim 100$  covans. Furthermore, the method of third differences applied on a small sample of tracks did not change the results significantly. Hence no correction for  $C$  and  $S$  shaped distortion has been applied and the value of  $\bar{D}$  may contain a small contribution of large scale distortion. The mean values of  $\bar{D}$  (total) (including noise) obtained by individual observers for the various cell sizes are given in Table II.

TABLE II. — Values of  $\bar{D}$  ( $\mu\text{m}$ ) and  $\bar{\alpha}$  for the various observers.

Microscope	$\bar{D}_5$ ( $\mu\text{m}$ )	$\bar{D}_{10}$	$\bar{D}_{15}$	$\bar{D}_{20}$	$\bar{\alpha}_{10}^5$	$\bar{\alpha}_{15}^5$	$\bar{\alpha}_{20}^{10}$
M. 40151	0.233	0.427	0.694	1.023	0.00613	0.00614	0.00623
M. 4024	0.266	0.458	0.738	1.145	0.00566	0.00608	0.00690
M. 40135	0.259	0.504	0.815	1.178	0.00810	0.00763	0.00722
M. 4046	0.286	0.532	0.820	1.159	0.00755	0.00704	0.00665
Mean Value of $\bar{\alpha}$					0.00720 $\pm 0.00009$	0.00692 $\pm 0.00012$	0.00675 $\pm 0.00014$
$\bar{D}$ Coulomb	0.121	0.354	0.663	1.034			

The cell sizes are in units of 100  $\mu\text{m}$ . The standard deviation has been calculated assuming  $\sigma = 0.8/\sqrt{n}$  where  $n$  is the number of independent cells.

In the same table we give also the values of  $\bar{D}$  due to Coulomb scattering alone for a nominal energy of 4.5 GeV (using the scattering constant of VOYVODIC and PICKUP<sup>(8)</sup>).

It is immediately apparent that for cell sizes larger than 1000  $\mu\text{m}$  multiple Coulomb scattering accounts for more than one half of the total signal. According to the results of LOHRMANN and TEUCHER a cell size of  $\sim 7$  mm



would be required in order to obtain a signal/noise ratio of two whereas in this stack a cell size of  $1500\text{ }\mu\text{m}$  seems sufficient. We have also tried to estimate the magnitude of spurious scattering and its dependence on  $t$  in our emulsions. Since it has been shown by LOHRMANN and TEUCHER that the distribution of  $D$  values due to spurious scattering alone is approximately Gaussian we may use the following relation:

$$(3) \quad \bar{D}_{ss}^2 = \bar{D}_{total}^2 - \bar{D}_{coulomb}^2 - \bar{D}_{noise}^2$$

in order to determine its magnitude. For  $\bar{D}$  (noise) we have taken the value of the total noise determined from the calibration of the microscopes as mentioned in Sect. 1.

In Fig. 2 we have plotted the values of  $\bar{D}_{ss}$ , together with the results of

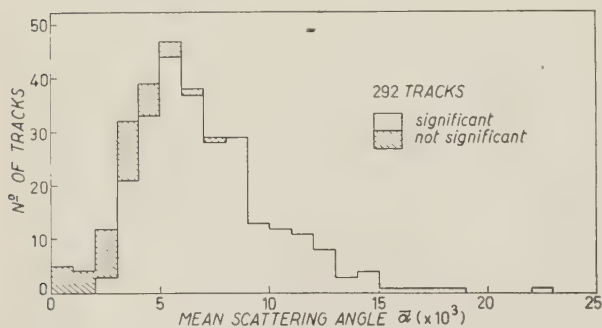


Fig. 2. — Spurious scattering as a function of cell size for various stacks. The mean second difference  $\bar{D}$  for pure Coulomb scattering is also shown for comparison. The experimental points are for cell sizes 5, 10, 15 and 20 (in units of  $100\text{ }\mu\text{m}$ ) but, for clarity, some have been slightly shifted parallel to the  $x$ -axis.

the values for  $\bar{\alpha}$  obtained for individual tracks do not satisfy equation (2), the mean value of  $\bar{\alpha}$  obtained for the whole sample has been calculated from the corresponding mean values of  $\bar{D}$  and is significant.

The skewness apparent in Fig. 3 is partly to be attributed to the fact that each value of  $\bar{\alpha}$  has been determined from only seven independent cells. Moreover, a few tracks which may have been exceptionally affected by spurious scattering would produce a similar effect.

The discrepancy of about 12% between the energy values as determined by relative scattering, and by measurements on individual tracks could be due to two causes:

a) As previously mentioned no correction for  $C$  shaped distortion has

the other authors, as a function of cell size. As may be seen the magnitude of spurious scattering in our stack is smaller by a factor of about 1.2 at  $t=5$  and it appears to increase with cell size as  $t^{0.5}$  only. The errors plotted are the statistical errors in the determination of the spurious scattering. The distribution of the values of  $\bar{\alpha}$  obtained for overlapping cells  $t=10$  and  $t=20$  from 292 tracks is given in Fig. 3. Although some of



been applied; since this distortion varies as  $t^2$  even a small contribution from this source will probably account for part of this discrepancy.

b) The influence of spurious scattering for the cell sizes used is not quite negligible.

It appears therefore that the criteria of significance in the choice of a basic cell size, as mentioned in Sect. 1, are not sufficient to ensure that the contribution of all spurious effects to the total signal is negligible. However a systematic error of about 12% at energies of 5 GeV does not seem very serious for most experiments considered at present.

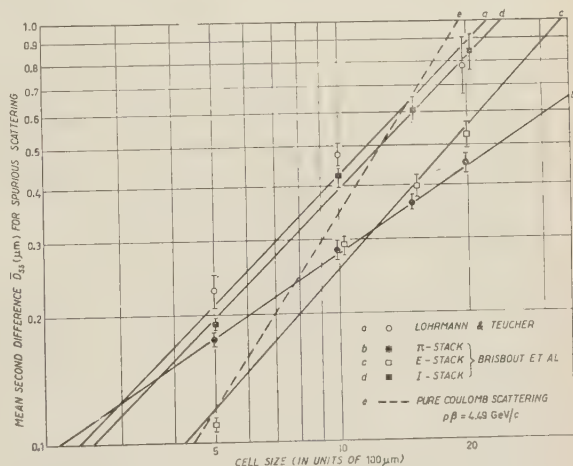


Fig. 3. — The distribution of  $\bar{\alpha}$ -values for individual tracks of 4.5 GeV  $\pi$ -mesons. These were calculated, from the observed second differences for cell sizes  $t = 10$  and  $t = 20$ , by the method of overlapping cells. The mean value observed is  $\bar{\alpha} = .00675$  deg. per  $100 \mu\text{m}$ .

The standard deviation for individual tracks is  $\sigma$  (observed) = .00315 and  $\sigma$  (expected) = .00243.

### 3. — Scattering Measurements on Tracks of High Energy Cosmic Ray Particles.

In the previous section we have seen that, at least in the particular stack exposed to the Bevatron, it is possible to determine reliably the energy of particles up to about 5 GeV by multiple scattering. In order to arrive at more general conclusions it seemed necessary to accumulate additional evidence from other plates.

For this purpose two stacks of stripped emulsions have been chosen and the multiple scattering has been determined on long tracks ( $> 1.5$  cm per plate) produced by high energy cosmic ray particles. These tracks were due to: a) particles producing nuclear disintegrations whose energy could be roughly estimated from the opening angle of the shower particles, and b) heavy primaries whose energy could be determined from the relative scattering of their fragmentation products.

These tracks were found in various parts of the stacks and each traced through several emulsions. Scattering measurements were made in every

emulsion so that in general the parameter  $\bar{\alpha}$  represents an average of the observations made in several emulsions. In some cases where large *C* shaped distortion was apparent «*q* corrections»<sup>(9)</sup> have been applied. The relevant data of these measurements are summarized in Tables III and IV. Whenever

TABLE III. — *Results of scattering measurements in E-stack.*

Energy	$\bar{\alpha}_{10}^5$	$\bar{\alpha}_{15}^5$	$\bar{\alpha}_{20}^{10}$	$\bar{D}_5^{es}$ ( $\mu\text{m}$ )	$\bar{D}_{10}^{26}$	$\bar{D}_{15}^{es}$	$\bar{D}_{20}^{es}$
7 GeV/nucleon	—	—	0.0029	0.009	0.175	0.28	0.33
5 GeV/nucleon	—	0.0058	0.0046	0.18	0.390	0.55	0.73
100 GeV	—	—	0.0055	0.19	0.46	0.67	0.79
100 GeV	—	0.0024	—	0.05	0.08	0.08	0.08
Weighted Mean Values: of $\bar{D}^{es}$ ( $\mu\text{m}$ )				0.11	0.29	0.40	0.53

Total track length = 32 cm, in 13 emulsions.

TABLE IV. — *Results of scattering measurements in I-stack.*

Energy	$\bar{\alpha}_{10}^5$	$\bar{\alpha}_{15}^5$	$\bar{\alpha}_{20}^{10}$	$\bar{D}_5^{es}$	$\bar{D}_{10}^{es}$	$\bar{D}_{15}^{es}$	$\bar{D}_{20}^{es}$
$\geq 5$ GeV/nucleon	0.012	0.0080	—	0.29	0.68	—	—
5 GeV/nucleon	—	0.0068	0.0066	0.22	0.42	0.76	1.07
14 GeV/nucleon	0.0056	0.0063	0.0065	0.13	0.33	0.65	1.01
10 GeV/nucleon	—	—	—	0.18	0.32	0.40	0.51
7 GeV/nucleon	0.0077	—	—	0.17	0.44	0.58	0.72
Weighted Mean Values of $\bar{D}^{es}$ ( $\mu\text{m}$ )				0.19	0.42	0.61	0.83

Total track length = 26.6 cm, in 18 emulsions.

the criteria of significance (eq. (2)) have not been fulfilled the particular values of  $\bar{\alpha}$  are omitted from the tables.

We also tried to obtain an estimate of the spurious scattering  $\bar{D}_{ss}$ , in a manner similar to that described in the previous section. We have eliminated from the total signal the grain and reading noise obtained by repeating the measurements on each track after displacing it by 50  $\mu\text{m}$  from the original position along its direction, and also the stage noise obtained from the calibration of our microscopes. Since in the case of heavy primary tracks the contribution due to Coulomb scattering alone was in general not negligible we have also subtracted from  $\bar{D}$  (total) the true signal as derived from relative scattering of the fragmentation products. In one case, where a lower

(9) P. H. FOWLER: *Phil. Mag.*, **41**, 169 (1950).

limit for the true energy of only 5 GeV/nucleon could be obtained, the values of  $\bar{D}_{ss}$  have been computed for cell sizes up to 1000  $\mu\text{m}$  only.

The weighted mean of the values of  $\bar{D}_{ss}$  obtained in each stack are given in Fig. 2. It is clear that the spurious scattering is significantly different in the three stacks. Moreover, as mentioned by the other authors, appreciable fluctuations may occur between various parts of the same stack.

#### 4. - Conclusions.

Our results differ from those of BISWAS *et al.* LOHRMANN and TEUCHER, and FAY, chiefly in that the spurious scattering in two of our stacks is lower by a factor 2 at higher cell sizes.

In these plates reliable estimates of energy up to 5 GeV can be obtained by multiple scattering measurements on flat tracks using a basic cell size of one mm.

It is understood that individual tracks will occasionally exhibit spurious scattering much larger than the average value for the stacks. However for systematic investigations on groups of particles the average value of spurious scattering is the determining factor and can be taken into account by adopting the following procedure.

In the stack where a systematic investigation of high energy phenomena is planned, a careful examination of spurious scattering in various parts of the stack should be made on tracks of particles of high energy. If the proposed investigation on a group of particles is made in the same parts of the stack the mean value of spurious scattering may then be subtracted. While higher energies will become accessible to measurement, great care must be exercised in the interpretation of results obtained in this way.

\* \* \*

We wish to express our indebtedness to Professor C. F. POWELL for extending to us the hospitality of his laboratory.

This experiment would not have been possible without the kind cooperation of Professor W. H. BARKAS and his group at Berkeley, especially Dr. H. H. HECKMAN, who exposed for us the  $\pi$ -meson stack and supplied us with the relevant data.

We are thankful to several of our colleagues in this laboratory, especially Dr. C. J. WADDINGTON, and Dr. M. W. FRIEDLANDER for useful discussions.

C.D. wishes to thank the Government of Ceylon and P.B.J. the Department of Scientific and Industrial Research for maintenance grants.

## RIASSUNTO (\*)

Lo scattering spurio è stato esaminato in tre pacchi di emulsioni pelate; uno di questi è stato esposto al fascio di mesoni  $\pi$  di 4.5 GeV di Berkeley, gli altri due alla radiazione cosmica. Misure di scattering multiplo eseguite su traiettorie piane di particelle di alta energia mostrano che lo scattering spurio in due di questi pacchi è considerevolmente minore di quello ottenuto da BISWAS *et al.*, LOHRMANN e TEUCHER, e FAY, e che si possono eseguire misure attendibili fino a 5 GeV (per particelle a carica singola) servendosi di una cella base di 1 mm. Lo scattering spurio è chiaramente funzione della qualità del pacco. Si propone un procedimento atto ad eliminare lo scattering spurio che in casi particolari permette di estendere le misure a energie superiori.

---

(\*) Traduzione a cura della Redazione.

## On the Pion Annihilation of Nucleon-Antiproton Pairs.

D. AMATI and B. VITALE (\*)

*Istituto di Fisica dell'Università - Roma*

*Istituto Nazionale di Fisica Nucleare - Sezione di Roma*

(ricevuto il 30 Marzo 1956)

**Summary.** — The pion annihilation of antiproton-nucleon pairs in bound  $S$ -states (singlet and triplet) are analyzed taking into account conservation law and selection rules previously founded. With a statistical model for the valuation of transition matrix elements the ratio of three pion to two pion annihilation is calculated and, for the  $3\pi$  annihilation, the angular distributions and energy spectrum of the final mesons. Finally some considerations are done about the annihilation of the pair from isotopic spin eigenstates.

### 1. — Introduction.

Several experiments with counter devices <sup>(1,2)</sup> and with nuclear emulsions <sup>(3)</sup> have brought us, in the last few months, a noticeable amount of experimental evidence on the existence of a heavy negative particle, with protonic mass, strongly interacting with nuclear matter. The interpretation of such events in terms of a new unstable kind of negative hyperon has been ruled out both by the experimental value of the mass,  $1840 \pm 90$  <sup>(1)</sup>, and by theoretical arguments based on Gell-Mann's model (see O. CHAMBERLAIN *et al.* <sup>(3)</sup>). The simplest interpretation of the existing data consists, therefore, in the identification of the observed events either as records of the passage

---

(\*) Now at the Department of Mathematical Physics, University of Birmingham.

<sup>(1)</sup> O. CHAMBERLAIN, E. SEGRÈ, C. WIEGAND and T. YPSILANTIS: *Phys. Rev.*, **100**, 947 (1955).

<sup>(2)</sup> J. M. BRABANT, B. CORK, N. HOROWITZ, B. J. MOYER, J. J. MURRAY, R. WALLACE and W. A. WENZEL: *Phys. Rev.*, **101**, 498 (1956).



of antiprotons through the system of counters <sup>(1)</sup>, or as interactions of antiprotons with nuclei <sup>(2,3)</sup>.

This interpretation is also supported by the fact that these particles, interacting with the nuclear matter, give rise to one or more pions; displaying therefore properties that had already been foreseen for the interaction of antinucleons with nucleons, followed by a pion annihilation of the nucleon-antinucleon pairs.

The characteristic features of the annihilation processes may prove to be of great importance for the study of the nucleon-antinucleon interaction; we will analyze and discuss, in the next section, the experimental data, and try to get some answers to the different problems involved. Furthermore, in Sect. 3, we shall give an explicit calculation of the most relevant features of the pion annihilation of nucleon-antiproton physical pairs (isotopic spin mixtures), namely, the ratio between two and three pion annihilation, the angular distribution and energy spectrum of the pions, assuming the pair to be in *S* state (singlet or triplet) and using simplifying statistical assumptions. In Sect. 4 we shall briefly consider the possibility of annihilation from isotopic spin eigenstates.

## 2. — Analysis of the Existing Experimental Data.

Some of the antiproton properties can be obtained from the counter data; they can be summed up as follows:

*a*) The mass of the negative particle is very near the protonic mass, and is the protonic mass within the experimental errors <sup>(1)</sup>.

*b*) The occurrence of annihilation in flight is almost certain; otherwise, it is impossible to explain the highest pulses obtained in the apparatus of BRABANT *et al.* <sup>(2)</sup> with particles of only about 450 MeV. If it is assumed that all the particles selected by the Čerenkov counters as «negative protons», and giving no response in the glass counter (events NO), correspond to antiprotons passing through the glass counter without interacting or annihilating, then the total cross section for antiprotons of an average energy of about 350 MeV is of the order of the geometric cross section.

<sup>(3)</sup> E. AMALDI, C. CASTAGNOLI, G. CORTINI, C. FRANZINETTI and A. MANFREDINI: *Nuovo Cimento*, **1**, 492 (1955); M. TEUCHER, H. WINZELER and E. LOHRMANN: *Nuovo Cimento*, **3**, 228 (1956); O. CHAMBERLAIN, W. W. CHUPP, G. GOLDBABER, E. SEGRÈ, C. WIEGAND, E. AMALDI, G. BARONI, C. CASTAGNOLI, C. FRANZINETTI and A. MANFREDINI: *Nuovo Cimento*, **3**, 447 (1956); R. D. HILL, S. D. JOHNSON and F. T. GARDNER: *Phys Rev.* **101**, 907 (1956).

c) The run «absorber in», corresponding to annihilations, presumably, at rest, presents higher individual pulses (being a lowest limit to the total energy released by the annihilation process) than the run «absorber out», corresponding to annihilation in flight. This can be easily understood as a consequence of the absorption, by the black bottom of the glass counter, of the annihilation products, going preferentially forward in the case «absorber out». Besides it may also be a variation of the pion multiplicity with the total energy of the nucleon-antiproton pairs in their center of mass system.

The nuclear plate data can be summed up as follows:

a) Several events produced by the annihilation of antiprotons coming to rest in the emulsion have been observed <sup>(3)</sup>; the time of flight is always rather short ( $10^{-11} \div 10^{-12}$  etc.).

Recently, in the nuclear emulsion exposed to the antiproton beam of the Cosmotron, the Berkley group has found some events interpreted as antiproton annihilation in flight <sup>(4)</sup>.

b) Pions certainly come out from the annihilation stars; it seems rather improbable that they are produced always by secondary collisions within the nucleus that has captured the antiproton (as it would be the case if the antiproton annihilated within the nucleus, sharing its rest mass energy and its nucleon partner's only among the other nucleons; or in the case of electromagnetic annihilation). The multiplicity of this pion production is, however, rather uncertain. The first Rome event, for instance <sup>(3)</sup>, may be explained as if one meson, disappearing, excited the nucleus.

c) The absorption takes place in heavy nuclei and, probably, also in light nuclei.

d) Recent results seem to indicate a total interaction cross section for the antiproton of the order of twice the geometrical <sup>(4)</sup>.

So high a total cross section is not completely unexpected. JOHNSON <sup>(5)</sup>, in lowest order perturbation theory with renormalized meson lines, found an elastic cross section of the order of 1/10 of the geometrical one; recently, considerations on scalar static interactions gave a total cross section of the order of, or greater than, the geometrical one <sup>(6)</sup>.

In the case of negative pion capture from nuclei, the life time for nuclear absorption from the continuum is very long compared to the slowing down time, even for geometrical cross section <sup>(7)</sup>; in that case, the process in com-

<sup>(4)</sup> Presented by O. CHAMBERLAIN at the *New York meeting of the American Physical Society* of February 1956.

<sup>(5)</sup> K. A. JOHNSON: *Phys. Rev.*, **96**, 1659 (1954).

<sup>(6)</sup> H. P. DUERR and E. TELLER: *Phys. Rev.*, **101**, 494 (1956).

<sup>(7)</sup> See, for instance, R. E. MARSHAK: *Meson Physics* (New York, 1952), Chapter 5.

petition with capture is the spontaneous decay. For antiprotons, the competition can be only between capture and subsequent annihilation, on one side, and annihilation from the continuum, on the other side. The former process will predominate, if the slowing down time is shorter than the time corresponding to its mean free path for annihilation in condensed matter. Both times depend on the inverse of the density of the medium (at least in first approximation, and for the first of the three steps of slowing down, which is by far the most important<sup>(8)</sup>). For the antiproton, supposed to interact with a geometrical cross section, both times are of the same order of magnitude:  $10^{-8}$  s in liquid hydrogen,  $10^{-10}$  s in nuclear emulsion, and in the high density density glass of the BRABANT *et al.* experiment (the times above are for antiprotons entering the medium with a kinetic energy of  $\sim 450$  MeV). We can therefore expect to find both annihilations in flight and at rest, with a ratio not very different from 1.

When the annihilation takes place in flight, two problems are of some interest: first, the dependence of the pion multiplicity on the total energy of the nucleon-antiproton pair in their center of mass system; second, and related to the first problem, the influence of the production of mesons by ordinary mechanism on the pion multiplicity. In the second case, indeed, the two yields of pions have to be considered as different if the interaction volume for the annihilation is different from the interaction volume for meson production in nucleon-nucleon collisions.

When the annihilation takes place at rest in heavy nuclei, owing to the strong Coulomb field and to the great mass of the antiproton, it seems rather improbable that the antiproton will reach some definite low orbit before annihilation. However this possibility is more likely in the annihilation at rest in hydrogen and possibly in light nuclei.

In a recent work L. M. BROWN and M. PESHKIN<sup>(9)</sup> conclude that an appreciable fraction of Bevatron antiprotons ( $\sim 450$  MeV) can be stopped in hydrogen and form a bound system in a low orbit.

It would be important, for a better understanding of the nucleon-antinucleon forces, to know if the nucleon-antiproton system reaches effectively states of definite orbital and intrinsic angular momentum. This possibility, and the particular states that could be involved, are so strongly dependent on the characteristic of the interaction that it seems useless to speculate now on them, without more experimental data. We have, however, tried to determine some of the characteristic features of the annihilation, in the assumption that the antiproton reaches a state of definite orbital and intrinsic angular momentum,

---

(<sup>8</sup>) E. FERMI and E. TELLER: *Phys. Rev.*, **72**, 399 (1947).

(<sup>9</sup>) We thank Drs. L. M. BROWN and M. PESHKIN to have sent us their work prior to publication.

namely singlet or triplet  $S$ . The comparison with the experimental data, as soon as more is available, may help us in proving, or disproving, the existence of such states. The hope is that, due to the numerous selection rules operating during the annihilation <sup>(10)</sup>, processes starting from such states shall present very peculiar features, characterizing them from the annihilations from the continuum or from other states. The annihilation from the continuum has been recently analysed, with the help of statistical assumptions <sup>(11)</sup>. We have not considered other modes of annihilation as, for instance, that into two  $K$ -mesons; this possibility is studied by GATTO in a forthcoming paper.

### 3. — Statistical Analysis of the Annihilation Processes.

In this section we shall study the two and three pion annihilation of a nucleon-antiproton pair in  $S$  state; the possible final particles and states as deriving from conservation laws (total angular momentum, parity, charge conjugation and charge symmetry) are listed in Tables V and VI of A. The nucleon and the antiproton will be here considered as to form a system with assigned charges (physical system), this means that the initial state will be an isotopic spin mixture.

In the following we shall indicate with an index  $\lambda$  the type of annihilation reaction we are considering;  $\lambda$  specifies therefore the initial particles, their state and the number and charge of the final pions.

The method we shall use in order to compute transition probabilities will be similar to the statistical one introduced by FERMI <sup>(12)</sup> for the production of mesons by nucleons. We shall suppose that the  $N - \bar{N}$  annihilation will excite, in an interaction volume  $\Omega$  (of radius  $\mathcal{R}$  in the C.M. system) all the degrees of freedom compatible with the general conservation rules. After some time this excitation will « freeze » and one of the possible degrees of freedom will be « gained » in the final state. We shall suppose that the square of the matrix element for the transition to a definite final state will be proportional to the probability of finding that state in  $\Omega$  (being the state normalized to 1 in a large normalization volume  $V$ ). The proportionality constant will obviously depend on the quantum numbers that characterize the reaction; in what follows we shall indicate it by  $A_J$ .

**3'1.  $2\pi$  annihilation.** — Let  $\mathbf{r}_1$ ,  $\mathbf{p}_1$ ,  $\mathbf{r}_2$  and  $\mathbf{p}_2$  be the co-ordinates and momenta of the two final pions. Introducing relative co-ordinates

$$(1) \quad \mathbf{r} = \frac{1}{2}(\mathbf{r}_2 - \mathbf{r}_1), \quad \mathbf{P} = \mathbf{p}_2 - \mathbf{p}_1,$$

<sup>(10)</sup> D. AMATI and B. VITALE: *Nuovo Cimento*, **2**, 719 (1955). In the following we shall refer to this paper as A.

<sup>(11)</sup> R. GATTO: *Nuovo Cimento*, **3**, 468 (1956).

<sup>(12)</sup> E. FERMI: *Progr. Theor. Phys.*, **5**, 570 (1950).



then in the C.M. system

$$(2) \quad p = 2\left(\left(\frac{1}{2}E\right)^2 - m^2\right)^{\frac{1}{2}},$$

where  $E$  is the total energy at disposal and  $m$  the meson mass.

The transition probability for a reaction  $\lambda$  will be <sup>(13)</sup>

$$(3) \quad W_2^\lambda = 2\pi |H_2^\lambda|^2 \frac{\varrho_2 \varepsilon_\lambda}{2!},$$

where  $\varrho_2$ , density of final states (for definite angular momentum eigenfunctions) is given by:

$$(4) \quad \varrho_2 = \frac{L}{\pi} \frac{dp}{dE} = \frac{L}{\pi} \frac{E}{p},$$

where  $L$  is the radius of the normalization volume  $V$ .

The coefficient  $\varepsilon_\lambda$  is given by the isotopic spin multiplicity and by the projections of the initial and final physical states in eigenstates of the total isotopic spin.

The 2 pions annihilation is only possible from  $^3S$  state of the  $\bar{N} - N$  system ( $P$  state of the final mesons); in that case and within the framework of the statistical hypothesis we stated at the beginning of this section

$$(5) \quad |H_2^\lambda|^2 = A_1 \int_{\Omega} |\psi_1^m(\mathbf{r})|^2 d\mathbf{r},$$

where

$$(6) \quad \psi_l^m(\mathbf{r}) = \frac{p^2}{L} j_l(pr) Y_l^m(\cos \theta),$$

( $j_l$  is the spherical Bessel function). It is evident that  $|H_2^\lambda|^2$  does not depend on  $m$ , so that the average over  $m$  gives again (5).

In the following it will be convenient to define

$$(7) \quad a_l(x) = j_l^2(x) - j_{l-1}(x)j_{l+1}(x).$$

Then, if  $\mathcal{R}$  is the radius of the volume of interaction:

$$(8) \quad |H_2^\lambda|^2 = A_1 \mathcal{R}^3 \frac{p^2}{L} a_1(p\mathcal{R}),$$

<sup>(13)</sup> We shall always put  $\hbar = c = 1$ .



and from (3), (4) and (8):

$$(9) \quad W_2^\lambda = A_1 \mathcal{R}^3 a_1(p\mathcal{R}) E p \varepsilon_\lambda.$$

The coefficients  $\varepsilon_\lambda$  are already given in table II of A; in this case the isotopic spin of the final states (two pions in  $P$  wave) can only be  $T = 1$ , and we have

$$(10) \quad \varepsilon_\lambda = \frac{1}{2} \quad \text{for } \bar{p}p, \quad \varepsilon_\lambda = 1 \quad \text{for } \bar{p}n,$$

and obviously 0 for the annihilations into  $2\pi^0$ .

In the case we are considering, the total energy will be nearly equal to the sum of the rest masses of the nucleon and the antinucleon; in the numerical computations we shall take  $E = 2M$  ( $M$  is the nucleon mass). Hereafter we shall use the GeV as the unit of energy.

The calculations were done taking for  $\mathcal{R}$  two values: half the Compton wave length of the pion and the Compton wave length of the nucleon. These can be considered in some way as the extreme values for the radius of the interaction volume. For

$$\mathcal{R} = \frac{1}{2m} = 3.6 \quad \text{we obtained} \quad W_2 = 3.75A_1,$$

and for

$$\mathcal{R} = \frac{1}{M} = 1.07 \quad W_2 = 0.43A_1.$$

**3.2.  $3\pi$  annihilation.** — Let  $\mathbf{r}_i$ ,  $\mathbf{p}_i$  ( $i = 1, 2, 3$ ) be the co-ordinates and momenta of the three final mesons, the charge assignation will follow, for each reaction  $\lambda$  the order used in Tables V and VI of A. We shall make use of the co-ordinate system defined by <sup>(14)</sup>:

$$(11) \quad \begin{cases} \mathbf{R} = \sqrt{\frac{1}{3}}(\mathbf{r}_1 + \mathbf{r}_2 + \mathbf{r}_3), \\ \mathbf{r} = \sqrt{\frac{1}{2}}(\mathbf{r}_2 - \mathbf{r}_1), \\ \mathbf{r}' = \sqrt{\frac{2}{3}}(\mathbf{r}_3 - \frac{1}{2}(\mathbf{r}_1 + \mathbf{r}_2)). \end{cases}$$

Their conjugate momenta are given by:

$$(12) \quad \begin{cases} \mathbf{P} = \sqrt{\frac{1}{3}}(\mathbf{p}_1 + \mathbf{p}_2 + \mathbf{p}_3), \\ \mathbf{p} = \sqrt{\frac{1}{2}}(\mathbf{p}_2 - \mathbf{p}_1), \\ \mathbf{p}' = \sqrt{\frac{2}{3}}(\mathbf{p}_3 - \frac{1}{2}(\mathbf{p}_1 + \mathbf{p}_2)). \end{cases}$$

<sup>(14)</sup> For properties of this system we refer to E. FABRI: *Nuovo Cimento*, **11**, 479 (1954).

Let  $E$  be the total energy in the C.M. system (defined by  $\mathbf{p} = 0$ ) and  $\mathbf{u}$ ,  $\mathbf{u}'$ ,  $\mathbf{p}$ ,  $\mathbf{p}'$  the unit vectors and the moduli of  $\mathbf{p}$  and  $\mathbf{p}'$ ; for each reaction  $\lambda$  the final state will depend on  $\mathbf{p}'$ ,  $\mathbf{u}$  and  $\mathbf{u}'$  <sup>(15)</sup>. If  $w_3^\lambda(\mathbf{p}', \mathbf{u}, \mathbf{u}') d\mathbf{p}' d\mathbf{u} d\mathbf{u}'$  is the transition probability to a state characterized by  $\mathbf{p}'$ ,  $\mathbf{u}$  and  $\mathbf{u}'$ , the three pion annihilation probability as function of  $\mathbf{p}'$  and  $\cos \alpha = \mathbf{u} \cdot \mathbf{u}'$  will be given by

$$(13) \quad w_3^2(\mathbf{p}', \cos \alpha) d\mathbf{p}' d\cos \alpha = \left( \int \int w_3^\lambda(\mathbf{p}', \mathbf{u}, \mathbf{u}') \delta(\mathbf{u} \cdot \mathbf{u}' - \cos \alpha) d\mathbf{u} d\mathbf{u}' \right) d\mathbf{p}' d\cos \alpha.$$

The final state, which is an eigenfunction of  $\mathbf{J}^2$ , can be developed in eigenstates of  $\mathbf{l}^2 = (\mathbf{r} \cdot \mathbf{p})^2$  and  $\mathbf{l}'^2 = (\mathbf{r}' \cdot \mathbf{p}')^2$ . Consistently with the statistical hypothesis stated before we will assume the statistical independence of the  $l'$  waves in the interaction volume; this means that the freezing can find the phase differences of two distinct waves distributed at random among all the possible values. So the only significant result would be the average on all the phase differences. This just eliminates the interferences of different  $l'$  waves.

As will be shown later, each three pion annihilation reaction involves a single value of the total isotopic spin  $T$ . In the following we shall do a further simplification taking the transition matrix element as independent of the final isotopic spin configuration corresponding to the same value of  $T$ . The possibility of different configurations will be taken into account by the isotopic spin multiplicity coefficient  $\varepsilon_\nu$ . Then

$$(14) \quad w_3^\lambda(\mathbf{p}', \mathbf{u}, \mathbf{u}') d\mathbf{p}' d\mathbf{u} d\mathbf{u}' = 2\pi \sum_{l'} |H_{3,l'}^\lambda(\mathbf{p}', \mathbf{u}, \mathbf{u}')|^2 \frac{Q_3 \varepsilon_\lambda}{3!},$$

where  $\varrho_3$  the density of final states, is given by

$$(15) \quad \varrho_3 = \frac{L^2}{\pi^2} \frac{dp}{dE} d\mathbf{p}' d\mathbf{u} d\mathbf{u}'.$$

In the summation of (14) must be considered only those values of  $l'$  that are consistent with the conservation laws; they are specified in Tables V and VI of A.

With the use of our statistical basic assumption we arrive to

$$(16) \quad |H_{3,l'}^\lambda(\mathbf{p}', \mathbf{u}, \mathbf{u}')|^2 = A_\lambda \eta_{l\nu}(p, p') |Z_{l\nu}^{JM}(\mathbf{u}, \mathbf{u}')|^2,$$

where

$$(17) \quad \eta_{l\nu}(p, p') = \frac{p^2 p'^2}{L^2} \int_{\Omega} r^2 r'^2 j_l^2(pr) j_l^2(p'r') dr dr':$$

<sup>(15)</sup>  $p$  will be a function of  $p'$  and  $\cos \alpha = \mathbf{u} \cdot \mathbf{u}'$ .

The function  $Z_{lv}^{MJ}$  is given by

$$(18) \quad Z_{lv}^{MJ}(\mathbf{u}, \mathbf{u}') = \sum_{m, m'} C_{lv}(JM | mm') Y_l^m(\mathbf{u}) Y_l^{m'}(\mathbf{u}'),$$

the  $C_{lv}(JM | mm')$  are the Clebsch-Gordan coefficients. Being  $\Omega$  defined as a sphere of radius  $\mathcal{R}$  in the  $\mathbf{r}_1, \mathbf{r}_2, \mathbf{r}_3$  C.M. system, we take as limits of integration in (17) the values <sup>(16)</sup>

$$(19) \quad r'_{\max} = \sqrt{\frac{3}{2}}\mathcal{R}, \quad r_{\max} = \mathcal{R},$$

obtaining

$$(20) \quad \eta_{lv}(p, p') = \left(\frac{3}{2}\right)^{\frac{3}{2}} \frac{\mathcal{R}^6}{L^2} p^2 p'^2 a_l(p\mathcal{R}) a_l(\sqrt{\frac{3}{2}}p'\mathcal{R}),$$

and then

$$(21) \quad w_3^j(p', \mathbf{u}, \mathbf{u}') d p' d \mathbf{u} d \mathbf{u}' = A_j \int \frac{\sqrt{3}}{2} \frac{1}{2\pi} \mathcal{R}^6 p^2 p'^2 \sum_l a_l(p\mathcal{R}) a_l(\sqrt{\frac{3}{2}}p'\mathcal{R}) \cdot Z_{lv}^{JM}(\mathbf{u}, \mathbf{u}')^2 \varepsilon_\lambda d p' d \mathbf{u} d \mathbf{u}'.$$

The integration of (13) can be readily performed observing <sup>(14)</sup> that the same result is obtained by integrating only over  $\mathbf{u}'$ , taking  $\mathbf{u}$  as quantization axis and then summing over  $M$ . In this way we obtain

$$(22) \quad w_3^j(p', \cos \alpha) d p' d \cos \alpha = \sqrt{\frac{3}{2}} \frac{A_j \mathcal{R}^6}{(2J+1)} \sum_l a_l(p\mathcal{R}) a_l(\sqrt{\frac{3}{2}}p'\mathcal{R}) (2l+1) \cdot (\sum_M |C_{lv}(JM | 0M) Y_l^M(\cos \alpha)|^2) p^2 p'^2 \frac{d p}{d E} \varepsilon_\lambda d p' d \cos \alpha.$$

In order to find the coefficients  $\varepsilon_\lambda$  let us analyze the final states. If  $X$  and  $T$  indicate respectively the space and isotopic spin dependence, the three possible completely symmetrized  $3\pi$  states are given by

$$\Psi_1 = \Psi_X^s \Psi_T^s, \quad \Psi_2 = \sqrt{\frac{1}{2}}(\Psi_X' \Psi_T' + \Psi_X'' \Psi_T''), \quad \Psi_3 = \Psi_X^a \Psi_T^a,$$

where the  $\Psi^s$  are completely symmetric in 1, 2, 3,  $\Psi^a$  completely antisymmetric, and  $\Psi'$  and  $\Psi''$  transform according to the representation  $D$  (characterized by Young tableaux  $\square$ ).  $\Psi_T^s$ ,  $\Psi_T'$  and  $\Psi_T''$  are eigenfunctions of total

<sup>(16)</sup> From the transformation relations (11) and from the definition of  $\Omega$  one can readily see that while  $r'_{\max} = \sqrt{\frac{3}{2}}\mathcal{R}$ , the value  $r_{\max}$  is not a constant but depends on  $r'$  and the angle between  $r$  and  $r'$ . Moreover  $\sqrt{\frac{1}{2}}\mathcal{R} < r_{\max} < \sqrt{2}\mathcal{R}$ , so that owing to the indefiniteness of  $\mathcal{R}$  we can take, within the rather qualitative aim of this calculation, the value  $r_{\max} = \mathcal{R}$ .

isotopic spin  $T = 1$  and it is easy to see that for total charge zero ( $T_3 = 0$ ) they are symmetric for the exchange  $\pi^+ \rightleftharpoons \pi^-$ , so that when  $T_3 = 0$  they are also eigenfunctions of the charge conjugation operator  $U$  with eigenvalue  $u = +1$ . Conversely,  $\Psi_\tau^a$  is simultaneous eigenfunction of  $T$  (with  $T = 0$ ) and of  $U$  with  $u = -1$ . So a  $p\bar{p}$  system with  $u = +1$  can only annihilate into 3 pions if  $T = 1$ , and if  $u = -1$  only if  $T = 0$ . So for  $p\bar{p}$  in the  $^1S$  state we have two final possible states  $\Psi_1$  and  $\Psi_2$ ; in the  $^3S$  case only the state  $\Psi_3$ . For the  $\bar{p}n$  system we have only  $T = 1$  and then  $\Psi_1$  and  $\Psi_2$  as possible final states.

The decomposition of the physical states in states of definite isotopic spin symmetry has been already done in A, the results where summed up in Table III. In this way we obtain for the  $3\pi$  annihilation processes of physical  $p\bar{p}$  and  $\bar{p}n$  systems (isotopic spin mixtures) the coefficients  $\varepsilon_\lambda$  given in Table I.

TABLE I.

Initial particles	Initial state	Final particles	$\varepsilon_\lambda$
$\bar{p}p$	$^1S$	$\pi^0 \pi^0 \pi^0$	3/10
$\bar{p}p$	$^1S$	$\pi^+ \pi^- \pi^0$	7/10
$\bar{p}p$	$^3S$	$\pi^+ \pi^- \pi^0$	5/10
$\bar{p}n$	$^1S$	$\pi^- \pi^- \pi^+$	13/10
$\bar{p}n$	$^1S$	$\pi^0 \pi^0 \pi^-$	7/10

In Table II are listed the values of  $w_3^2(p', \cos \alpha)/A_J \varepsilon_\lambda$  calculated for  $\mathcal{R} = 1/2m$  for each value of  $p'$  and  $\cos \alpha$ . The first number corresponds to the annihilation of a  $^1S$  state and the second to a  $^3S$ . As in the  $2\pi$  annihilation we used  $E = 2M$  and we took the GeV as the energy unity.

Because of the selection rules only a few terms in the sum (22) are needed for  $\mathcal{R} = 1/2m$ , and within an error of a few percent, only the terms ( $ss$ ), ( $dd$ ) and ( $pp$ ) must be taken into account. Integrating numerically  $w_3^2(p', \cos \alpha)$  over  $p'$  and  $\cos \alpha$ , using the values of  $\varepsilon_\lambda$  given in table I and the results previously obtained for the two meson annihilation we obtain the following values for the total probability of transition  $W^\lambda$ .

For  $\bar{p}p$  in  $^3S$  state we have the competition of two and three pion annihilation: the branching ratio in this case is  $W_3/W_2 = 0.16$ . The distribution in  $\cos \alpha$  (normalized to 1 for  $\cos \alpha = 0$ ), and  $p'$  (normalized so that its integration on  $p'$  is equal to ten), calculated with  $\mathcal{R} = 1/2m$ , are given in Tables IV and V. The calculations were also performed for  $\mathcal{R} = 1/M$ ; for the branching ratio of three to two pion annihilation of the  $^3S$  state of  $\bar{p}p$  was obtained  $W_3/W_2 = 10^{-4}$  and for the angular and energy distributions the values given in Tables IV' and V' (with the same normalizations as for Tab. IV and V).

TABLE II.

$P'$	$\cos \alpha$				
	0.0	0.3	0.6	0.9	1.0
0.00	0.00	0.00	0.00	0.00	0.00
	0.00	0.00	0.00	0.00	0.00
0.20	0.24	0.24	0.24	0.24	0.24
	0.02	0.02	0.01	0.00	0.00
0.40	0.61	0.61	0.59	0.62	0.63
	0.27	0.25	0.18	0.05	0.00
0.60	0.78	0.74	0.71	0.83	0.94
	0.77	0.70	0.50	0.15	0.00
0.80	0.86	0.81	0.75	0.88	1.18
	0.82	0.76	0.57	0.18	0.00
1.00	0.96	0.98	1.08	1.26	1.44
	0.27	0.27	0.27	0.08	0.00
1.10	0.62	0.69	1.01	2.53	4.13
	0.03	0.02	0.03	0.07	0.00
1.118	0.00	0.00	0.00	0.00	00.0
	0.00	0.00	0.00	0.00	0.00

TABLE III.

Initial particles	Initial state	Final particles	$W^\lambda$
$\bar{p}p$	$1S$	$\pi^0 \pi^0 \pi^0$	$0.46 A_0$
$\bar{p}p$	$1S$	$\pi^+ \pi^- \pi^0$	$1.08 A_0$
$\bar{p}p$	$3S$	$\pi^+ \pi^-$	$1.88 A_1$
$\bar{p}p$	$3S$	$\pi^+ \pi^- \pi^0$	$0.30 A_1$
$\bar{p}n$	$1S$	$\pi^- \pi^- \pi^+$	$2.00 A_0$
$\bar{p}n$	$1S$	$\pi^0 \pi^0 \pi^-$	$1.08 A_0$
$\bar{p}n$	$3S$	$\pi^- \pi^0$	$3.75 A_1$

TABLE IV.

$\cos \alpha$	0.0	0.3	0.6	0.9	1.0
For initial $1S$ states	1.00	6.99	1.01	1.36	1.74
For initial $3S$ states	1.00	0.91	0.70	0.23	0.00



TABLE V.

$p'$	0.00	0.20	0.40	0.60	0.80	1.00	1.10	1.118
For initial $^1S$ states	0.00	0.31	0.79	0.99	1.08	1.39	1.57	0.00
For initial $^3S$ states	0.00	0.07	0.63	1.80	1.90	0.77	0.10	0.00

TABLE IV'.

$\cos \alpha$	0.0	0.3	0.6	0.9	1.0
For initial $^1S$ states	1.00	1.03	1.09	1.29	1.40
For initial $^3S$ states	1.00	1.05	1.03	0.40	0.00

TABLE V'.

$p'$	0.00	0.20	0.40	0.60	0.80	1.00	1.10	1.118
For initial $^1S$ states	0.00	0.21	0.69	1.17	1.54	1.47	1.05	0.00
For initial $^3S$ states	0.00	0.03	0.36	1.29	2.33	0.71	0.17	0.00

3'3. *Conclusions.* — As expected the value of  $W_3/W_2$  is strongly dependent on  $\mathcal{R}$  <sup>(17)</sup>, and this fact prevents reliable predictions about the relative importance of the two and three pion annihilation; we can only infer that in the only  $S$  state where both annihilations are possible, i.e. the  $^3S$   $\bar{p}p$ , the  $2\pi$  annihilation will be dominant over the  $3\pi$  by a factor of order of magnitude probably greater than 10.

The general features of the energy and angular distribution do not depend strongly on  $\mathcal{R}$ ; this fact allows us to note some peculiarities in the  $3\pi$  annihilations that, with the help of future experimental results, would possibly throw some light about the possible bound states of nucleon-antinucleon pairs and

(17) If we use the approximate expressions of the spherical Bessel functions for small values of the argument from (7) we obtain

$$a_l(x) \sim \frac{2x^{2l}}{(2l+1)!!(2l+3)!!}.$$

With this approximation, which is only good for small values of  $\mathcal{R}$  (let say  $\mathcal{R}$  not greater than 1) we see from (9) and (22) for initial  $^3S$  states  $W_3/W_2 \propto \mathcal{R}^5$ .

the forces among them. From Tables IV and V we see that in the annihilation of the  $^1S$  state of a nucleon-antinucleon system we should find preferentially three colinearly outgoing mesons ( $\cos \alpha \sim 1$ ); in the  $\pi^+\pi^-\pi^0$  annihilation of  $\bar{p}p$  in  $^1S$ , the  $\pi^+$  and  $\pi^-$  will tend to come out in the same direction and the  $\pi^0$  in the opposite with about half of the total kinetic energy available. A similar thing happens for the annihilation of the  $^1S$   $\bar{p}n$  system: in this case the two equally charged mesons will tend to come out together and the other in the opposite direction. For the  $\pi^+\pi^-\pi^0$  annihilation of the  $^3S$   $\bar{p}p$  system, the small values of  $\cos \alpha$ , are preferred and the values of  $p'$  near  $p' = 0.7$ . This means that each meson will preferentially have  $\frac{1}{3}$  of the total kinetic energy available and that they will tend to be distributed at nearly  $120^\circ$  to one another.

#### 4. — Remarks on the Annihilation of Isotopic Spin Eigenstates.

Let  $l$ ,  $s$  and  $T$  be orbital angular momentum, spin and isotopic spin of the initial pair. In Sect. 3.3 we have shown that a nucleon-antinucleon pair with  $T_3 = 0$  can annihilate into three pions only if the charge conjugation quantum number is given by  $u = -(-1)^T$ . From Table IV of A we see that  $u = (-1)^{l+s}$ , then in order to annihilate into three pions,  $l$ ,  $s$  and  $T$  must be related by  $(-1)^{l+s+T+1} = 1$ . As can be immediately verified this last result is true also for  $T_3 = \pm 1$  (it reduces to  $(-1)^{l+s} = 1$ ).

Conversely, to annihilate into  $2\pi$  the necessary condition  $(-1)^{l+s+T} = 1$  must be satisfied; this fact is an immediate consequence of the total symmetrization of the  $2\pi$  state and of results listed in Table IV of A <sup>(18)</sup>.

Hence if there would exist nuclear bound states characterized by definite values of the total isotopic spin then, for each of those states, there would not be competition between two and three pion annihilation. If this would be the case, the ratio of occurrence of  $2\pi$  to  $3\pi$  annihilation could differ radically from that calculated for physical states (isotopic spin mixtures).

A simplified case, somewhat opposite to the case of physical particles, would be that of a nuclear bound state split into two levels characterized by different values of  $T$ , the mean life for annihilation in each level being quite smaller than the lifetime for the transition from one level to the other. If one level gives  $2\pi$  annihilation and the other  $3\pi$ , the two modes of annihilation would be of nearly equal probability, in contrast to the rather smaller probability of the  $3\pi$  annihilation found for the case of a physical pair.

At first sight the possibility of nuclear bound states seems unlikely because

(18) Added in proof. These results were also obtained, independently, by T. D. LEE and C. N. YANG, *Nuovo Cimento* **3**, 749 (1956).

of the great probability of annihilation from a low Coulomb orbit. However this problem is tied to that of the nucleon-antinucleon interaction which, at present, is very obscure. To the clarification of the issue would help an experimental investigation of the pion multiplicity of protonium annihilation.

\* \* \*

We are grateful to Prof. B. FERRETTI for his criticism; one of us (B.V.) wishes to thank Prof. R. E. PEIERLS for his kind hospitality at his Department and a useful discussion.

### *Added in proof.*

After sending this letter we have read a letter of I. JA. POMERANČUK (*Žu Éksper. Teor. Fiz. SSSR*, **30**, 423 1956) where many of the relations contained in our letter are also obtained. At high energy, POMERANČUK foresees  $a) = c)$ , and  $b)$  negligible with respect to  $c)$ .

### RIASSUNTO

Si studia l'annichilamento, in due e in tre mesoni  $\pi$ , di coppie antiprotone-nucleone in stato  $S$  (singoletto e tripletto). Con un modello di tipo statistico per il calcolo degli elementi di matrice per le transizioni, si valuta la relazione tra le sezioni d'urto per annichilamento in due e tre mesoni, e per quest'ultimo caso si ricavano le distribuzioni angolari e gli spettri energetici. Nel calcolo si tengono in conto le leggi di conservazione e le regole di selezione previamente trovate. Infine si fanno alcune considerazioni sulla possibilità di annichilamento di coppie in autostati dello spin isotopico.

## The Structure of the Nucleon.

S. FUBINI

*Istituto di Fisica dell'Università - Torino*  
*Istituto Nazionale di Fisica Nucleare - Sezione di Torino*

(ricevuto il 5 Aprile 1956)

**Summary.** — We derive from the fixed source meson theory an exact relation connecting the structure of the physical nucleon to the meson-nucleon scattering amplitudes. General formulae are obtained for the charge and current densities of the meson cloud of the nucleon. Using these results it is possible to obtain an upper limit of 5.5 meson masses for the cut-off and of 1.65 for the average number of mesons in the cloud. The nucleon magnetic moments take the correct experimental values  $\pm 1.9$  in correspondence of a cut-off to 5 meson masses.

### 1. — Introduction.

In this paper we shall use the fixed source meson theory in order to deduce an exact relation between the structure of the physical nucleon and the pion-nucleon phase-shifts. This relation enables one to calculate the expectation value in the physical nucleon state of any product of two meson field operators in terms of the renormalized coupling constant, the cut-off factor and the experimentally well known data on pion-nucleon scattering.

This result has many applications. First it allows to obtain the rigorous theoretical prediction for the nucleon magnetic moments and for the electron-nucleon scattering cross-sections (<sup>1,1b is</sup>). Secondly it can be used to study the

---

(<sup>1</sup>) Experiments on high energy electron proton scattering have been recently performed at STANFORD: R. HOFSTADTER and W. R. McALLISTER: *Phys. Rev.*, **98**, 217 (1955).

(<sup>1b is</sup>) Note added in proof. Results similar to ours have been obtained by H. MURAZAWA: *Phys. Rev.* **101** 1564 (1956) and by S. B. TREIMAN and R. G. SACHS: *Bull. Am. Phys. Soc.*, **2**, 169 (1956).

internal consistency of the fixed source meson theory <sup>(2)</sup>: we will show that it is possible to find an upper limit of 5.5 meson masses for the cut-off and of 1.65 for the average number of mesons in the nucleon cloud. Finally it gives a check of the various approximation methods applied until now to the fixed-source theory; this point will be treated in detail in a forthcoming publication.

## 2. — General Relations.

Since many of the results of I will be used here, all symbols not explicitly defined will have the same meaning as in that paper <sup>(3)</sup>.

In this section we want to calculate the expectation values in the physical nucleon state of the following operators

$$a_{k\alpha}^* a_{k'\alpha'}^* ; \quad a_{k\alpha}^* a_{k'\alpha'} ; \quad a_{k\alpha} a_{k'\alpha'} .$$

Let us use the identity

$$(\Psi_r, [HA]\Psi_r) = 0 ,$$

where  $A$  is any of the before mentioned operators and  $H = H_0 + H_I$  is the total Hamiltonian, renormalized in such a way that

$$(1) \quad H\Psi_r = 0 ,$$

thus we obtain:

$$(2) \quad \begin{cases} (\omega_k + \omega_{k'}) (\Psi_r, a_{k\alpha}^* a_{k'\alpha'}^* \Psi_r) = - (\Psi_r, [V_{k\alpha} a_{k'\alpha'}^* + a_{k\alpha}^* V_{k'\alpha'}] \Psi_r) , \\ (\omega_k - \omega_{k'}) (\Psi_r, a_{k\alpha}^* a_{k'\alpha'} \Psi_r) = - (\Psi_r, [V_{k\alpha} a_{k'\alpha'} - a_{k\alpha}^* V_{k'\alpha'}^*] \Psi_r) , \\ (\omega_k + \omega_{k'}) (\Psi_r, a_{k\alpha} a_{k'\alpha'} \Psi_r) = - (\Psi_r, [V_{k\alpha}^* a_{k'\alpha'} + a_{k\alpha} V_{k'\alpha'}^*] \Psi_r) . \end{cases}$$

It can be shown easily that <sup>(4)</sup>:

$$(3) \quad a_{k\alpha} \Psi_r = \frac{-1}{\omega_k + H} V_{k\alpha}^* \Psi_r .$$

<sup>(2)</sup> See M. CINI and S. FUBINI: *Nuovo Cimento*, **3**, 764 (1956) quoted in the following as I.

<sup>(3)</sup> In the following all energies and momenta will be measured in units of the meson mass.

<sup>(4)</sup> This because:  $[Ha_{k\alpha}]\Psi_r = Ha_{k\alpha}\Psi_r = -\omega_k a_{k\alpha}\Psi_r - V_{k\alpha}^* \Psi_r$ .



By recalling that the  $a$  and  $V$  operators commute, we get:

$$(4) \quad \begin{cases} (\omega_k + \omega_{k'}) (\Psi_r, a_{k\alpha}^* a_{k'\alpha'}^* \Psi_{r'}) = \left( \Psi_r, \left[ V_{k'\alpha'} \frac{1}{\omega_{k'} + H} V_{k\alpha} + V_{k\alpha} \frac{1}{\omega_k + H} V_{k'\alpha'} \right] \Psi_{r'} \right), \\ (\omega_k - \omega_{k'}) (\Psi_r, a_{k\alpha}^* a_{k'\alpha'} \Psi_{r'}) = \left( \Psi_r, \left[ V_{k\alpha} \frac{1}{\omega_{k'} + H} V_{k'\alpha'}^* - V_{k\alpha} \frac{1}{\omega_k + H} V_{k'\alpha'}^* \right] \Psi_{r'} \right), \\ (\omega_k + \omega_{k'}) (\Psi_r, a_{k\alpha} a_{k'\alpha'} \Psi_{r'}) = \left( \Psi_r, \left[ V_{k\alpha}^* \frac{1}{\omega_{k'} + H} V_{k'\alpha'}^* + V_{k\alpha}^* \frac{1}{\omega_k + H} V_{k'\alpha'}^* \right] \Psi_{r'} \right). \end{cases}$$

Let us now use the definition (I.2) of the  $V_{k\alpha}$ :

$$(5) \quad \begin{cases} (\Psi_r, a_{k\alpha}^* a_{k'\alpha'}^* \Psi_{r'}) = -\frac{e(k, k')}{\omega_k + \omega_{k'}} \sum_{l'l'} \langle l\alpha, r | R(\omega_k) + \bar{R}(\omega_{k'}) | l'\alpha', r' \rangle k_l k'_{l'}, \\ (\Psi_r, a_{k\alpha}^* a_{k'\alpha'} \Psi_{r'}) = -\frac{e(k, k')}{\omega_k - \omega_{k'}} \sum_{l'l'} \langle l\alpha, r | R(\omega_k) - R(\omega_{k'}) | l'\alpha', r' \rangle k_l k'_{l'}, \\ (\Psi_r, a_{k\alpha} a_{k'\alpha'} \Psi_{r'}) = -\frac{e(k, k')}{\omega_k + \omega_{k'}} \sum_{l'l'} \langle l\alpha, r | \bar{R}(\omega_k) + R(\omega_{k'}) | l'\alpha', r' \rangle k_l k'_{l'}, \end{cases}$$

where

$$e(k, k') = \frac{2\pi r(k)r(k')}{(\omega_k + \omega_{k'})^{\frac{1}{2}}},$$

and

$$(6) \quad \langle l\alpha, r | R(\omega_k) | l'\alpha', r' \rangle = (f^0)^2 \left( \Psi_r, \sigma_l \tau_\alpha \frac{1}{\omega_k + H} \sigma_{l'} \tau_{\alpha'} \Psi_{r'} \right).$$

The operator  $\bar{R}$  is obtained from  $R$  by exchanging the meson-indexes:

$$(7) \quad \langle l\alpha, r | \bar{R}(\omega_k) | l'\alpha', r' \rangle = \langle l'\alpha', r | R(\omega_k) | l\alpha, r' \rangle.$$

We are therefore reduced to the calculation of the operator  $R(\omega_k)$ . This will be made by using the general results of I. Equation (I.9) can be written in the form:

$$(8) \quad \frac{-3}{p^3 v^2(p)} \langle l\alpha, r | \text{Im } T(\omega_p) | l'\alpha', r' \rangle = (f^0)^2 [\Psi_r, \sigma_l \tau_\alpha \delta(\omega_p - H) \sigma_{l'} \tau_{\alpha'} \Psi_{r'}].$$

We multiply eq. (8) by  $1/(\omega_p + \omega_k)$ , we integrate from 1 to  $+\infty$  and use

eqs. (I.11, 12, 13) together with the completeness identity:

$$\int_1^{\infty} \delta(\omega_p - H) d\omega_p + \sum_r \Psi_r (\Psi_r = 1),$$

as a final result we obtain:

$$(9) \quad R(\omega_k) = f^2 \frac{(1 - \sigma \cdot l)(1 - \tau \cdot t)}{\omega_k} - 3 \int_1^{\infty} \frac{\text{Im } T(\omega_p) d\omega_p}{p^3 v^2(p)(\omega_k + \omega_p)}.$$

We can write down explicitly the spin and isotopic spin dependence of  $R(\omega_k)$

$$(10) \quad R(\omega_k) = R_1(\omega_k) + R_2(\omega_k)(\sigma \cdot l + \tau \cdot t) + R_3(\omega_k)(\sigma \cdot l)(\tau \cdot t),$$

$$(10') \quad \bar{R}(\omega_k) = R_1(\omega_k) - R_2(\omega_k)(\sigma \cdot l + \tau \cdot t) + R_3(\omega_k)(\sigma \cdot l)(\tau \cdot t),$$

where (see eqs. (I.15, 16))

$$(11) \quad \left\{ \begin{array}{l} R_1(\omega_k) = + \frac{f^2}{\omega_k} + \beta_1(\omega_k) + 4\beta_2(\omega_k) + 4\beta_3(\omega_k), \\ R_2(\omega_k) = - \frac{f^2}{\omega_k} - \beta_1(\omega_k) - \beta_2(\omega_k) + 2\beta_3(\omega_k), \\ R_3(\omega_k) = + \frac{f^2}{\omega_k} + \beta_1(\omega_k) - 2\beta_2(\omega_k) + \beta_3(\omega_k), \end{array} \right.$$

$$(12) \quad \beta_i(\omega_k) = \frac{1}{3\pi} \int_1^{\infty} \frac{d\omega_p \text{Im } g_i(\omega_p)}{p^3 v^2(p)(\omega_p + \omega_k)}.$$

Equations (5), (10), (11) and (12) show that the expectation value of any bilinear form in the meson field is a simple function of the renormalized coupling constant  $f^2$  and of the three quantities  $\beta_1(\omega_k)$ ,  $\beta_2(\omega_k)$  and  $\beta_3(\omega_k)$ . For example the expectation value  $N$  of the total number of mesons in the nucleon cloud can be expressed in the form:

$$(13) \quad N = - \frac{3}{\pi} \int_0^{\infty} \frac{v^2(k) k^4}{\omega_p} \frac{d}{d\omega_k} [R_1(\omega_k)] dk.$$

In the next section we shall apply our results to the investigation of the electromagnetic properties of the nucleon.

### 3. — Electromagnetic Properties of the Nucleon.

It is well known <sup>(5)</sup> that the charge and current densities  $\varrho(\mathbf{x})$  and  $\mathbf{j}(\mathbf{x})$  of meson field are given by:

$$(14) \quad \varrho(\mathbf{x}) = \frac{ei}{2} \sum_{kk'} \frac{\exp[i(\mathbf{k} + \mathbf{k}')\mathbf{x}]}{(\omega_k \omega_{k'})^{\frac{1}{2}}} [(\omega_k - \omega_{k'})(a_{k1}a_{k'2} - a_{k1}^*a_{k'2}^*) - \\ - (\omega_{k'} + \omega_k)(a_{k1}^*a_{k2} - a_{k1}a_{k2}^*)],$$

$$(14') \quad j_\mu(\mathbf{x}) = \frac{ei}{2} \sum_{kk'} \frac{\exp[i(\mathbf{k} + \mathbf{k}')\cdot\mathbf{x}]}{(\omega_k \omega_{k'})^{\frac{1}{2}}} (k'_\mu - k_\mu) \cdot \\ \cdot [a_{k1}a_{k'2} + a_{k1}^*a_{k2}^* + a_{k1}^*a_{k'2} + a_{k1}a_{k2}^*].$$

The expectation values of  $\varrho(\mathbf{x})$  and  $\mathbf{j}(\mathbf{x})$  in the physical nucleon state will be obtained using eqs. (5), (10), (10')

$$(15) \quad \varrho(\mathbf{x}) = -8\pi\tau_z e \sum_{k,k'} \frac{v(k)v(k')(\mathbf{k} \cdot \mathbf{k}') \exp[i(\mathbf{k} + \mathbf{k}')\mathbf{x}]}{k^2 - k'^2} [R_2(\omega_k) - R_2(\omega_{k'})],$$

$$(15') \quad j_\mu(\mathbf{x}) = 8\pi\tau_z ei \sum_{k,k'} \frac{v(k)v(k')k_\mu(\mathbf{k} \wedge \mathbf{k}') \cdot \boldsymbol{\sigma} \exp[i(\mathbf{k} + \mathbf{k}')\mathbf{x}]}{k^2 - k'^2} \left[ \frac{R_3(\omega_k)}{\omega_k} - \frac{R_3(\omega_{k'})}{\omega_{k'}} \right].$$

For simplicity of notation the expectation values are denoted with the same symbols as the corresponding operators.

By transforming the sums into integrals <sup>(6)</sup> and performing the angular integrations we get ( $r = |\mathbf{x}|$ )

$$(16) \quad \varrho(\mathbf{x}) = \frac{-2\tau_z e}{\pi^3} \int_0^\infty \int_0^\infty \frac{v(k)k^3 dk v(k')k'^3 dk' j_1(kr)j_1(k'r)}{k^2 - k'^2} [R_2(\omega_k) - R_2(\omega_{k'})],$$

$$(16') \quad \mathbf{j}(\mathbf{x}) = \frac{-2\tau_z e}{\pi^3} \frac{\mathbf{x} \wedge \boldsymbol{\sigma}}{r^2} \int_0^\infty \int_0^\infty \frac{v(k)k^3 dk v(k')k'^3 dk' j_1(kr)j_1(k'r)}{k^2 - k'^2} \left[ \frac{R_3(\omega_k)}{\omega_k} - \frac{R_3(\omega_{k'})}{\omega_{k'}} \right],$$

<sup>(5)</sup> See e.g. G. WENTZEL: *Quantum Theory of Fields* (New York, 1949). This author uses a convention opposite to ours for the isotopic spin of the nucleons.

<sup>(6)</sup> Since the normalization volume has been taken equal to 1, the sums will be transformed as follows  $\sum_k \rightarrow \frac{1}{(2\pi)^3} \int d^3k$ .

where  $j_1$  is the spherical Bessel function defined by

$$j_1(\varrho) = \frac{\sin \varrho}{\varrho^2} - \frac{\cos \varrho}{\varrho}.$$

Formulae (16) can be used to study the scattering of high energy electrons by nucleons. This will be done in a future work. Here we want only to remark that, for values of  $r$  of the order of the meson Compton wave length (which are the most important for that problem)  $\varrho$  and  $j$  do not depend appreciably on the choice of the form factor  $u(k)$ .

The total charge

$$(17) \quad e \cdot Q \tau_z = \int \varrho(r) d^3x,$$

and the total magnetic moment

$$(17') \quad \frac{e}{2M} \mathcal{M} \tau_z = \frac{1}{2} \int \mathbf{x} \wedge \mathbf{j}(\mathbf{x}) d^3x,$$

of the meson cloud can be obtained from (15), (15') (7)

$$(18) \quad Q = + \frac{2}{\pi} \int_0^\infty \frac{v^2(k) k^4 dk}{\omega_k} \frac{d}{d\omega_k} [R_2(\omega_k)],$$

$$(18') \quad \mathcal{M} = - \frac{4}{3\pi} \int_0^\infty \frac{v^2(k) k^4 dk}{\omega_k} \frac{d}{d\omega_k} \left[ \frac{R_3(\omega_k)}{\omega_k} \right].$$

The importance of the meson contribution to the charge of the physical nucleon has been pointed out by M. CINI. By applying the total isotopic spin conservation law (8) he has shown that:

$$(19) \quad Q = \frac{1 - (1/\varrho_1)}{2}.$$

---

(7) One must recall the orthogonality property of the Bessel function  $j_1(x)$ :

$$\int_0^\infty j_1(kr) j_1(k'r) r^2 dr = \frac{\pi}{2k^2} \delta(k - k').$$

(8) Since in the fixed source theory angular momenta and isotopic spins are treated symmetrically, the conservation of the total angular momentum gives the same result as (18) and (19).

On the other hand  $1/q_1$  must satisfy to the inequality <sup>(9)</sup>

$$(20) \quad \frac{1}{q_1} \leq \frac{1}{3}.$$

Therefore  $Q$  must be smaller than  $\frac{2}{3}$ , in next section we will show that this gives a very stringent upper limit for the cut-off of the theory.

#### 4. - Numerical Results and Discussion.

In order to simplify the discussion we shall concentrate on the case of a square cut-off at  $\xi$ . We need now an estimate of the renormalized coupling constant  $f^2$  and of the three functions  $\beta_1(\omega_k)$ ,  $\beta_2(\omega_k)$ ,  $\beta_3(\omega_k)$ .

In a recent investigation <sup>(10)</sup> it has been shown that the value of the coupling constant suggested by experiment is

$$f^2 = 0.105.$$

In that same paper the  $\beta_i(\omega_k)$  (which appear also in the Low sum rule) have been estimated. Since the high energy contributions to the integrals (12) have been proved to be small, the  $\beta_i$  are completely determined by the low-energy region which depends on the experimentally well known pion-nucleon phase-shifts. In this way one obtains that  $\beta_1(\omega_k)$  and  $\beta_2(\omega_k)$  are negligible and that  $\beta_3(\omega_k)$  can be well approximated by

$$\beta_3(\omega_k) = \frac{0.020}{\omega_k + 1.8}.$$

<sup>(9)</sup> W. THIRRING: private communication. The inequality (20) can be proven as follows. Let us call  $\tau'$  the isotopic spin operator of the physical nucleon. Then the total isotopic spin of the meson cloud  $T$  will be given by

$$(A.1) \quad T = \frac{1}{2}(\tau' - \tau).$$

On the other hand, since in the physical nucleon state only states with  $T=0$  and  $T=1$  appear, we must have

$$(A.2) \quad (\Psi_r, T^2 \Psi_r) \leq 2.$$

Now eqs. (A.1) and I.11) give

$$(A.3) \quad (\Psi_r, T^2 \Psi_r) = \frac{1}{4} \left( 6 - \frac{6}{q_1} \right).$$

eq. (20) follows immediately from (A.2) and (A.3).

<sup>(10)</sup> M. CINI, S. FUBINI and A. STANGHELLINI: *Nuovo Cimento*, **3**, 1379 (1956).



Using these numerical values we have evaluated  $Q$ ,  $\mathcal{M}$ ,  $N$  in correspondence to different values of the cut-off  $\xi$ . Our results are listed in Table I:

TABLE I.

$\xi$	$Q$	$\mathcal{M}$	$N$	$1/e_1$
4.5	0.43	1.6	1.0	0.14
5.0	0.54	1.9	1.3	-0.08
5.5	0.67	2.1	1.65	-0.33

Table I together with eqs. (19) and (20) shows that  $\xi$  cannot be higher than 5.5. At the same time it shows that the total number of mesons  $N$  is higher than one only for  $\xi < 4.5$ . In I it has been proven that the one-meson approximation gives rise to strong inconsistencies and therefore the states with many mesons must be important. Thus it seems reasonable <sup>(11)</sup> to state that the acceptable values of  $\xi$  must lie between 4.5 and 5.5. This is confirmed by the calculation of the magnetic moment  $\mathcal{M}$  which takes its correct experimental value 1.9 for  $\xi = 5$ .

\* \* \*

The author is very grateful to Prof. M. CINI for useful advice and criticism and to Prof. W. THIRRING for an illuminating discussion.

<sup>(11)</sup> Some new results obtained by W. THIRRING and the present author allow to put these somewhat qualitative arguments on a firmer basis (see W. THIRRING: communication at the Rochester Conference, 1956).

## RIASSUNTO

Si ricava, a partire dalla teoria mesonica di sorgente fissa, una relazione esatta fra la struttura del nucleon fisico e le fasi dell'urto mesone-nucleone. Si ottengono delle formule generali per le densità di carica e di corrente della nuvola mesonica del nucleone. Questi risultati ci permettono di ottenere un limite superiore di 5.5 masse mesoniche per il taglio e di 1.65 per il numero medio di mesoni nella nuvola. Per un taglio a 5 masse mesoniche i momenti magnetici dei nucleoni assumono i valori  $\pm 1.9$ , in accordo con l'esperienza.

## Intergalactic Space and Cosmic Rays.

G. COCCONI (\*)

*Istituto di Fisica dell'Università - Bologna*

(ricevuto il 12 Aprile 1956)

**Summary.** — Arguments are presented suggesting that the most energetic particles observed in the Cosmic Radiation are accelerated outside the galaxy, in the intergalactic space. The problem of the Cosmic Ray acceleration in the intergalactic space is discussed and some possible models are presented.

### Introduction.

The problem of the origin of the Cosmic Radiation (C.R.) can be subdivided into two parts.

One deals with the problem of the acceleration of ions from rest to, say,  $10^{10}$  eV; the second with the subsequent acceleration of a small percentage of C.R. from  $10^{10}$  eV to the maxima energies observed, i.e.  $> 10^{18}$  eV.

It is probable that the first acceleration takes place in the neighborhood of stars, though the actual mechanism is still quite controversial. We are not going to discuss this topic here.

The opinions about the subsequent acceleration are also divided; however, there is a quite universal agreement that the highest energies cannot be reached through mechanisms operating in the neighborhood of the stars, but that the acceleration takes place in the interstellar space, through interaction of the already accelerated ions emitted by the stars with the turbulent conducting galactic gas.

The fundamental work on this subject is by FERMI (1); modifications to

---

(\*) On leave from Cornell University, Ithaca, N.Y., U.S.A.

(1) E. FERMI: *Phys. Rev.*, **75**, 1169 (1949).

the first model have been later proposed by FERMI himself <sup>(2)</sup> and by others <sup>(3-5)</sup>, but the assumption has always been made that the acceleration takes place within the galaxy, be it the flat disk determined by the population I stars, or the spheric object determined by the population II stars and the gas <sup>(6)</sup>.

However, the experimental evidence gained in the last years seems to suggest that at least the most energetic particles cannot be accelerated inside the galaxy, and that in a complete picture of the origin of C.R. a chapter must be added, dealing with the acceleration of C.R. in the Inter-Galactic Space (I.G.S.).

The present note is dedicated to this problem. In Sect. 1 the arguments will be presented that suggest the necessity of an inter-galactic acceleration. In Sect. 2 some considerations about the I.G.S. acceleration are presented.

## 1. - Arguments Against a Purely Galactic Origin of the Cosmic Radiation.

The experimental information most directly related to the origin of C.R. is the following:

a) The analysis of the Extensive Air Showers by means of several hundreds detectors spread over surfaces of the order of one square kilometer gives conclusive evidence that primary C.R. with energies up to  $10^{18} \div 10^{19}$  eV exist, and that their frequency corresponds to a power spectrum (integral) with exponent  $1.8 \div 2.0$  (CLARK, KRANSHAW, VERNOV) <sup>(7)</sup>. This is the same law that holds for lower energies. Hence, a single spectrum describes the frequency of the primary C.R. for energies from  $10^{11}$  to  $10^{18} \div 10^{19}$  eV.

b) All the systematic measurements thus far made on Extensive Air Showers produced by primaries of  $\sim 10^{17}$  eV (KRANSHAW, CLARK <sup>(7)</sup> and KRANSHAW <sup>(8)</sup>) suggest that the distribution in space of these particles is isotropic. If a sidereal anisotropy exists, the amplitude,  $\delta$ , of the first harmonic is probably not larger than 0.10 times the average intensity. For primaries of  $10^{10}$  to  $10^{15}$  eV the measurements done thus far give  $\delta < 10^{-3}$  (DAUDIN <sup>(9)</sup>).

<sup>(2)</sup> E. FERMI: *Ap. Journ.*, **119**, 1 (1954).

<sup>(3)</sup> P. MORRISON, S. OLBERT and B. ROSSI: *Phys. Rev.*, **94**, 440 (1954).

<sup>(4)</sup> C. Y. FAN: *Phys. Rev.*, **101**, 314 (1956).

<sup>(5)</sup> L. DAVIS: *Phys. Rev.*, **101**, 351 (1956).

<sup>(6)</sup> S. B. PIKELVER: *Dokl. Akad. Nauk SSSR*, **88**, 229 (1953); G. R. BURBIDGE: *Phys. Rev.*, **101**, 906 (1956).

<sup>(7)</sup> *Communications at the Guanajuato (Mexico) Meeting* (September 1955).

<sup>(8)</sup> J. K. KRANSHAW and H. ELLIOT: *Proc. Phys. Soc.*, **A 69**, 102 (1956).

<sup>(9)</sup> J. DAUDIN, P. AUGER, A. CACHON and A. DAUDIN: *Nuovo Cimento*, **3**, 1017 (1956).

c) Up to energies per nucleon of  $\sim 10^{14}$  eV the mass spectrum of the primary C.R. seems to remain unchanged, i.e., preponderantly composed of protons. Various arguments, in part based on experimental evidence, in part speculative, make it plausible that even at the highest energies ( $10^{18} : 10^{19}$  eV) the protons still are the most abundant particles in the primary C.R. <sup>(10)</sup>.

In the models proposed thus far, where the acceleration of C.R. takes place inside the galaxy, the three requirements listed above are met as follows:

1) By limiting the average life spent by C.R. in the galaxy to a time that corresponds to the crossing of no more than  $\sim 1 \text{ g} \cdot \text{cm}^{-2}$  of interstellar matter. This assures that the particles do not suffer nuclear collisions during their stay in the galaxy, an essential condition for explaining the existence of heavy ions in the primary C.R. with the abundances observed.

2) By diffusing the C.R. in the turbulent magnetic fields of the galaxy, fields with average magnitude of the order of  $10^{-6} : 10^{-5}$  gauss. This insures both the acceleration of the particles up to the highest energies with a power spectrum, and their isotropic distribution.

In order to see how the models so far proposed fit the experimental evidence, let us consider first the model in which the galaxy is a sphere of radius  $R = 5 \cdot 10^{22} \text{ cm}$  filled with gas of density  $\sim 10^{-25} \text{ g} \cdot \text{cm}^{-3}$ , in which C.R. diffuse at random <sup>(6)</sup>. In this case the anisotropy,  $\delta$ , can be easily correlated to the total path of the particles in the galaxy,  $L$ .

Following the method of MORRISON *et al.* <sup>(3)</sup>, the anisotropy is given by:

$$\delta = \frac{2(\psi_2 - \psi_1)}{\psi_1 + \psi_2},$$

where  $\psi_1$  and  $\psi_2$  are the fluxes of C.R. at the earth, going towards and away respectively from the centre of the galaxy. If  $S$  is the strength of the C.R. source, and  $\varrho_0$  the C.R. density in the galaxy, then:

$$4\pi R_s^2(\psi_2 - \psi_1) = \int_0^{R_s} S dV \quad \text{and} \quad \psi_1 + \psi_2 = \frac{1}{2}\varrho_0 v,$$

where  $R_s$  is the distance of the sun from the center of the galaxy ( $R_s \approx 3 \cdot 10^{22} \text{ cm}$ ),

<sup>(10)</sup> Actually the last point of c) is not of fundamental importance for the evaluation of the magnetic rigidity. If the primaries of the most energetic Extensive Air Showers are heavy nuclei, then the estimate of their energy from the secondaries observed at sea-level must be increased and their magnetic rigidity would not change substantially. Besides, a factor of 2 would come from the mass to charge ratio of stable nuclei. More important is the fact that at  $10^{13} : 10^{14}$  eV nucleon heavy nuclei have been observed roughly in the same proportion as observed at the lowest energies.

and  $v$  the velocity of C.R.;  $\varrho_0$  can be eliminated by observing that the ratio

$$\frac{L}{v} = T_0 = \text{average time spent by C.R. in the galaxy,}$$

is equal to the ratio between the total number of C.R. present in the galaxy and the total source output per unit time:

$$\frac{L}{v} = \frac{\int_0^R \varrho_0 dV}{\int_0^R S dV} \approx \frac{\frac{4}{3} \pi R^3 \varrho_0}{\int_0^R S dV}.$$

This gives:

$$\delta = \frac{4R}{3L} \left( \frac{R}{R_s} \right)^2 \frac{\int_0^{R_s} S dV}{\int_0^R S dV} \approx \frac{4}{3} \frac{R_s}{L}.$$

Utilizing this relation one obtains the lower limits for  $L$  as given in Table I.

TABLE I.

Average energy (eV)	$\delta$ observed	
$U_1 = 10^{10}$	$< 10^{-3}$	$L_1 > 4 \cdot 10^{25} \text{ cm} = 4 \text{ g} \cdot \text{cm}^{-2}$
$U_2 = 10^{15}$	$< 10^{-3}$	$L_2 > 4 \cdot 10^{25} \text{ cm} = 4 \text{ g} \cdot \text{cm}^{-2}$
$U_3 = 10^{17}$	$< 10^{-1}$	$L_3 > 4 \cdot 10^{23} \text{ cm} = 0.04 \text{ g} \cdot \text{cm}^{-2}$

The fact that  $L$  remains as large as at least several  $\text{g} \cdot \text{cm}^{-2}$  up to  $10^{15} \text{ eV}$  means that, in this model, the particles of  $10^{15} \text{ eV}$  from the moment of their injection to the final energy must cross a total thickness equivalent to

$$L_{\text{tot}} > L_1 \ln \frac{U_2}{U_1} \approx 10 L_1 = 40 \text{ g} \cdot \text{cm}^{-2}.$$

This is incompatible with the observed existence of heavy ions <sup>(11)</sup>. It is worth

<sup>(11)</sup> It seems that this point has been missed in the previous literature. What is usually quoted is  $L_1$  the average path length of *all* C.R. in the galaxy, i.e., of the particles with average energy  $\sim U_1$ . When particles of energy  $U_2$  are actually observed, their average path length is  $\ln(U_2/U_1)$  times larger than the average path length of all particles.



noticing that we are evaluating lower limits, since no sidereal anisotropy has been actually observed thus far.

The evaluation of  $L_{\text{tot}}$  is based only on the asymmetry; actually it must be proved that the particles in question can cover that length while diffusing inside the galaxy.

If the average magnetic field in the turbulent elements of the galaxy is  $H$  gauss, and  $U$  (eV) is the (relativistic) energy of the particles, the radius of curvature in such a field for a particle of charge  $e$  is  $r = U/300H$  cm. This is also the lower limit for the dimensions of the diffusing elements. The m.f.p. between collisions must be somewhat larger, say:

$$\lambda \approx 2\pi U/300H.$$

The particles being accelerated over the whole volume, the average displacement before leaving the galaxy will be  $\approx aR$ , with  $a \approx \frac{1}{3}$ , and the average number of collisions in the galaxy will be:

$$N = \left( \frac{aR}{\lambda} \right)^2.$$

This corresponds to a total length:

$$L_{\text{tot}} = N\lambda = \frac{6 \cdot 10^{40}}{U} \text{ cm},$$

if  $H = 5 \cdot 10^{-6}$  gauss is used. For  $U = 10^{15}$  eV and  $U = 10^{17}$  eV the values of  $L$  given by this equation barely stay within the limits given in Table I. This means that the spherical galaxy, even if evenly packed with diffusing elements is barely able to hold the most energetic C.R. for the time required to mask, at the earth, the effect of the empty space.

The same arguments are even more radically against any model in which it is assumed that the random diffusion takes place in a disk-shaped galaxy or in the spiral arms.

In more recent models, however, the acceleration is not attributed to random collisions, but to series of coherent collisions against pairs of moving shock waves <sup>(2-4)</sup>, or to « betatron » collisions <sup>(5)</sup>. In these cases an overall magnetic field along the spiral arms of  $\sim 5 \cdot 10^{-6}$  gauss prevents the escaping of C.R. from the sides, and allows it only at the end of the spiral arms. The evaluation of the anisotropy expected depends then essentially on the detailed features of the magnetic field <sup>(12)</sup>. Probably it would be possible to imagine

<sup>(12)</sup> L. DAVIS: *Phys. Rev.*, **96**, 743 (1954).

a situation such that the experimental data known thus far can be satisfied. However, we want to remark that in a field of  $5 \cdot 10^{-6}$  gauss a proton of  $10^{18} \div 10^{19}$  eV has a radius of curvature of  $10^{21} \div 10^{22}$  cm, even larger than the cross dimensions of the spiral arm. How can a particle not only be confined, but also be accelerated in the spiral arms at these energies?

Another argument that applies to all galactic models is the following. The exponent  $\gamma$  of the integral spectrum of C.R. remains practically the same ( $\sim 1.8$ ) from  $10^{11}$  eV to  $10^{19}$  eV.

In all galactic theories this is considered as due to the fact that the energy of each C.R. in the galaxy increases exponentially with the number  $N$  of collisions between the particle and the accelerating turbulences:

$$U = U_0 \exp[\beta^2 N],$$

while the probability  $P$  of staying inside the galaxy decreases exponentially with  $N$ ,

$$P = P_0 \exp[-N/N_1],$$

where  $\beta$  is proportional to the velocity of the accelerating turbulence and  $N_1$  is the average number of collisions before escaping from the galaxy. Combining the two expressions, one gets:

$$P = P_0 \left( \frac{U_0}{U} \right)^{1/\beta^2 N_1}, \quad \text{so that} \quad \gamma = \frac{1}{\beta^2 N_1}.$$

The constancy of  $\gamma$  means that the product  $\beta^2 N_1$  is independent of energy for  $10^{11}$  eV  $< U < 10^{18}$  eV. If both  $\beta$  and  $N_1$  remain constant, then the difficulties discussed before become worse, because the smallest maximum anisotropy ( $\delta < 10^{-3}$ ) would apply also to the highest energies.

It is more plausible to assume that at small energies the C.R. are scattered more, i.e., that the turbulent fields are not all of the same strength; this would mean that  $N_1$  decreases when the energy increases, and  $\beta$  correspondingly increases. But this is just the opposite of what is expected of any of the proposed accelerating mechanisms; i.e., that in a collision the percent gain of the C.R. energy should increase as the energy of the C.R. increases.

We can conclude that all the arguments presented strongly suggest that at least part of the cosmic radiation comes from outside the galaxy.

We want to emphasize that the strength of these arguments is limited only by the inadequacy of the observational material and that any reasonable extrapolation would make them even more compelling.

For instance, it is quite sensible to expect that the energy spectrum extends well beyond the  $10^{18} \div 10^{19}$  eV to which the present experimental possibilities limit our knowledge. In such a case, the mechanisms «ad hoc» barely able to justify the existence of the maxima energies observed thus far will become totally inadequate, and more general properties of the Universe will have to be investigated.

## 2. — Some Consequences of the Intergalactic Acceleration.

a) Let us first consider the problem of the amount of matter crossed by C.R. moving in the Inter-Galactic Space.

The value of the density of matter in I.G.S. is still in question. However, it is admitted that it must be several orders of magnitude smaller than that in the galaxy. The values most frequently quoted range between  $10^{-27}$  and  $10^{-30}$  g·cm<sup>-3</sup>.

The upper limit to the total thickness of matter crossed by C.R. being  $\sim 1$  g·cm<sup>-2</sup>, these densities correspond to path lengths of  $10^{27} \div 10^{30}$  cm, and for relativistic particles to times of  $10^9 \div 10^{12}$  years.

The first of these figures is smaller than the so called age of the Universe ( $\sim 10^{10}$  years), but the second is quite larger, so we can conclude that likely the movement of C.R. in the intergalactic spaces is not limited by time.

b) Let us now assume that the I.G.S. is empty, and that each galaxy is emitting a flux,  $q$  (erg s<sup>-1</sup>), of C.R. equal to that emitted by our own galaxy. Then,

$$q = \frac{q_0 \omega}{T_0},$$

where:  $q_0$  = average energy density of C.R. in the galaxy,

$\omega$  = volume of the galaxy,

$T_0$  = average life of C.R. in the galaxy  $\approx 10^7$  years.

What is then the average energy density of C.R.,  $q$ , in the intergalactic space?

If  $T$  is the average life of the particles in the Universe, and  $\Omega$  the average volume of I.G.S. surrounding each galaxy ( $\Omega \approx 10^7 \omega$ ):

$$q \approx \frac{qT}{\Omega} = q_0 \frac{\omega}{\Omega} \frac{T}{T_0} \approx 10^{-7} q_0 \frac{T}{T_0}.$$

The value of  $T$  depends on the model chosen for the Universe. An infinite

static Universe gives  $T = \infty$  and  $q \rightarrow q_0$ ; this is the Cosmic Ray analogue of the Olbers' paradox for the visible light <sup>(13)</sup>.

For an Universe expanding with the recession constant

$$h \approx \frac{1}{10^{10} \text{ years}}, \quad \text{one has} \quad T \approx \frac{1}{h} = 10^{10} \text{ years}.$$

For a steady state Universe, with the same recession constant <sup>(13)</sup>, again  $T \approx 10^{10}$  years.

The most accepted models of the Universe being of these last kinds, we conclude that, if there is no acceleration in the I.G.S.:

$$q \approx 10^{-4} q_0.$$

Thus any mechanism capable of accelerating C.R. in the I.G.S. has, to start with, a flux of C.R. up to the highest galactic energies,  $10^4$  times smaller than that in the galaxies themselves, or larger.

This can be of help in providing a mechanism of acceleration with the injection of particles of high energy <sup>(14)</sup>.

c) If the acceleration takes place through interaction of the C.R. with moving magnetic fields (Fermi-like mechanism), the strength of the fields must satisfy the condition:

$$(1) \quad Hd \geq 10^{17} \text{ gauss} \cdot \text{cm},$$

where  $H$  is the average value of the field, and  $d$  its dimension.

The overall field of our galaxy has  $Hd \approx 5 \cdot 10^{16}$  gauss·cm, and if this value is representative for all galaxies, the galaxies themselves are barely able to participate in this kind of acceleration. In fact, the transparency of our galaxy to the most energetic C.R. constitutes the main argument against these particles being of galactic origin.

A mechanism of acceleration by means of the interaction of C.R. with the magnetic fields of two galaxies, (our own and the Magellanic clouds) has been proposed by HEIDMAN <sup>(15)</sup>. In the specific case, HEIDMAN does not try to explain the highest energies we are considering here, but it is conceivable that in other systems of galaxies, e.g., the colliding galaxies responsible for the strongest source of radio emission, conditions can arise where the highest energies can be achieved.

<sup>(13)</sup> See e.g., H. BONDI: *Cosmology* (Cambridge, 1952).

<sup>(14)</sup> Actually it is likely that  $T_0$ , the average life of C.R. in the galaxy, decreases as the energy of the particles increases; for very energetic particles, therefore,  $q$  is probably larger than  $10^{-4}q_0$ ; for the extreme energies, in fact,  $q \approx q_0$ .

<sup>(15)</sup> J. HEIDMAN: Private communication.

The lack of anisotropy observed for C.R. requires however that these sources are numerous and quite uniformly distributed in the Universe. Besides, if the volume of the accelerating region is limited to a small fraction of the space, the efficiency of production of C.R. must correspondingly increase.

A mechanism operating throughout the volume of the I.G.S. would be more appealing. Let us suggest two models of this kind.

Model one is based on the assumption that in the I.G.S. « clouds » of ionized gas exist with random velocities and dimensions such as to create magnetic fields satisfying condition (1). These clouds would then be capable of accelerating C.R. as in the Fermi model. Condition (1) is demanding; e.g., it requires clouds of  $\sim 10^{23}$  cm diameter moving with random velocities of  $3000 \text{ km s}^{-1}$ , assuming equipartition between kinetic and magnetic energy (density of intergalactic matter  $10^{-28} \text{ g} \cdot \text{cm}^{-3}$ ).

How well these conditions are met by the intergalactic gas is difficult to say. It seems likely that the gas is weakly ionized and that turbulences exist in it, because the galaxies with their magnetic fields move in it with random velocities not much smaller than the value quoted above. More experimental evidence is of course necessary.

The second model postulates the emission by the galaxies of electromagnetic waves of very low frequency, say 1 cycle per second, and high amplitude, say  $10 \text{ V} \cdot \text{cm}^{-1}$ .

The density of the intergalactic free electrons is low enough to allow the propagation of these waves, and any C.R. injected with the right phase could have its energy increased by the factor <sup>(16)</sup>

$$g = 1 + \left( \frac{eE\lambda}{\pi mc^2} \right)^2,$$

where:  $E$  = max. electric field,

$\lambda$  = wave length,

$m$  = mass of the accelerated particle.

With the field and the frequency quoted,  $g \approx 30$  for protons. Of course, when the injection occurs with the wrong phase the energy of the C.R. is decreased by the same factor, but what matters is that some of the galactic C.R. can gain energy.

There is no experimental evidence for the existence in the I.G.S. of such electromagnetic waves. An extrapolation of many orders of magnitude of the spectra observed for the radio-waves emitted by the galaxies could give

<sup>(16)</sup> E. McMILLAN: *Phys. Rev.*, **79**, 498 (1950).



numbers not in disagreement with those quoted, but of course such extrapolation is completely arbitrary.

What we want to point out in presenting these models is that, it is possible to think of mechanisms by which C.R. can be further accelerated in the I.G.S. without invoking very unusual phenomena.

A serious difficulty in envisaging an intergalactic acceleration of C.R. stays, in our opinion, in the time scale. It seems that the statistical mechanisms, as, e.g., those described before, are too slow to give an average gain in energy of the many orders of magnitude required in a time as *small* as the age of the Universe ( $\sim 10^{10}$  years).

However, our ignorance of both the properties of the I.G.S. and of the structure of the Universe are such that these difficulties cannot be considered unsurmountable.

As a conclusion, we think that problems of this kinds are now ripe for discussion and that, from the experimental point of view, researches that could give more information about the properties of C.R. particles of energies of  $10^{18}$  eV and greater are worth pursuing.

\* \* \*

The author wants to thank K. GREISEN for long discussions on the subject, and L. DAVIS, J. HEIDMAN and P. MORRISON for helpful suggestions.

The author is grateful to the Guggenheim Foundation whose grant made his stay in Bologna possible.

---

#### RIASSUNTO

Vari risultati sperimentali suggeriscono che almeno la parte più energica della radiazione cosmica non sia tutta contenuta ed accelerata nella galassia, ma sia invece comune a tutto l'universo e probabilmente accelerata negli spazi intergalattici. L'evidenza sperimentale è presentata nella prima parte, mentre nella seconda vengono discusse alcune conseguenze della presenza negli spazi intergalattici della radiazione cosmica ed esaminati alcuni meccanismi che potrebbero essere responsabili della sua accelerazione.

## NOTE TECNICHE

### Light Pulses Excited by $\alpha$ Particles in Argon. A Gaseous Scintillation Detector.

M. FORTE

*Laboratori CISE - Milano*

(ricevuto il 13 Marzo 1956)

**Summary.** — The light pulses produced by the passage of individual  $\alpha$ -particles through gases have been detected and analyzed by means of a suitable experimental technique. In Part I, the time shape of pulses obtained with argon of various purities is studied with respect to the mechanism of photon production. In Part II, we deal with the possibilities of the particle detectors based on the gas scintillation. A scintillation chamber filled with argon was found to be suitable for the spectral analysis of  $\alpha$ -particles, yielding a 13% resolution at  $\sim 5$  MeV, for instance. The resolving time of this instrument is a very short one.

#### Introduction.

The luminescence caused by the passage of  $\alpha$ -particles through gases has been studied in many works with the method of measuring the integral intensity of the light produced by a beam of particles <sup>(1)</sup>.

With the progress of the photomultiplier technique the accuracy of such measurements was improved <sup>(2)</sup>.

An interesting development in these works, made possible by the high sensitivity of photo-multipliers, consists in the method of revealing the luminescence produced by individual  $\alpha$ -particles in the gas under consideration. This was done by MUEHLHAUSE in 1953 <sup>(3)</sup> who utilized both the visible and the UV component of the luminescence, by covering the phototube surface with a proper wavelength shifter (stilbene or NaI).

<sup>(1)</sup> R. AUDUBERT and S. LORMEAU: *Compt. Rend.*, **228**, 318 (1949).

<sup>(2)</sup> A. GRÜN and E. SCHOPPER: *Zeits. f. Naturfor.*, **6a**, 698 (1951); A. WARD: *Proc. Phys. Soc.*, **67a**, 841 (1954).

<sup>(3)</sup> C. MUEHLHAUSE: *Phys. Rev.*, **91**, 495 (1953).

The aim of the present work is to describe and discuss the measurements made by us in the case of argon of various purities.

The first part concerns the study of the  $\alpha$ -pulse shapes with respect to the mechanism of photon production, and the results are considered in connection with those obtained in previous researches on photons produced in argon excited by Townsend avalanches.

In the second part some possible applications of this method in the realization of  $\alpha$ -particle spectrometers are described and the possibilities of such instruments in comparison with those of conventional types are discussed.

## Study of Light Emission.

### 1. — The Scintillation Chamber.

These measurements have been made with a cylindrical scintillation chamber 4 cm high and of 5 cm diameter (Fig. 1.). The walls are stainless steel and are lined internally with copper sheeting covered with white enamel that serves as light diffuser.

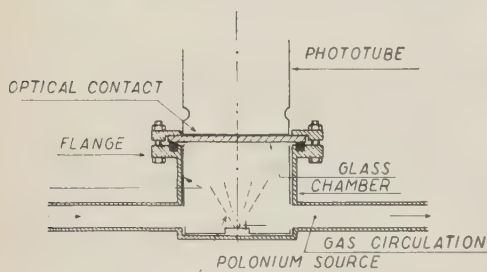


Fig. 1. — Scheme of the chamber and geometrical arrangement used for the measurements of the  $\alpha$  scintillations in gases.

The chamber is closed from above with glass. Vacuum and pressure are assured by means of a flange with a polyethylene gasket.

On the external face of the glass disc is placed the head of the photomultiplier.

On a support at the bottom of the chamber, a thin layer of a few sq. mm which emits a 1000  $\alpha$ -particles per minute, is deposited. This disc, driven from the outside by a

source can be screened with a small magnet.

### 2. — Vacuum and Filling Apparatus.

The chamber is connected with an apparatus which serves to evacuate the chamber itself, to purify the argon and to prepare gas mixtures.

This apparatus is shown in Fig. 2. Its containers and conductors are made of metal: so are the valves, joints and gaskets. The use of grease and mastic is avoided.

A silicone oil diffusion pump, connected in series with a rotating pump permits a vacuum of  $10^{-5}$  mm<sub>Hg</sub>, which is measured by a Penning ionization gauge. The pressure of the gases introduced in the apparatus is measured with a Bourdon manometer.

The scintillation chamber is inserted in a circuit of conductors in which the

gas is made to circulate. This circuit includes a furnace containing turnings of calcium and magnesium alloy (90% Ca - 10% Mg) which, if heated to 400-500 °C, allows the circulation and the purification of argon.

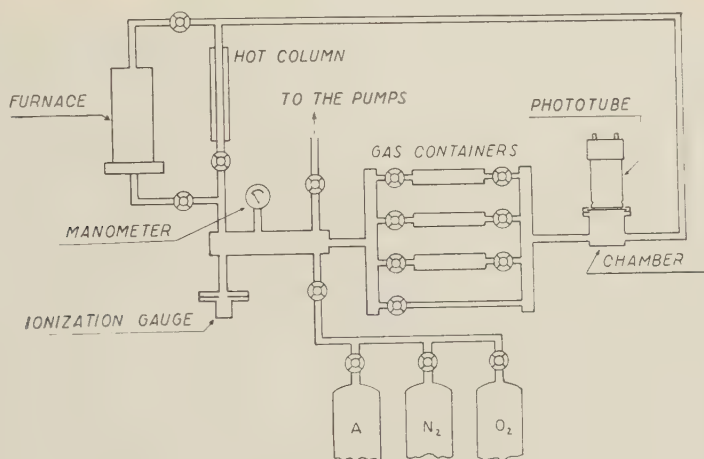


Fig. 2. — Filling and mixing apparatus, with a purification circuit.

It also includes a series of containers in which it is possible to enclose other gases that are to be mixed with argon.

When it is needed to use a mixture containing gas that can be adsorbed by the furnace, the latter is eliminated from the circuit and in such case the gas circulation is maintained by an electrically-heated vertical column inserted parallel to the furnace. Thus a rapid mixing of the introduced gases is obtained.

### 3. — Conversion of UV Photons.

When excited with  $\alpha$ -particles the gases studied by us emit photons that are mostly ultraviolet. To convert these photons into light detectable by the photomultiplier, sodium salicylate has been used, as a fluorescent substance. This salt, excited by UV light, emits fluorescent light in the blue region of the spectrum <sup>(4)</sup>, to which the photomultiplier used by us has a good relative sensitivity. The fluorescence quantum yield is practically constant for an exciting wave length of 850 to 2500 Å <sup>(5)</sup>. Sodium salicylate has been applied as a methyl alcohol solution on the enamelled surface of the light diffuser.

By evaporating the solvent, a layer, almost opaque, was formed, that stuck well to the surface. The internal surface of the glass that closes the chamber

<sup>(4)</sup> J. DE MONT: *Fluorochemistry* (New York, 1945), p. 201.

<sup>(5)</sup> E. INN: *Spectrochim. Acta*, **2**, 2 (1955).

was coated with a similar technique by a very thin and transparent layer of sodium salicilate.

The layers described remain unchanged over a long time even in vacuum, due to the negligible vapour pressure of sodium salicilate.

#### 4. - Electrical Devices and Measuring Methods.

The light emission produced by individual  $\alpha$ -particles has been registered with a photomultiplier E.M.I. 6262. The electric pulses at the output of the photomultiplier have been studied with respect to amplitude and duration. For measuring the amplitude, the pulses were sent to a conventional amplification chain through a time constant  $RC \cong 200 \mu\text{s}$  which is much greater than the duration of a single pulse, that never exceeded a few  $\mu\text{s}$ .

The corresponding voltage pulses at the output of the amplifier were measured in Volt by means of an oscillograph Cossor, model 1035.

The time development of single pulses was studied by using a faster amplification chain, consisting in a cathode follower and an amplifier model 600. The rise time of this chain was  $\sim 5 \cdot 10^{-8}$  s and the time constant at the input could be variated from  $1 \cdot 10^{-7}$  to  $10^{-6}$  s in order to obtain a suitable pulse resolution.

The pulses at the output of the amplifiers have been observed, depending on their duration, by means of an oscillograph with synchroscope Dumont mod. 248, using sweep durations of 5 and 25  $\mu\text{s}$ , or by means of a faster oscillograph, using sweep durations of 0.2, 0.6 and 2  $\mu\text{s}$ .

A few pulses of each type were registered photographically.

#### 5. - Experimental Results with Pure Argon.

For these measurements the apparatus was filled with argon of a purity exceeding 99.9%.

Throughout a series of measurements the argon was made to circulate through the furnace described. It is known <sup>(6)</sup> that by this method the argon is purified of most of foreign gases and is kept from contamination with organic vapours, so that it reaches a point where the fraction of molecular impurities is some  $10^{-4}$  or less.

The pressures used were of 80-100  $\text{cm}_{\text{Hg}}$ .

Under these conditions, pulses of  $\alpha$ -particles were observed and measured that were much higher than the dark pulses of the photomultiplier, with good reproducibility.

By comparing the pulses of individual  $\alpha$ -particles with dark pulses due to single electrons from the photocathode, the former were estimated as due to about 25 photoelectrons each.

The rise time of pulses observed with the oscillograph was found to be about  $1.5 \cdot 10^{-7}$  s at the indicated pressure.

<sup>(6)</sup> L. COLLI and U. FACCHINI: *Phys. Rev.*, **88**, 987 (1952).



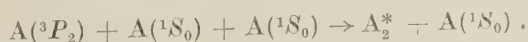
The study of the pulse duration was carried out with various pressures between 50 and 100 cm<sub>Hg</sub>. It was found that for this range the decay time of pulses was constant within experimental errors. The value thus obtained was  $2.5 \div 3 \mu\text{s}$  (Fig. 3).



Fig. 3. — The decay of an  $\alpha$  pulse in pure argon, 80 cm<sub>Hg</sub>, showing a decay time of  $\sim 3 \mu\text{s}$  (time markers: 1  $\mu\text{s}$  each).

## 6. — Discussion of Results.

The order of magnitude found for the pulse duration suggests the hypothesis that the photon emission implies the decay of a metastable level, by the same type of process which accounts for the emission of UV photons in pure argon excited with electron avalanche. This phenomenon was studied extensively by L. COLLI<sup>(?)</sup>, who suggest the following mechanism to explain the emission: the metastable level  $^3P_2$  produces by three-body collisions the formation of an excited argon molecule  $A_2^*$  according to



A three-body collision accounts for the conservation of momentum and energy.

An UV photon is emitted in the transition from the excited molecular

(?) L. COLLI: *Phys. Rev.*, **95**, 892 (1954).

state of argon to the fundamental state:



The emission intensity  $I$  versus time was experimentally found well represented by the formula

$$I = C \left( \exp \left[ -\frac{t}{\tau_A} \right] - \exp \left[ -\frac{t}{\tau_M} \right] \right),$$

were, under the considered scheme,  $\tau_A$  is the time constant for the formation of the molecules  $A_2^*$  and  $\tau_M$  is the lifetime of the molecular state.

The experimental observations of this process determined that:

$$\tau_A \simeq \frac{1}{10p^2} \text{ s}, \quad (p: \text{ pressure in mm}_{\text{Hg}}),$$

and

$$\tau_M \simeq 3.5 \text{ } \mu\text{s}.$$

We note that in our case, too, the decay time of photon emission is independent of the pressure, and that our results are in good quantitative agreement with the measurements reported above.

This enhances the hypothesis that in pure argon excited with high energy  $\alpha$ -particles, the photon emission is, at least for the most part, due to a process of the same nature as that observed in the case of excitation produced by electron avalanche.

## 7. - Measurements with Mixtures of Argon and $N_2$ , $O_2$ , $CO_2$ .

It was expected that small amounts of molecules of foreign gases in argon, would produce quenching collisions on the excited argon atoms or molecules, which would result in a reduction of the intensity and of the duration of the light emitted by argon.

The energies of excited argon atoms and molecules may in some cases be stored by the foreign molecules during the quenching collisions, and be partly emitted as photons of different energies.

These hypotheses account, qualitatively, for the results obtained in the following measurements with mixtures of pure argon with  $N_2$ ,  $O_2$ ,  $CO_2$ :

The concentrations of  $N_2$ ,  $O_2$ ,  $CO_2$  were determined by pressure measurements. Due to the little accuracy of this method, the percentages shown in Table I, left column, are to be considered as informative. The total pressure of the gas was 80-90  $\text{cm}_{\text{Hg}}$ .

In Table I, left side, are given the pulse amplitudes and their relative values with respect to the amplitudes obtained with pure argon. At the right side are indicated the pulse rise times and decay times.

With percentages from 0.5 to 2.5% of  $N_2$ , a progressive reduction both in the amplitudes and in the rise and decay times was observed. For instance, by introducing 0.5% of  $N_2$  in pure A, the pulse amplitudes diminished by about 50% and the decay time became  $\sim 0.5 \text{ } \mu\text{s}$  (Fig. 4). The addition of a few ten thousandths of  $O_2$  and  $CO_2$  produced effects of the same type.

TABLE I. - Amplitudes and durations of light pulses measured with the sodium salicylate UV converter.

PULSE AMPLITUDES			PULSE DURATIONS		
Phototube EMI 6262 Supply voltage 1070 Volt Amplification gain $\sim 470$ Time constant $RC \sim 200 \mu s$			Rise time of electric circuit $\sim 5 \cdot 10^{-8} s$		
Gas composition	Pulse amplitude Volt	Relative amplitude	Rise time $\tau_r \cdot 10^{-6} s$	Decay time $\tau_d \cdot 10^{-6} s$	Time constant $RC \cdot 10^{-6} s$
A (99.99%)	50	100	0.15	$2.5 \pm 3$	1; 0.2
A + O <sub>2</sub> [N <sub>2</sub> ] %					
0.5	25	50	0.15	0.5	1; 0.2
1	17	35	0.1	0.25	0.2; 0.1
2	15	30	0.07	0.15	0.1
A + O <sub>2</sub> [O <sub>2</sub> ] %					
0.05	17	35	0.05	0.1	0.1
0.15	12	25	0.05	0.1	0.1
0.4	7	15	0.05	0.1	0.1
A + CO <sub>2</sub> [CO <sub>2</sub> ] %					
0.03	15	30	0.05	0.1	0.1
0.07	10	20	0.05	0.1	0.1
0.15	7	15	—	—	—
A + N <sub>2</sub> + O <sub>2</sub> [N <sub>2</sub> ]% [O <sub>2</sub> ]%					
2 0.25	10	20	0.05	0.1	0.1
2 0.75	5	10	0.05	0.1	0.1
A + N <sub>2</sub> + O <sub>2</sub> [N <sub>2</sub> ]% [O <sub>2</sub> ]%					
2 0.05	10	20	0.05	0.1	0.1
2 0.15	8	15	0.05	0.1	0.1

A more accurate study of this effect was not possible because in most cases the rise and decay of the pulses under observation seemed limited by the rise time and time constant of the electronic circuit, i.e.  $5 \cdot 10^{-8}$  and  $10^{-7}$  s respectively.

Mixtures of three components were studied: the addition of a few thousandths of O<sub>2</sub> or a few ten thousandths of CO<sub>2</sub> to a mixture of A<sub>2</sub> + 2% N<sub>2</sub> reduced critically the emission intensity.

This chamber (Fig. 6) is cylindrical, 5 cm wide and 3.5 cm, terminating in a cone.

It is closed by a glass disc by means of a flange with a polyethylene gasket. Its walls are of silvered brass.

The chamber is provided with a cock at the bottom, so that it may be closed off and removed from the rest of the system.

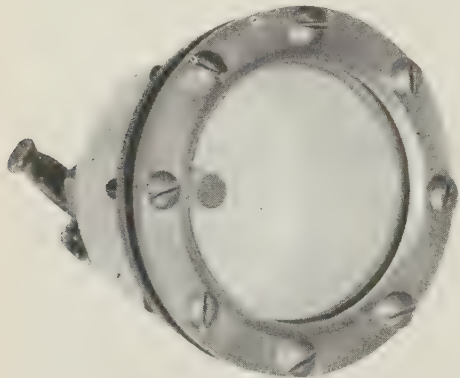


Fig. 6. — A view of the scintillation chamber: the sodium salicilate coating and the  $\alpha$  source at the bottom can be seen.

The  $\alpha$ -particle source is placed on a stainless steel disc of 5 mm diameter, attached to one end of the cock that is inserted in the lower part of the chamber.

The  $\alpha$  source used is polonium.

The internal surface and geometry of the chamber were studied with view to uniformity and better collection of the light. For this purpose a different coating technique from that described in Sect. 3 was usefully employed.

An opaque and very white coating was obtained by spraying a saturated solution of sodium salicilate in methyl alcohol on the chamber walls that had

been heated to over 100 °C. This sodium salicilate layer was used both as an UV converter and a light diffuser.

The light pulses produced in the chamber by  $\alpha$ -particles were analyzed by a photomultiplier, type Dumont 6292, the photocathode of which was placed in optical contact with the chamber window.

The amplitude and duration of the pulses at the output of the photomultiplier were measured by means of the electric apparatus and methods described in Sect. 1. Spectra of the amplitudes of the pulses, that were suitably shaped by a reflexion line, were obtained by means of a 99-channel pulse analyzer.

## 10. — Measurement Results.

Preliminary results indicated that the spread of the  $\alpha$ -pulse amplitudes depended on the pressure of the filling argon. It should be noted that such spreading is partly due to a geometrical effect on the collection of light by the UV converter, that happens because the  $\alpha$ -tracks, along which the UV photons are emitted, are not collimated. This effect can be reduced by confining the  $\alpha$ -particle paths within a little space around the source, using a high gas pressure. On the other hand it was observed that, in our conditions, the increase in the pressure caused an appreciable reduction in the mean amplitude of the pulses. This effect can probably be attributed to the increased quenching of the excited argon molecules by impurities.

This results in a reduction of the mean number of the photoelectrons emitted

by the photocathode per each  $\alpha$ -particle, i.e. in a worse statistical distribution of the pulse amplitudes of the output of the photomultiplier.

In our conditions, the convenient pressures were found to be 150-200 cm<sub>Hg</sub>.

A spectrum of pulse amplitudes obtained in the above described manner is shown in Fig. 7. The distribution has a symmetrical shape, and its full width at half maximum is  $\sim 13\%$ .

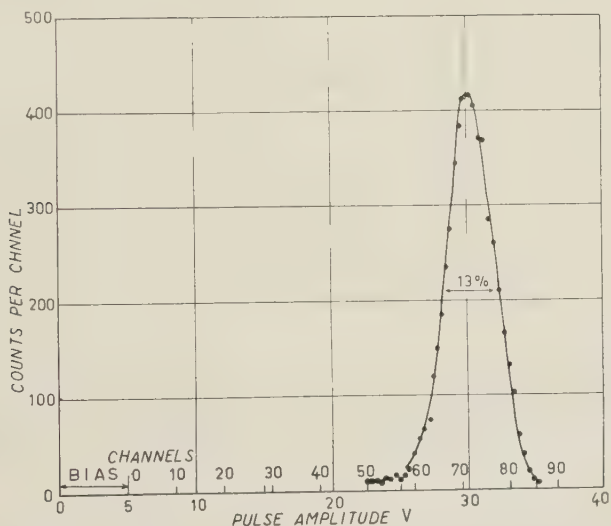


Fig. 7. — Pulse spectrum of  $\alpha$ -particles from a thin Polonium source (pulse cut off at  $2\ \mu\text{s}$ ).

In this case an estimate was made of the number of photoelectrons liberated at the cathode of the phototube during each scintillation: under the assumption that the statistical values of this number follow a Poisson distribution, the relative standard deviation of the pulses at the end of the multiplier, measured by us, implies that the average value is more than  $\sim 300$ .

A number of the same order has been found by comparing the  $\alpha$ -pulses with the dark pulses produced by single electrons from the cathode.

This permits the assumption that above neglected causes for spread, such as geometrical effects on the light collection, are less effective than the purely statistical deviation.

In this case too, it was interesting to examine the shape of the individual pulses. The rise of the pulses appeared limited by the rise time of the electronic chain of  $\sim 5 \cdot 10^{-8}$  s.

The duration of pulses were of some  $10^{-7}$  s, much shorter than those of some  $\mu\text{s}$  observed with highly purified argon, as described in Sect. 4.

## 11. — Testing Other UV Converters.

We have experimented with the same material used by Boicourt and coll. as UV converter: a transparent film of polystyrene with 5% of tetraphenylbutadiene was applied to the silvered walls of our scintillation chamber.



Measurements with this converter gave results that are not very different from those obtained with the sodium salicilate converter, though the pulse amplitude obtained was about half.

It was observed that soon after the chamber had been filled, the pulses decreased appreciably.

This may indicate that such converters contaminate the argon (<sup>8</sup>).

## 12. - Possibilities of the Scintillation Chamber.

**12.1. Constancy of operation.** - The measurements obtained with the scintillation chamber having a converter of sodium salicilate were not always exactly reproducible in various fillings, probably because of uncontrollable quantities of impurities contained in the filling argon. However, once the chamber was filled its responsive characteristics remained constant for many days.

In particular, pulse spectra obtained over a period of a few days were in excellent agreement.

**12.2. Counting rate.** - The principle on which the gaseous scintillation counter is based and the sufficiently high statistics in the generation of each pulse make it permissible to suppose that this instrument furnishes a counting rate approaching 100% (<sup>9</sup>), at least at not-too-low energies.

**12.3. Energy and time resolution.** - In order to compare this instrument with those of current use, it may be observed that the scintillation chamber permits an energy resolution qualitatively comparable with that of crystal spectrometers (<sup>10</sup>), while it cannot compete with the ionization chamber when a refined analysis is required.

On the other hand the resolving time of the scintillation chamber is expected to be considerably shorter with respect to the ionization chamber and to inorganic scintillators [ZnS, NaI (Tl) etc.] owing to the fact that the pulses of the former instrument have a rise time not more than some  $10^{-8}$  s, versus some  $10^{-6}$  s of the ionization chamber and ZnS, and some  $10^{-7}$  s of the NaI(Tl).

We can conclude that the scintillation chamber may be used, with simple and easy technique, as a counter and as a spectrometer for  $\alpha$ -particles (or, in a like manner, for other heavy particles). The characteristics of its response may offer advantages in some types of work, particularly where a good time resolution is required.

\* \* \*

We are very indebted to prof. G. BOLLA for his interest and to prof. U. FACCHINI for his useful suggestions and stimulations.

Thanks are due to Dr. B. DE MICHELIS for his help in some measurements.

(<sup>10</sup>) A definitely better resolution can be obtained with some kind of crystals cooled at low temperature (liquid nitrogen) though this requires careful technique and less simple operation: see B. HAHN: *Helv. Phys. Acta*, **26**, 271 (1953).

## RIASSUNTO

Si descrivono metodi per rivelare ed analizzare gli impulsi di luce prodotti dal passaggio di singole particelle  $\alpha$  nei gas. Nella Parte I si studia l'andamento temporale di impulsi ottenuti con argon di varie purezze ed i risultati si mettono in relazione con il meccanismo di produzione dei fotoni. Nella Parte II, si tratta dell'utilizzazione di questi impulsi per la realizzazione di strumenti rivelatori di particelle  $\alpha$ . Si descrive una camera a scintillazione funzionante con argon, che consente l'analisi spettrale di particelle  $\alpha$  con una risoluzione che è dell'ordine del 13% a  $\sim 5$  MeV, ed offre un tempo risolutivo particolarmente breve.

## Échelle binaire rapide.

D. T. JOVANOVIĆ

*Institut de Recherches Nucléaires Boris Kidrič - Vinča Belgrade, Yougoslavie (\*)*

(ricevuto il 15 Marzo 1956)

**Resumé.** — On décrit une échelle binaire rapide et les procédés de mesure utilisés pour en contrôler le fonctionnement. Le temps de résolution de l'échelle, déterminé par la méthode de paires d'impulsions, est égal à 35  $\mu$ s.

### 1. — Introduction.

En physique nucléaire les événements à étudier se produisent suivant une loi statistique; par suite, deux événements consécutifs peuvent être séparés par un intervalle de temps très court, la limite inférieure de cet intervalle étant la simultanéité des deux événements. Cependant chaque circuit de comptage (ainsi que les circuits de détection) possède un temps de résolution fini, ce qui provoque des pertes de comptage. La limite supérieure de la fréquence moyenne de répétition des impulsions, ou taux de comptage, susceptible d'être atteinte, est d'autant plus grande que le temps de résolution est plus faible, et que le pourcentage de pertes toléré est plus élevé; on admet en général 1% de pertes de comptage (dans certains cas particuliers cette tolérance peut être étendue jusqu'à 10%) <sup>(1)</sup>.

Certaines expériences effectuées avec des accélérateurs pulsés exigent des taux de comptage instantanés très élevés. D'autre part, la possession d'un circuit bistable rapide est intéressante pour beaucoup d'autres usages et notamment pour la construction de sélecteurs de temps multicanaux, ou de commutateurs électroniques, de façon à obtenir une bonne précision sur la détermination des intervalles de temps <sup>(2)</sup>. Ainsi, pour ces différentes raisons, l'étude de l'échelle binaire rapide, faisant l'objet de cet article, a été entreprise.

(\*) Cet article rend compte d'un travail effectué au Commissariat à l'Energie Atomique, Centre d'Etudes Nucléaires de Saclay (S. & O.).

(1) L. J. RAINWATER et C. S. WU: *Nucleonics*, **1**, 10 (Oct. 1947).

(2) R. PARSHARD et A. SAGAR: *Rev. Sci. Instr.*, **25** 395 (1954).

Les échelles binaires rapides décrites dans la littérature récente sont dérivées du circuit bien connu d'Eccles-Jordan. Il est possible d'augmenter la rapidité d'une échelle binaire en limitant les excursions des plaques et des grilles à l'aide de diodes polarisées<sup>(3)</sup>. L'utilisation de « cathode-followers » pour effectuer les deux liaisons de plaques aux grilles est également susceptible d'apporter une amélioration notable à la rapidité de l'échelle binaire. V. FITCH<sup>(4)</sup> utilisant simultanément ces deux procédés, est parvenu à faire fonctionner une échelle à une fréquence de 14 MHz à l'aide d'une tension sinusoïdale.

Il existe deux méthodes différentes pour mesurer le temps de résolution d'une échelle. On peut utiliser pour l'attaquer, soit un régime périodique (en général sinusoïdal), soit des paires d'impulsions produites sous une fréquence de récurrence relativement basse; les impulsions de chaque paire sont alors séparées par un intervalle de temps réglable. Les deux méthodes n'aboutissent pas à la même valeur du temps de résolution. Toutefois la méthode des paires d'impulsions nous semble préférable parce qu'elle est plus proche des conditions d'utilisation en régime statistique.

Afin d'utiliser la seconde méthode, nous avons dû construire spécialement un générateur de paires d'impulsions rapides qui sera également décrit.

## 2. — Description de l'échelle.

Le schéma de l'échelle binaire est représenté par la Fig. 1. Comme l'échelle de V. FITCH<sup>(4)</sup>, elle utilise des diodes limiteuses et des « cathodes-followers »; elle en diffère sur plusieurs points:

- mode de liaison entre plaques et grilles de la bascule,
- retour des diodes de grille sous basse impédance,
- utilisation de pentodes pour le circuit bistable,
- absence de découplage aux bornes de la résistance commune de cathodes,
- tensions de l'alimentation de l'échelle.

Les anodes des lampes  $V_3$  et  $V'_3$  attaquent directement les grilles des « cathodes-followers » de liaison  $V_1$  et  $V_2$ . Les grilles de la bascule sont reliées à une prise sur les résistances cathodiques de  $V_1$  et  $V_2$ . Les diodes limiteuses au germanium,  $X_3$  et  $X_4$ , sont polarisées à l'aide du « cathode-follower »  $V_4$ . Le potentiomètre  $P_2$  permet de choisir convenablement la tension de polarisation des diodes pour obtenir le plus faible temps de résolution (\*). Le potentiomètre  $P_1$  est destiné au réglage de la symétrie du circuit. Il est du type bobiné et son inductance introduit une surcompensation des circuits d'anode. L'échelle est attaquée par des impulsions négatives à travers les diodes au germanium,  $X_1$  et  $X_2$ .

(3) B. CHANCE *et al.*: *Waveforms* (New York, 1949), p. 607.

(4) V. FITCH: *Rev. Sci. Instr.*, **20**, 942 (1949).

(\*) En pratique on règle la tension de cathode de  $V_4$  légèrement au dessous de la valeur maximum qui permette encore un fonctionnement correct de l'échelle binaire.

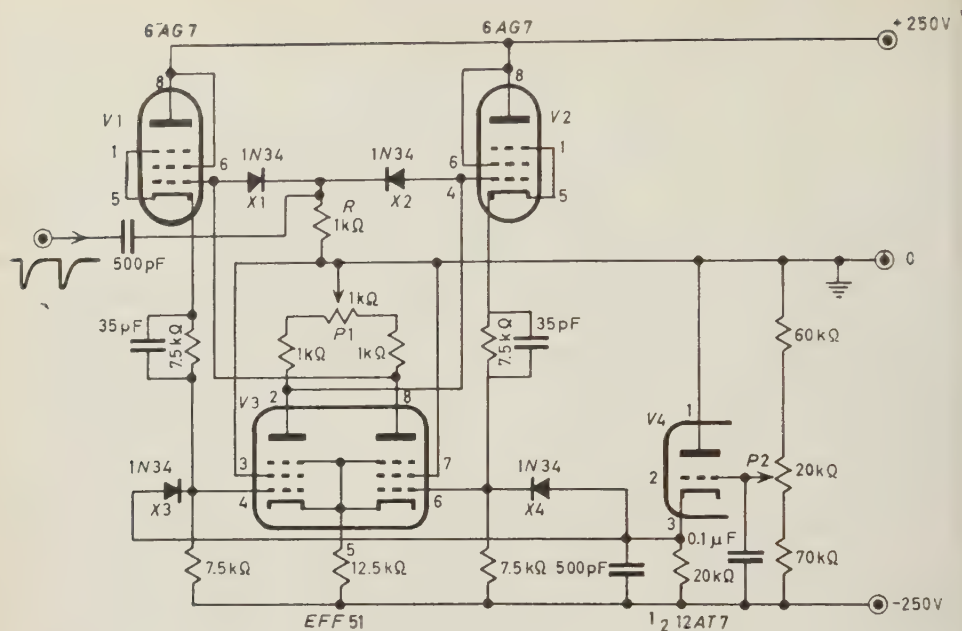


Fig. 1.

### 3. — Procédé de mesure du temps de résolution. Le générateur de paires d'impulsions.

Pour étudier le fonctionnement de l'échelle, les impulsions d'attaque doivent avoir une amplitude réglable et être aussi brèves que possible; le déphasage doit pouvoir être réglé d'une façon commode.

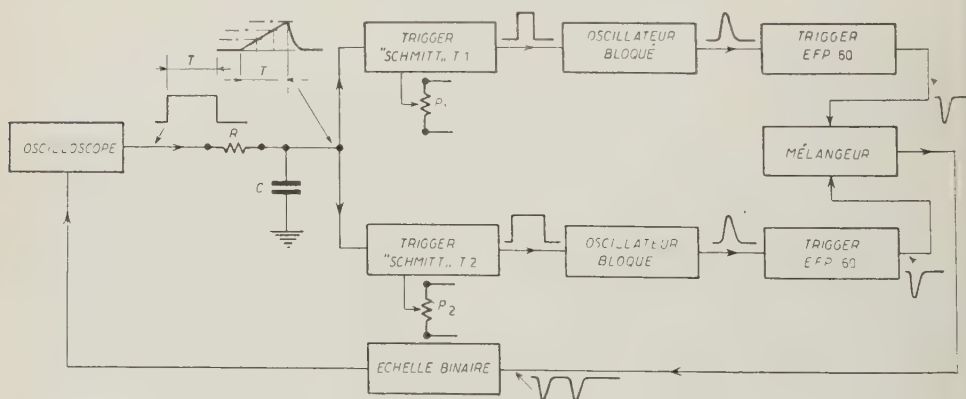
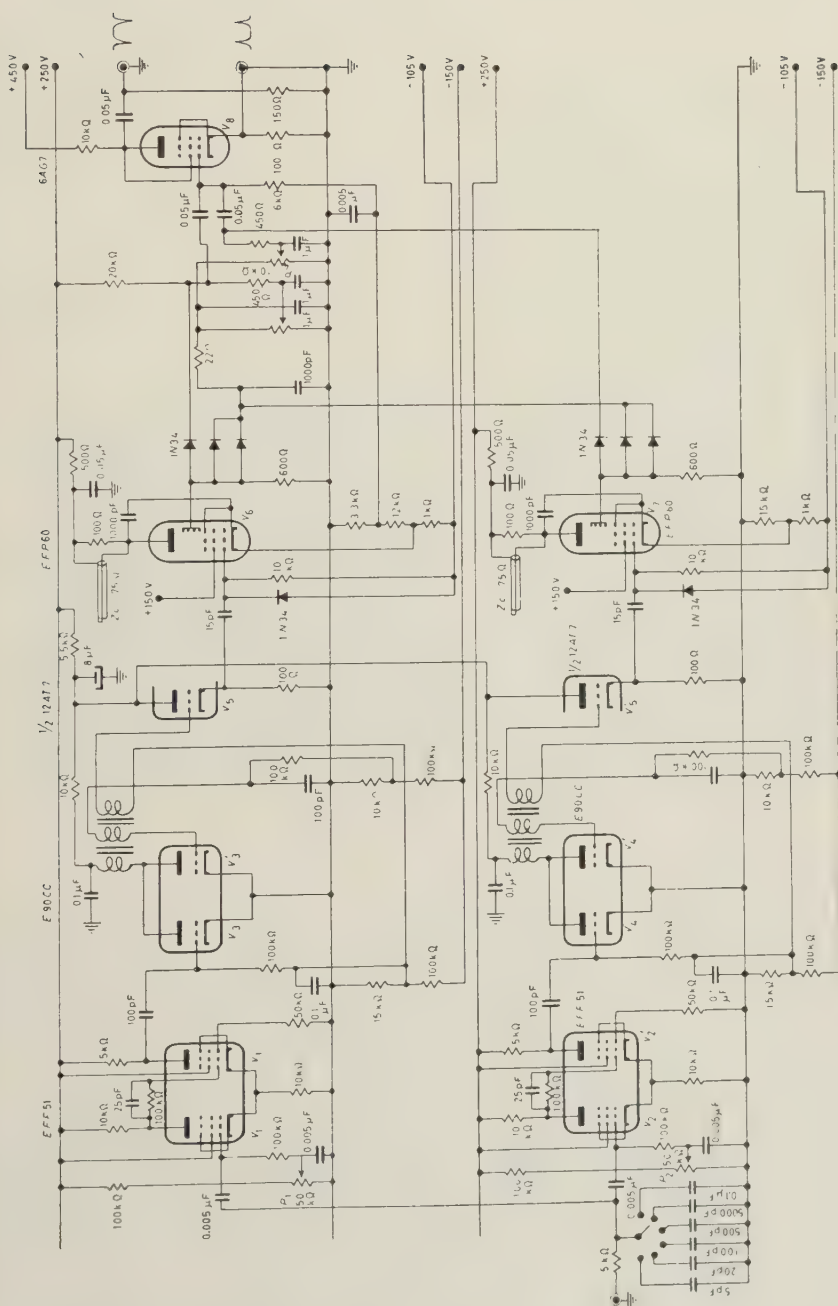


Fig. 2.

La Fig. 2. montre le schéma fonctionnel de l'appareillage utilisé pour la mesure du temps de résolution de l'échelle par la méthode des paires d'impulsions. L'oscillographe (Tektronix 517) dont la base de temps est déclenchée





par un générateur intérieur, délivre sur la sortie « + Gate », une impulsion positive de durée égale à celle du balayage. Cette impulsion positive est intégrée par un circuit RC pour obtenir la tension en dent de scie, qui est appliquée à deux monovibrateurs,  $T_1$  et  $T_2$ , dont le seuil est réglable. En faisant varier l'un des seuils par rapport à l'autre, on modifie le déphasage entre les impulsions fournies par les monovibrateurs. Deux oscillateurs bloqués mettent en forme ces impulsions afin d'attaquer convenablement des pentodes à émission secondaire du type EFP 60, destinées à engendrer des impulsions très étroites. Ces dernières sont appliquées, après mélange, à l'échelle à essayer. La mesure du temps de résolution est effectuée à l'aide de la base de temps calibrée (\*). Les signaux d'entrée et de sortie de l'échelle binaire, ainsi que les signaux en différents points du générateur peuvent être observés d'une façon très commode, le synchronisme entre le balayage et le phénomène à étudier étant parfaitement assuré. La fréquence de répétition des paires d'impulsions est déterminée par le générateur intérieur de l'oscillographe et est comprise entre 15 Hz et 15 kHz.

La Fig. 3 donne le schéma détaillé du générateur. La vitesse de montée de la dent de scie est réglée par le commutateur d'entrée qui permet de choisir entre un certain nombre de constantes de temps d'intégration. Les circuits des monovibrateurs et des oscillateurs bloqués sont bien connus. Les trois enroulements du transformateur de l'oscillateur bloqué possèdent chacun 10 spires bobinées sur un tore de mumétal au molybdène. Les générateurs d'impulsions courtes sont similaires à celui qui est décrit par F. H. WELLS<sup>(5)</sup>; afin d'obtenir des impulsions de durée inférieure à 50  $\mu$ s, la résistance de dynode a dû être légèrement réduite, et un coaxial d'impédance caractéristique faible a été utilisé dans l'anode. Les amplitudes des impulsions sont contrôlées indépendamment l'une de l'autre à l'aide des potentiomètres  $P_3$  et  $P_4$ . La largeur à la base des impulsions à la sortie du circuit mélangeur est égale à 30  $\mu$ s environ; leur polarité peut être soit positive, soit négative, et leur amplitude maximum à la sortie est égale à 12 V.

#### 4. — Résultats obtenus.

Avec l'échelle binaire dont le schéma est représenté par la Fig. 1, et en utilisant la méthode décrite, le temps de résolution a été trouvé égal à 35  $\mu$ s. La Fig. 4a montre les photographies des signaux d'attaque et de sortie de l'échelle correspondant à ce temps de résolution. La Fig. 4b représente le fonctionnement de l'échelle lorsque les impulsions d'attaque sont séparées par 200  $\mu$ s.

Afin d'avoir la certitude que le fonctionnement de l'échelle demeurerait toujours correct immédiatement après le premier cycle, la méthode des paires d'impulsions a été étendue à des trains de quatre impulsions déphasables entre elles. Cela a été obtenu par l'utilisation de deux générateurs de paires d'im-

(\*) Cette calibration a été vérifiée à l'aide d'un coaxial dont les caractéristiques étaient connues.

(5) F. H. WELLS: *Nucleonics*, 10, 28 (Avr. 1952).

pulsions identiques à celui décrit ci-dessus, le mélange étant effectué sur une résistance commune de  $150\ \Omega$ , qui remplace la résistance  $R$  de la Fig. 1. En raison de l'augmentation de capacité introduite par les câbles de liaison, la durée des impulsions d'attaque est légèrement élargie. La Fig. 5 représente les signaux de sortie de l'échelle pour différentes configurations des quatre impulsions d'entrée. Les Fig. 5a, 5b et 5c sont obtenues respectivement avec deux, trois et quatre impulsions séparées par l'intervalle de temps minimum qui permet le fonctionnement correct de l'échelle binaire; cet intervalle de temps a été trouvé égal à  $50\ \mu\text{s}$  dans les trois cas.

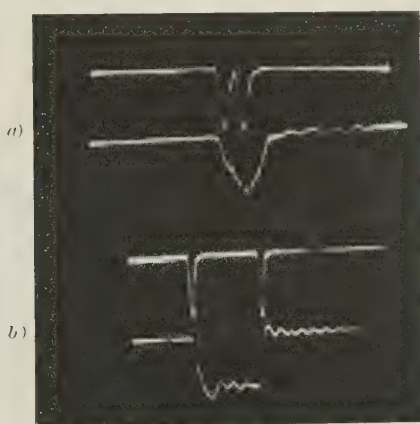


Fig. 4.

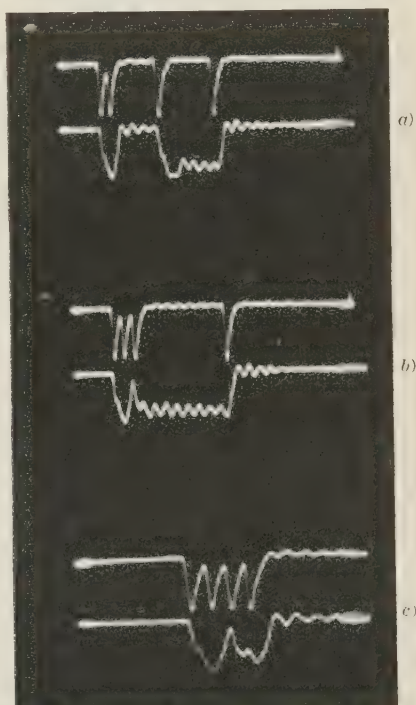


Fig. 5.

Le temps de résolution réel, pour un train de quatre impulsions, est probablement inférieur à  $50\ \mu\text{s}$  du fait que le générateur ne fournit plus des impulsions suffisamment brèves pour mesurer des temps de résolution plus courts, comme on peut le voir sur la Fig. 5.

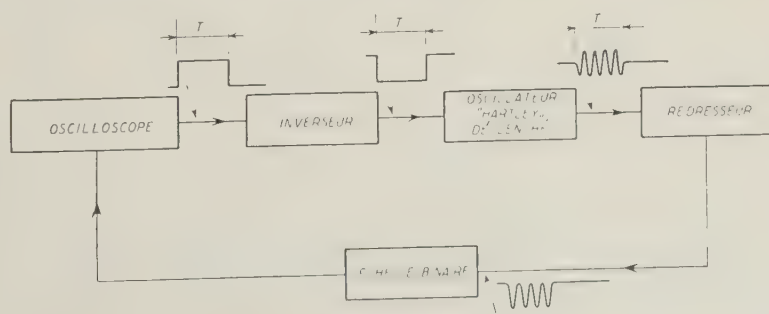


Fig. 6.

Enfin nous avons voulu mesurer le temps de résolution de l'échelle lorsqu'elle est attaquée par un train d'impulsions périodiques. Dans ce but nous avons utilisé le schéma fonctionnel montré par la Fig. 6. De même que dans la méthode précédente (Fig. 2), les impulsions positives de durée  $T$  sont prises sur l'oscilloscope (Tektronix 517) à la sortie « + Gate », elles sont inversées pour pouvoir attaquer un oscillateur Hartley déclenché<sup>(6)</sup>. Les impulsions fournies par l'oscillateur sont redressées et appliquées à l'échelle. La méthode est intéressante, mais nous n'avons pas pu en tirer tout le profit du fait que l'amplitude des signaux d'attaque décroissait en fonction de la fréquence. La Fig. 7

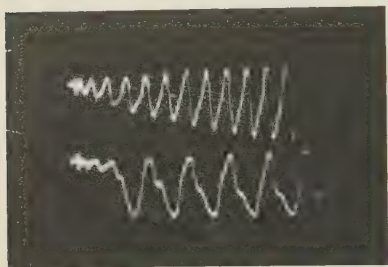


Fig. 7.

montre le fonctionnement à 16 MHz, fréquence limite pour laquelle l'amplitude est encore suffisante pour déclencher l'échelle binaire.

## 5. — Conclusion.

L'échelle binaire réalisée comporte 4 tubes dont un double, et nécessite deux sources de tension, l'une de  $-250$  V (débit 50 mA), l'autre de  $+250$  V (débit 30 mA). Le temps de résolution mesuré par la méthode des paires d'impulsions est égal à 35  $\mu$ s. En régime périodique la valeur réelle de ce temps n'est pas connue, mais il a été établi qu'elle était inférieure à 50  $\mu$ s. Les impulsions d'entrée doivent posséder une amplitude minimum de 7 V pour déclencher l'échelle, mais pour obtenir le temps de résolution indiqué, il est nécessaire d'avoir des amplitudes supérieures à 11 V.

Pour améliorer la méthode de mesure du temps de résolution en régime périodique, présentée par la Fig. 6, on se propose d'utiliser, à la suite de l'oscillateur, les circuits de mise en forme et de sortie (EFP 60 + 6AG7) existant dans le générateur de paires d'impulsions, représenté par le Fig. 3.

\* \* \*

Je remercie vivement Monsieur M. SURDIN, Chef du Service des Constructions Electriques, qui m'a donné la possibilité de réaliser ce travail; Messieurs H. GUILLOX et V. KOSTIĆ pour les discussions utiles qui ont eu lieu au cours de l'étude; le Commissariat à l'Energie Atomique qui m'a autorisé à publier cet article.

(6) B. CHANCE *et al.*: *Waveforms* (New York, 1949), p. 143.

## RIASSUNTO (\*)

Si descrive una scala binaria rapida e i sistemi di misura adottati per controllarne il funzionamento. Il tempo di risoluzione della scala, determinato col metodo delle coppie d'impulsi è di 35  $\mu$ s.

(\*) Traduzione a cura della Redazione.

# LETTERE ALLA REDAZIONE

(La responsabilità scientifica degli scritti inseriti in questa rubrica è completamente lasciata dalla Direzione del periodico ai singoli autori)

## Production of the Joshi Effect in Oxygen under the Near Infrared.

S. R. MOHANTY, K. R. K. RAO and T. R. BHAT

*Physico-Chemical Laboratories, Banaras Hindu University, Banaras, India*

(ricevuto il 15 Febbraio 1956)

Preliminary studies with chemical filters and the Kodak Wratten filter 87 had established the occurrence of the Joshi effect <sup>(1)</sup> (the photovariation, enhancement  $+ \Delta i$  and diminution  $- \Delta i$ , of the current  $i$  through gases and vapours under electrical excitation) in oxygen under the near infrared <sup>(2,3)</sup>. The effect  $\pm \Delta i$  under this wave band has now been investigated in some detail as regards its dependence on the exciting potential ( $V$ ).

A fused silica Siemens' tube (transmission,  $0.75 \div 2.78$  and  $3.22 \div 4.40 \mu\text{m}$ ) was degassed in vacuum at  $400^\circ\text{C}$  for 10 hours. It was next filled with pure oxygen at 26 mm<sub>Hg</sub> pressure ( $31^\circ\text{C}$ ); mercury vapour was avoided by making use of tin, gold and liquid-air traps. The electrodes consisted of a 10 per cent aqueous solution of sodium chloride inside the inner tube, and a helix of bright copper wire on the outer tube (Fig. 1). The discharge tube was excited over  $1 \div 2$  kV (rms) of 50 Hz frequency.

The infrared source was the Stupakoff standard insulcon glower SL 54.1030 (emission maximum,  $2 \mu\text{m}$ ) placed at a distance of 25 cm. The radiations from the glower were passed through a Pola-

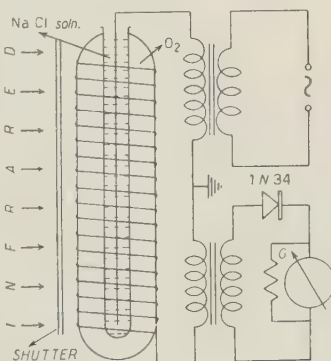


Fig. 1. -- Production of the Joshi Effect under the Infrared.

roid XRX10 non-polarizing filter (glass laminated) which transmitted the infrared to  $2.8 \mu\text{m}$  but completely absorbed the visible. The effect  $\pm \Delta i$  ( $= i_{\text{IR}} - i_{\text{D}}$ , where  $i_{\text{IR}}$  and  $i_{\text{D}}$  are the values of  $i$  under the infrared and in dark respectively) was observed at different  $V$  with a sensitive mirror galvanometer ( $G$ ) actuated by a crystal (1N34, Sylvania).

A representative set of results is shown graphically in Fig. 2. The posi-

<sup>(1)</sup> S. S. JOSHI: *Proc. Indian Sci. Congr.*, Chemistry Section, Presidential Address, 70 (1943).

<sup>(2)</sup> S. R. MOHANTY and SATYA PRAKASH: *Proc. Indian Sci. Congr.*, Physics Section, Part III, Abstract 43 (1950).

<sup>(3)</sup> T. D. PRASADA RAO: *M. Sc. Thesis*, Banaras Hindu University (1953).



tive effect  $+ \Delta i$  diminishes with increase in  $V$  to change sign at an inversion potential  $V_i$ ; beyond  $V_i$ , the negative effect  $- \Delta i$  first increases and then diminishes. Thus,  $+ \Delta i$  was 37.8 per cent at 1.07 kV. Increase in  $V$  to 1.2 kV

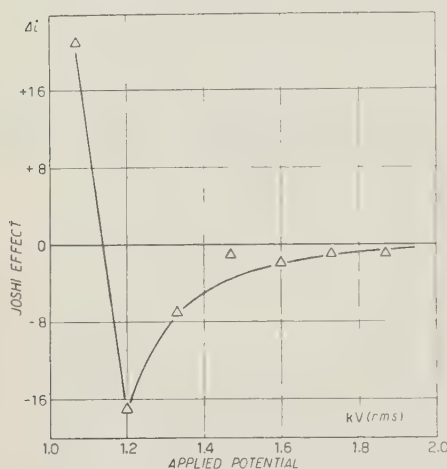


Fig. 2. — Potential Variation of the Joshi Effect under the Infrared.

resulted in the production of 13.9 per cent  $- \Delta i$  which diminished to 0.5 per cent at 1.87 kV. It is significant that the potential dependence of  $\pm \Delta i$  under the infrared is essentially similar to that obtaining with other frequencies ( $\nu$ ) in the electromagnetic spectrum (<sup>4</sup>). Thus, *ceteris paribus* total radiations ( $3700 \div 7800 \text{ \AA}$ ) from a 300 W 200 V tungsten filament (in glass) lamp produced at 1.07 kV a current suppression  $- \Delta i$  of 98.7 per cent which diminished to 7.7 per cent at 1.87 kV. That, at 1.07 kV, the system exhibited  $- \Delta i$  in the visible whilst  $+ \Delta i$  was obtained under the infrared is in agreement with the earlier findings (<sup>5,6</sup>) in these Laboratories that  $V_i$  varies inversely with  $\nu$  and the inten-

sity of the incident radiations.

According to HARRIES and VON ENGEL (<sup>7</sup>), the external light is strongly absorbed by, and causes the dissociation of, the molecules in an adsorbed layer on the electrode walls. Attachment by the atoms of the secondary electrons from these walls brings about  $- \Delta i$ . The dissociation energy of oxygen into normal atoms is 5.11 eV, corresponding to about  $2400 \text{ \AA}$  (<sup>8</sup>). That  $- \Delta i$  should occur in oxygen in the near infrared and the visible, despite non-occurrence of photodissociation, shows that the Harries and von Engel mechanism is untenable. Furthermore, the mechanism does not account for the production of  $+ \Delta i$ , and the observed co-occurrence (<sup>4</sup>) of  $+ \Delta i$  and  $- \Delta i$ . The theory of the phenomenon due to JOSHI (<sup>9,10</sup>) postulates, on the other hand, electron liberation due to the external light from an activated layer of electrons, etc., on the electrode walls. Capture of these photoelectrons by the electronegative elements in the discharge forms slow moving negative ions which reduce  $i$  mainly as a space charge effect. The photo-electrons which escape capture, and their secondaries, provided the field is favourable, cause  $+ \Delta i$ . The occurrence of  $\pm \Delta i$  under the near infrared shows, in agreement with Joshi's findings, that the electrode layer is characterized by a low work function (<sup>9,10,11</sup>).

\*\*\*

Grateful thanks of the authors are due to Prof. S. S. JOSHI for his kind interest and valuable suggestions, and to Mr. L. V. KANNAN for his assistance.

(<sup>7</sup>) W. L. HARRIES and A. VON ENGEL: *Journ. Chem. Phys.*, **19**, 514 (1951); *Proc. Phys. Soc. (London)*, B **64**, 916 (1951).

(<sup>8</sup>) G. HERZBERG: *Zeits. Phys. Chem.*, B **4**, 223 (1929).

(<sup>9</sup>) S. S. JOSHI: *Proc. Indian Sci. Congr.*, Physics Section, Part III, Abstract 26 (1946); Abstract 25 (1947).

(<sup>10</sup>) S. S. JOSHI: *Current Sci.*, **16**, 19 (1947).

(<sup>11</sup>) S. R. MOHANTY: *Nuovo Cimento*, **2**, 1107 (1955).

(<sup>4</sup>) S. R. MOHANTY: *Journ. Chem. Phys.*, **23**, 1533 (1955).

(<sup>5</sup>) S. R. MOHANTY and P. S. RAO: *Proc. Phys. Soc. (London)*, B **68**, 177 (1955).

(<sup>6</sup>) S. R. MOHANTY and P. S. RAO: *Journ. Sci. Res. Banaras Hindu University*, **5** (2), 106 (1954-55).

## On a High Energy Electronic Shower.

L. BARBANTI SILVA, C. BONACINI, C. DEPIETRI, I. IORI (\*), G. LOVERA (+),  
R. PERILLI FEDELI e A. ROVERI

*Istituto di Fisica dell'Università - Modena*

(+) *Istituto Nazionale di Fisica Nucleare - Sezione di Torino*

(ricevuto il 30 Marzo 1956)

Several examples of high energy cascade showers, consisting of electron pairs, have been recently investigated<sup>(1,6)</sup>. Their analysis is interesting in view of a possible check of the laws of quantum electrodynamics<sup>(7)</sup>.

An event which appears to be of the same type has been observed during the systematic scanning of a stack of n. 40 stripped emulsions Ilford G5 ( $6 \times 6''$ ,  $600 \mu\text{m}$  thick), flown at 93 000 ft during the Texas flights (January 1955).

The event initiates in the sheet of emulsion n. 27 with a very energetic pair of electrons; it develops with a

rapid increase of the number of pairs through 27 sheets of emulsion and leaves the stack after a path of about 4.8 cm: then, it consists of about 56 pairs. The scanning in the backward direction is in progress, but so far we have not yet found any event related with the shower.

In Table I the distances are referred, from the origin of the first pair, and the radial distance from the axis of the shower core, for the starting points of the first 21 pairs, on a range of 3.35 cm, (corresponding to about 1.15 radiation lengths, on assuming for the radiation length in the nuclear emulsion a value of 2.9 cm).

The starting points of the ten pairs immediately succeeding the first one, and, in addition too, those of the pairs n. 14, 15, 20, are indistinguishable from the other tracks that fill the core (i.e. at the origin of the pairs n. 10 and 11, the core is filled with more than ten tracks within a diameter of about  $1.8 \mu\text{m}$ ); they have been identified merely by means of grain counting measurements. The half cone including all these pairs is of about  $10^{-4}$  rad.

The measurements accomplished by the ionization method proposed by PER-

(\*) Now at Istituto di Fisica del Politecnico di Milano (Corso di Fisica Nucleare Applicata).

(1) M. SCHEIN, D. M. HASKIN and M. C. GLASSER: *Phys. Rev.*, **95**, 855 (1954).

(2) A. DEBENEDETTI, C. M. GARELLI, L. TALLONE, M. VIGONE, and G. WATAGHIN: *Nuovo Cimento*, **12**, 954 (1954); **2**, 220 (1955); **3**, 226 (1956).

(3) A. MILONE: *Pisa Conference*, June 1955.

(4) M. MIESOWICZ, W. WOLTER and O. STANISZ: *Pisa Conference*, June 1955.

(5) M. KOSHIBA and M. F. KAPLON: *Phys. Rev.*, **100**, 327 (1955).

(6) E. LOHRMANN: in print.

(7) G. WATAGHIN: *Proceedings of the Rochester Conference on High Energy Physics*, February 1955; *Mexico Conference*, September 1955.

TABLE I.

Pair	$x$ (cm)	$d$ ( $\mu\text{m}$ )	Pair	$x$ (cm)	$d$ ( $\mu\text{m}$ )	Pair	$x$ (cm)	$d$ ( $\mu\text{m}$ )
1	0	0	8	2.30	$< 0.9$	15	2.90	$< 1.1$
2	0.2	$< 0.2_5$	9	2.49	$< 0.9$	16	3.20	2.9
3	$0.47_5$	$< 0.4$	10	$2.54_5$	$< 0.9$	17	3.27	22.7
4	1.10	$< 0.5_5$	11	$2.54_5$	$< 0.9$	18	3.28	12.5
5	1.32	$< 0.6_5$	12	2.81	1.5	19	3.31	$1.3_5$
6	1.77	$< 0.8_5$	13	$2.86_5$	6.5	20	3.32	$< 0.6_5$
7	2.27	$< 0.9$	14	2.90	$< 1.1$	21	$3.32_5$	$2.4_5$

$x$ : distance for the point of production of the first pair.

$d$ : radial distance for the axis of the shower core.

KINS<sup>(8)</sup> seem to indicate an energy of about  $10^{11}$  eV for pair n. 2.

In Fig. 1 the development of the shower in the first 3.35 cm is represented schematically. The opening angle of the

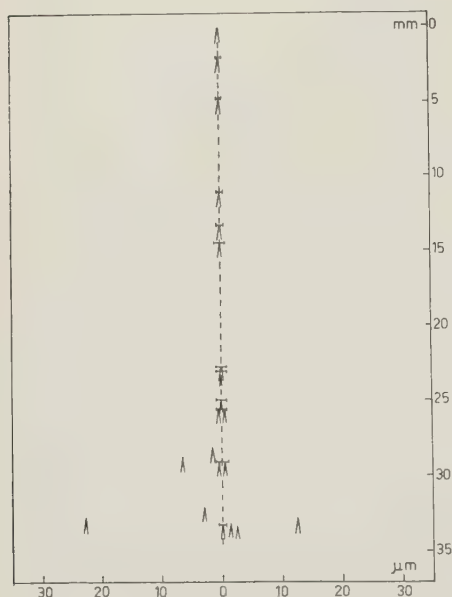


Fig. 1.

pairs in the drawing is not at all related to the true value, the determination of which is not possible for most of the pairs. The segments perpendicular to the

shower axis represent the diameter of the core in correspondence with the probable starting points of the pairs, whose origin is not directly observable.

In the first  $2.54_5$  cm, five tracks leave the core: one of them in the path between the starting points of the pairs n. 4 and 5; three between the pairs n. 6 and 7; and one between the pairs n. 7 and 8. After the origin of pair n. 11, the lateral spreading of the shower increases remarkably.

The measurements are in progress in the last section of the path of the shower (between 3.35 cm and the exit point): and we hope to be able to recognize more thoroughly the peculiar features of the event, after the completion of these preliminary data.

\* \* \*

The event has been observed by Dr. R. PERILLI FEDELI.

We thank Prof. G. WATAGHIN for his continuous interest and stimulating discussions.

We express our gratitude to Dr. A. ROBERTS, ONR London, who organized the Texas flight, and to Dr. Y. GOLDSCHMIDT-CLERMONT, CERN Geneva.

We are indebted to Prof. J. CRUSSARD, Prof. N. DALLAPORTA, Prof. F. G. HOUTERMANS, Prof. G. P. S. OCCHIALINI, Prof. C. F. POWELL, Prof. A. ROSTAGNI, for their help and assistance in the various operations concerning our stack.

<sup>(8)</sup> D. H. PERKINS: *Phil. Mag.*, **46**, 1146 (1955).

## Electron Production in Showers of Energies Between 10 and 100 GeV.

K. SITTE

*Department of Physics, Technion - Israel Institute of Technology, Haifa*

(ricevuto il 30 Marzo 1956)

Two facts lend a particular interest to the quantitative study of electron production in nuclear interactions with energies between 10 and 100 GeV:

1) It provides a check on the importance of the production of secondaries heavier than  $\pi$ -mesons. Since at present no efficient and undelayed mechanism of transfer of energy from K-particles or hyperons to the electron component is known, the fraction of primary energy which appears in the electron cascade will decrease in this energy region if, as it is claimed by some authors <sup>(1)</sup>, the energy given to the heavy secondaries increases with the primary energy and becomes about equal to that given to the  $\pi$ -mesons. Results of an earlier experiment contradicting this view have already been reported <sup>(2)</sup>.

2) Since it is somewhat easier to measure the total energy in the electron component than that in the charged

$\pi$ -mesons, it is tempting to use such a study for a determination of the degree of inelasticity of the collision, i.e. of the fraction of the primary energy transferred to all secondaries. On this point, some discrepancies appear to exist between earlier cloud chamber data <sup>(3)</sup>, and results obtained by VERNOV *et al.* <sup>(4)</sup> and by BERTOLINO <sup>(5)</sup> by other methods.

Cloud chamber photographs taken in a recent experiment <sup>(6)</sup> have, therefore, been re-examined with the aim to determine both the number of  $\pi^0$ -mesons emitted, and their total energy as a function of the primary energy. The chamber used in this work had been fitted with a light-material «producer plate» (Li, C or Al), and with eight  $\frac{1}{4}$  inch lead plates. In the re-examination, 298 showers initiated in the roof of the chamber or in the light-element plates, and 232 events starting in one of the upper lead plates, were analyzed. The primary energy was determined

<sup>(1)</sup> R. R. DANIELS and D. H. PERKINS: *Report on the International Congress on Cosmic Radiation, Bagnères de Bigorre*, p. 159 (1953); J. H. MULVEY: *Report on the International Congress on Cosmic Radiation, Bagnères de Bigorre*, p. 198 (1953).

<sup>(2)</sup> K. SITTE, F. E. FRÖHLICH and I. NADLHAFT: *Phys. Rev.*, **97**, 166 (1955).

<sup>(3)</sup> For literature, cf. N. M. DULLER and W. D. WALKER: *Phys. Rev.*, **93**, 215 (1954).

<sup>(4)</sup> E.g. S. N. VERNOV: *International Conference on Cosmic Radiation, Guanajuato* (1955).

<sup>(5)</sup> G. BERTOLINO: *Nuovo Cimento*, **3**, 141 (1956).

<sup>(6)</sup> J. G. ASKOWITH and K. SITTE: *Phys. Rev.*, **97**, 159 (1955).

from the «*F*-plot» in the way described before (<sup>3,6</sup>), but in the new analysis the showers were classified in three energy groups: from 10 to 20 GeV (average 16 GeV for showers initiated in light elements, and 15 GeV for those from lead); from 20 to 40 GeV (averages 27 and 26 GeV, respectively), and above 40 GeV (averages 48 and 45 GeV). No statistically significant differences were found for showers from different producer materials, and in some of the fol-

experimental errors. In calculating from the number of pairs observed under the lead plate, the number of  $\pi^0$ -mesons actually emitted, two limiting factors must, however, be taken into account: 1) that the pair may not be detected if the energy of the originating photon is lower than a certain minimum (as it is always for a photon emitted backward) and 2) that the choice of a particular cone in the laboratory system (aperture 30°) excludes a certain fraction of

TABLE I.

Primary Energy (GeV)	Light Elements			Lead			All Showers		
	$N^\pm$	$N^0$	$R$	$N^\pm$	$N^0$	$R$	$N^\pm$	$N^0$	$R$
10 ÷ 20	3.43 ±.14	1.47 ±.06	0.43 ±.03 <sub>5</sub>	3.35 ±.14	1.37 ±.06	0.41 ±.03 <sub>5</sub>	3.40 ±.10	1.43 ±.05	0.42 ±.03
20 ÷ 40	4.24 ±.16	1.70 ±.07	0.40 ±.03 <sub>5</sub>	4.08 ±.19	1.76 ±.07	0.43 ±.04	4.18 ±.12	1.74 ±.06	0.41 ±.03 <sub>5</sub>
> 40	5.46 ±.32	2.45 ±.20	0.45 ±.06	5.51 ±.43	2.48 ±.22	0.45 ±.06	5.47 ±.26	2.47 ±.20	0.45 ±.04

Average number of charged secondaries  $N^\pm$ , average number of neutral secondaries  $N^0$ , and neutral-to-charged ratio  $R = N^0/N^\pm$ , for the three primary energy groups.

lowing tables, all events are lumped together in the three energy groups (with averages of 15.5, 26.5 and 47 GeV.)

Wherever the geometry of the shower was such that it appeared possible to recognize all particles emitted within a cone of 30° aperture after traversal of the first lead plate, the number of electron pairs under this plate was counted. The number of  $\pi^0$ -mesons was computed from it, for an average path length of 1.17 cascade units (light-material showers) or 1.75 cascade units (lead showers), in the customary way. Corrections for secondary cascade processes must be applied but are rather small, so that their uncertainties do not seriously affect the

photons emitted in backward direction in the center of mass system. Under the circumstances of the present experiment, the two conditions lead to limitations in the *C*-system which are very nearly identical, and vary only slightly with the energy.

The results are summarized in Table I. The uncertainties given for the neutral-to-charged ratio  $R = N^0/N^\pm$  include the statistical standard deviation and estimated errors due to doubtful identification, geometrical factors. The data obtained clearly indicate that there is no appreciable variation with the primary energy of this ratio, and are in accord with earlier determinations in the low-



energy range <sup>(7,8)</sup>, and with those of the Bombay and Rochester groups at high energies <sup>(9,10)</sup>, but differ from the results  $R = 0.25$  reported by the Bristol group <sup>(11)</sup>.

In order to determine the energy

maximum, the number of electrons varies only slowly with depth; and 3) over a wide energy range, the number of electrons at the cascade maximum is very nearly proportional to the primary energy. It follows from these facts that

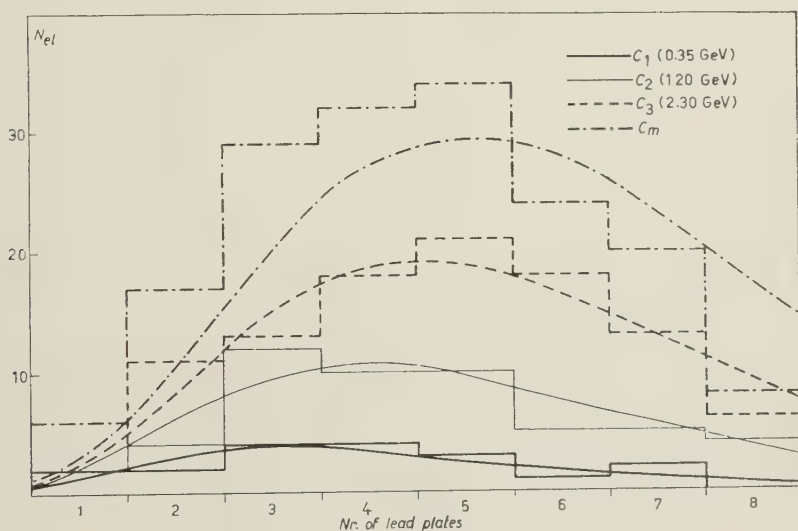


Fig. 1. — Histogram of the number of electrons  $N_{el}$  in three separate cascades  $C_1$  (0.35 GeV),  $C_2$  (1.20 GeV),  $C_3$  (2.30 GeV), and in the «mixed» cascade  $C_m$ , under the eight lead plates. The smooth curve  $C_m$  is calculated for a single cascade with an initiating photon energy of 3.85 GeV.

transferred to the electron component, it was decided to make use of three well-known facts on cascade development which make it possible to avoid the frequently impossible task of disentangling individual cascades and analyzing them separately: 1) the position of the cascade maximum varies only logarithmically with the energy; 2) near the cascade

even in a «mixed» cascade originated by several photons, the number of electrons at its maximum development is a good measure of the total primary energy—i.e., the sum of the energies of all photons—provided only that the photon spectrum is not too uncommon. This was checked on fourteen examples where the geometry of the event permitted a complete analysis of the individual cascades. A typical and rather extreme case is represented in Fig. 1. Here there electron cascades could be distinguished and their examination gave initiating photon energies of 0.35, 1.20 and 2.30 GeV. Histograms, and the curves according to the tables of JÁNOSSY and MESSEL <sup>(12)</sup>,

<sup>(7)</sup> G. SALVINI and Y. B. KIM: *Phys. Rev.*, **88**, 40 (1952).

<sup>(8)</sup> F. E. FROELICH, E. M. HARTH and K. SITTE: *Phys. Rev.*, **87**, 504 (1952).

<sup>(9)</sup> D. LAL, YASH PAL and RAMA: *Suppl. Nuovo Cimento*, **12**, 347 (1954).

<sup>(10)</sup> M. KOSHIBA and M. F. KAPLON: *Phys. Rev.*, **97**, 193 (1955).

<sup>(11)</sup> R. R. DANIELS, J. H. DAVIES, J. H. MULVEY and D. H. PERKINS: *Phil. Mag.*, **43**, 753 (1952); J. M. MULVEY: *Proc. Roy. Soc.*, **221**, 367 (1954).

<sup>(12)</sup> LEONIE JÁNOSSY and H. MESSEL: *Proc. Roy. Irish Acad.*, A **15**, 217 (1951).

are shown as  $C_1$ ,  $C_2$  and  $C_3$ . If, instead, the total number of electrons in each shelf is plotted—as in histogram  $O_m$ —the maximum number of electrons gives an initiating energy of 4.25 GeV: only slightly larger than the correct total of 3.85 GeV. Similar agreement was found in all fourteen cases, with deviations generally not exceeding  $\pm 10\%$ . Within this uncertainty it was, therefore, felt safe to ascribe to the total electron component the energy computed from the maximum number of electrons in the «mixed» cascade. Of course, slight corrections for backward emission have still to be applied.

Table II shows the results. The first column gives the primary energies,  $\langle E_p \rangle$ , the second the total energy  $\langle E_{el} \rangle$  of the electron component obtained after all

TABLE II.

$\langle E_p \rangle$ (GeV)	$\langle E_{el} \rangle$ (GeV)	$\langle f \rangle$
$15.5 \pm 0.5$	$3.30 \pm 0.5$	$0.71 \pm 0.11$
$26.5 \pm 0.7$	$5.80 \pm 0.7$	$0.73 \pm 0.09$
$47.0 \pm 2.1$	$9.50 \pm 1.9$	$0.67 \pm 0.14$

Average energy in the electron component  $\langle E_{el}^e \rangle$ , and fraction of energy transferred to all secondaries  $\langle f \rangle$ , as a function of the primary energy  $\langle E_p \rangle$ .

corrections, and the third the fraction  $\langle f \rangle$  of the primary energy transferred

to all secondaries, calculated with the neutral-to-charged ratios of Table I, and under the assumption that the average energy per secondary does not depend on its charge. The uncertainties of the primary energy are taken from the graphs, those of  $\langle E_{el} \rangle$  include statistical standard deviations and the estimated errors of the method,  $\pm 10\%$ . Again no significant trend is in evidence; if all the data are combined, a degree of inelasticity  $\langle f \rangle = 0.71 \pm 0.05$  is obtained. This is in better agreement with the cloud chamber work mentioned above (3) than with the data given by VERNOV (4) or by BERTOLINO (5). However, it must be stressed that the absolute values quoted depend critically on the validity of the «F-plot» method used to determine the primary energy, and while arguments for its correctness have been discussed in an earlier paper (6), the possibility of a systematical error of some  $10 \div 20\%$  cannot be entirely ruled out. Clearly, such an error would lead to an underestimate of  $\langle E_p \rangle$ , and hence to an overestimate of  $\langle f \rangle$ . However, while the absolute value of the degree of inelasticity in this energy region may thus still be somewhat in doubt—perhaps with a slightly higher probability for the larger figure—it appears certain that like the neutral-to-charged ratio, the inelasticity is practically constant for primary energies between 10 and 100 GeV.

Two Examples of Rare  $K^+$ -Decays in Emulsion (\*).

R. CESTER, T. F. HOANG (+), M. F. KAPLON, G. YEKUTIELI (×)

*Department of Physics, University of Rochester - Rochester New York,*

(ricevuto il 4 aprile 1956)

In the course of an unbiased systematic scan (by the on track method) in a stack of stripped emulsion for  $K^+$ -mesons exposed to the 270 MeV/c focused  $K^+$  beam of the Brookhaven Cosmotron we have observed two relatively rare examples of  $K^+$  decay. The first event is shown in a reproduction facsimile in Fig. 1 and is interpreted as the decay at rest,  $K_{\pi 2}^+ \rightarrow \pi^+ + \pi^0 (\rightarrow e^+ + e^- + \gamma)$ ; the second is shown in Fig. 2 and is interpreted as the decay in flight of a  $\tau^+$  meson,  $\tau^+ \rightarrow 2\pi^+ + \pi^-$ .

The first event (Fig. 1) is particularly significant as it gives independent support to our procedure of distinguishing between the  $K_{\mu 2}$  and  $K_{\pi 2}$  decay modes in emulsion on the basis of ionization alone (1). Our emulsion stacks were cross-irradiated with 1.5 GeV  $\pi^-$  mesons and all ionization measurements were carefully made and normalized with respect

to this beam (the normalized blob or grain density being denoted by  $\bar{b}$  or  $\bar{g}$ ). In the event of Fig. 1 the singly charged secondary had a dip angle of  $11^\circ$  with respect to the emulsion plane,  $\bar{b} = 1.14 \pm .04$  and a value of  $p\beta c = 174 \pm 25$  MeV. The lower and upper tracks of the pair ( $e_L$  and  $e_U$ ) had respectively dip angles of  $13^\circ$  and  $22^\circ$ , blob densities of  $1.03 \pm .04$  each and  $p\beta c$  values of  $60 \pm 16$  and  $135 \pm 20$  MeV. The low value of  $\bar{b}$  combined with  $p\beta c$  establishes their identity as electrons (plateau is 1.03). The mass of the secondary is determined to be  $(1.03 \pm .14) \mu$ , where  $\mu$  is the  $\pi$  rest mass. This, coupled with the closeness of the measured  $p\beta c$  to that expected for the  $K_{\pi 2}$  ( $p\beta c = 169$  MeV) strongly suggests this mode.

The event can be analyzed as follows. Since momentum and energy is not conserved with the visible charged particles, at least one neutral particle (we designate it as  $X^0$ ) must have been emitted. Its rest mass is given by

$$M_{X^0} = [(M_{K^-} - E_{\pi^-} - E_{e^+} - E_{e^-})^2 - (p_{\pi} + p_{e^+} + p_{e^-})^2]^{\frac{1}{2}}.$$

The spatial angles between the  $\pi^+$  and

(\*) This research was supported in part by the U. S. Atomic Energy Commission and the Office of Scientific Research of the Air Research and Development Command, U. S. Air Force.

(+) On leave from Laboratoire LEPRINCE-RINGUET, École Polytechnique, Paris.

(×) Now at Weizmann Institute of Science, Rehovoth, Israel.

(†) T. F. HOANG, M. F. KAPLON and G. YEKUTIELI: *Phys. Rev.* (in press.)

the electron pair were determined to be

$$\theta_{\pi e_L} = 168^\circ 15' \pm 1.5^\circ$$

and

$$\theta_{\pi e_U} = 169^\circ 45' \pm 1.5^\circ.$$

Using the measured values of  $p\beta c$  and the well known  $K^+$  rest mass of 494 MeV

at first sight to be a 4 prong star of which one of the prongs ( $b$ ) is observed to be a  $\pi^-$  meson. However the track labelled  $\tau$  is observed to increase its ionization in the direction of the «star». At the «star» it has a  $\bar{g} = 3.85 \pm .13$  and a  $p\beta c = 86 \pm 12$  MeV. This is consistent with the measured values of  $\bar{g}$  and  $p\beta c$  of stopping K-mesons in our emulsions when measured at the same

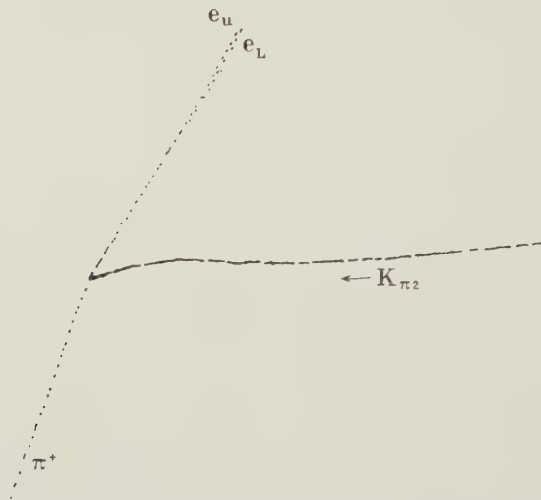


Fig. 1. — A facsimile drawing of an event interpreted as the decay,  $K_{\pi_2}^+ \rightarrow \pi^+ + \pi^0 (\rightarrow e^+ + e^- + \gamma)$ .

we find  $0 \leq M_{X^0} \leq 88$  MeV. This means that (in terms of known particles)  $X^0$  must have zero rest mass. With the assumption of only the one missing neutral particle we have two possibilities; (i) a radiative decay (internally converted) of a  $K_{\pi_2}^+$  or (ii) the decay  $K_{\pi_2}^+ \rightarrow \pi^+ + \pi^0 (\rightarrow \gamma + e^+ + e^-)$ . The first possibility (i) can be rejected immediately since that case requires  $M_{X^0} = \mu^0$ ,  $\mu^0 = 135$  MeV and we are left only with the second case (ii). We could of course either invent a new electromagnetic interaction to give the decay to  $\pi^+ + e^+ + e^- + \gamma$  directly or invent a new decay mode such as  $\pi^+ + e^+ + e^- + 2\nu$  but since the event can be minimally interpreted in terms of (ii) we consider this to be the correct interpretation.

The event of Fig. 2, might appear

distance from entrance to the stack. In view of the fact that a nucleon of this energy could not make a single  $\pi$ -meson, the event must represent either the interaction or decay in flight of a K-meson. Since there is no evidence to date for  $K^+$  interactions in which the  $K^+$ -mass is used for excitation it is important <sup>(2)</sup> to see whether this event is consistent with a decay in flight. Since the incoming particle is positively charged and one of the outgoing is observed to be negative the possibility of a  $\tau^+$  decay in flight suggests itself.

(<sup>2</sup>) One of the strong features of the Gell-Mann scheme which has been so successful in its characterization of the strange particles is the prediction that the  $K^+$  rest mass is conserved in nuclear interactions.

We can proceed to test this assumption by determining the mass of the parent (labeled  $\tau$ ) and its  $Q$ -value for  $3\pi$  decay. The range of track  $b$  is 14.5 mm corresponding to a kinetic energy of 28.5 MeV. The direction co-

to be  $76.8 \pm 2$  MeV. The velocity of the  $\tau$  at the point of decay is .384c corresponding to a  $p\beta c = 78.5$  MeV in good agreement with the measured value of  $86 \pm 12$  MeV. We conclude that the event is a  $\tau^+$  decay in flight and note

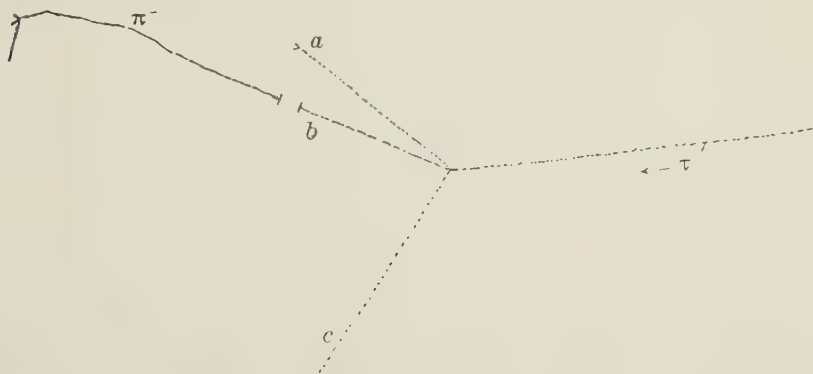


Fig. 2. — A facsimile drawing of an event interpreted as a  $\tau^+$  ( $\rightarrow 2\pi^- + \pi^+$ ) decay in flight.

sines of tracks  $a$ ,  $b$ , and  $c$  with respect to the incoming track (defining the  $X$ -direction) are  $\mathbf{a} = (.530, .521, .669)$ ,  $\mathbf{b} = (.759, .429, -.489)$  and  $\mathbf{c} = (.586, -.777, -.230)$  given in  $X, Y, Z$  order. An application of momentum conservation (using only track  $b$ ) determines the momenta of  $a$ ,  $c$  and  $\tau$  and with the assumption that  $a$  and  $c$  are  $\pi$ -mesons, their energies are also determined. The mass of  $\tau$  can then be calculated from its momentum and energy and yields a value of  $495.3 \pm 6$  MeV, in excellent agreement with other measurements; the  $Q$ -value of the decay is determined

that the accuracy of the mass determination is comparable with that obtained in elastic  $K^+p$  scatterings and that of the  $Q$ -value is comparable to that obtained from  $\tau^+$  decays at rest.

\*\*\*

We wish to thank the Mrs. J. MILKS, V. MILLER and B. SHERWOOD for their assistance in scanning the emulsions and to express our appreciation to Dr. G. COLLINS and the staff of the Cosmotron Laboratory for their assistance in obtaining the exposure.



## Sul limite classico della teoria di una particella di Dirac.

P. BOCCHIERI e A. LOINGER

*Istituto di Fisica dell'Università - Pavia*  
*Istituto Nazionale di Fisica Nucleare - Sezione di Milano*

(ricevuto il 10 Aprile 1956)

È noto che della teoria di Dirac di una particella sono state date due equivalenti formulazioni matematiche: la consueta formulazione spinoriale e la formulazione tensoriale di Whittaker e Ruse <sup>(1)</sup>. Recentemente TAKABAYASI <sup>(2)</sup> ha ripreso in esame la questione della trascrizione tensoriale dell'equazione di Dirac, fermando la sua attenzione sul problema di una particella muoventesi in un campo elettromagnetico assegnato; egli osserva che la  $\psi$  è univocamente determinata in ogni punto dello spazio e in ogni istante del tempo una volta che siano dati i valori, in ogni punto e in ogni istante, di opportuni covarianti costruiti mediante la  $\psi$ , la  $\bar{\psi}$  e le  $\gamma$ , e deduce poi dall'equazione di Dirac delle equazioni di moto per tali covarianti.

In un lavoro successivo <sup>(3)</sup> TAKABAYASI studia il limite classico («  $\hbar \rightarrow 0$  ») della sua trascrizione tensoriale, ottenendo una teoria classica di una particella dotata di spin.

Ora, un risultato siffatto è piuttosto sorprendente, in quanto la formulazione di TAKABAYASI è (come deve essere) completamente equivalente alla solita formulazione spinoriale e, d'altro canto, quest'ultima descrive nel suo limite classico una particella *priva di spin*, come ha mostrato PAULI (1932), usando un ragionevole « Ansatz » alla W.K.B. per la  $\psi$ . (Si noti che questo risultato conferisce ulteriore pregio alla teoria di Dirac, poichè una teoria classica di modello corpuscolare deve descrivere, per essere fisicamente corretta, una particella priva di spin, come è stato dimostrato da BOHR (1931) mediante l'analisi di un opportuno esperimento alla Stern e Gerlach <sup>(4)</sup>).

Osserviamo d'altra parte, a ulteriore chiarimento della questione, che alla stessa conclusione di PAULI si può giun-

<sup>(1)</sup> E. T. WHITTAKER: *Proc. Roy. Soc.*, A **158**, 38 (1937); H. S. RUSE: *Proc. Roy. Soc. Edinburgh*, **57**, 97 (1937).

<sup>(2)</sup> T. TAKABAYASI: *Prog. Theor. Phys.*, **13**, 106, 222 (1955); *Nuovo Cimento*, **3**, 233 (1956).

<sup>(3)</sup> T. TAKABAYASI: *Nuovo Cimento*, **3**, 242 (1956).

<sup>(4)</sup> Se si prescinde dall'effettiva grandezza  $\hbar/2$  dello spin si può costruire una teoria classica relativistica, indipendente da ogni modello particolareggiato, di una particella dotata di spin, come ha fatto KRAMERS (1934) nell'intento soprattutto di mostrare che la cosiddetta anomalia del rapporto giromagnetico  $m_0c/e$  è un effetto di relatività e non di quantizzazione. Nella teoria di Kramers non si fa alcuna ipotesi sul reale valore dello spin. Una considerazione analoga vale anche per la meccanica spinoriale classica di Proca (1954).

gere, *indipendentemente da ogni* « *Ansatz* », se ci si limita all'esame del caso particolare di un elettrone di Dirac *libero*.

Infatti per una particella libera, per esempio in quiete macroscopica e a spin orientato nel senso positivo dell'asse  $x_3$ , i valori di aspettazione delle parti  $\xi_i$  di « *Zitterbewegung* » delle coordinate  $x_i$ , sono <sup>(5)</sup>:

$$|\xi_1\rangle = \frac{\hbar}{2m_0c} \cos\left(\frac{2m_0c^2}{\hbar} t\right);$$

$$|\xi_2\rangle = \frac{\hbar}{2m_0c} \sin\left(\frac{\hbar}{2m_0c^2} t\right);$$

$$|\xi_3\rangle = 0;$$

ma da queste equazioni è evidente che per  $\hbar \rightarrow 0$  è  $\langle |\xi_1\rangle \rangle \rightarrow \langle |\xi_2\rangle \rangle \rightarrow 0$ , ossia nel

limite classico sparisce la « *Zitterbewegung* » e con essa, come è ovvio, anche lo spin.

Viene pertanto il sospetto che nel lavoro di TAKABAYASI citato in <sup>(3)</sup> il limite classico non sia stato eseguito correttamente: in effetti, il suddetto autore ha eseguito il limite in questione servendosi di un procedimento sbrigativo, consistente sostanzialmente nel cancellare dal sistema delle sue equazioni tensoriali di moto (e condizioni supplementari) i termini proporzionali ad  $\hbar$ ; ma è ben noto dalla teoria delle equazioni differenziali che un procedimento del genere, anche se in taluni casi può fornire risultati corretti, è del tutto ingiustificato in linea di principio.

In conclusione, ci sembra si possa tranquillamente riaffermare che nel limite classico una particella di Dirac *non* è dotata di spin.

<sup>(5)</sup> Vedi, per esempio, H. HÖNL e A. PAPA-  
PETROU: *Zeits. f. Phys.*, **116**, 153 (1940).

## Fluttuazioni statistiche nei conteggi di gruppi di granuli e di lacune nelle emulsioni nucleari.

G. LOVERA

*Istituto di Fisica dell'Università - Modena*  
*Istituto Nazionale di Fisica Nucleare - Sezione di Torino*

(ricevuto il 10 Aprile 1956)

Parecchi lavori sono stati dedicati, di recente, a trattazioni statistiche del processo di formazione delle tracce di particelle ionizzanti nelle emulsioni nucleari; ed alle fluttuazioni connesse (<sup>1,14</sup>), sulle

quali verte la presente nota (una bibliografia più estesa è riportata in alcuni dei lavori qui citati).

Precisamente, le considerazioni seguenti si riferiscono soltanto alle frequenze dei gruppi di granuli (blob), o, indifferentemente, di tutte le lacune (senza imporre un limite inferiore non nullo alla lunghezza di una lacuna), nei riguardi delle loro fluttuazioni statistiche. I vari modelli proposti per la formazione delle tracce hanno portato a differenti espressioni, per lo scarto quadratico medio da cui sono affette le misure basate su conteggi di gruppi di granuli e di lacune, per quanto, in alcuni casi singoli (<sup>12,13</sup>), si sia fatto rilevare che certe espressioni sono, in pratica, numericamente equivalenti (<sup>15</sup>).

(<sup>1</sup>) G. LOVERA: *Ric. Scient.*, **13**, 677 (1942).

(<sup>2</sup>) A. C. COATES: *Photographic Sensitivity* (London, 1951), p. 320.

(<sup>3</sup>) P. E. HODGSON: *Brit. Journ. Appl. Phys.*, **3**, 11 (1952).

(<sup>4</sup>) L. JAUNEAU, F. HUG-BOUSSER: *Journ. de Phys. et le Rad.*, **13**, 465 (1952).

(<sup>5</sup>) L. BARBANTI-SILVA, C. BONACINI, C. DE PIETRI, G. LOVERA, R. PERILLI FEDELI and A. ROVERI: *Atti. Sem. Mat. Fis. Univ. Modena*, **5**, 213 (1952).

(<sup>6</sup>) W. W. HAPP, T. E. HULL and A. H. MORRIS: *Can. Journ. Phys.*, **30**, 699 (1952).

(<sup>7</sup>) M. DELLA CORTE, M. RAMAT and L. RONCHI jr.: *Nuovo Cimento*, **10**, 509, 958 (1953); M. DELLA CORTE: *Nuovo Cimento*, **12**, 28 (1954).

(<sup>8</sup>) C. O'CEALLAIGH: *Proc. Bagnères Confer.*, p. 73 (1953); *Suppl. Nuovo Cimento*, **12**, 412 (1954); CERN: *Recommendations for Standardisation*, BS. 11 (1954).

(<sup>9</sup>) G. LOVERA: *Nuovo Cimento*, **12**, 154 (1954); I. IORI, G. LOVERA and A. ROVERI: *Atti Sem. Mat. Fis. Univ. Modena*, **7**, (1954); I. IORI and A. ROVERI: *Nuovo Cimento*, **2**, 165 (1955).

(<sup>10</sup>) A. J. HERZ and G. DAVIS: *Austral. Journ. Phys.*, **8**, 129 (1955).

(<sup>11</sup>) J. M. BLATT: *Austral. Journ. Phys.*, **8**, 248 (1955).

(<sup>12</sup>) G. LOVERA: *Atti Acc. Sci. Lett. Arti Modena*, **13**, 143 (1955).

(<sup>13</sup>) C. CASTAGNOLI, G. CORTINI and A. MANFREDINI: *Nuovo Cimento*, **2**, 301 (1955).

(<sup>14</sup>) P. H. FOWLER and D. H. PERKINS: *Phil. Mag.*, **46**, 587 (1955); R. R. DANIEL and D. H. PERKINS: *Proc. Roy. Soc.*, **A 221**, 351 (1954).

(<sup>15</sup>) Le due espressioni considerate nei lavori (<sup>9</sup>) e (<sup>10</sup>), e corrispondenti rispettivamente ai casi  $F=1$  e  $F=2$  del modello di Herz e Davis, secondo la notazione di BLATT (<sup>11</sup>), di-

In effetti, è facile mostrare che se si scrive lo scarto quadratico medio  $\sigma_a$  relativo ad una misura singola della frequenza  $a$  di gruppi (o di lacune) su di un segmento di traccia di lunghezza  $t$  prefissata, nella forma

$$(1) \quad \sigma_a^2 = a \left( 1 - h \frac{a}{a_{\max}} \right)$$

(dove  $a_{\max}$  è il valore massimo per il quale passa la frequenza  $a$  dei gruppi o delle lacune, sulla lunghezza  $t$  prescelta, al crescere del potere ionizzante specifico delle particelle che producono le tracce), i vari modelli portano a valori di  $h$  o costanti, o variabili molto lentamente con la densità della traccia e quindi compresi entro limiti assai ristretti, sicché è possibile, agli effetti pratici, conferire ad  $h$  nella (1) un opportuno valore medio: inoltre, i valori di  $h$  per i vari modelli sono assai prossimi fra loro. Queste conclusioni valgono nell'ipotesi, generalmente soddisfatta, che la lunghezza  $t$  del segmento di traccia sul quale si effettua la misura sia grande rispetto al diametro medio  $2\gamma$  del granulo sviluppato, sicché siano trascurabili termini dell'ordine di  $2\gamma/t$ .

Parecchi modelli statistici sono stati trattati in un ampio lavoro di BLATT <sup>(11)</sup>, e perciò a questo lavoro verrà fatto riferimento, per i casi in esso contemplati, nel passare in rassegna le espressioni ed i valori di  $h$  per i vari modelli.

1) Modello a spaziatura variabile, di O'CEALLAIGH <sup>(8)</sup> [BLATT, parte III del lavoro citato <sup>(11)</sup>, caso (a)]. Risulta facilmente:

$$(2) \quad h = \frac{2}{e} \cong 0.736.$$

2) Estensione, secondo FOWLER e

scendono dalla distribuzione dei granuli sviluppati, oppure di quelli di AgBr primitivi: si tratta di due presupposti che hanno entrambi un ovvio significato fisico.

PERKINS <sup>(14)</sup>, del modello a spaziatura variabile, di O'CEALLAIGH. Eseguendo calcoli numerici mediante la formula (3) del lavoro di FOWLER e PERKINS (che fornisce lo scarto quadratico medio per conteggi di gruppi o di lacune), in base ai valori sperimentali riportati dagli autori stessi, si trova che  $h$  varia tra  $2/e \cong 0.736$  e circa 0.715, al crescere della densità della traccia dal valor minimo al valore limite corrispondente a  $g \cong \cong 5000 \text{ mm}^{-1}$  (il parametro  $g$  è il coefficiente dell'esponente, nella formula che rappresenta la distribuzione delle lunghezze delle lacune). In particolare, per una densità della traccia compresa tra il valore minimo e quello corrispondente ad  $a_{\max}$ ,  $h$  si mantiene praticamente costante sul valore 0.736.

3) Modello tipo Happ, Hull e Morish, secondo BLATT [l. c. <sup>(11)</sup>, parte III, caso (b)], cioè estensione del modello a spaziatura costante, di O'Ceallaigh, al caso in cui i granuli sviluppati abbiano diametri non tutti uguali, bensì presentanti una certa distribuzione statistica. Si trova:

$$(3) \quad h = 2 \frac{k}{k + \frac{1}{2}} \left( \frac{2k+1}{2k+2} \right)^{2k+2} \left( \frac{k+1}{k + \lambda\gamma_0} \right)$$

( $k$ ,  $\gamma_0$ : parametri inerenti alla distribuzione dei raggi dei granuli sviluppati;  $\lambda$ : densità di probabilità della presenza di un granulo di AgBr reso sviluppabile). Per i valori  $k = 10$ ,  $\gamma_0 = 0.3 \mu\text{mm}$  prescelti da BLATT,  $h$  varia da 0.753 a 0.719 per  $\lambda\gamma_0$  compreso tra 0 e  $k/(2k+1)$ , cioè 10/21 (corrispondente ad  $a_{\max}$ ), e da 0.719 a 0.655 per  $\lambda\gamma_0$  compreso tra 10/21 e 1.5. Per  $k$  tendente ad infinito, si ricade, ovviamente, nel modello di O'Ceallaigh, e  $h$  tende a  $2/e$ .

4) Modello a spaziatura costante, di HERZ e DAVIS <sup>(10)</sup> [BLATT, l. c. <sup>(11)</sup>, parte III, caso (e)]. Si ha:

$$(4) \quad h = \frac{I^T}{(I^T - 1)^{T-1}}$$

(dove  $\Gamma$  è il massimo intero contenuto nel rapporto, supposto costante, tra il diametro di un granulo singolo dopo lo sviluppo, ed il diametro del granulo di AgBr primitivo). In particolare si trova:

$$\begin{array}{cccc} \Gamma = & 1 & 2 & 3 & \infty \\ h = & 0.750 & 0.741 & 0.738 & 2/e (\cong 0.736). \end{array}$$

5) Modificazione del modello a spaziatura costante nel senso di considerare variabile, con una certa distribuzione statistica, il numero  $n'$  di cellette elementari (contenenti ciascuna un granulo di AgBr suscettibile di essere reso sviluppabile) compreso sulla lunghezza  $t$  del segmento di traccia prescelto per la misura <sup>(12)</sup>. Si ottiene:

$$(5) \quad h = \left[ 2\Gamma + \frac{\bar{n}'}{n'_{\max}} \left( 2 - \frac{\bar{n}'}{n'_{\max}} \right) \right] \frac{\Gamma^{\Gamma}}{(\Gamma + 1)^{\Gamma+1}}$$

(dove  $\Gamma$  ha il significato già precisato; e  $\bar{n}'$ ,  $n'_{\max}$  sono rispettivamente il numero medio, ed il numero massimo di cellette elementari sul segmento di traccia prescelto).

TABELLA I. - Valori di  $h$  secondo la (5).

$\bar{n}'/n'_{\max}$	$\Gamma = 1$	$\Gamma = 2$	$\Gamma = 3$
0.7424	0.733	0.731	0.731
0.5	0.688	0.704	0.712

Il valore  $\bar{n}'/n'_{\max} = 0.7424$  corrisponde al caso considerato nel lavoro citato <sup>(12)</sup>, di  $\bar{n}' = 275$  e  $n'_{\max} = 370.4$  granuli di AgBr su 100  $\mu\text{mm}$ ; ed il valore 0.5 è stato scelto in base alla considerazione che il cammino medio di una particella ionizzante entro un granulo di AgBr è pressochè uguale al cammino medio nella intercapedine di gelatina tra due granuli di AgBr successivi <sup>(14)</sup>.

Poichè lo scarto quadratico medio della distribuzione dei valori di  $n'$ , calcolato secondo il modello statistico di RUARK e DEVOL <sup>(16)</sup>, nei casi qui considerati risulta piccolo rispetto a  $\bar{n}'$  ed a  $n'_{\max} - \bar{n}'$ , viene giustificato il fatto di considerare costante  $\Gamma$  al variare di  $n'$ , sempre che non si presenti una discontinuità di  $\Gamma$  in corrispondenza di  $n' = \bar{n}'$  o nella immediata prossimità di questo valore. La validità della (5) è perciò subordinata al fatto di considerare praticamente improbabile il verificarsi, fisicamente, di una discontinuità di  $\Gamma$  nella situazione suddetta, per un determinato trattamento di sviluppo subito dall'emulsione: questa ipotesi non appare, del resto, meno giustificata delle altre schematizzazioni necessariamente introdotte nei vari modelli, rispetto alla struttura effettiva dell'emulsione e delle tracce.

Le considerazioni ed i risultati suesposti, permettono di concludere che, essendo il valore di  $a_{\max}$  un dato determinabile sperimentalmente in modo diretto, l'impiego della (1) con un'opportuna scelta del valore di  $h$  (che le deduzioni teoriche fanno prevedere prossimo a  $0.70 \div 0.75$  circa) presenta, dal punto di vista pratico, il vantaggio di consentire il calcolo di  $\sigma_a$ , indipendentemente da qualsiasi modello inerente alla formazione delle tracce. Entro queste conclusioni si inquadrano, in modo soddisfacente, i dati di misure precedenti <sup>(9)</sup>.

È facile l'estensione delle presenti considerazioni al caso di conteggi delle sole lacune con lunghezza eccedente un certo valore minimo prescelto, sempre che il massimo della frequenza, previsto teoricamente, sia pure accessibile alle misure sperimentali.

<sup>(16)</sup> A. RUARK e L. DEVOL: *Phys. Rev.*, **49**, 355 (1936).



# Note on the Angular Correlation in the Decays of Hyperfragments.

P. ZIELIŃSKI

*Polish Academy of Sciences, Institute of Nuclear Research - Warsaw*

(ricevuto l'11 Aprile 1956)

The analysis of hyperfragment decays yields valuable information concerning both the structure of hyperfragments and the properties of « new particles » bound in them — in an overwhelming majority of cases of  $\Lambda^0$  hyperons. The available experimental data are so scanty however, that apart from the binding energies of  $\Lambda^0$  in the hyperfragments any more definite conclusions are difficult to be drawn. There are suggestions from the analysis of the non-mesonic decay of hyperfragments indicating frequent emission of two fast nucleons <sup>(1)</sup>, there are also suggestions related to their mesonic decays and concerning the structure of hyperfragments <sup>(2,5)</sup>. In the

present note we want to draw attention to some other possibility in analysing the data of the mesonic decays of hyperfragments.

Classifying the 37 cases of the mesonic decay of hyperfragments known from the literature, according to the reaction involved, we have:

- two body decays of the type  $\pi^- + \text{residual nucleus}$ : 10 cases;
- three body decays of the type  $\pi^- + \mu + \text{residual nucleus}$ : 17 cases;
- three body decays involving the neutral particle emission or four body decays: 10 cases.

The two body decay cases yield information concerning the binding energies — the others may provide also information on the decay process itself.

Among these, the most frequent decay of the type:  $\pi^- + \mu + \text{residual nucleus}$  suggests a simple interpretation.

As pointed out by CRUSSARD *et al.* <sup>(3)</sup> this mode of decay seems to indicate that we can picture a hyperfragment

<sup>(1)</sup> P. CIOK, M. DANYSZ and J. GIERULA: *Nuovo Cimento*, **11**, 436 (1954).

<sup>(2)</sup> During the performing of this analysis I have received the preprint of the work: *About the  $\Lambda$ -Nucleon Force* from Prof. R. GATTO, in which the need for an analysis of angular distributions in hyperfragment decays is emphasized. I am indebted to Prof. GATTO for sending me the preprints and private communications.

<sup>(3)</sup> J. CRUSSARD, V. FOCHE, G. KAYAS, L. LEPRINCE-RINGUET, D. MORELLET, F. RENARD and J. TREMBLEY: *Report of the Conference in Pisa* (1955), p. 481.

<sup>(4)</sup> W. F. FRY, J. SCHNEPS and M. S. SWAMI: *Disintegration of Hyperfragments*, II (preprints). I am indebted to Prof. FRY and his collaborators

for sending us the preprint of their work prior to publication.

<sup>(5)</sup> K. GOTSTEIN, B. ROEDERER, J. ROEDERER, N. VARSHNEYA and P. WALOSCHKE: *Report of the Conference in Pisa* (1955), p. 265.

as a stable fragment associated with a  $\Lambda^0$ -particle. The present experimental evidence does not contradict this suggestion.

FRY *et al.* <sup>(4)</sup> [see also GOTTSTEIN *et al.* <sup>(5)</sup>] consider that due to the low binding energies of the  $\Lambda^0$ -particle in the lightest hyperfragments one can neglect the interaction between the products of decay of the  $\Lambda^0$  i.e. the  $\pi^-$ , the proton and the residual nucleus in this kind of decay process. Under this assumption, the vector sum of the  $\pi^-$  and proton momenta yields the momentum of the  $\Lambda^0$ -particle within the hyperfragment.

Extending this way of approach we

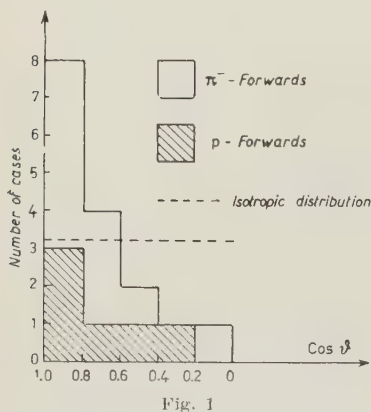


Fig. 1

can find moreover not only the momentum of the  $\Lambda^0$  but also the angle  $\theta$  between the direction of flight of the

$\Lambda^0$  within hyperfragment and the direction of decay of the  $\Lambda^0$ -particle in its rest frame. The figure shows the frequency distribution of the angle  $\theta$  for the 16 cases of this decay mode enabling the analysis <sup>(3,6)</sup>.

The histogram obtained seems to indicate a strong forward and backward correlation.

If the assumption involved is, approximately, correct and the selection bias of the decay mode is not important — one can partly look for cause of such an effect in the higher spins of  $\Lambda^0$ -particles.

\* \* \*

I wish to express my gratitude to prof. M. DANYSZ and dr. J. GIERULA for introducing me to the analysis of hyperfragments and for helpful suggestions. My thanks are also due to dr. J. DABROWSKI for a discussion.

<sup>(6)</sup> R. D. HILL, E. O. SALANT, M. WIDGOTT, L. S. OSBORNE, A. PEVSNER, D. M. RITSON, J. CRUSSARD and W. D. WALKER: *Phys. Rev.*, **94**, 797 (1954); J. E. NAUGLE, E. P. NEY, P. S. FREIER and W. B. CHESTON: *Phys. Rev.*, **96**, 1383 (1954); M. BALDO, G. BELLIBONTI, M. CEC-CARELLI, M. GRILLI, B. SECHI and G. T. ZORN: *Nuovo Cimento*, **1**, 1180 (1955); F. ANDERSON, G. LAWLOR and T. E. NEVIN: *Nuovo Cimento*, **2**, 605 (1955); « G-STACK »: *Report of the Conference in Pisa* (1955), p. 505; J. D. SORRELS, G. H. TRILLING and R. B. LEIGHTON: *Phys. Rev.*, **100**, 1484 (1955).

**Interactions of  $K^-$  Mesons with Hydrogen Nuclei at 50 to 110 MeV.**

N. N. BISWAS, L. CECCARELLI-FABBRICHESI, M. CECCARELLI (\*), M. CRESTI (-)

K. GOTTSTEIN, N. C. VARSHNEYA and P. WALOSCHEK

*Max-Planck-Institut für Physik - Göttingen*

(ricevuto il 13 Aprile 1956)

Among the interactions of  $K^+$ -mesons with different nuclei, those with free protons are of the greatest interest in connection with the problem of K-nucleon forces. The study of these interactions together with that of other fundamental interactions may also lead to an independent determination of various properties of heavy mesons, e.g. spin, parity, isotopic spin, which at present could be deduced only from the production and decay properties.

At present, however, the study of the K-p scattering is very difficult due to the extreme rarity of useful events <sup>(1)</sup>.

In this paper we present the preliminary results of a scanning program of the Göttingen group, in which 12 clear K-p collisions have been found and analyzed in detail.

The procedure used for finding these events is that of «along the track» scanning in two stacks exposed to the

Berkeley K-beam as described by us in a previous paper <sup>(2)</sup>. However, for some time the method of following all tracks to their ends has been substituted by a faster method in which the tracks are followed only down to the point corresponding to an energy of about 50 MeV. One sixth of the total number of tracks has been followed to the ends and carefully scrutinized under oil immersion in order to determine the proton and pion contamination of the K-beam.

In Fig. 1 is shown the energy spectrum of the K-primaries, namely, the lengths of tracks followed in the various energy intervals. The total length of track followed is 124 m between the energies of 50 and 110 MeV and 162 m between 0 and 110 MeV. In the same figure the shaded squares correspond to the primary energies of our K-p collisions.

In Table I are presented 11 K-p collisions having primary energies between 50 and 110 MeV and scattering angles greater than 15°. For this minimum angle and energy the proton range is

(\*) On leave from the University of Padova.

(-) At present at the Istituto di Fisica dell'Università di Padova.

<sup>(1)</sup> At present only two events have been published: W. W. CHUPP, G. GOLDBABER, S. GOLDBABER, W. JOHNSON and J. E. LANNUTTI: *Phys. Rev.*, **99**, 1042 (1955).<sup>(2)</sup> N. N. BISWAS, L. CECCARELLI-FABBRICHESI, M. CECCARELLI, K. GOTTSTEIN, N. C. VARSHNEYA and P. WALOSCHEK: *Nuovo Cimento*, **3**, 825 (1956).

Event No.	K-energy at coll. point (from that of the secondaries)	Energy of primary K (from energy distribution of K-beam) (MeV)	Scattering angle in the c.m.s. (degrees)	Scattered K-meson Track			
				Angle with the primary (degrees)	Range ( $\mu$ m)	Momentum (MeV/c)	Transverse Momentum (MeV/c)
3378	100 $\pm$ 2	91 $\pm$ 7	24.5 $\pm$ 1	16 $\pm$ 0.5	48 038 $\pm$ 1 500	323.5 $\pm$ 3.2	8.8
2414	62.5 $\pm$ 1.5	63 $\pm$ 8	31 $\pm$ 4	18.3 $\pm$ 0.7	20 400 $\pm$ 900	249.2 $\pm$ 3.3	7.7
3836	55.8 $\pm$ 1.1	63 $\pm$ 8	31 $\pm$ 1.5	19.0 $\pm$ 0.5	16 666 $\pm$ 500	234.5 $\pm$ 2.1	7.7
3599	61.7 $\pm$ 1.4	61 $\pm$ 8	54 $\pm$ 1	35.5 $\pm$ 0.5	15 630 $\pm$ 470	230 $\pm$ 1.6	13.3
3937	68.4 $\pm$ 1.7	58 $\pm$ 9	59 $\pm$ 1	38.5 $\pm$ 1	16 755 $\pm$ 630	234.8 $\pm$ 2.7	14.1
3622	81 $\pm$ 1.5	77 $\pm$ 7	80 $\pm$ 1	54 $\pm$ 0.5	15 915 $\pm$ 550	231.3 $\pm$ 2.4	18.8
584	73.3 $\pm$ 2.0	76 $\pm$ 7	85 $\pm$ 2	59 $\pm$ 0.7	11 520 $\pm$ 650	210 $\pm$ 3	18.8
3775	67.2 $\pm$ 2.2	73 $\pm$ 10	89 $\pm$ 1	61 $\pm$ 1	17 055 $\pm$ 650	236.1 $\pm$ 2.7	20.0
4361	51.4 $\pm$ 1.0	57 $\pm$ 9	107 $\pm$ 2	76 $\pm$ 0.5	3 240 $\pm$ 100	145 $\pm$ 1.5	14.1
565	58.6 $\pm$ 1.0	60 $\pm$ 8	126 $\pm$ 3	96.5 $\pm$ 1	1 796 $\pm$ 125	122.2 $\pm$ 2.4	12.2
3651	74.5 $\pm$ 1.7	77 $\pm$ 7	130.5 $\pm$ 1	98.5 $\pm$ 1	2 350 $\pm$ 160	132.1 $\pm$ 2.5	13.3
624	30.4 $\pm$ 1.0	46 $\pm$ 11	41.5 $\pm$ 1	27.5 $\pm$ 0.7	5 020 $\pm$ 220	164.5 $\pm$ 2	7.7

greater than 35  $\mu$ m and so the check on the coplanarity and the transverse momentum can be made easily. In the same table also a clear event at lower energy is presented; a few other possible

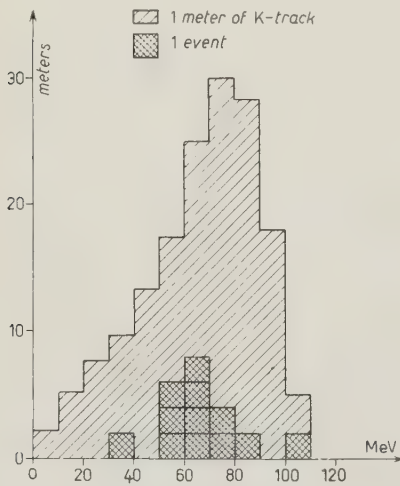


Fig. 1.

events at lower angles have however been excluded because of the difficulty of making these usual tests, and the possibility of scanning biases.

The criteria used in the identification of the K-p collisions are the tests of coplanarity, and the equality of the K and p transverse momenta, tests which are well satisfied in all the events of Table I as evident from the last two columns. The few cases in which the momentum balance is rather less satisfactory can easily be explained by greater errors of measurement due to the unfavourable geometry of the event. The non-occurrence of events with small significant deviations from coplanarity and simultaneously from the balance of transverse momentum indicates that the probability of some of the 12 events being due to collisions with nucleons bound to complex nuclei is negligible.

In all events except No. 3775, both the K and the proton stop in the stack. The ranges and the corresponding errors have been calculated according to the procedure used in the G-stack experiment <sup>(3)</sup>, being decreased by 4% in order to take into account a reasonable

<sup>(3)</sup> « G-STACK COLLABORATION ». Appendix I, *Nuovo Cimento*, **2**, 1063 (1955).

e with primary reces)	Proton Track			Deviation from		Observer
	Range ( $\mu$ m)	Momentum (MeV/c)	Transverse Momentum (MeV/c)	Coplanarity (degrees)	Transverse Momentum balance (MeV/c)	
$\pm 1$	$130 \pm 6$	$89.3 \pm 1.3$	$87.3 \pm 1.2$	$1.5 \pm 2.0$	$1.9 \pm 3.2$	Mrs. BAUMBACH
$\pm 0.7$	$72 \pm 8$	$74.2 \pm 3$	$71.3 \pm 3$	$0.2 \pm 1.0$	$6.7 \pm 5$	Mrs. BAUMBACH
$\pm 0.5$	$89 \pm 3.5$	$79.5 \pm 1$	$76.1 \pm 1.0$	$2.0 \pm 2.0$	$0.4 \pm 2.2$	Mrs. FAY
$\pm 0.5$	$700 \pm 50$	$147.8 \pm 3.5$	$131.2 \pm 3.2$	$1.0 \pm 2.0$	$2.3 \pm 3.7$	Miss ARNDT
$\pm 1$	$805 \pm 50$	$154.0 \pm 2.8$	$133.5 \pm 2.8$	$1.0 \pm 1.0$	$12.5 \pm 4.7$	Miss FECHNER
$\pm 0.5$	$4038 \pm 130$	$244.4 \pm 2.4$	$187 \pm 2.3$	$0.5 \pm 1.5$	$0 \pm 3.2$	Miss BISCHOFF
$\pm 0.5$	$3810 \pm 220$	$240 \pm 3.5$	$178.5 \pm 3.0$	$1.5 \pm 1.0$	$1.5 \pm 5.0$	Miss FECHNER
$\pm 0.5$	$8400 \pm 700$	$302.4 \pm 7.0$	$214 \pm 5.2$	$0.5 \pm 1.5$	$7.0 \pm 6.1$	Mrs. BAUMBACH
$\pm 0.5$	$3840 \pm 120$	$241 \pm 2.2$	$138.5 \pm 2.3$	$0.5 \pm 1.5$	$2.0 \pm 2.7$	Miss v. HEYDEBRECK
$\pm 1$	$7196 \pm 260$	$289.1 \pm 3.0$	$134 \pm 4.6$	$0.5 \pm 2.0$	$12 \pm 5.2$	Miss LEVIN
$\pm 1$	$11410 \pm 400$	$330.5 \pm 3.4$	$137 \pm 5$	$1.0 \pm 1.5$	$6.0 \pm 5.8$	Mrs GOTTSTEIN
$\pm 0.5$	$99 \pm 10$	$82.0 \pm 2.5$	$77.1 \pm 2.6$	$2.0 \pm 1.5$	$1.3 \pm 3.8$	Mrs GOTTSTEIN

moisture content (60%) of the emulsion, and the energies and the momenta have been obtained from the tables of FAY *et al.* (4). The proton of event No. 3775 traverses 6.4 mm of emulsion and escapes from the stack with a residual range of  $2.0 \pm 0.6$  mm, as estimated by the scattering and the gap-density measurements. In the case of event 3937 the proton suffers a large angle scattering possibly with some energy loss near its end. No correction in the range of the proton has, however, been made for this. In eleven cases the K-particle exhibits a clear thin secondary at the end of its track; in event 3622 no secondary can be seen but this is most probably a consequence of the fact that the K-meson stops very near the surface of one emulsion.

The energies of the colliding mesons have been computed, both from the K and proton energies after the collision and from the momentum dispersion curve of the focussed particles. The agreement between the two values is reasonably

good considering the rather wide spread in the ranges of our sample of K-mesons for a given nominal momentum. This can be considered as an additional check on the correct identification of the events.

The angles of scattering in the center of mass system have been obtained from those in the laboratory system from the curves of Pedretti (5). In Fig. 2 is shown the angular distribution for the first 11 K-p collisions in the c. o. m. system per unit solid angle. Each hatched rectangle corresponds to one event.

In spite of little statistical significance of our results, it may be justified to make a few remarks here. Since the Rutherford scattering contribution is certainly small, the distribution of Fig. 2 can be attributed mostly to the nuclear and shadow scattering. The distribution would then suggest that the differential cross-section of scattering is somewhat peaked in the forward direction.

(4) H. FAY, K. GOTTSTEIN and K. HAIN: *Suppl. Nuovo Cimento*, **2**, 234 (1954).

(5) E. PEDRETTI: *Curves privately circulated by the Bologna group. Nuovo Cimento* **3**, 956 (1956).



The mean free path for K-p scattering comes out to be  $11.3 \pm 3.4$  m (in case of 11 events, 50-110 MeV) and  $13.5 \pm 3.9$  m (in case of 12 events, 0-110 MeV). Taking a hydrogen content of  $0.053 \text{ g/cm}^3$  the total cross-section is found to be

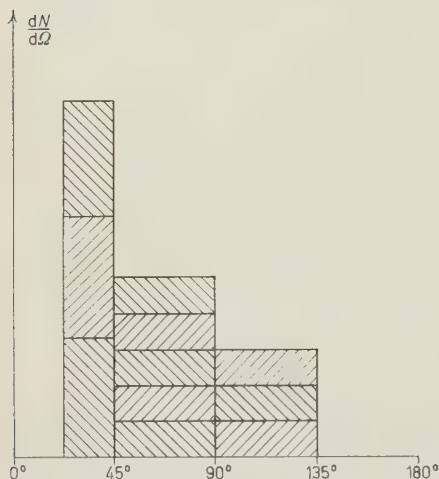


Fig. 2.

$27 \pm 8$  and  $23 \pm 7$  mb respectively. With the value of  $95 \pm 16$  cm for the m. f. p. of  $K^+$ -mesons in nuclear emulsion determined by LANNUTTI *et al.* <sup>(6)</sup>, these authors calculate the K-N cross-section to be equal to 6 mb. This value seems to be too low compared to our value of  $\sim 25$  mb, for K-p interaction. It should, however, be noted that in computing the K-N cross-section from the total nuclear cross-section these authors have assumed that the K-p and K-n cross-sections are equal, and also that they are not strongly energy dependent. In absence of any experimental data in favour of these assumptions these calculations may not necessarily be expected to lead to a

precise estimate. Moreover, the mean free path of 95 cm has been obtained by these authors <sup>(6)</sup> on the assumption that the differential cross-section is isotropic down to small angles. If, however, a forward scattering would exist the value of the K-nucleus cross-section would be underestimated and so also the value of the K-N cross-section <sup>(7)</sup>.

In scattering experiments on heavy nuclei, the existence of a preferentially forward scattering may not be easy to detect, in particular at low energies, because of a very great contribution due to Rutherford scattering. Small angle nuclear scatterings in the energy range with which we are here concerned will in general not be followed by the emission of other ionizing particles nor will the energy of the K-particles be noticeably decreased, and therefore a distinction between Rutherford and nuclear scatterings cannot be made on these grounds. In addition, the number of interactions with small momentum transfer to the nucleon which would seem to be frequent in the elementary collisions, may be strongly limited in a complex nucleus by the Pauli exclusion principle.

It is our intention to continue this program in order to obtain better statistics.

\* \* \*

This experiment was possible due to the kind co-operation of the Berkeley group who exposed the emulsions to the Bevatron for us. We are particularly indebted for this to Drs. E. J. LOFGREN, R. W. BIRGE and D. H. STORK.

We are grateful to Prof. W. HEISEN-

<sup>(6)</sup> J. E. LANNUTTI, W. W. CHUPP, G. GOLDHABER, S. GOLDHABER, E. HELMY, E. ILOFF, A. PEVSNER and D. M. RITSON: Privately circulated preprint.

<sup>(7)</sup> Preliminary results of our group would indicate a slightly shorter m.f.p. of  $K^+$ -mesons in nuclear emulsions, namely  $68 \pm 11$  cm. This value would correspond to an elementary K-N cross-section of about 9 mb, if the calculation is made using the same assumptions as in <sup>(6)</sup>.

BERG for his kind interest and encouragement, to Dr. G. QUARENI for useful discussions and suggestions, and to Drs. G. LÜDERS and K. NISHIJIMA who read the manuscript.

Several of us are indebted to various personalities and institutions for scholarship or maintenance grants:

M. CE. to Prof. W. HEISENBERG, N. N. B. to the Government of India, and

P. W. to the Akademischer Austauschdienst, Bonn. The latter also wishes to thank the Argentine Comision Nacional de la Energia Atomica for leave of absence. M. CR. thanks Prof. A. ROSTAGNI for granting him leave of absence from Padua University.

The Deutsche Forschungsgemeinschaft has supported our work by the purchase of microscopes.

## Strange Particles and the Conservation of Isotopic Spin.

A. GAMBA

*Istituto di Fisica dell'Università - Torino*  
*Istituto Nazionale di Fisica Nucleare - Sezione di Torino*

(ricevuto il 25 Aprile 1956)

In a paper under the same title CASE, KARPLUS and YANG<sup>(1)</sup> have recently investigated the following problem: «Does invariance under a finite group of rotations in isotopic spin space provide enough symmetry to furnish a basis for the classification of elementary particles and to account for all experimental evidence of charge independence?».

Their conclusion is in the affirmative; they point out three different possibilities in the tetrahedral, octahedral, and icosahedral groups respectively. Such theories suggest also attractive possibilities for introducing in a more satisfying way the «strangeness» quantum number.

The question came to the attention of the authors, because, as they state, «so far all experimental evidence for charge independence, direct or indirect, concerns only systems with relatively few states whose equivalence under isotopic spin rotation does not require the symmetry implied by the full group». We cannot agree on this point. We want

to show, for example, that any process involving one nucleon and one pion, by general principles, must either be charge dependent, or charge independent with respect to the full group, so that any intermediate invariance of the type investigated by CASE, KARPLUS and YANG has no physical meaning.

The argument runs as follows: in order to have a restricted invariance in isotopic spin space under a finite group of rotations, the transition matrix for a process ought to be invariant with respect to such a finite group, but *not* invariant with respect to the full group (otherwise the theory reduces to the usual one). The proof is then simply to show that such a matrix cannot be constructed out of the four isotopic spin matrices for the nucleon (the unit matrix 1, and the vector matrix  $\tau_\mu$ ) and the nine isotopic spin matrices for the pion (the unit matrix 1, the vector  $M_\mu$ , and the symmetrical tensor with vanishing trace  $N_{\mu\nu}$ , built up with the products  $M_\mu M_\nu$ ).

Group theory is used throughout; the notation for representations is that of CASE, KARPLUS and YANG.

(<sup>1</sup>) K. M. CASE, R. KARPLUS and C. N. YANG: *Phys. Rev.*, **101**, 874 (1956).

Look now to the following Table:

Rotation group	Representation to which belong the (isotopic spin) matrices for the:		Invariant matrices for the group (*)	Kronecker products which originate the invariants (+)
	<i>nucleon</i>	<i>pion</i>		
Full	$D_0, D_1$	$D_0, D_1, D_2$	$\alpha, \beta$	$D_0 \times D_0, D_1 \times D_1$
Tetrahedral	$\Gamma_0, \Gamma_1$	$\Gamma_0, \Gamma_{1A}, \Gamma'_0, \Gamma''_0, \Gamma_{1B}$	$\alpha, \beta, \gamma$	$\Gamma_0 \times \Gamma_0, \Gamma_1 \times \Gamma_{1A}, \Gamma_1 \times \Gamma_{1B}$
Octahedral	$\Gamma_0, \Gamma_1$	$\Gamma_0, \Gamma_1, \Gamma'_1, \Gamma^*_1$	$\alpha, \beta$	$\Gamma_0 \times \Gamma_0, \Gamma_1 \times \Gamma_1$
Icosahedral	$\Gamma_0, \Gamma_1$	$\Gamma_0, \Gamma_1, \Gamma_2$	$\alpha, \beta$	$\Gamma_0 \times \Gamma_0, \Gamma_1 \times \Gamma_1$

(\*)  $\alpha = 1, \beta = \mathbf{r} \cdot \mathbf{M}, \gamma = \tau_x M_y M_z + \tau_y M_z M_x + \tau_z M_x M_y$ .

(+) The 1st representation is in the isotopic spin space of the nucleon, the 2nd one in the isotopic spin space of the pion.

The only invariant matrices for the octahedral and icosahedral groups are  $\alpha$  and  $\beta$ . Since these are invariants also for the full rotation group, one is led back to the usual theory. The tetrahedral group seems to be better off, since  $\gamma$  is not an invariant for the full group.

However, such a matrix is ruled out by charge conservation, as can be easily verified by direct calculation: for

example it would allow processes like:  $\pi^+ + n \rightarrow \pi^- + n$ .

We have not considered processes in which more than one pion and one nucleon intervene, although such analysis could be easily carried on with similar methods. The purpose of this letter was only to show the general principles, underlying the concept of charge independence, which one cannot easily dispense with or modify.

## Sull'affinità metilica dei chinoni.

G. GIACOMETTI

*Istituto di Chimica Fisica dell'Università - Padova*

(ricevuto il 26 Aprile 1956)

In una serie di recenti lavori <sup>(1)</sup> SZWARC ha illustrato un metodo molto elegante per misurare le velocità relative delle reazioni di somma di radicali metilici a vari tipi di accettori, come gli idrocarburi aromatici ed i chinoni. Tali velocità relative vengono da lui espresse in una scala convenzionale e chiamate « affinità metiliche » della molecola in questione.

A prima vista tali misure non possono dire molto circa la posizione nel composto accettore che viene attaccata dal radicale nella fase primaria della reazione. Nondimeno, nel caso dei chinoni, lo SZWARC ammette che la somma avvenga inizialmente ad un doppio legame C=C dell'anello chinonico, sulla base di considerazioni effettuate sui suoi dati di affinità metiliche. A esemplificare il suo ragionamento prendiamo i tre composti p-benzochinone (I), 1-naftochinone (II), e antrachinone (III) per i quali le affinità metiliche sono dell'ordine (I) > (II) > (III). SZWARC sostiene che la diminuzione di reattività è spiegabile con l'ipotesi di attacco primario a doppi

legami, C=C dell'anello chinonico che vengono ad essere schermati, parzialmente in (II) e completamente in (III), dalla presenza degli anelli condensati. Ora, questo modo di vedere sembra un po' troppo aprioristico, nel senso che non solo impone l'ipotesi di non attacco all'ossigeno, ma anche quella di non attacco ai doppi legami aromatici degli anelli condensati, mentre è noto che il metile si somma facilmente agli stessi idrocarburi aromatici.

Lo scopo di questa nota è di dimostrare come, senza alcuna ipotesi sulla regione di attacco, sia possibile correlare l'ordine delle reattività con opportuni indici strutturali elettronici delle molecole, in modo che la posizione di attacco ne segua come logica conseguenza e risulti essere l'ossigeno chinonico piuttosto che il carbonio dei doppi legami.

Una correlazione di tal genere è già stata fatta dal COULSON <sup>(2)</sup> per gli idrocarburi aromatici, sulla base di due criteri molto ben stabiliti, nell'ambito del metodo degli orbitali molecolari: da una parte, coll'indice di valenza libera del-

<sup>(1)</sup> M. SZWARC e coll.: *Journ. Am. Chem. Soc.*, **76**, 3439, 5981 (1954); **77**, 1949, 4468 (1955).

<sup>(2)</sup> C. A. COULSON: *Journ. Chem. Soc.*, **1955**, 1435.



l'atomo al quale avviene l'attacco del radicale (più grande l'indice più grande la reattività); dall'altra, colla cosiddetta « energia di polarizzazione a radicale » (più grande l'energia minore la reattività). Questi due criteri permettono ovviamente di individuare la posizione preferita di attacco, come quella a maggior indice di valenza libera e a minor energia di polarizzazione.

Nel nostro caso il problema risulta un po' complicato dalla presenza dei due eteroatomi dei quali non si può tener conto che in un modo semiempirico nel quadro del metodo LCAO, MO. L'ostacolo può essere però aggirato partendo dalla considerazione degli idrocarburi isoaromatici con i chinoni (i cosiddetti chinondimetani) e applicando il II criterio a questi; si può poi mostrare con buona approssimazione che i risultati qualitativi non cambiano con l'introduzione degli eteroatomi.

Il primo criterio perde invece parecchio del suo significato quando si è in presenza di eteroatomi poichè l'indice di valenza per questi non è definito. Ciò nonostante possiamo anche qui avere una idea di come vanno le cose esaminando gli indici dei chinondimetani. Per le posizioni corrispondenti all'ossigeno si ha <sup>(3)</sup>: per il p-benzochinondimetano 0.974, per l'1-4naftochinondimetano 0.942, per l'antrachinondimetano 0.912, in accordo colle reattività sperimentali  $I > II > III$ . Per le posizioni negli anelli aventi indice maggiore si ha invece rispettivamente: 0.462, 0.467 (pos. o-), 0.438 (pos. α-), valori molto minori dei precedenti e che predicono un ordine di reattività  $II \geq I > III$  in disaccordo coll'esperienza.

Una maggiore sicurezza ci verrà dall'applicazione del secondo criterio.

La Tabella mostra i valori, per i chinoni considerati, della « energia di pola-

rizzazione a radicale » dei chinondimetani corrispondenti, nel caso che l'attacco avvenga: a) al carbonio corrispondente all'ossigeno, b) al carbonio degli anelli avente il massimo indice di valenza.

TABELLA (\*).

Composti	(a)	(b)
(I) p-benzochinondimetano	1.20 +	2.20 +
(II) 1,4-naftochinondimetano	1.30 ×	2.17 +
(III) antrachinondimetano	1.43 ×	~2.67 +

(\*) I valori delle energie sono espressi, secondo le solite convenzioni, in unità di  $\beta$  e a meno del termine coulombiano.

+ C. A. COULSON: *Trans. Farad. Soc.*, **47**, 553 (1951).

× Calcolati dai valori di indice di legame riportati da A. PULLMAN e B. PULLMAN [*Les théories électroniques de la Chimie Organique* (Paris), p. 605] e dalle energie dei radicali date da J. SYRKEN e M. DIATKINA [*Acta Physicochim. URSS*, **21**, 641 (1946)].

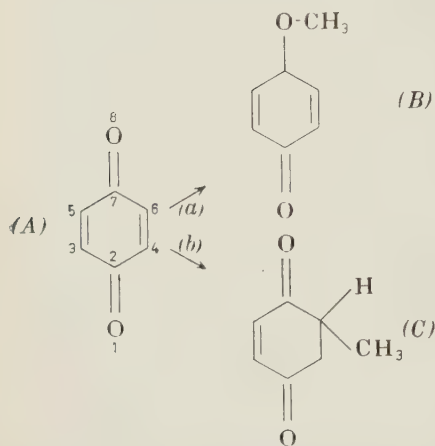
+ Calcolati durante il presente lavoro. L'energia totale  $\pi$  per il radicale derivante dall'attacco di tipo (b) su III è stata valutata approssimativamente, ma è certamente corretta entro i limiti necessari alle nostre conclusioni.

Anche qui i risultati mostrano inequivocabilmente maggiore reattività delle posizioni (a) rispetto alle (b) e predicono correttamente l'ordine di reattività ( $I > II > III$ ) per (a) e non per (b) che risulta invece  $II \geq I > III$  in accordo con quanto indicato dagli indici di valenza.

Possiamo ora mostrare che questa risposta non viene essenzialmente cambiata se si considera la perturbazione portata alla struttura elettronica dei chinondimetani dalla sostituzione degli ossigeni al posto dei gruppi  $\text{CH}_2$ .

(<sup>3</sup>) A. PULLMAN e B. PULLMAN: *Les Théories Électroniques de la Chimie Organique* (Paris, 1952), p. 604-5.

Basterà esemplificare sul p-benzo-chinone:



Si può usare il metodo introdotto da COULSON e LONGUET-HIGGINS che ho già descritto nei suoi particolari in una precedente nota (<sup>4</sup>). Indichiamo con  $A^+$ ,  $B^+$  e  $C^+$  i rispettivi composti non perturbati e con  $\delta\alpha$  e  $\delta\beta$  le perturbazioni coulombiana e di scambio dovute all'introduzione degli ossigeni. La perturbazione più importante, dovuta a  $\delta\alpha$ , (del tipo  $\sum q_i \delta\alpha$ ), agisce nello stesso modo su  $A^+$ ,  $B^+$  e  $C^+$  dato che le  $q_i$  sono tutte unitarie (\*), e quindi non altera le energie di polarizzazione; la perturbazione  $\delta\beta$  (che è al più dell'ordine  $0.5\beta < 0$  per l'ossigeno, ma in genere si può considerare minore se non addirittura trascu-

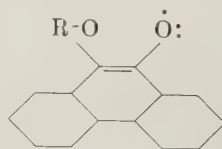
rare) è del tipo  $2\sum p_{rs}\delta\beta$ . Le energie di polarizzazione vengono così modificate:

$$(E_B - E_A) = (E_{B^+} - E_{A^+}) + (4p_{1,2}^{A^+} - 2p_{1,2}^{B^+})\delta\beta$$

$$(E_C - E_A) = (E_{C^+} - E_{A^+}) + (4p_{1,2}^{A^+} - 2p_{1,2}^{C^+} - 2p_{7,8}^{C^+})\delta\beta$$

con ovvio significato dei simboli. Ora, con buona approssimazione, possiamo porre  $p_{1,2}^{B^+} \approx p_{1,2}^{C^+}$ , per cui l'energia di polarizzazione ( $E_C - E_A$ ) viene diminuita all'incirca di  $|2p_{7,8}^{C^+}\delta\beta|$  in più rispetto a ( $E_B - E_A$ ). Inoltre  $p_{7,8}$  è dell'ordine di 0.8 qualunque sia la struttura del composto, dato che si tratta di un legame terminale. Quindi prendendo per  $\delta\beta$  il valore limite di  $0.5\beta$ , pur avendosi uno spostamento dell'energia di polarizzazione di  $\sim 0.8\beta$  a favore di C, questo non sarà tale da invertire il senso preferenziale di attacco stabilito dalla Tabella che è in tutti i casi favorevole a B per valori maggiori di  $0.8\beta$ .

È interessante notare, a supplemento delle nostre conclusioni, che nel caso del fenantrenchinone sono stati isolati composti stabili di somma con radicali alchilici aventi la struttura (<sup>5</sup>):



(<sup>4</sup>) G. GIACOMETTI: *Rend. Accad. Lincei*, VIII, 17, 379 (1954).

(\*) Va considerato naturalmente, nel computo della perturbazione coulombiana, anche il legame semplice  $O-CH_3$  di (B), benché non faccia parte del sistema coniugato.

(<sup>5</sup>) P. KARRER: *Trattato di Chimica Organica* (Firenze, 1942), p. 673.

Interactions of  $K^-$  Particles.

A. J. HERZ, R. M. MAY, J. H. NOON, B. J. O'BRIEN and N. SOLNTSEFF

The F.B.S. Falkiner Nuclear Research and Adolph Basser Computing Laboratories.  
School of Physics (\*), The University of Sydney - Sydney, N.S.W., Australia

(ricevuto il 29 Aprile 1956)

In a recent publication <sup>(1)</sup> we gave report on the interactions in flight of data on the interactions of  $K^-$  particles  $K^-$  particles found by systematic scanning which had come to rest in nuclear-

TABLE I.

	Frequency (%) or Ratio				
	Observed  (%)	Calculated for $\Lambda^0/\Sigma =$			
		1	3	10	20
Emitted Particle	$\pi^-$	10 to 20	23	24	25
	$\pi^+$	0 to 6	4.2	2.0	0.8
Ratio of Emission Frequencies $\pi^-/\pi^+$	$> 1.6$	5.5	12	31	62
	(GEORGE <i>et al.</i> <sup>(1)</sup> ) $< \sim 7$ (GOLDHABER <i>et al.</i> <sup>(2)</sup> )				

research emulsion. In this letter we give some further discussion, and we also

In our work on interactions at rest we found that only about two to four percent of the events showed the emission of charged hyperons, and on this

(\*) Also supported by the Nuclear Research Foundation within the University of Sydney.  
<sup>(1)</sup> E. P. GEORGE, A. J. HERZ, J. H. NOON and N. SOLNTSEFF: *Nuovo Cimento*, **3**, 94 (1956).

<sup>(2)</sup> G. GOLDHABER: Private communication (1955).

fact we based the conclusion that in the reaction



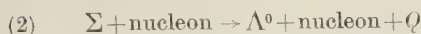
the branching ratio  $\Lambda^0/\Sigma$  for the production of  $\Lambda^0$  and  $\Sigma$  hyperons must lie some-

where between 1 and 10. However, in our argument we overlooked the possibility that  $\Sigma$  hyperons can be converted into  $\Lambda^0$  hyperons if they collide with a nucleon inside the parent nucleus (this was pointed out to us by R. GATTO).

TABLE II.

No.	$p\beta$ at star (MeV)	K.E. at star (MeV)	Event type	Identity and K.E. (MeV)	Remarks
1	115	60	$2+0_K$	p: 9 p: 8  17	
2	120	65	$4+0_K$	p: 6 p: 9 p: 58 p: 11  84	
3	120	65	$1+1_K$	p: 36 ? $\pi$ : 150  186	Total visible energy release including $\pi$ mass > 320 MeV
4	103	55	$5+0_K$	p: 7 p: 39 p: 5 p: 5 p: 8  64	
5	80	41	$2+0_K$	p: 44 p: 12 56	
6	78	48	$3+0_K$	p: 6 p: 17 p: 31  54	

The reaction involved is



and it is a fast reaction according to the Gell-Mann scheme, subject, of course, to the requirement of charge conservation. Owing to this possibility, the number of  $\Sigma$  hyperons observed to be emitted is probably less than the number produced in the primary reaction.

Because of the uncertainties in making allowances for the internal conversion of  $\Sigma$  hyperons and for the internal absorption of both  $\Lambda^0$  and  $\Sigma$  particles, it seems preferable to use the observed  $\pi^-/\pi^+$  ratio as an indicator of the ratio  $\Lambda^0/\Sigma$  in the basic reaction, for this ratio is fairly independent of secondary processes occurring in the parent nucleus. Our own data are given in Table I (taken from GEORGE *et al.*, 1956 <sup>(1)</sup>), and experimental data on the  $\pi^-/\pi^+$  ratio given by other workers (e.g. GOLDHABER <sup>(2)</sup>) are roughly similar. Although the statistics are not satisfactory because of the large number of  $\pi$  mesons whose charge could be of either sign, they favour a basic  $\Lambda^0/\Sigma$  ratio of the order of unity. The low observed frequency of emission of hyperons must then be due to internal collisions of the particles with nucleons in which they are converted according to reaction (2) or absorbed.

During part of our work we paid particular attention to interactions in flight. Six such events were found during this period, and we derive a mean free path of  $(16.3^{+10.1}_{-6.1})$  cm in nuclear research emulsion, consistent with a geo-

metric interaction cross-section. This figure is an average for the kinetic-energy range zero to 135 MeV, and all star-type events are included, but single scatters are not.

Details of the interacting particles and of the events produced are given in Table II; the total observed path length of these  $K^-$  particles is 17.3 cm. At the same time, 13  $K^-$  particles with a total path length of 57.3 cm were observed to come to rest and give rise to  $\sigma K$  stars. Particles coming to rest without visible decay or interaction ( $QK$  events) were not included in the statistics: instead we assumed that  $QK$  events constitute 29 % of all  $K^-$  absorptions at rest <sup>(1)</sup>, and corrected the observed path length accordingly.

It is of interest to note that the visible energy release in all but one of the events reported here is greater than the kinetic energy of the incident  $K^-$  particle. This shows that the  $K^-$  particle is absorbed in the majority of cases. On the other hand, the visible energy release is quite small compared with the rest mass of the  $K^-$  meson, and this suggests that in the energy range considered (0 to 135 MeV) the basic reaction is the same as for interactions at rest (equation (1)).

\* \* \*

We would like to acknowledge the contribution of Dr. E. P. GEORGE to the preliminary stages of the work reported in this letter. Thanks are due to Prof. H. MESSEL for arranging the excellent facilities and financial support.



# The Strength of Field Equations.

F. E. MAUGER

*King's College - London*

(ricevuta il 29 Aprile 1956)

In a note on the strength of field equations <sup>(1)</sup> Einstein's number  $D_n$  was used when evaluating the strengths of certain covariant systems. Since then HLAVATY has pointed out that this number must be incorrect since  $D_n$ , where

$$D_n = 4 \binom{4}{n} + 3 \binom{3}{n} + 2 \binom{2}{n} + 1 ,$$

gives, for  $n = 1$ , the number 30. This should equal the number of restrictions that may be applied to the first derivatives of the metric tensor  $g_{\mu\nu}$  at a point by a suitable coordinate transformation. However it is well known that all forty first derivatives can be made to vanish at a point.

To obtain the correct number we consider the general transformation of the non-symmetric tensor  $g_{\mu\nu}$  in the form

$$(1) \quad g'_{\mu\nu} = \frac{\partial x^\alpha}{\partial x'^\mu} \frac{\partial x^\beta}{\partial x'^\nu} g_{\alpha\beta} ,$$

together with the co-ordinate transformation

$$(2) \quad x^\varepsilon = a_\sigma^\varepsilon x'^\sigma ,$$

where  $a_\sigma^\varepsilon$  is a function of the co-ordinates. Equation (1) becomes, with this transformation

$$g'_{\mu\nu} = a_\mu^\alpha a_\nu^\beta g_{\alpha\beta} ,$$

so that sixteen conditions may be applied to the sixteen components of  $g_{\mu\nu}$  since there are sixteen components of  $a_\sigma^\varepsilon$ . Now we consider the transformation of the

<sup>(1)</sup> F. E. MAUGER: *Nuovo Cimento*, **2**, 330 (1955).

first derivatives in the form

$$(3) \quad \frac{\partial g'_{\mu\nu}}{\partial x'^{\sigma}} = \frac{\partial x^{\alpha}}{\partial x'^{\mu}} \frac{\partial x^{\beta}}{\partial x'^{\nu}} \frac{\partial x'^{\gamma}}{\partial x'^{\sigma}} \frac{\partial g_{\alpha\beta}}{\partial x'^{\gamma}} + \frac{\partial x^{\alpha}}{\partial x'^{\mu}} \frac{\partial^2 x^{\beta}}{\partial x'^{\nu} \partial x'^{\sigma}} g_{\alpha\beta} + \frac{\partial x^{\beta}}{\partial x'^{\nu}} \frac{\partial^2 x^{\alpha}}{\partial x'^{\sigma} \partial x'^{\mu}} g_{\alpha\beta},$$

and the transformation

$$(4) \quad x^{\varepsilon} = x'^{\varepsilon} + \frac{1}{2} a_{\mu\nu}^{\varepsilon} x'^{\mu} x'^{\nu}.$$

At the origin

$$\frac{\partial x^{\varepsilon}}{\partial x'^{\mu}} = \delta_{\mu}^{\varepsilon}, \quad \text{and} \quad \frac{\partial^2 x^{\varepsilon}}{\partial x'^{\mu} \partial x'^{\nu}} = a_{\mu\nu}^{\varepsilon}.$$

The transformation (4) leaves the sixteen undifferentiated components as they were and only alters the first derivatives. Thus we have at the origin the transformation

$$\frac{\partial g'_{\mu\nu}}{\partial x'^{\sigma}} = \frac{\partial g_{\mu\nu}}{\partial x^{\sigma}} + a_{\sigma\mu}^{\alpha} g_{\alpha\nu} + a_{\sigma\nu}^{\beta} g_{\beta\mu}.$$

Here there are forty arbitrary coefficients so we may make forty of the first derivatives vanish at a point. Similarly at the second stage we may use the transformation

$$x''^{\varepsilon} = x'^{\varepsilon} + \frac{1}{3!} a_{\mu\nu\sigma}^{\varepsilon} x'^{\mu} x'^{\nu} x'^{\sigma}.$$

This leaves the terms of order zero and one as they were and alters the second derivatives. Here we have eighty coefficients and one hundred and sixty second derivatives.

More generally, at the  $n$ -th stage there are  $16 \binom{4}{n}$  coefficients and  $4 \binom{4}{n+1}$  co-ordinate restrictions may be applied. Thus Einstein's number  $D_n$  is changed to  $B_n$  where

$$B_n = 4 \binom{4}{n+1}.$$

This change in the number of possible restrictions that may be applied at a point has the effect of increasing the apparent strength of covariant systems of field equations, measured with  $D_n$ , by a value  $\binom{4}{n} \frac{3}{n}$  for large  $n$ . Thus the strength of one set of Einstein's field equations and the strength of Stevenson's set, both determined using  $D_n$  in the paper previously mentioned, become  $\binom{n}{4} \frac{42}{n}$  and  $\binom{n}{4} \frac{48}{n}$  respectively.

## LIBRI RICEVUTI E RECENSIONI

PIERRE GRIVET - *La résonance paramagnétique nucléaire* - Editò dal Centre National de la Recherche Scientifique, Paris 1955 - 297 pagine, 140 figure.

Si tratta di un'opera redatta sotto la direzione di P. GRIVET da gruppi francesi e svizzeri che si sono dedicati alle risonanze magnetiche nucleari. Gli autori sono: R. GABILLARD, Y. AYANT, M. SOUTIF, J. C. EXTERMANN, M. BUYLEBODIN, G. B. BÉNÉ, P. M. DENIS.

Dopo una breve presentazione di C. J. GORTER e una introduzione di GRIVET i due primi capitoli espongono in maniera chiara e abbastanza approfondita le teorie fondamentali sulla risonanza magnetica nucleare, e cioè la teoria macroscopica e la teoria quantistica. Buona parte del libro è quindi dedicata alla descrizione particolareggiata di alcuni metodi e dispositivi sperimentali per la osservazione e lo studio del fenomeno: dispositivi originali di Bloch e Purcell, e alcune varianti, metodo di Torrey, metodo degli echi, altri dispositivi.

Il penultimo dispositivo tratta delle risonanze quadrupolari e l'ultimo è una esposizione critica delle diverse teorie proposte per spiegare le regolarità osservate nella distribuzione dei momenti nucleari nella tavola periodica degli elementi.

Il libro non è, e non ha probabilmente la pretesa di essere, una rassegna completa. Accanto agli argomenti fondamentali vengono poste in rilievo questioni particolari di cui si sono occupati alcuni degli autori. Fra queste i «pre-

battimenti» e i battimenti modulati, che vengono presentati, forse un po' ottimisticamente, come fenomeni capaci di fornire indicazioni abbastanza precise sul tempo di rilassamento trasversale.

Altre questioni di notevole interesse, come la struttura delle righe di risonanza nei cristalli, gli spostamenti della frequenza di risonanza dovuti allo schermaggio elettronico e a effetti chimici sono poco più che accennate.

Anche se non fornisce un quadro completo ed equilibrato dello stato attuale delle ricerche nel campo delle risonanze magnetiche nucleari, il libro ha tuttavia pregi notevoli. I vari argomenti sono per lo più ben rielaborati e ben presentati. I numerosi particolari tecnici possono interessare vivamente chi lavora sperimentalmente in questo campo.

Notevole una tabella che raccoglie dati ottenuti da vari autori sugli spin, i momenti magnetici e i momenti elettrici quadrupolari dei nuclei.

L. GIULOTTO

A. VON ENGEL - *Ionized gases*; pagine x + 277, Oxford University Press, London 1955.

L'argomento del volume è di notevole interesse in quanto, come sottolinea l'Autore nella prefazione, la comprensione di molti problemi in vari campi della fisica, anche più avanzata, sono basati sulla chiara conoscenza della complessa fenomenologia della conduzione in un gas

ionizzato. Il volume espone e studia questa fenomenologia da un punto di vista sostanzialmente pratico, nel senso che cerca di dare nella descrizione dei fenomeni un panorama principalmente interpretativo, richiamando od illustrando i principi fondamentali coinvolti in un determinato processo, e rimandando alla bibliografia, e qualche volta all'Appendice, per maggiori dettagli teorici che giustifichino rigorosamente le leggi esposte.

La visione generale così offerta dall'Autore permette che la lettura del libro possa essere proficua per tutte le persone che abbiano interesse all'argomento anche con una cultura non eccessivamente specializzata, in quanto i concetti esposti e la metodologia di calcolo usata sono acquisiti già da uno studente del III anno di una Facoltà scientifica. D'altra parte la vasta bibliografia, molto aggiornata, può tornar utile, oltrechè a coloro che desiderano approfondire qualche argomento particolare, anche a ricercatori in questo campo. Il carattere introduttivo e pratico del volume è accentuato dall'abbondanza dei grafici, tabelle numeriche, esempi, nonchè dalla succinta descrizione delle modalità di misura di numerose delle grandezze fondamentali in gioco nella fenomenologia descritta, cose che permettono anche al lettore non versato nel campo in questione di formarsi facilmente delle idee sull'andamento quantitativo dei fenomeni descritti.

L'Autore, dopo un primo capitolo in cui espone la cronologia delle varie tappe della ricerca nel campo della conduzione dei gas ionizzati, ed un secondo in cui dà un panorama generale, si addentra nell'analisi del complesso dei fenomeni coinvolti nel processo della conduzione. Il terzo capitolo è dedicato all'esposizione delle numerose cause di produzione di particelle cariche, mentre i quattro capitoli successivi prendono in esame il comportamento e le interazioni delle particelle cariche esistenti in un ambiente

gassoso. Gli ultimi tre capitoli sono dedicati alla ionizzazione in campo elettrico, alla scarica a bagliore e a quella ad arco. Il campo dei fenomeni trattati è molto vasto e la lettura del volume può essere di utilità a coloro che si occupano anche delle questioni tecniche più avanzate e diverse, dalle camere a ionizzazione agli spettrometri di massa, dai contatori di particelle alla microscopia elettronica.

M. CHIOZZOTTO

MAURICE DUMAS — *Les épreuves sur échantillon*, C.N.R.S., Paris, 1955.

Col crescente affermarsi e diffondersi dei procedimenti statistici di prove su campioni, in particolare per collaudi di accettazione e per il controllo continuativo delle produzioni in serie, è sempre più sentita la necessità di trattazioni che spieghino in modo semplice e pratico le tecniche da applicare e i calcoli da eseguire per rispondere ai quesiti più frequenti nelle condizioni più usuali.

A tali finalità risponde — tra altri — il volumetto di M. DUMAS, recentemente apparso nella collana di monografie del Centre d'Études Mathématiques en vue des applications » del C.N.R.S., e precisamente nella sezione A (Application des théories mathématiques) iniziata col « Calcul des Probabilités » di R. FORTET. I riferimenti a tale opera, che fa larga parte ai fondamenti teorici dei metodi descritti nel volumetto di cui si parla, e quelli ad altre esposizioni più esaurienti dello stesso DUMAS, di DUMAS-MAHEU e di MOTHES, giovano a rendere meno sensibili, o almeno più facilmente rimediabili, le inevitabili manchevolezze di una esposizione in cui le questioni concettuali, pur non potendosi del tutto ignorare, non possono trovare adeguato chiarimento.

Molto indovinata, ai fini di facilitare

la ricerca di quello che serve caso per caso fra i numerosi metodi descritti, appare la disposizione della materia, consistente nel considerare quattro problemi tipici (1°, della stima; 2°, dei col laudi di accettazione; 3°, dei confronti; 4°, del controllo statistico della produzione), trattandone dapprima in generale, nel Cap. II, e poi riprendendoli ordinatamente e dettagliatamente con riferimento a prove qualitative (risposta *si* o *no*, o « bianco »-« nero ») nel Cap. III, e a prove quantitative (risposta data da misure) in cui si tratti di accertare la dispersione (ossia la costanza delle misure) nel Cap. IV-1, oppure la dispersione ed insieme la media, nel Cap. IV-2. Precedono e seguono succinte indicazioni teoriche e pratiche, fra cui un utile repertorio contenente, per le principali regole, non solo i riferimenti alla trattazione ma anche un cenno brevissimo sull'impostazione e i risultati.

Peccato che alcuni riferimenti risultino errati (ad esempio, nel n. 136 i rinvii ai nn. 213 e 223 vanno corretti in 313 e 323; in diversi altri casi non ho trovato come l'indicazione andrebbe corretta; forse vi è stato un rimaneggiamento di numerazioni dopo la stesura?).

Quanto alle note questioni controverse riguardanti la concezione e l'impostazione teorica dei problemi, l'A. riferisce imparzialmente sui vari punti di vista non trascurando però, ove occorra, sia pur di sfuggita, di chiarire le diversità di significato e valore fra i metodi che rifuggono dalla considerazione di una probabilità iniziale (o « a priori ») e non consentono pertanto alcuna conclusione sulla probabilità finale (o « a posteriori »), e quelli invece in cui tale considerazione interviene, nel senso classico, od in quello di una « legge virtuale » (o degenerare) (concetto questo che costituisce il più personale apporto del DUMAS (1937) allo studio teorico di tali problemi).

B. DE FINETTI

D. HALLIDAY - *Introductory Nuclear Physics*. II Edizione, 1955. Un volume in-8° di 493 pagine. John Wiley & Sons, Inc., New York; Chapman & Hall, Limited, London.

Questo libro di Halliday, ora alla seconda edizione, ha lo scopo di presentare i capitoli più importanti della Fisica Nucleare in una rassegna per quanto possibile organica. Fin dalla prima pagina infatti l'A. avverte che per ora le nostre conoscenze nel campo della Fisica Nucleare sono da considerarsi come delle isole smarrite in un mare di fatti debolmente correlati tra di loro.

Nei primi capitoli vengono introdotti i concetti base necessari alla comprensione sia fenomenologica che quantitativa degli argomenti svolti nelle parti successive. Gli sviluppi matematici più laboriosi sono rimandati alle appendici. Vengono poi presentati una serie di argomenti, come il passaggio delle particelle cariche e dei quanti gamma nella materia, loro rivelazione, la fisica dei neutroni ecc. In questi capitoli, a nostro avviso, non sempre risulta soddisfacente lo sforzo di sintesi compiuto dall'A.; egli infatti è costretto dalle esigenze di spazio, a condensare in poche pagine accanto alla descrizione minuziosa delle tecniche sperimentali, anche la interpretazione teorica dei fatti osservati. Ciò induce il lettore inesperto a sottovalutare, in qualche caso, il peso concettuale di taluni sviluppi teorici.

Non manca un capitolo, invero molto condensato, sulle macchine acceleratrici di particelle cariche. Il volume si chiude con un capitolo sui Raggi Cosmici nel quale si fa cenno anche alle particelle subnucleari di recente scoperte: mesoni pesanti ed iperoni.

È difficile giudicare quale grado di cultura specifica sia necessaria alla comprensione di questo libro. Certamente esso risulterebbe poco comprensibile a



studenti che non avessero compiuto almeno il primo biennio universitario di studi matematici e fisici. Dubitiamo per altro che esso possa riuscire utile a lettori che non abbiano già una certa preparazione sugli argomenti trattati. Viceversa sembra che questo libro, specie negli Stati Uniti, sia considerato come una ottima introduzione didattica allo studio della Fisica nucleare. Ciò ci conduce a pensare alla diversa impostazione didattica delle Facoltà Scientifiche Americane rispetto alle nostre, dove si tende a dare agli studi un carattere prevalentemente formativo e molto meno sintetico o informativo.

I. F. QUERCIA

D. J. LITTLER, J. F. RAFFLE - *An Introduction to Reactor Physics* (x + 196 pagg., Pergamon Press, London, 1955), 25 s.

Questo volumetto, pubblicato dalla Pergamon Press per la U.K. Atomic Energy Authority, condensa in circa 200 pagine le nozioni essenziali della fisica dei reattori. Esso non presuppone nel lettore alcuna preparazione specifica nel campo della fisica nucleare, ma solo quei fondamenti generali di cultura scientifica, che sono comuni a fisici sperimentali e ad ingegneri di ogni ramo ed anche agli studenti universitari degli ultimi anni di tali corsi di laurea. È quindi effettivamente destinato ad essere usato come manuale per una prima introduzione sull'argomento.

I primi cinque capitoli (48 pagine) riassumono (partendo dagli atomi democratici e da Dalton) quelle nozioni di fisica nucleare che gli Autori ritengono indispensabili per una comprensione della struttura e del funzionamento dei reattori. Sarebbe troppo pretendere che questa breve premessa fosse qualcosa di più di uno schematico elenco di risultati.

È anzi nostra impressione che un lettore effettivamente digiuno di fisica nucleare possa servirsene solo come guida per studiare i vari argomenti su trattati più estesi, indicati del resto alla fine di ciascun capitolo.

La parte centrale del libro, costituita dai capitoli dal sesto al tredicesimo (98 pagine), è dedicata ai fondamenti della teoria dei reattori. Dopo un capitolo sulle reazioni a catena ed uno sulla diffusione dei neutroni, gli Autori espongono i metodi usati per calcolare le dimensioni critiche in un reattore ad uranio naturale e grafite, raffreddato a gas. Due capitoli sono poi dedicati alla cinetica del reattore e ai fenomeni associati al funzionamento di regime di quest'ultimo. Il sedicesimo capitolo è dedicato alle interazioni delle radiazioni con la materia e alla schermatura biologica dei reattori.

L'ultima parte del libro (35 pagine) è costituita da tre capitoletti che trattano rispettivamente dei rivelatori di radiazioni, delle alterazioni prodotte dall'irraggiamento sulla materia, delle misure di distanza di diffusione e delle esperienze esponenziali. Seguono tre brevi appendici, una delle quali sui danni biologici dell'irraggiamento e relative dosi di sicurezza.

Caratteristica di questo volume è la notevole concisione e la continua aderenza allo scopo che gli Autori si sono proposti, quello di mostrare al lettore come si giunga al calcolo di un reattore del tipo considerato. Questa concisione, a volte forse eccessiva, è indubbiamente un pregio per il lettore che ha già una certa familiarità coi metodi della fisica matematica e coi concetti fondamentali della fisica dei neutroni; può, viceversa, offrire talora ostacoli non indifferenti al lettore non iniziato non per mancanza di chiarezza nell'esposizione, ma per ciò che il libro non dice, in quanto non strettamente necessario allo scopo. In altre parole, il lettore che pensa col suo cer-

vello potrà usare con molto vantaggio questo bel volumetto, ma dovrà spesso andare a cercare la risposta agli interrogativi che gli si presentano in volumi più estesi.

M. AGENO

E. BAUER — *Champs de vecteurs et de tenseurs. Introduction à l'électromagnétisme*. Masson et C<sup>ie</sup>, Editeurs, Paris, 1955, pagg. VII+204.

Il volume è dedicato al calcolo vettoriale e tensoriale e ne comprende anche le principali applicazioni in fisica classica. Il capitolo primo tratta i vettori e i tensori, le operazioni su di essi e comprende alcune applicazioni elementari alla elasticità, alla cinematica, ed alla cristallografia. Il capitolo secondo tratta i campi di vettori e di tensori ed i vari teoremi di Gauss, di Stokes etc. L'autore fa uso contemporaneamente della notazione sintetica e di quella analitica. Il capitolo successivo comprende lo studio dei campi newtoniani (rotore nullo) e dei campi laplaciani (divergenza nulla). Nel capitolo quarto, più astratto, viene sviluppata la teoria dei tensori e dei campi di tensori in uno spazio qualunque. Il capitolo quinto dà le applicazioni al campo elettromagnetico, contiene dei cenni di relatività ristretta, e due note sono dedicate una alla interpretazione del magnetismo, l'altra alla equazione dei potenziali.

I vari argomenti sono svolti in forma corretta e con chiarezza. Si nota una certa sproporzione tra la preparazione matematica minuta e piuttosto avanzata e la limitatezza delle questioni fisiche trattate. Malgrado il sufficiente svolgimento del calcolo differenziale assoluto il volume non comprende alcun elemento di relatività generale. L'elettromagnetismo è svolto in modo assiomatico, cercando di ridurre all'essenziale le leggi fondamentali e descrivendone pochissime

esperienze: presentazione che può essere corretta per un fisico matematico, ma che risulta certamente pericolosa per un fisico cui continueremo a consigliare per la sua preparazione i volumi del Becker.

In conclusione possiamo dire che è certamente un pregio del volume quello di esporre i metodi del calcolo vettoriale e tensoriale accompagnandoli da illustrazioni fisiche e, per chi avesse da apprendere tali metodi, il libro è senz'altro consigliabile.

R. GATTO

CARLO MIRANDA — *Equazioni alle derivate parziali di tipo ellittico*. Springer-Verlag, Berlin-Göttingen-Heidelberg, pagg. VIII-222, 1955, DM. 28.80.

L'Autore dà una organica esposizione dei risultati attualmente noti nel campo delle equazioni differenziali a derivate parziali di tipo ellittico. Non è quindi facile accennare a tutte le questioni trattate, che vanno dalla teoria dei potenziali e dai classici problemi di Dirichlet, di Neumann, di derivata obliqua ai problemi misti, allo studio delle equazioni di ordine superiore al secondo e dei sistemi di equazioni, alle ricerche relative all'analiticità delle soluzioni di equazioni di tipo ellittico lineari o non lineari, alla esistenza e alla distribuzione degli autovalori per equazioni dipendenti da un parametro ecc. Non mancano cenni a questioni collaterali, quali il collegamento con la teoria delle funzioni di variabile complessa o ipercomplessa o con i problemi variazionali.

Accanto a questo ampio quadro di risultati c'è una rapida esposizione dei metodi più usati, che l'Autore svolge nel caso dei problemi di Dirichlet, Neumann e della derivata obliqua relativi ad una sola equazione di secondo ordine, limitandosi a dare qualche accenno alle ulteriori estensioni.

Sono esposti in particolare: il metodo di Giraud per la traduzione dei problemi al contorno in equazioni integrali di seconda specie; i metodi di analisi funzionale lineare introdotti da CACCIOPOLI, PICONE, WEYL (la cui esposizione è preceduta da una accurata discussione del concetto di soluzione generalizzata); i metodi di topologia funzionale, fondati su formule di maggiorazione a priori, dovuti a BERNSTEIN, HOFF, SCHAUDER, LÉRAY, CACCIOPOLI (di cui si mostra l'utilità anche nel campo delle equazioni non lineari). Per il metodo di minimo invece si rimanda alla classica trattazione di Courant-Hilbert, mentre per quello della « Kernel-Function » si rinvia alla monografia di BERGMANN e SCHIFFER.

L'opera è scritta in uno stile molto conciso che ha permesso di condensare un contenuto così vasto in meno di duecento pagine, senza rinunciare al rigore ed alla chiarezza dell'esposizione; ricchissima ed aggiornata la bibliografia comprendente oltre seicento lavori, nitida ed estremamente curata la veste tipografica.

E. DE GIORGI

L. BRILLOUIN e M. PARODI — *Propagation des ondes dans les milieux périodiques*. Masson et C<sup>ie</sup> e Dunod Editeurs, Paris, 1956, p. 347.

Questo volume di Brillouin e Parodi è in sostanza il rifacimento con varie aggiunte, del precedente volume di Brillouin *Wave Propagation in Periodic Structures* apparso nel 1946 nella collezione della Mc Graw-Hill. Gli autori si propongono di esporre alcuni principali problemi di origine fisica diversa ma che si risolvono con metodi matematici simili. Questi problemi riguardano la propagazione di onde (elastiche, elettromagnetiche, elettroniche) in diversi mezzi a struttura periodica e conducono ad equazioni analoghe.

Il primo capitolo è una introduzione storica alla propagazione delle onde ela-

stiche in un reticolo a una dimensione. I primi risultati furono infatti dovuti a Newton, Eulero, Daniele Bernoulli e Lagrange. I successivi tre capitoli comprendono la discussione dei reticoli a una dimensione. Viene dapprima discussa la natura della dipendenza della frequenza dal numero di onde per un tale reticolo: questo già illustra il concetto di « zona » che tanta importanza riveste nel caso pluridimensionale. Il più semplice esempio trattato è quello di un reticolo di particelle identiche, che serve ad illustrare la nozione di frequenza di taglio. Inoltre il confronto dei risultati con quelli di un filtro elettrico passabasso permette di formulare in termini generali la corrispondenza tra i filtri meccanici e i filtri elettrici. Altre analogie acustiche e magnetiche vengono anche accennate. Un esempio è il reticolo di cloruro di sodio ad una dimensione il cui studio semplificato mostra già l'esistenza di due branche per la dipendenza della frequenza dal numero di onde (branca acustica e branca ottica) e, quindi, di due bande passanti e due di arresto. Anche per questo caso viene discusso il corrispondente elettrico ed illustrata l'analogia. Viene anche illustrato in generale il caso di reticoli di molecole poliatomiche. Il quinto capitolo contiene una digressione sui concetti di velocità di propagazione dell'energia in una struttura reticolare, di flusso di energia, e sull'importante concetto di impedenza caratteristica. Il capitolo successivo è dedicato ai problemi ai limiti ed alle strutture periodiche finite. Una introduzione matematica tratta dei polinomi di Gegenbauer, che vengono presentati come una generalizzazione dei polinomi di Legendre. Con il loro ausilio viene trattato il calcolo delle frequenze proprie in particolari reticoli limitati i cui analoghi elettrici sono molto conosciuti. La nozione di filtro viene ritrovata come particolare caso limite di tali reticoli in cui si faccia aumentare indefinitamente il numero delle cellule. Gli esempi meccanici illustrati non sono del tutto

accademici, ma in alcuni casi sono stati impiegati per spiegare il comportamento di certi composti aciclici formati da lunghe catene di radicali  $\text{CH}_3$  e  $\text{CH}_2$ . Il capitolo settimo tratta i reticoli a due dimensioni. Dopo una introduzione sulle nozioni di reticolo diretto e reticolo reciproco ed una digressione sulle funzioni periodiche di più variabili viene mostrato come lo studio della dipendenza della frequenza dal vettore d'onda porta ad introdurre il concetto di zona, ed il problema della costruzione effettiva delle zone di vario ordine nel reticolo reciproco viene trattato in tutti i dettagli. Viene quindi affrontato il problema della propagazione delle onde nel reticolo, supposto illimitato o, nel caso sia limitato, sostituito con uno ciclico. La trattazione viene svolta in approssimazione perturbativa e porta a ritrovare la presenza di una onda riflessa di grande ampiezza nel caso in cui siano soddisfatte le condizioni di Bragg. Il caso fisicamente importante dei reticoli a tre dimensioni è svolto nel capitolo ottavo su linee analoghe al caso a due dimensioni. Viene riportata l'interpretazione di Ewald nel reticolo reciproco della condizione di Bragg, viene svolta la teoria della propagazione delle onde nel reticolo, vengono studiate le principali strutture e le loro zone ed accennato al metodo di Wigner-Seitz. Il resto del capitolo tratta il problema della distribuzione delle frequenze in un cristallo reale e la termodinamica del cristallo (alla Debye ma con le due temperature caratteristiche). Il capitolo successivo tratta della equazione di Mathieu e della sua generalizzazione di Hill: viene illustrato l'esempio di un oscillatore con eccitazione parametrica (gli autori usano il termine « oscillatore autoeccitato » che di solito però viene usato a designare casi non lineari del tutto diversi). I tre capitoli successivi sono dedicati alla propagazione delle onde lungo le linee elettriche ed allo studio dei filtri elettrici. La descrizione matematica dei quadrupoli usa l'algebra delle matrici cosiddette di qua-

drupolo. Vengono ritrovati i concetti fondamentali di quadrupolo inverso, di impedenza caratteristica etc., e studiata la propagazione in catene di quadrupoli e i vari tipi di bande. Le linee elettriche continue vengono introdotte come catene di quadrupoli infinitesimi e sono discussi i casi più semplici. Viene poi illustrato l'uso dei polinomi di Gegenbauer nello studio dei filtri elettrici. I restanti due capitoli sono dedicati alle guide per onde lente ed al moto degli elettroni in campi periodici in movimento. La limitazione ad onde lente, cioè con velocità di fase minore di quella della luce è suggerita dalla recente applicazione di onde trasversali magnetiche lente negli acceleratori lineari. Il problema della interazione degli elettroni con l'onda è impostato in termini classici e quantistici e ricondotto ad una equazione di Mathieu.

La varietà degli argomenti trattati, pur avendo tutti una profonda parentela quale si rivela dalla identica natura dei metodi matematici impiegati, la semplicità della esposizione, fanno la lettura di questo libro senz'altro raccomandabile. Le eventuali critiche riguardano al più alcuni punti minori e di dettaglio. Ad esempio la introduzione delle matrici di Pauli nella teoria dei filtri è svolta in maniera quasi forzata ed inessenziale. Inoltre è personale opinione di chi recensisce che l'uso dei polinomi di Gegenbauer nello studio dei reticoli lineari e nello studio dei filtri elettrici non corrisponda a nessuna effettiva esigenza formale: la scelta di opportune variabili angolari permette una trattazione altrettanto semplice. L'esposizione in certi punti poteva essere più concisa, specie nella riproduzione dei passaggi algebrici, e la bibliografia è piuttosto limitata. Tuttavia questi appunti riguardano aspetti non essenziali dell'opera e nulla tolgono ai suoi numerosi pregi.

La lettura di questo libro risulterà molto istruttiva soprattutto a quanti non conoscono il precedente volume di Brillouin sullo stesso soggetto.

R. GATTO



IL NUOVO CIMENTO

---

INDICI  
DEL VOLUME III - SERIE X  
1956

PRINTED IN ITALY





# INDICE SISTEMATICO

## PER NUMERI SUCCESSIVI DEL PERIODICO

N. 1, 1° GENNAIO 1956

Z. Koba - Velocity of the Dirac Electron . . . . .	pag. 1
I. I. SHERIF - The Molecular Heats of Gases from the Aspects of Heat Transfer . . . . .	" 6
E. SILVA and J. GOLDBERG - Photodisintegration of Samarium . . . . .	" 12
V. DE SABBATA and A. SUGIE - A Collective Model for the Nuclear-Photo-Reactions . . . . .	" 16
A. BONETTI, R. LEVI SETTI, M. PANETTI, G. ROSSI e G. TOMASINI - Lo spettro di energia degli elettroni di decadimento dei mesoni $\mu$ in emulsione nucleare . . . . .	" 33
B. CHINAGLIA and F. DEMICHELIS - Photographic Methods in $\gamma$ -Ray Scintillation Spectroscopy . . . . .	" 51
E. LOHRMANN and M. TEUCHER - Spurious Scattering in Nuclear Emulsions . . . . .	" 59
I. KAY and H. E. MOSES - The Determination of the Scattering Potential from the Spectral Measure Function. - II. Point Eigenvalues and Proper Eigenfunctions . . . . .	" 66
H. H. HECKMAN, F. M. SMITH and W. H. BARKAS - The Masses of Positive K-Particles . . . . .	" 85
E. P. GEORGE, A. J. HERZ, J. H. NOON and N. SOLNTSEFF - Nuclear Interactions of Negative K-Mesons in Nuclear-Research Emulsion . . . . .	" 94
G. R. MACLEOD - Cosmic Ray Showers of Wide Extent . . . . .	" 118
J. RAYSKI - On a Bilocal Interpretation of Isotopic Spin . . . . .	" 126
M. SCHEIN, D. M. HASKIN and R. G. GLASSER - Heavy Unstable Particles Produced in the High Energy Pion Beam of the Berkeley Bevatron . . . . .	" 131
G. BERTOLINO - On Cosmic Rays Jets . . . . .	" 141
F. DEMICHELIS and L. A. RADICATI - $\beta$ - $\gamma$ Angular Correlation of $^{214}_{83}\text{Bi}$ . . . . .	" 152
A. TOMASINI - Excitation of Nuclei by Absorption of $\pi$ -Mesons (III) . . . . .	" 160
G. COSTA and L. TAFFARA - On the Spin and Parity of the $\tau$ -Meson . . . . .	" 169
M. DEUTSCHMANN, M. CRESTI, W. D. B. GREENING, L. GUERRIERO, A. LORIA and G. ZAGO - An Anomalous $V^0$ Event . . . . .	" 180
F. AMMAN and L. DADDA - Design of the Pole Faces for Circular Particle Accelerators with the Electrolytic Tank . . . . .	" 184
C. B. A. McCUSKER and B. G. WILSON - The Rate of Extensive Showers of High Electron Density at Sea Level . . . . .	" 188
M. J. BRINKWORTH and B. ROSE - A Measurement of the Direction of the Polarization Produced in the Scattering of 135 MeV Protons . . . . .	" 195

A. BRACCI, C. COCEVA, L. COLLI and R. DUGNANI LONATI - Experimental Measurements on Double Compton Effect . . . . .	pag. 203
---	----------

*Lettere alla Redazione:*

Z. KOBA - Supplementary Remark on My Previous Note « Velocity of the Dirac Electron » . . . . .	» 214
M. SCHARFF, G. GJELDAKER and S. SØRENSEN - Three Examples of Complete $\tau$ -Decay . . . . .	» 214
S. R. MOHANTY - Energetics of Elimination of Adsorbed Gases from Dielectric Surfaces Under Electrodeless Discharge . . . . .	» 219
P. BOCCHIERI e A. LOINGER - Un'osservazione sulla condizione supplementare dell'elettrodinamica . . . . .	» 221
E. R. CAIANIELLO - Number of Feynman Graphs and Convergence . . . . .	» 223
A. DEBENEDETTI, C. M. GARELLI, L. TALLONE, M. VIGONE and G. WATAGHIN - A High Energy Shower . . . . .	» 226
M. TEUCHER, H. WINZELER and E. LOHRMANN - A Possible Example of Production and Annihilation of an Antiproton . . . . .	» 228
<i>Libri ricevuti e Recensioni</i> . . . . .	» 231

N. 2. 1° FEBBRAIO 1956

T. TAKABAYASI - Hydrodynamical Description of the Dirac Equation . . . . .	pag. 233
T. TAKABAYASI - New Classical Spin Theory as the Limit of the Dirac Equation . . . . .	» 242
S. ALTSHULER - Ingoing Waves in the Final State of Ionization Problems . . . . .	» 246
Y. ORLOV - The Non-linear Theory of Betatron Oscillations in the Strong-Focusing Synchrotron (I) . . . . .	» 252
W. KRÓLIKOWSKI and J. RZEWUSKI - On « Potentials » in the Theory of Quantized Fields . . . . .	» 260
I. KAY and H. E. MOSES - The Determination of the Scattering Potential from the Spectral Measure Function. - III. Calculation of the Scattering Potential from the Scattering Operator for the One-Dimensional Schrödinger Equation . . . . .	» 276
G. DI CAPORIACCO and M. GIOVANNOZZI - Cloud Chamber Study of Cosmic Ray Electronic Showers Under Dense Materials (II) . . . . .	» 305
R. GATTO - Charge Properties of the Weak Decay Interactions of the New Particles . . . . .	» 318
G. DIAMBRINI PALAZZI - A Magnetic Differential Probe. Its Employment for the Determination of the Static Median Magnetic Surface in the Gap of a Synchrotron . . . . .	» 336
I. BARDUCCI - Diffusion Coefficient of N in $\alpha$ -Fe . . . . .	» 350
G. FIDECARO and A. M. WETHERELL - Notes on the Design of Distributed Amplifiers . . . . .	» 359
F. PORRECA - On the Causes Affecting the Phase Grating Permanence, at the Stopping of the Ultrasounds . . . . .	» 371

F. DEMICHELIS, R. A. RICCI and G. TRIVERO - Investigations on the $\beta$ -Decay of $^{208}_{81}\text{Tl}(\text{ThC}'')$ . . . . .	pag. 377
P. SEN - A Simple Non-Local Quantum Electrodynamics . . . . .	» 390
J. M. BLATT and S. T. BUTLER - Some Comments on $K^-$ Interactions at Rest . . . . .	» 409
A. SALAM - On Generalised Dispersion Relations . . . . .	» 424
G. MORPURGO - On the Inelastic Scattering of Electrons from $^{12}\text{C}$ . . . .	» 430
R. S. LIOTTA - Covariant Canonical Equations for a Classical Field (I) . .	» 438
O. CHAMBERLAIN, W. W. CHUPP, G. GOLDBABER, E. SEGRÈ, C. WIEGAND, E. AMALDI, G. BARONI, C. CASTAGNOLI, C. FRANZINETTI and A. MANFREDINI - On the Observation of an Antiproton Star in Emulsion Exposed at the Bevatron . . . . .	» 447
R. GATTO - About the Capture and Annihilation of Antiprotons . . . .	» 468

*Note Tecniche:*

C. COTTINI, E. GATTI, G. GIANNELLI and G. ROZZI - Minimum Noise Pre-Amplifier for Fast Ionization Chambers . . . . .	» 473
--	-------

*Lettere alla Redazione:*

L. LEVI - Osservazioni sopra il processo di accrescimento a spirale in cristalli di bifosfato di ammonio (ADP). . . . .	» 484
T. TIETZ - The Solution of the Schrödinger Equation for an Approximate Atomic Field . . . . .	» 486
G. PUPPI and A. STANGHELLINI - Some Considerations of the Phase-Shift Analysis in the $(p^+p^+)$ Scattering . . . . .	» 491
B. NAGEL - A Remark on Quantum Electrodynamics with Non-Vanishing Photon Mass and Lamb Shift Calculations . . . . .	» 496
R. GATTO - About the $\Lambda^0$ -Nucleon Force . . . . .	» 499
D. A. TIDMAN - A quantum Theory of Refractive Index, Čerenkov Radiation and Ionization Loss . . . . .	» 503
PH. ROSSELET, R. WEILL et M. GAILLOUD - Production d'un hyperfragment par capture d'un hypéron négatif . . . . .	» 505

<i>Addendum</i> . . . . .	» 510
---------------------------	-------

<i>Libri ricevuti e Recensioni</i> . . . . .	» 511
--	-------

N. 3, 1° MARZO 1956

ADEL DA SILVEIRA - On the Theory of Spin-Two Particles . . . . .	pag. 513
E. P. WIGNER - Relativistic Invariance in Quantum Mechanics . . . . .	» 517
KEN-ITI GOTÔ - Quantization of Non-Linear Fields . . . . .	» 533
H. T. FLINT and E. M. WILLIAMSON - A Relativistic Theory of a Charged Particle in an Electromagnetic and Gravitational Field . . . . .	» 551

M. DEUTSCHMANN, M. CRESTI, W. D. B. GREENING, L. GUERRIERO, A. LORIA and G. ZAGO - Angular Correlations in $V^0$ Type Decays . . . . .	pag. 566
B. BROWMIK, D. EVANS, I. J. VAN HEERDEN and D. J. PROWSE - On the Spin of Artificially Produced $\tau$ -Mesons . . . . .	» 574
C. CEOLIN and N. DALLAPORTA - On a Possible Scheme for Heavy Unstable Particles . . . . .	» 586
F. DUIMIO - Un possibile schema generale di interazioni tra particelle elementari . . . . .	» 595
S. J. GOLDSACK and W. O. LOCK - The Capture of Negative Hyperons . . . . .	» 600
A. SALAM and W. GILBERT - On Generalized Dispersion Relations (II) . . . . .	» 607
P. SEN - A Mass Spectrum from a Field Theory Model of the Non-Local Theory . . . . .	» 612
P. BOCCHERI e A. LOINGER - La condizione supplementare del campo di Stückelberg . . . . .	» 626
E. HILLMAN and G. H. STAFFORD - Polarization Effects in Neutron-Proton Scattering at 98 MeV . . . . .	» 633

*Note Tecniche:*

P. POHL - A Simple Threefold Coincidence Circuit Using Only One EQ 80 (6 BE 7) Valve . . . . .	» 642
---	-------

*Lettere alla Redazione:*

W. B. CHESTON - Absorption of $K^-$ -Particles by Nuclei . . . . .	» 645
A. M. BAPTISTA et J. P. GALVÃO - Au sujet du volume sensible des compteurs de Geiger-Müller à cathode externe . . . . .	» 647
C. L. COWAN jr., F. B. HARRISON, L. M. LANGER and F. REINES - A Test of Neutrino-Antineutrino Identity . . . . .	» 649
O. SKJEGGESTAD and S. O. SØRENSEN - Mesonic Decay in Flight of a Triton Hyperfragment . . . . .	» 652
B. BERTOTTI - Gravitational Motion and Hamilton's Principle . . . . .	» 655
J. C. POLKINGHORNE - On the Integral Equation for the Heisenberg Current Operator . . . . .	» 658
A. BISI, S. TERRANI and L. ZAPPA - Radiation from $^{178}\text{W}$ . . . . .	» 661
B. BOSCO and R. STROFFOLINI - Meson-Meson Interaction from a Field- Theoretical Model . . . . .	» 662
R. GATTO - A Possible Method for Determining the Spins of the $\Sigma$ and of the $\Lambda$ . . . . .	» 665

<i>Libri ricevuti e Recensioni</i> . . . . .	» 669
--	-------

N. 4, 1° APRILE 1956

E. GROSSETTI - Determination of the Ultrasonic Absorption Coefficient in Liquids by the Thermal Method . . . . .	pag. 673
T. FULTON and R. G. NEWTON - Explicit Non-Central Potentials and Wave Functions for Given $S$ -Matrices . . . . .	» 677



M. B. PALMA-VITTORELLI, M. U. PALMA, D. PALUMBO and F. SGARLATA – Evidenced for a Double Covalent Bond from Paramagnetic Reso- nance, Optical Absorption and X-Ray Data . . . . .	pag. 718
J. CRUSSARD, V. FOUCHÉ, J. HENNESSY, G. KAYAS, L. LEPRINCE-RINGUET, D. MORELLET and F. RENARD – K-Mesons in Emulsions Exposed to a 6.2 GeV Proton Beam . . . . .	» 731
T. D. LEE and C. N. YANG – Charge Conjugation, a New Quantum Number $G$ , and Selection Rules Concerning a Nucleon-Antinucleon System . . . . .	» 749
G. BERTOLINI, M. BETTONI and E. LAZZARINI – $^{160}\text{Tb}$ Decay . . . . .	» 754
M. CINI and S. FUBINI – General Properties of the Fixed Source Meson Theory . . . . .	» 764
H. UMEZAWA, Y. TOMOZAWA, M. KONUMA and S. KAMEFUCHI – High Energy Behaviour of Renormalizable Fields . . . . .	» 772
G. BERTOLINI, M. BETTONI and E. LAZZARINI – Gamma-Gamma Angular Correlation in $^{46}\text{Ti}$ . . . . .	» 800
P. BASSI and F. FERRARI – The « $N$ » Component of Cosmics Rays in Re- lation to Oscillations of the Atmosphere . . . . .	» 806

*Note Tecniche:*

E. PICCIOTTO et F. SALVETTI – Comptage d' $\alpha$ à basse température; une méthode pour éviter la diffusion du Radon . . . . .	» 815
--	-------

*Lettere alla Redazione:*

E. LOHRMANN – Measurements on High Energy Electron Showers . . . . .	» 820
E. LOHRMANN – Meson Production at Very High Energies . . . . .	» 822
N. N. BISWAS, L. CECCARELLI-FABBRICHESI, M. CECCARELLI, K. GOTTSTEIN, N. C. VARSHNEYA and P. WALOSCHEK – On the Properties of $\tau^\pm$ -Mesons . . . . .	» 825
P. BOCCHERI, A. LOINGER e G. M. PROSPERI – Campi fermionici e metodo di quantizzazione di Feynman . . . . .	» 832
P. BUDINI – On Cut-Off and Non-Local Theories . . . . .	» 835
Y. EISENBERG, S. ROSENDORFF and Y. YEIVIN – A Note on the Analysis of $\tau$ -Meson Events . . . . .	» 837
B. LÜTHI and J. L. OLSEN – A New Effect in the Magnetoresistance of Aluminium . . . . .	» 840

<i>Libri ricevuti e Recensioni</i> . . . . .	» 842
--	-------

N. 5, 1<sup>o</sup> MAGGIO 1956

N. N. BOGOLJUBOV and D. V. ŠIRKOV – Charge Renormalization Group in Quantum Field Theory . . . . .	pag. 845
W. CZYŻ and J. SAWICKI – Polarization of Nucleons from Photonuclear Reactions . . . . .	» 864
H. KÜMMEL – Die Eigenschaften der quantentheoretischen Phasenraum- dichte . . . . .	» 870
G. EDER – Zerfall eines gebundenen $\Lambda^0$ -Teilchens . . . . .	» 880
G. EDER – Zur Photonvielfacherzeugung . . . . .	» 885

T. BASSANI, E. MONTALDI and F. G. FUMI - Electronic States of Diatomic Molecules: the $O_2^+$ Molecular Ion . . . . .	pag. 893
M. A. TONNELAT - Les équations approchées de la théorie du champ unifié d'Einstein-Schrödinger . . . . .	» 902
TSAI-CHÜ - Star Produced by the Capture of a Hyperon $\Sigma^-$ . . . . .	» 921
G. J. WADDINGTON - Observation on the Multiply Charged Particles of the Cosmic Radiation . . . . .	» 930
E. PEDRETTI - Kinematics of the Reaction $K + P \rightarrow \pi + \Sigma$ and of the Elastic Scattering $K + P \rightarrow K + P$ . . . . .	» 956
E. MINARDI - Su una teoria bilocale dell'interazione tra una particella con spin $\frac{1}{2}$ e il campo elettromagnetico . . . . .	» 968
D. PARK - The Theorem on Incoming Waves . . . . .	» 979
F. GÜRSEY - On a Conform-Invariant Spinor Wave Equation . . . . .	» 988
A. BISI, E. GERMAGNOLI and L. ZAPPA - Solid Scintillators for Beta Ray Spectrometry . . . . .	» 1007
J. DAUDIN, P. AUGER, A. CACHON et A. DAUDIN - Sur les variations diurnes en temps solaire et en temps sidéral des grandes gerbes de l'air . . . . .	» 1017
U. FARINELLI and A. GAMBA - Entropy in Quantum Mechanics . . . . .	» 1033
B. D'ESPAGNAT et J. PRENTKI - Interactions faibles des hyperons et des mésons lourds . . . . .	» 1045
S. KAMEFUCHI and H. HUMEZAWA - On the Limit of Applicability of Quantum Electrodynamics . . . . .	» 1060
G. MORPURGO - The Evidence from Angular Correlations on the Spin of the $\Lambda^0$ . . . . .	» 1069
L. F. LANDOVITZ and J. LEITNER - A Model for $\Lambda^0$ - $\theta^0$ Production . . . . .	» 1093
P. BUDINI - On the Pion-Nucleon Interaction . . . . .	» 1104
I. FILOSOFO, I. MODENA, E. POHL and J. POHL-RÜHLING - The Increase in the Total Cosmic Ray Intensity and in the Positive Excess due to the Solar Flare of 23rd February 1956 . . . . .	» 1112

*Note Tecniche:*

D. BLANC et R. VISIE - Le coefficient de température et la stabilité thermique des compteurs de Geiger-Müller autocoupeurs contenant une vapeur organique . . . . .	» 1119
---	--------

*Lettere alla Redazione:*

S. K. BHATTACHERJEE and S. RAMAN - A Note on the Decay of $^{185}\text{W}$ . . . . .	» 1131
B. JOUVET - On the Meaning of Fermi Coupling . . . . .	» 1133
T. TATI and H. TATI - On $\Lambda^0$ -Binding Energies in Hyperfragments . . . . .	» 1136
N. BRENE - A $\tau$ -Decay with a Secondary of Extremely Low Energy . . . . .	» 1140
R. GATTO - Remarks on the Absorption of Negative K-Mesons by Protons . . . . .	» 1142
K. SITE - Note on the Technique of Experiments on Air Shower Time Variations . . . . .	» 1145
Y. PAL VARSHNI - Dependence of Alpha Disintegration Energy on Proton and Neutron Numbers . . . . .	» 1148
A. DE MARCO, A. MILONE and M. REINHARZ - The Flux of the Helium Component of the Primary Cosmic Radiation at Geomagnetic Latitude $41^\circ \text{N}$ . . . . .	» 1150

F. BACHELET and A. M. CONFORTO - Increase of Cosmic Ray Intensity Associated with the Solar Flare of February 23, 1956 . . . . .	pag. 1153
K. PINKAU - The Conversion Length of High Energy Photons . . . . .	» 1156
C. CASTAGNOLI, C. FRANZINETTI and A. MANFREDINI - Probable Evidence for $Y_0$ -Events . . . . .	» 1159
G. BERTOLINI, M. BETTONI and E. LAZZARINI - Gamma-gamma Angular Correlation in $^{160}\text{Dy}$ . . . . .	» 1162
S. DEUTSCH - Radioactivité $\alpha$ spécifique des plaques Ilford pour recherches nucléaires - II. Activité de surface . . . . .	» 1166
F. HÄNNI, CH. LANG, M. TEUCHER, H. WINZELER and E. LOHRMANN - On the Mass of the $K^-$ -Meson . . . . .	» 1169
P. E. ARGAN and A. GIGLI - A New Detector of Ionizing Radiation. The Gas Bubble Chamber . . . . .	» 1171
<i>Libri ricevuti e Recensioni</i> . . . . .	» 1173

## N. 6, 1° GIUGNO 1956

P. G. BERGMANN - Introduction of « True Observables » into the Quantum Field Equations . . . . .	pag. 1177
I. POMERANČUK - Vanishing of Renormalized Charge in Quantum Electrodynamics and in Meson Theory . . . . .	» 1186
L. BASS - Radiation with a Finite Rest-Mass and the Heat Balance of the Earth . . . . .	» 1204
W. TOBOCMAN - Transition Amplitudes as Sums over Histories . . . . .	» 1213
H. HAKEN - Kopplung nichtrelativistischer Teilchen mit einem quantisierten Feld . . . . .	» 1230
A. CARRELLI and E. GROSSETTI - On Thermoelastic Waves in Liquids . . . . .	» 1254
C. C. GROSJEAN - A High Accuracy Approximation for Solving Multiple Scattering Problems in Infinite Homogeneous Media . . . . .	» 1262
G. TORALDO DI FRANCIA - Electromagnetic Cross-Section of a Small Circular Disc with Unidirectional Conductivity . . . . .	» 1276
K. PINKAU - Observations on Electromagnetic Cascades in Nuclear Emulsion . . . . .	» 1285
G. N. FOWLER - On the Ionization Loss of Fast $\mu$ -Mesons . . . . .	» 1316
P. E. ARGAN and A. GIGLI - Remarks on the Operation of the Diffusion Cloud Chamber - II . . . . .	» 1337
J. A. McLENNAN Jr. - Conformal Invariance and Conservation Laws for Relativistic Wave Equations for Zero Rest Mass . . . . .	» 1369
M. CINI, S. FUBINI and A. STANGHELLINI - The Coupling Constant of $p$ -Wave Pion-Nucleon Scattering . . . . .	» 1380
P. BROVETTO and S. FERRONI - On the Production of Heavy Mesons in the Nucleon-Nucleon Collision at Energies Near the Threshold . . . . .	» 1387
H. PRIMAKOFF - Exclusion Principle Inhibition of Bound Hyperon Mesonic Decay . . . . .	» 1394
F. A. BRISBOUT, C. DAHANAYAKE, A. ENGLER, P. H. FOWLER and P. B. JONES - Spurious Scattering in Nuclear Emulsions . . . . .	» 1400
D. AMATI and B. VITALE - On the Pion Annihilation of Nucleon-Antiproton Pairs . . . . .	» 1411
S. FUBINI - The Structure of the Nucleon . . . . .	» 1425
G. COCCONI - Intergalactic Space and Cosmic Rays . . . . .	» 1433

*Note Tecniche:*

M. FORTE - Light Pulses Excited by $\alpha$ -Particles in Argon. A Gaseous Scintillation Detector . . . . .	pag. 1443
D. I. JOVANOVIĆ - Échelle binaire rapide . . . . .	» 1456

*Lettere alla Redazione:*

S. R. MOHANTY, K. R. K. RAO and T. R. BHAT - Production of the Joshi Effect in Oxygen Under the Near Infrared . . . . .	» 1463
L. BARBANTI-SILVA, C. BONACINI, C. DE PIETRI, I. IORI, G. LOVERA, R. PERILLI-FEDELI and A. ROVERI - On a High Energy Electronic Shower . . . . .	» 1465
K. SITTE - Electron Production in Showers of Energies between 10 and 100 GeV . . . . .	» 1467
R. CESTER, T. F. HOANG, M. F. KAPLON and G. YEKUTIELI - Two Examples of Rare $K^+$ -Decays in Emulsion . . . . .	» 1471
P. BOCCHERI e A. LOINGER - Sul limite classico della teoria di una particella di Dirac . . . . .	» 1474
G. LOVERA - Fluttuazioni statistiche nei conteggi di gruppi di granuli e di lacune nelle emulsioni nucleari . . . . .	» 1476
P. ZIELIŃSKI - Note on the Angular Correlation in the Decays of Hyperfragments . . . . .	» 1479
N. N. BISWAS, L. CECCARELLI-FABBRICHESI, M. CECCARELLI, M. CRESTI, K. GOTTSTEIN, N. C. VARSHNEYA and P. WALOSCHEK - Interactions of $K^+$ Mesons with Hydrogen Nuclei at 50 to 110 MeV . . . . .	» 1481
A. GAMBA - Strange Particles and the Conservation of Isotopic Spin . . . . .	» 1486
G. GIACOMETTI - Sull'affinità metilica dei chinoni . . . . .	» 1488
A. J. HERZ, R. M. MAY, J. H. NOON, B. J. O'BRIEN and N. SOLNTSEFF - Interactions of $K^-$ -Particles . . . . .	» 1491
F. E. MAUGER - The Strength of Field Equations . . . . .	» 1494
<i>Libri ricevuti e Recensioni</i> . . . . .	» 1496
<i>Indici del Volume III, Serie X, 1956</i> . . . . .	» 1503

## INDICE PER AUTORI

Le sigle L., N.T. e N.d.L., si riferiscono rispettivamente alle *Lettere alla Redazione*, alle *Note Tecniche* e alle *Note di Laboratorio*.

ALTSHULER S. - Ingoing Waves in the Final State of Ionization Problems . . . . .	pag. 246
AMALDI E. (vedi CHAMBERLAIN O.) . . . . .	» 447
AMATI D. and B. VITALE - On the Pion Annihilation of Nucleon-Antiproton Pairs . . . . .	» 1411
AMMAN F. and L. DADDA - Design of the Pole Faces for Circular Particle Accelerators with the Electrolytic Tank . . . . .	» 184
ARGAN P. E. and A. GIGLI - A New Detector of Ionizing Radiation. The Gas Bubble Chamber (L.) . . . . .	» 1171

ARGAN P. E. and A. GIGLI - Remarks on the Operation of the Diffusion Cloud Chamber - II . . . . .	pag. 1337
AUGER P. (vedi DAUDIN J.) . . . . .	» 1017
BACHELET F. and A. M. CONFORTO - Increase of Cosmic Ray Intensity Associated with the Solar Flare of February 23, 1956 (L.) . . . . .	» 1153
BAPTISTA A. M. et J. P. GALVAO - Au sujet du volume sensible des compteurs de Geiger-Müller (L.) . . . . .	» 647
BARBANTI SILVA L., C. BONACINI, C. DE PIETRI, I. IORI, G. LOVERA, R. PERILLI FEDELI and A. ROVERI - On a High Energy Electronic Shower (L.) . . . . .	» 1465
BARDUCCI I. - Diffusion Coefficient of N in $\alpha$ -Fe . . . . .	» 350
BARKAS W. H. (vedi HECKMANN H.: H.) . . . . .	» 85
BARONI G. (vedi CHAMBERLAIN O.) . . . . .	» 447
BASS L. - Radiation with a Finite Rest-Mass and the Heat Balance of the Earth . . . . .	» 1204
BASSANI T., E. MONTALDI and F. G. FUMI - Electronic States of Diatomic Molecules: the $O_2^+$ Molecular Ion . . . . .	» 893
BASSI P. and F. FERRARI - The « N » Component of Cosmic Rays in Relation to Oscillations of the Atmosphere. . . . .	» 806
BATTACHERJEE S. K. and S. RAMAN - A Note on the Decay of $^{185}W$ (L.) . . . . .	» 1131
BERGMANN P. G. Introduction of « True Observables » into the Quantum Field Equations . . . . .	» 1177
BERTOLINI G., M. BETTONI and E. LAZZARINI - $^{169}Tb$ Decay . . . . .	» 754
BERTOLINI G., M. BETTONI and E. LAZZARINI - Gamma-Gamma Angular Correlation in $^{64}Ti$ . . . . .	» 800
BERTOLINI G., M. BETTONI and E. LAZZARINI - Gamma-Gamma Angular Correlation in $^{160}Dy$ (L.) . . . . .	» 1162
BERTOLINO G. - On Cosmic Ray Jets. . . . .	» 141
BERTOTTI B. - Gravitational Motion and Hamilton's Principle (L.) . . . . .	» 655
BETTONI M. (vedi BERTOLINI G.) . . . . .	» 754
BETTONI M. (vedi BERTOLINI G.) . . . . .	» 800
BETTONI M. (vedi BERTOLINI G.) (L.) . . . . .	» 1162
BHAT T. R. (vedi MOHANTY S. R.) (L.) . . . . .	» 1463
BHOWMIK B., D. EVANS, I. J. VAN HEERDEN and D. J. PROWSE - On the Spin of Artificially Produced $\tau$ -Mesons . . . . .	» 574
BISI A., E. GERMAGNOLI and L. ZAPPA - Solid Scintillators for Beta Ray Spectrometry. . . . .	» 1007
BISI A., S. TERRANI and L. ZAPPA - Radiation from $^{178}W$ (L.) . . . . .	» 661
BISWAS N. N., L. CECCARELLI-FABBRICHESI, M. CECCARELLI, K. GOTTSTEIN, N. C. VARSHNEYA and P. WALOSCHEK - On the Properties of $\tau^+$ -Mesons (L.) . . . . .	» 825
BISWAS N. N., L. CECCARELLI-FABBRICHESI, M. CECCARELLI, M. CRESTI K. GOTTSTEIN, N. C. VARSHNEYA and P. WALOSCHEK - Interaction of $K^+$ -Mesons with Hydrogen Nuclei at 50 to 110 MeV (L.) . . . . .	» 1481
BLANC D. et R. VISTE - Le coefficient de température et la stabilité thermique des compteurs de Geiger-Müller autocoupeurs contenant une vapeur organique (N. T.) . . . . .	» 1119
BLATT J. M. and S. T. BUTLER - Some Comments on $K^-$ -Interactions at Rest . . . . .	» 409
BOCCHIERI P. e A. LOINGER - Un'osservazione sulla condizione supplementare dell'elettrodinamica (L.) . . . . .	» 221



BOCCHIERI P. e A. LOINGER - La condizione supplementare del campo di Stückelberg . . . . .	pag. 626
BOCCHIERI P. e A. LOINGER - Sul limite classico della teoria di una particella di Dirac (L.) . . . . .	» 1474
BOCCHIERI P., A. LOINGER e G. M. PROSPERI - Campi fermionici e metodo di quantizzazione di Feynman (L.) . . . . .	» 832
BOGOLJUBOV N. N. and D. V. ŠIRKOV - Charge Renormalization Group in Quantum Field Theory . . . . .	» 845
BONACINI C. (vedi BARBANTI SILVA L.) (L.) . . . . .	» 1465
BONETTI A., R. LEVI-SETTI, M. PANETTI, G. ROSSI e G. TOMASINI - Lo spettro di energia degli elettroni di decadimento dei mesoni $\mu$ in emulsione nucleare . . . . .	» 33
BOSCO B. and R. STROFFOLINI - Meson-Meson Interaction from a Field-Theoretical Model (L.) . . . . .	» 662
BRACCI A., C. COCEVA, L. COLLI and R. DUGNANI LONATI - Experimental Measurements on Double Compton Effect. . . . .	» 203
BRENE N. - A $\tau$ -Decay with a Secondary of Extremely Low Energy (L.) . . . . .	» 1140
BRINKWORTH M. J. and B. ROSE - A Measurement of the Direction of the Polarization Produced in the Scattering of 135 MeV Protons . . . . .	» 195
BRISBOUT F. A., C. DAHANAYAKE, A. ENGLER, P. H. FOWLER and P. B. JONES - Spurious Scattering in Nuclear Emulsions . . . . .	» 1400
BROVETTO P. and S. FERRONI - On the Production of Heavy Mesons in the Nucleon-Nucleon Collisions at Energies Near the Threshold . . . . .	» 1387
BUDINI P. - On Cut-Off and Non-Local Theories . . . . .	» 835
BUDINI P. - On the Pion-Nucleon Interaction . . . . .	» 1104
BUTLER S. T. (vedi BLATT J. M.) . . . . .	» 409
CACHON A. (vedi DAUDIN J.) . . . . .	» 1017
CAIANIELLO E. R. - Number of Feynman Graphs and Convergence (L.) . . . . .	» 223
CARRELLI A. and E. GROSSETTI - On Thermoelastic Waves in Liquids . . . . .	» 1254
CASTAGNOLI C. (vedi CHAMBERLAIN O.) . . . . .	» 447
CASTAGNOLI C., C. FRANZINETTI and A. MANFREDINI - Probable Evidence for $Y_0$ -Events (L.) . . . . .	» 1159
CECCARELLI M. (vedi BISWAS N. N.) (L.) . . . . .	» 825
CECCARELLI M. (vedi BISWAS N. N.) (L.) . . . . .	» 1481
CECCARELLI-FABBRICHESI L. (vedi BISWAS N. N.) (L.) . . . . .	» 825
CECCARELLI-FABBRICHESI L. (vedi BISWAS N. N.) (L.) . . . . .	» 1481
CEOLIN C. and N. DALLAPORTA - On a possible Scheme for Heavy Unstable Particles . . . . .	» 586
CHAMBERLAIN O., W. W. CHUPP, G. GOLDBABER, E. SEGRÈ, C. WIEGAND, E. AMALDI, G. BARONI, C. CASTAGNOLI, C. FRANZINETTI and A. MANFREDINI - On the Observation of an Antiproton Star in Emulsion Exposed at the Bevatron . . . . .	» 447
CESTER R., T. F. HOANG, M. F. KAPLON and G. YEKUTIELI - Two Examples of Rare $K^+$ -Decay in Emulsion (L.) . . . . .	» 1471
CHESTON W. B. - Absorption of $K^-$ -Particles by Nuclei (L.) . . . . .	» 645
CHINAGLIA B. and F. DEMICHELI - Photographic Methods in $\gamma$ -Ray Scintillation Spectroscopy . . . . .	» 51
CHUPP W. W. (vedi CHAMBERLAIN O.) . . . . .	» 447
CINI M. and S. FUBINI - General Properties of the Fixed Source Meson Theory . . . . .	» 764

CINI M., S. FUBINI and A. STANGHELLINI - The Coupling Constant of $p$ -Wave Pion-Nucleon Scattering . . . . .	pag. 1380
COCCONI G. - Intergalactic Space and Cosmic Rays . . . . .	" 1433
COCEVA C. (vedi BRACCI A.) . . . . .	" 203
COLLI L. (vedi BRACCI A.) . . . . .	" 203
CONFORTO A. M. (vedi BACHELET F.) (L.) . . . . .	" 1153
COSTA G. and L. TAFFARA - On the Spin and Parity of the $\tau$ -Meson . . . . .	" 169
COTTINI C., E. GATTI, G. GIANNELLI and G. ROZZI - Minimum Noise Pre-Amplifier for Fast Ionization Chambers (N. T.) . . . . .	" 473
COWAN C. L. jr., F. B. HARRISON, L. M. LANGER and F. REINES - A Test of Neutrino-Antineutrino Identity (L.) . . . . .	" 649
CRESTI M. (vedi DEUTSCHMANN M.) . . . . .	" 180
CRESTI M. (vedi DEUTSCHMANN M.) . . . . .	" 566
CRESTI M. (vedi BISWAS N. N.) (L.) . . . . .	" 1481
(RUSSARD J., V. FOUCHÉ, J. HENNESSY, G. KAYAS, L. LEPRINCE-RINGUET, D. MORELLET and F. RENARD - K-Mesons in Emulsions Exposed to a 6.2 GeV Proton Beam . . . . .	" 731
CZYŻ W. and J. SAWICKI - Polarization of Nucleons from Photonicuclear Reactions . . . . .	" 864
DADDA L. (vedi AMMAN F.) . . . . .	" 184
DAHANAYAKE C. (vedi BRISBOUT F. A.) . . . . .	" 1400
DALLAPORTA N. (vedi CEOLIN C.) . . . . .	" 586
DAUDIN A. (vedi DAUDIN J.) . . . . .	" 1017
DAUDIN J., P. AUGER, A. CACHON et A. DAUDIN - Sur les variations diurnes en temps solaire et en temps sidéral des grandes gerbes de l'air . . . . .	" 1017
DEBENEDETTI A., C. M. GARELLI, L. TALLONE, M. VIGONE and G. WATAGHIN - A High Energy Shower (L.) . . . . .	" 226
DE SABBATA V. and A. SUGIE - A collective Model for the Nuclear Photo-Reaction. . . . .	" 16
DE SILVEIRA ADEL - On the Theory of Spin-Two Particles . . . . .	" 513
D'ESPAGNAT B. et J. PRENTKI - Interactions faibles des hypérons et des mésons lourds . . . . .	" 1045
DE MARCO A., A. MILONE and M. REINHARZ - The Flux of the Helium Component of the Primary Cosmic Radiation at Geomagnetic Latitude $41^\circ$ N (L.) . . . . .	" 1150
DEMICHELS F. (vedi CHINAGLIA B.) . . . . .	" 51
DEMICHELS F. and L. A. RADICATI - $\beta$ - $\gamma$ Angular Correlation of $^{214}_{83}\text{Bi}$ . . . . .	" 152
DEMICHELS F., R. A. RICCI and G. TRIVERO - Investigations on the $\beta$ -Decay of $^{208}_{81}\text{Po}(\text{ThC}')$ . . . . .	" 377
DE PIETRI C. (vedi BARBANTI SILVA L.) (L.) . . . . .	" 1465
DEUTSCH S. - Radioactivité $\alpha$ spécifique des plaques Ilford pour recherches nucléaires - II. Activité de surface (L.) . . . . .	" 1166
DEUTSCHMANN M., M. CRESTI, W. D. B. GREENING, L. GUERRIERO, A. LORIA and G. ZAGO - An Anomalous $V^0$ Event . . . . .	" 180
DEUTSCHMANN M., M. CRESTI, W. D. B. GREENING, L. GUERRIERO, A. LORIA and G. ZAGO - Angular Correlations in $V^0$ -Type Decays . . . . .	" 566
DIAMBRINI PALAZZI G. - A Magnetic Differential Probe. Its Employment for the Determination of the Static Median Magnetic Surface in the Gap of a Synchrotron . . . . .	" 336
DI CAPORIACCO G. and M. GIOVANNOZZI - Cloud Chamber Study of Cosmic Ray Electronic Showers under Dense Materials (II) . . . . .	" 305

DUGNANI LONATI R. (vedi BRACCI A.) . . . . .	pag. 203
DUIMIO F. - Un possibile schema generale di interazioni tra particelle elementari . . . . .	» 595
EDER G. - Zerfall eines gebundenen $\Lambda^0$ -Teilchens . . . . .	» 880
EDER G. - Zur Photonvielfacherzeugung . . . . .	» 885
EISENBERG Y., S. ROSENDORFF and Y. YEIVIN - A Note on the Analysis of $\tau$ -Meson Events (L.) . . . . .	» 837
ENGLER A. (vedi BRISBOUT F. A.) . . . . .	» 1400
EVANS D. (vedi BHOWMIK B.) . . . . .	» 574
FARINELLI U. and A. GAMBA - Entropy in Quantum Mechanics . . . . .	» 1033
FERRARI F. (vedi BASSI P.) . . . . .	» 806
FERRONI S. (vedi BROVETTO P.) . . . . .	» 1387
FIDECARO G. and A. M. WETHERELL - Notes on the Design of Distributed Amplifiers . . . . .	» 359
FILOSOFO I., I. MODENA, E. POHL and J. POHL-RÜHLING - The Increase in the Total Cosmic Ray Intensity and in the Positive Excess due to the Solar Flare of 23-rd February 1956 . . . . .	» 1112
FLINT H. T. and E. M. WILLIAMSON - A Relativistic Theory of a Charged Particle in an Electromagnetic and Gravitational Field . . . . .	» 551
FORTE M. - Light Pulses Excited by $\alpha$ -Particles in Argon. A Gaseous Scin- tillation Detector (N.T.) . . . . .	» 1443
FOUCHÉ V. (vedi CRUSSARD J.) . . . . .	» 731
FOWLER G. N. - On the Ionization Loss of Fast $\mu$ -Mesons . . . . .	» 1316
FOWLER P. H. (vedi BRISBOUT F. A.) . . . . .	» 1400
FRANZINETTI C. (vedi CHAMBERLAIN O.) . . . . .	» 447
FRANZINETTI C. (vedi CASTAGNOLI C.) (L.) . . . . .	» 1159
FUBINI S. (vedi CINI M.) . . . . .	» 754
FUBINI S. (vedi CINI M.) . . . . .	» 1380
FUBINI S. - The Structure of the Nucleon . . . . .	» 1425
FULTON T. and R. G. NEWTON - Explicit Non-Central Potentials and Wave Functions for Given $S$ -Matrices . . . . .	» 677
FUMI F. G. (vedi BASSANI T.) . . . . .	» 893
GAILLOUD M. (vedi ROSSELET PH.) (L.) . . . . .	» 505
GALVÃO J. P. (vedi BAPTISTA A. M.) (L.) . . . . .	» 647
GAMBA A. (vedi FARINELLI U.) . . . . .	» 1033
GAMBA A. - Strange Particles and the Conservation of Isotopic Spin (L.) . . . . .	» 1486
GARELLI C. M. (vedi DEBENEDETTI A.) (L.) . . . . .	» 226
GATTI E. (vedi COTTINI C.) (N. T.) . . . . .	» 473
GATTO R. - Charge Properties of the Weak Decay Interactions of the New Particles . . . . .	» 318
GATTO R. - About the Capture and Annihilation of Antiprotons . . . . .	» 468
GATTO R. - About the $\Lambda^0$ -Nucleon Force (L.) . . . . .	» 499
GATTO R. - A Possible Method for Determining the Spins of the $\Sigma$ and the $\Lambda$ (L.) . . . . .	» 665
GATTO R. - Remarks on the Absorption of Negative K-Mesons by Pro- tons (L.) . . . . .	» 1142
GEORGE E. P., A. J. HERZ, J. H. NOON and N. SOLNTSEFF - Nuclear Inter- actions of Negative K-Mesons in Nuclear-Research Emulsion . . . . .	» 94
GERMAGNOLI E. (vedi BISI A.) . . . . .	» 1007
GIACOMETTI G. - Sull'affinità metilica dei chinoni (L.) . . . . .	» 1488

GIANNELLI G. (vedi COTTINI C.) (N. T.) . . . . .	pag. 473
GIGLI A. (vedi ARGAN P. E.) (L.) . . . . .	» 1171
GIGLI A. (vedi ARGAN P. E.) . . . . .	» 1337
GILBERT W. (vedi SALAM A.) . . . . .	» 607
GIOVANNONZI M. (vedi DI CAPORACCO G.) . . . . .	» 305
GJELDAKER G. (vedi SCHARFF M.) (L.) . . . . .	» 216
GLASSER R. G. (vedi SCHEIN M.) . . . . .	» 131
GOLDEMBERG J. (vedi SILVA E.) . . . . .	» 12
GOLDHABER G. (vedi CHAMBERLAIN O.) . . . . .	» 447
GOLDSACK S. J. and W. O. LOCK - The Capture of Negative Hyperons . . . . .	» 600
GOTTSTEIN K. (vedi BISWAS N. N.) (L.) . . . . .	» 825
GOTTSTEIN K. (vedi BISWAS N. N.) (L.) . . . . .	» 1481
GREENING W. D. B. (vedi DEUTSCHMANN M.) . . . . .	» 180
GREENING W. D. B. (vedi DEUTSCHMANN M.) . . . . .	» 566
GROSJEAN C. C. - A High Accuracy Approximation for Solving Multiple Scattering Problems in Infinite Homogeneous Media . . . . .	» 1262
GROSSETTI E. - Determination of the Ultrasonic Absorption Coefficient in Liquids by the Thermal Method . . . . .	» 673
GROSSETTI E. (vedi CARRELLI A.) . . . . .	» 1254
G-STACK COLLABORATION - On the Masses and Modes of Decay of Heavy Mesons Produced by Cosmic Radiation . . . . .	» 510
GUERRIERO L. (vedi DEUTSCHMANN M.) . . . . .	» 180
GUERRIERO L. (vedi DEUTSCHMANN M.) . . . . .	» 566
GÜRSEY F. - On a Conform-Invariant Spinor Wave Equation . . . . .	» 988
HAKEN H. - Kopplung nichtrelativistischer Teilchen mit einem quanti- sierten Feld . . . . .	» 1230
HÄNNI F., CH. LANG, M. TEUCHER, H. WINZELER and E. LOHRMANN - On the Mass of the K-Meson (L.) . . . . .	» 1169
HARRISON F. B. (vedi COWAN C. L. jr.) (L.) . . . . .	» 649
HASKIN D. M. (vedi SCHEIN M.) . . . . .	» 131
HECKMANN H. H., F. M. SMITH and W. H. BARKAS - The Masses of Positive K-Particles . . . . .	» 85
HENNESSY J. (vedi CRUSSARD J.) . . . . .	» 731
HERZ A. J. (vedi GEORGE E. P.) . . . . .	» 94
HERZ A. J., R. M. MAY, J. H. NOON, B. J. O'BRIEN and N. SOLNTSEFF - Interactions of K-Particles (L.) . . . . .	» 1491
HILLMAN E. and G. H. STAFFORD - Polarization Effects in Neutron-Proton Scattering at 98 MeV . . . . .	» 633
HOANG T. F. (vedi CESTER R.) (L.) . . . . .	» 1471
IORI I. (vedi BARBANTI SILVA L.) (L.) . . . . .	» 1465
JONES P. B. (vedi BRISBOUT F. A.) . . . . .	» 1400
JOUVET B. - On the Measuring of Fermi Coupling (L.) . . . . .	» 1133
JOVANOVIĆ D. I. - Échelle binaire rapide (N.T.) . . . . .	» 1456
KAMEFUCHI S. and H. UMEZAWA - On the Limit of Applicability of Quantum Electrodynamics . . . . .	» 1060
KAMEFUCHI S. (vedi UMEZAWA H.) . . . . .	» 772
KAPLON M. F. (vedi CESTER R.) (L.) . . . . .	» 1471
KAY I. and H. E. MOSES - The Determination of the Scattering Potential from the Spectral Measure Function (II) - Point Eigenvalues and Proper Eigenfunctions . . . . .	» 66



KAY I. and H. E. MOSES - The Determination of the Scattering Potential from the Spectral Measure Function - (III) Calculation of the Scattering Potential from the Scattering Operator for the One-Dimensional Schrödinger Equation . . . . .	pag. 276
KAYAS G. (vedi CRUSSARD J.) . . . . .	» 731
KEN-ITI GOTÔ - Quantization of Non-Linear Fields . . . . .	» 533
KOBA Z. - Velocity of the Dirac Electron. . . . .	» 1
KOBA Z. - Supplementary Remarks on My Previous Note « Velocity of the Dirac Electron » (L.) . . . . .	» 215
KONUMA M. (vedi UMEZAWA H.) . . . . .	» 772
KRÓLIKOWSKI W. and I. RZEWUSKI - On « Potentials » in the Theory of Quantized Fields . . . . .	» 260
KÜMMEL H. - Die Eigenschaften der quantentheoretischen Phasenraum-dichte . . . . .	» 870
LANDOVITZ L. F. and J. LEITNER - A Model for $\Lambda^0$ - $\theta^0$ Production . . . . .	» 1093
LANG CH. (vedi HÄNNI F.) (L.) . . . . .	» 1169
LANGER L. M. (vedi COWAN C. L. Jr.) . . . . .	» 649
LAZZARINI E. (vedi BERTOLINI G.) . . . . .	» 754
LAZZARINI E. (vedi BERTOLINI G.) . . . . .	» 800
LAZZARINI E. (vedi BERTOLINI G.) (L.) . . . . .	» 1162
LEE T. D. and C. N. YANG - Charge Conjugation, a New Quantum Number $G$ , and Selection Rules Concerning a Nucleon-Antinucleon System . . . . .	» 749
LEITNER J. (vedi LANDOVITZ L. F.) . . . . .	» 1093
LEPRINCE-RINGUET L. (vedi CRUSSARD J.) . . . . .	» 731
LEVI L. - Osservazioni sopra il processo di accrescimento a spirale in cristalli di bifosfato di ammonio (ADP) (L.) . . . . .	» 484
LEVI-SETTI R. (vedi BONETTI A.) . . . . .	» 33
LIOTTA R. S. - Covariant Canonical Equations for a Classical Field (I) . . . . .	» 438
LOCK W. O. (vedi GOLDSACK S. J.) . . . . .	» 600
LOHRMANN E. and M. TEUCHER - Spurious Scattering in Nuclear Emulsions . . . . .	» 59
LOHRMANN E. (vedi TEUCHER M.) (L.) . . . . .	» 228
LOHRMANN E. - Measurements on High Energy Electron Showers (L.) . . . . .	» 820
LOHRMANN E. - Meson Production at Very High Energies (L.) . . . . .	» 822
LOHRMANN E. (vedi HÄNNI F.) (L.) . . . . .	» 1169
LOINGER A. (vedi BOCCHIERI P.) (L.) . . . . .	» 221
LOINGER A. (vedi BOCCHIERI P.) . . . . .	» 626
LOINGER A. (vedi BOCCHIERI P.) (L.) . . . . .	» 832
LOINGER A. (vedi BOCCHIERI P.) (L.) . . . . .	» 1474
LORIA A. (vedi DEUTSCHMANN M.) . . . . .	» 180
LORIA A. (vedi DEUTSCHMANN M.) . . . . .	» 566
LOVERA G. (vedi BARBANTI SILVA L.) (L.) . . . . .	» 1465
LOVERA G. - Fluttuazioni statistiche nei conteggi di gruppi di granuli e di lacune nelle emulsioni nucleari (L.) . . . . .	» 1476
LÜTHI B. and J. L. OLSEN - A New Effect in the Magnetoresistance of Aluminium (L.) . . . . .	» 840
MACLEOD G. R. - Cosmic Ray Showers of Wide Extent . . . . .	» 118
MANFREDINI A. (vedi CHAMBERLAIN O.) . . . . .	» 447
MANFREDINI A. (vedi CASTAGNOLI C.) (L.) . . . . .	» 1159
MAUGER F. E. - The Strength of Field Equations (L.) . . . . .	» 1494
MAY R. M. (vedi HERZ A. J.) (L.) . . . . .	» 1491
MCCUSKER C. B. A. and G. B. WILSON - The Rate of Extensive Showers of High Electron Density at Sea Level. . . . .	» 188



McLENNAN J. A. Jr. — Conformal Invariance and Conservation Laws for Relativistic Wave Equations for Zero Rest Mass . . . . .	pag. 1360
MILONE A. (vedi DE MARCO A.) (L.) . . . . .	» 1150
MINARDI E. — Su una teoria bilocale dell'interazione tra una particella con spin $1/2$ e il campo elettromagnetico . . . . .	» 968
MODENA I. (vedi FILOSOFO I.) . . . . .	» 1112
MOHANTY S. R. — Energetics of Elimination of Adsorbed Gases from Dielectric Surfaces Under Electrodeless Discharge (L.) . . . . .	» 219
MOHANTY S. R., K. R. K. RAO and T. R. BHAT — Production of the Joshi Effect in Oxygen Under the Near Infrared (L.) . . . . .	» 1463
MONTALDI E. (vedi BASSANI G.) . . . . .	» 893
MORELLET D. (vedi CRUSSARD J.) . . . . .	» 731
MORPURGO G. — On the Inelastic Scattering of Electrons from $^{12}\text{C}$ . . . . .	» 430
MORPURGO G. — The Evidence from Angular Correlations on the Spin of the $\Lambda^0$ . . . . .	» 1069
MOSES H. E. (vedi KAY I.) . . . . .	» 66
MOSES H. E. (vedi KAY I.) . . . . .	» 276
NAGEL B. — A Remark on Quantum Electrodynamics with Non-Vanishing Photon Mass and Lamb Shift Calculations (L.) . . . . .	» 496
NEWTON R. G. (vedi FULTON T.) . . . . .	» 677
NOON J. H. (vedi GEORGE E. P.) . . . . .	» 94
NOON J. H. (vedi HERZ A. J.) (L.) . . . . .	» 1491
O'BRIEN B. J. (vedi HERZ A. J.) (L.) . . . . .	» 1491
OLSEN J. L. (vedi LÜTHI B.) (L.) . . . . .	» 840
ORLOV Y. — The Non Linear Theory of Betatron Oscillations in the Strong Focusing Synchrotron (I) . . . . .	» 252
PALMA M. U. (vedi PALMA-VITTORELLI M. B.) . . . . .	» 718
PALMA-VITTORELLI M. B., M. U. PALMA, D. PALUMBO and F. SGARLATA — Evidence for a Double Covalent Bond from Paramagnetic Resonance, Optical Absorption and X-Ray Data . . . . .	» 718
PALUMBO D. (vedi PALMA-VITTORELLI M. B.) . . . . .	» 718
PAL VARSHNI Y. — Dependence of Alpha Disintegration Energy on Proton and Neutron Numbers (L.) . . . . .	» 1148
PANETTI M. (vedi BONETTI A.) . . . . .	» 33
PARK D. — The Theorem of Incoming Waves . . . . .	» 979
PEDRETTI E. — Kinematics of the Reaction $K + P \rightarrow \pi + \Sigma$ and of the Elastic Scattering $K + P \rightarrow K + P$ . . . . .	» 956
PERILLI FEDELI R. (vedi BARBANTI SILVA L.) (L.) . . . . .	» 1465
PICCIOTTO E. and F. SALVETTI — Comptage d' $\alpha$ à basse température; une méthode pour éviter la diffusion du Radon (N. T.) . . . . .	» 815
PINKAU K. — The Conversion Length of High Energy Photons (L.) . . . . .	» 1156
PINKAU K. — Observations on Electromagnetic Cascades in Nuclear Emulsion . . . . .	» 1285
POHL E. — A Simple Threefold Coincidence Circuit Using Only One EQ80 (6 BE 7) Valve (N. T.) . . . . .	» 642
POHL E. (vedi FILOSOFO I.) . . . . .	» 1112
POHL-RÜHLING J. (vedi FILOSOFO I.) . . . . .	» 1112
POLKINGHORNE J. C. — On the Integral Equation for the Heisenberg Current Operator (L.) . . . . .	» 658
POMERANČUK I. — Vanishing of Renormalized Charge in Quantum Electrodynamics . . . . .	» 1186
PORRECA F. — On the Causes Affecting the Phase Grating Permanence at the Stopping of the Ultrasounds . . . . .	» 371

PRENTKY J. (vedi D'ESPAGNAT B.) . . . . .	pag. 1045
PRIMAKOFF H. — Exclusion Principle Inhibition of Bound Hyperon Mesonic Decay . . . . .	» 1394
PROSPERI G. M. (vedi BOCCHIERI P.) (L.) . . . . .	» 832
PROWSE D. J. (vedi BHOWMIK B.) . . . . .	» 574
PUPPI G. and A. STANGHELLINI — Some Considerations of the Phase-Shift Analysis in the $(p^+p^+)$ Scattering (L.) . . . . .	» 491
RADICATI L. A. (vedi DEMICHELIS F.) . . . . .	» 152
RAMAN S. (vedi BATTACHERJEE S. K.) (L.) . . . . .	» 1131
RAO K. R. K. (vedi MOHANTY S. R.) (L.) . . . . .	» 1463
RAYSKI J. — On a Bilocal Interpretation of Isotopic Spin . . . . .	» 126
REINES F. (vedi COWAN C. L. jr.) (L.) . . . . .	» 649
REINHARZ M. (vedi DE MARCO A.) (L.) . . . . .	» 1150
RENARD F. (vedi CRUSSARD J.) . . . . .	» 731
RICCI R. A. (vedi DEMICHELIS F.) . . . . .	» 377
ROSE B. (vedi BRINKWORTH M. J.) . . . . .	» 195
ROSSELET PH., R. WEILL et M. GAILLOUD — Production d'un hyperfragment par capture d'un hypéron négatif (L.) . . . . .	» 505
ROSSI G. (vedi BONETTI A.) . . . . .	» 33
ROVERI A. (vedi BARBANTI SILVA L.) (L.) . . . . .	» 1465
ROZZI G. (vedi COTTINI C.) (N. T.) . . . . .	» 473
RZEWUSKI I. (vedi KROLIKÓWSKI W.) . . . . .	» 260
SALAM A. — On Generalized Dispersion Relations . . . . .	» 424
SALAM A. and W. GILBERT — On Generalized Dispersion Relations (II) . . . . .	» 607
SALVETTI F. (vedi PICCIOTTO E.) (N. T.) . . . . .	» 815
SAWICKI J. (vedi Czyż W.) . . . . .	» 864
SCHARFF M., G. GJELDAKER and S. SØRENSEN — Three Examples of Complete $\tau$ -Decay (L.) . . . . .	» 216
SCHEIN M., D. M. HASKIN and R. G. GLASSER — Heavy Unstable Particles Produced in the High Energy Pion Beam of the Berkeley Bevatron . . . . .	» 131
SEGRÈ E. (vedi CHAMBERLAIN O.) . . . . .	» 447
SEN P. — A Simple Non-Local Quantum Electrodynamics . . . . .	» 390
SEN P. — A Mass Spectrum from a Field Theory Model of the Non-Local Theory . . . . .	» 612
SGARLATA F. (vedi PALMA-VITTORELLI M. B.) . . . . .	» 718
SHERIF I. I. — The Molecular Heats of Gases from the Aspects of Heat Transfer . . . . .	» 6
SILVA E. and J. GOLDBERG — Photodisintegration of Samarium . . . . .	» 12
ŠIRKOV D. V. (vedi BOGOLJUBOV N. N.) . . . . .	» 845
SITTE K. — Note on the Technique of Experiments on Air Shower Time Variations (L.) . . . . .	» 1145
SITTE K. — Electron Production in Showers of Energies between 10 and 100 GeV (L.) . . . . .	» 1467
SKJEGGESTAD O. and S. O. SØRENSEN — Mesonic Decay in Flight of a Triton Hyperfragment (L.) . . . . .	» 652
SMITH F. M. (vedi HECKMANN H. H.) . . . . .	» 85
SOLNTSEFF N. (vedi GEORGE E. P.) . . . . .	» 94
SOLNTSEFF N. (vedi HERZ A. J.) (L.) . . . . .	» 1493
SØRENSEN S. (vedi SCHARFF M.) (L.) . . . . .	» 216
SØRENSEN S. O. (vedi SKJEGGESTAD O.) (L.) . . . . .	» 652

STAFFORD G. H. (vedi HILLMAN E.) . . . . .	pag. 633
STANGHELLINI A. (vedi PUPPI G.) (L.) . . . . .	" 491
STANGHELLINI A. (vedi CINI M.) . . . . .	" 1380
STROFFOLINI R. (vedi BOSCO B.) (L.) . . . . .	" 662
SUGIE A. (vedi DE SABBATA V.) . . . . .	" 16
TAFFARA L. (vedi COSTA G.) . . . . .	" 169
TAKABAYASI T. - Hydrodynamical Description of the Dirac Equation . . . . .	" 233
TAKABAYASI T. - New Classical Spin Theory as the Limit of the Dirac Equation . . . . .	" 242
TALLONE L. (vedi DEBENEDETTI A.) (L.) . . . . .	" 226
TATI H. (vedi TATI T.) (L.) . . . . .	" 1136
TATI T. and H. TATI - On $\Lambda^0$ Binding Energies in Hyperfragments (L.) . . . . .	" 1136
TERRANI S. (vedi BISI A.) (L.) . . . . .	" 661
TEUCHER M. (vedi LOHRMANN E.) . . . . .	" 59
TEUCHER M., H. WINZELER and E. LOHRMANN - A Possible Example of Production and Annihilation of an Antiproton (L.) . . . . .	" 228
TEUCHER M. (vedi HÄNNI F.) (L.) . . . . .	" 1169
TIDMAN D. A. - A Quantum Theory of Refractive Index, Cerenkov Radiation and Ionization Loss (L.) . . . . .	" 503
TIETZ T. - The Solution of the Schrödinger Equation for an Approximate Atomic Field (L.) . . . . .	" 486
TOBOCMAN W. Transition Amplitudes as Sums over Histories . . . . .	" 1213
TOMASINI G. (vedi BONETTI A.) . . . . .	" 33
TOMASINI A. - Excitation of Nuclei by Absorption of $\pi$ -Mesons (III) . . . . .	" 160
TOMOZAWA Y. (vedi UMEZAWA H.) . . . . .	" 772
TONNELAT M. A. - Les équations approchées de la théorie du champ unifié d'Einstein-Schrödinger . . . . .	" 902
TORALDO DI FRANCIA G. - Electromagnetic Cross-Section of a Small Circular Disc with Unidirectional Conductivity . . . . .	" 1276
TRIVERO G. (vedi DEMICHELIS F.) . . . . .	" 377
TSAI-CHÜ - Star Produced by the Capture of a Hyperon . . . . .	" 921
UMEZAWA H., Y. TOMOZAWA, M. KONUMA and S. KAMEFUCHI - High Energy Behaviour of Renormalizable Fields . . . . .	" 772
UMEZAWA H. (vedi KAMEFUCHI S.) . . . . .	" 1060
VAN HEERDEN I. J. (vedi BHOWMIK B.) . . . . .	" 574
VARSHNEYA N. C. (vedi BISWAS N. N.) (L.) . . . . .	" 825
VARSHNEYA N. C. (vedi BISWAS N. N.) (L.) . . . . .	" 1481
VIGONE M. (vedi DEBENEDETTI A.) (L.) . . . . .	" 226
VISTE R. (vedi BLANC D.) (N. T.) . . . . .	" 1119
VITALE B. (vedi AMATI D.) . . . . .	" 1411
WADDINGTON G. J. - Observation on the Multiply Charged Particles of the Cosmic Radiation . . . . .	" 930
WALOSCHEK P. (vedi BISWAS N. N.) (L.) . . . . .	" 825
WALOSCHEK P. (vedi BISWAS N. N.) (L.) . . . . .	" 1481
WATAGHIN G. (vedi DEBENEDETTI A.) (L.) . . . . .	" 226
WEILL R. (vedi ROSSELET PH.) (L.) . . . . .	" 505
WETHERELL A. M. (vedi FIDECARO G.) . . . . .	" 359
WIEGAND C. (vedi CHAMBERLAIN O.) . . . . .	" 447
WIGNER E. P. Relativistic Invariance in Quantum Mechanics . . . . .	" 517
WILLIAMSON E. M. - (vedi FLINT H. T.) . . . . .	" 551

WILSON G. B. (vedi McCUSKER C. B. A.) . . . . .	pag. 188
WINZELER H. (vedi TEUCHER M.) (L.) . . . . .	» 228
WINZELER H. (vedi HÄNNI F.) (L.) . . . . .	» 1169
YANG C. N. (vedi LEE T. D.) . . . . .	» 749
YEKUTIELI G. (vedi CESTER R.) (L.) . . . . .	» 1471
ZAGO G. (vedi DEUTSCHMANN M.) . . . . .	» 180
ZAGO G. (vedi DEUTSCHMANN M.) . . . . .	» 566
ZAPPA L. (vedi BISI A.) (L.) . . . . .	» 661
ZAPPA L. (vedi BISI A.) . . . . .	» 1007
ZIELIŃSKI P. — Note on the Angular Correlation in the Decays of Hyper- fragments (L.) . . . . .	» 1479

## INDICE ANALITICO PER MATERIE

### APPARATI E STRUMENTI E TECNICA SPERIMENTALE

Coefficient de température et la stabilité thermique des compteurs de Geiger-Müller autocoupeurs contenant une vapeur organique (N.T.), <i>D. Blanc et R. Viste</i> . . . . .	pag. 1119
Comptage d' $\alpha$ à basse température: une méthode pour éviter la diffusion du Radon (N.T.), <i>E. Picciotto and F. Salvetti</i> . . . . .	» 815
Design of Distributed Amplifiers. <i>G. Fidecaro and A. M. Wetherell</i> . . . . .	» 359
Design of the Pole Faces for Circular Particle Accelerators with the Electrolytic Tank, <i>F. Amman and L. Dadda</i> . . . . .	» 184
Échelle binaire rapide (N.T.), <i>D. T. Jovanović</i> . . . . .	» 1456
Fluttuazioni statistiche nei conteggi di gruppi di granuli e di lacune nelle emulsioni nucleari (L.), <i>G. Lovera</i> . . . . .	» 1476
Light Pulses Excited by $\alpha$ -Particles in Argon. A Gaseous Scintillation Detector (N.T.), <i>M. Forte</i> . . . . .	» 1443
Magnetic Differential Probe. Its Employment for the Determination of the Stadic Median Magnetic Surface in the Gap of a Synchrotron, <i>G. Diambrini Palazzi</i> . . . . .	» 336
Minimum Noise Pre-Amplifier for Fast Ionization Chambers (N.T.), <i>C. Cottini, E. Gatti, G. Giannelli and G. Rozzi</i> . . . . .	» 473
New Detector of Ionizing Radiation. The Gas Bubble Chamber (L.), <i>P. E. Argan and A. Gigli</i> . . . . .	» 1171
Non Linear Theory of Betatron Oscillations in the Strong Focusing Synchrotron (I), <i>Y. Orlov</i> . . . . .	» 252
Operation of the Diffusion Cloud Chamber - II, <i>P. E. Argan and A. Gigli</i> . . . . .	» 1337
Photographic Methods in $\gamma$ -Ray Scintillation Spectroscopy, <i>B. Chinaglia and F. Demichelis</i> . . . . .	» 51
Radioactivité $\alpha$ spécifique des plaques Ilford pour recherches nucléaires. - II. Activité de surface (L.), <i>M. Deutsch</i> . . . . .	» 1166
Simple Threefold Coincidence Circuit Using only One EQ 80 (6 BE 7) Valve (N.T.), <i>E. Pohl</i> . . . . .	» 642
Solid Scintillators for Beta Ray Spectrometry, <i>A. Bisi, E. Germagnoli and L. Zappa</i> . . . . .	» 1007



Spurious Scattering in Nuclear Emulsion, <i>F. A. Brisbout, C. Dahanayake, A. Engler, P. H. Fowler and P. B. Jones</i> . . . . .	pag. 1400
Spurious Scattering in Nuclear Emulsions, <i>E. Lohrmann and M. Teucher</i> »	59
Technique of Experiments on Air Shower Time Variations (L.), <i>K. Sitte</i> »	1145
Volume sensible des compteurs de Geiger-Müller (L.), <i>A. M. Baptista et J. P. Galvão</i> . . . . .	» 647

## COSMICA (RADIAZIONE)

Cloud Chamber Study of Cosmic Ray Electronic Showers under Dense Materials - II, <i>G. Di Caporiacco and M. Giovannozzi</i> . . . . .	pag. 305
Cosmic Ray Jets, <i>G. Bertolino</i> . . . . .	» 141
Cosmic Ray Showers of Wide Extent, <i>G. R. Macleod</i> . . . . .	» 118
Electron Production in Showers of Energies between 10 and 100 GeV. (I.), <i>K. Sitte</i> . . . . .	» 1467
Flux of the Helium Component of the Primary Cosmic Radiation at Geomagnetic Latitude 41° N (L.), <i>A. De Marco, A. Milone and M. Reinharz</i> . . . . .	» 1150
High Energy Electronic Showers (L.), <i>L. Barbanti-Silva, C. Bonacini, C. Depietri, I. Iori, G. Lovera, R. Perilli-Fedeli and A. Roveri</i> . .	» 1465
High Energy Shower (L.), <i>A. Debenedetti, C. M. Garelli, L. Tallone, M. Vigone and G. Wataghin</i> . . . . .	» 226
Increase of Cosmic Ray Intensity Associated with the Solar Flare of February 23, 1956 (L.), <i>F. Bachelet and A. M. Conforto</i> . . . . .	» 1153
Increase in the Total Cosmic Ray Intensity and in the Positive Excess due to the Solar Flare of 23rd February 1956, <i>I. Filosofo, I. Modena, E. Pohl and J. Pohl-Ruhling</i> . . . . .	» 1112
Intergalactic Space and Cosmic Rays, <i>G. Cocconi</i> . . . . .	» 1433
Measurements on High Energy Electron Showers (L.), <i>E. Lohrmann</i> .	» 820
« N » Component of Cosmic Rays in Relation to Oscillations of the Atmosphere, <i>P. Bassi and F. Ferrari</i> . . . . .	» 806
Observations on Electromagnetic Cascades in Nuclear Emulsions, <i>K. Pinkau</i> . . . . .	» 1285
Observations on the Multiply Charged Particles of the Cosmic Radiation, <i>G. J. Waddington</i> . . . . .	» 930
Rate of Extensive Showers of High Electron Density at Sea Level, <i>O. B. A. McCusker and G. B. Wilson</i> . . . . .	» 188
Variations diurnes en temps solaire et en temps sidéral des grandes gerbes de l'air, <i>J. Daudin, P. Auger, A. Cachon et A. Daudin</i> . . . . .	» 1017

## ELETTRODINAMICA E TEORIE DEI CAMPI

Bilocal Interpretation of Isotopic Spin, <i>J. Rayski</i> . . . . .	pag. 126
Campi fermionici e metodo di quantizzazione di Feynman (L.), <i>P. Bocchieri, A. Loinger e G. M. Prosperi</i> . . . . .	» 832
Charge Conjugation, a New Quantum Number <i>G.</i> and Selection Rules concerning a Nucleon-Antinucleon System, <i>T. D. Lee and C. N. Yang</i> .	» 749
Charge Renormalization Group in Quantum Field Theory, <i>N. N. Bogoljubov and D. V. Sirkov</i> . . . . .	» 845



Condizione supplementare del campo di Stückelberg, <i>P. Bocchieri e A. Loinger</i> . . . . .	pag. 626
Conform-Invariant Spinor Wave Equation, <i>F. Gursey</i> . . . . .	» 988
Conformal Invariance and Conservation Laws for Relativistic Wave Equations for Zero Rest Mass, <i>J. A. McLennan jr.</i> . . . .	» 1360
Conversion Length of High Energy Photon (L.), <i>K. Pinkau</i> . . . .	» 1156
Coupling Constant of <i>p</i> -Wave Pion-Nucleon Scattering, <i>M. Cini, S. Fubini and A. Stanghellini</i> . . . . .	» 1380
Covariant Canonical Equation for a Classical Field - I, <i>R. S. Liotta</i> .	» 438
Cut-Off and Non-Local Theories, <i>P. Budini</i> . . . . .	» 835
Determination of the Scattering Potential from the Spectral Measure Function. - II. Point Eigenvalues and Proper Eigenfunctions, <i>I. Kay and H. E. Moses</i> . . . . .	» 66
Determination of the Scattering Potential from the Spectral Measure Function. - III. Calculation of the Scattering Potential from the Scattering Operator for the One-Dimensional Schrödinger Equation, <i>I. Kay and H. E. Moses</i> . . . . .	» 276
Eigenschaften der quantentheoretischen Phasenraumdichte, <i>H. Kummel</i> .	» 870
Experimental Measurements on Double Compton Effect, <i>A. Bracci, C. Coceva, L. Colli and R. Dugnani Lonati</i> . . . . .	» 203
Explicit Non-Central Potentials and Wave Functions for given <i>S</i> -Matrices, <i>T. Fulton and R. G. Newton</i> . . . . .	» 677
Generalized Dispersion Relations, <i>A. Salam</i> . . . . .	» 424
Generalized Dispersion Relations. II, <i>A. Salam and W. Gilbert</i> . . . .	» 607
General Properties of the Fixed Source Meson Theory, <i>M. Cini and S. Fubini</i> . . . . .	» 764
High Energy Behaviour of Renormalizable Fields, <i>H. Umezawa, Y. Tomozawa, M. Konuma and S. Kamefuchi</i> . . . . .	» 772
Ingoing Waves in the Final State of Ionization Problems, <i>S. Altshuler</i> .	» 246
Integral Equation for the Heisenberg Current Operator (L.), <i>J. C. Polkinghorne</i> . . . . .	» 658
Introduction of « True Observables » into the Quantum Field Equations, <i>P. G. Bergmann</i> . . . . .	» 1177
Kopplung nichtrelativistischer Teilchen mit einem quantisierten Feld, <i>H. Haken</i> . . . . .	» 1230
Limit of Applicability of Quantum Electrodynamics, <i>S. Kamefuchi and H. Umezawa</i> . . . . .	» 1060
Mass Spectrum from a Field Theory Model of the Non-Local Theory, <i>P. Sen</i> . . . . .	» 612
Meaning of Fermi Coupling (L.), <i>B. Jowet</i> . . . . .	» 1133
Meson-Meson Interaction from a Field Theoretical Model (L.), <i>B. Bosco and R. Stroffolini</i> . . . . .	» 662
Number of Feynman Graphs and Convergence (L.), <i>E. R. Caianiello</i> .	» 223
Osservazione sulla condizione supplementare dell'elettrodinamica (L.), <i>P. Bocchieri e A. Loinger</i> . . . . .	» 221
Photonvielfacherzeugung, <i>G. Eder</i> . . . . .	» 885
Pion-Nucleon Interaction, <i>P. Budini</i> . . . . .	» 1104
« Potentials » in the Theory of Quantized Fields, <i>W. Królikowski and J. Rzewuski</i> . . . . .	» 260
Quantization of Non-Linear Fields, <i>Ken-Iti Goto</i> . . . . .	» 533

Radiation with a Finite Rest-Mass and the Heat Balance of the Earth, <i>L. Bass</i> . . . . .	pag. 1204
Relativistic Invariance in Quantum Mechanics, <i>E. P. Wigner</i> . . . . .	» 517
Remark on Quantum Electrodynamics with Non-Vanishing Photon Mass and Lamb Shift Calculations (L.), <i>B. Nagel</i> . . . . .	» 496
Simple Non-Local Quantum Electrodynamics, <i>P. Sen</i> . . . . .	» 390
Strength of Field Equations (L.), <i>F. E. Mauger</i> . . . . .	» 1494
Structure of the Nucleon, <i>S. Fubini</i> . . . . .	» 1425
Teoria bilocale dell'interazione tra una particella con spin $\frac{1}{2}$ e il campo elettromagnetico, <i>E. Minardi</i> . . . . .	» 968
Test of Neutrino-Antineutrino Identity (L.), <i>C. L. Cowan jr., F. B. Harrison, L. M. Langer and F. Reines</i> . . . . .	» 649
Theorem of Incoming Waves, <i>D. Park</i> . . . . .	» 979
Theory of Spin-Two Particles, <i>De Silveira Adel</i> . . . . .	» 513
Vanishing of Renormalized Charge in Quantum Electrodynamics, <i>I. Po- merančuk</i> . . . . .	» 1186
Transition Amplitudes as Sums over Histories, <i>W. Tobočan</i> . . . . .	» 1213

## LIQUIDI E SOLIDI

Diffusion Coefficient of N in $\alpha$ -Fe, <i>I. Barducci</i> . . . . .	pag. 350
Double Covalent Bond from Paramagnetic Resonance, Optical Absorp- tion and X-Ray Data, <i>M. B. Palma-Vittorelli, M. U. Palma, D. Pa- lumbo and F. Sgarlata</i> . . . . .	» 718
New Effect in the Magnetoresistance of Aluminium (L.), <i>B. Lüthi and J. L. Olsen</i> . . . . .	» 840
Processo di accrescimento a spirale in cristalli di bifosfato di ammonio (ADP) (L.), <i>L. Levi</i> . . . . .	» 484
Thermoelastic Waves in Liquids, <i>A. Carrelli and E. Grossetti</i> . . . . .	» 1254

## MESONI PESANTI E IPERONI

Absorption of $K^-$ -Particles by Nuclei (L.), <i>W. B. Cheston</i> . . . . .	pag. 645
Analysis of $\tau$ -Meson Events (L.), <i>Y. Eisenberg, S. Rosendorff and Y. Yeivin</i> . . . . .	» 837
Angular Correlation in the Decays of Hyperfragments (L.), <i>P. Zieliński</i> . . . . .	» 1479
Angular Correlations in $V^0$ Type Decays, <i>M. Deutschmann, M. Cresti, W. D. B. Greening, L. Guerriero, A. Loria and G. Zago</i> . . . . .	» 566
Anomalous $V^0$ Event, <i>M. Deutschmann, M. Cresti, W. D. B. Greening, L. Guerriero, A. Loria and G. Zago</i> . . . . .	» 180
Capture of Negative Hyperons, <i>S. J. Goldsack and W. O. Lock</i> . . . . .	» 600
Charge Properties of the Weak Decay Interactions of the New Particles, <i>R. Gatto</i> . . . . .	» 318
Comments on $K^-$ -Interactions at Rest, <i>J. M. Blatt and S. T. Butler</i> . . . . .	» 409
Evidence from Angular Correlations on the Spin of the $\Lambda^0$ , <i>G. Morpurgo</i> . . . . .	» 1069
Exclusion Principle Inhibition of Bound Hyperon Mesonic Decay, <i>H. Primakoff</i> . . . . .	» 1394
Heavy Unstable Particles Produced in the High Energy Pion Beam of the Berkeley Bevatron, <i>M. Schein, D. M. Haskin and R. G. Glasser</i> . . . . .	» 131

Kinematics of the Reaction $K + P \rightarrow \pi + \Sigma$ and of the Elastic Scattering $K + P \rightarrow K + P$ , <i>E. Pedretti</i> . . . . .	pag. 956
K-Mesons in Emulsions Exposed to a 6.2 GeV Proton Beam, <i>J. Crussard, V. Fouché, J. Hennessy, G. Kayas, L. Leprince-Ringuet, D. Morellet and F. Renard</i> . . . . .	» 731
$\Lambda^0$ Binding Energies in Hyperfragments (L.), <i>T. Tati and H. Tati</i> . . . . .	» 1136
$\Lambda^0$ Nucleon Force (L.), <i>R. Gatto</i> . . . . .	» 499
Interactions faibles des hyperons et des mésons lourds, <i>B. d'Espagnat et J. Prentki</i> . . . . .	» 1045
Interactions of $K^+$ -Mesons with Hydrogen Nuclei at 50 to 110 MeV (L.), <i>N. N. Biswas, L. Ceccarelli-Fabbrichesi, M. Ceccarelli, M. Cresti, K. Gottstein and N. C. Varshneya</i> . . . . .	» 1481
Interactions of $K^-$ -Particles (L.), <i>A. J. Herz, R. M. May, J. H. Noon, B. J. O'Brien and N. Solntseff</i> . . . . .	» 1491
Mass of the K-Meson (L.), <i>F. Hänni, Ch. Lang, M. Teucher, H. Wintelzer and E. Lohrmann</i> . . . . .	» 1169
Masses and Modes of Decay of Heavy Mesons Produced by Cosmic Radiation, <i>G-Stack Collaboration</i> . . . . .	» 510
Masses of Positive K-Particles, <i>H. H. Heckmann, F. M. Smith and W. H. Barkas</i> . . . . .	» 85
Mesonic Decay in Flight of a Triton Hyperfragment (L.), <i>O. Skjeggstad and S. O. Sørensen</i> . . . . .	» 652
Mesonic Decay of Hyperfragments (L.), <i>H. P. Fowler and K. H. Hansen</i> . . . . .	» 1495
Model for $\Lambda^0$ - $\theta^0$ Production, <i>L. F. Landovik and J. Leitner</i> . . . . .	» 1093
Nuclear Interactions of Negative K-Mesons in Nuclear Research Emulsion, <i>E. P. George, A. J. Herz, J. K. Noon and N. Solntseff</i> . . . . .	» 94
Possibile schema generale di interazioni tra particelle elementari, <i>F. Duimio</i> . . . . .	» 595
Possible Method for Determining the Spins of the $\Sigma$ and of the $\Lambda$ (L.), <i>R. Gatto</i> . . . . .	» 665
Possible scheme for Heavy Unstable Particles, <i>C. Ceolin and N. Dal-laporta</i> . . . . .	» 586
Probable Evidence for $Y_0$ -Events (L.), <i>C. Castagnoli, C. Franzinetti and A. Manfredini</i> . . . . .	» 1159
Production of Heavy Mesons on the Nucleon-Nucleon Collisions at Energies Near the Threshold, <i>P. Brovetto and S. Ferroni</i> . . . . .	» 1387
Production d'un hyperfragment par capture d'un hyperon négatif (L.), <i>Ph. Rosselet, R. Weill and M. Gaillard</i> . . . . .	» 505
Properties of $\tau^+$ -Mesons (L.), <i>N. N. Biswas, L. Ceccarelli-Fabbrichesi, M. Ceccarelli, K. Gottstein, N. C. Varshneya and P. Waloschek</i> . . . . .	» 825
Remarks on the Absorption of Negative K-Mesons by Protons (L.), <i>R. Gatto</i> . . . . .	» 1142
Spin and Parity of the $\tau$ -Meson, <i>G. Costa and L. Taffara</i> . . . . .	» 169
Spin of Artificially Produced $\tau$ -Mesons, <i>B. Bhowmick, D. Evans, I. J. Van Heerden and D. J. Prowse</i> . . . . .	» 574
Star Produced by the Capture of a Hyperon, <i>Tsai-Chü</i> . . . . .	» 921
Strange Particles and the Conservation of Isotopic Spin (L.), <i>A. Gamba</i> . . . . .	» 1486
Three Examples of Complete $\tau$ -Decay (L.), <i>M. Scharff, G. Gjeldaker and S. Sørensen</i> . . . . .	» 216
Two Examples of Rare $K^+$ -Decay in Emulsion (L.), <i>R. Cester, T. F. Hoang, M. F. Kaplan and G. Yekutieli</i> . . . . .	» 1471

$\tau$ -Decay with a Secondary of Extremely Low Energy (L.), <i>N. Brene</i> . . .	pag. 1140
Zerfall eines gebundenen $\Lambda^0$ Teilchens, <i>G. Eder</i> . . . . .	» 880

MESONI ( $\pi$  E  $\mu$ )

Ionization Loss of Fast $\mu$ -Mesons, <i>G. N. Fowler</i> . . . . .	pag. 1316
Meson Production at Very High Energies (L.), <i>E. Lohrmann</i> . . . . .	» 822
Spettro di energia degli elettroni di decadimento dei mesoni $\mu$ in emulsion nucleare, <i>A. Bonetti, R. Levi Setti, M. Panetti, G. Rossi e G. Tomasini</i> . . . . .	» 33

## MOLECOLE

Affinità metilica dei chinoni (L.), <i>G. Giacometti</i> . . . . .	pag. 1488
Electronic States of Diatomic Molecules: the $O_2^+$ Molecular Ion, <i>T. Basiani, E. Montaldi and F. G. Fumi</i> . . . . .	» 893
Molecular Heats of Gases from the Aspects of Heat Transfer, <i>I. I. Sherif</i> . . . . .	» 6

## NUCLEI (FISICA NUCLEARE)

Capture and Annihilation of Antiprotons, <i>R. Gatto</i> . . . . .	pag. 468
Collective Model for the Nuclear Photoreaction, <i>V. De Sabbata and A. Sugie</i> . . . . .	» 16
Considerations of the Phase-Shift Analysis in the ( $p$ - $p$ ) Scattering (L.), <i>G. Puppi and A. Stanghellini</i> . . . . .	» 491
Dependence of Alpha Disintegration Energy on Proton and Neutron Numbers (L.), <i>Y. Pal Varshni</i> . . . . .	» 1148
Excitation of Nuclei by Absorption of $\pi$ -Mesons. III, <i>A. Tomasini</i> . . . . .	» 160
Inelastic Scattering of Electrons from $^{12}C$ , <i>G. Morpurgo</i> . . . . .	» 430
Measurement of the Direction of the Polarization Produced in the Scattering of 135 MeV Protons, <i>M. J. Brinkworth and B. Rose</i> . . . . .	» 195
Observations of an Antiproton Star in Emulsion Exposed at the Bevatron, <i>O. Chamberlain, W. W. Chupp, G. Goldhaber, E. Segré, C. Wiegand, E. Amaldi, G. Baroni, C. Castagnoli, C. Franzinetti and A. Manfredini</i> . . . . .	» 447
Photodisintegration of Samarium, <i>E. Silva and J. Goldenberg</i> . . . . .	» 12
Pion Annihilation of Nucleon-Antiproton Pairs, <i>D. Amati and B. Vitale</i> . . . . .	» 1411
Polarization Effects in Neutron-Proton Scattering at 98 MeV, <i>E. Hillman and G. H. Stafford</i> . . . . .	» 633
Polarization of Nucleons from Photonuclear Reactions, <i>W. Czyż and J. Sawicki</i> . . . . .	» 864
Possible Example of Production and Annihilation of an Antiproton (L.), <i>M. Teucher, H. Winzeler and E. Lohrmann</i> . . . . .	» 228

## ONDE ELETTROMAGNETICHE

Electromagnetic Cross-Section of a Small Circular Disc with Unidirectional Conductivity, <i>G. Toraldo di Francia</i> . . . . .	pag. 1276
---	-----------



## QUANTISTICA (MECCANICA)

Entropy in Quantum Mechanics, <i>U. Farinelli and A. Gamba</i> . . . . .	pag. 1033
Hydrodynamical Description of the Dirac Equation, <i>T. Takabayasi</i> . . . . .	» 233
Limite classico della teoria di una particella di Dirac (L.), <i>P. Bocchieri and A. Loinger</i> . . . . .	» 1474
New Classical Spin Theory as the Limit of the Dirac Equation, <i>T. Takabayasi</i> . . . . .	» 242
Quantum Theory of Refractive Index, Čerenkov Radiation and Ionization Loss (L.), <i>D. A. Tidman</i> . . . . .	» 503
Solution of the Schrödinger Equations for an Approximate Atomic Field (L.), <i>T. Tietz</i> . . . . .	» 486
Supplementary Remarks on My Previous Note « Velocity of the Dirac Electron » (L.), <i>Z. Koba</i> . . . . .	» 214
Velocity of the Dirac Electron, <i>Z. Koba</i> . . . . .	» 1

## RADIOATTIVITÀ

$\beta$ - $\gamma$ Angular Correlation of $^{214}_{83}\text{Bi}$ , <i>F. Demichelis and L. A. Radicati</i> . . . . .	pag. 152
$^{160}\text{Tb}$ Decay, <i>G. Bertolini, M. Bettoni and E. Lazzarini</i> . . . . .	» 754
Gamma-Gamma Angular Correlation in $^{160}\text{Dy}$ (L.), <i>G. Bertolini, M. Bettoni and E. Lazzarini</i> . . . . .	» 1162
Gamma-Gamma Angular Correlation in $^{46}\text{Ti}$ , <i>G. Bertolini, M. Bettoni and E. Lazzarini</i> . . . . .	» 800
Investigations on the $\beta$ -Decay of $^{208}_{81}\text{Tl}(\text{ThC}'')$ , <i>F. Demichelis, R. A. Ricci and G. Trivero</i> . . . . .	» 377
Note on the Decay on $^{185}\text{W}$ (L.), <i>S. K. Battacherjee and S. Raman</i> . . . . .	» 1131
Radiation from $^{178}\text{W}$ (L.), <i>A. Bisi, S. Terrani and L. Zappa</i> . . . . .	» 661

## RELATIVITÀ GENERALE

Équations approchées de la théorie du champ unifié d'Einstein Schrödinger, <i>M. A. Tonnelat</i> . . . . .	pag. 902
Gravitational Motion and Hamilton's Principle (L.), <i>B. Bertotti</i> . . . . .	» 655
Relativistic Theory of a Charged Particle in an Electromagnetic and Gravitational Field, <i>H. T. Flint and E. M. Williamson</i> . . . . .	» 551

## SCARICHE NEI GAS

Energetics of Elimination of Adsorbed Gases from Dielectric Surfaces under Electrodeless Discharge, <i>S. R. Mohanty</i> . . . . .	pag. 219
Production of the Joshi Effect in Oxygen under the Near Infrared (L.), <i>S. R. Mohanty, K. R. K. Rao and T. R. Bhat</i> . . . . .	» 1463

## SCATTERING MULTIPLO E IONIZZAZIONE

High Accuracy Approximation for Solving Multiple Scattering Problems in Infinite Homogeneous Media, <i>C. C. Grosjean</i> . . . . .	pag. 1262
---	-----------

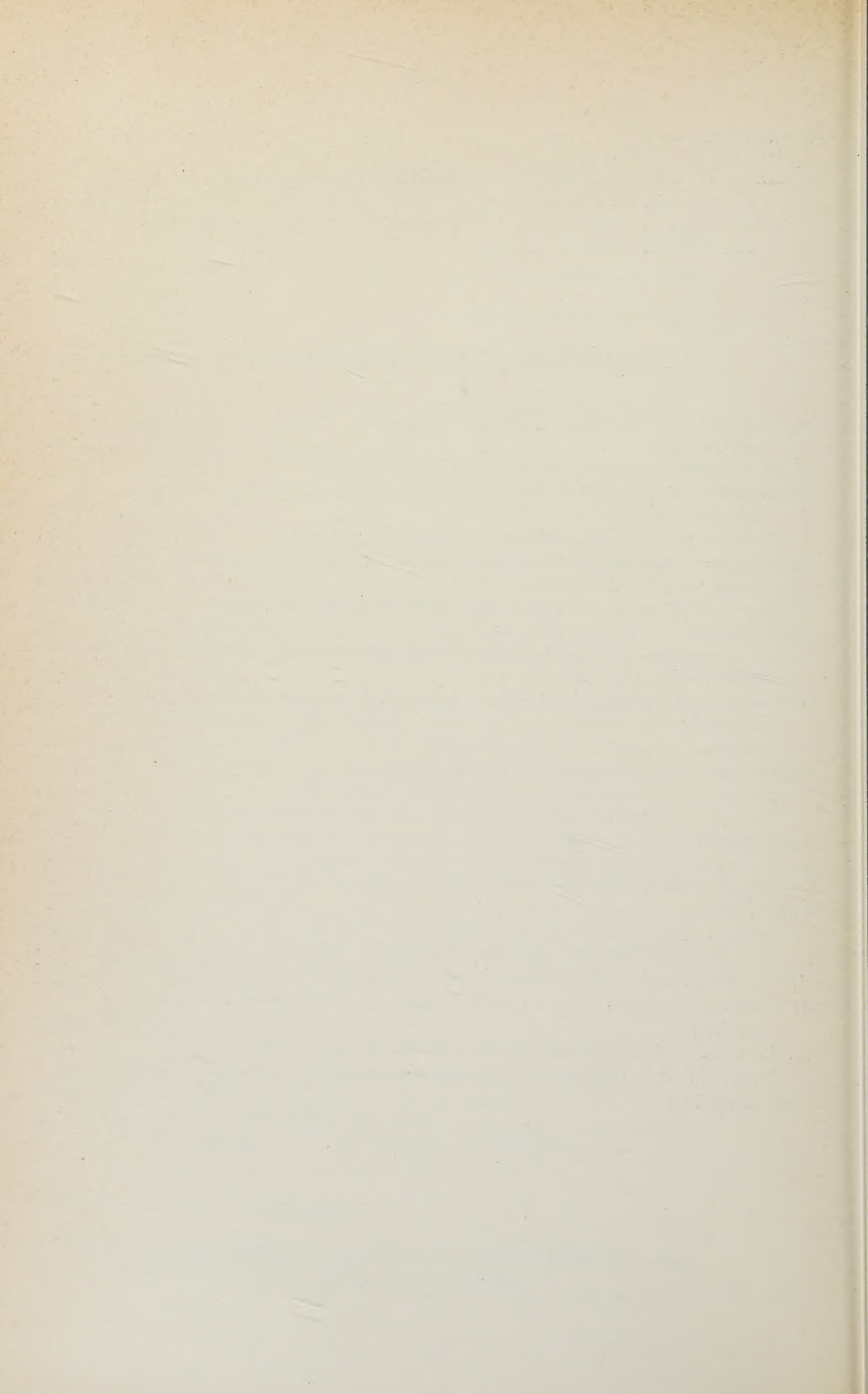


## ULTRASUONI

Causes Affecting the Phase Grating Permanence at the Stopping of the Ultrasounds, <i>F. Porreca</i> . . . . .	pag. 371
Determination of the Ultrasonic Absorption Coefficient in Liquids by the Thermal Method, <i>E. Grossetti</i> . . . . .	» 673

## INDICE DELLE RECENSIONI

H. SCHEIBEÉ und F. SEIDE — <i>Lecher Lehrbuch der Physik für Mediziner und Biologen</i> . . . . .	pag. 231
W. B. FRETTER — <i>Introduction to Experimental Physics</i> . . . . .	» 231
M. GOEPPERT MEYER and J. H. D. JENSEN — <i>Elementary theory of nuclear shell structure</i> . . . . .	» 511
J. DIEUDONNÉ — <i>La Géométrie des groupes classiques</i> . . . . .	» 669
R. COURANT — <i>Vorlesungen über Differential- und Integralrechnung - I. Funk- tionen einer Veränderlichen</i> . . . . .	» 669
P. SAMUEL — <i>Méthodes d'Algèbre abstraite en Géométrie algébrique</i> . . . .	» 670
H. HARTMANN — <i>Die Chemische Bindung</i> . . . . .	» 671
A. E. CRAWFORD — <i>Ultrasonic Engineering with Particular Reference to High Power Applications</i> . . . . .	» 842
G. POMILJ e D. NAPOLITANI — <i>Piano degli esperimenti ed elaborazione pro- babilistica dei risultati con particolare riguardo alla sperimentazione in biologia</i> . . . . .	» 843
H. HERMES — <i>Einführung in die Verbandstheorie</i> . . . . .	» 1173
W. THIRRING — <i>Einführung in die Quantenelektrodynamik</i> . . . . .	» 1174
L. COLLATZ — <i>Numerische Behandlung von Differentialgleichungen</i> . . . . .	» 1174
THE PHYSICAL SOCIETY, LONDON — <i>The Physics of the Ionosphere</i> . . . . .	» 1175
R. T. COX — <i>Statistical mechanics of irreversible change</i> . . . . .	» 1176
P. GRIVET — <i>La résonance paramagnétique nucléaire</i> . . . . .	» 1496
A. VON ENGEL — <i>Ionized Gases</i> . . . . .	» 1496
M. DUMAS — <i>Les épreuves sur échantillon</i> . . . . .	» 1497
D. HALLIDAY — <i>Introductory Nuclear Physics</i> . . . . .	» 1498
D. J. LITTLER and J. F. RAFFLE — <i>An Introduction to Reactor Physics</i> . . .	» 1499
E. BAUER — <i>Champs de vecteurs et de tenseurs. Introduction à l'électroma- gnétisme</i> . . . . .	» 1500
C. MIRANDA — <i>Equazioni alle derivate parziali di tipo ellittico</i> . . . . .	» 1500
L. BRILLOUIN and M. PARODI — <i>Propagation des ondes dans les milieux périodiques</i> . . . . .	» 1501



---

Fine del Volume III, Serie X, 1953

---

PROPRIETÀ LETTERARIA RISERVATA

---

Direttore responsabile: G. POLVANI

Tipografia Compositori - Bologna

Questo fascicolo è stato licenziato dai torchi il 28-V-1956

